Doctoral thesis

Doctoral theses at NTNU, 2022:353

Christian Fredrik Sætre

Orbital Stabilization of Nonlinear Underactuated Systems

NTNU
Norwegian University of Science and Technology
Thesis for the Degree of
Philosophiae Doctor
Faculty of Information Technology and Electrical
Engineering
Department of Engineering Cybernetics

NTNU
Norwegian University of
Science and Technology

Christian Fredrik Sætre

Orbital Stabilization of Nonlinear Underactuated Systems

Thesis for the Degree of Philosophiae Doctor

Trondheim, December 2022

Norwegian University of Science and Technology
Faculty of Information Technology and Electrical Engineering
Department of Engineering Cybernetics

NTNU
Norwegian University of
Science and Technology

NTNU
Norwegian University of Science and Technology

Thesis for the Degree of Philosophiae Doctor

Faculty of Information Technology and Electrical Engineering
Department of Engineering Cybernetics

ISBN 978-82-326-5510-6 (printed ver.)
ISBN 978-82-326-6639-3 (electronic ver.)
ISSN 1503-8181 (printed ver.)
ISSN 2703-8084 (online ver.)

Doctoral theses at NTNU, 2022:353

Printed by NTNU Grafisk senter

Abstract

Orbital stabilization is a particular form of set stabilization, where the control objective is to induce, via time-invariant state-feedback, an asymptotically stable *orbit* in the resulting closed-loop system. Here an orbit is understood as the set of all the states traced out by a solution of an autonomous system. The problem of orbital stabilization of a motion, *the orbital stabilization problem*, is therefore equivalent to the problem of ensuring the asymptotic orbital (Poincaré) stability of a particular solution of the controlled system. It constitutes a fundamental motion control objective, and can be formulated for a variety of different motions in terms of their associated orbits, including equilibria (trivial orbits), limit cycles (periodic orbits), point-to-point motions (heteroclinic orbits), etc.

Among the benefits of orbital stabilization is that it preserves the autonomy of the closed-loop system. It therefore has a relaxed control objective compared to trajectory tracking: Whereas a trajectory tracking controller aims to converge to an ever-evolving point in state space (i.e. a curve in time–state space), an orbitally stabilizing controller only needs to ensure convergence to the curve this point traces out in state space. This makes orbital stabilization well-suited for executing specific motions of highly nonlinear and underactuated systems, for which non-feedback-linearizable and non-minimum phase dynamics are common.

This thesis is devoted to the study of the orbital stabilization problem. It provides contributions along three main lines: 1) projection- and linearization-based methods for designing orbitally stabilizing feedback for various forced motions of a rich class of nonlinear, control-affine dynamical systems; 2) procedures for planning forced orbits of a class of underactuated mechanical systems; and 3) a technique that allows one to add a sliding mode control–based robustifying feedback extension to an existing orbitally stabilizing controller for trivial and periodic motions. A series of numerical experiments demonstrate the effectiveness of the proposed methods, including executing point-to-point maneuvers of the "butterfly" robot, generating orbitally stable symmetric walking gaits of a three-link compass biped with two degrees of underactuation, and inducing up-right oscillations in an underactuated cart-pendulum system subject to unknown perturbations.

Keywords: Orbital Stabilization, Orbital Stability, Underactuated Mechanical Systems, Transverse Linearization, Sliding Mode Control, Motion Planning.

Preface

This thesis is the culmination of the research I conducted during my doctoral studies at the Department of Engineering Cybernetics, NTNU, from August 2017 to December 2021. The research has been funded by the Research Council of Norway as part of the project "Dynamic manipulation for industrial and service robotics applications", grant number 262363, under the supervision of Prof. Anton Shiriaev.

Acknowledgments

First and foremost, I would like to thank my supervisor, Prof. Anton Shiriaev. Our discussions have been a great source of learning, and I will be forever grateful that you introduced me to the topics and problems from which the key ideas in this thesis have evolved.

I would also thank everyone I have collaborated with the last few years. In particular, I would like to thank Dr. Ahmed Chemori for the opportunity of a research stay in the beautiful city of Montpellier; Prof. Leonid Fridman for teaching me about sliding mode control; and Prof. Leonid Freidovich for his keen eye and insightful comments. I would also like to thank everyone at the Department of Engineering Cybernetics, as well as all the anonymous reviewers of my papers for their valuable comments and suggestions.

Last, but definitely not least, I am especially grateful to my partner, Siri, and my family for all their patience, encouragement and support during these last few years.

Publications

The thesis is partly based on the following publications:

I. C.F. Sætre, A.S. Shiriaev, and T. Anstensrud. 'Trajectory optimization and orbital stabilization of underactuated Euler-Lagrange systems with impacts'. *Proceedings of the 18th European Control Conference (ECC).* IEEE. pp. 758–763, 2019.

C.F.S. conceptualized the paper and derived the mathematical statements. C.F.S. implemented and performed the numerical experiments. C.F.S. wrote and prepared the original draft. A.S. supervised the work. All authors reviewed the original draft and contributed to the revision of the paper.

II. C.F. Sætre, A.S. Shiriaev, S. Pchelkin, and A.Chemori. 'Excessive transverse coordinates for orbital stabilization of (underactuated) mechanical systems'. *Proceedings of the 1st Virtual European Control Conference*

(ECC). IEEE. pp. 895–900, 2020.

C.F.S. conceptualized the paper and derived the mathematical statements. C.F.S. implemented and performed the numerical experiments. C.F.S. wrote and prepared the original draft. A.S. and A.C. supervised the work. All authors reviewed the original draft and contributed to the revision of the paper.

III. C. F. Sætre and A. Shiriaev. 'On excessive transverse coordinates for orbital stabilization of periodic motions'. *Proceedings of the IFAC World Congress 2020.* Vol. 52. 2. IFAC-PapersOnLine. pp. 9250–9255, 2020.

C.F.S. conceptualized the paper and derived the mathematical statements. C.F.S. implemented and performed the numerical experiments. C.F.S. wrote and prepared the original draft. A.S. supervised the work. Both authors reviewed the original draft and contributed to the revision of the paper.

IV. C. F. Sætre and A. Shiriaev. 'On orbital stabilization as an alternative to reference tracking control'. *Proceedings of the 16th International Workshop on Advanced Motion Control (AMC).* IEEE. pp. 91–97, 2020.

C.F.S. conceptualized the paper and derived the mathematical statements. C.F.S. implemented and performed the numerical experiments. C.F.S. wrote and prepared the original draft. A.S. supervised the work. Both authors reviewed the original draft and contributed to the revision of the paper.

V. C. F. Sætre, A. Shiriaev, L.B. Freidovich, S.V. Gusev, and L.M. Fridman. 'Robust orbital stabilization: A Floquet theory–based approach'. *International Journal of Robust and Nonlinear Control* Vol. 31.16, pp. 8075–8108, 2021.

Inspired in part by the ideas in the patent application of L.B.F. and S.V.G., C.F.S. and A.S conceptualized the paper. C.F.S. derived the mathematical statements. C.F.S. implemented and performed the numerical experiments. C.F.S. wrote and prepared the original draft. A.S. and L.M.F. supervised the work. All authors reviewed the original draft and contributed to the revision of the paper.

VI. C. F. Sætre and A. Shiriaev. 'Orbital stabilization of point-to-point maneuvers in underactuated mechanical systems'. *Accepted for publication in Automatica.* Preprint available at the arXiv: arXiv:2102.04966. 2022.

C.F.S. conceptualized the paper and derived the mathematical statements. C.F.S. implemented and performed the numerical experiments. C.F.S. wrote and prepared the original draft. A.S. supervised the work. Both authors reviewed the original draft and are contributing in regard to the revisions of the paper.

Contents

Chapter 1

Introduction

1.1 Background and motivation

Industrial robots are arguably one of humanity's greatest technological innovations. For several decades already, they have been successfully utilized in factories around the world to automate dangerous and repetitive tasks, with benefits ranging from increased productivity and lowered costs, to improved product quality and manufacturing reliability. Their success partly comes to the task they are set to solve. Indeed, many of the standard applications where industrial robots are utilized in industry today, including basic welding, painting and pick-and-place operations, can most often be considered as almost pure kinematic problems. In such cases, both the problems of motion planning and motion control are well understood, and there exists a large variety of simple, safe and reliable methods that may be applied which are available in most standard textbooks on the subject. This has allowed industrial robotics manufacturers to produce off-the-shelf robots which are easy to install, easy to program and reliable to use.

While purely kinematic considerations are often sufficient for the most standard tasks, there are nevertheless almost always certain benefits of also considering some properties of the *dynamics* of the robotic system. For example, model-based cancellation of certain dynamical aspects (e.g., gravity compensation or inverse-dynamics control) can enhance accuracy and performance, whereas force/impedance control allows robotics systems to also perform contact-based tasks, such as drilling and milling operations. However, with robotic systems nowadays expected to perform ever more complex tasks and to execute increasingly difficult maneuvers, rather than just simply compensating for- or removing dynamical aspects of the system, there has been an increased focus on instead *exploiting* these aspects

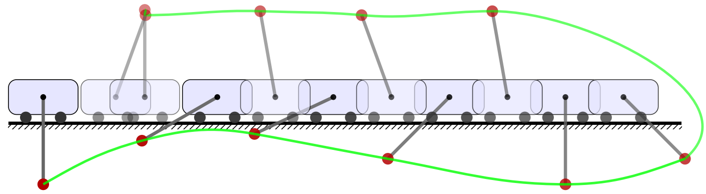

(a) Swinging up an unactuated pendulum on a cart.

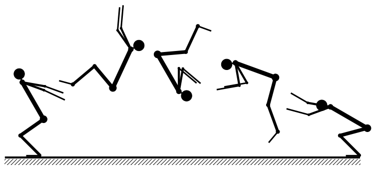

(b) Executing a backflip.

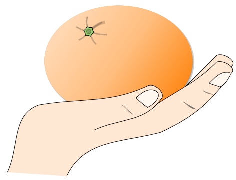

(c) Manipulating an orange.

Figure 1.1: Examples of some highly dynamic and underactuated tasks.

to solve the task at hand. In fact, certain tasks and behaviors are inherently dynamic by their very nature. Consider, for instance, the following problems: swinging up an unactuated pendulum on a cart (Fig. 1.1(a)); having a humanoid robot perform a backflip (Fig. 1.1(b)); or the problem of maneuvering a compliant object, say an orange (Fig. 1.1(c)), on the palm of a robotic hand. To successfully execute the desired behavior for such tasks, the complex interplay between the internal- and external forces acting on the system needs to be continuously shaped as to maintain a certain balance that ensures the correct time evolution of its states.

From dynamic walking [1, 2] to dynamic manipulation [3–5], utilizing the dynamical properties of a system potentially allows for a massive increase in the possible motions it can perform, and consequently the tasks it can solve. It may also be used to improve the system's energy efficiency, and might even allow for an increase in its workspace [6].

The challenges of underactuation

While the benefits and potential of harnessing a system's inherent dynamical properties are clearly vast, so, too, are the challenges faced by the control engineer tasked with ensuring that the intended dynamic behavior is executed both safely and reliably. Consider, for instance, tasks such as those depicted in Figure 1.1. Not only are the equations of motion of such systems often highly nonlinear, but they are also *underactuated* [7–12], meaning simply that the system has fewer independent controls than it has degrees of freedom. This effectively limits the control influence one has upon the system at any given time instant. Compared to systems which are fully actuated, underactuation therefore brings with it two main challenges: First, it restricts the space of feasible maneuvers which the system can execute. Second, it generally prohibits the use simplifying strategies such a feedback linearization.[1] To better illustrate this fact, consider the fully-actuated version of the cart-pendulum system shown in Figure 1.1(a). In theory, *any* continuous evolution of its states can be achieved, and the systems can both be steered to- and be at rest at any of its configurations. Its underactuated counterpart with a passive pendulum, on the other hand, can only execute those motions which comply with the dynamical constraints which arise due to the system's underactuation. Moreover, it can only be at rest with the pendulum in either its upright or downright position.

Separate model-based motion planning and control design

While the last few decades have seen a surge in new data-driven (model-free), learning-based design methods to tackle such problems (see, e.g., [14, 15]), some of the most well-known, state-of-the-art applications, including the parkouring Atlas robot [16], still predominantly adhere to methods in-line with the more classical model-based approaches. Roughly speaking, such approaches are generally divided into two steps: First, one uses a mathematical model of the system to plan a nominal, open-loop motion; and then, in the second step, one designs a model-based feedback controller to compensate for uncertainties and the perturbations that inevitably will occur in practice. There are of course a multitude of different ways to solve either of these steps. However, the most common types of approaches are arguably those following the reference-trajectory tracking methodology. In these methods, on first finds a desired motion, represented by a time-varying reference trajectory, using, for example, some form of trajectory optimization approach such as collocation- or shooting-based methods [17–21]. Then, in the second step, one designs (by some means) a time-varying tracking controller which ensures that the reference trajectory is (uniformly) asymptotically stable.

Due to the time-varying nature of the reference-tracking methodology, any such scheme will necessarily have an inherent "timing" property stemming from the tracking controller always attempting to have the system in specific configurations at specific time instants. Whilst this property may be vital in some applications, it can make trajectory tracking less suited for others. In the case of an underactuated system, for instance, trying to

[1] More general strategies, e.g., partial (input-output) feedback linearization [13], can also be of limit use in the general case, due to both the need of nonlinear coordinate–control transformations and the possibility of unstable (non-minimum phase) zero dynamics.

minimize the distance to the trajectory in state space while simultaneously attempting to enforce the timing of the motion, puts, roughly speaking, extra strain on the (limited) control action that is available. Moreover, the inherent timing-property of any such control scheme means that, even if just slightly delayed, the system might be momentarily driven away from the nominal motion in state space in order to instead "catch up in time" (see [22] for an excellent illustrative example in this regard).

Orbital stabilization: ensuring the orbital stability of a motion

For certain motion control tasks, especially those in which one wants to make use of a system's dynamical properties, it may instead be the closeness to the desired motion in the state space of the system which is of paramount importance, whereas the "timing" of the motion is of less importance (if important at all). Compared to the reference (trajectory) tracking problem, this allows for a relaxation of the control objective by essentially removing a dimension: the time dimension. More specifically, one can instead try to find a completely time-invariant, (static) state-feedback control law such that the resulting autonomous closed-loop system admits the desired motion as an asymptotically stable *orbit*. Namely, as an invariant, non-self-intersecting curve in the system's state space corresponding to the desired motion, to which all neighboring trajectories converge.

We call this concept of both generating and stabilizing (via feedback) a specific desired motion, while simultaneously preserving the system's autonomy, *orbital stabilization*; while the problem of finding such a control law is referred to as an *orbital stabilization problem*. This concept is heavily linked to the well-established notion of (asymptotic) *orbital stability* of a solution to an autonomous (dynamical) system [23–28]. Indeed, orbital stabilization of a motion can be considered as the problem of rendering the desired motion an (asymptotically) orbitally stable solution of the closed-loop system; or equivalently, the asymptotic stabilization of the orbit traced out by the solution in the system's state space.

General-purpose methods for orbital stabilization

A variety of methods have been proposed that (at least partly) solve the orbital stabilization problem for particular types of motion and/or for different classes of dynamical systems. For instance, in the case of equilibrium points (i.e. trivial orbits), it is known that Lyapunov's stability notion coincides with orbital stability [29] (see also Sec. 2.2). Thus, for (forced) equilibrium points, the orbital stabilization problem coincides with the reference tracking problem (which, in turn, condenses down to a constant set-point regulation problem), for which there are a vast and varied number of differ-

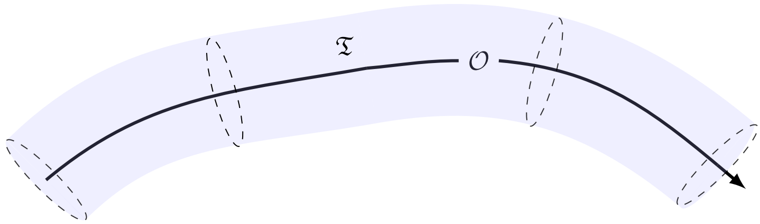

Figure 1.2: Illustration of a positively invariant tube $\mathfrak{T}$ surrounding the orbit $\mathcal{O}$.

ent control methods and -strategies available. The body of work regarding the stabilization of periodic orbits is also quite extensive, see, e.g., [30–38] to name but a few (some of these methods are covered in more detail in Section 3.4). Nevertheless, there is still a need for general-purpose methods which are both applicable to a large class of underactuated, nonlinear dynamical systems, as well as methods which can be utilized to stabilize other orbits than just trivial and periodic ones. Of particular interest are methods which simultaneously provide a time-invariant, strict (local) *Lyapunov function* [23, 39–43]. Indeed, besides just its value in regard to stability and robustness analysis, knowledge of such a function also allows for the use of robustification techniques such as Lyapunov redesign [44]. Moreover, it can be used to obtain a conservative estimate of the region of attraction under the control law, in the form of a positively invariant (tubular) neighbourhood of the nominal motion, as illustrated in Figure 1.2.

Linearization-based control design

In the case of a linearly stabilizable equilibrium point, it is well known that both an exponentially stabilizing control law and a quadratic (local) Lyapunov function can be obtained from the Jacobian linearization about this point. Depending on the nonlinearity of the system, the region of attraction under such a controller may of course be fairly local (although effective numerical methods for finding estimates of the region of attraction exist; see [42]). Regardless, linearization remains an integral part of nonlinear control theory. This is not only due to the fact that it is applicable to a large class of systems, but also because it allows one to utilize well-established tools from linear systems theory for both control design and stability analysis.

In regard to the problem of executing known nontrivial motions of a highly nonlinear, underactuated system (consider, e.g., tasks such as those depicted in Fig. 1.1), it might not make sense to speak of anything else than the *local* stability of the motion. Hence, any method which allows for the construction of a feedback controller rendering the motion asymptotically orbitally stable within a small neighbourhood surrounding it (see Fig. 1.2) is necessarily of great value. The linear system obtained from linearizing a system about the nontrivial target motion is, however, of little use in this regard. Not only is the linear system time-varying, but it can only be stabilized by a time-varying controller in general. This raises the following key question: How can one use linearization-based techniques to construct a time-invariant orbitally stabilizing control law for nontrivial motions?

Projection operators, transverse coordinates and -linearization

In [22], Hauser and Hindman proposed a method allowing the orbital stabilization problem[2] to be solved for feedback linearizable systems (see also [45–48] for some further extensions of this approach). The key idea proposed therein was to convert a linear trajectory tracking controller into a controller stabilizing the trajectory's orbit by using a particular projection of the system states onto the desired orbit, a so-called *projection operator* as we will refer to it in this thesis. This projection operator recovered the corresponding "time" to be used, thus eliminating the controller's time dependence. Thus the former tracking error instead became a *transverse* error—a weighted measure of the distance from the current state to the orbit. Moreover, this allowed one to transform the positive definite, time-varying Lyapunov function for the desired trajectory under the tracking controller into a time-invariant, positive semidefinite Lyapunov function for the orbit.

New arguments which allows one to extend the applicability of such an approach to a more general class of dynamical systems is naturally of particular interest in regard to a general-purpose method for solving the orbital stabilization problem. For this purpose, one can find inspiration in the rich history surrounding the problem of characterizing the (in-)stability of a motion. Specifically, for periodic orbits, it has long been known (see, e.g., [23, 24, 27, 49]) that strict contraction in the directions transverse to the orbit corresponds to the contraction of all neighboring solutions towards the orbit itself; see also [50–52]. Moreover, the occurrence of this contraction can be established by assessing the stability of the origin of a set of so-called *transverse coordinates* [30, 34, 41, 53]. These are (local) coordinates which

[2]The concept of a *maneuver* is introduced in [22]. That is, a non-self-intersecting curve in state–control space corresponding to a specific (forced) motion. While the projection of each maneuver upon state space defines a unique orbit, there might not (especially for systems not affine in the controls) be a unique maneuver for each (forced) orbit. Thus, the concept of *maneuver regulation* considered in [22] is equivalent to the concept of orbital stabilization as we consider it in this thesis.

evolve upon- and span some continuously evolving transverse hypersurface, a so-called *moving Poincaré Section* [54, 55], of dimension one less than the dimension of the state space. The exponential (in-)stability of the origin of such coordinates can, in turn, be determined from the linearization of their dynamics along the nominal orbit [26], a so-called *transverse linearization* [34, 41, 56].

Projection-based (excessive transverse) coordinates

It is upon the bedrock-combination of projection operators, transverse coordinates and the concept of a transverse linearization which most of the methods we will present in this thesis for solving the orbital stabilization problem are built. While such a combination allows one to compute a linearization which can be used to design orbitally stabilizing feedback, knowledge of a set of transverse coordinates evolving upon a moving Poincaré section, and whose zero-level set provides an implicit representation of the non-vanishing orbit, is necessarily a prerequisite in this regard. While there exist several methods for obtaining such a set of coordinates (see e.g., [30, 31, 34, 38, 53, 57], to name but a few), they are often applicable only to a specific class of dynamical systems. Moreover, their construction can vary significantly depending on the orbit and may also require additional numerical steps.

As an alternative, one can instead consider an *excessive* set of transverse coordinates. In fact, given knowledge of a regular parameterization of the orbit and a projection operator, one can always obtain a generic set of such coordinates. For instance, the projection-based function corresponding to the difference between the current state and its projection (through the projection operator) onto the orbit, acts as an excessive set of coordinates upon the moving Poincaré section defined by the projection operator. In the work of Pchelkin et al. [38], such coordinates were used to design two families of orbitally stabilizing controllers for fully-actuated robot manipulators. To determine the orbital stability of a motion, a linear auxiliary system corresponding to the transverse linearization was used. However, this auxiliary system was not explicitly defined, but stated in the form of a matrix equation which needed to be solved numerically.

Among the contributions of this thesis is to provide explicit expressions for the transverse linearization of such excessive coordinates, in the form of a system of differential-algebraic equations. In fact, we show that such a linearization is equivalent to the linearization obtained by Leonov [26, 58] (see also [59]) in relation to his work on determining the (in-)stability of motions in both the orbital and Zhukovsky sense. Even though this allows for effective and generic methods for designing orbitally stabilizing feedback controllers, it has surprisingly not, at least to author's best knowledge, been directly utilized for this purpose before. Furthermore, due to the structure of the aforementioned projection-based functions, it is in fact natural to view such a linearization along a non-trivial orbit (rather than about a reference trajectory) as a continuation of the (Jacobian) linearization about an equilibrium point. Indeed, we will in this thesis see that this allows one to develop methods for solving orbital stabilization problems formulated for a variety of different motions, such as those corresponding to a forced equilibrium point (trivial orbits), limit cycles (periodic orbits), point-to-point motions (heteroclinic orbits), and hybrid cycles (hybrid periodic orbits).

The need for additional robustness

In addition to the methods we will present in this thesis, there exist several other methods for designing orbitally stabilizing feedback for different classes of systems in the literature (some prominent methods in regard to periodic orbits were listed earlier in the introduction). These methods all share a primary goal: to simultaneously generate and stabilize self-induced motions (e.g. oscillations) via time-invariant continuous state-feedback. This means that, in general, a precise mathematical model of the system to be controlled is required for these methods to be successfully applied. Indeed, since the resulting closed-loop system is autonomous, any unknown disturbance or model discrepancies (e.g., due to unmodelled dynamics or uncertain parameters), may significantly alter its behavior. Thus, if not taken into consideration, unknown perturbations can result in a change of both the shape and location of the induced orbit, even rendering it unstable. Yet, with the exception of a few methods that are either only applicable for a very limiting class of systems [36] or only ensure asymptotic orbital stability of some of the system's states [37], most orbital stabilization methods for non-trivial orbits are not designed specifically with robustness in mind.

This lack of robustness can be problematic, as uncertainty and unknown disturbances will often be an inherent part of many such tasks. Consider, for example, the problem of rolling a compliant object, say, an orange, on the palm of a robotic hand (see Fig. 1.1(c)). In such a dynamic manipulation problem, trying to accurately model all the complex phenomena which occur due to the contact between the hand and the compliant object when it is in motion is not only a daunting task, it will often be infeasible in practice. A more realistic strategy is to use a model of the system which is "good enough" in the aforementioned two-step procedure, and then complementing it by a *robust* controller. That is, to use the available mathematical model to both find an approximate ("almost feasible") motion and to design a nominal feedback for it, whereas the remaining disturbances and uncertainties are lumped together and compensated for by a robustifying feedback extension.

Adding robustifying extensions based on sliding mode control

Regarding the problem of designing the aforementioned robustifying feedback extension, the sliding mode control (SMC) methodology [60–63] is especially well suited due to its insensitivity to bounded perturbations satisfying a matching condition. It consists of two main steps: 1) the construction of a vector-valued *switching function*, whose zero-level set defines a *sliding manifold/surface* on which the system has desired properties; and 2) the design of a control law which ensures that the sliding manifold is reached in finite time despite of any matched perturbations.

There exist a large array of different strategies [62–66] to solve the latter problem, provided that a switching function with an appropriate relative degree is given and the perturbation has certain known attributes (bounded, Lipschitz continuous, etc.). Thus the question which is of most interest in regard to the topics in this thesis is the following: How to construct a time-invariant switching function that defines a sliding manifold upon which the system's states converges to a desired orbit?

In [67], Freidovich and Gusev proposed a series of general steps for finding such a switching function for (underactuated) mechanical systems: 1) Construct a linear feedback controller stabilizing the transverse linearization while simultaneously ensuring the existence of a real invariant subspace of the closed-loop system, whose co-dimension equals the number of independent controls; 2) Construct a continuous full-rank left annihilator of this subspace; 3) Construct a switching function from this annihilator using a set of transverse coordinates and a projection operator.

Inspired by this approach, we propose in this thesis a similar method, where we instead add to an existing orbitally stabilizing feedback controller a robustifying feedback extension. The switching functions is designed with the particular property that the first-order approximation system under the *equivalent control* in sliding mode [60, 62] corresponds to the first-order approximation of the perturbation-free system under the nominal orbitally stabilizing feedback controller. This allows for a novel robustification procedure for orbitally stabilizing feedback, which is applicable to both trivial- and periodic orbits, as well as to a large class of nonlinear dynamical systems, including underactuated mechanical systems.

1.2 Contributions and outline of the thesis

1.2.1 Summary of contributions

The aim of this thesis is to study and develop methods for orbital stabilization of various forced motions of dynamical systems, with a particular focus on underactuated mechanical systems.

A summary of the main contributions of this thesis follows:

- A new motion control problem, *the orbital stabilization problem*, is formulated. It incorporates the problem of ensuring, via the use of feedback control, asymptotic orbital stability of a variety of different motions.

- Constructive procedures for solving the orbital stabilization problem for periodic motions, point-to-point motions, as well as hybrid periodic motions in a class of hybrid systems.

- Methods for planning various orbits of underacted mechanical systems.

- Procedures for adding robustifying feedback extensions to existing control laws which orbitally stabilizes trivial- or periodic orbits.

Scope and limitations

We only consider systems of ordinary differential equations which are affine in the control variables, and whose state space is $\mathbb{R}^n$. Measurements of all the states of the system under consideration are assumed to be available.

In an attempt to make the material accessible also to readers having limited knowledge of differential geometry, we have tried to keep notation and terminology which are not inline with basic calculus to a minimum.

1.2.2 Outline

A summary of each chapter in this thesis follows.

Chapter 2. Preliminaries: The Stability of Orbits

Some preliminaries concepts relating to the stability of orbits of autonomous (dynamical) systems are presented. This includes orbits and their properties, some relevant stability definitions such as the notion of orbital stability, as well as some classical methods for assessing the stability of orbits, e.g. the use of linearization, the Andronov–Vitt theorem, and Leonov's method.

Chapter 3. The Orbital Stabilization Problem

We formulate the orbital stabilization problem, as well as introduce some necessary assumptions and key concepts. We also outline the basic ideas and general lines of the suggested approaches for solving the orbital stabilization problem for various types of orbits. Moreover, we provide some simple, motivating examples, and draw connections to some related concepts.

Chapter 4. Orbital Stabilization of Periodic Motions

The problem of stabilizing periodic orbits is considered. Some key concepts are introduced and reviewed, including projection operators and transverse coordinates. It is shown that combining these two concepts allows for a local change of coordinates in a vicinity of the periodic orbit, thus essentially separating the transverse- and tangential dynamics. We further demonstrate how this allows for the design of exponentially orbitally stabilizing control laws via convex optimization. Of particular importance, we study so-called projected differential Lyapunov- and Riccati equations which arise from the transverse linearization corresponding to a generic set of projection-based excessive transverse coordinates.

Chapter 4 is partly based on [68, 69]. The main contributions are:

- Explicit expressions for the transverse linearization for an excessive set of transverse coordinates are provided; see Proposition 4.30 and Corollary 4.31 in Section 4.5.
- Projected differential Lyapunov equations for assessing the stability of periodic orbits; see Theorem 4.41 in Section 4.6.2.
- Projected differential Riccati–based equations for constructing orbitally stabilizing feedback by solving a semidefinite programming problem; see Proposition 4.44 and Proposition 4.46 in Section 4.6.3.

Chapter 5. Applications to Underactuated Mechanical Systems

A procedure based on so-called *synchronizations function* for planning orbits of underacted mechanical systems is proposed. In this regard, properties of the *reduced dynamics* associated with the synchronization functions are reviewed and studied. We also study a specific set of projection-based excessive transverse coordinates and provide expressions for the corresponding transverse linearization for more general mechanical systems.

Chapter 5 is partly based on [70, 71]. The main contributions are:

- A synchronization function–based method for planning periodic- and heteroclinic orbits of mechanical systems with one degree of underactuation; see Theorem 5.16 Theorem 5.18 and Theorem 5.18 in Section 5.3.

- Explicit expressions for the transverse linearization corresponding to a particular excessive set of transverse coordinates; see Proposition 5.22 in Section 5.4.

Chapter 6. Orbital Stabilization of Point-to-Point Maneuvers

The problem of exponential stabilization, via continuous static state-feedback, of a heteroclinic orbit corresponding to a so-called point-to-point maneuver is considered. To achieve this, a specific parameterization of the motion and a particular projection operator are introduced. Roughly speaking, this allows one to "merge" the Jacobian linearization at the equilibria on the boundaries with a transverse linearization along the orbit. This, in turn, provides a method for computing stabilizing control gains offline by solving a semidefinite programming problem. The resulting nonlinear controller, which exponentially stabilizes both the orbit and the final equilibrium point, is locally Lipschitz continuous and requires no discontinuous switching.

Chapter 6 is based on [71]. The main contributions are:

- Sufficient conditions ensuring that a (locally Lipschitz continuous) feedback controller orbitally stabilizes the orbit of a known point-to-point maneuver of a nonlinear control-affine system; see Theorem 6.10 in Section 6.3.4.

- A constructive procedure allowing for the design of such feedback by solving a semidefinite programming problem; see Proposition 6.12 in Section 6.3.4.

- Arguments facilitating the generation of orbitally stable point-to-point motions of a ball rolling between any two points upon the frame of the "butterfly" robot; see Proposition 6.13 in Section 6.4

Chapter 7. Orbital Stabilization of Cycles in Hybrid Systems

The problem of stabilizing hybrid cycles of a class of hybrid dynamical systems is considered. Moreover, a numerical framework for constructing such forced hybrid cycles of underactuated mechanical systems with jumps is also presented. Specifically, we use synchronization functions to rewrite a trajectory optimization problem, where parts of the dynamical constraints arising due to the system's underactuation are reduced to a single equation in integral form. This allows for the discretization of the planning problem into a parametric nonlinear programming problem using some numerical quadrature.

Chapter 7 is partly based on [72]. The main contributions are:

- A statement allowing one to design an orbitally stabilizing feedback for hybrid periodic orbit of a hybrid dynamical system using semidefinite programming problem is provided; see Theorem 7.2 in Section 7.2.2.
- A series of constructive steps allowing one to effectively search for hybrid periodic orbits of a class of underactuated hybrid mechanical systems using nonlinear programming; see Section 7.3.

Chapter 8. Robust Orbital Stabilization via Sliding Mode Control

We present a method that allows one to add a robustifying feedback extension to an existing feedback orbitally stabilizing trivial or periodic orbits. The approach utilizes the sliding-mode control (SMC) methodology. Thus, if found, the feedback extension can be applied as to completely compensate for any model uncertainties and external disturbances satisfying a matching condition. The main contribution of the chapter is a constructive procedure for designing the time-invariant switching function used in the SMC synthesis. More specifically, in the case of a periodic orbit, its zero-level set (the sliding manifold) is designed using a real Floquet–Lyapunov transformation to locally correspond to an invariant subspace of the Monodromy matrix of a transverse linearization. This ensures asymptotic stability of the periodic orbit when the system is confined to the sliding manifold sufficiently close to the orbit.

Chapter 8 is based on [73]. The main contributions are:

- A procedure and conditions allowing for the robustification of a known controller which exponentially stabilizes an equilibrium point; see Lemma 8.2 and Proposition 8.6 in Section 8.2.
- A procedure and conditions allowing for the robustification of an existing controller which exponentially stabilizes a periodic orbit; see Theorem 8.21 and Proposition 8.27 in Section 8.4.

1.3 Notation

Sets

We denote by $\mathbb{R}$, $\mathbb{R}_{\geq 0}$ and $\mathbb{R}_{>0}$ the set of real numbers, the nonnegative reals and the strictly positive reals, respectively. We use $\mathbb{R}^{n\times m}$ (resp. $\mathbb{C}^{n\times m}$) to denote the set of all real (resp. complex) $n\times m$ matrices, with $\mathbb{R}^n=\mathbb{R}^{n\times 1}$; $\mathbb{M}^n$ is the set of all real, symmetric $n\times n$ matrices and ($\mathbb{M}^n_{\succeq 0}$) $\mathbb{M}^n_{\succ 0}$ the set of all real, symmetric, positive (semi-) definite matrices.

Matrix and vector notation

For column vectors $x\in\mathbb{R}^n$ and $y\in\mathbb{R}^m$, we use $\mathrm{col}(x,y)=[x^\mathsf{T},y^\mathsf{T}]^\mathsf{T}$. For two points, $a,b\in\mathbb{R}^n$, we denote $\mathfrak{L}(a,b):=\{a+(b-a)\iota,\ \ \iota\in[0,1]\}$, i.e. the set of all points lying one the line segment connecting a and b. We denote by $\mathbf{I}_n$ the $n\times n$ identity matrix; $\mathbf{0}_{n\times m}$ is used to denote an $n\times m$ matrix of zeros, with $\mathbf{0}_n=\mathbf{0}_{n\times n}$; while $\mathbb{1}_{n\times m}$ denotes a matrix containing only ones. $A^\mathsf{T}\in\mathbb{R}^{m\times n}$ denotes the transpose of $A\in\mathbb{R}^{n\times m}$. For a square, nonsingular matrix $A\in\mathbb{R}^{n\times n}$, we use A^{-1} to denote its inverse matrix, while $A^{-\mathsf{T}}$ denotes the transpose of the inverse of A: $A^{-\mathsf{T}}=(A^{-1})^\mathsf{T}=(A^\mathsf{T})^{-1}$. We denote by $A^\dagger\in\mathbb{R}^{m\times n}$ the unique pseudoinverse of $A\in\mathbb{R}^{n\times m}$, which satisfies the following four properties: 1) $A^\dagger AA^\dagger=A^\dagger$; 2) $AA^\dagger A=A$; 3) $(AA^\dagger)^\mathsf{T}=AA^\dagger$; 4) $(A^\dagger A)^\mathsf{T}=A^\dagger A$. The smallest and largest eigenvalues of a symmetric matrix $\Lambda\in\mathbb{R}^{n\times n}$ are denoted $\lambda_{\min}(\Lambda)$ and $\lambda_{\max}(\Lambda)$, respectively. Given $M\in\mathbb{C}^{n\times n}$, we denote by $\overline{M}$ its (element-wise) complex conjugate. We use $M\succeq 0$ to indicate that the square matrix M is positive semidefinite (PSD), while it is positive definite (PD) if $M\succ 0$.

Function notation

For a scalar function, f, we denote by $f^n(x)$ its nth power at x, i.e. $f^2(x)=\big(f(x)\big)^2$ (any abuse of this notation such as, e.g., the inverse $f^{-1}(f(x))=x$, will generally be clear from the context). We say that a function $f:\mathbb{R}^n\to\mathbb{R}^m$ is of class $\mathcal{C}^r$ (or $\mathcal{C}^r$-smooth) if all its partial derivatives are r-times continuously differentiable with respect to its arguments. For a mapping $h:X\to\mathbb{R}^m$ which is $\mathcal{C}^k$-smooth on its domain X, we also use the notation $h\in\mathcal{C}^k(X,\mathbb{R}^m)$. If $f\in\mathcal{C}^1(\mathbb{R}^n,\mathbb{R}^m)$, then we denote by $Df(x)$ its $m\times n$ Jacobian matrix evaluated at $x\in\mathbb{R}^n$, while if $f\in\mathcal{C}^2(\mathbb{R}^n,\mathbb{R})$, then $D^2f(x)$ will be used to denote its $n\times n$ Hessian matrix at $x\in\mathbb{R}^n$. For $f\in\mathcal{C}^0(\mathbb{R},\mathbb{R})$, we write $f(y)=O(|y|)$ (resp. $f(y)=o(|y|)$) to denote that f is such that $|f(y)|/|y|$ is bounded (resp. vanishes) as $|y|\to 0$.

Norms and distance measures

For $x, y \in \mathbb{R}^n$, we denote $\langle x, y\rangle = x^{\mathsf{T}}y = \sum_{i=1}^{n} x_i y_i$. We use $\|\cdot\|$ and $\|\cdot\|_\Lambda$ to denote the Euclidean norm and the Λ-weighted norm, respectively; that is, $\|x\| = \sqrt{\langle x, x\rangle}$ and $\|x\|_\Lambda = \sqrt{\langle x, \Lambda x\rangle}$ for any $x \in \mathbb{R}^n$ and some $\Lambda \in \mathbb{M}^n_{\succeq 0}$. For $x \in \mathbb{R}^n$ and $\mathcal{O} \subset \mathbb{R}^n$, we use the following set distance notation: $\mathrm{dist}(\mathcal{O}, x) := \inf_{y\in\mathcal{O}} \|x - y\|$. We denote the open n-ball of radius $\epsilon > 0$ centered at $x \in \mathbb{R}^n$ by $\mathcal{B}_\epsilon(x) := \{y \in \mathbb{R}^n : \ \|x - y\| < \epsilon\}$.

Special functions

$\mathrm{sgn}(\cdot) : \mathbb{R} \to \{-1, 0, 1\}$ denotes the signum function; $\mathrm{sat}_a^b(\cdot) : \mathbb{R} \to [a, b]$ is the saturation function with lower- and upper bounds a and b, i.e. $\mathrm{sat}_a^b(x) = \max\big(a, \min(x, b)\big)$, with $\mathrm{sat}(x) = \mathrm{sat}_{-1}^{1}(x)$; while for some $x \in \mathbb{R}$ and $\alpha \in \mathbb{R}_{\geq 0}$ we denote $\lceil x \rfloor^\alpha = \mathrm{sgn}(x)\,|x|^\alpha$. We use $\mathrm{atan2}(y, x)$ to denote the four-quadrant arctangent function.

Differential equations, differentiation and linearization notation

For a system of ordinary differential equations, $\dot{x}(t) = f(x(t))$, where the independent variable t represents time, we denote $\dot{x}(t) = \frac{d}{dt}x(t)$. We will commonly abuse notation and write $x = x(t)$. We will also some times use $x(t)$ (or $x(\cdot)$), as well as $x(t; x_0)$, to denote a solution satisfying $x(t_0) = x_0$, whenever this is clear from the context.

If the vector-valued function $\chi = \chi(t) \in \mathbb{R}^n$ is the state of a smooth dynamical system, i.e. $\dot{\chi} = h(\chi)$, then $\boldsymbol{\delta}_\chi = \boldsymbol{\delta}_\chi(t) \in \mathbb{R}^n$ is used to denote the state of the linearization (first-order approximation) of the dynamics of $\chi(\cdot)$ about some nominal solution. This nominal solution, normally one upon an orbit, is generally clear from the context.

If $s \mapsto h(s)$ is differentiable at $s \in \mathcal{S} \subseteq \mathbb{R}$, then we use $h'(s) = \frac{d}{ds}h(s)$.

Chapter 2

Preliminaries: The Stability of Orbits

In this chapter, we present some preliminary concepts in relation to the stability of orbits of autonomous systems. We introduce different types of orbits and study their properties. We then compare the stability definitions of Lyapunov, Poincaré and Zhukovsky in regard to the problem of quantifying the stability of orbits. We also briefly review some classical methods and tools for assessing their stability, including the use of linearizations and characteristic exponents, Poincaré sections and first-return maps. Furthermore, we introduce the moving coordinate systems of Zubov and Urabe, leading to the theory of transverse coordinates and the concept of a transverse linearization, as well as study the extensions of this theory obtained by Leonov.

2.1 Orbits of autonomous systems

Consider an autonomous system of ordinary differential equations:

$$\dot{x} = f(x). \tag{2.1}$$

Here $x = x(t) \in \mathbb{R}^n$ denotes the states at time $t \in \mathbb{R}_{\geq 0}$, the state space is $\mathbb{R}^n$ and $\dot{x}(t) = \frac{d}{dt}x(t)$. It will be assumed that the vector field $f : \mathbb{R}^n \to \mathbb{R}^n$ is $\mathcal{C}^2$ everywhere on $\mathbb{R}^n$, such that both the local existence and uniqueness of the solutions of (2.1) are ensured by the Picard–Lindelöf theorem [74].

Let $x_\star : \mathbb{R}_{\geq 0} \to \mathbb{R}^n$ denote a solution of the dynamical system (2.1), that is $\dot{x}_\star(t) = f(x_\star(t))$, which is well defined for all $t \geq 0$. We will refer to the curve the solution traces out as it evolves in time–state space as its *trajectory*, while the state curve obtained from its projection upon state space, given by the set

$$\mathcal{O} := \{x \in \mathbb{R}^n : \ x = x_\star(t), \ t \in \mathbb{R}_{\geq 0}\}, \tag{2.2}$$

will be referred to as its *orbit*[1] [24, 25, 74]. Whereas the trajectory is associated with both the solution $x_\star(\cdot)$ and the initial time instant t_0, the corresponding orbit is inherently time-invariant and therefore completely insensitive to shifts in time. Indeed, this can be readily seen by noting that, for any $\tau \geq 0$, it still holds that $\dot{x}_\star(t+\tau) = f(x_\star(t+\tau))$, with $x_\star(t+\tau)$ consequently an alternative (time) parameterization of $\mathcal{O}$.

The time-insensitivity of autonomous systems with a locally Lipschitz right-hand side can also be used to derive another key property of their orbits: they cannot have any self-intersections. This is just a straightforward consequence of the uniqueness of solutions and that, if $y = z \in \mathcal{O}$, then evidently $f(y) = f(z)$. Hence for (2.1), there exists one, and only one, orbit passing through a point $x \in \mathbb{R}^n$ [24, Thm. 4.1].

As orbits are defined by the solutions upon them, the behaviors of their defining solutions can be used to classify orbits into certain families. Such families ranges from those corresponding to chaotic or aperiodic behaviors, such as *strange attractors* [75–77], *chaotic modes* [78], and *invariant (limit) tori* [26, 79]; to the more familiar types of behaviors such as the following four types of orbits (see also Figure 2.1), which are of more relevance to this thesis:

- *Trivial (or fixed) orbits:* An orbit which consists of a single point, namely, an equilibrium point $x_e \in \mathbb{R}^n$ of (2.1), i.e. $f(x_e) \equiv \mathbf{0}_{n\times 1}$;
- *Periodic orbits (or cycles):* A nontrivial orbit whose defining solutions are periodic; that is, there exists some $T > 0$, such that $x_\star(t+T) = x_\star(t)$ and $\|f(x_\star(t))\| \neq 0$ for all $t \geq 0$;
- *Heteroclinic orbits:* An orbit whose limit points corresponds to two distinct fixed points of a dynamical system;
- *Homoclinic orbits:* A nontrivial orbit which approaches the same fixed point in both forward- and negative time.

[1] While the notions of a solution's orbit and its trajectory are some times used interchangeably in the literature, we will in this thesis make this clear distinction as to further highlight the conceptual difference between trajectory tracking and orbital stabilization.

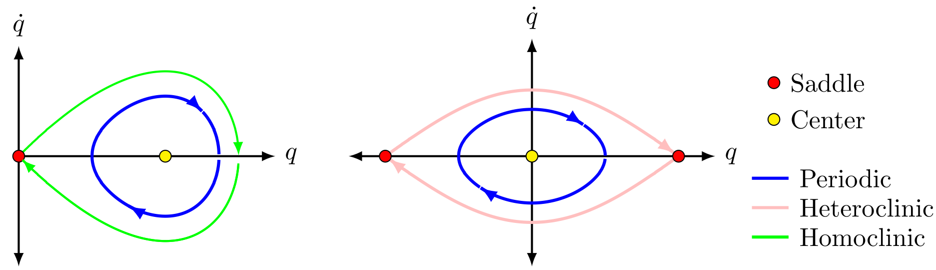

Figure 2.1: Illustration of various planar orbits of a second-order scalar system.

Both trivial- and periodic orbits are examples of *closed* orbits, as if the the system is initialized at a point on the orbit, then its states will eventually return to this point within a finite amount of time. We say that a closed orbit is *isolated* if there are no other closed orbits in its immediate vicinity. Of particular note are *limit cycles*, which are isolated non-trivial periodic orbits [76, 77, 80]. We say that a limit cycle is stable (resp. unstable) if it is the limit set of all its neighboring orbits in forward (resp. reverse) time.

Unlike fixed- and periodic orbits, a heteroclinic- and homoclinic orbit of a system with a locally Lipschitz right-hand side cannot be closed, as by starting within its interior, the equilibrium point(s) on the boundaries can only be reached within an infinite (forward- or reverse) amount of time. For such orbits, the point which is reached in an infinite reverse (or backward) amount of time, i.e. its "starting point", is referred to as an *α-limit point*, whereas its *ω-limit point* is the point which is reached in an infinite (forward) amount of time, i.e. its "end point".

Since the main aim of this thesis is to provide methods for stabilizing certain types of orbits, we need to define what we mean when we speak of the stability of an orbit. We therefore introduce three basic stability notions in the next section, and briefly discuss their strengths and limitations in regard to different types of orbits.

2.2 Lyapunov- vs Orbital- vs Zhukovsky stability

There exist a variety of different definitions of stability, intended for specific application or to capture certain peculiarities in behaviors of the solutions of dynamical systems; see, e.g., [23, 26, 40, 44, 75, 76, 81, 82]. Regardless of this variety, for autonomous systems there are three fundamental definitions which remain the basic ones: Lyapunov stability [83], Orbital (Poincaré) stability [84] and Zhukovsky stability [85]. Among these three stability notions, it is Lyapunov's definition which is the most widely known and commonly used, insofar that is has become almost synonymous with the notion of stability altogether. While it may be applied to a variety of different sets and systems, we state it here in terms of a specific solution of an autonomous system:

Definition 2.1. (Lyapunov stability) A solution $x_\star(t)$ of (2.1) is said to be

1. *(Lyapunov) stable* if, for any $\epsilon > 0$, there exists a $\delta = \delta(\epsilon) > 0$, such that for all solutions $x(\cdot; x_0)$, $x(0; x_0) = x_0$, of (2.1) satisfying $\|x_0 - x_\star(0)\| < \delta$, it is implied that $\|x(t; x_0) - x_\star(t)\| < \epsilon$ for all $t \geq 0$;

2. *Asymptotically (Lyapunov) stable*, if it is stable (in Lyapunov's sense), and, moreover, $\|x(t; x_0) - x_\star(t)\| \to 0$ as $t \to \infty$;

3. *Exponentially (Lyapunov) stable* if there exist positive constants δ, C, λ such that $\|x_0 - x_\star(0)\| < \delta$ implies $\|x(t; x_0) - x_\star(t)\| \leq C \exp(-\lambda t)$ for all $t \geq 0$.

This notion of stability therefore requires trajectories to stay close not only in state space, but to also do so in a form of synchrony as they evolve in time. The requirement of such a time-related synchrony is obviously too stringent for certain behaviors, making Lyapunov's notion ill-suited as a way of characterizing stability in some cases. For instance, a solution upon a non-trivial periodic orbit cannot be asymptotically stable in the sense of Lyapunov (see, e.g., [28] or Theorem 81.1 in [23]), even though the orbit itself is. Indeed, this well-known fact can be derived simply by noting that, due to the system's autonomy, if one shifts a solution in time, then one obviously just obtains a new, phase-shifted solution which traces out the same curve (orbit) in state space. As a consequence, the original solution and its phase-shifted counterpart can never intersect each other, and thus the distance between them can never go to zero. More technically, this corresponds to the fact that, for any $y_0, z_0 \in \mathcal{O}_p$ satisfying $0 < \|y_0 - z_0\| < \delta$, both $x(\cdot; y_0)$ and $x(\cdot; z_0)$ remain on $\mathcal{O}_p$ for all $t \geq 0$, but $\|x(t; y_0) - x(t; z_0)\| \geq \bar{\epsilon}(\delta) > 0$ even as $t \to \infty$, regardless of how small δ is taken.

In such cases, a more well suited notion of stability is the one introduced by Poincaré [84], commonly referred to as *orbital-* or *Poincaré stability.* Essentially, rather than looking at the distance between the perturbed solutions and the nominal one as they evolve in time as in Lyapunov's definition, one instead looks at the distance of perturbed solutions to the nominal orbit (2.2) using the set-distance measure

$$\mathrm{dist}(\mathcal{O}, x) := \inf_{y \in \mathcal{O}} \|x - y\| . \tag{2.3}$$

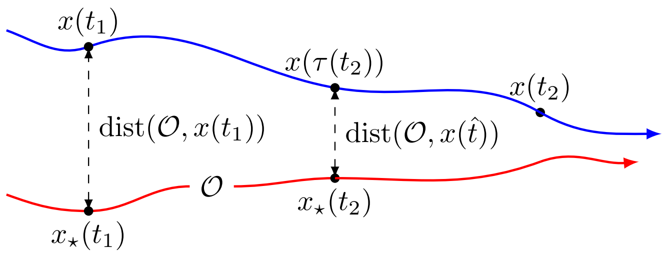

Figure 2.2: Illustration of two trajectories which remain close in space but where the perturbed, blue trajectory $x(\cdot)$ at time t_2 has "run away from" the nominal, red trajectory $x_\star(\cdot)$. This can be resolved by introducing a homeomorphism $\tau : \mathbb{R}_{\geq 0} \to \mathbb{R}_{\geq 0}$ which effectively also "aligns" the trajectories at all time moments.

Thus orbital stability of a solution just means the (Lyapunov) stability of the orbit it defines. Its definition follows [23–28, 44].

Definition 2.2. (Orbital stability) A solution $x_\star(t)$ of (2.1) is said to be

1. *Orbitally stable* if, for any $\epsilon > 0$, there exists a $\delta = \delta(\epsilon) > 0$, such that for all solutions $x(\cdot; x_0)$, $x(0; x_0) = x_0$, of (2.1) satisfying $\mathrm{dist}(\mathcal{O}, x_0) < \delta$, it is implied that $\mathrm{dist}(\mathcal{O}, x(t; x_0)) < \epsilon$ for all $t \geq 0$;

2. *Asymptotically orbitally stable*, if it is orbitally stable, and, moreover, $\mathrm{dist}(\mathcal{O}, x(t; x_0)) \to 0$ as $t \to \infty$;

3. *Exponentially orbitally stable* if there exist positive constants δ, C, λ such that $\mathrm{dist}(\mathcal{O}, x_0) < \delta$ implies $\mathrm{dist}(\mathcal{O}, x(t; x_0)) \leq C \exp(-\lambda t)$ for all $t \geq 0$.

As previously stated, one may consider orbital stability simply as the Lyapaunov stability of the orbit $\mathcal{O}$ instead of one of its defining solutions $x_\star(\cdot)$, thus ignoring the (time) parameterization altogether. As seen in Figure 2.2, this directly avoids the aforementioned problem of trajectories never converging to-, or even "running away from" a nominal trajectory as time evolves, even though they remain arbitrarily close, or eventually converge to the nominal trajectory's orbit in state space.

Figure 2.2 also illustrates another way to resolve the problem of time-parameterized trajectories "running away from" each other even though they remain arbitrarily close in state space: By introducing a scalar function $\tau(\cdot)$ acting as a reparametrization—a "rescaling of time"—of one (-or both) of the solutions, aligning them in space by effectively "slowing down-" or "speeding up" their evolution, thus possibly avoiding the running-away-from-each-other effect. This idea of using reparametrizations to study a solution's stability is due to Zhukovsky [85], and is therefore commonly referred to as *Zhukovsky stability* [26, 76, 86]. Zhukovsky's notion of stability, which implies orbital stability, is of relevance to this thesis due to its conceptual similarities with the methods we will utilize to design orbitally stabilizing feedback controllers.[2] We provide its definition next.

Definition 2.3. (Zhukovsky stability [26, 29, 54, 75, 76]) Introduce the following set of homeomorphisms:

$$\mathrm{Hom} := \{\tau(\cdot) |\ \tau : [0, +\infty) \to [0, +\infty),\ \tau(0) = 0\}. \tag{2.4}$$

A solution $x_\star(t)$ of (2.1) is said to be

1. *Zhukovsky stable* if, for any $\epsilon > 0$, there exists a $\delta = \delta(\epsilon) > 0$ and a function $\tau \in \mathrm{Hom}$, such that for all solutions $x(\cdot; x_0)$, $x(0; x_0) = x_0$, of (2.1) satisfying $\|x_0 - x_\star(0)\| < \delta$, it is implied that $\|x(\tau(t); x_0) - x_\star(t)\| < \epsilon$ for all $t \geq 0$;

2. *Asymptotically Zhukovsky stable*, if it is Zhukovsky stable, and, moreover, $\|x(\tau(t); x_0) - x_\star(t)\| \to 0$ as $t \to \infty$;

3. *Exponentially Zhukovsky stable* if there exist positive constants δ, C, λ and a $\tau \in \mathrm{Hom}$ such that $\|x_0 - x_\star(0)\| < \delta$ implies $\|x(\tau(t); x_0) - x_\star(t)\| \leq C \exp(-\lambda t)$ for all $t \geq 0$.

Zhukovsky stability can therefore be seen as a middle ground between Lyapunov stability and orbital stability: it is not as strong as Lyapunov stability in general as it does not require all solutions to be aligned in the time dimension, but therefore also not as strict; yet it is stricter, and therefore also stronger than orbital stability in general, as it considers the distance to a time-scaled solution rather than the whole orbit. Indeed, we have the following string of implications:

Proposition 2.4 ([75]). *For a solution $x_\star(\cdot)$ of* (2.1)*, Lyapunov (asymptotic) stability implies Zhukovski (asymptotic) stability, and Zhukovski (asymptotic) stability implies orbital (asymptotic) stability.*

For certain types of orbits, some of these stability notions also coincide.

Proposition 2.5 ([75]). *For an equilibrium point of* (2.1)*, the notions of Lyapunov-, orbital- and Zhukovsky stability coincide; while for a periodic orbit, the notions of orbital stability and Zhukovsky stability are equivalent.*

[2]The notion of Zhukovsky stability is also of relevance in applications in which orbital stability has certain limitations, including the stabilization of quasi-periodic orbits, e.g. limit tori, and for studying the (in-)stability of attractors; see, e.g., [26, 79].

While the notion of orbital stability of a solution, or rather the stability of its orbit, will suffice for the applications we will consider in this thesis—our aim is, after all, *orbital* stabilization—the ideas of Zhukovsky is, as we mentioned previously, conceptually important. Indeed, we will later see in Section 2.4.2 that this idea of reparameterization of perturbed trajectories can be used to both derive and prove several statements regarding the stability of certain types of solutions and their orbits. Such statements include important results such as the Andronov–Vitt theorem [87], and its generalizations by Demidovich [88] and Leonov [54], which provide sufficient conditions stated in terms of the *characteristic exponents* of the *linearized*-, or so-called *first-order variational* system along the nominal solution.

2.3 Linearization and the first-order variational system

Linearization is one of the few general tools for analyzing the stability of solutions of nonlinear systems. It is based on the first method of Lyapunov [83], in which one attempts to study the characteristic stability properties of the nonlinear system (2.1) close to $\mathcal{O}$ by analyzing its linearization (first-order approximation) along the nominal solution $x_\star(t)$. The motivation for this comes from studying the behavior of solutions to the nonlinear system for small initial perturbations Δx_0 away from $x_\star(0)$. Since the vector field $f(\cdot)$ is assumed to be (twice) continuously differentiable, the time-evolution of the perturbation stemming from Δx_0, which we denote $\Delta x(t) := x(t) - x_\star(t)$, is then governed by the differential equation [25, 89]

$$\frac{d}{dt}\Delta x = A(t)\Delta x + \Xi(t, \Delta x).$$

Here $A(t) := Df(x_\star(t))$, while

$$\|\Xi(\cdot, \Delta x)\| = O(\|\Delta x\|^2) \quad \text{as} \quad \|\Delta\| \to 0,$$

which, in turn, implies $\Xi(t, \mathbf{0}_{n\times 1}) = \mathbf{0}_{n\times 1}$, $\partial\Xi(t, \Delta x)/\partial\Delta x|_{\Delta x = \mathbf{0}_{n\times 1}} = \mathbf{0}_n$.

The *first-order variational system*, also referred to as the *first approximation system*, or even just as the *linearization* of (2.1) along $\mathcal{O}$, is the following linear, continuous, time-varying system [25, 74, 76, 90, 91]:

$$\dot{\boldsymbol{\delta}}_x = A(t)\boldsymbol{\delta}_x. \tag{2.5}$$

Here the notation $\boldsymbol{\delta}_x \in \mathbb{R}^n$ may be viewed as the first-order component of any perturbations away from the nominal solution.[3] Denoting by $\Phi(\cdot)$ the

[3] We will utilize the notation $\boldsymbol{\delta}_\chi = \boldsymbol{\delta}_\chi(t)$ throughout this thesis to denote the state of the linearization of the dynamics of a function $\chi = \chi(t)$ about some specified solution.

state-transition matrix (STM) of the linear time-varying system (2.5), i.e. the unique fundamental matrix solution to the initial-value problem [81]

$$\dot{\Phi}(t, t_0) = A(t)\Phi(t, t_0), \quad \Phi(t_0, t_0) = \mathbf{I}_n, \tag{2.6}$$

then the perturbation as a function of time will be of the form

$$\Delta x(t) = \Phi(t, t_0)\left[\Delta x_0 + \int_{t_0}^{t} \Phi(t_0, \tau)\Xi(\tau, \Delta x(\tau))d\tau\right].$$

It therefore seems natural to attempt to study the local stability characteristics of the nominal solution by trying to assess the long-term behavior of the state-transition matrix of the variational system. That is, we want to try to extract the behavior of the solutions $x(\cdot)$ of (2.1) starting close to $\mathcal{O}$, by looking at the behavior of the solutions of (2.5), specifically their exponential growth or -decay. Since the solutions of the variational system correspond to the linearly independent columns of Φ, one can for this purpose study their *characteristic exponents.*

Definition 2.6 (Characteristic exponent [25, 83, 89])**.** The number (or the symbols $\pm\infty$), given by the formula $\limsup_{t\to+\infty} \frac{1}{t} \ln \|h(t)\|$ is called the characteristic exponent of the continuous function $h : [0, \infty) \to \mathbb{R}^n$.

Let us, for example, consider the simplest type of orbit: an equilibrium point $x_e \in \mathbb{R}^n$ of (2.1). As is well known (see, e.g., [81, Property 4.1]), the state-transition matrix can in this case be obtained analytically using the matrix exponential [92]: $\Phi(t, t_0) = \exp(A(t - t_0))$ where $A := Df(x_e)$. It follows that the characteristic exponents of the variational system must be equal to the eigenvalues of A. From this, the widely known necessary and sufficient condition for the exponential stability of an equilibrium point of (2.1) can be derived [44, 74, 92]:

Proposition 2.7. *An equilibrium point $x_e \in \mathbb{R}^n$ of* (2.1)*, i.e. a trivial orbit, is locally exponentially stable if, and only if, all the eigenvalues of the Jacobian matrix $A := Df(x_e)$ have strictly negative real parts.*[4]

In the case of an equilibrium point, one can in fact extract more information from the linearization. Indeed, if the equilibrium point x_e is exponentially stable, and therefore hyperbolic, it is implied by the Hartman–Grobman theorem [74, 94, 95] that there is a homeomorphism (in fact a

[4]We will refer to a matrix A satisfying the the conditions of the Proposition as a *Hurwitz* matrix [93].

diffeomorphism if f is $\mathcal{C}^2$ [96]) between the solutions of the linearized system and those of the nonlinear system in a neighborhood of x_e. This has also been called the *Principle of the Stability in the First Approximation*; see [23, Thm. 28.1].

2.3.1 Periodic orbits and the Andronov–Vitt theorem

Unlike an equilibrium point, in the case of a periodic orbit one must also take into account the fact that, since the nominal solution is non-vanishing, so is the vector field along it. Hence, one of the characteristic exponents must always be equal to one; a fact which is readily seen by noting that $\frac{d}{dt}f(x_\star(t)) = A(t)f(x_\star(t))$, and $\limsup_{t\to+\infty}\frac{1}{t}\ln\|f(x_\star(t))\| \equiv 0$ as $f(x_\star(\cdot))$ is everywhere bounded. It turns out, however, that the orbit's stability nevertheless may some times be determined from the remaining $(n-1)$ characteristic exponents of the variational system. This important fact follows from the Andronov–Vitt theorem [23, 25, 26, 28, 49, 76, 97].

Theorem 2.8 (Andronov–Vitt)**.** *A non-trivial, T-periodic solution $x_\star(t) = x_\star(t+T)$ of* (2.1) *is asymptotically orbitally stable if the first-order variational system* (2.5) *has one simple zero characteristic exponent and the remaining $(n-1)$ characteristic exponents have strictly negative real parts.*

By introducing the so-called *Monodromy matrix* $\mathfrak{M} \in \mathbb{R}^{n\times n}$, defined by

$$\mathfrak{M} := \Phi(T, 0), \tag{2.7}$$

then it is clear that the conditions of the Andronov–Vitt theorem may be equivalently stated in terms of the so-called *characteristic multipliers*, which are the eigenvalues of $\mathfrak{M}$.

Corollary 2.9. *A non-trivial periodic orbit $\mathcal{O}$ is asymptotically stable if the Monodromy matrix $\mathfrak{M}$ has one eigenvalue equal to unity, and its remaining $(n-1)$ eigenvalues have magnitudes strictly less than one.*

As the following theorem demonstrates, these conditions are in fact both necessary and sufficient for the exponential orbital stability of $x_\star(\cdot)$.

Theorem 2.10 (Hauser & Chung [41])**.** *A periodic orbit $\mathcal{O}$ of* (2.1) *is exponentially stable if, and only if, $(n-1)$ of the eigenvalues of Monodromy matrix $\mathfrak{M} := \Phi(T, 0)$ have magnitudes which are strictly less than one.*

2.3.2 Beyond periodic orbits: The notion of regularity

It is now natural to ask whether this property, namely the strict negativeness of $(n-1)$ of the characteristic exponents, generalizes to all bounded, non-vanishing orbits of (2.1). It turns out that this depends on the the so-called *regularity* of the corresponding variational system [23, 54, 83, 88, 89].

Definition 2.11 ([23, 54, 89])**.** Denote by $\lambda_1 \geq \lambda_2 \geq \cdots \geq \lambda_n$ the n characteristic exponents of (2.5) (its *spectrum*) and let $\Lambda = \sum_{i=1}^{n} \lambda_i$. We say the linear system (2.5) is *regular* if the number Γ, defined by

$$\Gamma = \Lambda - \liminf_{t\to\infty} \frac{1}{t} \int_0^t \operatorname{Tr} A(\tau) d\tau, \tag{2.8}$$

is exactly equal to zero.

It was shown by Lyapunov [83] that the origin of the system

$$\dot{z} = \mathcal{A}(t)z + h(t,z), \quad z \in \mathbb{R}^{\bar{n}}, \tag{2.9}$$

where $\mathcal{A} \in \mathcal{C}^0(\mathbb{R}_{\geq 0}, \mathbb{R}^{\bar{n}\times\bar{n}})$ is bounded, while $h \in \mathcal{C}^1$ satisfies $\|h(t,0)\| = 0$ and $\|\partial h(t,z)/\partial z\| = O(\|z\|^{\upsilon})$ for $\upsilon > 0$, is exponentially stable if the linear part is regular and all its characteristic exponents have negative real parts.[5] It was later shown by Perron [98] that the requirement of the regularity of the linear part is substantial [89].

Examples of regular linear systems include all continuous systems with constant or periodic coefficients [89]. Due to this, it is also implied that all so-called (real) *reducible* systems are regular; that is, systems for which there exists a nonsingular matrix function $L : \mathbb{R}_{\geq 0} \to \mathbb{R}^{n\times n}$, with both $L(t)$ and $\dot{L}(t)$ continuous and bounded for all $t \in \mathbb{R}_{\geq 0}$, such that the matrix $F = L(t)\mathcal{A}(t)L^{-1}(t) + \dot{L}(t)L^{-1}(t)$ is constant. Indeed, from the coordinate transformation $y(t)) = L(t)z(t)$, we obtain

$$\dot{y} = Fy + L(t)h(t, L^{-1}(t)y),$$

which is therefore regular as its linear part is constant. Hence (2.9) must be regular too due to the boundedness of $L(t)$. The following corresponds to Theorem 25 in the work of Massera [39]:

Theorem 2.12. *If $\mathcal{A}$ is reducible and all the eigenvalues of F have strictly negative real parts, then there is a number $M > 0$, such that, for any function $h(\cdot)$ satisfying $\|h(t,z)\| \leq M\,\|z\|$ uniformly in t in a neighborhood of the origin, the origin of* (2.9) *is uniformly asymptotically stable.*

These results are however not directly applicable to linearizations along a bounded, non-vanishing (not necessarily periodic) solution due to the zero characteristic exponent. Nevertheless, similarly to the Andronov–Vitt theorem, Demidovich [88] showed that if the linearization is regular and

[5] An alternative, yet highly related notion for the asymptotic stability of the time-varying system (2.9) can be stated using Bol exponents; see, e.g., [76].

$(n-1)$ of the characteristic exponents have strictly negative real parts, then the solution is asymptotically orbitally stable. This was generalized even further by Leonov [54], which proved the following statement (in which we use the same notation as in Def. 2.11) using similar methods to those we will present in sections 2.4.2 and 2.4.3.

Theorem 2.13 ([54])**.** *A bounded, non-vanishing solution of* (2.1) *is asymptotically Zhukovsky (and therefore orbitally) stable if* $\lambda_2 + \Gamma < 0$.

2.4 Tools for assessing the stability of periodic orbits

A conclusion that can be drawn from both the Andronov–Vitt theorem, its generalization Theorem 2.13, as well as Theorem 2.10, is that the exponential stability of a periodic orbit must be equivalent to the exponential stability of some $(n-1)$-dimensional subsystem of the variational system. Indeed, the stability of the nominal orbit is in fact equivalent to the stability of the dynamics *transverse* to its flow—a fact which plays a key role in the proofs of many of the aforementioned statements. In this section, we will therefore briefly cover some key tools for analyzing the stability of periodic orbits which are based on studying the behavior of solutions in the directions transverse to the orbit's flow.

Let $x_\star(t) = x_\star(t+T)$ now denote a bounded, T-periodic solution satisfying $\|\dot{x}_\star(t)\| > 0$ for all $t \geq 0$, and denote by

$$\mathcal{O} := \{x \in \mathbb{R}^n : \ x = x_\star(t), \ t \in [0, T)\} \tag{2.10}$$

the corresponding closed orbit. In the following, we will look at some methods for studying stability of $\mathcal{O}$, including the classical method of using Poincaré first-return maps (Sec. 2.4.1), the orthonormal moving coordinates systems of Zubov and Urabe (Sec 2.4.2), as well as Leonov's extension and his differential matrix inequality (Sec. 2.4.3). These methods, even though they are derived in slightly different ways, nevertheless have some strong similarities to- and interesting connections with the methods we will introduce in Chapter 4 to design orbitally-stabilizing feedback controllers.

2.4.1 The Poincaré first-return map and Poincaré sections

A classical approach for assessing the stability of a periodic orbit is the Poincaré first-return map [28, 55, 76, 84]. Given a point $x_\star \in \mathcal{O}$, the main idea of this method is to constructs a smooth, $(n-1)$-dimensional hypersurface $\mathfrak{S}$, a so-called *Poincaré section*, which is transversal to $\mathcal{O}$ about $x_\star$.[6] Due

[6] Here transversality means that $\mathfrak{n}^\top(x) f(x_\star) \neq 0$ for all $x \in \mathfrak{S}$, with $\mathfrak{n}(x)$ the normal vector of $\mathfrak{S}$ at a point $x \in \mathfrak{S}$.

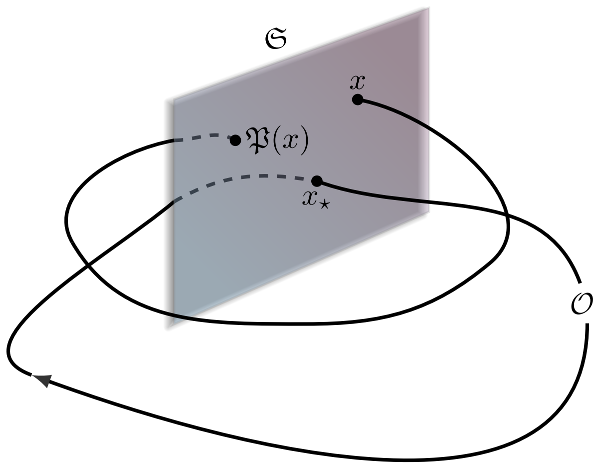

Figure 2.3: Illustration of a Poincaré Section $\mathfrak{S}$ and the return map $\mathfrak{P} : \mathfrak{S} \to \mathfrak{S}$.

to the continuous dependence of solutions upon the initial conditions (on a finite time interval) [25, 44, 80], there will always be a sufficiently small region $\mathfrak{S}_0 \subset \mathfrak{S}$ of $x_\star$, such that all solutions crossing $\mathfrak{S}_0$ will eventually intersect $\mathfrak{S}$ again within a finite amount of time. This means that for any solution of $x(\cdot) = x(\cdot; x_0)$ of (2.1) that satisfies $x_0 \in \mathfrak{S}_0$, there is a mapping $\mathfrak{P} : \mathfrak{S}_0 \to \mathfrak{S}$ from which one can retrieve the point of first return where $x(\cdot)$ intersects $\mathfrak{S}$ again.

The function $\mathfrak{P}(\cdot)$, which is illustrated in Figure 2.3, is the so-called *Poincaré first-return map*. It defines a discrete system, given by the difference equation

$$x_{\mathfrak{S}}[i+1] = \mathfrak{P}\left(x_{\mathfrak{S}}[i]\right), \quad x_{\mathfrak{S}}[\cdot] \in \mathfrak{S}, \tag{2.11}$$

where $x_{\mathfrak{S}}[i]$ is the point of the i-th intersection with the surface $\mathfrak{S}$ of some trajectory $x(\cdot)$ of (2.1). Naturally, $x_\star$ is a fixed point of the Poincaré map $\mathfrak{P}(\cdot)$, such that the stability of the orbit $\mathcal{O}$ can be determined by studying the stability of the fixed point $x_\star$ of the difference equation (2.11). Indeed, it is well known that $\mathcal{O}$ is (asymptotically) stable if, and only if, $x_\star \in \mathfrak{S}$ is a (asymptotically) stable fixed point of the the map $\mathfrak{P}(\cdot)$ [74, Lemma 12.2]. Moreover, the exponential stability of $\mathcal{O}$ can be verified by linearizing the map $\mathfrak{P}$ at $x_\star$ and checking that all the characteristic multipliers (the eigenvalues of its differential $d\mathfrak{P}$) lie strictly inside the complex unit circle [55, 74] (cf. Theorem 2.10). Note here that these multipliers are equivalent to $(n-1)$ of the eigenvalues of the Monodromy matrix (see (2.7)).

While Poincaré maps have been successfully applied as a control design–tool for various applications in the literature (see, e.g., the notion of controlled Poincaré maps in [76], or its application to the stabilization of hybrid cycles in [99]; see also the references in [55]), the technique's discrete nature does not allow one to properly analyze the stability properties along the whole orbit, thus limiting its use for constructive (orbitally stabilizing) feedback design [55, 57]. Indeed, as Poincaré map–based analysis only provides information about the contraction (or expansion) of the first-return points upon the chosen Poincaré section, it does not provide a continuous representation of the dynamical system's behavior along the whole orbit. Furthermore, the Poincaré map can seldom be found analytically, and its construction, which generally must be done for the closed-loop system, will require integrating over the whole periodic, and can therefore often be numerically expensive.

However, some of the shortcomings of the Poincaré map–technique, such as only being applicable to periodic orbits and not providing a continuous representation along the whole orbit, can be overcome by exploiting the idea of the Poincaré section. Suppose, for instance, that rather than having the hyperplane transverse to a single, fixed point on the orbit, we instead "force" the Poincaré section to continuously evolve along its flow while still staying transverse to it. As we will see, such an object, coined a *moving Poincaré section* by Leonov [54], allows one to study the behavior of perturbed trajectories along whole orbit by defining a coordinate system upon these sections. One can therefore study the stability of the orbit by studying just the transversal components of these perturbed trajectories which lie upon the moving Poincaré section.

2.4.2 The moving coordinate systems of Zubov and Urabe

Our aim will now be to obtain a continuous representation of the system's behavior and stability characteristic within some tubular neighborhood the periodic orbit. For this purpose, we will in this section consider the similar methods introduced separately by Zubov [27] and Urabe [24, 49] (see also [23, 25, 41, 91]), whereas in Section 2.4.3 we will consider the extensions and generalizations of this approach obtained by Leonov [26, 54, 59]. Note that similar types of approaches were also utilized by Borg [50], and later by Hartman and Olech [51] to provide similar conditions for the asymptotic orbital stability of a periodic solution.

The key idea which is used in the derivation of these methods is many ways similar to concept of reparameterizations of trajectories as in the definition of Zhukovsky stability (see Definition 2.3). Roughly speaking, by aligning perturbed trajectories with the nominal one in state space using a reparametrization, one can introduce a moving coordinate system where $(n-1)$ of the corresponding coordinates span the space which is directly orthogonal to the orbit's flow. Thus a continuous representation of the transversal components of any small perturbation away from the periodic orbit is obtained. This, in turn, allows one to assess the orbit's stability characteristics through the study of the corresponding *transverse dynamics*—the dynamics of the $(n-1)$ orthogonal (transverse) coordinates. Moreover, from the corresponding *transverse linearization*, which is short for the linearization of the transverse dynamics [41, 55], one can possibly determine the exponential (in-)stability of the orbit as well.

Constructing a moving Poincaré section

In order to construct such a coordinate system, we first denote $f_\star(t) := f(x_\star(t))$, and define the hyperplane

$$\hat{\Pi}_t := \left\{ x \in \mathbb{R}^n : \ f_\star^{\mathsf{T}}(t)(x - x_\star(t)) = 0 \right\}.$$

Since $f(\cdot)$ is twice continuously differentiable, the curvature along the curve traced out by the nominal (bounded) solution must necessarily be bounded. We can therefore always find some number $\delta > 0$ such that the parts of the hyperplanes $\hat{\Pi}_t$, $t \in [0, T)$, which are contained within an open, tubular δ-neighborhood of the orbit $\mathcal{O}$,

$$\mathcal{T}_\delta := \{ x \in \mathbb{R}^n : \ \mathrm{dist}(\mathcal{O}, x) < \delta \},$$

are all disjoint. That is, by defining, for some $\delta > 0$, the hypersurface

$$\Pi_t := \hat{\Pi}_t \cap \mathcal{T}_\delta, \tag{2.12}$$

then $\hat{\Pi}_{t_1} \cap \hat{\Pi}_{t_2} = \emptyset$ for all $t_1, t_2 \in [0, T)$, $t_1 \neq t_2$.

Since the family of hyperplanes defined by Π_t continuously evolve along with the flow of the orbit, the surfaces Π_t therefore correspond to a moving Poincaré section as defined in [54]; see also [55].

Reparametrization à la Zhukovsky

Our aim will now be to construct a coordinate system upon the moving Poincaré section Π_t in which the resulting coordinates, whose origin correspond to the orbit, continuously evolve upon- and span this section as it evolves along $\mathcal{O}$. As a consequence, the orbital stability of the nominal solution—or equivalently, the stability of the orbit itself—can be determined from the stability of the origin of this coordinate system.

To this end, let $x(t) = x(t; x_0)$ denote a solution of (2.1). For the sake of simplicity, and without loss of generality, we will slightly abuse notation and take the starting point of the nominal time-parameterized solution $x_\star(\cdot)$ upon $\mathcal{O}$ such that $x_0 = x(0) \in \Pi_0$. At some time instant, we then define the function

$$y_\perp(t) := x(\tau(t)) - x_\star(t), \tag{2.13}$$

where $\tau \in \mathrm{Hom}$ is such that $x(\tau(t)) \in \Pi_t$, with the set Hom as defined in (2.4). Now, due to the continuous dependence of solutions upon the initial conditions, together with the continuous differentiability of Π_t, the following can be inferred: If $x_0 \in \Pi_0$, and therefore $\|x_{\mathbf{0}} - x_\star(0)\| < \delta$, then we can always find a $\mathcal{C}^1$ function $\tau \in \mathrm{Hom}$ and a time instant $\hat{t} \in \mathbb{R}_{>0}$, such that $x(\tau(t)) \in \Pi_t$ for all $t \in [0, \hat{t})$; see also, e.g., [54, Lemma 1].

As a consequence, in the particular case when $x_\star(\cdot)$ is Zhukovsky stable (see Def. 2.3), we can, for $\|y_\perp(0)\|$ sufficiently small, let $\hat{t} \to \infty$, such that $y_\perp(t)$ then is well defined on whole of $\mathbb{R}_{\geq 0}$. The following statement, corresponding to Lemma 2 in [54], summarizes the above.

Lemma 2.14. *If the solution $x_\star(\cdot)$ is stable in the sense of Zhukovski, then there exists a real number $\delta > 0$, such that for any solution $x(t) = x(t; x_0)$ of* (2.1) *satisfying $x_0 \in \Pi_0 \subset \mathcal{T}_\delta$, there is a $\mathcal{C}^1$ function $\tau \in$ Hom such that $x(\tau(t)) \in \Pi_t$ for all $t \geq 0$.*

Here the condition that $x(\tau(t)) \in \Pi_t$ for all $t \geq 0$ of course, in turn, implies that the function $y_\perp(t)$, defined by (2.13), is well defined on $\mathbb{R}_{\geq 0}$.

Even in the absence of Zhukovski stability, we can utilize the function $y_\perp(\cdot)$ to study the orbit's stability characteristics, though of course $y_\perp(\cdot)$ might not then be well defined for all $t \geq 0$. Indeed, we may in this case nevertheless always take $\delta > 0$ sufficiently small as to guarantee that $\hat{t}$ exceeds the solution's period T; see Lemma 4.1 [26].

Derivation of the transverse dynamics

Suppose now that the function $y_\perp(t)$ given by (2.13) is well defined on $\hat{\mathcal{T}} := [0, \hat{t})$ for some $\hat{t} \geq T > 0$. By the definition of Π_t, this implies

$$f_\star^{\mathsf{T}}(t) y_\perp(t) = 0$$

for all t in $[0, T)$. It follow that, at any time instant inside $\hat{\mathcal{T}}$, the relation

$$\dot{f}_\star^{\mathsf{T}}(t) y_\perp(t) + f_\star^{\mathsf{T}}(t) \dot{y}_\perp(t) = 0 \tag{2.14}$$

holds. Here both $\dot{f}_\star(t) = A(t) f_\star(t) = Df(x_\star(t)) f_\star(t)$ and

$$\dot{y}_\perp(t) = (f \circ x \circ \tau)(t) \dot{\tau}(t) - f_\star(t)$$

are easily derived using the chain rule. Inserting this into (2.14), we obtain

$$\dot{\tau} = \frac{\|f_\star(t)\|^2 - \dot{f}_\star^\mathsf{T}(t) y_\perp(t)}{f_\star^\mathsf{T}(t) f(y_\perp(t) + x_\star(t))}, \tag{2.15}$$

and hence

$$\dot{y}_\perp = \frac{\|f_\star(t)\|^2 - \dot{f}_\star^\mathsf{T}(t) y_\perp}{f_\star^\mathsf{T}(t) f(y_\perp + x_\star(t))} f(y_\perp + x_\star(t)) - f_\star(t), \qquad f_\star^\mathsf{T}(t) y_\perp = 0. \tag{2.16}$$

Notice here that, even though $y_\perp \in \mathbb{R}^n$, this system is of order $(n-1)$ due to the orthogonality constraint $f_\star^\mathsf{T}(t) y_\perp = 0$. This motivates searching for an equivalent set of coordinates of reduced order as to directly circumvent this orthogonality condition altogether.

Constructing an orthonormal coordinate system

In order to find such reduced-order coordinates, let the $\mathcal{C}^1$ matrix-valued function $N_\perp : \mathbb{R}_{\geq 0} \to \mathbb{R}^{n \times (n-1)}$ be such that $N(t) := \left[f_\star(t) / \|f_\star(t)\|, N_\perp(t) \right]$ is an orthonormal matrix for all $t \geq 0$, i.e. $N^{-1}(t) = N^\mathsf{T}(t)$. It can easily be verified that

$$\begin{aligned} \frac{d}{dt}\left(\frac{f_\star(t)}{\|f_\star(t)\|} \right) &= \left(\mathbf{I}_n - \frac{f_\star(t) f_\star^\mathsf{T}(t)}{\|f_\star(t)\|^2} \right) A(t) \frac{f_\star(t)}{\|f_\star(t)\|}, \\ \dot{N}_\perp(t) &= -\left(I_n - N_\perp(t) N_\perp^\mathsf{T}(t) \right) A^\mathsf{T}(t) N_\perp(t). \end{aligned}$$

With this in mind, we consider now the transformation

$$y_\perp(t) = N_\perp(t) z_\perp, \quad z_\perp(t) \in \mathbb{R}^{n-1}, \tag{2.17}$$

which evidently is equivalent to $x(\tau(t)) = x_\star(t) + N_\perp(t) z_\perp(t)$. Thus $z_\perp(t)$ acts as coordinates upon the moving Poincaré section Π_t, whose coordinate axes correspond to the columns of $N_\perp$. Differentiating both sides of (2.17) and using (2.16), together with the fact that $\left\| N_\perp^\mathsf{T}(t) f_\star(t) \right\| = 0$, we obtain

$$\dot{z}_\perp = N_\perp^\mathsf{T}(t) \frac{\|f_\star(t)\|^2 - \dot{f}_\star^\mathsf{T}(t) N_\perp(t) z_\perp}{f_\star^\mathsf{T}(t) f(N_\perp(t) z_\perp + x_\star(t))} f(N_\perp(t) z_\perp + x_\star(t)) - N_\perp^\mathsf{T}(t) \dot{N}_\perp(t) z_\perp \tag{2.18}$$

where we also have used $N_\perp^\dagger := (N_\perp^\mathsf{T} N_\perp)^{-1} N_\perp^\mathsf{T} = N_\perp^\mathsf{T}(t)$.

Clearly, due to the definition of the function $y_\perp$ (see (2.13)) and the transformation (2.17), the characteristic stability properties of the systems (2.16) and (2.18), besides being equivalent to each other, are also inherently linked to the orbit's local stability characteristics. The following statement, which can be derived from Theorem 25 in [27], clearly demonstrates this fact.

Proposition 2.15. *The orbit $\mathcal{O}$ is (asymptotically) stable for* (2.1) *if, and only if, the origins of the systems* (2.16) *and* (2.18) *are (asymptotically) stable.*

In order to asses the exponential stability of the periodic orbit $\mathcal{O}$, we can attempt to linearize the transverse dynamics (2.16) and (2.18) along the orbit's flow. This gives rise to another type of linearization than the one considered in Section 2.3, commonly referred to as a *transverse linearization.*

Transverse linearization

Consider again (2.16). As shown in [26, 54], we can, for x sufficiently close to $\mathcal{O}$, expand the right-hand side of (2.16) as to rewrite it in the following equivalent form (see also [59] for further details):

$$\dot{y}_\perp = A_\perp(t)y_\perp + O(\|y_\perp\|^2), \qquad f_\star^\mathsf{T}(t)y_\perp = 0. \tag{2.19}$$

Here

$$A_\perp(t) := \left(\mathbf{I} - \frac{f_\star(t)f_\star^\mathsf{T}(t)}{\|f_\star(t)\|^2}\right)A(t) - \frac{f_\star(t)f_\star^\mathsf{T}(t)}{\|f_\star(t)\|^2}A^\mathsf{T}(t).$$

Similarly, for (2.18), we can utilize (2.19) together with the fact that

$$N_\perp^\mathsf{T}(t)\dot{N}_\perp(t) = \mathbf{0}_{n-1},$$

as to rewrite (2.18) on the following form:

$$\dot{z}_\perp = \mathcal{A}_\perp(t)z_\perp + O(\|z_\perp\|^2), \quad \mathcal{A}_\perp(t) := N_\perp^\mathsf{T}(t)A(t)N_\perp(t). \tag{2.20}$$

The linearizations of (2.19) and (2.20), namely their first-order approximation systems, can therefore readily be obtained. For (2.19) this obviously corresponds to the following linear-periodic system of differential-algebraic equations:

$$\dot{\boldsymbol{\delta}}_{y_\perp} = A_\perp(t)\boldsymbol{\delta}_{y_\perp}, \tag{2.21a}$$

$$0 = f_\star^\mathsf{T}(t)\boldsymbol{\delta}_{y_\perp}; \tag{2.21b}$$

while for (2.20), it is given by

$$\dot{\boldsymbol{\delta}}_{z_\perp} = \mathcal{A}_\perp(t)\boldsymbol{\delta}_{z_\perp}. \tag{2.22}$$

Since these two linear system are related through the orthonormal coordinate transformation (2.17), their characteristic exponent are necessarily equivalent. Moreover, using e.g. Lemma 2.1 in [25], we can further relate this back to the characteristic exponents of the variational system (2.5).

Indeed, one can easily verify that if $\boldsymbol{\delta}_x(t)$ is a solution to the variational system (2.5), then

$$\boldsymbol{\delta}_{y_\perp}(t) = \left(\mathbf{I}_n - \frac{f_\star(t) f_\star^\top(t)}{\|f_\star^\top(t)\|^2}\right)\boldsymbol{\delta}_x(t) \tag{2.23}$$

is a solution to (2.21) [29, Lemma 2], which turn relates to a solution of (2.22) through the transformation $\boldsymbol{\delta}_{y_\perp}(t) = N_\perp(t)\boldsymbol{\delta}_{z_\perp}(t)$. We may therefore conclude the following:

Lemma 2.16. *If the periodic orbit $\mathcal{O}$ is exponentially stable, then the $(n-1)$ characteristic exponents of the variational system* (2.5) *with strictly negative real parts are equivalent to the $(n-1)$ characteristic exponents of the transverse linearizations* (2.21) *and* (2.22)*.*

Using the above lemma, it is interesting to note that one can obtain a statement analogous to the Andronov–Vitt theorem. More specifically, as one can validate (see, e.g., [54]) that the following relation always holds

$$\frac{d}{dt}\left(\frac{f_\star(t)}{\|f_\star(t)\|^2}\right) = A_\perp(t)\frac{f_\star(t)}{\|f_\star(t)\|^2}; \tag{2.24}$$

it can be deduced that the linear, T-periodic system $\dot{w} = A_\perp(t)w$ has one simple zero characteristic exponent, whereas the remaining $(n-1)$ characteristic exponents are equivalent to those of the transverse linearization (2.21) (cf. Theorem 2.8). Therefore, by invoking Theorem 2.10, we can infer the following important fact: The exponential orbitally stability of the nominal solution is equivalent to the asymptotic stability of the transverse linearizations. Or stated even more clearly:

Theorem 2.17. *The periodic orbit $\mathcal{O}$ is exponentially stable for* (2.1) *if, and only if, the origins of the linear, T-periodic systems* (2.21) *and* (2.22) *are asymptotically stable.*

One way of assessing the asymptotic (exponential) stability of (2.21) and (2.22) is to compute their characteristic exponents and then utilize Lemma 2.16. In the case of (2.22), this is done by computing its Monodromy matrix (see (2.7)); whereas for (2.21), one computes the Monodromy matrix of the system $\dot{w} = A_\perp(t)w$ and disregards one of its unitary eigenvalues. Such an approach is necessarily equivalent to both the Andronov–Vitt theorem and the Poincaré first-return map, thus providing lower- and upper bounds on the (local) exponential contraction through exponents with the smallest and largest magnitudes. However, this also means that it has the exact same drawbacks, in the sense that it does not provide continuous representation of this contraction at all points along the nominal orbit.

For this purpose, Lyapunov's second (direct) method—in which one searchers for a *Lyapunov function*—is better suited. Even though such a function will necessarily be time-varying when considering either of transverse dynamics, it can nevertheless be used to demonstrate the exponential stability of the orbit (see, e.g. [44, Thm. 4.10]). Moreover, in the case of the system (2.18), such a function can be derived using the corresponding transverse linearization (2.22) by solving a *periodic Lyapunov differential equation* (PLDE). Indeed, by combining Theorem 2.17 with the Extended Lyapunov lemma in the work of Bittanti et al. [100], we can readily state the following.

Proposition 2.18 (Periodic Lyapunov Differential Equation). *The periodic orbit $\mathcal{O}$ is exponentially stable if, and only if, for each continuous, T-periodic matrix-valued function $Q : \mathbb{R}_{\geq 0} \to \mathbb{M}^{(n-1)}_{\succ 0}$, the the Periodic Lyapunov differential equation,*

$$\dot{L}_\perp(t) + \mathcal{A}_\perp^\top(t) L_\perp(t) + L_\perp(t)\mathcal{A}_\perp(t) + Q(t) = \mathbf{0}_{(n-1)}, \tag{2.25}$$

has a T-periodic, $\mathcal{C}^1$-smooth solution $L_\perp : \mathbb{R}_{\geq 0} \to \mathbb{M}^{(n-1)}_{\succ 0}$.[7] □

If a matrix function $L_\perp(\cdot)$ satisfying the conditions in Proposition 2.18 exists, then $\mathcal{V}_\perp(t, z_\perp) = z_\perp^\top L_\perp(t) z_\perp$ is a Lyapunov function for (2.20), with its time derivative of the form $\dot{\mathcal{V}}_\perp = -z_\perp^\top Q(t) z_\perp + O(\|z_\perp\|^3)$. It is therefore possible to use $\mathcal{V}_\perp$ to not only estimate the rate of contraction at certain points about $\mathcal{O}$, but to also provide a conservative estimate of the region of attraction, given as an invariant tube enveloping $\mathcal{O}$, within which all solutions of the nonlinear system (2.1) exponential converge to $\mathcal{O}$.

A certain drawback in regard to using (2.22) and PLDE for this purpose, is that it requires the construction of the orthonormal basis $N_\perp(\cdot)$. The transverse linearization (2.21), on the other hand, does not require the formation of this basis; yet finding a similar condition to the PLDE to assess its exponential stability is not as straightforward due to the orthogonality constraint (2.21b). The most basic condition which takes into account this constraint is the one obtained by Borg in [50] (see also [26, 51, 101]). As we are interested in the stability of only particular solutions in this thesis, we formulate next a statement following directly from Borg's more general result:

[7] The positive definiteness of $Q(\cdot)$ and $L(\cdot)$ can be relaxed to positive semi-definiteness of $L_\perp(\cdot)$ and the detectability of the pair $(\mathcal{A}_\perp(\cdot), Q(\cdot))$.

Theorem 2.19. *Suppose that for all $t \in [0, T)$ and all $\chi \in \Pi_t$, the following inequality is satisfied:*

$$\frac{1}{2}\chi^{\mathsf{T}}\left[A_{\perp}^{\mathsf{T}}(t) + A_{\perp}(t)\right]\chi = \chi^{\mathsf{T}} A(t)\chi < 0. \tag{2.26}$$

Then the nominal periodic solution $x_\star(t)$ of the autonomous system (2.1) *is asymptotically orbitally stable.*

A further a generalization of Borg's result was later obtained by Hartman and Olech [51], requiring a less strict condition upon the right-hand side of (2.26).[8] Even still, the condition (2.26) is quite limiting in that it requires strict contraction in all directions which lie in cross sections which are orthogonal to the nominal orbit's flow. Naturally, we would like to relax this as to instead allow contraction of some ellipsoidal-shaped tube such as that which can be obtained from Proposition 2.18, rather than the circular tube corresponding to (2.26). Such a condition was obtained by Leonov (see, e.g., [26, 58]), in which the orthogonality condition (2.21b) simultaneously was relaxed to just a *transversality condition*, thus extending it to a larger family of transverse linearizations and providing alternative ways of assessing the orbit's exponential stability.

We briefly cover Leonov's method in the next sections, although note that the derivations we present differs slightly from those in [26] as to highlight its connection with the methods we will present in Chapter 4 to construct orbitally stabilizing feedback controllers.

2.4.3 Leonov's method

Consider a $\mathcal{C}^1$ function $\pi^{\mathsf{T}} : \mathbb{R}^n \to \mathbb{R}^n$ which is such that if $\mathcal{P}(t) := \pi(x_\star(t))$, then $\mathcal{P}(t)f_\star(t) = 1$ for all $t \geq 0$. Similarly to the previous section, we use this to define a hypersurface of the form

$$\tilde{\Pi}_t := \{x \in \mathbb{R}^n : \ \mathcal{P}(t)(x - x_\star(t)) = 0\} \cap \mathcal{T}_\delta, \tag{2.27}$$

with $\delta > 0$ taken sufficiently small as to guarantee that the surfaces are all disjoint for any pair of different time instants on $[0, T)$. Note that, as opposed to Π_t (see (2.12)), the hypersurface $\tilde{\Pi}_t$ is only required to be orthogonal to $\mathcal{P}(t)$, and will therefore only be transverse to $f_\star(t)$ in general.

Proceeding in a similar manner to the previous derivation, we let $x(t) = x(t; x_0)$ denote a solution to (2.1) which is such that $x_0 \in \tilde{\Pi}_0$. At some time instant, we then define

$$x_\perp(t) := x(\tilde{\tau}(t)) - x_\star(t) \tag{2.28}$$

[8] Note that both the methods of Borg [50] and Hartman and Olech [51] also provides conditions for the existence of a limit cycle, not only its stability; see Section 3.4.

where $\tilde{\tau} \in \mathrm{Hom}$ is such that $x(\tau(t)) \in \tilde{\Pi}_t$. Taking the δ-tube $\mathcal{T}_\delta$ sufficiently small, we can by [26, Lemma 4.1] here as well, at least for $\|x_\perp\|$ sufficiently small, ensure the existence of a $\mathcal{C}^1$ function $\tilde{\tau} \in \mathrm{Hom}$ such that $x(\tilde{\tau}(t)) \in \tilde{\Pi}_t$ for all $t \in [0, T)$. Thus sufficiently close to $\mathcal{O}$, we can consider the system

$$\dot{x}_\perp = \tilde{A}_\perp(t)x_\perp + O(\|x_\perp\|^2), \quad \mathcal{P}(t)x_\perp = 0, \tag{2.29}$$

where

$$\tilde{A}_\perp(t) := (\mathbf{I}_n - f_\star(t)\mathcal{P}(t))\, A(t) - f_\star(t) D\pi(x_\star(t)). \tag{2.30}$$

Note that the matrix function $\tilde{A}_\perp$ is equivalent to $A_\perp$ if $\mathcal{P}(t) \equiv f_\star^{\mathsf{T}}(t)/\left\|f_\star(t)\right\|^2$. It follows that the corresponding transverse linearization is given by

$$\dot{\boldsymbol{\delta}}_{x_\perp} = \tilde{A}_\perp(t)\boldsymbol{\delta}_{x_\perp}, \tag{2.31a}$$
$$0 = \mathcal{P}(t)\boldsymbol{\delta}_{x_\perp}. \tag{2.31b}$$

Combing Theorem 2.17 with Theorem 4.2 in [26] we obtain the following.

Theorem 2.20. *The exponential stability of the periodic orbit $\mathcal{O}$ of* (2.1) *is equivalent to the exponential stability of the origin of* (2.31)*.*

Recall now one of our current goals: to construct a method for assessing the stability of (2.31), or equivalently that of (2.21), similar to how the PLDE can be used in regard to the reduced-order coordinates (see Proposition 2.18). For this purpose, we consider next the method proposed in [26] (see also [58]), which can be used to derive both the Andronov–Vitt theorem, as well as Borg's condition (and even more still; see [26]).

Let $\lambda : \mathbb{R}_{\geq 0} \to \mathbb{R}$ denote a continuous, T-periodic scalar function, and consider a bounded, T-periodic matrix-valued function $W : \mathbb{R}_{\geq 0} \to \mathbb{M}^n$ which is $\mathcal{C}^1$ and nonsingular for all $t \geq 0$. Suppose that for all $t \in [0, T)$ and all $\chi \in \tilde{\Pi}_t$, the following inequality is satisfied:

$$\chi^{\mathsf{T}} \left[\dot{W}(t) + \tilde{A}_\perp^{\mathsf{T}}(t)W(t) + W(t)\tilde{A}_\perp(t) - \lambda(t)W(t)\right] \chi \leq 0. \tag{2.32}$$

Further suppose that there exists a pair of finite sequences $\{\kappa_j\}$, $\{t_j\}$, $j \in J \subset \mathbb{N}$, satisfying, for all $j \in J$,

$$\kappa_j < 0 \quad \text{and} \quad 0 < t_{j+1} - t_j. \tag{2.33}$$

Then the following statement, which is a slightly simplified version of the ones found in [26, 58], can be stated.

Theorem 2.21. *Suppose* $\chi^\mathsf{T} W(t)\chi > 0$ *for all* $t \geq 0$ *and all* $\chi \in \tilde{\Pi}_t \backslash \{0\}$, *with* W *satisfying* (2.32). *Further suppose that there exists a pair of sequences of the form* (2.33), *such that*

$$\int_{t_j}^{t_{j+1}} \lambda(t)dt \leq \kappa_j \tag{2.34}$$

holds for all $j \in J$. *Then the nominal periodic orbit,* $\mathcal{O}$, *of the autonomous system* (2.1) *is exponentially stable.*

Roughly speaking, if the conditions of Theorem 2.21 are met, then, for x sufficiently close to $\mathcal{O}$, the positive semi-definite function $V := x_\perp^\mathsf{T} W(t) x_\perp$ is exponentially decreasing on "average" when evaluated over some series of finite time intervals of the form (2.33), with the averaged rate of decay over the j-th interval bounded by κ_j. Here the transversality condition is taken into account by only requiring the inequality (2.32) to hold for $\chi \in \tilde{\Pi}_t$.

Later, in Section 4.6, we will further make use of the fact that $(\mathbf{I}_n - f_\star(t)\mathcal{P}(t))\chi = \chi$ if $\chi \in \tilde{\Pi}_t$, in order to instead construct from (2.32) a differential linear matrix inequality which can be solved using semi-definite programming.

Chapter 3

The Orbital Stabilization Problem

In this chapter, we formulate the orbital stabilization problem, introduce the notion of so-called s-parameterized orbits, as well as provide an overview of the control structure we will later use to solve the orbital stabilization problem. We also show how certain well-known control methods can be viewed as orbital stabilization, as well as discuss certain related concepts.

3.1 Problem Formulation

Consider a nonlinear, time-invariant, control-affine system of the form:

$$\dot{x} = f(x) + B(x)u. \tag{3.1}$$

Here $x = x(t) \in \mathbb{R}^n$ denotes the state vector, $\mathbb{R}^n$ is the state space, $\dot{x}(t) = \frac{d}{dt}x(t)$, and $u \in \mathbb{R}^m$ is a vector of independent control inputs. For now, it will be assumed that both the vector field $f : \mathbb{R}^n \to \mathbb{R}^n$ and the columns of the matrix-valued function $B : \mathbb{R}^n \to \mathbb{R}^{n\times m}$, denoted $b_i : \mathbb{R}^n \to \mathbb{R}^n$, are at least $\mathcal{C}^2$-smooth (twice continuously differentiable) on $\mathbb{R}^n$.

In a single sentence, one may describe the *orbital stabilization problem* as follows: The problem of simultaneously generating and stabilizing, via time-invariant feedback, a desired (forced) *orbit*[1] of the dynamical system (3.1). That is, to construct some mapping $k : \mathbb{R}^n \to \mathbb{R}^m$, such that closed-loop system under the control law $u = k(x)$ admits the desired motion as

[1]Recall from Section 2.1 that an orbit is the set of all points along the curve traced out by a solution of an autonomous dynamical systems. Thus orbital stabilization is just particular type of *set stabilization*, in which the invariant set under consideration is an orbit of the closed-loop system.

an asymptotically stable orbit. A preliminary assumption of the existence of such an orbit must therefore be made. In addition to its existence, will will also assume knowledge of a particular parameterization of the orbit.

3.1.1 The notion of an s-parameterized orbit

Knowledge of a triplet of functions (x_s, u_s, ρ) satisfying the following properties will generally be assumed.

Assumption 3.1. Given some connected interval $\mathcal{S} \subseteq \mathbb{R}$ and a finite (possibly empty) set of isolated points $\mathcal{S}_e \subset \mathcal{S}$, there exist three continuous functions

$$x_s : \mathcal{S} \to \mathbb{R}^n, \quad u_s : \mathcal{S} \to \mathbb{R}^m \quad \text{and} \quad \rho : \mathcal{S} \to \mathbb{R}_{\geq 0}, \tag{3.2}$$

such that, by defining

$$\mathcal{F}(s) := x_s'(s) = \frac{d}{ds} x_s(s), \tag{3.3}$$

these functions have the following properties:

P1 $x_s(\cdot)$ is of class $\mathcal{C}^2$, while $u_s(\cdot)$ and $\rho(\cdot)$ are $\mathcal{C}^1$ on $\mathcal{S} \backslash \mathcal{S}_e$; (*smoothness*)

P2 $\rho(s) > 0$ for all $s \in \mathcal{S} \backslash \mathcal{S}_e$, and $\rho(s_e) = 0$ for all $s_e \in \mathcal{S}_e$; (*time scaling*)

P3 $\|\mathcal{F}(s)\| > 0$ for all $s \in \mathcal{S}$; (*regularity*)

P4 $x_s : \mathcal{S} \to \mathbb{R}^n$ is one-to-one; (*non-self-intersecting*)

P5 $\mathcal{F}(s)\rho(s) = f(x_s(s)) + B(x_s(s))u_s(s)$ for all $s \in \mathcal{S}$. (*feasibility*)

Before further explaining the implication of each of these properties, we first note that knowledge of some functions satisfying the properties of Assumption 3.1 allows us to introduce the concept of a so-called *maneuver* of the dynamical system (3.1) as defined in [22]. Namely, the state–control curve

$$\mathcal{M} := \{(x, u) \in \mathbb{R}^n \times \mathbb{R}^m : \quad x = x_s(s), \quad u = u_s(s), \quad s \in \mathcal{S}\}. \tag{3.4}$$

Note, however, that since $B(\cdot)$ has been assumed to have full rank, one can always find the unique function $u_s(s)$ from Property **P5** given the knowledge of the pair $(x_s(s), \rho(s))$. Hence, instead of the maneuver $\mathcal{M}$, we may instead just consider its projection upon state space, namely its *orbit*:[2]

$$\mathcal{O} := \{x \in \mathbb{R}^n : \quad x = x_s(s), \quad s \in \mathcal{S}\}. \tag{3.5}$$

[2]Consequently, as was previously mentioned in the Introduction, the concept of *maneuver regulation*, as it appears in [22], is here equivalent to the stabilization of $\mathcal{O}$.

As we throughout this thesis will consider various maneuvers and their orbits having a parameterization of the form as in Assumption 3.1, we give it a name:

Definition 3.2 (s-parameterization)**.** A triplet (x_s, u_s, ρ) as in (3.2) having the properties described in Assumption 3.1 will be referred to as an ($\mathcal{C}^1$-smooth) s *-parameterization* of the maneuver $\mathcal{M}$ and its orbit $\mathcal{O}$.

Properties of an s-parameterized orbit

Since the orbit $\mathcal{O}$ generally only exists in the presence of some control signal, we will generally refer to it as a *forced* orbit of the dynamical system (3.1). Due to Assumption 3.1, one can infer that it has the following properties:

- by **P1**, $\mathcal{O}$ is a $\mathcal{C}^2$-smooth, one- or zero dimensional submanifold of $\mathbb{R}^n$;
- by **P2** and the regularity condition **P3**, it vanishes only for (isolated) points s_e in a zero-measure set $\mathcal{S}_e \subset \mathcal{S}$ for which $\rho(s_e) \equiv 0$;
- by **P4**, $\mathcal{O}$ is an embedded submanifold of $\mathbb{R}^n$ and consequently has a tubular neighborhood (of some radius $\epsilon > 0$) within which each point has a unique orthogonal projection onto $\mathcal{O}$;
- by **P5**, it is a controlled invariant set of (3.1), meaning that it can be rendered (positively) invariant.

Here the latter point, which corresponds to the maneuver $\mathcal{M}$ being consistent with the dynamics (3.1), can be easily verified by deriving a time parameterization of $\mathcal{M}$. Such a parameterization can be obtained by viewing the curve parameter $s = s(t)$ as a solution to the following autonomous differential equation (see **P2**):

$$\dot{s} = \rho(s). \tag{3.6}$$

Hence, by the chain rule we have

$$\dot{x}_s(s(t)) = x_s'(s(t))\dot{s}(t) = \mathcal{F}(s(t))\rho(s(t)).$$

Denoting by $x_\star(t) := x_s(s(t))$ and $u_\star(t) := u_s(s(t))$, we therefore obtain, by inserting the above into left-hand side of the expression in Property **P5**,

$$\dot{x}_\star(t) = f(x_\star(t)) + B(x_\star(t))u_\star(t), \tag{3.7}$$

which clearly demonstrates that $\mathcal{M}$ is consistent with the dynamics (3.1).

In the case of non-vanishing orbit, e.g. periodic ones (recall the concept of an *orbit* from Section 2.1), one may therefore view an s-parameterization as a time-scaled parameterization à la [102–104]. For instance, $x_\star(t)$ and $x_s(s(t))$ are clearly equivalent (up to a time shift) if $\rho \equiv 1$ for all $s \in \mathcal{S}$. The main difference between a time-parameterization and an s-parameterization therefore arises for orbits which vanish at certain points (i.e, orbits containing equilibrium points). Indeed, while $\|\dot{x}_s(s(t))\| \equiv 0$ for any $s(t) \in \mathcal{S}$ such that $\rho(s(t)) \equiv 0$, the key aspect of such an s-parameterization is that both Property **P2** and the regularity property **P3** hold, by allowing $\rho(\cdot)$ to vanish. This property is vital to our approach, as it will allow us to construct a state-dependent projection onto the maneuver, which by **P1** and **P5** is well-defined in a vicinity of $\mathcal{O}$.

In the case of non-vanishing orbits, it is therefore natural to ask whether there are any benefits (apart from generality of course) of considering an s-parameterization of the orbit (3.5) instead of just using a time parameterization? While there are admittedly no major benefits to be made beyond flexibility of the representation, there are several subtle advantages from which the control engineer may benefit. In particular, it allows one to work with a fixed interval $\mathcal{S}$, rather than an orbit-dependent time interval. The benefits of this range from an easy and compact representation of the motion, to streamlining both motion planning- and control design procedures, consequently making it both easier to construct and implement orbitally stabilizing feedback. Some of the benefits in regard to control design and -implementation will be made apparent in the examples in the next sections. To also demonstrates some of the benefits of using such a parameterization for motion planning, we consider next a simple example, after which we will properly formulate the orbital stabilization problem.

Example 3.1. Consider the second-order system

$$\begin{aligned}\ddot{\theta} &= -L\sin(\varphi),\\ \ddot{\varphi} &= u,\end{aligned}$$

where $\theta, \varphi, u \in \mathbb{R}$ and $L > 0$. As this system has two degrees of freedom, corresponding to (θ, φ), but only a single actuator, u, it is said to be *underactuated* by one degree. Our aim is to find some solution of the form $\theta_s(s) = \varphi_s(s) = a\cos(s)$ given some $a > 0$, with $s = s(t) \in [0, 2\pi)$ satisfying (3.6) for some strictly positive function $\rho(\cdot)$. Due to the system's underactuation, however, the function $\rho(\cdot)$ cannot be any; rather, since

$$\ddot{\theta}_s(s) = \ddot{\varphi}_s(s) = -a\left[\rho'(s)\sin(s) + \rho(s)\cos(s)\right]\rho(s), \quad \rho'(s) = \frac{d}{ds}\rho(s),$$

we have from the above expression for $\ddot{\theta}$ that it must be the solution to

$$a\rho'(s)\rho(s)\sin(s) + a\rho^2(s)\cos(s) - L\sin(a\cos(s)) = 0; \tag{3.8}$$

whereas from $\ddot{\varphi} = u$ the corresponding nominal control input is $u_s(s) = -L\sin(a\cos(s))$. Now, by multiplying (3.8) by $\sin(s)$, we can rewrite it as

$$\frac{d}{ds}\left(\frac{1}{2}a\rho^2(s)\sin^2(s) - \frac{L}{a}\cos(a\cos(s))\right) = 0.$$

Hence, along any solution of the form $\theta_s(s) = \varphi_s(s) = a\cos(s)$, the relation

$$\frac{1}{2}a\rho^2(s)\sin^2(s) + \frac{L}{a}\left[\cos(a) - \cos(a\cos(s))\right] = 0$$

must hold for all $s \in [0, 2\pi)$. The positive solution is therefore

$$\rho(s) = \sqrt{2L\left[\cos(a\cos(s)) - \cos(a)\right]/(a^2\sin^2(s))},$$

which by utilizing L'Hôptial's rule can be shown to be strictly positive and well defined for all $s \in [0, 2\pi)$. We have thus obtained a family of such a-dependent s-parameterizations without ever having to compute the time period of the oscillations.

3.1.2 Formulating the orbital stabilization problem

Suppose Assumption 3.1 holds, and denote by $\mathcal{O} \subset \mathbb{R}^n$ the corresponding forced orbit defined by (3.5). Let $\mathcal{N}_\delta(\mathcal{O})$ denote a δ-neighborhood of $\mathcal{O}$, defined according to

$$\mathcal{N}_{\mathcal{O}}(\delta) := \{x \in \mathbb{R}^n : \quad \mathrm{dist}(\mathcal{O}, x) < \delta\}, \tag{3.9}$$

where

$$\mathrm{dist}(\mathcal{O}, x) := \inf_{y \in \mathcal{O}} \|x - y\|.$$

The orbital stabilization problem can then be formulated:

Problem 3.3 (The orbital stabilization problem)**.** *For* (3.1)*, construct a control law $u = k(x)$, where $k : \mathbb{R}^n \to \mathbb{R}^m$ is locally Lipschitz continuous on a sufficiently large neighborhood of $\mathcal{O}$ and $\mathcal{C}^1$-smooth almost everywhere therein, such that $\mathcal{O}$ is an asymptotically stable set of the closed-loop system*

$$\dot{x} = f(x) + B(x)k(x). \tag{3.10}$$

Namely, for any real number $\epsilon > 0$, there is a $\delta = \delta(\epsilon) > 0$, such that for all solutions $x(\cdot)$ of (3.10) *satisfying $x(t_0) \in \mathcal{N}_\delta(\mathcal{O})$, it is implied that both*

- $x(t) \in \mathcal{N}_\epsilon(\mathcal{O})$ *for all* $t \geq t_0$ *(*stability*),*
- $\text{dist}(\mathcal{O}, x(t)) \to 0$ *as* $t \to \infty$ *(*attractivity*).*

Remark 3.4. Most often in this thesis, we will be concerned with the problem of *exponential* orbital stabilization, in which we want to ensure

$$\text{dist}(\mathcal{O}, x(t)) \leq Ce^{-\lambda(t-t_0)} \tag{3.11}$$

holding for all $t \geq t_0$ if $\text{dist}(\mathcal{O}, x(t_0)) \leq \delta$, given some real numbers $\delta, C, \lambda > 0$.

The essence of the orbital stabilization problem is therefore to only consider the distance to a desired forced orbit rather than the distance to a specific (time-varying) solution. Indeed, orbital stabilization is tightly linked to the notion of the orbital stability of a solution which we considered in Section 2.2.

Before we introduce some key concepts and consider a few simple examples showing some of the benefits of orbital stabilization, let us provide a brief, general overview of the methods we will use to solve the orbital stabilization problem.

3.2 Overview of the suggested control structure

Let an s-parameterization, $x_s : \mathcal{S} \to \mathcal{O}$, of a desired orbit $\mathcal{O}$ be given (see Def. 3.2). The (static) state-feedback control laws $u = k(x)$ we will present in this thesis for solving the corresponding orbital stabilization problem generally have a particular structure. Specifically, they can be decomposed into three separate parts:

$$k(x) = u_{nom}(x) + u_{fb}(x) + u_{rob}(x). \tag{3.12}$$

Roughly speaking, u_{nom} is a "nominal" feedback part which must be satisfying $u_{nom}(x_s(s)) \equiv u_s(s)$ for all $s \in \mathcal{S}$, and is therefore somewhat analogous to a feedforward term (it is of course not truly a feedforward due to its dependence on the system's state); u_{fb} is the stabilizing feedback part, ensuring convergence to the orbit $\mathcal{O}$; while u_{rob} is a (possibly discontinuous) robustifying feedback extension which can be added to compensate for uncertainties in the mathematical model or to reject unknown disturbances. A block-diagram overview of the control structure is shown in Figure 3.1.

By omitting the feedback extension u_{rob}, the control laws we will most commonly use throughout this thesis have the following type of structure:

$$u = u_s\big(p(x)\big) + K\big(p(x)\big)e(x). \tag{3.13}$$

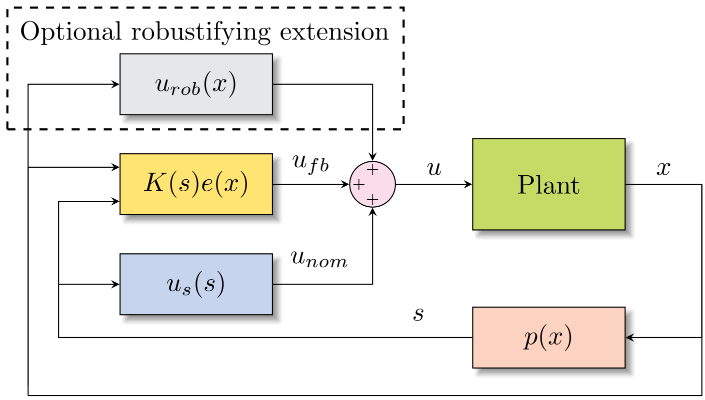

Figure 3.1: Block diagram of the proposed control structures (3.12)–(3.13).

Here $x \mapsto p(x)$, $p : \mathfrak{X} \subseteq \mathbb{R}^n \to \mathcal{S}$, is a so-called *projection operator*, which in a vicinity of the orbit projects the current states onto the orbit as to retrieve the corresponding value of the curve parameter s to be used in the control law. The continuous matrix-valued function $K : \mathcal{S} \to \mathbb{R}^{m\times N}$ correspond to the feedback-gains, with N either equal to n or $(n-1)$; while the function $e : \mathbb{R}^n \to \mathbb{R}^N$ is such that its zero-level set provides an implicit representation of the orbit. For example, in the case of non-vanishing orbits (e.g. periodic ones), we will commonly use the subscript notation $e_\perp$, as e then corresponds to a vector of so-called (excessive) *transverse coordinates*, which we will study in depth in Chapter 4.

Note that, since we will assume throughout this thesis that exact measurements of all the system's states are available, the implementation of a control law of the form (3.13) is straightforward in general:

Step 1: Given x, compute $p = p(x)$ and $e = e(x)$;

Step 2: Compute $u_s(p)$ and $K(p)$ (e.g. using splines or lookup tables depending on their complexity);

Step 3: Take $u = u_s(p) + K(p)e$.

To both motivate the use of orbital stabilization and to illustrate some of the aforementioned key concepts, will compare it to reference tracking in the next example.

Example 3.2. (The "catch-up" effect) Consider the double integrator

$$\ddot{q} = u, \quad q(t), u(t) \in \mathbb{R}, \quad \dot{q} = \frac{d}{dt}q. \tag{3.14}$$

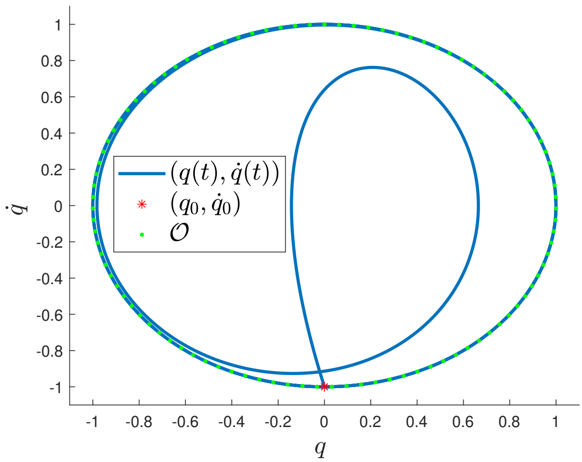

Figure 3.2: Shows the "catch-up" effect obtained for the double-integrator system in Example 3.2 under the control law (3.17) with $a = \omega = 1$ and $k_p = k_d = 2$.

Suppose we want the unit-mass particle $q \in \mathbb{R}$ to move in a sinusoidal fashion with amplitude $a > 0$ and frequency $\omega > 0$, such that the curve it traces out in state space corresponds to the following periodic orbit:

$$\mathcal{O} = \{(q, \dot{q}) = (a\sin(\omega t), a\omega\cos(\omega t)),\ t \in [0, 2\pi/\omega)\}\,. \tag{3.15}$$

To this end, let us consider the following reference trajectory lying on $\mathcal{O}$:

$$q_\star(t) = a\sin(\omega t). \tag{3.16}$$

We can then define the tracking error $\epsilon(t) := q(t) - a\sin(\omega t)$ and utilize some regular reference tracking controller; for example, taking

$$u_{PD} = -a\omega^2\sin(\omega t) - k_p\epsilon - k_d\dot{\epsilon} \tag{3.17}$$

results in the error dynamics

$$\ddot{\epsilon} = -k_p\epsilon - k_d\dot{\epsilon},$$

which are exponentially stable for any $k_p, k_d > 0$. However, the controller (3.17) has an explicit dependence on time due to the reference signal $r(t) = a\sin(\omega t)$ appearing in the computations of the error, ϵ, its time derivative, as well as in the feedforward term. Thus the closed-loop system is time-varying, not autonomous. As a consequence, if we for instance start the system with, say, the initial conditions $(q_0, \dot{q}_0) = (0, -a\omega) \in \mathcal{O}$, the system will experience a "catch-up" effect as shown in Figure 3.2, in which the states are momentarily driven away from the orbit. This happens because of the initial velocity error being equal to $\dot{\epsilon}_0 = -2a\omega$ even though the system is initialized directly on the desired orbit (3.15).

Let us now attempt to instead solve this task using an orbitally-stabilizing feedback controller based on transverse coordinates and a projection operator. We will propose for this purpose two methods: the first using a single transverse coordinate, and the second utilizing an *excessive* set of transverse coordinates.

A single transverse coordinate: We begin by noting that the desired trajectory (3.16) is the solution to the following initial-value problem (IVP):

$$\ddot{q} = -\omega^2 q, \quad (q(0), \dot{q}(0)) = (0, a\omega).$$

Using here the identity $2\ddot{q} = \frac{d}{dq}\dot{q}^2$ [105], we can integrate the above IVP and rearrange it in order to obtain a function $I : \mathbb{R}^2 \to \mathbb{R}$, defined by

$$I(q, \dot{q}) := \frac{1}{2}\dot{q}^2 + \frac{1}{2}\omega^2(q^2 - a^2), \tag{3.18}$$

which must be equal to zero at all points on $\mathcal{O}$. The function $I(\cdot)$ is in fact a *transverse coordinate*, namely: it vanishes on the orbit, is non-zero away from it, and the transpose of its gradient, given by $DI(q, \dot{q}) = [\omega^2 q, \dot{q}]$, is evidently locally orthogonal to the nominal orbit's flow:

$$DI(q_\star(t), \dot{q}_\star(t)) f(x_\star(t)) = \begin{bmatrix} \omega^2 a \sin(\omega t) & a\omega\cos(\omega t) \end{bmatrix} \begin{bmatrix} a\omega\cos(\omega t) \\ -a\omega^2 \sin(\omega t) \end{bmatrix} \equiv 0.$$

It follows that if we can asymptotically stabilize its origin, then we will simultaneously asymptotically stabilize the orbit.

An example of such an orbitally-stabilizing control law is the following:

$$u_I = -\omega^2 q - k_I \dot{q} I, \quad k_I > 0. \tag{3.19}$$

This nonlinear feedback controller, whose derivation is similar to Fradkov's speed-gradient method [106], is obtained from Proposition 4.12 which we will state and prove in Section 4.4; see also Sec. II in [107] where the same controller is equivalently derived, but from the point of view of energy levels and the Hamiltonian.

Whilst this approach of using the coordinate I and the controller (4.21) will indeed orbitally stabilize the periodic orbit within some non-zero neighborhood, it is very case specific. That is to say, the system, in addition to being scalar, is both fully actuated and has trivial dynamics. We therefore present a more general approach utilizing an *excessive* number of transverse coordinates next.

Excessive transverse coordinates: We begin by observing that the orbit (3.15) can be written in the form of an s-parameterization satisfying Assumption 3.1:

$$\begin{aligned} q_s(s) &= a\sin(s) &&=: \phi(s), \\ \dot{q}_s(s) &= a\cos(s)\omega &&=: \phi'(s)\rho(s), \\ \dot{s} &= \omega &&=: \rho(s). \end{aligned} \tag{3.20}$$

Thus the curve parameter $s \in \mathcal{S} := [0, 2\pi)$ can be considered simply a re-scaling of time along $\mathcal{O}$, that is $s = \omega t$. Noting that

$$|s - \operatorname{atan2}(\omega q_s(s), \dot{q}_s(s))| \equiv 0 \quad \forall s \in \mathcal{S},$$

one can, for example, utilize the projection operator

$$p(q, \dot{q}) = \operatorname{atan2}(\omega q, \dot{q}), \tag{3.21}$$

where $\operatorname{atan2}(\cdot)$ denotes the four-quadrant arctangent function.

Using the short-hand notation $p = p(q, \dot{q})$, one has with this parameterization several natural candidates for transverse coordinates, including:

$$y = q - \phi(p), \tag{3.22a}$$

$$\dot{y} = \dot{q} - \phi'(p)\dot{p}, \tag{3.22b}$$

$$z = \dot{q} - \phi'(p)\rho(p), \tag{3.22c}$$

$$\xi = \dot{p} - \rho(p). \tag{3.22d}$$

So which should we pick? Or just as importantly, how many of them do we need to consider? Namely, if $e_\perp = e_\perp(q, \dot{q})$ is the vector of transverse coordinates, whose origin we want to stabilize, what should its dimension be? By simple reasoning, as the system has two states, $(q, \dot{q})$, and since we already have one coordinate which retrieves the curve parameter upon the orbit, i.e. the projection operator $p = p(q, \dot{q})$, it is implied that $e_\perp$ has to be of unit dimension for there to exist a well-defined (local) diffeomorphism $(q, \dot{q}) \mapsto (p, e_\perp)$. Hence, there exists at most one independent transverse coordinate at any given time. The only candidate always satisfying this among the possible coordinates in (3.22) is ξ, which takes the place of the previously defined coordinate I; that is $\hat{I} = \frac{1}{2}(\dot{p} + \rho(p))\xi$. However, note that it is dependent upon the time-derivative of the projection operator, $\dot{p} = \frac{\partial p}{\partial q}\dot{q} + \frac{\partial p}{\partial \dot{q}}\ddot{q}$, which in turn is dependent on $\ddot{q}$.

Thus, suppose we instead take[3] $e_\perp = \mathrm{col}(y, z)$; that is, an *excessive* number of coordinates. It is clear that, even though the triplet (p, y, z) can have at most two independent elements at any given time, if we stabilize the origin of the excessive coordinates $e_\perp$, we simultaneously stabilize the periodic orbit. For example, as we will prove later in this thesis (see Proposition 4.36 in Section 4.5.3), the following control law

$$u = -\omega^2 a \sin(s) - k_y y - k_z z \tag{3.23}$$

exponentially stabilizes stabilizes the orbit (3.15) for any two constants $k_y, k_z \in \mathbb{R}$ with $k_z > 0$. The proof we will later present is based on the *transverse linearization* associated with $e_\perp$, which simply means the linearization (first-order approximation) of its dynamics along the orbit $\mathcal{O}$. Thus the above stability result is of course only guaranteed to hold locally. Nevertheless, it is quite surprising that it is true regardless of the value of k_y, although taking $k_y > 0$ is likely advantageous in terms of the convergence rate. It is also important to note that even though the structure of the controller (3.23), which is of the form (3.13), is reminiscent of the reference tracking controller (3.17), it is an inherently nonlinear controller due to the definition of the projection operator (3.21).

To further demonstrate the differences, we compare these two orbitally-stabilizing control laws to the reference-tracking control law (3.17) in a numerical simulation example next.

Simulation: Consider again the scalar particle example (3.14), but suppose its true mass is in fact 1.5 kg and that it is also subject to an unknown dry-friction term:

$$\frac{3}{2}\ddot{q} = u - 2\mathrm{sgn}(\dot{q}). \tag{3.24}$$

The task remains the same as before: to converge to the periodic orbit (3.15). We compared for this purpose the following three controllers: the u_{PD}-controller (3.17) with $(k_p, k_d) = (4, 4)$; the u_I-controller (3.19) with $k_I = 1$; and the u_{yz}-controller (3.23) with $(k_y, k_z) = (4, 4)$.[4]

Figure 3.3 shows the obtained phase portraits and control inputs from numerically simulating the system (3.24) when starting at

$$(q_0, \dot{q}_0) = (0, -3a\omega/2) \quad \text{with} \quad a = \pi/2 \quad \text{and} \quad \omega = \pi.$$

[3]Note that one cannot simply replace the coordinate z with $\dot{y}$. Not only would this also require one to compute $\ddot{q}$, but as shown in [38], the gradients of both y and $\dot{y}$ loose rank at the same points along $\mathcal{O}$, and so $(y, \dot{y})$ are not valid excessive transverse coordinates.

[4]The controller gains are here picked rather arbitrary in order to best illustrate the concept of orbital stabilization compared to reference tracking, and have therefore not been chosen specifically with the goal of optimizing performance in mind.

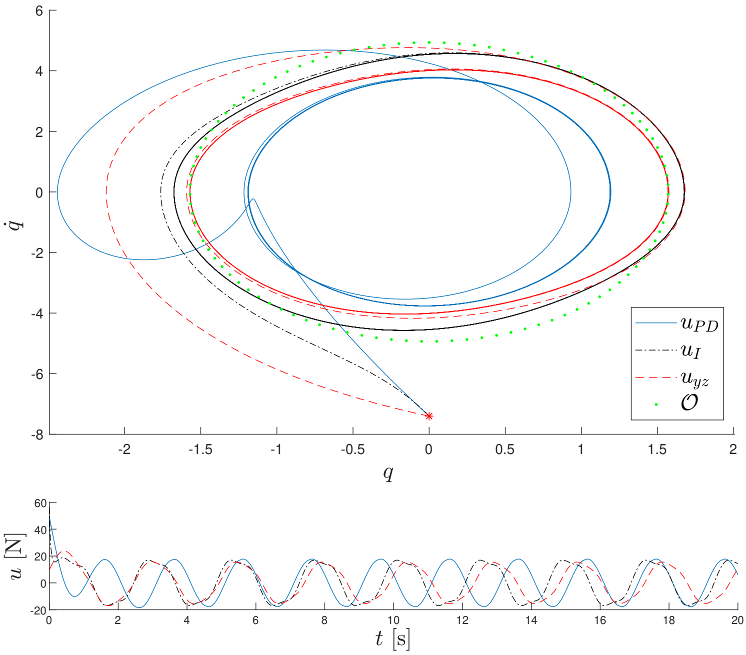

Figure 3.3: Phase portrait and control input from the comparison between a reference tracking PD-controller (—) and two orbitally stabilizing controllers using, respectively, one (-·-) and two (- -) transverse coordinates. The green, dotted line (···) corresponds to the nominal orbit.

It is clear that, whereas the orbitally stabilizing controllers u_I and u_{yz} gradually converge close to the orbit in ways one might argue are quite natural, the reference tracking (feedforward+PD)-controller takes a much more aggressive action and a significant detour (corresponding to the previously mentioned "catch-up" effect), before eventually converging to a perturbed orbit.

3.3 Classic control methods viewed as orbital stabilization

With the aim of providing some intuition and motivation for the methods we will present in this thesis, we will in this section demonstrate how some well-known classical control methods can be viewed as solving an orbital stabilization problem.

Reference tracking viewed as orbital stabilization

As we have previously stated, given knowledge of an s-parameterization as by Assumption 3.1, one can always retrieve a time-parameterized reference trajectory, in the form of a pair of time-varying functions $(x_\star(t), u_\star(t))$. This of course means that one always has the option of restating the motion-control problem as a *reference-tracking control problem* (RTCP), e.g. as the one we considered in Example 3.2. Recall that in the quintessential RTCP, the goal is to design some time-varying control law $u = \tilde{k}(x,t)$ which renders the origin of the *tracking error*, $\epsilon(t) := x(t) - x_\star(t)$, (uniformly) asymptotically stable. In contrast to orbital stabilization, the resulting differential equations governing the error dynamics will therefore in general be non-autonomous, possibly making the tasks of analyzing and/or stabilizing the origin somewhat more intricate.

One can, of course, utilize the common trick of augmenting the state as to"autonomize" the system, and consequently the error dynamics, thus transforming the RTCP into an orbital stabilization problem. More specifically, one can introduce the augmented state $\chi := \mathrm{col}(t, x)$, with $\dot{\chi}_1 = 1$ and $\chi_1(t_0) = t_0$. Thus a new reference trajectory can then be defined: $\chi_\star(s) := \mathrm{col}(s, x_\star(s))$. Here the curve parameter $s \in \mathbb{R}_{\geq 0}$ can be recovered from a projection of the augmented states onto the desired state curve $\chi_\star(\cdot)$ through the now trivial projection operator:

$$p(\chi) = [1, 0, \ldots, 0]\chi.$$

From a practical point of view, there is of course little to be gained from this augmented state representation. Indeed, as the first row of the augmented error variable $\mathcal{E}(\chi) := \chi - \chi_\star\big(p(\chi)\big)$ is trivially zero, the resulting error dynamics necessarily cannot be asymptotically stable; in fact, only a subspace of at most the same dimension as the original system can be stabilized. Moreover, such a control strategy will, if not modified in some way, still be relentless in its pursuit of ensuring the "timing" of the motion, rather than purely minimizing just the distance to the desired state curve as an orbitally stabilizing feedback would. Nevertheless, viewing RTCP as an orbital stabilization problem for the augmented state may provide some intuition for the concepts we will use later on, specifically where the stabilization problem is reduced to only stabilizing certain (transverse) subspaces.

Critical- or over damped PD control

Consider once again the double-integrator system (3.14), that is

$$\ddot{q} = u, \quad q(t), u(t) \in \mathbb{R}. \tag{3.14}$$

Rather than wanting to stabilize, say, a particular periodic orbit, our aim is now to stabilize the origin $q = 0$ of (3.14). We can in fact pose this as an orbital stabilization problem, where the main task is not to stabilize the trivial orbit at the origin per se, but instead the task is that of stabilizing the dual orbit(s) formed by the unbounded curve $\dot{q} = -\kappa q$ for some $\kappa > 0$. Indeed, if the system's states are confined to this curve, then they will evidently converge to the origin at an exponential rate. Or in other words: the origin is exponentially stable relative to this orbit. By designing a control law which exponentially stabilizes the orbit, we can therefore conclude the exponential stability of $q = 0$ by using a reduction principle [108–110].

To this end, we introduce the scalar function

$$\sigma := \dot{q} + \kappa q. \tag{3.25}$$

As the dual orbit $\mathcal{O}$ can be defined by its zero-level set,

$$\mathcal{O} := \{(q, \dot{q}) \in \mathbb{R} \times \mathbb{R} : \quad \sigma(q, \dot{q}) = 0\},$$

it is a transverse coordinate. We will now show that by stabilizing $\mathcal{O}$ using a control law of the form (3.13), it naturally leads to a pole-placement scheme in which the both eigenvalues of the closed-loop system are real, and where the damping response may be viewed in terms of the curve $\mathcal{O}$ and the second nullcline, which together enclose a positively-invariant region of the phase plane to which all solutions converge.

To this end, we first note that the dynamics of σ is governed by

$$\dot{\sigma} = \ddot{q} + \kappa \dot{q} = u + \kappa(\sigma - \kappa q),$$

and that we may also write $\dot{q} = -\kappa q + \sigma$. Let $x = \mathrm{col}(q, \dot{q})$ and consider

$$u = u_{nom}(x) - \mu\sigma, \quad \mu > 0. \tag{3.26}$$

Here u_{nom} is the mapping which equals the "nominal" control input on $\mathcal{O}$ if $\sigma \equiv 0$, which can be obtained by setting $\dot{\sigma} = 0$ and solving for u. There are two basic options for u_{nom}: 1) use the "feedback-linearizing" option $u_{nom} = -\kappa\dot{q}$; or 2) the "feedforward" version $u_{nom} = \kappa^2 q$. For example, by opting for 1), one just needs to take $\mu > 0$ to ensure that the origin is globally exponentially stable as it results in $\dot{\sigma} = -\mu\sigma$.

In regard to the methods we will present in thesis, however, it is the second "feedforward" option which is of most interest. Using the notation from sections 3.1 and 3.2, the resulting control law will then be of the form

$$u = \rho'(s)\rho(s) + K_{\perp}(s)(x - x_s(s)), \quad s = p(x), \tag{3.27}$$

where

$$\rho(s) = -\kappa s, \quad K_\perp(s) = [k_1(s), k_2(s)] \quad \text{and} \quad x_s(s) = \mathrm{col}(s, \rho(s)).$$

Here a variety of projection operators are possible, such as, for example, the orthogonal projection onto $\mathcal{O}$, given by $p(x) = q - \dot{q}/\kappa$. It leads to

$$u = \kappa(\kappa + k_2(s))q + (1/\kappa)(k_1(s) - \kappa^2)\dot{q},$$

such that for a constant $K_\perp$ it is required that $k_1 < \kappa^2$ and $k_2 < -\kappa$.

Let us, however, in the following consider the perhaps simplest choice of projection operator, namely:

$$p(x) = q. \tag{3.28}$$

Clearly k_1 is now arbitrary, such that for $k_2 = -\mu$, we have

$$u = \kappa^2 q - \mu\sigma. \tag{3.29}$$

Since this leads to

$$\begin{aligned} \dot{q} &= -\kappa q + \sigma, \\ \dot{\sigma} &= (\kappa - \mu)\sigma, \end{aligned}$$

we must evidently take $\mu > \kappa$ in order to avoid the existence of other equilibria and to ensure stability. Indeed, one can easily show that the eigenvalues of the closed-loop system are then given by

$$\lambda^2 + \mu\lambda + \kappa(\mu - \kappa) = 0 \implies \lambda = -\frac{\mu}{2} \pm \frac{1}{2}\sqrt{\mu^2 - 4\kappa(\mu - \kappa)} = -\frac{\mu}{2} \pm \frac{1}{2}|\mu - 2\kappa|,$$

which are both strictly negative and real as $0 < \kappa < \mu$, thus leading to an critically damped response if $\mu \equiv 2\kappa$, or an overdamped response otherwise.[5] This response can also be understood geometrically by the fact that, since no solution can cross the curve $\mathcal{O}$, all solutions must enter and then remain within the region in the second and forth quadrants of the phase plane enclosed by $\mathcal{O}$ and the second nullcline corresponding to $u = 0$, which is given by the set $\mathfrak{n}_2 = \{\dot{q} = (\kappa^2 - \mu\kappa)q/\mu\}$.

One can of course utilize these ideas to stabilize any curve of the form $\dot{q} = \rho(q)$, where is a $\rho(\cdot)$ is a smooth function such that $q\rho(q) < 0$ for all $q \neq 0$. For example, $u = 2\kappa^2 e^q(e^q - 1)/(e^q + 1)^3 - \mu\big(\dot{q} + \kappa(e^q - 1)/(e^q + 1)\big)$ brings the states onto the sigmoid curve $\dot{q} = -\kappa(e^q - 1)/(e^q + 1)$.

[5] If $u = b(\kappa^2 q - \mu\sigma)$ for some $0 < b < 1$, then an underdamped response can occur if μ is not taken sufficiently large. This is due to the controller overshooting the curve $\dot{q} = -\kappa q$ as the the "nominal control"-part $b\kappa^2 q$ is no longer sufficient as to render $\mathcal{O}$ positively invariant.

Integral extension: By adding an integral action to (3.29), i.e.

$$u = \kappa^2 q - \mu\sigma - \eta \int_0^t \sigma(\tau)d\tau, \tag{3.30}$$

and then defining $\varphi_1 = \int_0^t \sigma(\tau)d\tau$, $\varphi_2 = \sigma$, the origin of

$$\begin{aligned}\dot{\varphi}_1 &= \varphi_2,\\ \dot{\varphi}_2 &= -\eta\varphi_1 - (\mu - \kappa)\varphi_2\end{aligned}$$

is evidently exponentially stable for $\kappa >$ only if $\mu, \eta > 0$ and $\mu > \kappa$.[6]

Classical sliding mode control

In case the right-hand side of (3.14) also contain some unknown perturbation, then there is no longer any guarantee that the linear PD-like control laws considered previously will be stabilizing. In such cases, the classical first-order *sliding mode control* methodology may be better suited due to its complete insensitivity to bounded perturbations satisfying a matching condition [62, 63, 66, 111]. This insensitivity is achieved through utilizing a discontinuous (relay) feedback, such as

$$u = u_{nom}(x) - \mu\lceil\sigma\rfloor^0, \tag{3.31}$$

where $\lceil\sigma\rfloor^\alpha = \operatorname{sgn}(\sigma)\,|\sigma|^\alpha$. Of course, due to the unknown perturbation and the discontinuous control which is applied to the system, it will generally no longer be true that $\dot{\sigma} \equiv 0$ even though the states have been successfully forced onto $\mathcal{O}$ in finite time. Nevertheless, the so-called *equivalent control* introduced by Utkin [60, 111, 112]—which in some sense can be considered as the "average" of the applied discontinuous control signal needed to keep the system confined to $\mathcal{O}$—will still be of the form $u_{eq} = \rho'(q)\rho(q)$ (see (3.27)). Thus instead of evolving along $\mathcal{O}$ in the usual sense, one can consider the system as being brought into a mode of sliding along the orbit $\mathcal{O}$, with the system's solutions then understood in the sense of Filippov [113, 114] (see also [115]). Within this framework, the transverse coordinate σ is therefore commonly referred to as the *sliding variable*, while its zero-level set, i.e. the orbit $\mathcal{O}$, is referred to as the sliding surface/manifold as it is rendered finite-time attractive [66].

[6] Assuming $q(0) = 0$, the series type PID controller (3.30) can be rewritten as a parallel PID controller: $u = -k_p q - k_d \dot{q} - k_i \int_0^t q(\tau)d\tau$ with $k_p := (\mu\kappa + \eta - \kappa^2)$, $k_d := \mu$ and $k_i := \eta\kappa$. By the Routh-Hurwitz criterion [92], it is well know that the PID controller is stabilizing if and only if $k_d, k_i > 0$ and $k_p k_d > k_i$. The first conditions evidently correspond to $\mu > 0$ and $\kappa\eta > 0$, whereas the second can be shown to be equivalent to $\mu\kappa(\mu - \kappa) > \eta(\kappa - \mu)$, which holds only if $\mu > \kappa$.

Adding a robustifying feedback extensions to a PD controller

It is important to remark that if the second-order system is of the form $\ddot{q} = u + \Delta(q, \dot{q}, t)$, with $\Delta(\cdot)$ containing both the uncertainties in the system's model and any unknown disturbances, then one is not forced to abandon the continuous PD controller (3.29) completely in favor of the sliding mode control law (3.31). Rather, one can combine the two, thus essentially settling upon a compromise between the continuous and gradual convergence of the PD controller, and the discontinuous, but disturbance-rejecting capabilities of the sliding mode controller.

In order to demonstrate this possibility, which we will study in more detail in Chapter 8, let us take $u = (1 - 2\eta)\kappa^2 q - 2\eta\kappa\dot{q} + v$ with $\eta > 1/2$. Here the first two terms correspond to an over- or critically damped PD controller (i.e. (3.29) with $\mu = 2\eta\kappa$), while $v \in \mathbb{R}$ is a robustifying feedback extension to be designed. Hence, in regard to (3.12), this corresponds to $u_{nom} = \kappa^2 q$, $u_{fb} = -2\eta\kappa\sigma = -2\eta\kappa(\dot{q} + \kappa q)$, and $u_{rob} = v$.

Letting again $x = \mathrm{col}(q, \dot{q})$, we may then write

$$\dot{x} = \begin{bmatrix} 0 & 1 \\ (1 - 2\eta)\kappa^2 & -2\eta\kappa \end{bmatrix} x + \begin{bmatrix} 0 \\ 1 \end{bmatrix} [v + \Delta(x, t)] =: A_{cl}x + B[v + \Delta(x, t)].$$

Notice here that the eigenvalues of A_{cl} are $\lambda_1 = -\kappa$ and $\lambda_2 = -\kappa(2\eta - 1)$, whose corresponding left eigenvectors are $S_1 = [(2\eta - 1)\kappa, 1]$ and $S_2 = [\kappa, 1]$, respectively, i.e. $S_i A_{cl} = \lambda_i S_i$,. This can be equivalently reformulated as follows: each S_i annihilates an A_{cl}-invariant, one-dimensional subspace of $\mathbb{R}^2$. Specifically, $S_i w_j = 0$ where $w_j \in \mathbb{R}^2$, $j \in \{1, 2\}\backslash\{i\}$, is a right eigenvector of A_{cl}, i.e. $A_{cl} w_j = \lambda_j w_j$.

Let us define the scalar functions $\sigma_i := S_i x$, $i = 1, 2$. Note that σ_2 corresponds to the function we have previously defined in (3.25). Clearly

$$\dot{\sigma}_i = S_i \dot{x} = \lambda_i S_i x + S_i B[v + \Delta(x, t)] = \lambda_i \sigma_i + [v + \Delta(x, t)],$$

from which the following can be concluded: If $v = v(x)$ can be designed as to confine the system's states to the subspace annihilated by either S_1 or S_2, i.e. induce a sliding mode on $\sigma_i = 0$, then the equivalent control will be $v_{eq} = -\Delta(x, t)$. In this regard, suppose, for example, that $|\Delta(x, t)| \leq \Delta_M + \delta\,|\sigma_i|$ for constants $\Delta_M, \delta \geq 0$, with $\delta < |\lambda_i|$. Then one can, to this end, for instance take $v = -\zeta\lceil\sigma_i\rfloor^0$, with $\zeta > \Delta_M$, as to ensure that the sliding surface $\Sigma_i := \{\sigma_i = 0\}$ is reached in finite time. Moreover, if $x_i(t) \in \Sigma = \mathrm{span}\,(w_j)$ for all $t \geq t_0 \geq 0$, with $j \in \{1, 2\}\backslash\{i\}$, then $x(t) = e^{\lambda_j(t - t_0)}x(t_0)$ in the ideal sliding mode [60].

Terminal sliding mode control

If we loosen the smoothness requirement upon the mapping $x_s(\cdot)$, then we may also consider a slightly more general curve than those corresponding to the zero-level set of (3.25). For instance, let us consider

$$\sigma = \dot{q} + \kappa\lceil q\rfloor^{\alpha} \tag{3.32}$$

where $\alpha \geq 1/2$ and with $\lceil\sigma\rfloor^{\alpha} = \operatorname{sgn}(\sigma)\,|\sigma|^{\alpha}$ as before. Note that for $\alpha \equiv 1$ this corresponds to (3.25). If, on the other hand, $\alpha \in [1/2, 1)$, then the system is in a so-called *terminal mode* [116] if its solutions are confined to $\mathcal{O} = \{\sigma = 0\}$, meaning simply that they will reach the origin within a finite amount of time; see, e.g., [117, 118].

In a similar manner to (3.26), let us consider a control law of the form $u = u_{\star}(x) - \mu\lceil\sigma\rfloor^{\beta}$. Using the fact that $\frac{d}{dq}\lceil q\rfloor^{\alpha} = \alpha\,|q|^{\alpha-1}$, we find

$$\dot{q} = -\kappa\lceil q\rfloor^{\alpha} + \sigma \tag{3.33a}$$
$$\dot{\sigma} = u + \kappa\alpha|q|^{\alpha-1}\dot{q} = u + \kappa\alpha|q|^{\alpha-1}(-\kappa\lceil q\rfloor^{\alpha} + \sigma). \tag{3.33b}$$

This motives the following choice: $u = -\kappa\alpha\,|q|^{\alpha-1}\,\dot{q} - \mu\lceil\sigma\rfloor^{0}$. For some $\alpha \in [1/2, 1)$, this corresponds to the so-called singular terminal sliding mode controller [116, 119]; see also [120] for its non-singular counterpart.

Let us try to obtain an alternative control law by instead taking inspiration from control structure (3.13). To this end, we note that the equivalent control on

$$\mathcal{O} = \{x = x_s(s) := \operatorname{col}(s, \rho(s)), \quad s \in \mathbb{R}\},$$

where $\rho(s) = -\kappa\lceil s\rfloor^{\alpha}$, is given by $u_{eq}(s) = \rho'(s)\rho(s) = \alpha\kappa^2\lceil s\rfloor^{2\alpha-1}$. In the spirit of (3.27)-(3.28), we may therefore instead consider [7]

$$u = \alpha\kappa^2\lceil q\rfloor^{2\alpha-1} - \mu\lceil\sigma\rfloor^{\frac{2\alpha-1}{\alpha}}. \tag{3.34}$$

This results in

$$\dot{q} = -\kappa\lceil q\rfloor^{\alpha} + \sigma \tag{3.35a}$$
$$\dot{\sigma} = \left(\alpha\kappa|q|^{\alpha-1} - \mu|\sigma|^{\frac{\alpha-1}{\alpha}}\right)\sigma, \tag{3.35b}$$

[7] If the states either lie above the terminal curve (3.32) in the second quadrant, or below it in the fourth, then the control law (3.34) will always drive the states across the vertical $\dot{q}$-axis. This can however be avoided by taking inspiration from the nonlinear damping approach in [121]. Specifically, we can modify (3.34) as follows: $u = \alpha\kappa^2\lceil q\rfloor^{2\alpha-1} - \mu\lceil\sigma\rfloor^{\frac{2\alpha+a-1}{\alpha}} / \,|q|^{a}$,with $\mu = \alpha\kappa^{\frac{1-a}{\alpha}} + \rho$ and $\rho > 0$. It has an unbounded gain for any $a \geq 0$, in effect making the $\dot{q}$-axis into a barrier which no solution can cross.

which is homogeneous of degree $(\alpha - 1)$ with respect to the dilation $(1, \alpha)$ [112]. Taking

$$\mu = \alpha\kappa^{\frac{1}{\alpha}} + \rho, \quad \rho > 0, \tag{3.36}$$

we have, whenever $y \equiv 0$, that

$$\dot{\sigma} = \left(\alpha\kappa|q|^{\alpha-1} - \mu\left|\kappa\lceil q\rfloor^{\alpha}\right|^{\frac{\alpha-1}{\alpha}}\right)\sigma = -\frac{\rho}{\kappa^{\frac{\alpha-1}{\alpha}}}\lceil\sigma\rfloor^{\frac{2\alpha-1}{\alpha}},$$

thus ensuring that the origin is the only fixed point. Similarly to the PD controller (3.27), all solutions will therefore enter the region in the second and forth quadrants of the phase plane enclosed by the second nullcline, corresponding to $u = 0$ with u as in (3.34), and the curve $\mathcal{O}$, from which they cannot escape, thus ensuring the attractivity of the origin. In fact, since the second nullcline can easily be verified to be given by

$$\mathfrak{n}_2 = \left\{(q, \dot{q}) \in \mathbb{R}^2 : \quad \dot{q} + c\lceil q\rfloor^{\alpha} = 0\right\} \quad \text{where} \quad c := \kappa - \left(\frac{\alpha\kappa^2}{\mu}\right)^{\frac{\alpha}{2\alpha-1}},$$

which is itself evidently a terminal ("finite-time") curve if μ is taken according to (3.36). Thus all the closed-loop system's solutions are squeezed between two terminal surfaces, implying therefore convergence to the origin in finite time. Indeed, using instead homogeneity-based arguments, we have, due to the homogeneity of (3.35) and the above established attractivity of the origin, that the origin is globally asymptotically stable by Proposition 6.1 in [122], whereas for $\alpha \in [1/2, 1)$, its finite-time stability follows by Theorem 7.1 therein.[8]

Energy-based control

Consider the following second-order, underactuated system:

$$\ddot{q} = u, \tag{3.37a}$$

$$\ddot{\theta} = \sin(\theta) - \cos(\theta)u. \tag{3.37b}$$

It corresponds to the well-known cart-pendulum system after a partially feedback-linearizing controller [13] has been applied [123, 124]. The task at hand is to stabilize some given constant energy-level set, $E_\star$, of the pendulum, whose upright position corresponds to $\theta = 0$, while keeping the cart's position, q, at the zero position.

[8]Similarly to the possible underdamped response of the PD controller stated in Footnote 5, if $u = b(\alpha\kappa^2\lceil q\rfloor^{2\alpha-1} - \mu\lceil\sigma\rfloor^{\frac{2\alpha-1}{\alpha}})$ for some $0 < b < 1$, then one might instead obtain a twisting-like behavior, a so-called *twisting mode* [116].

We have already seen how transverse coordinates could be use to regulate the particle system to a certain energy level (see (3.18)). In a similar manner, we therefore define the following transverse coordinate:

$$I = \frac{1}{2}\omega^2 + \cos(\theta) - E_\star.$$

Its derivative with respect to time is

$$\dot{I} = -\omega\cos(\theta)u.$$

Similarly to (3.19) (see also Proposition 4.12), it has been shown by Åström and Furuta in [125] that by taking $u = u_I$, with

$$u_I = k_I\omega\cos(\theta)I,$$

the pendulum's energy will be driven towards its desired value $E_\star$. Moreover, by adding a simple PD extension stabilizing the cart subsystem, for example

$$u = \kappa^2 q - (\kappa + k_\sigma)\sigma + k_I\omega\cos(\theta)I \quad \text{where} \quad \sigma := \dot{q} + \kappa q, \quad \kappa, k_\sigma > 0,$$

it was shown by Chung and Hauser [123] that one can in fact achieve exponential stability of the orbit

$$\mathcal{O} := \left\{(q,\dot{q}) = (0,0), \quad E(\theta,\dot{\theta}) = E_\star\right\}.$$

It was further demonstrated by Spong [124] that by taking $E_\star = 1$, i.e. the energy level at upright position of the pendulum, the same controller can be used to execute a swing-up maneuver.

The analysis used in [123] was heavily linked to the methods we will utilize in this thesis. Indeed, it was based on the fact that q, $\dot{q}$ (or alternatively σ) and I are transverse coordinates for the orbit, such that its exponential stability could be assessed using the corresponding transverse linearization.

3.4 Alternative methods and related concepts

Energy shaping–based approaches

In the last example, we saw that several well-known energy-based approaches [123–125] corresponded to orbital stabilization. Indeed, any energy shaping–based approach utilizing a time-invariant control law will generally fall under the umbrella of orbital stabilization as we consider it in this thesis. Naturally, this has lead to the development of energy-based methods tailored toward orbital stabilization. Of particular note are the approaches of Ortega, Romero and Yi et al., including their Immersion and invariance–based approach [32, 126] and Mexican sombrero energy-assignment method [35]; see also [127, 128]. However, whereas the promising ´´Mexican-sombrero" method is applicable to a large class of nonlinear systems, the Immersion and invariance–based method is more of an orbit-generation approach than an orbital stabilization method. This is due to the orbit which is induced in the closed-loop system being dependent on the initial conditions; hence, it is not an orbital stabilization method as by our definition in this thesis.

Path following and maneuvering

We have seen that the orbital stabilization problem in some sense can be considered as a relaxation of the reference-tracking problem by removing its inherent time dependence. For certain applications, however, such as motion control of second-order systems, it is possible to relax the problem even further by instead considering it as a *path-following problem*. In path following, the motion-control problem is generally decoupled into two parts [129–131]:[9] in the primary part—the *geometric task*—one wants to ensure convergence to the desired *path*, often given as a geometric curve in some output space parameterized by a scalar *path variable*; while in the secondary part—the *dynamic assignment task*—the goal is to ensure a certain behavior upon the path, e.g. some specific velocity profile.

It has shown by Aguiar and his collaborators [132, 133] that while trajectory-tracking control has certain limitations in the case of non-minimum phase systems, these limitations can be overcome by instead using path-following techniques. Indeed, as the geometric- and dynamic tasks are decoupled in path following, one can essentially treat the path variable as an additional control variable by changing its dynamics on-the-fly through a cleverly selected *timing law*. Orbital stabilization may therefore be viewed as a middle ground between reference-trajectory tracking and path following: While the timing law is neither fixed nor strictly evolving with time as in reference tracking, it is completely and uniquely determined by the system's states, and therefore not as flexible as in path following, where it essentially can be chosen freely. However, in the case of underactuated mechanical systems, not all speed assignments are necessarily feasible along some specific path (especially if it is a curve in state space). This makes it difficult to actually utilize the extra freedom of path following, thus instead

[9] The notion of *maneuvering* is instead used the works of Skjetne and his collaborators [130, 131] to clearly distinguish it from pure path following. Note that, while they, too, are inspired by the notion of a *maneuver* introduced by Hauser and Hindman [22] as we mentioned earlier in the Introduction, they do not consider it as a pure state-control curve as we do in this thesis. Rather, they separate the problem into two parts: the primary task of pure path following and a secondary dynamic assignment task upon the path.

motivating the more tractable concept of orbital stabilization.

Virtual holonomic constraint–based methods

For underactuated mechanical systems, the virtual holonomic constraint (VHC)–based methods are among the most prominent both in terms of orbit generation and -stabilization. While the term "virtual constraint" seems to have been first coined by Canudas-de-Wit in [134], the conceptual ideas originates from the early works of Grizzle and his collaborators [135–137] on bipedal robot locomotion. Roughly speaking, by assuming the invariance of certain artificial relations between the system's generalized coordinates, so-called *virtual* (*holonomic*) *constraints*, one reduces the dynamic constraints arising due to the system's underactuation down to a set of second-order equations in a single variable, with the number of equations equaling the system's degree of underactuation [138–140]. This reduction therefore paves the way for the development of effective methods to solve the problem of orbit generation.

At the same time, the VHC approach also facilitates the constructions of orbitally stabilizing feedback.[10] In the aforementioned early work on biped locomotion (see, e.g., [99]), the problem of gait stabilization was achieved by partly relying on the impact occurring at the end of a gait cycle when the foot strikes the ground. Canudas-de-Wit [141] suggested an approach in which parameters in the virtual constraints are dynamically changed using an adaptive-like law as to ensure convergence to a periodic orbit, although this orbit cannot be directly specified in advance. In the works of Shiriaev and collaborators [33, 142], it was shown that for any periodic orbit found using the VHC approach there exist natural candidates for transverse coordinates, for which the transverse linearization can be computed analytically [34, 55]. Thus, by pairing this method with a projection operator (see Section 3.2) to ensure the controllers time-independence, one obtains a constructive procedure for solving the orbital stabilization problem. Some examples this scheme being successfully utilized can be found in [143–145].

Transverse feedback linearization

A concept which is highly related to the methods we will present in thesis as to achieve orbital stabilization is the notion of *transverse feedback lineariz-*

[10] In the VHC literature, there are two common ways to consider the resulting motion-control problem: as an orbital stabilization problem or the as the problem of ensuring strict invariance of the so-called *constraint manifold* [139, 140]. In the work of Mohammadi et al. [31], a method using particular dynamic VHC is suggested as to solve these two tasks simultaneously, by essentially allowing the constraint manifold to change through the dynamically-defined VHC which eventually converges to its nominal value.

ation. This concept was first introduced by Banaszuk and Hauser [30], and later studied in detail by Nielsen and his collaborators [146–149]. When applicable, this powerful technique allows one to find a particular set of transverse coordinates, which together with a specific feedback transformation reduces the corresponding transverse dynamics to a controllable, time-variant linear system, thus essentially trivializing the problem of feedback design. However, similarly to standard feedback-linearizing controllers for nonlinear systems, there are aspects of this technique which limits its use for highly nonlinear and underactuated systems: 1) the method is sensitive to uncertainties in the mathematical model; and most importantly, 2) both checking if a system is in fact transversely feedback linearizable and deriving the resulting transformations are non-trivial tasks in general. In regard to latter point, the transverse linearization–based approaches we will present in this thesis will generally be easier to utilize and applicable to a larger class of systems, but at the expense of a more difficult feedback-design problem.

Contraction analysis

Linearizing the dynamics of a set of transverse coordinates along a target orbit is an important part of the methods we suggest for orbital stabilization in this thesis. The (transverse) linearization which is then obtained also has several strong connections to the "standard" linearization along the nominal motion, the so-called *first-order variational system* which we discussed in Section 2.3. However, to compute both of these types of linearizations, knowledge of the nominal motion is necessarily required.

One can of course attempt to carry out a linearization along any arbitrary solution of the dynamical system. In fact, carrying out such a "linearization" without specifying a particular solution leads to a general variational system, some times referred to as the *differential-* or *incremental dynamics*, which can be used to study the *contraction* between all neighboring within some domain. This is the key idea behind *contraction analysis* [101, 150–152], which can be used to simultaneously determine both the existence and exponential stability of a particular types of orbits, including fixed points [51, 150, 153] and limit cycles [26, 50–52, 154–157].

While there are strong structural similarities between several of these methods and those in this thesis, the relaxation of not fixing the orbit means that control design based on contraction analysis generally requires one to solve a matrix-valued partial differential equation. Such a controller, if found, in general brings with it advantageous compared to a controller designed from a first-order approximation. However, it may be significantly harder to design for nonlinear systems than a linearization-based control law. Thus, while there exist effective methods for its use in trajectory tracking of fully-actuated systems (see, e.g., [158, 159]), these methods are of limited use for orbital stabilization of underactuated systems at present.

Chapter 4

Orbital Stabilization of Periodic Motions

In this chapter, we present methods for solving the orbital stabilization problem for periodic orbits. We study some key concepts which will be used throughout this thesis, including projection operators, (excessive) transverse coordinates, and projected differential Lyapunov- and Riccati equations.

4.1 Introduction

The theory and methods outlined in Chapter 2 provided several powerful tools for assessing the stability characteristics of an orbit. Yet, those tools cannot be directly utilized to design feedback controllers which solve an (nontrivial) orbital stabilization problem due to their time dependence.

In this chapter, we will propose methods aimed at solving the orbital stabilization problem which are greatly inspired by many of the underlying ideas of the methods considered in Chapter 2. In particular, we will introduce a pair of completely time-invariant mappings, corresponding to a set of (excessive) transverse coordinates and a projection operator as we briefly considered in Chapter 3. This allows for a local change of coordinates in a vicinity of a periodic orbit, which essentially separates the transverse- and tangential dynamics. Moreover, we will show that the resulting transverse linearization along the orbit has the same structure as the linearizations derived by Zubov, Urabe and Leonov. Similarly to Chapter 2 (see Prop. 2.18 and Thm. 2.21), it will be shown that the orbit's stability is ensured by the existence of a solution to a certain Lyapunov differential equation, whereas an orbitally stabilizing feedback can be constructed from a solution to a certain Riccati differential equation.

Of particular importance, we consider in this chapter a generic set of projection-based excessive transverse coordinates. We derive the resulting transverse linearization, which is on the form of a system of linear differential-algebraic equations. It is shown that this linearized system is not stabilizable if one omits the algebraic part (a transversality conditions), and that it shares several characteristics with the corresponding variational system and a certain linear comparison system. We further introduce so-called projected differential Lyapunov- and Riccati equations. These allows one to validate an orbit's stability or to search for an orbitally stabilizing feedback controller using semidefinite programming.

Note that while we mainly limit our focus to periodic orbits in this chapter, many of the statements will be extended in the later chapters to other types of orbits as well.

Outline: The chapter is organized as follows: We discuss some preliminaries and formulate the problem in Section 4.2. We then define and study so-called projection operators in Section 4.3. In Section 4.4 we introduce the notion of transverse coordinates. A particular set of excessive transverse coordinates are then introduced and studied in Section 4.5. These are in turn used in Section 4.6 to design stabilizing feedback for periodic orbits.

4.2 Problem formulation

Consider a control-affine system of the form

$$\dot{x} = f(x) + B(x)u. \tag{4.1}$$

As in Chapter 3, we denote by $x(t) \in \mathbb{R}^n$ the state vector at time $t \in \mathbb{R}_{\geq 0}$ and by $u \in \mathbb{R}^m$ the controls. While it will still be assumed that the vector field $f : \mathbb{R}^n \to \mathbb{R}^n$ is $\mathcal{C}^2$-smooth, we will now only assume that the columns of the matrix-valued function $B : \mathbb{R}^n \to \mathbb{R}^{n\times m}$, denoted $b_i : \mathbb{R}^n \to \mathbb{R}^n$, are locally Lipschitz continuous on any domain of interest.

As we are mainly (although not exclusively) concerned with the stabilization of periodic orbits in this chapter, we will assume the existence of a non-trivial closed orbit $\mathcal{O} \subset \mathbb{R}^n$ of the undriven (i.e. $u = 0$) system (4.1). That is, we assume the undriven system admits a $\mathcal{C}^2$-smooth periodic solution, $x_\star(t+T) = x_\star(t)$, of some finite minimal periodicity $T > 0$. Hence,

$$\dot{x}_\star(t) = f(x_\star(t)) \quad \text{and} \quad \|f(x_\star(t))\| > 0$$

both hold for all t in $[0, T)$. The main problem we are looking to solve in this chapter can then be stated:

Problem 4.1 (Stabilizing a periodic oscillation)**.** *Find a $\mathcal{C}^1$-smooth matrix-valued function $k : \mathbb{R}^n \to \mathbb{R}^m$, satisfying $\|k(y)\| = 0$ for all $y \in \mathcal{O}$, such that, under the control law*

$$u = k(x), \tag{4.2}$$

the closed-loop system (4.1) *admits the periodic orbit*

$$\mathcal{O} = \{x \in \mathbb{R}^n : \ x = x_\star(t), \quad t \in [0, T)\}$$

as an exponentially stable limit cycle.

Remark 4.2. The above implies that the periodic orbit corresponds to a self-induced (alternatively, self-excited or -sustained) oscillation of the undriven system. However, in most applications, the desired operating mode might only exist in the presence of some nominal control input, and thus corresponds to a forced (or controlled invariant) oscillation. In light of this, suppose that the columns of $B(\cdot)$ are $\mathcal{C}^2$. Then the periodic orbit $\mathcal{O}$ may in fact be considered as a forced orbit of some "original" system

$$\dot{x} = f_0(x) + B(x)u_0, \quad f_0 \in \mathcal{C}^2(\mathbb{R}^n, \mathbb{R}^n). \tag{4.3}$$

That is to say, there then exists some $\mathcal{C}^2$ mapping $U_\star : \mathbb{R}^n \to \mathbb{R}^m$ such that

$$\dot{x}_\star(t) = f_0(x_\star(t)) + B(x_\star(t))U_\star(x_\star(t)).$$

Thus (4.1) may then in turn corresponds to (4.3) by taking

$$u_0 = W(x) + u \quad \text{and} \quad f(x) := f_0(x) + B(x)W(x),$$

for some $W \in \mathcal{C}^2(\mathbb{R}^n, \mathbb{R}^m)$ satisfying $U_\star(x_\star(t)) \equiv W(x_\star(t))$ for all $t \in [0, T)$.

Rather than considering the time-parameterization, $x_\star(t)$, we will in the sequel assume that a specific s-parameterization (see Assumption 3.1) is known.

Assumption 4.3. The undriven ($u = 0$) system (4.1) has a bounded, nontrivial periodic solution $x_\star(t) = x_\star(t + T)$ of minimal periodic $T > 0$. Moreover, given $\mathcal{S} := [0, s_T)$ for some $s_T > 0$, there is a $\mathcal{C}^2$-smooth mapping $x_s : \mathcal{S} \to \mathcal{O}$ and a solution $s : [0, T) \to \mathcal{S}$ to

$$\dot{s} = \rho(s), \quad \rho \in \mathcal{C}^1(\mathcal{S}, \mathbb{R}_{>0}), \tag{4.4}$$

such that

$$x_\star(t) \equiv x_s(s(t))$$

holds for all $t \in \mathcal{I} := [0, T)$. □

Given such a parameterization, namely

$$x_s : \mathcal{S} \to \mathcal{O}, \quad \mathcal{S} \ni s \mapsto x_s(s), \tag{4.5}$$

we may of course equivalently define the periodic orbit $\mathcal{O}$ by

$$\mathcal{O} := \{x \in \mathbb{R}^n : \; x = x_s(s), \quad s \in \mathcal{S}\}. \tag{4.6}$$

Using the same notation as in Section 3.1, we also denote

$$\mathcal{F}(s) := \frac{d}{ds} x_s(s), \tag{4.7}$$

such that the following series of relations must hold for all $t \in \mathcal{I}$:

$$\dot{x}_\star(t) = f(x_\star(t)) = \big(f \circ x_s\big)(s(t))\big) = \frac{d}{dt} x_s(s(t)) = \mathcal{F}(s(t))\rho(s(t))$$

Consequently, $\|\mathcal{F}(s)\| > 0$ holds for all $s \in \mathcal{S}$, ensuring the regularity of the above s-parameterization.

Remark 4.4. As to allow one to extend the above s-parameterization also beyond the time interval $[0, T)$, it can sometimes be useful to alternatively view $x_s : \mathbb{R}_{\geq 0} \to \mathcal{O}$ and $\rho : \mathbb{R}_{\geq 0} \to \mathbb{R}_{>0}$ as s_T-periodic functions, with $s : \mathbb{R}_{\geq 0} \to \mathbb{R}_{\geq 0}$ a diffeomorphism similar to the function $\tau(\cdot)$ which is used in the definition of Zhukovsky stability (see Def. 2.3); e.g., $x_s(s(\hat{t} + T)) = x_s(s(\hat{t}) + s_T) = x_s(s(\hat{t}))$ for some $\hat{t} \in [0, T)$.

Based on the methods we considered in the previous chapter, one might in light of the above remark wonder if there are any connections between such an s-parameterization and the reparameterizations utilized in Zhukovsky's stability notion. The short answer to this question is: no. Yet the observant reader might recall our previous claim that there are similarities between Zhukovsky's reparametrizations and the method we will utilize to solve the orbital stabilization problem. So what is this connection, if not through the s-parameterization? To answer this, let us recall something previously stated in Chapter 3. Namely, that parameterizations of the form (4.5) also help facilitate the construction of a *projection operator*, $x \mapsto p(x) \in \mathcal{S}$, for the orbit. It is in fact these operators which make our approach conceptually similar to Zhukovsky's reparametrizations, in the sense that it naturally aligns, in some sense, perturbed trajectories with the nominal one. This property is a vital part of our approach, as it can be used to both ensure the time-invariance of the designed control laws, to define different families of (excessive) transverse coordinates, as well as to construct time-invariant Lyapunov functions for the orbit. We therefore properly define and discuss the properties of such operators next.

4.3 Projection operators

We begin with a definition.

Definition 4.5 (Projection operator)**.** Let the orbit $\mathcal{O}$ be closed (i.e. trivial or periodic) and denote by $x_s : \mathcal{S} \to \mathcal{O}$ an s-parameterization of $\mathcal{O}$. A $\mathcal{C}^1$-mapping $p : \mathfrak{X} \to \mathcal{S}$, which is well defined[1] within a neighborhood[2] $\mathfrak{X} \subset \mathbb{R}^n$ of $\mathcal{O}$, is said to be a *projection operator* with respect to $\mathcal{O}$ if it is a left inverse of $x_s(\cdot)$, that is $s = p(x_s(s))$ for all $s \in \mathcal{S}$. □

Remark 4.6. We will most often assume that p is of class $\mathcal{C}^2$ in this thesis.

Given a projection operator $p(\cdot)$ as by Definition 4.5, we will use $\mathcal{P} : \mathcal{S} \to \mathbb{R}^{1\times n}$ to denote its Jacobian matrix (i.e. the transpose of its gradient) evaluated along the orbit:

$$\mathcal{P}(s) := Dp(x_s(s)). \tag{4.8}$$

The main motivation for introducing such an operator is that it allows us to define a state projection $x_p : \mathfrak{X} \to \mathcal{O}$ onto $\mathcal{O}$, defined by the composition

$$x_p(x) := (x_s \circ p)(x). \tag{4.9}$$

Clearly, by the left-inverse property of $p(\cdot)$, the function $x_p(\cdot)$ is idempotent and thus satisfies the projection condition: $(x_p \circ x_p)(x) = x_p(x)$ for all $x \in \mathfrak{X}$. This, in turn, allows us to define the following *projected-distance* (or simply "error") function

$$e(x) := x - x_p(x), \tag{4.10}$$

which necessarily acts as a measure of the distance to the orbit within $\mathfrak{X}$. Indeed, its zero-level set evidently contains $\mathcal{O}$.

In the case of non-vanishing orbits, for example a periodic one as (4.6), the function $e_\perp = e(x)$ corresponds to what we will refer to as *excessive transverse coordinates* in this thesis, and which we will study in depth in Section 4.6 (see also (2.13)).

One can of course also consider (4.10) in the case of an equilibrium point. The following simple example shows how a projection operator then can trivially be defined together with an s-parameterization.

Example 4.1. Let $\mathcal{O}_e$ be a trivial orbit consisting of a single, isolated equilibrium point $x_e \in \mathbb{R}^n$, i.e. $\mathcal{O}_e = \{x_e\}$ and $f(x_e) = \mathbf{0}_{n\times 1}$. In this case,

[1] By well defined, it is meant that $p(x)$ has a unique value for all x in $\mathfrak{X}$.

[2] We refer to an open, connected set (a *domain*) $\mathcal{N} \subset \mathbb{R}^n$ containing a compact, connected set $\mathcal{O} \subset \mathbb{R}^n$ as a *neighborhood* of $\mathcal{O}$.

it is evident that $x_p(x) = x_e$ regardless of $x_s(\cdot)$ and $p(\cdot)$, which must be of the form $\{s_e\} \ni s \mapsto x_s(s) = s\mathcal{F}$ and $p(x) = s_e$ for some scalar $s_e \in \mathbb{R}$ and non-zero vector $\mathcal{F} \in \mathbb{R}^n$, satisfying $s_e\mathcal{F} = x_e$. Since

$$\dot{e} = f(e + x_p) + B(e + x_p)u$$

describes the time evolution of the function $e = x - x_p(x)$, it follows that

$$\dot{\boldsymbol{\delta}}_e = Df(x_e)\boldsymbol{\delta}_e + B(x_e)u,$$

describes the evolution of the first-order components of e about the origin. That is, the above linear, time-invariant system is the linearization of the dynamics of e "along" $\mathcal{O}$, which, since the orbit is trivial, is equivalent to the regular Jacobian linearization of (4.1) about x_e.

Relation to moving Poincaré sections and reparametrizations à la Zhukovsky

As previously stated, the purpose of a projection operator is simple: Within some tubular neighborhood, it allows one to project the current states onto the nominal orbit and consequently define some measure of distance to it. Consider, for instance, the set

$$\Pi(s) := \{x \in \mathfrak{X} : \; p(x) = s\}. \tag{4.11}$$

It contains all the states in the neighborhood $\mathfrak{X}$ of $\mathcal{O}$ which are mapped to some particular point $s \in \mathcal{S}$. As illustrated in Figure 4.1, in the case of a non-vanishing orbit, this set is a $(n-1)$-dimensional hypersurface, whose geometry is clearly dependent on the choice of $p(\cdot)$. This surface corresponds to a *moving Poincaré section* as we briefly discussed in Section 2.4.2 (see also [54, 55]). Indeed, it moves along with the orbit's flow and is everywhere locally transverse to it, with $\mathcal{P}^{\mathsf{T}}(s)$ the normal vector to its tangent space at $x_s(s)$, which we denote by $\mathbf{T}\Pi(s)$.

In order to further illustrate this transversality property in the case of non-vanishing orbits, we notice that, by the left-inverse property of a projection operator, i.e. $p(x_s(s)) = s$, the chain rule implies

$$\frac{d}{ds}p(x_s(s)) = \mathcal{P}(s)\mathcal{F}(s) = \frac{d}{ds}s = 1. \tag{4.12}$$

This does not mean that $\mathcal{P}^{\mathsf{T}}(s)$ is necessarily in the span of $\mathcal{F}(s)$. Rather, as the following simple statement demonstrates, it just implies that $\mathcal{P}$ must be a left inverse of $\mathcal{F}$.

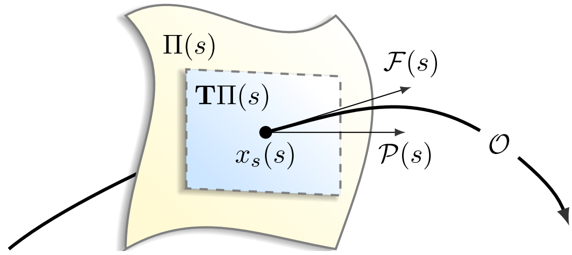

Figure 4.1: Illustration of the moving Poincaré section $\Pi(s)$. Its tangent space, $\mathbf{T}\Pi(s)$, at $x_s(s)$ corresponds to the blue-shaded region which is orthogonal to $\mathcal{P}^{\mathsf{T}}(s)$.

Claim 4.7. *Denote by $\theta(s) \in (-\frac{\pi}{2}, \frac{\pi}{2})$ the angle between $\mathcal{P}^{\mathsf{T}}(s)$ and $\mathcal{F}(s)$ in their common plane. Then there exists a $\mathcal{C}^0$ vector-valued function $q_\perp^{\mathsf{T}} : \mathcal{S} \to \mathbb{R}^n$ of unit length, satisfying $q_\perp(s)\mathcal{F}(s) \equiv 0$ for all $s \in \mathcal{S}$, such that*

$$\mathcal{P}(s) = \frac{\mathcal{F}^{\mathsf{T}}(s)}{\|\mathcal{F}(s)\|^2} + \tan(\theta(s))\frac{q_\perp(s)}{\|\mathcal{F}(s)\|}. \tag{4.13}$$

Proof. There always exist continuous, scalar functions $a(s)$ and $b(s)$ allowing us to factorize $\mathcal{P}$ as follows: $\mathcal{P}(s) = a(s)\frac{\mathcal{F}^{\mathsf{T}}(s)}{\|\mathcal{F}(s)\|} + b(s)q_\perp(s)$. By (4.12) we have $\mathcal{P}\mathcal{F} = \|\mathcal{P}\|\|\mathcal{F}\|\cos(\theta) = 1$, implying that $a(s) = 1/\|\mathcal{F}(s)\|$. Thus $\|\mathcal{P}(s))\|^2 = 1/\|\mathcal{F}(s)\|^2 + b^2(s) = 1/\left(\|\mathcal{F}(s)\|^2\cos(\theta(s)\right)$. Solving for $b(\cdot)$, one finds $b^2(s) = \frac{1-\cos^2(\theta(s))}{\cos^2(\theta(s))\|\mathcal{F}(s)\|^2}$, such that one can take $b(s) = \tan(\theta(s))/\|\mathcal{F}(s)\|$. □

Let us now also briefly comment upon the aforementioned similarities between the use of projection operators and the reparameterization used in the definition of Zhukovsky stability (see Def. 2.3). Recall that Zhukovsky's stability notion utilizes parameterizations to "align" perturbed trajectories in space, as to avoid their possible divergence in time. More technically, following the methods we considered in sections 2.4.2-2.4.3, this amounts to finding a homeomorphism $\tau : \mathbb{R}_{\geq 0} \to \mathbb{R}_{\geq 0}$ such that, for any perturbed trajectory $x(\cdot)$ lying close to $\mathcal{O}$, the function $(x \circ \tau)(\cdot)$ at some time $t \geq 0$ lies on some hypersurface Π_t (locally) transverse to $x_\star(t)$. Now, if such a function $\tau(\cdot)$ is known, then we also know the surface (the moving Poincaré section) $\Pi_{(\cdot)}$. Thus we may view the above from an equivalent, yet slightly different perspective: For some point x lying close to $\mathcal{O}$, if we can determine to which section $\Pi_{(\cdot)}$ it belongs, then we can determine the corresponding point on $\mathcal{O}$, or equivalently the corresponding "nominal time instant" $t \in [0, T)$. For example, if $x(t_1) \in \Pi_{t_2}$, with $t_1 \geq 0$ and $t_2 \in [0, T)$, then one should take $x_\star(t_2)$. Notice that this is in fact what a projection operator does: it retrieves the corresponding "nominal time instant" (for some time-scaled curve parameter) for all points lying close to $\mathcal{O}$. This has, for the purpose of control design, the benefit that it allows one to define the aforementioned distance measure, further allowing for the design of time-invariant orbitally-stabilizing feedback controllers. Indeed, such a feedback, if found, then results in an autonomous closed-loop system which admits the desired periodic solution as an asymptotically stable limit cycle.

Note, however, that there are certain limitations to such a scheme in the general case. The perhaps most clear example of this are orbits which returns to points arbitrarily close to itself, such as invariant tori (see, e.g., the example in [79]). The concept of projection operators may nevertheless still be utilized in the synthesis of an orbitally-stabilizing feedback, but since this only results in orbitally stable solutions upon the nominal orbit, which may *not* be Zhukovsky stable, convergence can only be ensured to some arbitrary point upon the orbit. This issue may partly be remedied, though, by allowing the projection operator to have memory (making it dynamic), by essentially moving its codomain as solutions evolve along the orbit.

Some statements for finding and computing projection operators

For a pair of points $a, b \in \mathbb{R}^n$, recall the line-segment notation: $\mathfrak{L}(a, b) := \{a + (b - a)\iota,\ \iota \in [0, 1]\}$. In regard to finding a projection operator for a given non-vanishing orbit, we provide the following preliminary statement:

Lemma 4.8. *Suppose there exists a $\mathcal{C}^k$ function $h : \mathbb{R}^n \times \mathcal{S} \to \mathbb{R}$ which for all $s \in \mathcal{S}$ satisfies*

$$h(x_s(s), s) \equiv 0 \quad \textit{and} \quad \frac{\partial h}{\partial s}(x, s)\bigg|_{x=x_s(s)} \neq 0. \tag{4.14}$$

Then, within a sufficiently small tubular neighborhood $\mathfrak{X} \subset \mathbb{R}^n$ of the orbit $\mathcal{O}$, there exists a unique $\mathcal{C}^k$ mapping $p : \mathfrak{X} \to \mathcal{S}$ such that

$$h(x, p(x)) = 0 \quad \textit{and} \quad \mathfrak{L}(x, x_p(x) \subset \mathfrak{X}$$

both hold for all $x \in \mathfrak{X}$, with $Dp(x) = \left[-\left(\frac{\partial h}{\partial s}(x, s)\right)^{-1} \frac{\partial h}{\partial x}(x, s)\right]\Big|_{s=p(x)}$ therein.

Proof. The statement is essentially just a reformulation of the implicit function theorem [160, 161]. The hypothesis of the lemma ensure that for each point $y \in \mathcal{O}$, there is an open neighborhood of y within which a unique $\mathcal{C}^k$-smooth solution exists. For $\mathfrak{X}$ taken sufficiently small, the requirement $\mathfrak{L}(x, x_p(x) \subset \mathfrak{X}$ therefore ensures the uniqueness of p within $\mathfrak{X}$. □

It follows that if a function $h(\cdot)$ satisfying the conditions of Lemma 4.8 is known, then one can, for $x \in \mathfrak{X}$, take $p(x)$ as the projection of the system's states onto $\mathcal{S}$. From this lemma we can also obtain the following statement (see also ([22, 45]), which for non-vanishing orbits provides a large family of such operators.

Proposition 4.9. *Let the smooth matrix-valued function $\Lambda : \mathcal{S} \to \mathbb{M}^n_{\succeq 0}$ be such that $\mathfrak{h}(s) := \Lambda(s)\mathcal{F}(s)$ is of class $\mathcal{C}^r$ on $\mathcal{S}$, and $\mathcal{F}^\mathsf{T}(s)\Lambda(s)\mathcal{F}(s) > 0$ holds for all $s \in \mathcal{S}$ Then there is an $\epsilon > 0$ and a neighborhood $\mathfrak{X} \subset \mathbb{R}^n$ of $\mathcal{O}$, with $\mathcal{B}_\epsilon(x_s(s)) \subset \mathfrak{X}$ for all $s \in \mathcal{S}$, where*

$$p(x) = \underset{\substack{s\in\mathcal{S} \\ \mathfrak{L}(x_s(s),x)\subset\mathcal{B}_\epsilon(x_s(s))}}{\arg\min} \Big[(x - x_s(s))^\mathsf{T}\Lambda(s)(x - x_s(s))\Big] \tag{4.15}$$

has a unique solution, such that $p : \mathfrak{X} \to \mathcal{S}$ is a $\mathcal{C}^r$-smooth projection operator. Moreover, its Jacobian matrix is

$$Dp(x) = \frac{\mathcal{F}^\mathsf{T}(p)\Lambda(p) - e_\perp^\mathsf{T}\Lambda'(p)}{\mathcal{F}^\mathsf{T}(p)\Lambda(p)\mathcal{F}(p) + e_\perp^\mathsf{T}\left[\frac{1}{2}\Lambda''(p)e_\perp - 2\Lambda'(p)\mathcal{F}(p) - \Lambda(p)\mathcal{F}'(p)\right]} \tag{4.16}$$

where $p = p(x)$ and $e_\perp = x - x_s(p(x))$, such that

$$\mathcal{P}(s) := Dp(x_\star(s)) = \frac{\mathcal{F}^\mathsf{T}(s)\Lambda(s)}{\mathcal{F}^\mathsf{T}(s)\Lambda(s)\mathcal{F}(s)}. \tag{4.17}$$

Remark 4.10. For Λ constant and positive definite, the fact that such an $\mathcal{C}^r$ operator necessarily exists if $x_s(\cdot)$ is $\mathcal{C}^{r+1}$ is similar to the unique nearest point property of $\mathcal{O}$; see, e.g., [162, 163].

Proof. Differentiating the terms inside the brackets in (4.15) with respect to s, we obtain the function

$$J(x, s) := (x - x_s(s))^\mathsf{T}\left[\Lambda'(s)(x - x_s(s)) - 2\Lambda(s)\mathcal{F}(s)\right]. \tag{4.18}$$

Since $\Lambda(\cdot)$ is positive semidefinite, it follows that any $p(x)$ which satisfies $J(x, p(x)) \equiv 0$ corresponds to a local minima of (4.15) since

$$\frac{\partial}{\partial s}J(x, s)\big|_{x=x_s(s)} = 2\mathcal{F}^\mathsf{T}(s)\Lambda(s)\mathcal{F}(s) > 0,$$

which also implies the left-inverse property, i.e. $s \equiv p(x_s(s))$, is satisfied for all $s \in \mathcal{S}$. Moreover, it allows us to invoke Lemma 4.8, which, together with $\mathfrak{L}(x_s(s), x) \subset \mathcal{B}_\epsilon(x_s(s)) \subset \mathfrak{X}$, guarantees the existence of a unique (but generally local) solution $p(x)$, whose Jacobian is given by (4.16). $\square$

While similar operators have been proposed before, they are often limited to Λ being constant [53], and commonly also requiring it to be positive definite [22], thus guarantee the uniqueness of such an operator even without the condition $\mathfrak{L}(x_s(s), x) \in \mathfrak{X}$. To motivate the above, we thus provide a simple example where neither hold everywhere.

Example 4.2. For $x = \mathrm{col}(x_1, x_2)$, let us again consider the unit circle: $x_s(s) = \mathrm{col}(\sin(s), \cos(s))$ with $\mathcal{S} := [0, 2\pi)$ and $\mathcal{F}(s) = \mathrm{col}(\cos(s), -\sin(s))$. Let us take for this curve a projection operator as in Proposition 4.9 with $\Lambda(s) = \mathrm{diag}(\cos^2(s), \sin^2(s))$. Even though $\Lambda(\cdot)$ is not everywhere positive definite on $\mathcal{S}$, it does satisfy $\mathcal{F}^\mathsf{T}(s)\Lambda(s)\mathcal{F}(s) > 0$. We have

$$(x - x_s(s))^\mathsf{T}\Lambda(s)(x - x_s(s)) = (x_1 - \sin(s))^2\cos^2(s) + (x_2 - \cos(s))^2\sin^2(s).$$

While the functions $J(x, s)$ is given by

$$\begin{aligned} J(x, s) =& \left[(x_2 - \cos(s))^2 - (x_1 - \sin(s))^2\right]\sin(s)\cos(s) \\ &+ 2\sin^3(s)(x_2 - \cos(s)) - 2\cos^3(s)(x_1 - \sin(s)). \end{aligned}$$

This shows that there is not a unique s such that $J(x, s) = 0$ if $x_1 = 0$ or $x_2 = 0$. Indeed, for $x_1 = 0$, both $s = 0$ and $s = \pi$ result in $J = 0$. However, by taking, say, $\mathfrak{X} = \{x \in \mathbb{R}^2 : \ \|x - x_s(s)\| < \epsilon, \ s \in \mathcal{S}\}$ for some $0 < \epsilon \ll 1$, the uniqueness of p taken according to (4.15) is guaranteed by the requirement that $\mathfrak{L}(x_s(s), x) \subset \mathfrak{X}$.

Some further comments on numerical methods and uniqueness

To apply most of the techniques we will propose in this thesis in practice, it is crucial that one is able to compute the projection operator online in real time. The complexity of this task will of course greatly depend upon the choice of operator; some times it can be computed directly from the state measurements (see, e.g., (3.21)), while other times it is implicitly defined, e.g. as in Proposition 4.9, thus requiring one to either solve an online optimization problem in real time or to use a dynamic approach as suggested in [22].

In the latter type of cases, the general way to solve the real-time optimization problem is to utilize some method built around either Newton's method or some quasi-Newton method [164]. To speed up convergence, one can also complement the optimization algorithm with a dynamic observer which provides initial conditions passed to the optimization solver.

Recently, another interesting two-step approach was proposed in [53] for projection operators of the form as in Proposition 4.9. By representing the

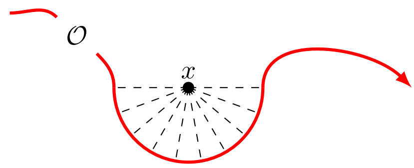

Figure 4.2: Illustrations of a singular point of an orthogonal projection operator.

curve $x_s(\cdot)$ as a B-spline of order N, with knots $\iota_0 \leq \iota_1 \leq \cdots \leq \iota_N$, one first finds the knot ι_j which results in the smallest value of (4.15) (or alternatively (4.18)). Then in the second step, one searches for the minimizer s of (4.18), but restricts the search to the interval $[\iota_{j-1}, \iota_{j+1}]$ (with $\iota_{0-1} = \iota_N$ and $\iota_{N+1} = \iota_0$). Here the latter step again requires some form of line search, with Brent's derivative-free method [165] suggested as an alternative in [53].

As previously stated in footnote 1, due to the assumed smoothness of the curve $x_s(\cdot)$, any projection operator as by Definition 4.5 will be well defined within some open neighborhood $\mathfrak{X}$ of $\mathcal{O}$, in the sense that it has a unique value which varies continuously with respect to the value of the states therein. However, in the case of a nontrivial periodic orbit, for each projection operator there must necessarily be at minimum one point in $\mathbb{R}^n$ at which its the value is not unique. For example, if the projection operator is taken as (4.15) with $\Lambda = \mathbf{I}_n$, that is $p(x) = \arg\min_{s\in\mathcal{S}} \|x - x_s(s)\|^2$, then singularities will occur at the centers of curvature along the orbit $\mathcal{O}$. This scenario is illustrated in Figure 4.2.

As was demonstrated in [166], there can be a remarkable difference in the size of the domain $\mathfrak{X}$ for different operators. Thus, in order to avoid sudden jumps in the projected value, ensuring a sufficiently large region $\mathfrak{X}$ should be among the key criteria used when deciding upon a projection operator.[3]

4.4 Transverse coordinates

It is the notion of so-called *excessive transverse coordinates*, or more generally the function $e = e(x)$ defined by (4.10), which will be our main focus both in this chapter as well as throughout the thesis. However, in order to both motivate the use of such coordinates and to highlight inherent structural similarities, we will in this section first introduce the notion of "regular" *transverse coordinates*, and demonstrate how they can be used to design orbitally stabilizing feedback controllers.

[3]Other key aspect which may be considered when choosing a projection operator in practice include structural simplicity, sensitivity to noise (e.g. its independence of estimated states), as well as how easy, fast and reliable it is to numerically compute.

As we saw in the previous section, we can—similarly to the moving coordinate systems we considered in sections 2.4.2 and 2.4.3—use projection operators to introduce transverse coordinates which continuously evolve upon- and spans Π along the whole orbit. Thus, as the name suggests, transverse coordinates are nothing more than (local) coordinates upon some moving Poincaré section (MPS), such that location of the MPS's origin and the transverse coordinates together constitute a local coordinate transformation. It is important to note that for the purpose of achieving orbital stabilization, one does not need to know this coordinate transformation exactly; all one needs to know is a projection operator, defining a MPS, and a function whose zero-level set locally provides an implicit representation of the orbit. It is this function we refer to as transverse coordinates.

Definition 4.11. A $\mathcal{C}^2$-smooth[4] vector-valued function $z_\perp : \mathbb{R}^n \to \mathbb{R}^{n-1}$ is a vector of *transverse coordinates* for a non-vanishing orbit $\mathcal{O}$ if $\|z_\perp(y)\| \equiv 0$ and $\operatorname{rank} Dz_\perp(y) = n-1$ for all $y \in \mathcal{O}$. □

Simply put, these conditions together ensure that there is some neighborhood of $\mathcal{N}$ of the orbit $\mathcal{O}$, such that the orbit can be defined by the zero-level set of $z_\perp(\cdot)$ evaluated therein. That is

$$\mathcal{O} = \{x \in \mathcal{N} : \ z_\perp(x) = 0\} \subseteq \{x \in \mathbb{R}^n : \ z_\perp(x) = 0\},$$

where the inclusion evidently can be replaced by an equality only if $\|z_\perp(y)\| = 0$ implies $y \in \mathcal{O}$. Since the magnitude of $z_\perp$ therefore provides some measure of the distance to the orbit, the characteristic local stability properties of the orbit $\mathcal{O}$ and the origin of $z_\perp(\cdot)$ are essentially equivalent inside $\mathcal{N}$.

Notice also that the above definition is made without any reference to a specific projection operator. This has an important implication: The MPS upon which these coordinates evolve can be different (even locally about a point on $\mathcal{O}$) to the MPS $\Pi(\cdot)$ induced by some arbitrary projection operator. Stated somewhat differently: a decrease in the magnitude of $z_\perp(x)$ for $x \in \mathcal{N}$ may not correspond to a decrease in the minimal distance (a geodesic) from x to $x_p(x)$ on $\Pi(p(x))$.

The fact that such transverse coordinates do not (necessarily) depend on the choice of projection operator, means that we can pair any p satisfying Definition 4.5 with any function $z_\perp$ satisfying Definition 4.11 to obtain a local coordinate transformation. As we will see later on, such a pairing may allow for the construction of time-invariant control laws that exponentially

[4]The requirement that the mapping is $\mathcal{C}^2$-smooth will be made more clear later in this sections when we will linearize the dynamics of $z_\perp$ along the orbit.

stabilize the origin (i.e., the zero value) of $z_\perp$, and thus necessarily provide a solution to Problem 4.1. This will normally require that $Dz_\perp(x)B(x)$ has full rank in a vicinity of the desired orbit (i.e. a vector relative degree–like condition).

Before we proceed to derive this coordinate transformation, it is important to remark that knowledge of a projection operator is not always needed to achieve orbital stabilization if one knows a vector of transverse coordinates. This is, for example, always the case when transverse feedback linearization [30, 146, 147] is applicable. It is also true in the case of the transverse coordinate $I(\cdot)$ utilized in the control law (3.19) considered in the Chapter 3. It was then claimed that this control law achieved asymptotically orbitally stable oscillations of the double integrator system in Example 3.2. The following statement, which is inspired by Fradkov's speed-gradient method [106], validates that claim.

Proposition 4.12. *Given some Lipschitz continuous mapping $f:\mathbb{R}\to\mathbb{R}$, let $w(t)=w(t+T)$, $T>0$, be a (bounded) periodic solution of the initial value problem*

$$\ddot{w}=f(w),\quad (w(0),\dot{w}(0))=(q_0,\dot{q}_0),\tag{4.19}$$

satisfying $|f(w(t))|^2+|\dot{w}(t)|^2>0$ for all $t\in[0,T)$. Then the scalar function $I=I(q,\dot{q})$, defined by

$$I:=\frac{1}{2}\dot{q}^2-\frac{1}{2}\dot{q}_0^2-\int_{q_0}^{q}f(\sigma)d\sigma,\tag{4.20}$$

is a transverse coordinate for the periodic orbit

$$\mathcal{O}:=\{(q,\dot{q})\in\mathbb{R}\times\mathbb{R}:\ (q,\dot{q})=(w(t),\dot{w}(t)),\ t\in[0,T)\}.$$

Moreover, taking in $u=u_I$, with

$$u_I:=f(q)-k_I\dot{q}I,\tag{4.21}$$

for some $k_I>0$, renders $q_*(t)=w(t)$ an asymptotically[5] orbitally stable solution of the scalar second-order system $\ddot{q}=u$, where $q,u\in\mathbb{R}$.

Remark 4.13. If, for instance, q belongs to $\mathbb{S}^1$ instead of $\mathbb{R}$, then there are certain periodic orbits which come in pairs, and $I(\cdot)$ is a transverse coordinate for both. For example, the orbits of both $w_+(t)=t \mod 2\pi$ and $w_-(t)=-t \mod 2\pi$ are locally orbitally stabilized by $u_I=-k_I\dot{q}(\dot{q}^2-1)$.

[5] We will see in the next section that the control law (4.21) is in fact exponentially orbitally stabilizing; see Example 4.4.

Proof. Let us first validate that $I(\cdot)$ is a transverse coordinate for the orbit $\mathcal{O}$. To this end, we first note that $\frac{d}{dt}\dot{w}^2 = 2\dot{w}\ddot{w} = \frac{d\dot{w}^2}{dw}\dot{w}$, from which we can infer the well-known relation $2\ddot{w} = \frac{d\dot{w}^2}{dw}$. Inserting this into (4.19) gives

$$\frac{1}{2}\frac{d}{dw}\dot{w}^2 = f(w).$$

Since this must hold along all solutions of the system, we can integrate both sides with respect to w to obtain that $\frac{1}{2}\dot{w}^2(t) - \frac{1}{2}\dot{w}^2(0) + \int_{w(0)}^{w(t)} f(\sigma)d\sigma \equiv 0$ must hold for all $t \geq 0$ along any solution $w(t)$ of (4.19). Hence $I(\cdot)$ vanishes on the orbit $\mathcal{O}$. Moreover, its Jacobian matrix $DI(q,\dot{q}) = [-f(q), \dot{q}]$ is everywhere orthogonal to the vector field $\mathrm{col}(\dot{q}, f(q))$ and has full rank on $\mathcal{O}$ since $\|DI\|^2 = |f(q)|^2 + |\dot{q}|^2$. Thus all the conditions in Definition 4.11 are met, and I is therefore a transverse coordinate. Moreover, $\mathrm{col}(\dot{q}, f(q))$ corresponds to the normal vector at any point upon the moving Poincaré section (which here is a curve in $\mathbb{R}^2$) to which $I(\cdot)$ belongs at a given time instant.

Now, if the controller is taken according to (4.21), straightforward computations show that $\dot{I} = -k_I\dot{q}^2 I$. Defining the $\mathcal{C}^1$ Lyapunov function candidate $V_I := \frac{1}{2}I^2$, we therefore obtain $\dot{V}_I = -k_I\dot{q}^2 I^2 \leq 0$, which is negative definite with respect to I as long as $|\dot{q}| \neq 0$. From the relation $|f(w(t))|^2 + |\dot{w}(t)|^2 > 0$ and the continuity of $f(\cdot)$, it follows that there exists some nonzero neighborhood of the orbit $\mathcal{O}$, within which $|\ddot{q}| > 0$ whenever $\dot{q} \equiv 0$. Indeed, if $\dot{q} \equiv 0$, then $\ddot{q} = f(q)$. Hence, by the Barbashin–Krasovskii–LaSalle invariance principle [167], we can conclude that the origin of the transverse coordinate I is locally asymptotically stable, which again implies that the orbit $\mathcal{O}$ is asymptotically stable. □

One might be tempted to apply the ideas in Proposition 4.12 to other types of orbits as well. Yet, as the following simple example demonstrates, the non-vanishing condition is essential for its applicability.

Example 4.3. Consider the following second-order system taken from [77]:

$$\ddot{w} = 2w - w^2.$$

This system admits a homoclinc orbit contained in the zero-level set of

$$I(w,\dot{w}) := \frac{1}{2}\dot{w}^2 + \frac{1}{3}w^3 - w^2,$$

shown by the bold, green line in Figure 4.3.[6] As is seen, the orbit both

[6]The phase portraits in Example 4.3 were generated using Pplane [168] in MATLAB.

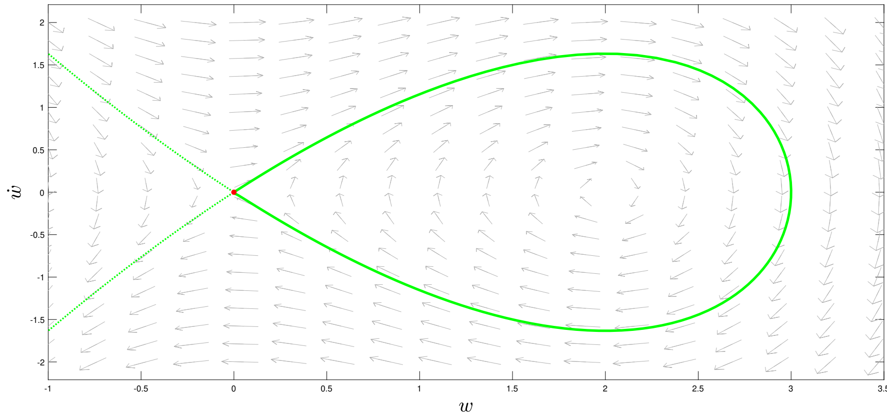

Figure 4.3: The homoclinic orbit considered in Example 4.3.

originates from- and eventually settles at the origin after looping around the center equilibrium point located at $(2, 0)$.

Since $DI(w, \dot{w}) = [w^2 - w, \dot{w}]$, the rank of the function $I(\cdot)$ is zero at the origin, meaning that it is not truly a transverse coordinate in the sense of Definition 4.11. More crucially, however, is the fact that some of the parts of its zero-level set lies outside of the homoclinic orbit, corresponding to the green, dashed lines in Figure 4.3. Thus it follows that, even though the control law (4.21) will ensure that all solution of $\ddot{q} = u_I$ starting inside the region enveloped by the orbit will asymptotically converge to it, there is necessarily a region of the phase plane where all solutions will diverge. To prove the existence of this unstable region, it suffices to note that u_I does not alter the saddle point located at the origin, and therefore the region simply corresponds to the eigenvector of the unstable eigenvalue of the linearization at this point.

One might, however, use similar ideas to that in Proposition 4.12 as to achieve orbital stabilization. For instance, to stabilize the homoclinic orbit, consider instead the function

$$\hat{I}(q, \dot{q}) := \frac{1}{2}\dot{q}^2 + \frac{1}{3}|q|^3 - \lceil q \rfloor^2$$

where $\lceil q \rfloor^\alpha = \mathrm{sgn}(q)\,|q|^\alpha$, and which crucially only vanishes on the orbit. As seen in Figure 4.4, one may then apply the locally Lipschitz control law,

$$\hat{u}_{\hat{I}} = 2|q| - \lceil q \rfloor^2 - k_{\hat{I}}\dot{q}\hat{I},$$

as to asymptotically stabilizes the orbit.

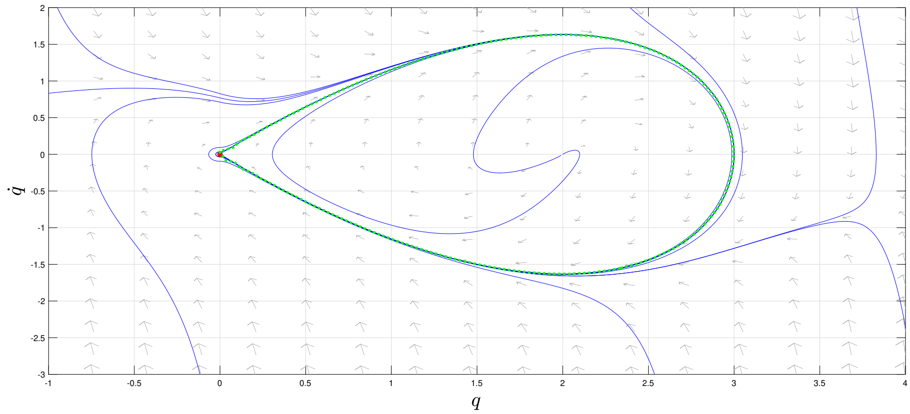

Figure 4.4: The homoclinic orbit considered in Example 4.3 stabilized by a non-smooth feedback.

4.4.1 Transverse linearization: a tool to assess exponential orbital stability

Similarly to what we saw in Section 2.4.2, the local exponential stability of a periodic orbit can be assessed from the stability of a *transverse linearization* [34, 41]. That is, the linearization of the dynamics of a vector of transverse coordinates along the nominal orbit. This makes a transverse linearizations a useful tool for the purpose of control design. Our aim now will therefore be to derive the transverse linearization associated with a vector-valued function, $z_\perp$, corresponding to a set of transverse coordinates.

To this end, we define

$$\mathcal{Z}_\perp(s) := Dz_\perp(x_s(s)), \tag{4.22}$$

which is the Jacobian matrix of the transverse coordinates evaluated along the orbit using the s-parameterization (see Assumption 4.3). As the following lemma shows, given any pairing of a projection operator as by Definition 4.5 and transverse coordinates as by Definition 4.11, they together constitute a valid set of local coordinates in a neighborhood of the orbit $\mathcal{O}$.

Lemma 4.14. *The mapping $x \mapsto (p(x), z_\perp(x))$ is a diffeomorphism in a vicinity of the orbit $\mathcal{O}$, with the elements of the Jacobian matrix of the inverse mapping $X : \mathcal{S} \times \mathbb{R}^{n-1} \to \mathbb{R}^n$, i.e. $x = X(p, z_\perp)$, evaluated at $x_s(s) \in \mathcal{O}$ given by*

$$\left.\frac{\partial X}{\partial p}\right|_{x=x_s(s)} = \mathcal{F}(s), \quad \left.\frac{\partial X}{\partial z_\perp}\right|_{x=x_s(s)} = (\mathbf{I}_n - \mathcal{F}(s)\mathcal{P}(s))\, \mathcal{Z}_\perp^\dagger(s). \tag{4.23}$$

Proof. Recall that the Jacobian of a projection operator evaluated along the orbit must satisfy $\mathcal{P}(s)\mathcal{F}(s) = 1$ for all $s \in \mathcal{S}$, whereas the Jacobian matrix, $\mathcal{Z}_\perp(s)$, of the transverse coordinates has full rank and must satisfy $\mathcal{Z}_\perp(s)\mathcal{F}(s) = \mathbf{0}_{n-1\times 1}$ as $\|z_\perp(x_s(s))\| = 0$. Thus the Jacobian matrix of the mapping $x \mapsto (p(x), z_\perp(x))$ evaluated at $x_s(s)$, given by

$$DX^{-1}(x_s(s)) = \begin{bmatrix} \mathcal{P}(s) \\ \mathcal{Z}_\perp(s) \end{bmatrix},$$

is nonsingular for all $s \in \mathcal{S}$. Now note that, for all $s \in \mathcal{S}$, the following relation holds:

$$\begin{bmatrix} \mathcal{P}(s) \\ \mathcal{Z}_\perp s \end{bmatrix} \begin{bmatrix} \mathcal{F}(s) & (\mathbf{I}_n - \mathcal{F}(s)\mathcal{P}(s))\, \mathcal{Z}_\perp^\dagger(s) \end{bmatrix} = \mathbf{I}_n.$$

Hence, by the inverse function theorem [160], the elements in (4.23) correspond to the Jacobian matrix of the inverse mapping at this point, and hence $x \mapsto (p(x), z_\perp(x))$ is a local diffeomorphism in a vicinity of $\mathcal{O}$. $\square$

Using this lemma, we may in turn derive the following statement, which shows the possibility of locally expanding certain functions in terms of some transverse coordinates:

Lemma 4.15. *A function $\phi : \mathbb{R}^n \to \mathbb{R}$, which is $\mathcal{C}^2$ in a neighborhood $\mathcal{N}$ of $\mathcal{O}$, can, in a vicinity of $\mathcal{O}$, be written in the form*

$$\phi(x) = \phi(x_p) + D\phi(x_p)(\mathbf{I}_n - \mathcal{F}(p)\mathcal{P}(p))\mathcal{Z}_\perp^\dagger(p)z_\perp(x) + O(\|z_\perp(x)\|^2), \quad (4.24)$$

where $x_p = x_p(x)$ and $p = p(x)$. Moreover, if $\phi(y) = 0$ for all $y \in \mathcal{O}$, then

$$\phi(x) = D\phi(x_p)\mathcal{Z}_\perp^\dagger(p)z_\perp(x) + O(\|z_\perp(x)\|^2). \quad (4.25)$$

Proof. Consider a point $q \in \mathcal{O}$, which in $(p, z_\perp)$-coordinates can be written as $q = X(\hat{s}, 0)$ for $\hat{s} = p(q) \in \mathcal{S}$. For each such point q, we can, at least inside a subset $\mathfrak{x}$ of $\mathfrak{X}$ containing $\mathcal{O}$, associate with it a set as in (4.11); namely $\Pi(\hat{s}) := \{x \in \mathfrak{x} : \; p(x) = \hat{s}\}$, where $\hat{s}$ satisfies $x_s(\hat{s}) \equiv q$, and with $\hat{\mathfrak{X}}$ such that, for any $x \in \hat{\mathfrak{X}}$ and all $\iota \in [0, 1]$, $\big(x + \iota\big[x_p(x) - x\big]\big) \subset \hat{\mathfrak{X}}$; i.e., all points on the line segment connecting $x \in \hat{\mathfrak{X}}$ and $x_p(x)$ lie within $\hat{\mathfrak{X}}$.

Now, since $x = X(p, z_\perp)$ is a local diffeomorphism and $\phi \in \mathcal{C}^2(\mathbb{R}^n, \mathbb{R})$, it follows from Taylor's theorem (see, e.g., [160, Thm. 2.1.33]) that we can expand and rewrite the function in terms of p and $z_\perp$ for any x upon some subset of $\Pi(\hat{s})$; that is, as $X(p, z_\perp) \to q$, we may write

$$\begin{aligned}\phi(x) =&\phi(x_p(x)) + D\phi(x_p(x))\frac{\partial X}{\partial z_\perp}\bigg|_{x=x_p(x)}(z_\perp(x) - z_\perp(q))\\ &+ D\phi(x_p(x))\frac{\partial X}{\partial p}\bigg|_{x=x_p(x)}(p(x) - \hat{s}) + O(\|X(p, z_\perp) - q\|^2).\end{aligned}$$

Since $z_\perp(q) = 0$ and $p(x) = \hat{s}$ for $x \in \Pi(\hat{s})$, this reduces to (4.24) using (4.23), while (4.25) is then implied by $\|D\phi(x_s(s))\mathcal{F}(s)\| = 0$. The statement then follows from the fact that this can readily be done for any $q \in \mathcal{O}$ and all x within a tubular neighborhood of the orbit where the diffeomorphism $x \mapsto (p(x), z_\perp(x))$ is well defined, due to the continuity of $\phi(\cdot)$, $p(\cdot)$ and $z_\perp(\cdot)$ therein. □

Notice here that, except for the computation of $x_p = x_s(p(x))$, the expression (4.25) for a function which vanishes on the orbit is independent of the projection operator. This is not too surprising, as if the rank of the gradient of the function ϕ evaluated along the orbit is everywhere equal to one, then ϕ would itself constitute a single transverse coordinate and hence must be independent of the choice of projection operator.[7] As a consequence, there is an equivalence between the local stability properties of all vectors of transverse coordinates as by Definition 4.11, in the sense that, given any two such vector-valued functions $y_\perp, z_\perp \in \mathbb{R}^{n-1}$, with $\mathcal{Y}_\perp(s) := Dy_\perp(x_s(s))$ and $\mathcal{Z}_\perp(s) := Dz_\perp(x_s(s))$, we can locally expand one in terms of the other to obtain:

$$y_\perp(x) = \mathcal{Y}_\perp(p(x))\mathcal{Z}_\perp^\dagger(p(x))z_\perp(x) + O(\|z_\perp(x)\|^2).$$

Hence, the first-order variations of these coordinates in a vicinity of $\mathcal{O}$ must satisfy

$$\boldsymbol{\delta}_{y_\perp} = \mathcal{Y}_\perp(s)\mathcal{Z}_\perp^\dagger(s)\boldsymbol{\delta}_{z_\perp},$$

with $s = s(t)$ and where the $(n-1)\times(n-1)$ matrix function $\mathcal{Y}_\perp(s)\mathcal{Z}_\perp^\dagger(s)$ is nonsingular for all $s \in \mathcal{S}$ as $\mathcal{F}(s)$ spans the nullspaces of both of the full-rank matrices $\mathcal{Y}_\perp(s)$ and $\mathcal{Z}_\perp(s)$.

[7] One may, however, define transverse coordinates which are indirectly dependent upon the choice of projection operator. That is, a mapping $y_\perp : \mathcal{S}\times\mathbb{R}^n \to \mathbb{R}^{n-1}$, such that $y_\perp(x) = y_\perp(p(x), x)$ is a vector of transverse coordinates for any $p(\cdot)$, and $D_s y_\perp(s, x) := \frac{\partial}{\partial s}y_\perp(s, x)$ satisfies $\|D_s y_\perp(s, x_s(s))\| \neq 0$ for all $s \in \mathcal{S}$, defines a family of *projection operator–based* transverse coordinates; see [70] for further details.

The "out-of-phase" convergence property

Recall that orbital stabilization does not guarantee that the system's states will converge to the orbit $\mathcal{O}$ in phase with the nominal solution $x_\star(t)$. Let us quickly demonstrate that this is indeed the case using the above statement.

Given a projection operator $p(\cdot)$ and transverse coordinates $z_\perp$, define

$$\psi(t) := \int_0^t (\dot{p}(x(\sigma)) - (\rho \circ p)(x(\sigma)))d\sigma. \tag{4.26}$$

In order to then derive the well-known phase-shift property of orbital stability, we can utilize Lemma 4.15 to write the dynamics of ψ in a vicinity of $\mathcal{O}$:

$$\dot{\psi} = Df_{\|}(x_p(x))z_\perp + Dp(x)B(x)u + O(\|z_\perp\|^2). \tag{4.27}$$

Here $f_{\|}(x) := Dp(x)f(x)$. From this, it is clear that $\dot{p} = \rho(p)$ whenever $z_\perp = u \equiv 0$ as expected, even though the system's states will generally not be in phase with the nominal solution after converging to the orbit.

Transverse linearization

Given a vector of transverse coordinates, $z_\perp$, consider now the corresponding *transverse dynamics* obtained from (4.1) using the chain rule:

$$\dot{z}_\perp = Dz_\perp(x)\left[f(x) + B(x)u\right].$$

Since here $\|Dz_\perp(y)f(y)\| = 0$ for all $y \in \mathcal{O}$, the transverse dynamics can be equivalently rewritten in small vicinity of the orbit $\mathcal{O}$ using Lemma 4.15 as

$$\dot{z}_\perp = Df_\perp(x_p(x))\mathcal{Z}_\perp^\dagger(p(x))z_\perp + Dz_\perp(x)B(x)u + O(\|z_\perp\|^2), \tag{4.28}$$

where $f_\perp(x) := Dz_\perp(x)f(x)$. From this, the transverse linearization—the first-order approximation (variational system) of the transverse dynamics along $\mathcal{O}$—can be readily obtained:

$$\dot{\boldsymbol{\delta}}_{z_\perp} = \mathcal{A}_\perp(s)\boldsymbol{\delta}_{z_\perp} + \mathcal{B}_\perp(s)u, \tag{4.29}$$

with $s = s(t)$ a solution to $\dot{s} = \rho(s)$ and where

$$\mathcal{A}_\perp(s) := Df_\perp(x_s(s))\mathcal{Z}_\perp^\dagger(s) \quad \text{and} \quad \mathcal{B}_\perp(s) := \mathcal{Z}_\perp(s)B(x_s(s)). \tag{4.30}$$

As previously stated, we can use this system to assess the exponential stabilizability of the orbit $\mathcal{O}$. Indeed, the following statement, corresponding to Part (a) of Theorem 12 in [31], confirms this fact (see also [41, 57]).

Theorem 4.16. *The periodic orbit $\mathcal{O}$, defined in* (4.6), *is exponentially stabilizable for* (4.1) *if, and only if, the linear, T-periodic system* (4.29) *is stabilizable.* □

A quadratic-like Lyapunov function for assessing exponential orbital stability

Although Theorem 4.16 allows one to determine from the transverse linearization (4.29) if one can exponentially stabilize a periodic orbit corresponding to Assumption 4.3 for (4.1) (and vice versa), it does not tell one how to directly use (4.29) to design an orbitally stabilizing feedback for (4.29). We will therefore show next that if the following assumption holds, then it is straightforward to design such a control law using projection operators.

Assumption 4.17. A continuous matrix-valued function $K_\perp : \mathcal{S} \to \mathbb{R}^{m\times n-1}$, satisfying $K_\perp(0) \equiv K_\perp(s_T)$, is known, which is such that the zero solution of (4.29) is rendered asymptotically stable under $u = K_\perp(s)\boldsymbol{\delta}_{z_\perp}$.

Using that $\dot{s} = \rho(s) > 0$ (see (4.4)), we immediately obtain the following statement, which can be useful for finding such a feedback $K_\perp$.

Corollary 4.18. *The origin of the linear, T-periodic system* (4.29) *is asymptotically stable under $u = K_\perp(s(t))\boldsymbol{\delta}_{z_\perp}$ for some continuous $K_\perp : \mathcal{S} \to \mathbb{R}^{m\times n-1}$, if, and only if, the point $\hat{z} = 0$ of the linear, s_T-periodic system*

$$\frac{d}{d\tau}\hat{z} = \frac{1}{\rho(\bar{\tau})}\Big[Df_\perp(x_s(\bar{\tau}))\mathcal{Z}_\perp^\dagger(\bar{\tau}) + \mathcal{Z}_\perp(\bar{\tau})B(x_s(\bar{\tau}))K_\perp(\bar{\tau})\Big]\hat{z}, \tag{4.31}$$

where $\bar{\tau} := \tau \mod s_T$, is asymptotically stable.

Remark 4.19. Note that in light of Remark 4.4, we have here utilized $\bar{\tau} := \tau \mod s_T$ to both highlight the s_T-periodicity of the right-hand side of (4.31) and to avoid abuse of notation. However, as one only needs to evaluate the right-hand side over the interval $[0, s_T)$ in order to assess the stability due to the s_T-periodicity, we will just utilize s instead of τ and $\bar{\tau}$ when encountering similar scenarios throughout the remainder of this thesis.

In [31] (see Part (b) of Theorem 12) it was shown that if Assumption 4.17 holds, then the control law $u = K_\perp(p(x))z_\perp(x)$, with $p(\cdot)$ some projection operator as by Definition 4.5, renders the periodic orbit $\mathcal{O}$ exponentially stable with respect to (4.1). However, the proof given in [31] utilizes Proposition 1.5 in [41], which assumes that the right-hand side of the closed-loop system is ($\mathcal{C}^1$-) smooth. Thus, while the additional requirements that $B(\cdot)$ and $K_\perp(\cdot)$ were differentiable would be sufficient to apply similar arguments to those in [41], such arguments are not directly applicable when assuming just continuity of $K_\perp(\cdot)$ on $\mathcal{S}$. Hence, for the sake of completeness, we will here provide an alternative route towards such a proof.

To this end, we assume that Assumption 4.17 holds and denote

$$\mathcal{A}_{cl}(s) := \mathcal{A}_\perp(s) + \mathcal{B}_\perp(s)K_\perp(s).$$

Recall from Proposition 2.18 (see also [41, 100]) that the asymptotic stability of (4.29) is equivalent to the existence of some $\mathcal{C}^1$-smooth, positive definite, T-periodic matrix function $L(t) = \mathcal{L}_\perp(s(t)$, satisfying

$$\mathcal{L}'_\perp(s(t))\rho(s(t)) = -\mathcal{A}_{cl}^\mathsf{T}(s(t))\mathcal{L}_\perp(s(t)) - \mathcal{L}_\perp(s(t))\mathcal{A}_{cl}(s(t)) - \mathcal{Q}_\perp(s(t)), \tag{4.32}$$

with $\mathcal{Q}_\perp : \mathcal{S} \to \mathbb{M}_{\succ 0}^{n-1}$ continuous and T-periodic. As the following statement demonstrates, this in fact implies the existence of a (local) strict Lyapunov function for the orbit with respect to (4.1), given a particular choice of projection operator (see also [41]).

Lemma 4.20. *Let Assumption 4.17 hold, and suppose the control law for* (4.1) *is taken as* $u = K_\perp(p(x))z_\perp(x)$ *for some projection operator* $p(\cdot)$ *as by Definition 4.5. Then for any matrix function* $\mathcal{Q}_\perp \in \mathcal{C}^0(\mathcal{S}, \mathbb{M}_{\succ 0}^{n-1})$*, satisfying* $\mathcal{Q}_\perp(0) \equiv \mathcal{Q}_\perp(s_T)$*, there is a unique matrix-valued function* $\mathcal{L}_\perp \in \mathcal{C}^1(\mathcal{S}, \mathbb{M}_{\succ 0}^{n-1})$ *that solves* (4.32) *for all* $s \in \mathcal{S}$*. Moreover, the function*

$$\mathcal{V}_\perp(x) = z_\perp^\mathsf{T}(x)\mathcal{L}_\perp(p(x))z_\perp(x) \tag{4.33}$$

is a local Lyapunov function for the orbit $\mathcal{O}$ *with respect to the closed-loop system* (4.1)*, in the sense that there exist numbers* $\mu, \nu \in \mathbb{R}_{>0}$*, such that* $\mathcal{V}_\perp(x) > 0$ *and* $\dot{\mathcal{V}}_\perp(x) < -\mu\mathcal{V}_\perp(x)$ *for all* $x \in \{x \in \mathfrak{X} : \ \mathcal{V}_\perp(x) < \nu\} \setminus \mathcal{O}$.

Proof. The existence and uniqueness of $\mathcal{L}_\perp$ is well known (see, e.g., Proposition 2.18 or [41, 100]). Moreover, the fact that there is some tubular neighborhood of $\mathcal{O}$, within which the locally positive semidefinite function $\mathcal{V}_\perp$ satisfies $\mathcal{V}_\perp > 0$, follows immediately from the definition of transverse coordinates (see Def. 4.11) and that $\mathcal{L}_\perp$ is positive definite.

To show that $\dot{\mathcal{V}}_\perp < -\mu\mathcal{V}$ also holds within such a neighborhood, we first note from (4.27) that $\dot{p} = \rho(p) + O(\|z_\perp\|)$, such that the time derivative of $\mathcal{V}_\perp$ is of the form

$$\dot{\mathcal{V}}_\perp(x) = -z_\perp^\mathsf{T}\mathcal{Q}_\perp(p)z_\perp + 2z_\perp^\mathsf{T}\mathcal{L}_\perp(p)\tilde{\mathcal{B}}_\perp(x)K_\perp(p(x))z_\perp(x) + O(\|z_\perp\|^3).$$

Here $\left\|\tilde{\mathcal{B}}_\perp(x)\right\| \leq l_B \|x - x_p(x)\|$ for some $l_B > 0$ holds in a vicinity of $\mathcal{O}$ since the columns of $B(\cdot)$ are locally Lipschitz. Moreover, as $\|x - x_p(x)\|$ is $O(\|z_\perp\|)$ by Lemma 4.15, we have $\dot{\mathcal{V}}_\perp(x) = -z_\perp^\mathsf{T}\mathcal{Q}_\perp(p)z_\perp + O(\|z_\perp\|^3)$. Hence, by standard arguments, there exist $\mu, \upsilon \in \mathbb{R}_{>0}$, such that $\dot{\mathcal{V}}_\perp(x) < -\mu\mathcal{V}_\perp(x)$ for all $x \notin \mathcal{O}$ satisfying $\|\mathcal{V}_\perp(x)\| < \upsilon$. This concludes the proof. $\square$

Remark 4.21. We will use this statement in Chapter 8.4.4 to design a robustifying feedback extension to compensate for any matched uncertainties and disturbances using a Lyapunov redesign technique.

From Lemma 4.20, the following statement, corresponding to Part (b) of Theorem 12 in [31], is readily obtained:

Theorem 4.22. *Let Assumption 4.17 hold. Then, given any projection operator* $p(\cdot)$ *as by Definition 4.5, the control law*

$$u = K_\perp(p(x))z_\perp(x) \tag{4.34}$$

exponentially stabilizes the orbit $\mathcal{O}$ *for* (4.1). □

Proof. By Lemma 4.20, there exist $\mu, \nu \in \mathbb{R}_{>0}$ such that $\dot{\mathcal{V}}_\perp(x) < -\mu\mathcal{V}_\perp(x)$ for all $x \notin \mathcal{O}$ satisfying $\mathcal{V}_\perp(x) < \nu$, with $\mathcal{V}_\perp$ defined in (4.33). The exponential stability of $\mathcal{O}$ can then be concluded using the comparison principle [169]. Indeed, let $v(t) := \mathcal{V}_\perp(x(t))$ such that $v(t) \leq v(t_0)e^{-\mu(t-t_0)}$ if $v(t_0) < \nu$ by the Comparison Lemma [44, Lemma 3.4]. From the definition of $\mathcal{V}_\perp$, this, in turn, implies the existence of $\bar{\mu}, \bar{\nu} \in \mathbb{R}_{>0}$, such that $\|z_\perp(x(t))\| \leq \|z_\perp(x(t_0))\| \, e^{-\bar{\mu}(t-t_0)}$ for all $t \geq t_0$ if $\|z_\perp(x(t_0))\| < \bar{\nu}$. Since an orthogonal projection $x_{p_o}(x)$ onto $\mathcal{O}$ is $O(\|z_\perp\|)$ by Lemma 4.15, together with the fact that $\mathrm{dist}(\mathcal{O}, x(t)) \equiv \|x(t) - x_{p_o}(x(t))\|$ within a sufficiently small tubular neighborhood of $\mathcal{O}$, the exponential stability of $\mathcal{O}$ (cf. Def. 2.2) thus follows. □

Example 4.4. We can use the transverse linearization to determine that the control law (4.21) in Proposition 4.12 is not only asymptotically stabilizing, but in fact is exponentially orbitally stabilizing. To this end, recall from the proof of Proposition 4.12 that $f_\perp(q, \dot{q}) = -k_I\dot{q}^2 I$, and hence

$$Df_\perp(q_\star(t), \dot{q}_\star(t)) = -k_I\dot{q}_\star^2(t)DI(q_\star(t), \dot{q}_\star(t))$$

as $I(q_\star(t), \dot{q}_\star(t)) \equiv 0$. Using (4.29), the transverse linearization is then found to be

$$\frac{d}{dt}\boldsymbol{\delta}_I = -k_I\dot{q}_\star^2(t)\boldsymbol{\delta}_I.$$

Since the nominal solution $q_\star(t) = w(t)$ is periodic and satisfies $|f(q_\star(t))|^2 + |\dot{q}_\star(t)|^2 > 0$, the characteristic exponent, given by $\frac{1}{T}\int_0^T(-k_I\dot{q}_\star^2(\sigma))d\sigma$, must be strictly negative, implying exponential stability. This, in turn, guarantees the (local) exponential stability of the orbit for the closed-loop system by Theorem 4.22.

4.4.2 Orbitally stabilizing feedback design

Periodic Riccati differential equation

In light of Theorem 4.22, the remaining question is therefore how to constructs a feedback that stabilizes the linearized transverse dynamics (4.29). Since the linear system is T-periodic (or s_T-periodic for (4.31)), one can, for instance, solve a *periodic Riccati differential equation* for this purpose.

Proposition 4.23 ([93, 170–173]). *Suppose there exists an s_T-periodic, $\mathcal{C}^1$-smooth matrix function $\mathcal{R}_\perp : \mathcal{S} \to \mathbb{M}^{(n-1)}_{\succ 0}$ satisfying, for all $s \in \mathcal{S}$, the periodic Riccati differential equation (PRDE)*

$$\begin{aligned}\rho(s)\mathcal{R}'_\perp(s) + \mathcal{A}^\mathsf{T}_\perp(s)\mathcal{R}_\perp(s) + \mathcal{R}_\perp(s)\mathcal{A}_\perp(s) + \mathcal{Q}_\perp(s) + \kappa(s)\mathcal{R}_\perp(s) \\ - \mathcal{R}_\perp(s)\mathcal{B}_\perp(s)\Gamma_\perp(s)\mathcal{B}^\mathsf{T}_\perp(s)\mathcal{R}_\perp(s) = \mathbf{0}_{(n-1)}\end{aligned} \tag{4.35}$$

where $\mathcal{Q} : \mathcal{S} \to \mathbb{M}^{(n-1)}_{\succ 0}$, $\Gamma_\perp : \mathcal{S} \to \mathbb{M}^m_{\succ 0}$, and $\kappa : \mathcal{S} \to \mathbb{R}_{\geq 0}$ are continuous and s_T-periodic. Then the control law (4.34) *with $K_\perp(\cdot)$ taken according to*

$$K_\perp(s) = -\Gamma(s)\mathcal{B}^\mathsf{T}_\perp(s)\mathcal{R}_\perp(s), \tag{4.36}$$

i.e. $u = K_\perp(p(x))z_\perp(x)$, renders the periodic orbit $\mathcal{O}$ exponentially stable with respect to the closed-loop system (4.1) *for any projection operator $p(\cdot)$.*

Gusev's SDP approach for solving the PRDE

Several methods have been proposed for solving the PRDE (4.35) in the literature, including the multi-shot methods of Varga [174, 175] and Gusev's approach [176, 177]; see also [178] for a comparison of these methods. The latter approach allows one to attempt to find a solution by solving a semidefinite program (SDP). Since we will utilize this approach later in this thesis, we will briefly outline its main ideas next.

Define the matrix-valued functional

$$\begin{aligned}\mathfrak{R}^\perp(\mathcal{R}_\perp, s) :=& \rho(s)\mathcal{R}'_\perp(s) + \mathcal{A}^\mathsf{T}_\perp(s)\mathcal{R}_\perp(s) + \mathcal{R}_\perp(s)\mathcal{A}_\perp(s) \\ &+ \mathcal{Q}_\perp(s) + \kappa(s)\mathcal{R}_\perp(s) - \mathcal{R}_\perp(s)\mathcal{B}_\perp(s)\Gamma_\perp(s)\mathcal{B}^\mathsf{T}_\perp(s)\mathcal{R}_\perp(s)\end{aligned} \tag{4.37}$$

corresponding to the left-hand side of (4.35). The following result corresponding to [179, Thm. 1] and [180, Thm. 5.3.4.], which are slight generalizations of the dual of Theorem 1 in [170], can then be stated.

Theorem 4.24 (Maximal solution to the PRDE). *Let $\mathcal{Q}_\perp(s) \in \mathcal{C}^0(\mathcal{S}, \mathbb{M}^{n-1})$, $\kappa = 0$ and $\Gamma = \mathbf{I}_m$, and suppose the pair $(\mathcal{A}_\perp, \mathcal{B}_\perp)$ is stabilizable. Further* *suppose that there exists an s_T-periodic matrix-valued function $\mathcal{R}(s)$ satisfying $\mathfrak{R}^{\perp}(\mathcal{R}(s), s) \succeq 0$ for all $s \in \mathcal{S}$. Then there exists a $\mathcal{R}_{\perp} \in \mathcal{C}^1(\mathcal{S}, \mathbb{M}^{n-1})$, called the maximum solution to the PRDE, which is s_T-periodic, as well as satisfies $\mathfrak{R}^{\perp}(\mathcal{R}_{\perp}(s), s) = 0$ and $\mathcal{R}_{\perp}(s) - \mathcal{R}(s) \succeq 0$ for all $s \in \mathcal{S}$.* □

From this theorem we can deduce the following: If $(\mathcal{A}_{\perp}, \mathcal{B}_{\perp})$ is stabilizable and $\mathcal{Q}(s) \in \mathbb{M}^{n-1}_{\succ 0}$, then the s_T-periodic matrix function $\mathcal{R}_{\perp} \in \mathcal{C}^1(\mathcal{S}, \mathbb{M}^{n-1})$ which has the largest trace (i.e. the sum of its eigenvalues) at all points on $\mathcal{S}$ among all the matrix functions satisfying $\mathfrak{R}^{\perp}(\mathcal{R}(s), s) \succeq 0$, is the unique positive-definite solution to the corresponding PRDE.

In order to use this as to formulate an SDP problem, one has to circumvent the term $\mathcal{R}\mathcal{B}_{\perp}\Gamma_{\perp}\mathcal{B}_{\perp}^{\mathsf{T}}\mathcal{R}$ as it is quadratic in $\mathcal{R}$. For this purpose, one can use the following well-known property of the Schur complement (see, e.g., [181, Th. 1.12]): $\mathfrak{R}^{\perp}(\mathcal{R}(s), s) \succeq 0$ if, and only if,

$$\mathfrak{R}^{\perp}_{SC}(\mathcal{R}(s), s) = \begin{bmatrix} \rho\mathcal{R}' + \mathcal{A}_{\perp}^{\mathsf{T}}\mathcal{R} + \mathcal{R}\mathcal{A}_{\perp} + \mathcal{Q}_{\perp} + \kappa\mathcal{R} & \mathcal{R}\mathcal{B}_{\perp} \\ \mathcal{B}_{\perp}^{\mathsf{T}}\mathcal{R} & \Gamma_{\perp}^{-1} \end{bmatrix} \succeq 0, \tag{4.38}$$

where we have omitted the s-argument to shorten the notation. With this in mind, let $\mathcal{R}(s)$ be taken as a real trigonometric polynomial of order $\mathfrak{m}$:

$$\mathcal{R}(s) = N_0 + \sum_{i=1}^{\mathfrak{m}} \left[N_i \sin(2i\pi s/s_T) + M_i \cos(2i\pi s/s_T) \right],$$

with the constant matrix coefficients, $N_0, N_i, M_i \in \mathbb{M}^{n-1}$, $i = 1, \ldots, \mathfrak{m}$. Let the $l+1$ unique points $s_0 = 0 < s_1 < s_2 < \cdots < s_l$, with $s_l < s_T$, dividing $\mathcal{S}$ into $l+1$ segments (these points may for example be evenly spaced or correspond to some Gauss points, etc.). The following SDP problem, with decision variables N_0, N_i, M_i, $i = 1, \ldots, \mathfrak{m}$, may then be formulated:

$$\begin{aligned} \max_{\substack{N_0, N_i, M_i \in \mathbb{M}^{n-1} \\ i=1,\ldots,\mathfrak{m}}} \quad & \sum_{j=0}^{l} \operatorname{Tr}\left(\mathcal{R}(s_j)\right) \\ \text{subject to} \quad & \mathfrak{R}^{\perp}_{SC}\big(\mathcal{R}(s_j), s_j)\big) \succeq 0, \quad j = 0, 1, \ldots, l. \end{aligned} \tag{4.39}$$

If a solution is found for properly chosen grid points and sufficiently large l, then one can take $\mathcal{R}_{\perp}(s) = \mathcal{R}(s)$ as an approximate solution to the PRDE (4.35) and design an LQR-based feedback by (4.36).

A differential LMI approach

As an alternative to solving the PRDE, one can instead utilize the following differential linear matrix inequality (DLMI) approach inspired by the LMI based method of [182] (see also [183–185]). It can be effectively solved using SDP, and has the additional benefit that it can be easily modified as to also be used for non-periodic orbits.

Proposition 4.25. *Suppose that for some smooth, scalar, s_T-periodic function $\lambda : \mathcal{S} \to \mathbb{R}_{>0}$, there exist a pair of s_T-periodic matrix functions $W_\perp \in \mathcal{C}^1(\mathcal{S}, \mathbb{M}^{n-1}_{\succ 0})$ and $Y_\perp \in \mathcal{C}^0(\mathcal{S}, \mathbb{R}^{m\times n-1})$, such that the linear matrix inequality*

$$\begin{aligned}\rho(s)W_\perp'(s) - W_\perp(s)\mathcal{A}_\perp^\mathsf{T}(s) - \mathcal{A}_\perp(s)W_\perp(s) \\ - Y_\perp^\mathsf{T}(s)\mathcal{B}_\perp^\mathsf{T}(s) - \mathcal{B}_\perp(s)Y_\perp(s) - \lambda(s)W_\perp(s) \succeq \mathbf{0}_{(n-1)}\end{aligned} \tag{4.40}$$

holds for all $s \in \mathcal{S}$. Then the control law (4.73)*, with $K_\perp(\cdot)$ taken as*

$$K_\perp(s) = Y_\perp(s)W_\perp^{-1}(s), \tag{4.41}$$

i.e. $u = K_\perp(p(x))z_\perp(x)$, exponentially stabilizes the orbit (4.6) *for* (4.1) *for any projection operator $p(\cdot)$ as by Definition 4.5.*

Proof. First note that $W_\perp \in \mathcal{C}^1(\mathcal{S}, \mathbb{M}^{n-1}_{\succ 0})$ ensures $W_\perp(s)$ being nonsingular for all $s \in \mathcal{S}$. Let us therefore consider $\mathcal{V}_\perp = \boldsymbol{\delta}_{z_\perp}^\mathsf{T} W_\perp^{-1}(s)\boldsymbol{\delta}_{z_\perp}$ as a Lyapunov function candidate for (4.29) under the control law $u = Y_\perp(s)H_\perp^{-1}(s)\boldsymbol{\delta}_{z_\perp}$. Using the well-known fact that $\frac{d}{ds}W_\perp^{-1}(s) = -W_\perp^{-1}(s)W_\perp'(s)W_\perp^{-1}(s)$, one can easily show that the time-derivative of $\mathcal{V}_\perp$ can be written as

$$\dot{\mathcal{V}}_\perp = \boldsymbol{\delta}_{z_\perp}^\mathsf{T} W_\perp^{-1}\Big[- \rho W_\perp' + W_\perp\mathcal{A}_\perp^\mathsf{T} + \mathcal{A}_\perp W_\perp + Y_\perp^\mathsf{T}\mathcal{B}_\perp^\mathsf{T} + \mathcal{B}_\perp Y_\perp\Big] W_\perp^{-1}\boldsymbol{\delta}_{z_\perp},$$

where we have omitted the functions arguments to shorten the notation. The inequality (4.40) therefore implies $\dot{\mathcal{V}}_\perp \le -\lambda(s)\mathcal{V}_\perp$. Hence, by the comparison lemma [44, Lemma 3.4], the zero solution of the closed-loop linearized transverse dynamics (4.29) is exponentially stable, such that the periodic orbit (4.6) is exponentially stable for the closed-loop system (4.1). □

4.4.3 Can other transverse coordinates be used instead?

Suppose one knows a $\mathcal{C}^1$-smooth mapping $k : \mathbb{R}^n \to \mathbb{R}^m$, satisfying $\|k(y)\| = 0$ for all $y \in \mathcal{O}$, which exponentially stabilizes the orbit. By the Andronov-Vitt theorem (Theorem 2.8), $n-1$ of the characteristic exponents of the T-periodic (first-order) variational system

$$\dot{\boldsymbol{\delta}}_x = [Df(x_s(s)) + B(x_s(s))Dk(x_s(s))]\,\boldsymbol{\delta}_x, \quad s = s(t), \tag{4.42}$$

must then have strictly negative real parts. It is therefore interesting to ask: Is it possible to relate this back to some specific set of transverse coordinates and some projection operator as to obtain a new stabilizing feedback? To provide an answer, we need only use Lemma 4.15 as to expand $k(\cdot)$ in terms of the given transverse coordinates as to obtain such a new exponentially orbitally stabilizing feedback by simply omitting the higher-order terms. For example, if for some transverse coordinates $z_\perp \in \mathbb{R}^{(n-1)}$ and a projection operator $p(\cdot)$, we instead take $u = Dk(x_p(x))\mathcal{Z}_\perp^\dagger(p(x))z_\perp(x)$, $x_p = x_s(p(x))$, then the variational system (4.42) remains the same. The following can therefore be concluded:

Proposition 4.26. *If a $\mathcal{C}^1$ mapping $k : \mathbb{R}^n \to \mathbb{R}^m$, satisfying $\|k(y)\| = 0$ for all $y \in \mathcal{O}$, is such that $u = k(x)$ exponentially stabilizes the orbit $\mathcal{O}$ for* (4.1)*, then for any projection operator $p(\cdot)$ (see Def. 4.5) and any vector of transverse coordinates $z_\perp(\cdot)$ (see Def. 4.11), the control law*

$$u = Dk(x_p(x))\mathcal{Z}_\perp^\dagger(p(x))z_\perp(x) \tag{4.43}$$

also exponentially stabilizes $\mathcal{O}$ with respect to (4.1)*.* □

4.5 Projection-based excessive transverse coordinates

Consider again the projection operator–based function which we considered in Section 4.5, namely

$$e_\perp := e_\perp(x) = x - x_p(x). \tag{4.44}$$

The following will now be assumed:

Assumption 4.27. The projection operator $p : \mathfrak{X} \to \mathcal{S}$ (see Def. 4.5) is $\mathcal{C}^2$.

In light of the discussion at the end of Section 4.3, the function $e_\perp$ is in many ways analogous to the coordinates of Zubov and Leonov considered in Chapter 2 (see (2.13) and (2.28)). Indeed, as $e_\perp$ is defined in terms of some projection operator $p(\cdot)$, it must, for any $x \in \mathfrak{X}$, lie upon the moving Poincaré section corresponding to the hypersurface formed by the set $\Pi(p(x))$ defined in (4.11). Yet, since the codomain of the function $e_\perp$ is $\mathbb{R}^n$, it is not a vector of transverse coordinates for a non-vanishing orbit $\mathcal{O}$ as by Definition 4.11. Instead, the function $e_\perp = e_\perp(x)$ is a vector of so-called *excessive transverse coordinates*: it is $\mathcal{C}^2$-smooth in $\mathfrak{X}$ (as p is $\mathcal{C}^2$), $\|e_\perp(y)\| \equiv 0$ and $\operatorname{rank} De_\perp(y) = n-1$ for all $y \in \mathcal{O}$ (cf. Definition 4.11).

Unlike a “standard” set of transverse coordinates, however, they cannot directly be used to obtain a local change of coordinates (see Lemma 4.14), as the map $x \mapsto e_\perp(x)$ is evidently not a diffeomorphism. To see this more clearly, consider the Jacobian matrix $De_\perp(x)$. It follows that, sufficiently close the orbit, a variation of the states, $\boldsymbol{\delta}_x$, relates to a variation of (4.44) through

$$\mathcal{E}_\perp(s) := De_\perp(x_s(s)) = \mathbf{I}_n - \mathcal{F}(s)\mathcal{P}(s); \tag{4.45}$$

that is,

$$\boldsymbol{\delta}_{e_\perp} = \mathcal{E}_\perp(s)\boldsymbol{\delta}_x, \tag{4.46}$$

where we have used the shorthand notation $s = s(t)$. Thus for (4.44) to be a valid (local) change of coordinates, the matrix function $\mathcal{E}_\perp(s)$ should necessarily be everywhere invertible, which it clearly cannot be. Even still, $\mathcal{E}_\perp(\cdot)$ has some key properties which will be readily utilized throughout this thesis. We summarize some of these properties in the next statement.

Lemma 4.28. *The matrix function $\mathcal{E}_\perp : \mathcal{S} \to \mathbb{R}^{n\times n}$, defined in* (4.45)*, is a projection matrix, that is $\mathcal{E}_\perp^2(s) = \mathcal{E}_\perp(s)$ for all $s \in \mathcal{S}$; its rank is always $(n-1)$; while $\mathcal{P}(s)$ and $\mathcal{F}(s)$ span its left- and right null spaces, respectively.*

Proof. Recalling from (4.12) the relation $\mathcal{P}(s)\mathcal{F}(s) = 1$, it is straightforward to validate that $\mathcal{P}(s)$ and $\mathcal{F}(s)$ are left- and right annihilators of $\mathcal{E}_\perp(s)$, respectively, and that $\mathcal{E}_\perp(s) = \mathcal{E}_\perp^2(s)$. Lastly, as $\mathcal{E}_\perp$ consists of a rank n matrix (i.e. $\mathbf{I}_n$) and a rank one matrix (i.e. $\mathcal{F}(s)\mathcal{P}(s)$), as well as the existence of the annihilators, implying its kernel is of dimension one, it follows that its rank is always $(n-1)$ by the rank-nullity theorem. □

Using the fact that $\mathcal{E}_\perp$ is a projection matrix, one can show, by computing the first-order Taylor expansion of (4.44) about $x_s(p(x))$, that

$$e_\perp = \mathcal{E}_\perp(p(x))e_\perp + \mathcal{F}(p(x))h(p(x), e_\perp) \tag{4.47}$$

must hold sufficiently close to $\mathcal{O}$, given some continuous scalar function $h(\cdot)$ satisfying $|h(\cdot, e_\perp)| = O(\|e_\perp\|^2)$. Hence $\mathcal{E}_\perp(s)\boldsymbol{\delta}_{e_\perp} = \mathcal{E}_\perp^2(s)\boldsymbol{\delta}_x = \boldsymbol{\delta}_{e_\perp}$, such that, by Lemma 4.28, the following relation must hold:

$$\mathcal{P}(s)\boldsymbol{\delta}_{e_\perp} = \mathcal{P}(s)\mathcal{E}_\perp(s)\boldsymbol{\delta}_{e_\perp} \equiv 0. \tag{4.48}$$

Letting $\mathbf{T}\Pi(s)$ denote the tangentspace about $x_s(s)$ of the moving Poincaré section $\Pi(s)$, defined in (4.11), then condition (4.48) implies $\boldsymbol{\delta}_{e_\perp}(t) \in \mathbf{T}\Pi(s(t))$. Similarly to the discussion at the end of Section 4.3, this allows us to infer that, sufficiently close to the nominal orbit, the coordinates (4.44) are orthogonal to the gradient of the projection operator $p(\cdot)$ and therefore locally transverse to the nominal orbit. Thus, even though they are an excessive set of transverse coordinates as rank $\mathcal{E}_\perp(s) = n - 1$, they can be used for the purpose of orbitally stabilizing feedback design. Indeed, as we will show shortly, the stability characteristics of their origin are in fact equivalent to that of any other set of transverse coordinates, and therefore also that of the nominal orbit. Thus, we will derive next the corresponding transverse linearization associated with $e_\perp$ along $\mathcal{O}$ in order to assess the stability of their zero-level set.

4.5.1 The corresponding transverse linearization

Similarly to how conventional transverse coordinates could be used to re-write a function in a neighborhood of the orbit (see Lemma 4.15), one can do this using these excessive transverse coordinates as well:

Lemma 4.29. *Any $\mathcal{C}^2$ function $\phi : \mathbb{R}^n \to \mathbb{R}$ can be written as*

$$\phi(x) = \phi(x_p(x)) + D\phi(x_p(x))\mathcal{E}_\perp(p(x))e_\perp(x) + O(\|e_\perp(x)\|^2) \tag{4.49}$$

within a neighborhood of $\mathcal{O}$. Moreover, if $\phi(y) = 0$ for all $y \in \mathcal{O}$, then

$$\phi(x) = D\phi(x_p(x))e_\perp(x) + O(\|e_\perp(x)\|^2). \tag{4.50}$$

Proof. Proceeding in a similar manner to the proof of Lemma 4.15, we have, according to Taylor's theorem [160], that the function ϕ can be equivalently rewritten in its "first-order approximation form" about some point $q \in \mathcal{O}$ (cf. Hadamard's lemma):

$$\phi(x) = \phi(q) + D\phi(q)(x - q) + O(\|x - q\|^2).$$

Consider now an arbitrarily large ball $\mathcal{B}$ centered at q. While the above form of $\phi(\cdot)$ necessarily holds for all x in $\mathcal{B}$ and beyond, let us consider only the slice of $\mathcal{B}$ contained in $\{x \in \hat{\mathfrak{X}} \subseteq \mathfrak{X} : \; p(x) = \hat{s}\}$ where $\hat{s}$ is such that $x_s(\hat{s}) \equiv q$ and with $\hat{\mathfrak{X}}$ as in the proof of Lemma 4.15; namely, $\mathcal{O} \subset \hat{\mathfrak{X}}$ and, for any $x \in \hat{\mathfrak{X}}$ and all $\iota \in [0, 1]$, $\big(x + \iota\big[x_p(x) - x\big]\big) \subset \hat{\mathfrak{X}}$. Upon this slice, we may then readily write $x_p(x)$ instead of q to obtain

$$\phi(x) = \phi(x_p(x)) + D\phi(x_p(x))e_\perp(x) + O(\|e_\perp(x)\|^2).$$

Since the projection operator $p(\cdot)$ is assumed to be $\mathcal{C}^2$ and well defined in $\mathfrak{X}$, this holds everywhere in $\hat{\mathfrak{X}}$. Using (4.47), it further simplifies to (4.50). Lastly, since $\phi(q) \equiv 0$ for all $q \in \mathcal{O}$ implies $\|D\phi(q)f(q)\| = \|D\phi(q)\mathcal{F}(p(q))\| \equiv 0$, we obtain (4.50). ◻

Taking the time-derivative of the function $e_\perp$ defined in (4.44), we obtain

$$\dot{e}_\perp = De_\perp(x)\dot{x} = De_\perp(x)f(x) + De_\perp(x)g(x)u. \tag{4.51}$$

We can therefore utilize Lemma 4.29 as to obtain the corresponding transverse linearization by isolating the linear part of the transverse dynamics (4.51). To this end, we denote by

$$A_s(s) := Df(x_s(s)) \quad \text{and} \quad B_s(s) := B(x_s(s)), \tag{4.52}$$

such that

$$\dot{\boldsymbol{\delta}}_x = A_s(s)\boldsymbol{\delta}_x + B_s(s)u \tag{4.53}$$

is the first-order variational system along $\mathcal{O}$ (see Section 2.3). Now, since $p(\cdot)$ and $f(\cdot)$ are both assumed to be $\mathcal{C}^2$, we can, for some x sufficiently close to $\mathcal{O}$, use (4.47) and Lemma 4.29 as to write the time derivative of $p = p(x)$ as

$$\begin{aligned}\dot{p}(x) = \rho(p) + \Big[f^{\mathsf{T}}(x_p)D^2p(x_p) + Dp(x_p)A_s(p)\Big]\mathcal{E}_\perp(p)e_\perp \\ + Dp(x)B(x)u + O(\|e_\perp\|^2),\end{aligned} \tag{4.54}$$

where $x_p = x_p(x)$. Similarly, by using that $\|De_\perp(q)f(q)\| = 0$ for all $q \in \mathcal{O}$, we may readily state the following:

Proposition 4.30. *Let Assumption 4.27 hold. Then within $\mathfrak{X}$, the time-derivative of the excessive transverse coordinates* (4.44)*, given by* (4.51)*, can be equivalently written as*

$$\dot{e}_\perp = A_\perp(p(x))e_\perp + B_\perp(p(x))u + \tilde{B}_\perp(x)u + O(\|e_\perp\|^2), \tag{4.55}$$

where $\tilde{B}_\perp(x) := De_\perp(x)B(x) - B_\perp(p(x))$, while

$$A_\perp(s) := \mathcal{E}_\perp(s)A_s(s) - \mathcal{F}(s)\mathcal{F}^{\mathsf{T}}(s)D^2p(x_s(s))\rho(s), \tag{4.56a}$$

$$B_\perp(s) := \mathcal{E}_\perp(s)B_s(s). \tag{4.56b}$$

□

Combining this with the transversality condition (4.48) for the variation of $e_\perp$ in a vicinity of the orbit, we immediately obtain the transverse linearization along $\mathcal{O}$ associated with $e_\perp$:

Corollary 4.31. *Let Assumption 4.27 hold and let $s = s(t) \in \mathcal{S}$ be a solution to* (4.4)*. Then the following linear-periodic system of differential-algebraic equations*

$$\dot{\boldsymbol{\delta}}_{e_\perp} = A_\perp(s)\boldsymbol{\delta}_{e_\perp} + B_\perp(s)u, \tag{4.57a}$$

$$0 = \mathcal{P}(s)\boldsymbol{\delta}_{e_\perp}, \tag{4.57b}$$

is the first-order approximation system of (4.51) *about the orbit $\mathcal{O}$ using the parameterization* (4.5). □

Notice that if we omit the control part, then (4.57) has the exact same structure as the linearization obtained by Leonov in [26] (cf.(2.31)). Indeed, as the following example demonstrates, the linearization (2.19) and its generalizations are also easily obtained through a specific choice of the projection operator.

Example 4.5. (Transverse linearization for a constant weighted projection) Suppose the projection operator is taken according to Proposition 4.9 for some constant matrix $\Lambda \in \mathbb{M}^n_{\succeq 0}$, that is

$$p(x) = \arg\min_{s\in\mathcal{S}} \left[(x - x_s(s))^{\mathsf{T}}\Lambda(x - x_s(s))\right] = \arg\min_{s\in\mathcal{S}} \|x - x_s(s)\|^2_\Lambda . \quad (4.58)$$

As we then have

$$Dp(x) = \frac{\mathcal{F}^{\mathsf{T}}(p)\Lambda}{\|\mathcal{F}(p)\|^2_\Lambda - e_\perp^{\mathsf{T}}\Lambda\mathcal{F}'(p)},$$

it is implied by (4.18) that $Dp(x)e_\perp(x) = 0$ must hold for all x within a tubular neighborhood of $\mathcal{O}$.

Now, from the transversality condition (4.57b) and the fact that $\mathcal{F}'(s)\rho(s) = A_s(s)\mathcal{F}(s) - \mathcal{F}(s)\rho'(s)$, the following relation can readily be obtained:

$$\mathcal{F}^{\mathsf{T}}(s)D^2p(x_s(s))\rho(s)\mathcal{E}_\perp(s) = \frac{\mathcal{F}^{\mathsf{T}}(s)A_s^{\mathsf{T}}(s)\Lambda}{\|\mathcal{F}(s)\|^2_\Lambda}\mathcal{E}_\perp(s).$$

Thus, using that $f(x_s(s)) = \mathcal{F}(s)\rho(s)$, the matrix function $A_\perp(\cdot)$ reduces to

$$A_\perp(s) = A_s(s) - \frac{f(x_s(s)))f^{\mathsf{T}}(x_s(s))}{\|f(x_s(s))\|^2_\Lambda}\left[\Lambda A_s(s) + A_s^{\mathsf{T}}(s)\Lambda\right]. \quad (4.59)$$

For $\Lambda = \mathbf{I}_n$ this evidently corresponds to (2.19); see also [23, 27, 29, 54, 59].

By studying (4.59), one can easily validate that the relation

$$\frac{d}{dt}\left(\frac{f(x_s(s))}{\|f(x_s(s))\|^2_\Lambda}\right) = A_\perp(s)\frac{f(x_s(s))}{\|f(x_s(s))\|^2_\Lambda} \quad (4.60)$$

holds (see, e.g., [54]). This means that for $u = 0$, the transverse linearization (4.55) would have the non-vanishing solution $f(x_s(s))/\|f(x_s(s))\|^2_\Lambda$ if we omitted the transversality condition (4.57b). As we will see next, this property is in fact shared by all transverse linearizations of the form (4.57). Hence, it is crucial that the transversality condition is taken into account when attempting to stabilize its origin.

4.5.2 Necessity of the transversality condition

Consider the linear system

$$\dot{\chi} = A_\perp(s)\chi + B_\perp(s)u \tag{4.61}$$

corresponding to (4.57) without the transversality condition (4.57b). As we claimed after Example 4.5, the undriven part of this system always has a non-vanishing solution.

Lemma 4.32. *The undriven ($u = 0$) linear-periodic system* (4.61) *has the solution $\mathcal{F}(s(t))$, while the remaining $(n-1)$ linearly-independent solutions can all be taken to be orthogonal to $\mathcal{P}(s(t))$.*

Proof. Inserting $\chi(t) = \mathcal{F}(s(t))$ into the above differential equation and using the shorthand notation $s = s(t)$, we obtain

$$\frac{d}{dt}\mathcal{F}(s) = \mathcal{E}_\perp(s)A_s(s)\mathcal{F}(s) - \mathcal{F}(s)\mathcal{F}^\top(s)D^2p(x_s(s))\mathcal{F}(s)\rho(s),$$

where $\frac{d}{dt}\mathcal{F}(s(t)) = \mathcal{F}'(s(t))\rho(s(t))$. By differentiating (4.12), i.e. the relation $\mathcal{P}(s)\mathcal{F}(s) \equiv 1$, with respect to s, it is implied that

$$\mathcal{F}^\top(s)D^2p(x_\star(s))\mathcal{F}(s) = -\mathcal{P}(s)\mathcal{F}'(s). \tag{4.62}$$

Using this and the relation $\mathcal{E}_\perp(s)\mathcal{F}(s) = \mathbf{0}_{n\times 1}$, together with the fact that

$$A_s(s)\mathcal{F}(s) = \mathcal{F}'(s)\rho(s) + \mathcal{F}(s)\rho(s),$$

which is obtained by differentiating $f(x_\star(s))$ with respect to s, the above can be equivalently rewritten in the following form:

$$\mathcal{F}'(s)\rho(s) = \mathcal{E}_\perp(s)\mathcal{F}'(s)\rho + \mathcal{F}(s)\mathcal{P}(s)\mathcal{F}'(s)\rho(s) = \mathcal{F}'(s)\rho(s).$$

This shows that $\mathcal{F}(\cdot)$ is indeed a solution, and as $\mathcal{F}$ is nonvanishing and bounded, the corresponding characteristic exponent must be equal to zero.

To show that the remaining linearly independent solutions can be taken to be orthogonal to $\mathcal{P}$, consider a full-rank matrix function $N_\perp : \mathbb{R}_{\geq 0} \to \mathbb{R}^{n\times(n-1)}$ satisfying $\|\mathcal{P}(s(t))N_\perp(t)\| = 0$ for all $t \geq 0$. It must satisfy

$$\mathcal{F}^\top(s(t))D^2p(x_\star(s(t)))N_\perp(t) + \mathcal{P}(s(t))N'_\perp(t) \equiv 0,$$

which can be achieved by taking $\frac{d}{dt}N_\perp = A_\perp(s(t))N_\perp$. □

The naturally question to then ask is whether it is possible to utilize feedback to suppress the solution $\mathcal{F}$ and asymptotically stabilize the origin of (4.61). If this were the case, then one could utilize standard techniques from linear control theory, such as LQR and differential Riccati equations, to stabilize the transverse dynamics, and consequently the periodic orbit. However, as the zero-level set of the variables $e_\perp = e_\perp(x)$ defines a one-dimensional manifold, namely the desired orbit $\mathcal{O}$, this is necessarily impossible. The following statement confirms this fact.

Proposition 4.33. *The origin of* (4.61) *is not stabilizable.*

Proof. Let (see Lem. 4.32)

$$U(t) := \big[\mathcal{F}(s(t)), N_\perp(t)\big] \tag{4.63}$$

denote a fundamental matrix of (4.61) for $u = 0$, i.e. $\dot{U} = A_\perp(t)U$, with $N_\perp$ satisfying $\mathcal{P}(s(t))N_\perp(t) \equiv \mathbf{0}_{1\times(n-1)}$ for all $t \geq 0$. It is easy to validate that its unique inverse is given by

$$U^{-1}(t) = \begin{bmatrix} \mathcal{P}(s(t)) \\ N_\perp^\dagger(t) \end{bmatrix}, \tag{4.64}$$

with $N_\perp^\dagger(t) := (N_\perp^\top(t)N_\perp(t))^{-1}N_\perp(t)\mathcal{E}_\perp(s(t))$ satisfying $\|N_\perp^\dagger(t)\mathcal{F}(s(t))\| \equiv 0$ for all $t \geq 0$ as in Lemma 4.32. Consider now the coordinate transformation $\chi = U(t)\eta$, with $\chi = \chi(t)$ a solution to the system (4.61). Differentiating with respect to time and inserting from (4.61), we obtain

$$A_\perp(s(t))U(t)\eta + B_\perp(s(t))u = A_\perp(s(t))U(t)\eta + U(t)\dot{\eta}.$$

Hence,

$$\dot{\eta} = U^{-1}(t)B_\perp(s(t))u = \begin{bmatrix} \mathcal{P}(s(t)) \\ N_\perp^\dagger(t) \end{bmatrix} \mathcal{E}_\perp(s(t))B(s(t))u = \begin{bmatrix} \mathbf{0}_{1\times n} \\ N_\perp^\dagger(t) \end{bmatrix} B(s(t))u,$$

where we have used the properties of $\mathcal{E}_\perp(\cdot)$ (see Lemma 4.28). It follows that $\eta_1(t) = \eta_1(0)$ for all $t \geq 0$, implying that $\mathcal{F}$ will remain a solution of (4.61) regardless of the control input. As a consequence, the origin of (4.61) cannot be stabilizable. □

In order to utilize the linearized transverse dynamics (4.57) to design orbitally stability feedback, we therefore either have to: 1) directly take into account the transversality condition; or 2) somehow circumvent the unstabilizable subspace of (4.61). A method inspired by Theorem 2.21 will be derived in Section 4.6.3 which is inline with 1), whereas we in the next section we will introduce a method, corresponding to 2), which is based on using a certain *comparison system* of (4.61). As we will see, this comparison system also shares several properties with both the corresponding transverse linearization and the variational system.

4.5.3 A comparison system and spectrum equivalence

Let us left-multiply both sides of (4.61) by the matrix function $\mathcal{E}_\perp(s)$. Utilizing the properties of $\mathcal{E}_\perp(\cdot)$ stated in Lemma 4.28, one can then rewrite the system on several different equivalent forms, with the following two singular descriptor system–like forms among them:

$$\mathcal{E}_\perp(s)\left[\dot{\chi} - \mathcal{E}_\perp(s)\left(A_s(s)\chi + B_s(s)u\right)\right] = \mathcal{E}_\perp(s)\left[\dot{\chi} - A_s(s)\chi - B_s(s)u\right] = 0. \tag{4.65}$$

Consider, therefore, the following linear-periodic *comparison system*:

$$\dot{w} = \mathcal{E}_\perp(s)A_s(s)w + \mathcal{E}_\perp(s)B_s(s)v, \;\; w \in \mathbb{R}^n, \;\; v \in \mathbb{R}^m. \tag{4.66}$$

It corresponds to the terms inside the brackets of the left-most expression in (4.65) being set to zero. Whenever the Hessian $D^2p(\cdot)$ vanishes at all points along the nominal orbit, then the system (4.66) is evidently equivalent to (4.61), i.e. to the transverse linearization without the transversality condition. In fact, even in the general case when the Hessian may not be zero, it has several interesting connections to both (4.61) and to the first-order variational system (4.53), which we recall is given by

$$\dot{\boldsymbol{\delta}}_x = A_s(s(t))\boldsymbol{\delta}_x + B_s(s(t))u. \tag{4.53}$$

In order to demonstrate this fact, we first define

$$\mu(t) := \exp\left(\int_0^t \mathcal{F}^{\mathsf{T}}(s(\tau))D^2p(x_s(s(\tau)))\mathcal{F}(s(\tau))\rho(s(\tau))d\tau\right), \tag{4.67}$$

where the functions $s(\cdot)$, $x_s(\cdot)$, etc., now are viewed in the light of Remark 4.4. Note that (4.62) also allows $\mu(t)$ to be equivalently written as

$$\mu(t) = \exp\left(\int_0^t -\mathcal{P}(s(\tau))\mathcal{F}'(s(\tau))\rho(s(\tau))d\tau\right).$$

In the case of a constant weighted projection as (4.58), we for instance have

$$\mathcal{P}(s)\mathcal{F}'(s) = \frac{\mathcal{F}^{\mathsf{T}}(s)\Lambda\mathcal{F}'(s)}{\|\mathcal{F}(s)\|_\Lambda^2} = \frac{1}{2}\frac{\frac{d}{ds}\|\mathcal{F}(s)\|_\Lambda^2}{\|\mathcal{F}(s)\|_\Lambda^2},$$

such that $\mu(t) = \ln(\|\mathcal{F}(s(t))/\mathcal{F}(s(0))\|_\Lambda)$, and therefore $\mu(T) \equiv 0$.

Using (4.67), we can derive the following relation between the sums of the characteristic exponents of the various systems.

Lemma 4.34. *The (minimal) sum of the characteristic exponents of the linear-periodic systems*

$$\dot{y} = A_s(s(t))y \quad \textit{and} \quad \dot{\chi} = A_\perp(s(t))\chi,$$

denoted by Σ, are the same, whereas for

$$\dot{w} = \mathcal{E}_\perp(s(t))A_s(s(t))w,$$

it is equal to $\Sigma + \ln(\mu(T))/T$. □

Proof. In the special case of an orthogonal projection, that is $\mathcal{P}(s) = \mathcal{F}^\mathsf{T}(s)/\|\mathcal{F}(s)\|$, the equivalence between the variational system (4.53) and the system (4.61) for $u \equiv 0$ was demonstrated in [54]. We will proceed along similar lines to derive the remaining relations.

Recall from Section 2.3.2 that for a regular linear system (e.g. constant or periodic) of the form $\dot{\sigma} = C(t)\sigma$, the sum of its characteristic exponents is given by the formula [89]

$$\Sigma(C) = \liminf_{t\to\infty} \frac{1}{t}\int_0^t \operatorname{Tr} C(\tau)d\tau \tag{4.68}$$

where $\operatorname{Tr} C$ denotes the trace of C, i.e. the sum of the elements on its main diagonal. Consider, therefore,

$$\Sigma(A_\perp) = \liminf_{t\to\infty} \frac{1}{t}\int_0^t \operatorname{Tr}\left[\mathcal{E}_\perp A_s - \mathcal{F}\mathcal{F}^\mathsf{T} D^2 p(x_s)\rho\right] d\tau,$$

where we have omitted some of the function arguments for the sake of readability. Let us also recall the following two properties of the trace operator: $\operatorname{Tr} CD = \operatorname{Tr} DC$ for any $C, D \in \mathbb{R}^{n\times n}$ and $\operatorname{Tr}(cd^\mathsf{T}) = d^\mathsf{T} c$ for $c, d \in \mathbb{R}^{n\times 1}$. This allows us to rewrite the above as to obtain

$$\Sigma(A_\perp) = \Sigma(A_s) - \liminf_{t\to\infty} \frac{1}{t}\int_0^t \left[\mathcal{P}A_s\mathcal{F} + \mathcal{F}^\mathsf{T} D^2 p(x_s)\mathcal{F}\rho\right] d\tau.$$

Since

$$\liminf_{t\to\infty} \frac{1}{t}\int_0^t \left[\mathcal{P}A_s\mathcal{F} + \mathcal{F}^\mathsf{T} D^2 p(x_s)\mathcal{F}\rho\right] d\tau = \liminf_{t\to\infty} \frac{1}{t}\int_0^t \frac{1}{\rho(s(\tau))}\frac{d}{d\tau}\rho(s(\tau))d\tau$$

reduces to $\liminf_{t\to\infty} \frac{1}{t}\ln(\rho(s(t))/\rho(0)) \equiv 0$, we have $\Sigma(A_s) \equiv \Sigma(A_\perp)$.

As to show $\liminf_{t\to\infty} \frac{1}{t}\int_0^t \operatorname{Tr}\mathcal{E}_\perp(s(\tau))A_s(s(\tau))d\tau = \Sigma + \ln(\mu(T))/T$, it suffices to note that we can write

$$\liminf_{t\to\infty} \frac{1}{t}\int_0^t \operatorname{Tr}\mathcal{E}_\perp(s(\tau))A_s(s(\tau))d\tau = \Sigma(A_\perp) + \liminf_{t\to\infty}\frac{1}{t}\ln(\mu(t)),$$

as well as that $\liminf_{t\to\infty}\frac{1}{t}\ln(\mu(t)) = \frac{1}{T}\ln(\mu(T))$ due to the periodicity of the integrand in the expression for $\mu(\cdot)$; see, e.g., [61]. □

Combining Lemma 4.34 and Lemma 4.32, we therefore arrive at the following statement, which analogous to the classical Poincaré test for planar systems [26, 80].

Proposition 4.35 (Poincaré-like test)**.** *Let $n = 2$. Then the periodic orbit $\mathcal{O}$ of the undriven system* (4.1) *is exponentially stable if $\int_0^{s_T}\frac{1}{\rho(\sigma)}A_\perp(\sigma)d\sigma <$ 0.*

To demonstrate its use, we revisit an example from Chapter 3.

Example 4.6. Consider again the task of stabilizing sinusoidal oscillations of the scalar double-integrator system $\ddot{q} = u$, but now on a slightly more general form by allowing for some smooth function $\rho : \mathcal{S} \to \mathbb{R}_{>0}$ rather than just $\rho = \omega \equiv \text{const}$. The nominal periodic orbit is then given by:

$$\mathcal{O} := \{q = a\sin(s),\ \dot{q} = a\rho(s)\cos(s),\ s \in [0, 2\pi)\}.$$

To stabilize this orbit, we will consider a control law of the form

$$u = u_\star(p) - k_y y - k_z z. \tag{4.69}$$

Here the projection operator $p = p(q, \dot{q})$ is the solution to the implicit equation $h(q, \dot{q}, s) = s - \operatorname{atan2}\left(\frac{q\rho(s)}{\dot{q}}\right)$; the nominal control $u_\star$ is given by

$$u_\star(s) := a\rho'(s)\rho(s)\cos(s) - a\rho^2(s)\sin(s);$$

while $y := q - a\sin(p)$ and $z := \dot{q} - a\rho(p)\cos(p)$. By Lemma 4.8, such a projection operator must in a neighborhood of $\mathcal{O}$ correspond to

$$Dp(q, \dot{q}) = \frac{\rho(s)}{\rho^2(s)q^2 + \dot{q}^2 - q\dot{q}\rho'(s)}\begin{bmatrix}\dot{q} & -q\end{bmatrix};$$

and hence

$$\mathcal{P}(s) = \frac{\begin{bmatrix}\cos(s)\rho(s) & -\sin(s)\end{bmatrix}}{a\rho(s) - a\rho'(s)\sin(s)\cos(s)}. \tag{4.70}$$

Letting $x = \mathrm{col}(q, \dot{q})$ and $e_\perp := \mathrm{col}(y, z)$, the closed-loop system can now be written in the following form:

$$\dot{x} = \mathcal{F}(p)\rho(p) + \hat{A}e_\perp := \begin{bmatrix} a\rho(p)\cos(p) \\ u_\star(p) \end{bmatrix} + \begin{bmatrix} 0 & 1 \\ -k_y & -k_z \end{bmatrix} e_\perp.$$

We can therefore infer that

$$A_\perp(s) := \mathcal{E}_\perp(s)\hat{A}\mathcal{E}_\perp(s) - \mathcal{F}(s)\mathcal{F}^\mathsf{T}(s)D^2p(x_s(s))\rho(s).$$

Recalling from (4.62) that $\mathcal{F}^\mathsf{T} D^2 p(x_s)\mathcal{F} = -\mathcal{P}\mathcal{F}'$, where

$$\begin{aligned} \mathcal{P}(s)\mathcal{F}'(s) &= \frac{2a\rho'(s)\sin(s)^2 - a\rho''(s)\sin(s)\cos(s)}{a\rho(s) - a\rho'(s)\sin(s)\cos(s)} \\ &= \frac{\frac{d}{ds}\left[\rho(s) - \rho'(s)\sin(s)\cos(s)\right]}{\rho(s) - \rho'(s)\sin(s)\cos(s)}, \end{aligned}$$

it follows that $\Sigma(A_\perp) = \Sigma(\mathcal{E}_\perp\hat{A}\mathcal{E}_\perp)$ as

$$\int_0^{s_T} \mathcal{P}(\sigma)\mathcal{F}'(\sigma)d\sigma = \left[\ln(\rho(s) - \rho'(s)\sin(s)\cos(s))\right]_0^{2\pi} \equiv 0,$$

which we note corresponds to $\mu(T) = 1$ (see (4.67)).

From the derivations in the above example, the control law (3.23) can in fact be obtained:

Proposition 4.36. *Let $\rho = \omega \equiv const.$ Then for any two constants $k_y, k_z \in \mathbb{R}$ with $k_z > 0$, the control law (4.69) renders $q_\star(t) = a\sin(\omega t)$ an exponentially orbitally stable solution of the scalar second-order system $\ddot{q} = u$.*

Proof. As in this case $\rho' = 0$, it is straightforward to show that

$$\mathrm{Tr}\left[(\mathcal{E}_\perp(s)\hat{A}(s)\mathcal{E}_\perp(s)\right] = \mathrm{Tr}\left[(\mathcal{E}_\perp(s)\hat{A}(s)\right] = -k_z\cos^2(s) + \frac{\sin(2s)}{2\omega}\left(\omega^2 - k_y\right).$$

Integrating with respect to s from 0 to 2π, we find that $\Sigma(A_\perp) < 0$ only if $k_z > 0$, such that the proposition follows from Proposition 4.35. □

In light of Lemma 4.34, one might wonder if there are additional relations between the solutions of (4.61) and the comparison system (4.66). In order to attempt to study the existence of such relations, we let, as in the last sections, the columns of $N_\perp(t) \in \mathbb{R}^{n\times(n-1)}$ correspond to $(n-1)$ independent solutions of the undriven system (4.61) satisfying $\|\mathcal{P}(s(t))N_\perp(t)\| \equiv 0$ for all $t \geq 0$. This allows us to state the following:

Lemma 4.37. *The nonsingular matrix function*

$$W(t) := \begin{bmatrix} \mathcal{F}(s(t))\mu(t) & N_\perp(t) + \mathcal{F}(s(t))\mu(t)L(t) \end{bmatrix} \begin{bmatrix} \mathcal{P}(s(0)) \\ N_\perp^\dagger(0) \end{bmatrix}, \tag{4.71}$$

with $\mu(\cdot)$ defined in (4.67) *and*

$$L(t) := \int_0^t \mu^{-1}(\tau)\mathcal{F}^\mathsf{T}(s(\tau))D^2p(x_s(s(\tau)))\rho(s(\tau))N_\perp(\tau)d\tau,$$

is the state transition matrix of the undriven ($v = 0$) comparison system (4.66)*.*

Proof. Consider the coordinate change $w = \hat{Y}(t)\phi$ with

$$\hat{Y}(t) = \begin{bmatrix} \mu(t)\mathcal{F}(s(t)), N_\perp(t) \end{bmatrix}. \tag{4.72}$$

By the properties of $\mathcal{E}_\perp(\cdot)$ (see Lemma 4.28), it is not difficult to show that $\hat{Y}(\cdot)$ is a fundamental matrix of the system

$$\frac{d}{dt}\hat{y} = \left[\mathcal{E}_\perp(s)A_s(s) - \mathcal{F}(s)\mathcal{F}^\mathsf{T}(s)D^2p(x_s(s))\rho(s)\mathcal{E}_\perp(s)\right]\hat{y},$$

and that its unique inverse is given by (cf. (4.64))

$$\hat{Y}^{-1}(t) = \begin{bmatrix} \mu^{-1}(t)\mathcal{P}(s(t)) \\ N_\perp^\dagger(t) \end{bmatrix}.$$

Hence $\dot{w} = \dot{\hat{Y}}(t)\phi + \hat{Y}(t)\dot{\phi}$ is equivalent to

$$\begin{aligned} \mathcal{E}_\perp(s)A_s(s)\hat{Y}(t)\phi = &\left[\mathcal{E}_\perp(s)A_s(s) - \mathcal{F}(s)\mathcal{F}^\mathsf{T}(s)D^2p(x_s(s))\rho(s)\mathcal{E}_\perp(s)\right]\hat{Y}(t)\phi \\ &+ \hat{Y}(t)\dot{\phi}. \end{aligned}$$

This implies that $\dot{\phi} = \hat{Y}^{-1}(t)\mathcal{F}(s)\mathcal{F}^\mathsf{T}(s)D^2p(x_s(s))\mathcal{E}_\perp(s)\hat{Y}(t)\phi$, which in turn reduces to

$$\dot{\phi} = \begin{bmatrix} 0 & \mu^{-1}(t)\mathcal{F}^\mathsf{T}(s(t))D^2p(x_s(s(t)))N_\perp(t) \\ \mathbf{0}_{(n-1)\times 1} & \mathbf{0}_{(n-1)} \end{bmatrix}\phi.$$

Thus $\phi_r = \mathrm{col}(\phi_2, \ldots, \phi_n)$ must be constant, whereas $\phi_1(t) = \phi_1(0) + L(t)\phi_r$. It follows that any solution of (4.66) (whenever $v = 0$) is of the form

$$w(t) = \hat{Y}(t)\begin{bmatrix} 1 & L(t) \\ \mathbf{0}_{(n-1)\times 1} & \mathbf{I}_{n-1} \end{bmatrix}\hat{Y}^{-1}(0)w(0) = W(t)w(0).$$

As $\mathcal{F}$ and the columns of $N_\perp$ are linearly independent, the statement follows. □

Looking at the state-transition matrix (4.71) of the undriven comparison system, it is clear that the zero solution of the linearized transverse dynamics (4.55) will be asymptotically stable if the part of all the solutions of (4.66) which lie in the subspace corresponding to the image of $\mathcal{E}_\perp(s(t))$ vanish. That is to say, if for any solution $w(t) = W(t)w(0)$ of (4.66) we have that $w_\perp(t) := \mathcal{E}_\perp(s(t))w(t)$ decays to zero under some feedback controller of the form $v = K(s)\mathcal{E}_\perp(s)w$, then the origin of the linearized transverse dynamic under $u = K(s)\boldsymbol{\delta}_{e_\perp}$ is asymptotically stable. We will in fact show that one can utilize this property as to design orbitally stabilizing using a specific comparison system in the next section. We will also derive some more general differential matrix equation–based methods for constructing such stabilizing feedback, which instead directly take into account the transversality condition.

4.6 Control design using excessive transverse coordinates

We have seen that the zero solution of the system obtained by omitting the transversality condition (4.57b) from the transverse linearization (4.57) cannot be asymptotically stabilized (Proposition 4.33). The main conclusion to be drawn from this is simply that one always has to take into account the transversality condition when attempting to design a orbitally stabilizing feedback controller. The simplest solution is of course to directly circumvent the transversality condition altogether by instead utilizing a minimal set of $(n-1)$ transverse coordinates as those we considered in Section 4.4. Indeed, such coordinates inherently satisfy the condition, and the stabilizability of the corresponding transverse linearization is equivalent to the exponential stabilizability of the nominal orbit; see Theorem 4.22. As previously stated, there exist several methods for obtaining such coordinates for different classes of systems; see, e.g., [30, 31, 34, 53, 57, 186]. However, their construction can be vary significantly depending on the nominal orbit, and may often require additional numerical steps.

As to provide a more general and streamlined alternative, we will here suggest methods which instead utilize the excessive transverse coordinates (4.44); that is,

$$e_\perp := x - x_p(x) = x - x_s(p(x)) \tag{4.44}$$

with p of class $\mathcal{C}^2$. More specifically, we are looking to find a continuous, s_T-periodic matrix function $K : \mathcal{S} \to \mathbb{R}^{m\times n}$, i.e. $K(0) \equiv K(s_T)$, such that the nonlinear control law

$$u = K(p(x))e_\perp \tag{4.73}$$

exponentially stabilizes the periodic orbit (4.6) for (4.1), thus consequently solving Problem 4.1. We will in the following suggest three approaches utilizing, respectively, the comparison system (4.66), the variational system (4.53) and the transverse linearization (4.57):

1. *A comparison-system approach*: Use the comparison system (4.66) corresponding to an orthogonal projection to directly design a stabilizing feedback;

2. *The Hauser and Hindman approach*: Design a stabilizing feedback directly for the variational system (4.53) and then combine it with a specific choice of projection operator;

3. *Projected differential Riccati-like equations*: Solve differential Riccati-like matrix equations directly for the transverse linearization (4.57) using the (projection) matrix function $\mathcal{E}_\perp(s)$ (see Lemma 4.28).

We start with the approach which utilizes the comparison system, while the two latter approaches are considered in Section 4.6.2 and Section 4.6.3.

4.6.1 The comparison system approach

Let the excessive transverse coordinates (4.44) now be taken such that they satisfy the orthogonality condition

$$\mathcal{F}^\mathsf{T}(p)e_\perp \equiv 0. \tag{4.74}$$

Recall from Example 4.5 that this is equivalent to the constant weighted projection (4.58) with $\Lambda = \mathbf{I}_n$, i.e. $p(x) = \arg\min_{s\in\mathcal{S}} \|x - x_s(s)\|^2$. By (4.59), we can therefore write

$$\dot{e}_\perp = A_\perp(p)e_\perp + De_\perp(x)B(x)u + \Delta(x),$$

where

$$A_\perp(s) = A_s(s) - \frac{f(x_s(s)))f^\mathsf{T}(x_s(s))}{\|f(x_s(s))\|^2}\left[A_s(s) + A_s^\mathsf{T}(s)\right], \tag{4.75}$$

and with the $\mathcal{C}^1$-smooth vector-valued function $\Delta(\cdot)$ satisfying (see [54])

$$\|\Delta(x)\| = O(\|e_\perp\|^2) \quad \text{and} \quad \mathcal{F}^\mathsf{T}(p)\Delta(x) \equiv 0.$$

As by (4.60) (see also [54]) the undriven system ($u \equiv 0$) without the orthogonality condition (4.74) then has the non-vanishing solution

$$\chi_\parallel(t) = \frac{(f \circ x_s(s))(t)}{\|(f \circ x_s(s))(t)\|^2} = \mathcal{P}^\mathsf{T}(s(t)) \tag{4.76}$$

whose characteristic exponent evidently is exactly zero, while the remaining $(n-1)$ solutions all satisfy $\mathcal{F}^{\mathsf{T}}(s(t))\chi_{\perp}^{i}(t)=0$, $i=1,\dots,n-1$.

Roughly speaking, we will show that if there exists a feedback of the form $v=K(s)w$ which "sufficiently" stabilizes the origin of the comparison system (4.66) (corresponding to the transverse linearization of the above system) for some $K\in\mathcal{C}^0\big(\mathcal{S},\mathbb{R}^{n\times m}\big)$, then the control law (4.73) will also asymptotically stabilize the origin of the transverse dynamics (4.51). Note that there are two main benefits of using such an approach for finding a stabilizing feedback for (4.57): 1) It circumvents the need to consider the uncontrollable subspace always present in (4.61); and 2) one avoids having to compute the Hessian $D^2p(\cdot)$. On the other hand, the existence of such a feedback is obviously not guaranteed.

In order to show that it may in fact some times exist, suppose that a continuous matrix function $K:\mathcal{S}\to\mathbb{R}^{m\times n}$, $K(0)=K(s_T)$, exists such that the largest characteristic exponents, λ_M, of the closed-loop system

$$\dot{w}=\Omega(s)A_{cl}(s)w \tag{4.77}$$

satisfies $\lambda_M<0$, where

$$A_{cl}(s):=A_s(s)+B_s(s)K(s); \tag{4.78}$$

that is, we assume (4.66) is stabilizable. Moreover, let $\mathfrak{W}(t)$ denote the state-transition matrix (see (2.6)) for this system:

$$\dot{\mathfrak{W}}(t)=\Omega(s(t))A_{cl}(s(t))\mathfrak{W}(t),\quad \mathfrak{W}(0)=\mathbf{I}_n. \tag{4.79}$$

Then, by a small modifications of theorems 2 and 4 in [89], there exist some number $C>0$ and a scalar functions $\zeta:[0,\infty)\to\mathbb{R}$, satisfying

$$\lim_{t\to\infty}\frac{1}{t}\int_{\tau}^{t}\zeta(\sigma)d\sigma=\lambda_M\quad\forall\tau\geq 0, \tag{4.80}$$

such that the following inequality holds:

$$\|\mathfrak{W}(t)\mathfrak{W}^{-1}(\tau)\|\leq C\exp\left(\int_{\tau}^{t}\zeta(\sigma)d\sigma\right)\quad\forall t\geq\tau\geq 0. \tag{4.81}$$

We can from this state the following:

Proposition 4.38. *Let $p(\cdot)$ be taken as to satisfy orthogonality condition* (4.74)*. Suppose that $\|A_s(s)\|\leq\alpha\in\mathbb{R}_{>0}$ for all $s\in\mathcal{S}$ and that the inequality*

$$\lambda_M<-C\alpha\leq 0 \tag{4.82}$$

holds, with C from (4.81)*. Then the control law* (4.73) *asymptotically stabilizes the orbit* (2.10) *of the dynamical system* (4.1)*.*

Proof. Let the matrix-function $N_\perp : \mathbb{R}_{\geq 0} \to \mathbb{R}^{n\times(n-1)}$ be such that that the columns of $N_\perp(0)$ form a normalized basis of the nullspace of $\mathcal{P}(0)$, i.e. $\|\mathcal{F}^\mathsf{T}(s(0))N_\perp(0)\| = 0$, and it is a solution to normalized adjoint equation

$$\dot{N}_\perp = -\left(\mathbf{I}_n - N_\perp N_\perp^\mathsf{T}\right) A_\perp^\mathsf{T} N_\perp,$$

where we have omitted the function arguments for readability. Using the fact that $N_\perp^\mathsf{T}(0)N_\perp(0) = \mathbf{I}_{(n-1)}$, one can easily check that both $N_\perp^\mathsf{T}(t)N_\perp(t) = \mathbf{I}_{(n-1)}$ and $\|\mathcal{P}(s(t))N_\perp(t)\| = 0$ then hold for all $t \geq 0$.

Let $N_\parallel(t) := \mathcal{F}(s(t))/\|\mathcal{F}(s(t))\|$ and define $N(t) = \left[N_\parallel(t), N_\perp(t)\right]$. Using that $\mathcal{E}_\perp(s) = (\mathbf{I}_n - N_\parallel N_\parallel^\mathsf{T})$, this matrix-valued function is evidently orthonormal for all $t \geq 0$, i.e. $N^\mathsf{T}(t)N(t) = \mathbf{I}_n$, and satisfies

$$\dot{N} = \left[(\mathbf{I}_n - N_\parallel N_\parallel^\mathsf{T})A_s N_\parallel N_\parallel^\mathsf{T} - (\mathbf{I}_n - N_\perp N_\perp^\mathsf{T})A_s^\mathsf{T}(\mathbf{I}_n - N_\parallel N_\parallel^\mathsf{T})\right] N.$$

Consider now the coordinate change $w = N(t)\gamma$, with $w = w(t)$ a solution of the comparison system (4.66). It can be shown that this results in

$$\dot{\gamma} = \begin{bmatrix} 0 & N_\parallel^\mathsf{T} A_s^\mathsf{T} N_\perp \\ \mathbf{0}_{n-1\times 1} & N_\perp^\mathsf{T} A_s N_\perp \end{bmatrix} \gamma + \begin{bmatrix} \mathbf{0}_{1\times m} \\ N_\perp^\mathsf{T} B_s \end{bmatrix} v, \tag{4.83}$$

which, by defining $\gamma_r := [\mathbf{0}_{n-1\times 1}, \mathbf{I}_{n-1}]\gamma$, we can write as

$$\begin{aligned} \dot{\gamma}_1 &= N_\parallel^\mathsf{T} A_s^\mathsf{T}(s) N_\perp \gamma_r \\ \dot{\gamma}_r &= N_\perp^\mathsf{T} A_s(s) N_\perp \gamma_r + N_\perp^\mathsf{T} B_s(s) v. \end{aligned}$$

Note that the above subsystems are not decoupled, implying that for certain triplets $(A_s(\cdot), B_s(\cdot), x_s(\cdot))$, its origin may be asymptotically stabilized. Thus, taking $v = K(s)w = K(s)N(s)\gamma$, we get $\dot{\gamma} = A_\gamma(t)\gamma$ with

$$A_\gamma(t) := \begin{bmatrix} 0 & N_\parallel^\mathsf{T} A_s^\mathsf{T} N_\perp \\ N_\perp^\mathsf{T} B K N_\parallel & N_\perp^\mathsf{T} A_{cl} N_\perp \end{bmatrix}.$$

Now, since $\mathfrak{W}(t)$ is the state transition matrix of the system

$$\dot{w} = \mathcal{E}_\perp(s(t))A_{cl}(s(t))w,$$

that is $w(t) = \mathfrak{W}(t)w_0$ and $\mathfrak{W}(0) = \mathbf{I}_n$, then $\Gamma(t) = N^\mathsf{T}(t)\mathfrak{W}(t)N(0)$ has the same characteristic exponents and is the state transition matrix of $\dot{\gamma} = A_\gamma(t)\gamma$.

Consider now the system (4.61) with $A_\perp$ according to (4.75) and with the feedback $u = K(s)\mathcal{E}_\perp(s)\chi$, where $\mathcal{E}_\perp(s)$ is introduced in order to ensure the transversality condition $\mathcal{F}^{\mathsf{T}}(s)\boldsymbol{\delta}_{e_\perp} \equiv 0$ holds. The time derivative of $\xi = N^{\mathsf{T}}(t)\chi$ is then

$$\dot{\xi} = A_\xi(t)\xi = A_\gamma(t)\xi + \begin{bmatrix} -N_\parallel A_s N_\parallel & -N_\parallel A_s^{\mathsf{T}} N_\perp \\ -N_\perp^{\mathsf{T}} B_s K N_\parallel & \mathbf{0}_{n-1} \end{bmatrix} \xi,$$

such that

$$\xi(t) = \Gamma(t)\xi_0 + \Gamma(t)\int_0^t \Gamma^{-1}(\tau)\tilde{A}(\tau)\xi(\tau)d\tau$$

where $\tilde{A}(t) := A_\xi(t) - A_\gamma(t)$. It is easy to validate that

$$\xi_*(t) = [1/\|(f \circ x_s(s))(t)\|, \mathbf{0}_{1\times(n-1)}]^{\mathsf{T}}$$

is a solution (corresponding to (4.76)), and therefore

$$\xi_*(0) = \Gamma^{-1}(t)\xi_*(t) - \int_0^t \Gamma^{-1}(\tau)\tilde{A}(\tau)\xi_*(\tau)d\tau.$$

It follows that one can take

$$\xi(0) = \kappa\xi_*(0) + [0, \xi_\perp^{\mathsf{T}}(0)]^{\mathsf{T}}, \quad \kappa := \xi_1(0)\|f(x_s(s_0))\|,$$

such that any solution can be written in the form

$$\xi(t) = \kappa\xi_*(t) + \Gamma(t)\begin{bmatrix} 0 \\ \xi_\perp(0) \end{bmatrix} + \Gamma(t)\int_0^t \Gamma^{-1}(\tau)\tilde{A}(\tau)(\xi(\tau) - c\xi_*(\tau))d\tau.$$

Thus the system has one solution corresponding to (4.76), i.e. $\xi_*(t)$, whose characteristic exponent equals zero, but which is not a solution to the system (4.57). Furthermore, due to the system being decoupled, we can find $(n-1)$ additional independent solutions of the form $\xi(t) = E\xi_\perp(t)$, with $E^{\mathsf{T}} := \begin{bmatrix}\mathbf{0}_{(n-1)\times 1} & \mathbf{I}_{n-1}\end{bmatrix}$ and where

$$\xi_\perp(t) = E^{\mathsf{T}}\Gamma(t)\big[E\xi_\perp(0) + \int_0^t \Gamma^{-1}(\tau)\tilde{A}(\tau)E\xi_\perp(\tau)d\tau\big].$$

Since any solution of (4.57) can be equivalently rewritten as $\boldsymbol{\delta}_{e_\perp}(t) = N_\perp(t)\xi_\perp(t)$, we need therefore only find conditions ensuring the asymptotic stability of the above solutions. To this end, utilizing (4.81) and the fact that $\|\tilde{A}E\| = \|N_\parallel A^{\mathsf{T}} N_\perp\| \leq \|A\| \leq \alpha$, we obtain

$$\|\xi_\perp(t)\| \leq C\psi(0,t)\|\xi_\perp(0)\| + C\alpha\int_0^t \psi(\tau,t)\|\xi_\perp\|d\tau,$$

where $\psi(\tau,t) := \exp\left(\int_\tau^t \zeta(\sigma)\ d\sigma\right)$. Thus, by defining $\phi(t) := \psi(t,0)\|\xi_\perp(t)\|$, the above inequality implies $\phi(t) \leq C\phi(0) + C\alpha \int_0^t \phi(\tau)d\tau$. This allows us to utilize Grönwall's lemma [44, 89] to obtain the inequality $\phi(t) \leq C\phi(0)\exp(C\alpha t)$, from which, in turn,

$$\|\xi_\perp(t)\| \leq C\|\xi_\perp(0)\| \exp\left(\int_0^t (\zeta(\sigma) + C\alpha)d\sigma\right)$$

can be deduced. By the hypothesis of the proposition, the largest characteristic exponent therefore has a strictly negative real part and hence the origin of (4.55) is asymptotically stable. □

Remark 4.39. The value of the above statement is not in the condition (4.82) per se. Rather, its importance is simply due to the fact that it shows the possibility of orbitally stabilizing the solution by designing a stabilizing feedback directly for the comparison system (4.66). Indeed, the condition (4.82) is by no means unique, and similar conditions can, as we will soon see, be stated using, for example, Lyapunov's second method. □

It is also of practical importance to note that if a controller $v = K(s)w$ stabilizing the origin of the comparison system (4.66) has been designed, then one does not need to check the conditions of the theorem. That is to say, one can instead utilize the Andronov–Vitt theorem on the first approximation system $\dot{\boldsymbol{\delta}}_x = (A_s(s) + B_s(s)K(s)\mathcal{E}_\perp(s))\boldsymbol{\delta}_x$ to validate that it will also be a stabilizing controller for (4.57); or, equivalently, check that the system (4.61) has $(n-1)$ characteristic multipliers within the unit circle. As yet another alternative, one can combine Lemma 4.34 and Lemma 4.37 to obtain the following statement which also can be utilized for this purpose.

Corollary 4.40. *If the system* (4.66) *under the control law* $v = K(s)\mathcal{E}_\perp(s)w$ *has one simple zero characteristic exponent and the remaining* $(n-1)$ *characteristic exponents have strictly negative real parts, then the control law* $u = K(p)e_\perp$ *asymptotically stabilizes the origin of the system* (4.55). □

Note that we illustrate the above scheme in an example in Section 4.6.4.

4.6.2 Projected Lyapunov differential equations

Inspired by Theorem 2.21, we next propose a series of differential matrix equations for either validating exponential orbital stability of the closed-loop system, or for constructing orbitally stabilizing feedback controllers. We will also demonstrate some connections to the methods proposed by Hindman and Hauser [22, 45, 46].

Projected differential Lyapunov equations

For some $\mathcal{C}^2$-smooth projection operator $p(\cdot)$, suppose the applied control law is of the form (4.73), i.e. $u = K(p(x))(x - x_p(x))$. Moreover, let $A_{cl}(s)$ be given by (4.78), that is $A_{cl}(s) := A_s(s) + B_s(s)K(s)$. The following can be used to assess if the control law is orbitally stabilizing:

Theorem 4.41. *Suppose that for some continuous, s_T-periodic PD matrix function $Q : \mathcal{S} \to \mathbb{M}^n_{\succ 0}$, there exists a $\mathcal{C}^1$ matrix function $L : \mathcal{S} \to \mathbb{M}^n_{\succ 0}$ satisfying, for all $s \in \mathcal{S}$, the* projected Lyapunov differential equation *(PrjLDE):*

$$\mathcal{E}_\perp^\mathsf{T}(s)\big[\rho(s)L'(s) + A_{cl}^\mathsf{T}(s)\mathcal{E}_\perp^\mathsf{T}(s)L(s) + L(s)\mathcal{E}_\perp(s)A_{cl}(s) + Q(s) \\ - \rho(s)L(s)\mathcal{F}(s)\mathcal{P}'(s) - \rho(s)\mathcal{P}^{\mathsf{T}\prime}(s)\mathcal{F}^\mathsf{T}(s)L(s)\Big]\mathcal{E}_\perp(s) = \mathbf{0}_n. \tag{4.84}$$

Then by taking in (4.1) *the control law* (4.73)*, the orbit $\mathcal{O}$, defined in* (2.10)*, is rendered exponentially stable with respect to the closed-loop system. Moreover, for any solution $L \in \mathcal{C}^1(\mathcal{S}, \mathbb{M}^n_{\succ 0})$ to* (4.84)*, the matrix function $L_\perp : \mathcal{S} \to \mathbb{M}^n_{\succeq 0}$, defined by*

$$L_\perp(s) = \mathcal{E}_\perp^\mathsf{T}(s)L(s)\mathcal{E}_\perp(s), \tag{4.85}$$

is unique and solves

$$\rho(s)L_\perp'(s) + A_{cl}^\mathsf{T}(s)L_\perp(s) + L_\perp(s)A_{cl}(s) + Q_\perp(s) = \mathbf{0}_n, \tag{4.86}$$

where $Q_\perp(s) = \mathcal{E}_\perp^\mathsf{T}(s)Q(s)\mathcal{E}_\perp(s)$.

Proof. The statement can essentially be derived from Theorem 2.21 (see Theorem 5.1 in [26] or Theorem 1 in [58]), as well as using the fact that the asymptotic stability of the transverse linearization implies exponential stability of the orbit. For the sake of completeness, however, we derive here a slightly different proof utilizing projection operators.

First note that by (4.55), we may write the closed-loop transverse dynamics when sufficiently close to $\mathcal{O}$ as

$$\dot{e}_\perp = \left[\mathcal{E}_\perp(p(x))A_{cl}(p(x)) - \Xi(p(x))\right]\mathcal{E}_\perp(p(x))e_\perp + O(\|e_\perp\|^2),$$

where $\Xi(s) := \mathcal{F}(s)\mathcal{P}'(s)\rho(s) = f^\mathsf{T}(x_s(s))D^2p(x_s(s))$. Further note that $\dot{L}(p(x)) = L'(p(x))\rho(p(x)) + O(\|e_\perp\|)$ by (4.54).

Consider now the positive semidefinite Lyapunov function candidate

$$V_\perp(x) = e_\perp^\mathsf{T}L(p(x))e_\perp. \tag{4.87}$$

Locally, it is equal zero only if $x \in \mathcal{O}$, and strictly positive otherwise. Using (4.47) and the above, the time derivative of $V_\perp = V_\perp(x)$ can be written as

$$\dot{V}_\perp = e_\perp^\mathsf{T}\mathcal{E}_\perp^\mathsf{T}(p)\Big[\rho(p)L'(p) + A_{cl}^\mathsf{T}(p)\mathcal{E}_\perp^\mathsf{T}(p)L(p) + L(p)\mathcal{E}_\perp(p)A_{cl}(p) \\ - L(p)\Xi(p) - \Xi^\mathsf{T}(p)L(p)\Big]\mathcal{E}_\perp(p)e_\perp + O(\|e_\perp\|^3),$$

with $p = p(x)$. Using (4.84), this is in turn equivalently to

$$\dot{V}_\perp = -e_\perp^\mathsf{T}\mathcal{E}_\perp^\mathsf{T}(p)Q(p)\mathcal{E}_\perp(p)e_\perp + O(\|e_\perp\|^3).$$

Hence, due to (4.47), this implies that there is an open tubular neighborhood $\mathcal{N}$ of $\mathcal{O}$, as well as a strictly positive constant $\lambda \in \mathbb{R}_{>0}$, such that the differential inequality $\dot{V}_\perp \leq -\lambda V_\perp$ holds for all $x \in \mathcal{N}$. By the comparison principle (see, e.g., [169, Theorem 1.1],[44, Lemma 3.4]), we therefore have that any ϵ-sublevel set of the form $\{x \in \mathcal{N} : V_\perp(x) \leq \epsilon\} \subseteq \mathcal{N}$ is forward invariant, and all solutions starting within it must converge to the orbit $\mathcal{O}$ exponentially.

What remains is therefore to show that, given a solution $L(\cdot)$ to (4.84), the postive semidefintie matrix function, $L_\perp$, given by (4.85), is unique and solves (4.86). Before showing this, however, first note that a solution to (4.84) will not be unique; indeed, given a solution $L_\perp(s)$ to (4.86), that is

$$L_\perp(s) = \mathcal{E}_\perp^\mathsf{T}(s)L_\perp(s)\mathcal{E}_\perp(s),$$

it can be shown that $\hat{L}(s) := L_\perp(s) + h_L(s)\mathcal{P}^\mathsf{T}(s)\mathcal{P}(s)$ will also satisfy (4.84) for an arbitrary smooth function $h_L : \mathcal{S} \to \mathbb{R}_{>0}$.

As to show that $L_\perp$ will be unique, we first note that

$$\mathcal{E}_\perp^\mathsf{T}L_\perp'\mathcal{E}_\perp = \mathcal{E}_\perp^\mathsf{T}\big[L' - L\mathcal{F}\mathcal{P}' - \mathcal{P}^{\mathsf{T}\prime}\mathcal{F}^\mathsf{T}L\big]\mathcal{E}_\perp,$$

where we have dropped the s-argument to shorten the notation. We may then rewrite the PrjLDE (4.84) as (4.86). Now let $N_\perp : \mathcal{S} \to \mathbb{R}^{n\times n-1}$ be a solution to

$$N_\perp{}'(s) = -\mathcal{F}(s)\mathcal{P}'(s)N_\perp(s), \quad \mathcal{P}(0)N_\perp(0) = \mathbf{0}_{1\times n-1}, \tag{4.88}$$

such that $\mathcal{P}(s)N_\perp(s) = \mathbf{0}_{1\times n-1}$ for all $s \in \mathcal{S}$. By Lemma 4.28 and the relation $\mathcal{P}\mathcal{F} \equiv 1$, this allows us to write $\mathcal{E}_\perp(s) = N(s)EN^{-1}(s)$ in which $E := \mathrm{diag}(0, \mathbf{I}_{n-1})$, $N(s) := \big[\mathcal{F}(s), N_\perp(s)\big]$ and $N^{-1}(s) = \big[\mathcal{P}^\mathsf{T}(s), (N_\perp^\dagger(s)\mathcal{E}_\perp(s))^\mathsf{T}\big]^\mathsf{T}$. Hence (4.84) is then equivalent to

$$EN^\mathsf{T}\big[\dot{L} + A_{cl}^\mathsf{T}N^{-\mathsf{T}}EN^\mathsf{T}\hat{L}_\perp + \hat{L}_\perp NEN^{-1}A_{cl} \\ - \dot{\mathcal{P}}^\mathsf{T}\mathcal{F}^\mathsf{T}L - L\mathcal{F}\dot{\mathcal{P}} + Q\big]NE = \mathbf{0}_n,$$

with $\dot{\mathcal{P}}(s) = f^{\mathsf{T}}(x_s(s))D^2p(x_s(s))$. It can be shown that the parts of this equation which are not trivially zero correspond to the following matrix differential equation:

$$\mathcal{A}^{\mathsf{T}}\mathcal{L}_\perp + \mathcal{L}_\perp\mathcal{A} + N_\perp^{\mathsf{T}}\big[\dot{L} - \dot{\mathcal{P}}^{\mathsf{T}}\mathcal{F}^{\mathsf{T}}L - L\mathcal{F}\dot{\mathcal{P}}\big]N_\perp + \mathcal{Q}_\perp = 0,$$

where $\mathcal{A}(s) := N_\perp^\dagger(s)\mathcal{E}_\perp(s)A_{cl}(s)N_\perp(s)$, while the matrix functions $\mathcal{L}_\perp(s) := N_\perp^{\mathsf{T}}(s)L(s)N_\perp(s)$ and $\mathcal{Q}_\perp(s) := N_\perp^{\mathsf{T}}(s)Q(s)N_\perp(s)$ evidently are both sufficiently smooth and positive definite (PD). Now using $\dot{N}_\perp = -\mathcal{F}\dot{\mathcal{P}}N_\perp$, one finds that

$$\dot{\mathcal{L}}_\perp = N_\perp^{\mathsf{T}}\left[\dot{L} - \dot{\mathcal{P}}^{\mathsf{T}}\mathcal{F}^{\mathsf{T}}L - L\mathcal{F}\dot{\mathcal{P}}\right]N_\perp.$$

We can therefore rewrite the above equation as

$$\dot{\mathcal{L}}_\perp(s(t)) = -\mathcal{A}^{\mathsf{T}}(s(t))\mathcal{L}_\perp(s(t)) - \mathcal{L}_\perp(s(t))\mathcal{A}(s(t)) - \mathcal{Q}_\perp(s(t)), \tag{4.89}$$

which is a T-periodic differential Lyapunov equation. As has been previously stated, it is known [100] (see Proposition 2.18) that such an equation has a unique PD solution $\mathcal{L}_\perp(\cdot)$ for any continuous, PD matrix function $\mathcal{Q}_\perp(\cdot)$ if, and only if, the T-periodic system

$$\frac{d}{dt}\vartheta_\perp = \mathcal{A}(s(t))\vartheta_\perp \tag{4.90}$$

is asymptotically stable. Hence, by the uniqueness of the pseudoinverse,

$$\begin{aligned} L_\perp(s) = \mathcal{E}_\perp^{\mathsf{T}}(s)L(s)\mathcal{E}_\perp(s) &= (N_\perp^\dagger(s)\mathcal{E}_\perp(s))^{\mathsf{T}}N_\perp^{\mathsf{T}}(s)L(s)N_\perp(s)N_\perp^\dagger(s)\mathcal{E}_\perp(s) \\ &= (N_\perp^\dagger(s)\mathcal{E}_\perp(s))^{\mathsf{T}}\mathcal{L}_\perp(s)N_\perp^\dagger(s)\mathcal{E}_\perp(s) \end{aligned}$$

is consequently also unique. □

Let us briefly try to provide some intuition behind the PrjLDE[8]. Simply put, by right- and left multiplying by $\mathcal{E}_\perp$ and its transpose, respectively, one obtains the projection upon the transverse subspace corresponding to the transversality condition (4.57b), thus avoiding the non-stabilizable subspace spanned by $\mathcal{F}$; see Lemma 4.32. Indeed, as shown in the proof of Theorem 4.41, the solution to the PrjLDE essentially corresponds to a solution to the periodic Lyapunov differential equation (PLDE) (4.89), which

[8] We use the abbreviation PrjLDE rather than PLDE to avoid any confusion with periodic Lyapunov equations [171]. Note also that, while there are obvious similarities, the PrjLDE should not be confused with the so-called projected (generalized continuous-time algebraic) Lyapunov equations of nonsingular descriptor systems as in [187].

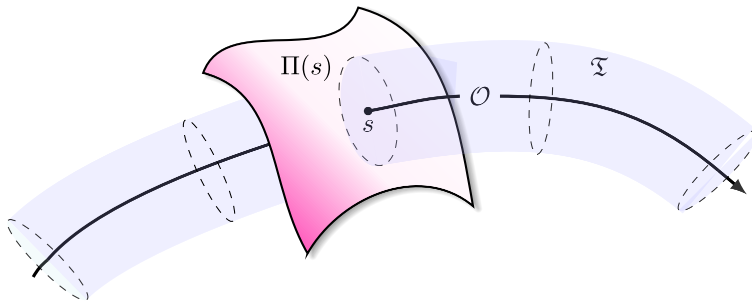

Figure 4.5: Illustration of the invariant tube $\mathfrak{T}$, defined in (4.91), corresponding to the interior of a level set of the Lyapunov function $V_\perp$ given by (4.87), with Π the moving Poincaré section defined in (4.11).

in turn is ensured by the asymptotic stability of the linear-periodic system (4.90). Clearly, the system (4.90) must correspond to the linearization of some vector of transverse coordinates, $z_\perp \in \mathbb{R}^{n-1}$, whose Jacobian matrix along the orbit is given by $\mathcal{Z}_\perp(s) = N_\perp^\dagger(s)\mathcal{E}_\perp(s)$ (cf. Theorem 4.22). A straightforward example of such coordinates would be the function $z_\perp(x) = N_\perp^\dagger(p(x))\mathcal{E}_\perp(p(x))e_\perp(x)$, which, for practical purposes, has the drawback of requiring the construction of a continuous representation, $N_\perp(\cdot) \in \mathbb{R}^{n\times(n-1)}$, of the nullspace of $\mathcal{P}(\cdot)$, i.e. (4.88).

Not only does a solution to the PrjLDE ensure that a feedback of the form (4.73) is exponentially orbitally stabilizing, it also provides a way of obtaining a rough estimate of its region of attraction using the Lyapunov function (4.87). Although beyond the scope of this thesis, one can search for the largest $\delta > 0$ such that $V_\perp$ is strictly decreasing within the open tube

$$\mathfrak{T} := \{x \in \mathfrak{X} : \ V_\perp(x) < \delta\}, \tag{4.91}$$

that is $\dot{V}_\perp < 0$ for all $x \in \mathfrak{T}\backslash\mathcal{O}$; see Figure. 4.5.

Relation to the method of Hindman and Hauser

As was mentioned in the thesis' introduction, Hauser and Hindman proposed a method in [22] which allows one to convert a trajectory tracking controller into an orbitally stabilizing control law using a particular projection operator for certain types of trajectories. While their result was limited to feedback-linearizable systems, one can use Theorem 4.41 as to readily extended their approach to more general nonlinear system, at the expense of more local results. In fact, the following statement, which can be seen as an extension of Theorem 2.1 in [22] (see also Theorem 1.2 in [46]), demonstrates that one can use their idea to design orbitally stabilizing feedback using only the variational system (4.53).

Proposition 4.42. *Let* $A_{cl}(\cdot) := A_s(s)+A_s(s)K(s)$ *for some* $K \in \mathcal{C}^0(\mathcal{S}, \mathbb{R}^{m\times n})$. *Suppose there exists a matrix function* $L \in \mathcal{C}^\infty(\mathcal{S}, \mathbb{M}^n_{\succ 0})$ *satisfying*

$$\rho(s)L'(s) + A_{cl}^\mathsf{T}(s)L(s) + L(s)A_{cl}(s) + Q(s) = \mathbf{0}_n \tag{4.92}$$

for some s_T*-periodic matrix function* $Q \in \mathcal{C}^0(\mathcal{S}, \mathbb{M}^n_{\succ 0})$. *If addition* $x_s(\cdot)$ *is of class* $\mathcal{C}^3$, *then by taking the projection operator as*

$$p(x) = \arg\min_{s\in\mathcal{S}} \Big[(x - x_s(s))^\mathsf{T} L(s)(x - x_s(s))\Big], \tag{4.93}$$

the control law

$$u = K(p(x))(x - x_p(x)) \tag{4.94}$$

exponentially stabilizes the periodic orbit $\mathcal{O}$ *for the closed-loop system* (4.1).

Proof. To prove the proposition, we need to show that the conditions of Theorem 4.41 are all satisfied for this particular choice of projection operator as long as (4.92) holds.

By taking $\Lambda(s) = L(s)$ in Proposition 4.9, the projection operator (4.93) is $\mathcal{C}^2$ within its domain if L is smooth and x_s is $\mathcal{C}^3$. Thus we have that the gradient of projection operator (4.93) evaluated along the orbit is given by (4.17). Hence, due to the properties of $\mathcal{E}_\perp$ (see Lemma 4.28), we have

$$\mathcal{F}^\mathsf{T}(s)L(s)\mathcal{E}_\perp(s) = \mathbf{0}_{1\times n}.$$

The PrjLDE (4.84) therefore reduces to

$$\mathcal{E}_\perp^\mathsf{T}(s)\Big[\rho(s)L'(s) + A_{cl}^\mathsf{T}(s)L(s) + L(s)A_{cl}(s) + Q(s)\Big]\mathcal{E}_\perp(s) = \mathbf{0}_n,$$

which is obviously satisfied if (4.92) holds. □

Is such feedback stabilizing if one changes the projection operator?

In light of Theorem 4.41 and Proposition 4.42, a natural question to now ask is whether or not one has to prespecify the projection operator before attempting to design a feedback controller. Or in other words: can one use a generic choice of operator satisfying Definition 4.5, e.g. an orthogonal projection such that (4.74), for control design, but utilize another projection operator in the applied control law? In fact, in their paper [46], Hindman and Hauser conjectured that this is indeed the case. While we cannot give a definitive answer to this question, we can at least partly answer it.

In this regard, the first thing to note is simply that one can of course directly change between different projection operators if their gradients evaluated along the orbit coincide. However, if this is not the case, then just a small modification to the feedback is needed in order to ensure that it is also stabilizing when using another operator. While this fact can be easily derived utilizing, e.g., Lemma 4.15 and the Andronov-Vitt theorem in a similar manner to how it was done for a minimal set of transverse coordinates to obtain Proposition 4.26, we provide here instead the following statement based on Theorem 4.41.

Proposition 4.43. *Suppose all the conditions in Theorem 4.41 are satisfied for some $\mathcal{C}^2$-smooth projection operator $p(\cdot)$ and a continuous matrix function $K : \mathcal{S} \to \mathbb{R}^{m\times n}$. Then for any other $\mathcal{C}^2$-smooth projection operator $\hat{p}(\cdot)$, the control law*

$$u = K(\hat{p})\big(\mathbf{I}_n - \mathcal{F}(\hat{p})\mathcal{P}(\hat{p})\big)\big(x - x_s(\hat{p})\big), \quad \hat{p} = \hat{p}(x), \tag{4.95}$$

where $\mathcal{P}(s) := Dp(x_s(s))$, exponentially stabilizes the orbit $\mathcal{O}$ for (4.1).

Proof. Let the positive definite (PD) matrix functions $L(\cdot)$ and $Q(\cdot)$ satisfy the PrjLDE (4.84) for the original operator $p(\cdot)$. Let $\hat{\mathcal{P}}(s) = D\hat{p}(x_s(s)$ and $\hat{\mathcal{E}}_\perp(s) = \mathbf{I}_n - \mathcal{F}(s)\hat{\mathcal{P}}(s)$, while note that $\mathcal{E}_\perp(s) = \mathbf{I}_n - \mathcal{F}(s)\mathcal{P}(s)$ remains as before. Define

$$\hat{L}(s) := \mathcal{E}_\perp^\mathsf{T}(s)L(s)\mathcal{E}_\perp(s) + \hat{\mathcal{P}}(s)\hat{\mathcal{P}}^\mathsf{T}(s),$$
$$\hat{Q}(s) := \mathcal{E}_\perp^\mathsf{T}(s)Q(s)\mathcal{E}_\perp(s) + \hat{\mathcal{P}}(s)\hat{\mathcal{P}}^\mathsf{T}(s).$$

Both $\hat{L}(s)$ and $\hat{Q}(s)$ are evidently PD for all $s \in \mathcal{S}$. Thus, if we can show that this pair of matrix functions satisfy the PrjLDE given the control law (4.95), then we may readily apply Theorem 4.41 to prove the statement.

To this end, we first note that $\hat{\mathcal{E}}_\perp^\mathsf{T}\big[\frac{d}{ds}(\hat{\mathcal{P}}\hat{\mathcal{P}}^\mathsf{T})\big]\hat{\mathcal{E}}_\perp = \mathbf{0}_n$, while

$$\frac{d}{ds}\mathcal{E}_\perp = -\mathcal{F}'\mathcal{P} - \mathcal{F}\mathcal{P}' = -\mathcal{F}\mathcal{P}'\mathcal{E}_\perp - \frac{1}{\rho}\mathcal{E}_\perp A_s\mathcal{F}\mathcal{P},$$

where we have used that $\rho' = \frac{d}{ds}(\mathcal{P}f(x_s)) = \mathcal{P}'\mathcal{F}\rho + \mathcal{P}A_s\mathcal{F}$. Hence

$$\hat{\mathcal{E}}_\perp^\mathsf{T}\hat{L}'\hat{\mathcal{E}}_\perp = \hat{\mathcal{E}}_\perp^\mathsf{T}\left[\mathcal{E}_\perp^\mathsf{T}L'\mathcal{E}_\perp + (\mathcal{E}_\perp')^\mathsf{T}L\mathcal{E}_\perp + \mathcal{E}_\perp^\mathsf{T}L\mathcal{E}_\perp'\right]\hat{\mathcal{E}}_\perp.$$

By defining $\hat{A}_{cl} = A_s + B_sK\mathcal{E}_\perp = A_{cl}\mathcal{E}_\perp + A_s\mathcal{F}\mathcal{P}$, as well as noting that $\mathcal{E}_\perp\hat{\mathcal{E}}_\perp = \mathcal{E}_\perp$, the expression $\hat{\mathcal{E}}_\perp\big[\rho\hat{L}' + \hat{A}_{cl}^\mathsf{T}\hat{\mathcal{E}}_\perp^\mathsf{T}\hat{L} + \hat{L}\hat{\mathcal{E}}_\perp\hat{A}_{cl}\big]\hat{\mathcal{E}}_\perp$ reduces to

$${\mathcal{E}_\perp}^\mathsf{T}\big[\rho L' + A_{cl}^\mathsf{T}\mathcal{E}_\perp^\mathsf{T}L + L\mathcal{E}_\perp A_{cl} - \rho L\mathcal{F}\mathcal{P}' - \rho{\mathcal{P}^\mathsf{T}}'\mathcal{F}^\mathsf{T}L\big]\mathcal{E}_\perp.$$

Lastly, by also observing that $\hat{\mathcal{E}}_\perp^\mathsf{T}(s)\hat{L}(s)\mathcal{F}(s)\hat{\mathcal{P}}'(s) = \mathbf{0}_n$, it is clear that $\hat{L}$ and $\hat{Q}$ are solutions to their respective PrjLDE if L and Q solves (4.84). $\square$

4.6.3 Projected differential Riccati equations

The PrjLDE in Theorem 4.41 allows one to assess if a feedback of the form (4.73) is exponentially orbitally stabilizing. Yet, it does not provide a way of constructing such a control law. For this purpose, one can instead utilize the following projected Riccati differential equations (PrjRDE).

Proposition 4.44. *Suppose that for some continuous, s_T-periodic function $\kappa : \mathcal{S} \to \mathbb{R}_{\geq 0}$ and s_T-periodic matrix functions $\mathcal{Q} \in \mathcal{C}^0(\mathcal{S}, \mathbb{M}^n_{\succ 0})$ and $\Gamma \in \mathcal{C}^1(\mathcal{S}, \mathbb{M}^m_{\succ 0})$, there exists a s_T-periodic, $\mathcal{C}^1$ matrix function $R : \mathcal{S} \to \mathbb{M}^n_{\succ 0}$ satisfying the projected periodic Riccati differential equation (PrjPRDE)*

$$\begin{aligned}\mathcal{E}_\perp^\mathsf{T}(s)\Big[\rho(s)R'(s) + A_\perp^\mathsf{T}(s)R(s) + R(s)A_\perp(s) + \mathcal{Q}(s) + \kappa(s)R(s) \\ - R(s)B_\perp(s)\Gamma(s)B_\perp^\mathsf{T}(s)R(s)\Big]\mathcal{E}_\perp(s) = \mathbf{0}_n\end{aligned} \tag{4.96}$$

for all $s \in \mathcal{S}$. Then the control law (4.73)*, with $K(\cdot)$ taken according to*

$$K(s) = -\Gamma(s)B_\perp^\mathsf{T}(s)R(s), \tag{4.97}$$

i.e. $u = K(p(x))e_\perp(x)$, renders the periodic orbit $\mathcal{O}$ exponentially stable with respect to the closed-loop system (4.1)*.*

Proof. Taking $L(\cdot)$ and $Q(\cdot)$ in Theorem 4.41 as

$$L(s) = R(s) \quad \text{and} \quad Q(s) = \mathcal{Q}(s) + \kappa(s)R(s) + R(s)B_\perp(s)\Gamma(s)B_\perp^\mathsf{T}(s)R(s),$$

one can easily validate that (4.84) is satisfied if (4.96). The statement then follows as $Q(\cdot)$ obviously is positive definite. □

Solving the PRDE using semidefinite programming

In order to solve (4.96), we propose an approach based on Gusev's method [176, 177] as we considered in Section 4.4.2 for solving the PRDE (4.35).

We begin by defining

$$\mathfrak{R}_{SC}(R(s), s) = \begin{bmatrix} \mathcal{E}_\perp^\mathsf{T}\left[\rho R' + A_\perp^\mathsf{T} R + RA_\perp + \mathcal{Q} + \kappa R\right]\mathcal{E}_\perp & \mathcal{E}_\perp^\mathsf{T} RB_\perp \\ B_\perp^\mathsf{T} R\mathcal{E}_\perp & \Gamma^{-1}\end{bmatrix}, \tag{4.98}$$

where we have omitted the s-argument to keep the notation short. Moreover, introduce the matrix-valued function $R(s) \in \mathbb{M}^n$ corresponding to a (real) trigonometric polynomial of order $\mathfrak{m}$:

$$R(s) = C_0 + \sum_{i=1}^{\mathfrak{m}} \left[C_i \sin(2i\pi s/s_T) + D_i \cos(2i\pi s/s_T)\right].$$

Here the unknown constant matrix coefficients $C_0, C_i, D_i \in \mathbb{M}^n$, $i = 1, \dots, \mathfrak{m}$ are to be found. Continuing as in Section 4.4.2, we let the $l+1$ unique points $s_0 = 0 < s_1 < s_2 < \cdots < s_l$, with $s_l < s_T$, divide $\mathcal{S}$ in to $l+1$ segments. The SDP problem we suggest for finding a solution to (4.96) can then be stated:

$$\begin{aligned} \max_{\substack{C_0, C_i, D_i \in \mathbb{M}^n \\ i=1,\dots,\mathfrak{m}}} \quad & \sum_{j=0}^{l} \Big[\mathrm{Tr}\left(\mathcal{E}_\perp^\mathsf{T}(s_j) R(s_j) \mathcal{E}_\perp(s_j)\right) - \mathcal{F}^\mathsf{T}(s_j) R(s_j) \mathcal{F}(s_j) \Big] \\ \text{s.t.} \quad & \mathfrak{R}_{SC}\big(R(s_j), s_j\big) \succeq 0, \quad j = 0, 1, \dots, l, \\ & R(s_j) \succeq 0, \qquad\qquad\quad\; j = 0, 1, \dots, l. \end{aligned} \tag{4.99}$$

Let us now show that a solution to this problem provides an approximate solution to the PrjPRDE. To this end, denote $Q_\perp(s) := \mathcal{E}_\perp^\mathsf{T}(s) Q(s) \mathcal{E}_\perp(s)$ and let the matrix function $N_\perp(s)$ be defined according to (4.88). The following statement can then be obtained by following the same steps as in the proof of Theorem 4.41.

Proposition 4.45. *For any solution $R \in \mathcal{C}^1(\mathcal{S}, \mathbb{M}^n_{\succ 0})$ to (4.96), the matrix function $R_\perp : \mathcal{S} \to \mathbb{M}^n_{\succeq 0}$, defined by*

$$R_\perp(s) = \mathcal{E}_\perp^\mathsf{T}(s) R(s) \mathcal{E}_\perp(s), \tag{4.100}$$

is unique and solves

$$\begin{aligned} \rho(s) R_\perp'(s) + A_s^\mathsf{T}(s) R_\perp(s) + R_\perp(s) A_s(s) + Q_\perp(s) + \kappa(s) R_\perp(s) & \\ - R_\perp(s) B_s(s) \Gamma(s) B_s^\mathsf{T}(s) R_\perp(s) = \mathbf{0}_n. & \end{aligned} \tag{4.101}$$

Moreover, such a solution to (4.101) is equivalent to the solution $\mathcal{R}_\perp(s) := N_\perp^\mathsf{T}(s) R(s) N_\perp(s) \in \mathbb{M}^{n-1}_{\succ 0}$ to the T-periodic PRDE

$$\begin{aligned} \dot{\mathcal{R}}_\perp(s(t)) + \mathcal{A}^\mathsf{T}(s(t)) \mathcal{R}_\perp(s(t)) + \mathcal{R}_\perp(s(t)) \mathcal{A}(s(t)) + \mathcal{Q}_\perp(s(t)) & \\ + \kappa(s) \mathcal{R}_\perp(s) - \mathcal{R}_\perp(s(t)) \mathcal{B}(s(t)) \Gamma(s(t))) \mathcal{B}^\mathsf{T}(s(t)) \mathcal{R}_\perp(s(t)) = \mathbf{0}_{n-1}, & \end{aligned} \tag{4.102}$$

where $\mathcal{Q}_\perp(s) := N_\perp^\mathsf{T}(s) Q(s) N_\perp(s)$, $\mathcal{A}(s) := N_\perp^\dagger(s) \mathcal{E}_\perp(s) A_s(s) N_\perp(s)$, and $\mathcal{B}(s) := N_\perp^\dagger(s) \mathcal{E}_\perp(s) B_s(s)$. □

In light of the above proposition, recall from Theorem 4.24 that a solution to (4.102) for $\kappa = 0$ is the so-called maximum solution with respect to the functional (4.37). Necessarily, any positive semidefinite solution to (4.101) of the form (4.100) must be maximal in a similar sense. In order to show how this motivates the SDP problem (4.99), we first recall that the properties of the Schur complement [181] ensures that $\mathfrak{R}_{SC}(R(s), s)$ is positive semidefinite if, and only if, the left-hand side of (4.96) is positive semidefinite. Thus a solution $R(s)$ to (4.96) implies that $R_\perp(s)$ defined by (4.100) is the maximal solution that solves (4.101), in the sense that, for any $\hat{R}(s)$, satisfying $\mathfrak{R}_{SC}(\hat{R}(s), s) \succeq 0$ for all $s \in \mathcal{S}$, one has $R_\perp(s) - \hat{R}_\perp(s) \succeq 0$ where $\hat{R}_\perp(s) = \mathcal{E}_\perp^{\mathsf{T}}(s)\hat{R}(s)\mathcal{E}_\perp(s)$. Hence, a solution to the SDP problem (4.99), if it exists, should, for properly chosen grid points, ensure that $R_\perp(s)$ is the maximal solution by maximizing the trace of $\mathcal{E}_\perp^{\mathsf{T}}(s_j)R(s_j)\mathcal{E}_\perp(s_j)$, whereas the uniqueness of this solution is ensured by adding the constraints $R(s_j) \succeq 0$ and subtracting $\mathcal{F}^{\mathsf{T}}(s_j)R(s_j)\mathcal{F}(s_j)$ in the objective function. Indeed, since if $R(s)$ solves (4.96), then so does $R_\perp(s)$ given by (4.100). The latter term in the objective function ensures that a solution $R(s)$ must have one zero eigenvalue, thus implying its uniqueness.

Differential LMI representation of the PRDE

As an alternative to the above projected Riccati equation, one can instead consider a differential linear matrix inequality (DLMI) similar to that in Proposition 4.25. Indeed, as the next statement clearly shows, by representing the matrix functions to be found as sums of basis functions, then the resulting matrix equations will be affine in all the unknown (decision) variables. Thus, by using a suitable transcription method, one can effectively search for an approximate solution using semidefinite programming.

Proposition 4.46. *Suppose that for some smooth, scalar, s_T-periodic function $\lambda : \mathcal{S} \to \mathbb{R}_{>0}$, there exist a pair of s_T-periodic matrix functions $W \in \mathcal{C}^1(\mathcal{S}, \mathbb{M}^n_{\succ 0})$ and $Y \in \mathcal{C}^0(\mathcal{S}, \mathbb{R}^{m\times n})$ satisfying, for all $s \in \mathcal{S}$, the linear matrix inequality:*

$$\begin{aligned}\rho(s)W'(s) - W(s)A_\perp^{\mathsf{T}}(s) - A_\perp(s)W(s) - Y^{\mathsf{T}}(s)B_\perp^{\mathsf{T}}(s) - B_\perp(s)Y(s) \quad (4.103)\\ - \lambda(s)[\mathcal{E}_\perp(s)W(s) + W(s)\mathcal{E}_\perp^{\mathsf{T}}(s)] \succeq 0.\end{aligned}$$

Then the control law (4.73)*, with $K(\cdot)$ taken according to*

$$K(s) = Y(s)W^{-1}(s), \tag{4.104}$$

i.e. $u = K(p(x))e_\perp(x)$, exponentially stabilizes the orbit (2.10) *for* (4.1)*.*

Proof. To prove the statement, we will show that the existence of such matrix-valued functions $W(\cdot)$, $Y(\cdot)$ implies that the conditions in Theorem 4.41 are satisfied. To this end, we take $L = W^{-1}$. Since $W(s)$ is symmetric and positive definite (SPD), it follows that $L(s)$, besides also being SPD, satisfies

$$\frac{d}{ds}L(s) = \frac{d}{ds}W^{-1}(s) = -W^{-1}(s)W'(s)W^{-1}(s) = -L(s)W'(s)L(s).$$

By inserting this into (4.84), we find that we can rewrite it as

$$\mathcal{E}_\perp^\top L\Big[-\rho W' + A_\perp^{cl} W + W(A_\perp^{cl})^\top + WQW\Big] L\mathcal{E}_\perp = \mathbf{0}_n, \tag{4.105}$$

with $A_\perp^{cl} := A_\perp + B_\perp Y W^{-1}$ and where we have dropped the s-argument to keep the notation short. Thus if we can show that a solution to (4.103) implies the existence of a continuous SPD matrix function $Q(\cdot)$, then we have proven the statement.

We proceed by noting that the continuity of the left-hand side of (4.103) implies the existence of a continuous, (symmetric) positive semidefinite matrix functions $G : \mathcal{S} \to \mathbb{M}^n_{\succeq 0}$, which allow us to replace the matrix inequality in (4.103) with an equality by adding it to the right-hand side. This, in turn, allows us the rewrite (4.105) as

$$\mathcal{E}_\perp^\top L\Big[-\lambda\big(\mathcal{E}_\perp W + W\mathcal{E}_\perp^\top\big) - G + WQW\Big] L\mathcal{E}_\perp = \mathbf{0}_n,$$

which further reduces to $-2\lambda\mathcal{E}_\perp^\top L\mathcal{E}_\perp - \mathcal{E}_\perp^\top LGL\mathcal{E}_\perp + \mathcal{E}_\perp^\top Q\mathcal{E}_\perp = \mathbf{0}_n$. Among the solutions to this matrix equations is $Q(s) = 2\lambda(s)L(s) + L(s)G(s)L(s)$, which is continuous and positive definite as desired. □

Note that, in a similar manner to how a solution R to (4.96) implies a unique solution $R_\perp = \mathcal{E}_\perp^\top R\mathcal{E}_\perp$ to (4.101), we will show in Chapter 7 that a solution pair (W, Y) to (4.103) implies a solution $(W_\perp, Y_\perp) = (\mathcal{E}_\perp W\mathcal{E}_\perp^\top, Y\mathcal{E}_\perp^\top)$ to a reduced projected differential LMI (see Proposition 7.6).

4.6.4 Illustrative example

For the purpose of comparing the use of the comparison system approach with the use of projected Riccati differential equations in regard to designing orbitally stabilizing feedback for periodic orbits, we will consider a simple example in this section. Specifically, we will consider the system

$$\dot{x}_1 = x_2 + x_1x_3 + x_1u \tag{4.106a}$$

$$\dot{x}_2 = -x_1 + x_2x_3 + x_2u \tag{4.106b}$$

$$\dot{x}_3 = u \tag{4.106c}$$

which for $u \equiv 0$ admits, for any $a > 0$, the periodic orbit

$$\mathcal{O}_a = \{x \in \mathbb{R}^3 \mid\, x_1^2 + x_2^2 = a^2,\ x_3 = 0\}. \tag{4.107}$$

The task of stabilizing such an orbit for the system (4.106) was considered by Banaszuk and Hauser in [30]. Using transverse feedback linearization, they showed that by taking $\theta = -\arctan(x_2/x_1)$, there exists a pair of transverse coordinates $z_\perp = \text{col}(z_\perp^1, z_\perp^2)$, with

$$z_\perp^1 := \log\left(\sqrt{x_1^2 + x_2^2}\right) - \log(a) - x_3 \quad \text{and} \quad z_\perp^2 := x_3,$$

such that $(x_1, x_2, x_3) \mapsto (\theta, z_\perp)$ is a diffeomorphism everywhere except $(x_1, x_1) = (0, 0)$. Indeed, in accordance with Definition 4.11, we evidently have $\|z_\perp(y)\| = 0$ and $\operatorname{rank} Dz_\perp(y) = 2$ for all $y \in \mathcal{O}_a$. Moreover, the dynamics of θ is trivial ($\dot{\theta} = 1$), while the transverse dynamics are linear:

$$\frac{d}{dt} z_\perp^1 = z_\perp^2, \qquad \frac{d}{dt} z_\perp^2 = u.$$

While this is clearly a convenient choice of coordinates, thus illustrating the possibility of finding a minimal set of coordinate that can greatly simplify control design, it also shows the challenge of finding a (convenient) set of coordinates even for such a simple, low dimensional system.

Let us therefore consider the alternative of instead using the excessive transverse coordinates (4.44). More specifically, let the parameterization of $\mathcal{O}_a$ be taken as $x_s(s) = \text{col}(a \sin(s), a \cos(s), 0)$ and let the projection operator be given by $p(x) = \text{atan2}\,(x_1, x_2)$ such that $\dot{s}(t) = \rho(s(t)) = 1$, where $\text{atan2}(\cdot)$ denotes the four-quadrant arctangent function. Since we consider $\rho \equiv 1$, this projection operator is therefore simply a radial projection onto $\mathcal{O}_a$, thus resulting in the satisfaction of the orthogonality condition (4.74).

Omitting the orthogonality condition in the linearized transverse dynamics (4.55) of the excessive coordinates $e_\perp = x - x_s(p(x))$, i.e. we consider (4.61), we obtain the following 2π-periodic system:

$$\frac{d}{ds}\chi = \begin{bmatrix} 0 & 1 & a\sin(s) \\ -1 & 0 & a\cos(s) \\ 0 & 0 & 0 \end{bmatrix} \chi + \begin{bmatrix} a\sin(s) \\ a\cos(s) \\ 1 \end{bmatrix} u. \tag{4.108}$$

Notice that it is equivalent to the variational system along the orbit. The corresponding comparison system (4.66) is given by

$$\frac{d}{ds} w = \begin{bmatrix} -\frac{\sin(2s)}{2} & \sin^2(s) & a\sin(s) \\ -\cos^2(s) & \frac{\sin(2s)}{2} & a\cos(s) \\ 0 & 0 & 0 \end{bmatrix} w + \begin{bmatrix} a\sin(s) \\ a\cos(s) \\ 1 \end{bmatrix} v. \tag{4.109}$$

For $a = 1$, we designed a stabilizing feedback controller for the comparison system, in which the found controller gains are shown in Figure 4.6. By

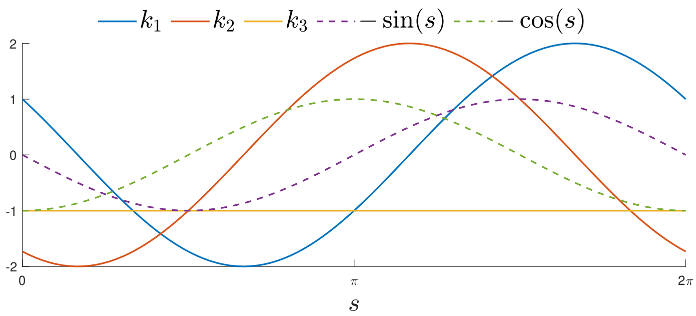

Figure 4.6: Stabilizing controller gains for (4.109).

writing $\frac{d}{ds}w = \mathcal{E}_\perp(s)A(s)w + B_\perp(s)v$, these gains correspond to the feedback matrix

$$K(s) = [k_1(s), k_2(s), k_3] = -B_\perp^\top(s)R_w(s)$$

with $R_w(s) = R_w^\top(s)$ the positive definite solution to the periodic Riccati differential equation:

$$\frac{d}{ds}R_w + A^\top \mathcal{E}_\perp^\top R_w + R_w \mathcal{E}_\perp A + I_3 - R_w B_\perp B_\perp^\top R_w = \mathbf{0}_3.$$

With this controller, the characteristic exponents of (4.108) were approximately $(0, -1.73, -1)$, implying the asymptotic stability of the orbit by Proposition 4.33; while for the system (4.109) they were approximately $(-0.86 \pm 0.5i, -1)$, showing it is indeed an orbitally stabilizing controller as we would expect from Proposition 4.38.

Let us now also demonstrate a certain limitation of Proposition 4.38 by instead considering the control law

$$u = -\begin{bmatrix}\sin(p(x)) & \cos(p(x)) & 1\end{bmatrix} e_\perp \tag{4.110}$$

which exponentially stabilizes the system (4.108), and consequently asymptotically stabilizes the orbit (4.107) for any $a > 0$. Indeed, it can be shown that the projected periodic Riccati differential equation

$$\mathcal{E}_\perp^\top \left[\frac{d}{ds}R + A_\perp^\top R + RA_\perp + \mathbf{I}_3 - RB_\perp B_\perp^\top R\right]\mathcal{E}_\perp = \mathbf{0}_3,$$

has a family of solutions given by

$$R(s) = \mathcal{E}_\perp^i(s)\begin{bmatrix}\frac{1}{a} & 0 & 0\\ 0 & \frac{1}{a} & 0\\ 0 & 0 & 1\end{bmatrix}\mathcal{E}_\perp^j(s) + k\begin{bmatrix}\cos^2(s) & -\frac{\sin(2s)}{2} & 0\\ -\frac{\sin(2s)}{2} & \sin^2(s) & 0\\ 0 & 0 & 0\end{bmatrix}$$

for any $k \in \mathbb{R}$ and $i, j \in \{0, 1\}$, such that $u = -B_\perp^\mathsf{T}(p)R(p)e_\perp$, corresponding to (4.110), is exponentially orbitally stabilizing by Proposition 4.44. On other hand, in accordance with Proposition 4.33, it can be shown that the closed-loop system, i.e. $A_\perp^{cl}(s) := A_\perp(s) - B_\perp(s)B_\perp^\mathsf{T}(s)R_\perp(s)$, without the orthogonality condition (4.74) has the solution $\mathcal{F}(s(t))$ with characteristic exponent equal to zero. Its two other independent solutions are $[0, 0, e^{-t}]^\mathsf{T}$ and $\left[\sin(s(t)), \cos(s(t)), le^{(a-1)t} + \frac{e^{-at}}{a-1}\right]^\mathsf{T}$ with $l \in \mathbb{R}$. Taking $l = 0$, their characteristic exponents equals -1 and $-a$, respectively, again implying the exponential stability of the nominal orbit.

Consider now the same control law implemented on the comparison system (4.109), that is

$$v = -\begin{bmatrix}\sin(s) & \cos(s) & 1\end{bmatrix} w.$$

It too has $\mathcal{F}(s)$ as a solution, while it can be shown that -1 and $-a$ are indeed the characteristic exponents of the two remaining independent solutions (although note that these solutions are different to those of (4.108) given above). We can therefore use Corollary 4.40 to validate that the control law is exponentially orbitally stabilizing, but we cannot utilize Proposition 4.38 for this purpose.

So why is not the origin of the comparison system (4.109) asymptotically stable under the controller (4.110)? It turns out that the existence of the solution $\mathcal{F}(s)$ is clear by noticing that $B_\perp(s)B_\perp^\mathsf{T}(s)R(s) \equiv \hat{K}(s)\mathcal{E}_\perp(s)$ where

$$\hat{K}(s) := \begin{bmatrix} a & 0 & a\sin(s) \\ 0 & a & a\cos(s) \\ \sin(s) & \cos(s) & 1 \end{bmatrix}.$$

Thus $K(s)w \equiv 0$ for any $w \in \operatorname{span}(\mathcal{F}(s))$. It follows that a controller asymptotically stabilizing the linearized transverse dynamics (4.57) will not necessarily asymptotically stabilize the comparison system (4.66). It is, however, interesting to note that all the characteristic exponents of both the systems $\dot{\hat{y}} = \big(A_\perp(s) - \hat{K}(s)\big)\hat{y}$ and $\dot{\hat{w}} = \big(\mathcal{E}_\perp(s)A(s) - \hat{K}(s)\big)\hat{w}$ have strictly negative real parts and sum to $(-2a - 1)$.

Chapter 5

Applications to Underactuated Mechanical Systems

In this chapter, we propose a procedure based on so-called synchronization functions for planning orbits of underacted mechanical systems. We also provide explicit expressions for the transverse linearization corresponding to the projection-based excessive transverse coordinates for a class of mechanical systems.

5.1 Introduction

While the methods we propose in this thesis are applicable to a broad class of nonlinear control systems, it is particularly *underactuated mechanical systems* [7–11] these methods are tailored to. This sub-category of mechanical control systems are defined by having fewer independent controls (actuators) than their degrees of freedom. As previously mentioned in the thesis' introduction, this means that any feasible motion of the system must comply with the dynamic constraints which arise due to the system's underactuation [33]. In general, this greatly restricts the space of feasible (forced) motions which the system can execute, thus making it especially important to have prior knowledge of a maneuver corresponding to the nominal motion one wishes to orbitally stabilize.

In order to search for such maneuvers, we will in this chapter study a constructive procedure heavily inspired by the so-called *virtual (holonomic) constraints* (VHC) approach [33, 55, 138] (see also [31, 139]), which provides an effective means to search for orbits of a class of underactuated mechanical systems. In the VHC approach, one assumes the invariance of certain relations between the generalized coordinates, parameterized by a scalar *motion generator*. Unlike a fully-actuated system where the dynamics of this motion generator essentially can be chosen freely, its time evolution must satisfy a series of second-order differential equations for underactuated systems.[1]

The main differences between the VHC approach and the one we will present in this chapter are the following: we do not assume that the synchronization parameter is a (known) function of the generalized coordinates, and, as we are looking to obtain an s-parameterization (see Assumption 4.3), we will require it to be monotonically increasing in time. This makes our approach conceptually similar to certain time-scaling approaches, such as the one suggested in [103] for finding time-optimal trajectories of fully-actuated systems using convex optimization (see also [38]). The main motivation for using such an approach also for systems with underactuation, is that it allows one to find a rich set of behavior even if the so-called *synchronization functions* (which are analogous to the virtual holonomic constraints) are represented by, say, polynomials of relatively low order, due to the additional flexibility of having a time-scaled synchronization parameter.

In the second part of this chapter, we consider the projection-based excessive transverse coordinates we studied in Section 4.5 for mechanical systems. These coordinates have previously been used by Pchelkin et al. in [38] for orbital stabilization of fully-actuated robot manipulators. There, a transverse linearization was used to show that a PD-like feedback with constant gains could be used to achieve orbitally stable motions of the system. However, they did not provide explicit expressions for the transverse linearization, requiring instead a matrix equation to be solved numerically. Among the contributions of this chapter is therefore to provide explicit expressions for the transverse linearization, thus avoiding the need to solve a matrix equation as in [38]. We also provide further generalizations compared to [38], including allowing for state-dependent projection operators, as opposed to only configuration-dependent ones, as well as consider a more general class of controlled (underactuated) mechanical systems.

Outline: The chapter is organized as follows: We introduce the considered class of underactuated mechanical systems in Section 5.2. In Section 5.3 we suggest a synchronization function–based method for finding orbits in un-

[1]It is interesting to note that, for completely passive (non-Euclidean) mechanical systems, recent work by Albu-Schäffer, Della Santina and collaborators (see, e.g., [188, 189]) related to the notion of Eigenmanifolds, have truly showed the possibility of exploiting the inherent structure of mechanical systems to find families of periodic motions, so-called *nonlinear modes*, which may be used to generate highly energy-efficient motions.

deractuated mechanical systems. In Section 4.5, we consider the projection-based excessive transverse coordinates for mechanical control systems, and derive explicit expressions for the transverse linearization. The problem of generating orbitally stable oscillations of the cart-pendulum system is considered as an illustrative example in Section 6.4.

5.2 (Underactuated) mechanical systems

We will now consider mechanical systems within the formalism of Lagrangian mechanics. We denote by $q = \mathrm{col}(q_1, \dots, q_{n_q}) \in \mathbb{R}^{n_q}$ a vector of n_q generalized coordinates of the system, and by $\dot{q} \in \mathbb{R}^{n_q}$ the corresponding generalized velocities. Furthermore, we denote by $u \in \mathbb{R}^m$ the vector of the m independent controls acting on the system, with their specific influence upon the system specified through the constant, full-rank coupling matrix $\mathbf{B}_u \in \mathbb{R}^{n_q \times m}$. Given a Lagrangian $\mathcal{L} : \mathbb{R}^{n_q} \times \mathbb{R}^{n_q} \to \mathbb{R}$ of the system, the equations of motion are governed by the Euler-Lagrange equations [190]:

$$\frac{d}{dt}\left(\frac{\partial \mathcal{L}(q, \dot{q})}{\partial \dot{q}}\right) - \frac{\partial \mathcal{L}(q, \dot{q})}{\partial q} = \mathbf{B}_u u. \tag{5.1}$$

Specifically, since we consider *mechanical* systems, the Lagrangian is taken as difference between the kinetic- and potential energy of the system, namely, $\mathcal{L}(q, \dot{q}) := \frac{1}{2}\dot{q}^T \mathbf{M}(q)\dot{q} - V(q)$. Here the smooth, scalar function $q \mapsto V(q)$ denotes the system's potential energy, while $\mathbf{M}(\cdot) \in \mathbb{M}^{n_q}_{\succ 0}$ denotes the smooth inertia matrix, whose ij-th element we denote by $\mathfrak{m}_{ij}(\cdot)$. This allows us to equivalently rewrite (5.1) in the commonly used *manipulator form*:

$$\mathbf{M}(q)\ddot{q} + \mathbf{C}(q, \dot{q})\dot{q} + \mathbf{G}(q) = \mathbf{B}_u u. \tag{5.2}$$

Here $\mathbf{G}(q) = \mathrm{col}(\partial V(q)/\partial q_1, \dots, \partial V(q)/\partial q_{n_q})$ is the vector of potential forces, e.g., gravitation forces; the matrix function $\mathbf{C}(q, \dot{q})$ corresponds to centrifugal and Coriolis terms, and can be partitioned into two parts,

$$\mathbf{C}(q, \dot{q}) = \mathbf{C}_1(q, \dot{q}) + \mathbf{C}_2(q, \dot{q}), \tag{5.3}$$

with the matrix functions $\mathbf{C}_1(\cdot)$ and $\mathbf{C}_2(\cdot)$ given by[2]

$$\mathbf{C}_1(q, \dot{q}) := \frac{d}{dt}\mathbf{M}(q) = \sum_{i=1}^{n_q} \frac{\partial \mathbf{M}(q)}{\partial q_i}\dot{q}_i, \tag{5.4a}$$

$$\mathbf{C}_2(q, \dot{q}) := -\frac{\partial^2 \mathcal{K}}{\partial \dot{q} \partial q} = -\frac{1}{2}\left[\frac{\partial \mathbf{M}(q)}{\partial q_1}\dot{q} \quad , \quad \dots \quad , \quad \frac{\partial \mathbf{M}(q)}{\partial q_{n_q}}\dot{q}\right]^{\mathsf{T}}. \tag{5.4b}$$

[2]Defining the matrix function $\mathbf{C}(\cdot)$ according to (5.3)-(5.4) will not in general guarantee that $\mathbf{N}(q, \dot{q}) := \dot{\mathbf{M}}(q) - 2\mathbf{C}(q, \dot{q})$ is skew symmetric; see, e.g. [190].

Note that by letting $x := \mathrm{col}(x_1, x_2) = \mathrm{col}(q, \dot{q})$ denote the state vector, such that the state space is $\mathbb{R}^n$ with $n := 2n_q$, then (5.2) can in turn be written in the form (4.1), i.e., $\dot{x} = f(x) + B(x)u$, by defining

$$f(x) := \begin{bmatrix} x_2 \\ -\mathbf{M}^{-1}(x_1)\left[\mathbf{C}(x_1, x_2)x_2 + \mathbf{G}(x_1)\right] \end{bmatrix}, \quad B(x) := \begin{bmatrix} \mathbf{0}_{n_q \times m} \\ \mathbf{M}^{-1}(x_1)\mathbf{B}_u \end{bmatrix}.$$

We will assume that the matrix functions in (5.2) satisfy the following properties, which are known to cover a large class of mechanical systems [190–192]:

Assumption 5.1. The following properties hold for the mechanical system (5.2):

i) $\mathbf{M}(q)$ is bounded, i.e. $\lambda_m \mathbf{I}_{n_q} \leq \mathbf{M}(q) \leq \lambda_M \mathbf{I}_{n_q}$ for all $q \in \mathbb{R}^{n_q}$, where the positive constants λ_m and λ_M denote the smallest and largest eigenvalues of $\mathbf{M}(q)$ for all $q \in \mathbb{R}^{n_q}$, respectively;

ii) $\mathbf{C}(q, \dot{q})$ satisfies the following properties: 1) $\mathbf{C}(q, \mathbf{z})\mathbf{y} = C(q, \mathbf{y})\mathbf{z}$; 2) $\|\mathbf{C}(q, \mathbf{z})\| \leq k_C \|\mathbf{z}\|$; and 3) $\mathbf{C}(q, a\mathbf{z}) = a\mathbf{C}(q, \mathbf{z})$, holding for all $q, \mathbf{z}, \mathbf{y} \in \mathbb{R}^{n_q}$, some constant $k_C > 0$ and any $a \in \mathbb{R}$;

iii) $\mathbf{G}(q)$ is upper and lower bounded for all $q \in \mathbb{R}^{n_q}$, i.e. there exists a scalar $g_M > 0$ such that $\|\mathbf{G}(q)\| \leq g_M$ for all $q \in \mathbb{R}^{n_q}$.

Another important characteristic of the system (5.1) is its degree of actuation: The system is said to be: *underactuated* if $m < n_q$, with degree of underactuation $n_q - m$; *fully actuated* if $m = n_q$; while it is said to be *redundantly actuated* if $m > n_q$. While we will mainly focus on *underactuated* mechanical control systems in this chapter, it is nevertheless important to note that the methods we will develop, especially those in Section 5.4, are also applicable to the other two classes as well.

5.3 Orbit generation using synchronization functions

Our main aim in this section will be to generate a non-trivial periodic orbit of (5.2) corresponding to an s-parameterized maneuver as by Definition 3.2.

Problem 5.2. *For $\mathcal{S} := [0, s_T) \subset \mathbb{R}_{\geq 0}$, find smooth, s_T-periodic functions*

$$x_s : \mathcal{S} \to \mathbb{R}^n, \quad u_s : \mathcal{S} \to \mathbb{R}^n, \quad \text{and} \quad \rho : \mathcal{S} \to \mathbb{R}_{>0}, \tag{5.5}$$

corresponding to an s-parameterization of the closed maneuver

$$\mathcal{M} := \{(x, u) \in \mathbb{R}^n \times \mathbb{R}^m : \quad x = x_s(s), \quad u = u_s(s), \quad s \in \mathcal{S}\}$$

as by Definition 3.2. That is, $x_s : \mathcal{S} \to \mathbb{R}^n$ traces out a non-self-intersecting curve, while

$$\rho(s) > 0, \quad \|\mathcal{F}(s)\| > 0 \quad \textit{and} \quad \mathcal{F}(s)\rho(s) = f(x_s(s)) + B(x_s(s))u_s(s),$$

hold for all $s \in \mathcal{S}$, where $\mathcal{F}(s) := x_s'(s) = \frac{d}{ds}x_s(s)$.

In order to solve Problem 5.2, we will propose a method heavily inspired by the *virtual holonomic constraints* approach of [33, 138]. We will however avoid using the terminology "virtual (holonomic) constraints", as our main aim is not the strict enforcement of such constraints per se. Indeed, this would correspond to ensuring the invariance of the so-called *constraint manifold* associated with the virtual constraints (see, e.g., [139]). Rather, we are looking to find a vector of so-called *synchronization functions*, whose sole purpose is to aid us in the search for an orbit of the mechanical system, which we later aim to stabilize using, for example, the techniques we considered in the previous chapter.

While we will mainly focus on periodic orbits in this chapter, it is important to note that the methods we will introduce in the following sections will also allow us to construct other types of orbits (maneuvers) as well (see, e.g., Sec. 5.3.4), which will be readily applied and orbitally stabilized in later chapters.

5.3.1 Synchronization functions

Since the mechanical system (5.2) is a second-order system, it is clear that for any smooth s-parameterized maneuver of this system (see Def. 3.2), the function $x_s : \mathcal{S} \to \mathcal{O}$ can be written in the following form:

$$x_s(s) := \mathrm{col}\big(\Phi(s), \Phi'(s)\rho(s)\big). \tag{5.6}$$

Here $\Phi(s) = \mathrm{col}(\phi_1(s), \dots, \phi_{n_q}(s))$ is a smooth vector-valued function such that $x_s(\cdot)$ traces out a (periodic or injective) curve in the state space of the system. As one may consider the generalized coordinates as being synchronized when confined to this curve, we will refer to the smooth scalar functions $\phi_i(\cdot)$ as *synchronization functions*. Moreover, the scalar function $\rho : \mathcal{S} \to \mathbb{R}_{\geq 0}$ may now, in addition to governing the dynamics of the curve parameter $s = s(t)$ through

$$\dot{s} = \rho(s),$$

be considered as to set the speed at which the curve formed by $\Phi(\cdot)$ is traversed.

Let us derive conditions upon $\Phi : \mathcal{S} \to \mathbb{R}^{n_q}$ which are necessary for it to correspond to a solution to Problem 5.2, beginning with $\|\mathcal{F}(s)\| > 0$. By direct calculation, one finds that

$$\|\mathcal{F}(s)\|^2 = \left\|\Phi'(s)\right\|^2 + \left\|\Phi''(s)\rho(s) + \Phi'(s)\rho'(s)\right\|^2. \tag{5.7}$$

For $\|\mathcal{F}(s)\| > 0$ to hold, it is clearly sufficient that

$$\|\Phi'(s)\|^2 + \|\Phi''(s)\|^2\rho^2(s) > 0 \quad \iff \quad \|\Phi'(s)\|^2 + \|\Phi''(s)\|^2 > 0, \tag{5.8}$$

which is a direct consequence of the requirement that $\rho(s) > 0$ for all $s \in \mathcal{S}$.

The next condition which needs to be satisfies is $\mathcal{F}(s)\rho(s) = f(x_s(s)) + B(x_s(s))u_s(s)$ for all $s \in \mathcal{S}$. This corresponds to the s-parameterized maneuver

$$\mathcal{M} = \{(x, u) \in \mathbb{R}^n \times \mathbb{R}^m : \ x = x_s(s), \quad u = u_s(s), \quad s \in \mathcal{S}\} \tag{5.9}$$

being consistent with the dynamics (5.2). Due to the particular structure of the vector-valued function $x_s(\cdot)$, this, in turn, is equivalent to the possibility of rendering the maneuver's orbit, given by

$$\mathcal{O} = \left\{(q, \dot{q}) \in \mathbb{R}^{n_q} \times \mathbb{R}^{n_q} : \ q = \Phi(s), \quad \dot{q} = \Phi'(s)\rho(s), \quad s \in \mathcal{S}\right\}, \tag{5.10}$$

(positively) invariant with respect to (5.2). For this to be the case, it is clear that the triplet (Φ, u_s, ρ) must satisfy, for all $s \in \mathcal{S}$, the relation

$$\mathfrak{A}(s)\rho'(s)\rho(s) + \mathfrak{B}(s)\rho^2(s) + \mathfrak{G}(s) = \mathbf{B}_u u_s(s), \tag{5.11}$$

where

$$\mathfrak{A}(s) := \mathbf{M}\big(\Phi(s)\big)\Phi'(s), \tag{5.12a}$$
$$\mathfrak{B}(s) := \mathbf{M}\big(\Phi(s)\big)\Phi''(s) + \mathbf{C}\big(\Phi(s), \Phi'(s)\big)\Phi'(s), \tag{5.12b}$$
$$\mathfrak{G}(s) := \mathbf{G}\big(\Phi(s)\big). \tag{5.12c}$$

For later, we note here that, by defining $\mathfrak{D}(s) := \mathbf{C}_2(\Phi(s), \Phi'(s)\big)\Phi'(s)$, i.e.

$$\mathfrak{D}(s) = -\frac{1}{2}\operatorname{col}\Bigg(\left\langle \Phi'(s), \left(\frac{\partial \mathbf{M}}{\partial q_1}\big(\Phi(s)\big)\right)\Phi'(s)\right\rangle, \dots \tag{5.13}$$
$$\dots, \left\langle \Phi'(s), \left(\frac{\partial \mathbf{M}}{\partial q_{n_q}}\big(\Phi(s)\big)\right)\Phi'(s)\right\rangle\Bigg),$$

then

$$\mathfrak{B}(s) = \mathfrak{A}'(s) + \mathfrak{D}(s). \tag{5.14}$$

Now, recall that $\mathbf{B}_u$ is assumed to have full rank. This implies that it has a family of full-rank left inverses, including its unique pseudoinverse $\mathbf{B}_u^{\dagger} := (\mathbf{B}_u^{\mathsf{T}}\mathbf{B}_u)^{-1}\mathbf{B}_u^{\mathsf{T}} \in \mathbb{R}^{n_q \times m}$. Since $\mathbf{B}_u^{\dagger}\mathbf{B}_u = \mathbf{I}_m$, the following is readily obtained by multiplying (5.11) from the left by $\mathbf{B}_u^{\dagger}$:

Lemma 5.3. *Suppose $\Phi \in \mathcal{C}^{\infty}(\mathcal{S}, \mathbb{R}^{n_q})$ and $\rho \in \mathcal{C}^{\infty}(\mathcal{S}, \mathbb{R}_{\geq 0})$ are known, and correspond to an s-parameterized maneuver $\mathcal{M}$ (see* (5.9)*) of* (5.2)*. Then*

$$u_s(s) = \mathbf{B}_u^{\dagger}\left[\mathfrak{A}(s)\rho'(s)\rho(s) + \mathfrak{B}(s)\rho^2(s) + \mathfrak{G}(s)\right] \tag{5.15}$$

corresponds to the function $u_s : \mathcal{S} \to \mathbb{R}^m$ on the maneuver. □

The key observation to be made from the above lemma is simply that a maneuver of the mechanical system (5.2) may be completely determined from the pair (Φ, ρ). Moreover, if the system is either fully- or redundantly actuated, i.e. $m \geq n_q$, then any such pair will in fact correspond to a feasible maneuver of (5.2); although note that it might not correspond to an orbit, as such a maneuver can then have self-intersections.[3] Further note that (5.15) may also be valid for certain non-smooth, continuous maneuvers. For instance, one may only require that $\rho(s)$ and the product $\rho'(s)\rho(s)$ are continuous on $\mathcal{S}$ (see the terminal sliding mode example in Section 3.3).

The reduced dynamics

While one in the fully-actuated case is more or less free to choose any pair (Φ, ρ) to construct a maneuver simply by taking u_s according to (5.15), only very specific such pairs correspond to a maneuver for an underactuated system. To demonstrate this fact for $m < n_q$, let $\mathbf{B}_u^{\perp} \in \mathbb{R}^{(n_q - m) \times n_q}$ denote some full-rank left annihilator of $\mathbf{B}_u \in \mathbb{R}^{n_q \times m}$, that is

$$\mathbf{B}_u^{\perp}\mathbf{B}_u = \mathbf{0}_m. \tag{5.16}$$

By multiplying both sides of (5.11) from the left by $\mathbf{B}_u^{\perp}(s)$, we obtain

$$\mathbf{B}_u^{\perp}\left[\mathfrak{A}(s)\rho'(s)\rho(s) + \mathfrak{B}(s)\rho^2(s) + \mathfrak{G}(s)\right] = \mathbf{0}_{m \times 1}. \tag{5.17}$$

Denoting by $\mathbf{b}_i^{\perp}$ the i-th row of $\mathbf{B}_u^{\perp}$, we can rewrite this as

$$\alpha_i(s)\rho'(s)\rho(s) + \beta_i(s)\rho^2(s) + \gamma_i(s) = 0, \quad i = 1, 2, \ldots, m, \tag{5.18}$$

[3] As the distance to the state curve of a maneuver with self-intersections will not everywhere be well defined, one cannot directly utilize the scheme we proposed in Chapter 4 based on transverse coordinates and projections operators. Note, however, that this can be resolved by allowing the projection operator to have memory; see Section 9.3.

where

$$\alpha_i(s) := \mathbf{b}_i^{\perp}\mathfrak{A}(s) \quad \beta_i(s) := \mathbf{b}_i^{\perp}\mathfrak{B}(s), \quad \text{and} \quad \gamma_i(s) := \mathbf{b}_i^{\perp}\mathfrak{G}(s). \tag{5.19}$$

Note here from (5.14) that

$$\beta_i(s) = \alpha_i'(s) + \delta_i(s) \quad \text{with} \quad \delta_i(s) := \mathbf{b}_i^{\perp}\mathfrak{D}\big(\Phi(s), \Phi'(s)\big). \tag{5.20}$$

The m equations in (5.18) can be considered as dynamical constraints which arise due to the system's underactuation, and which effectively impose restrictions upon which pairs (Φ, ρ) that correspond to feasible behaviors of the controlled mechanical system (5.2). We summarize the above in the next statement (see also Lemma 1 in [34] for a similar statement).

Proposition 5.4. *Consider a mechanical system* (5.2) *with* $n_q - m$ *degrees of underactuation. The smooth triplet* (x_s, u_s, ρ) *defined in* (5.5) *corresponds to an s-parameterized maneuver of this system on* $\mathcal{S}$ *if* $x_s(\cdot)$ *satisfies* (5.7), $u_s(\cdot)$ *satisfies* (5.15), *and the m equations in* (5.18) *hold for all* $s \in \mathcal{S}$. □

The method we propose for constructing such a (not necessarily periodic) maneuver involves three intertwined steps:

Step 1 Take the elements of $\Phi(s) = \mathrm{col}(\phi_1(s), \ldots, \phi_{n_q}(s))$ as the sum of a finite number of smooth basis functions (e.g. polynomials of some kind) which depend on a set of coefficients;

Step 2 For a specific choice of the coefficients of each $\phi_i(\cdot)$, search for a sufficiently smooth function $\rho : \mathcal{S} \to \mathbb{R}_{\geq 0}$ satisfying the m equations in (5.18) for all $s \in \mathcal{S}$;

Step 3 If such a function $\rho(\cdot)$ is found, take $u_s(\cdot)$ according to (5.15).

A key part of the procedure involves finding the function $\rho(\cdot)$ which should be strictly positive everywhere, except, possibly, at certain isolated points where all the functions $\gamma_i(\cdot)$ simultaneously vanish. In order to help us find such a function, we will make use of the following fact: For (5.18) to hold, any solution $s = s(t) \in \mathcal{S}$ of $\dot{s} = \rho(s)$ must also be the solution to the second-order equations

$$\alpha_i(s)\ddot{s} + \beta_i(s)\dot{s}^2 + \gamma_i(s) = 0, \quad i = 1, 2, \ldots, m, \tag{5.21}$$

where $\alpha_i(\cdot)$, $\beta_i(\cdot)$ and $\gamma_i(\cdot)$ are defined as in (5.19). We refer to the equations (5.21) as the *reduced dynamics* associated with the vector-valued function $\Phi(\cdot)$. Due to the significance of these equations, we will study some key properties of this type of second-order differential equation next.

5.3.2 Properties of the reduced dynamics

Consider the scalar second-order differential equation

$$\alpha(s)\ddot{s} + \beta(s)\dot{s}^2 + \gamma(s) = 0 \quad \text{where} \quad \beta(s) = \alpha'(s) + \delta(s). \tag{5.22}$$

If not otherwise stated, we will for simplicity's sake assume that α, δ and γ are all smooth functions on $\mathcal{S}$. Note, however, that when these functions correspond to the reduced dynamics (5.18), the functions $\alpha(\cdot)$, $\delta(\cdot)$ and $\gamma(\cdot)$ inherits the properties of $\Phi(\cdot)$, and are thus smooth if $\Phi(\cdot)$ is smooth.

As previously stated, or aim is to utilize the properties of the scalar second-order equation (5.22) in order to find a smooth scalar function $\rho : \mathcal{S} \to \mathbb{R}_{\geq 0}$, such that

$$\alpha(s)\rho'(s)\rho(s) + \beta(s)\rho^2(s) + \gamma(s) = 0 \tag{5.23}$$

holds for all $s \in \mathcal{S}$. That is, a solution $s = s(t) \in \mathcal{S}$ to

$$\dot{s} = \rho(s)$$

is also a solution to (5.22). To this end, we will in the following study some of the key properties of (5.22), most of which building upon or restating previously reported results (see, e.g., [33, 138, 193]), including its equilibrium points, singular points, and its integrability.

Equilibrium points

Let $s_e \in \mathcal{S}$ be an equilibrium point of (5.22), that is $\gamma(s_e) \equiv 0$. We may always associate with such a point a trivial solution to (5.23), namely a function $\rho(\cdot)$ for which $\rho(s_e) = 0$. Differentiating (5.23) with respect to s and evaluating it at $s = s_e$ for $\rho(s_e) = 0$, we find that

$$\alpha(s_e)(\rho'(s_e))^2 + \gamma'(s_e) = 0.$$

Hence if $\alpha(s_e) \neq 0$, then $\rho(s_e) \equiv 0$ can only occur at s_e if the function

$$\nu(s) := \gamma'(s)/\alpha(s) \tag{5.24}$$

satisfies $\nu(s_e) \leq 0$. We may also study the properties of such an equilibrium, specifically the *type* of the equilibrium (see, e.g, [23, Sec. 20] or [194]), by looking at the linear system

$$\ddot{z} = -\nu(s_e)z$$

obtained from the Jacobian linearization of (5.22) about $(s, \dot{s}) = (s_e, 0)$. The eigenvalues of this linear system are $\lambda = \pm\sqrt{-\nu(s_e)}$. Hence, by the Hartman–Grobman theorem (see Sec. 2.3), the equilibrium is a saddle point if $\mu(s_e) < 0$, while it has been shown in [138] (see Thm. 3 therein) that it is a center if $\nu(s_e) > 0$. This is summarized in the next statement.

Lemma 5.5 ([138]). *Let $s_e \in \mathcal{S}$ be an equilibrium point of* (5.22) *i.e.* $\gamma(s_e) \equiv 0$, *satisfying* $\alpha(s_e) \neq 0$. *Then s_e is a center if $\nu(s_e) > 0$ or a saddle if $\nu(s_e) < 0$.* □

Integrability

An important property of the equation (5.23) is the fact that it is integrable, with the integrating factor given by

$$\mu(s_r, s) := \frac{1}{2}\alpha(s)\Psi(s_r, s) \quad \text{with} \quad \Psi(s_r, s) := \exp\left\{\int_{s_r}^{s} \frac{2\delta(\sigma)}{\alpha(\sigma)} d\sigma\right\} \tag{5.25}$$

for any $s_r \in \mathcal{S}$. Namely, if $s = s(t)$ is a solution to (5.22) satisfying $s(t_0) = s_0$, then multiplying (5.22) by $\mu(s_0, s)$ yields

$$\mu(s_0, s)\left[\alpha(s)\ddot{s}^2 + \beta(s)\dot{s}^2 + \gamma(s)\right] = 0. \tag{5.26}$$

By using the identity $2\ddot{s} = \frac{d}{ds}\dot{s}^2$ [105, 138], the above is equivalent to

$$\frac{d}{ds}\left(\mu(s_0, s)\alpha(s)\dot{s}^2\right) + \mu(s_0, s)\gamma(s) = 0.$$

Denoting by $\dot{s}_0 = \dot{s}(t_0)$, and integrating the above over $[s_0, s]$, one obtains

$$\frac{1}{2}\Psi(s_0, s)\alpha^2(s)\dot{s}^2 - \frac{1}{2}\alpha^2(s_0)\dot{s}_0^2 + \int_{s_0}^{s} \Psi(s_0, \tau)\alpha(\tau)\gamma(\tau)d\tau \equiv 0. \tag{5.27}$$

Our aim will now be to use this relation to plan orbits of the reduced dynamics. In this regard, it is of course desirable that one can (numerically) compute the value of the expression on the left-hand side both accurately and effectively. However, due to the nested integrals appearing in the latter part of the expression, one generally needs to find a compromise between the speed and accuracy of the computation. Yet, it is important to note that for certain systems there are structural properties which can be exploited, with the perhaps most useful such property being the following:

$$\delta(s) = \beta(s) - \alpha'(s) \equiv 0 \quad \forall s \in \mathcal{S}. \tag{5.28}$$

Indeed, one can easily observe that this results in $\Psi(s) \equiv 1$ for all $s \in \mathcal{S}$, from which one can infer the following:

Lemma 5.6. *Suppose the condition* (5.28) *is satisfied for all $s \in \mathcal{S}$. Then*

$$\frac{1}{2}\alpha^2(s)\dot{s}^2 - \frac{1}{2}\alpha^2(s_0)\dot{s}_0^2 + \int_{s_0}^{s} \alpha(\tau)\gamma(\tau)d\tau \equiv 0 \tag{5.29}$$

is equivalent to (5.27). □

The expression (5.29) is quite useful in the sense that, even if one cannot compute its value analytically, one can nevertheless obtain an accurate approximate value both fast and effectively using some numerical quadrature, for example some Gaussian quadrature rule [195]. Indeed, we will later utilize this property in Chapter 7 to derive an optimization-based procedure for constructing periodic orbits of a class of hybrid mechanical systems.

In light of this, it is natural to ask: when does the (5.28) condition actually occur? To provide an answer to this question, we first observe from (5.20) that $\delta(\cdot)$ is a linear combination of the elements of $\mathfrak{D}(\cdot)$ (see (5.13)). Since the i-th row of $\mathfrak{D}(\cdot)$ has quadratic form with respect to $\partial \mathbf{M}(q)/\partial q_i$, it is evident that the conditions will be trivially true for all flat systems (i.e., systems whose inertia matrix $\mathbf{M}(\cdot)$ is constant). Furthermore, the condition will also hold for all systems with one degree of underactuation if its passive degree of freedom is the first in its kinematic chain; see [99, Proposition B.10]. This, in turn, corresponds to underactuated systems of Class-I according to the classification of Olfati-Saber [10].

Returning to the general expression (5.27), note that it is has a Lagrangian structure [196, 197]. Indeed, by defining, for any $s_0 \in \mathcal{S}$, the Lagrangian $\mathcal{L}_r = \mathcal{L}_r(s, \dot{s})$ by

$$\mathcal{L}_r = \frac{1}{2}\Psi(s_0, s)\alpha^2(s)\dot{s}^2 - \int_{s_0}^{s} \Psi(s_0, \tau)\alpha(\tau)\gamma(\tau)d\tau,$$

then (5.26) is clearly obtained by the Euler-Lagrange equation

$$\frac{d}{dt}\left(\frac{\partial \mathcal{L}_r}{\partial \dot{s}}\right) - \frac{\partial \mathcal{L}_r}{\partial s} = 0.$$

A key question which needs to be answered is then whether a solution to (5.26) corresponds to a solution to the reduced dynamics (5.22), and vice versa.[4] The following statement immediately provides an answer to the latter.

Theorem 5.7 ([33, 105])**.** *Suppose the function $\alpha : \mathcal{S} \to \mathbb{R}$ only vanishes at isolated points on $\mathcal{S}$. If the solution $(s(t), \dot{s}(t)) \in \mathcal{S} \times \mathbb{R}$ of* (5.22) *exists and is continuously differentiable, then* (5.27) *holds along this solution.* □

The main importance of Theorem 5.7 is due to the fact that it may be used to construct a single transverse coordinate (see, e.g., [33, 34, 198]).

[4] Although we only consider $\mathcal{S} \subseteq \mathbb{R}$ in this thesis, it is important to note that if, say, $\mathcal{S} = \mathbb{S}^1$ instead, then the relation between solutions of (5.26) and (5.22) is somewhat more intricate; see [140, 197].

However, as we have previously stated, rather than exploiting the integrability of the reduced dynamics to construct a transverse coordinate, we are in this thesis instead mainly interested in using this property to construct a particular solution corresponding to $\dot{s} = \rho(s) \geq 0$. Thus, to this end, we define, for some $a, b \in \mathbb{R}_{\geq 0}$, the function

$$I(s_a, s_b, a, b) := \Psi(s_a, s_b)\alpha^2(s_b)b^2 - \alpha^2(s_a)a^2 + 2\int_{s_a}^{s_b} \Psi(s_a, \tau)\alpha(\tau)\gamma(\tau)d\tau. \tag{5.30}$$

As the following statement then demonstrates, whenever the integrating factor is nonzero and well defined, we can evaluate (5.27) over a given interval by evaluating (5.30) on a series of subintervals.

Lemma 5.8. *For $s_a, s_b, s_c \in \mathcal{S}$, $s_a \leq s_b \leq s_c$, and $a, b, c \in \mathbb{R}_{\geq 0}$,*

$$I(s_a, s_c, a, c) = I(s_a, s_b, a, b) + \Psi(s_a, s_b)I(s_b, s_c, b, c) \tag{5.31}$$

holds for the function $I(\cdot)$ defined in (5.30).

Proof. By the definition of $\Psi(\cdot)$ (see (5.25)) it follows that

$$\Psi(s_a, s_c) = \Psi(s_a, s_b)\Psi(s_b, s_c),$$

and therefore

$$\begin{aligned}\int_{s_a}^{s_c} \Psi(s_a, \tau)r(\tau)d\tau &= \int_{s_a}^{s_b} \Psi(s_a, \tau)r(\tau)d\tau + \int_{s_b}^{s_c} \Psi(s_a, \tau)r(\tau)d\tau \\ &= \int_{s_a}^{s_b} \Psi(s_a, \tau)r(\tau)d\tau + \Psi(s_a, s_b)\int_{s_b}^{s_c} \Psi(s_b, \tau)r(\tau)d\tau\end{aligned}$$

where $r(\tau) := \alpha(\tau)\gamma(\tau)$. Hence, by adding and subtracting $\Psi(s_a, s_b)\alpha^2(s_b)b^2$ to the expression for $I(s_a, s_c, a, c)$, the relation (5.31) follows. $\square$

Using the function $I(\cdot)$ defined in (5.30), the question related to orbit generation which we are interested in answering may then be restated as follows: If

$$I(s_a, s_b, a, b) \equiv 0$$

for $[s_a, s_b] \subseteq \mathcal{S}$ and some $a, b \in \mathbb{R}_{\geq 0}$, does this this imply the existence of a smooth function $\rho : \mathcal{S} \to \mathbb{R}_{\geq 0}$, for which $\rho(s_a) = a$ and $\rho(s_b) = b$, that satisfies (5.23) for all $s \in [s_a, s_b]$? Essentially, this may viewed as the converse to the question which Theorem 5.7 answers. If it is true, then

$$\Psi(s_0, s)\alpha^2(s)\rho^2(s) - \alpha^2(s_0)\rho^2(s_0) + 2\int_{s_0}^{s} \Psi(s_0, \tau)\alpha(\tau)\gamma(\tau)d\tau \equiv 0 \tag{5.32}$$

holds for any pair of points $s_0, s \in [s_a, s_b]$. An answer is most easily obtained if $\alpha(s)$ does not vanish on $[s_a, s_b]$. Indeed, the reduced dynamics may then be viewed as a conservative, one-degree-of-freedom mechanical system [197], with $\frac{1}{2}\Psi(s_0, s)\alpha^2(s)\dot{s}^2$ its kinetic energy and $\Psi(s_0, s)\alpha(s)\gamma(s)$ the gradient of its potential energy. The equality (5.27) may then, in turn, be viewed as the conservation of energy along the solutions of this system:

Lemma 5.9. *If $\alpha(s) \neq 0$ on $[s_a, s_b] \subset \mathbb{R}$ and $I(s_a, s_b, a, b) \equiv 0$ for some $a, b \in \mathbb{R}_{\geq 0}$, with $I(\cdot)$ defined in* (5.30)*, then*

$$\rho(s) = \sqrt{\frac{\Psi^{-1}(s_a, s)}{\alpha^2(s)} \left[\alpha^2(s_a)a^2 - 2\int_{s_a}^{s} \Psi(s_a, \tau)\alpha(\tau)\gamma(\tau)d\tau\right]} \tag{5.33}$$

satisfies (5.23) *for all $s \in [s_a, s_b]$, as well as $\rho(s_a) = a$ and $\rho(s_b) = b$. If, moreover, $\rho(s) > 0$ for all $s \in [s_a, s_b]$, then $\rho(\cdot)$ is smooth on $[s_a, s_b]$.*

Remark 5.10. While (5.33) ensures that ρ is locally Lipschitz on the given interval, it is important to remark that it may not be everywhere smooth (or even $\mathcal{C}^1$) as it can enter into- and then leave a saddle point. For example, the function $\rho(s) = \sqrt{2(s - 1 + e^{-s})}$ satisfies

$$\rho'(s)\rho(s) + \frac{1}{2}\rho^2(s) - s = 0$$

for all $s \in \mathbb{R}$, but its derivative is discontinuous at the origin even though $\rho'(s)\rho(s) = 1 - e^{-s}$ is smooth.

Proof. That $\rho(s_a) = a$ and $\rho(s_b) = b$ is obvious. Differentiating (5.33) one finds that

$$2\Psi(s_a, s)\alpha(s)\left(\alpha(s)\rho'(s)\rho(s) + \beta(s)\rho^2(s) + \gamma(s)\right) = 0.$$

The condition $\alpha(s) \neq 0$ guarantees that $\Psi(s_a, s)$ will be nonzero and continuously differentiable (and therefore bounded) on the given interval. Hence (5.23) must hold. The smoothness of $\rho(\cdot)$ on $[s_a, s_b]$ follows directly from (5.23) and its derivative. □

In order to provide a more general answer, we also need to address the case when $\alpha(s)$ vanishes at certain points. Such points are referred to as *singular points* of (5.22). Clearly, their existence generally causes a vertical asymptote in the phase plane of (5.22) which no solution can cross. We are therefore looking to find conditions which ensures that there exists a "bridge" along which at least one solution of (5.22) can cross the asymptote. Moreover, we want to determine if it is still sufficient that $I(s_a, s_b, a, b) \equiv 0$ for a solution of the form (5.33) to exist. We consider next a particular family of such points.

Simple singular points

As previously stated, a singular point $s_s \in \mathcal{S}$ of (5.22) is a point at which $\alpha(s_s) = 0$. Supposing that (5.22) has a monotonically increasing solution $s = s(t)$ that also satisfies $\dot{s} = \rho(s)$, then

$$\beta(s_s)\rho^2(s_s) + \gamma(s_s) = 0$$

must hold at any such point. Since we require $\rho \in \mathbb{R}_{\geq 0}$, this implies

$$\rho(s_s) = \sqrt{\frac{-\gamma(s_s)}{\beta(s_s)}} = \sqrt{\frac{-\gamma(s_s)}{\delta(s_s) + \alpha'(s_s)}}. \tag{5.34}$$

Excluding the cases when s_s is an equilibrium of (5.22), i.e. we assume $|\gamma(s_s)| > 0$, then we can infer that the inequality

$$\gamma(s_s)\big(\delta(s_s) + \alpha'(s_s)\big) < 0 \tag{5.35}$$

must necessarily hold.

Another key question relating to singular points is what happens with the integrating factor (5.25) at such a point. Namely, do both of the limits $\lim_{s\to s_s^\pm} \mu(s\pm\epsilon, s) = 2^{-1} \lim_{s\to s_s^\pm} \big(\alpha(s_s)\Psi(s\pm\epsilon, s)\big)$ exist for some $\epsilon > 0$, and are they finite? Clearly this will be the case if $\lim_{s\to s_s} \Psi(s_r, s)$ is non-zero and finite. This, in turn, is ensured if s_s is a so-called *simple singular point*.

Definition 5.11 (Simple singular point)**.** A singular point $s_s \in \mathcal{S}$ of (5.22), i.e. $\alpha(s_s) \equiv 0$, where (5.35) holds is said to be *simple* if $\alpha'(s_s) \neq 0$ (i.e. it is isolated) and $\lim_{s\to s_s} \big[\delta(s)/\alpha(s)\big]$ exists and is finite.

Let $s = s(t)$, $s(t_0) = s_0$, be a monotonically increasing, twice continuously differentiable solution of (5.22), which at some time instant t_s crosses a simple singular point, i.e. $s(t_s) = s_s$. By Theorem 5.7, this implies

$$\frac{1}{2}\alpha^2(s_0)\dot{s}^2(t_0) - \int_{s_0}^{s_s} \Psi(s_0, \tau)\alpha(\tau)\gamma(\tau)d\tau \equiv 0.$$

Since it is monotonically increasing, there is a $\rho \in \mathcal{C}^1(\mathcal{S}, \mathbb{R}_{\geq 0})$ such that $\dot{s} = \rho(s)$. In fact, due to the above equality, we may in fact take ρ according to (5.35), as by L'Hôpital's rule:

$$\begin{aligned}
\lim_{s\to s_s} \rho^2(s) &= \lim_{s\to s_s} \frac{\Psi^{-1}(s_0, s)}{\alpha^2(s)} \left[\alpha^2(s_0)\rho^2(s_0) - 2\int_{s_0}^{s} \Psi(s_0, \tau)\alpha(\tau)\gamma(\tau)d\tau\right] \\
&= \lim_{s\to s_s} \frac{\frac{d}{ds}\big[\alpha^2(s_0)\rho^2(s_0) - 2\int_{s_0}^{s} \Psi(s_0, \tau)\alpha(\tau)\gamma(\tau)d\tau\big]}{\frac{d}{ds}\big[\Psi(s_0, s)\alpha^2(s)\big]} \\
&= -\frac{\gamma(s_s)}{\beta(s_s)}.
\end{aligned} \tag{5.36}$$

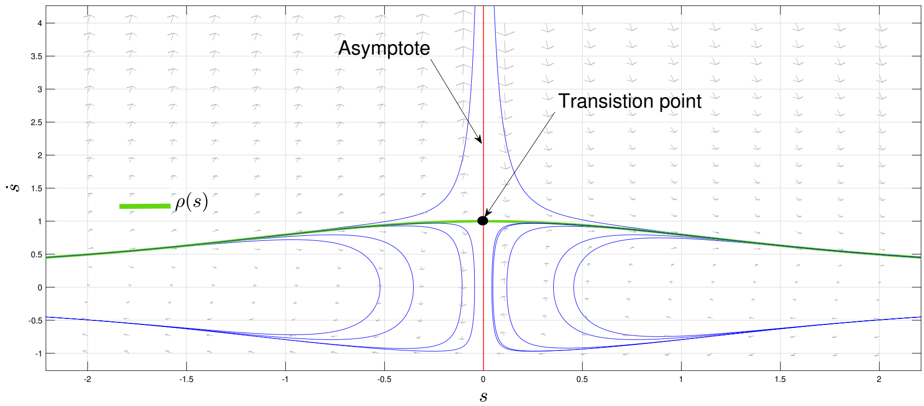

Figure 5.1: Shows the unique positive solution crossing the vertical asymptote corresponding to the simple singular point considered in Example 5.1.

Hence (5.34) is not violated.

It is also important to note that, in order to find $\rho'(s_s)$, one can compute the derivative of (5.23):

$$\alpha\rho''\rho + \alpha(\rho')^2 + \big(3\alpha' + 2\delta\big)\rho'\rho + \big(\alpha'' + \delta'\big)\rho^2 + \gamma' = 0,$$

where we have omitted the s-argument to shorten the notation. At the singular point, this reduces to

$$\big(3\alpha'(s_s) + 2\delta(s_s)\big)\rho'(s_s)\rho(s_s) + \big(\alpha''(s_s) + \delta'(s_s)\big)\rho^2(s_s) + \gamma'(s_s) = 0. \quad (5.37)$$

If here $3\alpha'(s_s)+2\delta(s_s) \equiv 0$ as well, then one computes the second derivative, and so on, until the coefficient in front of $\rho'(s_s)$ is nonzero.

In light of this, one might therefore wonder if a solution of the form (5.33) as in Lemma 5.9 can be found if the interior of the interval $[s_a, s_b]$ also contains a simple singular point? As the following example demonstrates, the answer to this question is in fact both yes and no.

Example 5.1. Consider the second-order system

$$s\ddot{s} + (1+s^2)\dot{s}^2 - 1 = 0$$

corresponding to the reduced dynamics (5.22) with $\alpha(s) = s$, $\delta(s) = s^2$ and $\gamma(s) = -1$. The point $s_s = 0$ is a simple singular point of this system: $\alpha(s_s) = 0$, $\alpha'(s_s) = 1$, $-\gamma(s_s)/\beta(s_s) = 1$ and $\delta(s)/\alpha(s) = s$. Moreover, since the function $\Psi(\cdot)$ defined in (5.25) is $\Psi(s_0, s) = e^{(s^2 - s_0^2)}$, the equality corresponding to (5.27) for this system is equivalent to

$$s^2 e^{(s^2-s_0^2)}\dot{s}^2 - s_0^2\dot{s}_0^2 + (1 - e^{(s^2-s_0^2)}) = 0.$$

Evaluating this at, say, $s = s_f = 1$ and $s_0 = -1$, we obtain $\dot{s}_f^2 = \dot{s}_0^2$. Thus, for any $\dot{s}_0 \geq 0$, one can always find some $\dot{s}(t)$ which makes the above equality hold even on the other side of the vertical asymptote caused by the singular point. However, as the previously attained identity $\dot{s}_f^2 = \dot{s}_0^2$ clearly shows, this will generally not correspond to a bounded orbit crossing the asymptote. In fact, even if the above equality is valid, it generally just implies the existence of two unbounded solutions which are mirrored about the vertical asymptote. Indeed, as can be seen in Figure 5.1, there exists one, and only one, bounded solution $s(t)$ which is monotonically increasing and which crosses the asymptote. This solution corresponds to the function $\rho(s) = \sqrt{(e^{s^2} - 1)/s^2 e^{s^2}}$, for which clearly $\lim_{s \to 0} \rho(s) = 1$.

Let us demonstrates the claims in the above example in a slightly more general and rigorous fashion. Specifically, let the interval $[s_a, s_b]$ contain a single simple singular point, s_s, on its interior, and suppose $I(s_a, s_b, a, b) \equiv 0$ for some $a, b \in \mathbb{R}_{\geq 0}$. Defining

$$\mathfrak{a}(x) := \frac{\Psi^{-1}(s_a, x)}{\alpha^2(x)} \left[\alpha^2(s_a) a^2 - 2 \int_{s_a}^{x} \Psi(s_a, \tau) \alpha(\tau) \gamma(\tau) d\tau \right],$$

$$\mathfrak{b}(y) := \frac{\Psi^{-1}(s_b, y)}{\alpha^2(y)} \left[\alpha^2(s_b) b^2 - 2 \int_{s_b}^{y} \Psi(s_b, \tau) \alpha(\tau) \gamma(\tau) d\tau \right],$$

one can easily validate that $\rho_a(s) = \mathfrak{a}(s)$ satisfies (5.23) on $[s_a, s_s)$, whereas $\rho_a(s) = \mathfrak{b}(s)$ satisfies (5.23) on $(s_s, s_b]$. We will show that while $I(s_a, s_b, a, b) \equiv 0$ in fact implies

$$\lim_{y \to s_s^+} \mathfrak{b}(y) - \lim_{x \to s_s^-} \mathfrak{a}(x) \equiv 0,$$

it does not necessarily imply that we can continuously merge the functions ρ_a and ρ_b into a single function ρ satisfying (5.23) on the whole of $[s_a, s_b]$. To this end, first note that $\alpha^2(s)$ is locally convex about s_s. Moreover, the terms inside the bracket in the expressions for the functions $\mathfrak{a}$ and $\mathfrak{b}$ are continuous, and their zero value would readily imply the limit in (5.36). In fact, due to Lemma 5.8, if either of the functions satisfy the latter case, then so does the other; that is, $\lim_{x \to s_s^-} \mathfrak{a}(x) = -\gamma(s_s)/\beta(s_s)$ if, and only if, $\lim_{y \to s_s^+} \mathfrak{b}(y) = -\gamma(s_s)/\beta(s_s)$. If, on the other hand, both of the terms inside the brackets are not zero, we may, due to the local convexity of α^2, replace the one-sided limits with two-sided limits in the above identity, such that we instead can check if $\lim_{s \to s_s} \mathfrak{b}(s) - \lim_{s \to s_s} \mathfrak{a}(s) \equiv 0$. Note that, since $\lim_{s \to s_s} \Psi^{-1}(s_b, s) = \Psi(s_s, s_b)$ and $\lim_{s \to s_s} \Psi^{-1}(s_a, s) = \Psi^{-1}(s_a, s_s)$, we may write

$$\mathfrak{b}(s) = \frac{\Psi^{-1}(s_a, s)}{\alpha^2(s)} \left[\Psi(s_a, s_b)\alpha^2(s_b)b^2 + 2\int_s^{s_b} \Psi(s_a, \tau)\alpha(\tau)\gamma(\tau)d\tau \right].$$

Adding and subtracting $\alpha^2(s_a)a^2 + 2\int_{s_a}^{2} \Psi(s_a, \tau)\alpha(\tau)\gamma(\tau)d\tau$ inside the brackets, this can be equivalently rewritten as

$$\mathfrak{b}(s) = \frac{\Psi^{-1}(s_a, s)}{\alpha^2(s)} \left[\alpha^2(s_a)a^2 - 2\int_{s_a}^{s} \Psi(s_a, \tau)\alpha(\tau)\gamma(\tau)d\tau \right],$$

where we have used that $I(s_a, s_b, a, b) \equiv 0$. Hence, $\lim_{s\to s_s} \mathfrak{b}(s) \equiv \lim_{s\to s_s} \mathfrak{a}(s)$. However, since $\alpha^2(s_a)a^2 - 2\int_{s_a}^{s_s} \Psi(s_a, \tau)\alpha(\tau)\gamma(\tau)d\tau$ is nonzero, the solutions on either side of the asymptote caused by the singular point are unbounded. We may from this conclude the following:

Proposition 5.12. *Let the interior of $\hat{\mathcal{S}} = [s_a, s_b] \subseteq \mathcal{S}$ contain a single simple singular point (see Def. 5.11. If $I(s_a, s_b, a, b) \equiv 0$ for some $a, b \in \mathbb{R}_{\geq 0}$, with $I(\cdot)$ given by* (5.30)*, then*

$$\rho(s) = \sqrt{\frac{2}{\alpha^2(s)} \int_s^{s_s} \Psi(s, \tau)\alpha(\tau)\gamma(\tau)d\tau} \tag{5.38}$$

satisfies (5.23) *for all $s \in [s_a, s_b]$. Moreover, $\rho(s_a) = a$ and $\rho(s_b) = b$ if*

$$\alpha^2(s_a)a^2 - 2\int_{s_a}^{s_s} \Psi(s_a, \tau)\alpha(\tau)\gamma(\tau)d\tau \equiv 0,$$

or equivalently $\alpha^2(s_b)b^2 - 2\int_{s_b}^{s_s} \Psi(s_b, \tau)\alpha(\tau)\gamma(\tau)d\tau \equiv 0$. □

From this, one can in turn deduce the following:

Corollary 5.13. *Let $\hat{s}_s$ and $\bar{s}_s$, $\hat{s}_s < \bar{s}_s$, denote two simple singular points of* (5.22)*, and suppose $\alpha(s) \neq 0$ for all $s \in (\hat{s}_s, \bar{s}_s)$. Then there exists a unique locally Lipschitz continuous function $\rho : [\hat{s}_s, \bar{s}_s] \to \mathbb{R}_{\geq 0}$ satisfying* (5.22) *on $[\hat{s}_s, \bar{s}_s]$ if $\int_{\hat{s}_s}^{\bar{s}_s} \Psi(\hat{s}_s, \tau)\alpha(\tau)\gamma(\tau)d\tau \equiv 0$.* □

Other types of singular points

In the case of simple singular points, we saw that there exists a unique (positive) solution of the reduced dynamics (5.22). As the following example demonstrates, there is also another family of feasible singular points. Unlike simple singular points, however, these points result in a loss of the uniqueness of the solutions to the reduced dynamics about them.

Example 5.2. Consider the following system:

$$s\ddot{s} + (1-d)\dot{s}^2 + 1 = 0.$$

It has a singular point at $s = s_s = 0$, and corresponds to (5.22) with $\alpha(s) = s$, $\delta(s) = -d$ and $\gamma(s) = 1$, such that $\alpha'(s_s) = 1$ and $-\gamma(s_s)/\beta(s_s) = 1/(d-1))$. Hence $d > 0$ is required (see (5.34)) for there to exist a transition point across the vertical asymptote at $s = s_s$. However, $\lim_{s\to s_s}(\delta(s)/\alpha(s))$ is clearly not well defined for this system, whereas

$$\Psi(s_0, s) = \exp\left\{2\int_{s_0}^{s} \frac{\delta(\tau)}{\alpha(\tau)} d\tau\right\} = \exp\left\{-2d\int_{s_0}^{s} \frac{1}{\tau} d\tau\right\} = \left(\frac{s_0}{s}\right)^{2d}$$

is unbounded when s approaches the singular point from either direction if $s_0 < 0$ for the left limit and $s_0 > 0$ for the right. We can nevertheless compute (5.27) everywhere else:

$$s^{(2-2d)}\dot{s}^2 - s_0^{(2-2d)}\dot{s}_0^2 + \frac{1}{1-d}\left[s^{(2-2d)} - s_0^{(2-2d)}\right].$$

For $d > 1$ we may therefore take

$$\rho(s) = \sqrt{s^{(2d-2)} s_0^{(2-2d)}\dot{s}_0^2 + \frac{1}{1-d}\left[s^{(2d-2)} s_0^{(2-2d)} - 1\right]}.$$

Note that then $\rho(s_s) = 1/\sqrt{d-1}$ regardless of the values of s_0 and $\dot{s}_0$. Differentiating the above expression with respect to s yields

$$\rho'(s) = \frac{1}{\rho(s)} s^{(2d-3)} s_0^{(2-2d)}\left[(d-1)\dot{s}_0^2 + 1\right].$$

Hence, we must further require that $d \geq 3/2$ for $\rho'(s)$ to be bounded at s_s, and $d > 3/2$ for it to be continuous.

The type of singular point considered in the above example has previously been considered by Surov and his collaborates in [193] (see also [199]). There, it was demonstrated that such singular points can be used to generate strange behaviors in mechanical systems, including making the passive pendulum in the Furuta pendulum system oscillate about the the horizontal line without crossing the vertical line.

This type of singular point is part of a large family of singular points where the uniqueness of the solutions to (5.22) is violated when approaching this point from one or both directions. Similarly to simple singular points, it is of course required that (5.35) holds, namely that $\gamma(s_s)\big(\delta(s_s)+\alpha'(s_s)\big) < 0$. However, whereas $\delta(s)/\alpha(s)$ is continuous about a simple singular point, it is unbounded (from at least one direction) for this family of singular points. For instance, whereas the uniqueness was broken from both sides in the above example, for the system

$$s^2\ddot{s} + (2s+d)\dot{s}^2 + g = 0$$

with constants $d, g \in \mathbb{R}$, it is violated only from the left if $d > 0$ and $g < 0$, or from the right if the signs are flipped. Thus the uniqueness of the solutions to (5.22) is violated for these types of singular points, in the sense that $(s, \dot{s}) = (s_s, \sqrt{-\gamma(s)/\beta(s_s)}$ is (locally) finite-time attractive from the left and/or finite-time repellent from the right with respect to (5.22). This, of course, does not necessarily mean that such a point is an attractor (resp. repeller) of the reduced dynamics, which also requires it being forward (resp. backward) invariant. Rather, if this uniqueness is broken on both sides, it means that all nearby solutions are funneled into this point when approaching it both from the left (i.e. in forward time) and from the right (i.e. in backward time).

Let us now derive some conditions which ensure that the uniqueness of solutions is violated at such a point. For brevity, we will only consider solutions approaching from the left. Then, for some $s_0 < s_s$ and $\eta \in \{0, 1, 2, 3\}$, with $\Psi(\cdot)$ defined in (5.25), the following requirements are the primary ones:

$$|\alpha^\eta(s)\Psi(s_0, s)| \to +\infty \quad \text{and} \quad \int_{s_0}^{s} \Psi(s,\tau)\alpha(\tau)\gamma(\tau)d\tau \to 0 \quad \text{as} \quad s \to s_s^-. \tag{5.39}$$

This can be observed by noticing from (5.32) that since

$$\rho_{\dot{s}_0}(s) = \sqrt{\Psi^{-1}(s_0, s)\alpha^{-2}(s)\left[\alpha^2(s_0)\dot{s}_0^2 - 2\int_{s_0}^{s}\Psi(s_0,\tau)\alpha(\tau)\gamma(\tau)d\tau\right]}$$

one then has $\lim_{s\to s_s^-}\rho_{\dot{s}_0}(s) = \sqrt{-\gamma(s_s)/\beta(s)}$ by L'Hôpital's rule, regardless of the value of $\dot{s}_0 > 0$.

The derivative of each such function $\rho_{\dot{s}_0}$ with respect to s is of course

$$\begin{aligned}
\rho'_{\dot{s}_0}(s) &= \frac{1}{\rho_{\dot{s}_0}(s)}\left[\frac{1}{2}\Psi(s_0,s)\alpha^2(s)\rho^2_{\dot{s}_0}(s)\frac{d}{ds}\left(\Psi^{-1}(s_0,s)\alpha^{-2}(s)\right) - \frac{\gamma(s)}{\alpha(s)}\right] \\
&= -\frac{1}{\rho_{\dot{s}_0}(s)}\left[\frac{\Psi(s_0,s)\alpha^2(s)\left(\beta(s)\right)\rho^2_{\dot{s}_0}(s)+\gamma(s)\big)}{\Psi(s_0,s)\alpha^3(s)}\right] \\
&= -\frac{\Big(\beta(s)\rho^2_{\dot{s}_0(s)}+\gamma(s)\Big)}{\rho_{\dot{s}_0}(s)\alpha(s)}
\end{aligned}$$

as before. But for it to be finite when approaching the singular point from the left, it is also required that

$$\lim_{s \to s_s^-} \frac{d}{ds} \left[\Psi^{-1}(s_0, s)\alpha^{-2}(s) \int_{s_0}^{s} \Psi(s_0, \tau)\alpha(\tau)\gamma(\tau)d\tau \right]$$

exists and is finite.

As previously stated, Theorem 1 in [193] provides sufficient conditions which ensures that the above requirements hold from both sides. We restate it here in a slightly different format using our notation:

Proposition 5.14. *[193] Suppose the interval $[s_a, s_b] \subseteq \mathcal{S}$ contains a single isolated singular point s_s within its interior, with $\alpha \in \mathcal{C}^3$ and $\beta, \gamma \in \mathcal{C}^2$ on (s_a, s_b). Further suppose that $\gamma(s_a) = \gamma(s_b) = 0$; $\gamma'(s_a) > 0$ and $\gamma'(s_b) < 0$; $\gamma(s) > 0$ for all $s \in (s_a, s_b)$; and that*

$$2\delta(s_s) < -3\alpha'(s_s) < 0. \tag{5.40}$$

Then for any positive, real numbers c and d, and points $s_c, s_d \in \mathcal{S}$, $s_c < s_s < s_d$, there exists a $\mathcal{C}^1$ scalar function $\rho(\cdot)$, which is strictly positive and satisfies (5.23) *over (s_c, s_d), such that $\rho(s_c) = c$ and $\rho(s_d) = d$.* □

Note that the requirement regarding the ends of the interval corresponding to equilibrium points of the reduced dynamics being of saddle type is not strictly required. Indeed, as the following example borrowed from [193] demonstrates, the equilibria can be replaced by simple singular points.

Example 5.3. Consider the reduced dynamics (5.22) with the functions

$$\begin{aligned}
\alpha(s) &= \cos(\phi_2(s))\phi_1'(s) + \phi_2'(s), \\
\beta(s) &= \cos(\phi_2(s))\phi_1''(s) + \phi_2''(s) - (\phi_1'(s))^2 \cos(\phi_2(s)) \sin(\phi_2(s)), \\
\gamma(s) &= -g \sin(\phi_2(s)),
\end{aligned}$$

where $g = 9.81\,\mathrm{m\,s^{-2}}$, such that $\delta(s) = -(\phi_1'(s))^2 \cos(\phi_2(s)) \sin(\phi_2(s)) + \phi_1'(s)\phi_2'(s) \sin(\phi_2(s))$. This corresponds to the Furuta pendulum system with unit link lengths given the vector of synchronization functions $\Phi(s) = \mathrm{col}\big(\phi_1(s), \phi_2(s)\big)$. For $\mathcal{S} = [0, 2\pi)$, we will consider

$$\phi_1(s) = -\frac{1}{2}(a + b\cos(s))^2 \quad \text{and} \quad \phi_2(s) = -c - d\cos(s)$$

for some constants $a, b, c, d \in \mathbb{R}_{\geq 0}$. Hence

$$\alpha(s) = \sin(s)\big[b\cos(\phi_2(s))(a + b\cos(s)) + d\big],$$

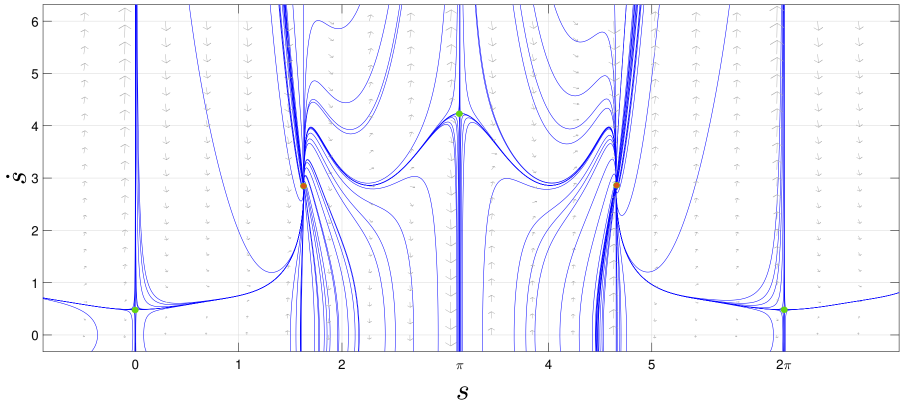

Figure 5.2: Shows the phase portrait of the reduced dynamics of the Furuta pendulum in Example 5.3. A unique positive solution can be seen which crosses both simple singular points, marked by green dots, and singular points of the type considered in [193], which are marked by red dots.

such that the sets $\mathfrak{S}_s = \{0, \pi, 2\pi\}$ and $\mathfrak{S}_x = \{s \in \mathcal{S} : \; b\cos(\phi_2(s))(a + b\cos(s)) + d = 0\}$ contain the system's singular points. Since

$$\delta(s) = b\sin^2(s)\sin(\phi_2(s))(a + b\cos(s))\big[d - 2b(a + b\cos(s))\cos(\phi_2(s))\big]$$

the elements of $\mathfrak{S}_s$ are therefore all simple singular points if $\mathfrak{S}_s \cap \mathfrak{S}_x = \emptyset$. Moreover, for any $s_s \in \mathfrak{S}_x$, one has $\delta(s_s) = -3d^2\sin^2(s_s)\tan(\phi_2(s_s))$.

Taking, for instance, $(a, b, c, d) = (1.5, 2, 2, 1)$ results in a pair of non-simple singular points lying within $(0, \pi)$ and $(\pi, 2\pi)$, respectively. The corresponding phase portrait of the resulting reduced dynamics is shown in Figure 5.2, in which the existence of a unique solution crossing all the singular points is apparent.

5.3.3 Conditions for the existence of a periodic orbit

Using the properties of the reduced dynamics derived in Section 5.3.2, we will now provide constructive statements that allows one to design s-parameterized maneuvers corresponding to periodic orbits. For simplicity's sake, we consider systems with only one degree of underactuation (i.e. $m = n_q - 1$), such that the reduced dynamics (5.21) correspond to a single equation of the form (5.22). Note, however, that the same arguments can also be used for systems with higher degrees of underactuation by further requiring that the remaining $m - 1$ equations in (5.21) also share the same solution; see [9, 34].

Let us begin by providing the following problem statement, whose solution evidently implies a solution to Problem 5.2.

Problem 5.15. *For $\mathcal{S} = [0, s_T) \subset \mathbb{R}_{\geq 0}$, find a strictly positive, smooth function $\rho : \mathcal{S} \to \mathbb{R}_{>0}$ which solves* (5.22) *and satisfies $\rho(0) \equiv \rho(s_T)$, where* (5.22) *is the reduced dynamics associated with the smooth, s_T-periodic vector of synchronization functions $\Phi : \mathcal{S} \to \mathbb{R}^{n_q}$, i.e. $\Phi(0) \equiv \Phi(s_T)$, with $m = n_q - 1$.*

The following statement is useful when attempting to search for an s-parameterized orbit of (5.22).

Theorem 5.16. *Let $\mathcal{S} := [0, s_T) \subset \mathbb{R}\geq 0$ and suppose the smooth function $\Phi : \mathcal{S} \to \mathbb{R}^{n_q}$ is such that $\Phi(s + s_T) \equiv \Phi(s)$ for all $s \in \mathcal{S}$. Further suppose that any singular point in the interval $\mathcal{S}$ is simple, and any equilibrium point is isolated and of center type. If in addition*

$$\int_0^{s_T} \frac{\delta(\tau)}{\alpha(\tau)} d\tau = \int_0^{s_T} \Psi(0, \tau)\alpha(\tau)\gamma(\tau) d\tau \equiv 0,$$

then there exists a smooth, strictly positive function $\rho : \mathcal{S} \to \mathbb{R}_{>0}$ satisfying $\rho(0) \equiv \rho(s_T)$, thus providing a solution to Problem 5.15.

Proof. If $\dot{s} = \rho(s)$, then for $\rho(0) \equiv \rho(s_T)$ to hold, it follows from (5.27) that

$$\frac{1}{2} \left[\Psi(s_0, s_T)\right] \alpha^2(0)\rho^2(0) + \int_{s_0}^{s_T} \Psi(s_0, \tau)\alpha(\tau)\gamma(\tau) d\tau \equiv 0$$

must hold. Here we have used the fact that $\alpha(s + s_T) = \alpha(s)$ since $\Phi(s + s_T) \equiv \Phi(s)$. Due to how $\Psi(\cdot)$ is defined, the Theorem's hypotheses together with Lemma 5.8 and Proposition 5.12 ensure that this holds and that such a bounded function $\rho(\cdot)$ exists. Lastly, since $\mathcal{S}$ only contains equilibrium points of type center, $\rho(\cdot)$ must be strictly positive and smooth due to (5.23) and its derivative (5.37). $\square$

If the conditions in Theorem 5.16 hold, then one of course still needs compute the function ρ in order to obtain the corresponding s-parameterized maneuver. In the cases when $\mathcal{S}$ contains no (simple) singular points, this is easily achieved using either (5.27) or by integrating (5.23). If the interval also contains simple singular points, then one can find the value of ρ at these points from (5.34) and ρ' from (5.37), and use (5.27) and (5.23) in between.

5.3.4 Conditions for the existence of a heteroclinic orbit

We will now demonstrate how one can use the properties of the reduced dynamics in order to also find *heteroclinic* orbits whenever $m = n_q - 1$. Specifically, for a pair of points (configurations) $q_\alpha \in \mathbb{R}^{n_q}$ and $q_\omega \in \mathbb{R}^{n_q}$, $q_\omega \neq q_\omega$ of (5.2), suppose there exist $u_\alpha, u_\omega \in \mathbb{R}^m$ such that $\mathbf{G}(q_\alpha) \equiv \mathbf{B}_\omega u_\alpha$ and $\mathbf{G}(q_\omega) \equiv \mathbf{B}_u u_\omega$. Denoting $x_\alpha = \mathrm{col}(q_\alpha, \mathbf{0}_{n_q \times 1})$ and $x_\omega = \mathrm{col}(q_\omega, \mathbf{0}_{n_q \times 1})$, the task we now aim to solve is the following:

Problem 5.17. *For $\mathcal{S} := [s_\alpha, s_\omega] \subset \mathbb{R}$, $s_\alpha < s_\omega$, find smooth functions $\Phi : \mathcal{S} \to \mathbb{R}^{n_q}$ and $\rho : \mathcal{S} \to \mathbb{R}_{\geq 0}$, such that the following criteria are satisfied for the system* (5.2)*:*

- $\Phi(s_\alpha) = q_\alpha$ *and* $\Phi(s_\omega) = q_\omega$*;*
- $\rho(s_\omega) = \rho(s_\omega) \equiv 0$*, as well as* $\rho(s) > 0$ *for all* $s \in (s_\alpha, s_\omega)$*;*
- *both* (5.7) *and* (5.19) *hold for all* $s \in \mathcal{S}$*.*

Using Lemma 5.3, a solution to Problem 5.17 implies the existence of a heteroclinic orbit of the reduced dynamics, which in turn corresponds to a so-called *point-to-point maneuver* of the mechanical system. (We will consider the problem of orbital stabilization of such maneuvers in Chapter 6). The subscripts "α" and "ω" are therefore used to denote that the equilibrium points on the boundaries are α- and ω-limit points of the induced orbit.

Recalling the definitions of $\nu(\cdot)$ and $\Psi(\cdot)$ given in (5.24) and (5.25), respectively, the following result provides a solution to the above problem.

Theorem 5.18. *Let the smooth vector-valued function $\Phi : \mathcal{S} \to \mathbb{R}^{n_q}$ be such that $\Phi(s_\alpha) = q_\alpha$, $\Phi(s_\omega) = q_\omega$, $\|\Phi'(s_\alpha)\| \neq 0$, $\|\Phi'(s_\omega)\| \neq 0$, $\nu(s_\alpha) \leq 0$ and $\nu(s_\omega) \leq 0$. Further suppose that the following conditions hold: $\alpha(s) \neq 0$ for all $s \in \mathcal{S}$; there exists a single point $s_e \in \mathrm{int}\, \mathcal{S}$ satisfying $\gamma(s_e) \equiv 0$, for which $\nu(s_e) > 0$; and*

$$\int_{s_\alpha}^{s_\omega} \Psi(s_0, \tau)\alpha(\tau)\gamma(\tau) d\tau \equiv 0. \tag{5.41}$$

Then there exists a unique smooth function $\rho : \mathcal{S} \to \mathbb{R}_{\geq 0}$, for which $\rho(s_\alpha) = \rho(s_\omega) \equiv 0$, satisfying both (5.22) *and $\rho(s) > 0$ for all $s \in (s_\alpha, s_\omega)$.*

Remark 5.19. As $\|\mathbf{G}(q_\alpha) - \mathbf{B}_u u_\alpha\| = \|\mathbf{G}(q_\omega) - \mathbf{B}_u u_\omega\| = 0$, a solution to Theorem 5.18 implies $\gamma(\hat{s}) \equiv 0$ for $\hat{s} \in \{s_\alpha, s_\omega\}$. Hence (5.23) is then trivially true at $\hat{s} \in \{s_\alpha, s_\omega\}$, while from its derivative with respect to s,

$$\alpha\rho''\rho + \alpha(\rho')^2 + \big(3\alpha' + 2\hat{\beta}\big)\rho'\rho + \big(\alpha'' + \hat{\beta}'\big)\rho^2 + \gamma' = 0,$$

one finds that $(\rho'(\hat{s}))^2 = -\gamma'(\hat{s})/\alpha(\hat{s})$. Thus, for s_α and s_ω to be hyperbolic (saddle) equilibrium points of (5.22), and consequently $\rho'(s_\alpha) > 0$ and $\rho'(s_\omega) < 0$, it is further required that $\nu(s_\alpha) < 0$ and $\nu(s_\omega) < 0$. From this, one can also easily deduce that the function $\gamma(s)/\alpha(s)$ then must change its sign an odd number of times over the open interval (s_α, s_ω). Considering only one sign change, the necessary existence of a point $s_e \in \operatorname{int}\mathcal{S}$ for which $\gamma(s_e) = 0$ and $\nu(s_e) > 0$ (i.e. a center) is evident.

Remark 5.20. Due to the requirement of a center on $\operatorname{int}\mathcal{S}$, Theorem 5.18 cannot be used to construct an s-parameterized point-to-point maneuver between two adjacent equilibria for systems where the equilibria of (5.22) are fixed. In light of Remark 5.19, one can in such cases instead attempt to use an alternative set of conditions which are based on $\alpha(s)$ changing its sign once over $\operatorname{int}\mathcal{S}$ instead of $\gamma(s)$. Such condition correspond to the particular type of non-simple singular points considered in [193] which were briefly discussed at the end of Section 5.3.2. Using Theorem 1 in [193], this corresponds to replacing the conditions in the second sentence in Theorem 5.18 with the following: $\nu(s_\alpha) < 0$ and $\nu(s_\omega) < 0$; $\gamma(s) > 0$ for all $s \in \operatorname{int}\mathcal{S}$; and there exists a single point $s_s \in \operatorname{int}\mathcal{S}$ satisfying $\alpha(s_s) \equiv 0$ and $\hat{\beta}(s_s) < -\frac{3}{2}\alpha'(s_s) < 0$.

Proof. The boundary conditions imposed on $\Phi(\cdot)$ are obvious, whereas those on $\Phi'(\cdot)$ are obtained directly from (5.7) by setting $\rho(s_\alpha) = \rho(s_\omega) = 0$. The condition $\alpha(s) \neq 0$ implies that the integrating factor (5.25) is both nonzero and bounded on $\mathcal{S}$, as well as ensures the uniqueness of the solutions to (5.22). Thus, using again $\rho(s_\alpha) = \rho(s_\omega) = 0$ in (5.32), the existence of a smooth function ρ which vanishes at the boundaries and satisfies (5.23) on $\mathcal{S}$ follows from [33, Thm. 1]. Since $\gamma(s) \neq 0$ for all $\operatorname{int}\mathcal{S}\backslash\{s_e\}$, and $\nu(s_e) > 0$, the function ρ^2 must be strictly positive on $\operatorname{int}\mathcal{S}$. This, in turn, guarantees (5.7) holding on the whole of $\operatorname{int}\mathcal{S}$. □

Heteroclinic orbits implied by Theorem 5.18 includes those corresponding to a separatrix of a pendulum-like equation. For example, the function $\rho(s) = \sqrt{2 - 2\cos(s)}$ would be the resulting solution for $\ddot{s} = \sin(s)$.

An example of a system having a heteroclinic orbit of the form as in Remark 5.20, on the other hand, would be $s\ddot{s} + (1-d)\dot{s}^2 - g(s^2 - s_e^2) = 0$, for $d > 3/2$ and $g, c > 0$. Specifically, it emerges from $s_\alpha = -s_e$, crosses the singular point at $s_s = 0$ with $\rho(s_s) = \sqrt{gs_e^2/(d-1)}$, and terminates at $s_\omega = s_e$. Notice, however, that for any solution of this system starting within the interior of the corresponding orbit, it will only approach $s_\alpha = -s_e$ in backward time as $t \to -\infty$, and s_ω in forward time as $t \to \infty$.

Although beyond the scope of this thesis, it is nevertheless important to mention that one may in fact also use this type of singular points to ensure that, say, s_α is finite-time repellent. For instance, let d, g and s_e be as above. Then the system $s\ddot{s} + (1-d)\dot{s}^2 - gs(s-s_e) = 0$ has a heteroclinic orbit connecting $s_\alpha = 0$ and $s_\omega = s_e$, on which the backward time it takes for any solution starting on its interior to reach $s_\alpha = 0$ is finite. Indeed, it can be shown that

$$\begin{aligned}\rho^2(s) &= 2gs^{2d-2}\int_{s_e}^{s}\sigma^{2-2d}(\sigma - s_e)d\sigma \\ &= g\left[\frac{(3-2d)s^2 - (4-2d)s_e s + s_e^{4-2d}s^{2d-2}}{(3-2d)(2-d)}\right].\end{aligned}$$

Thus if $d = 2$ and $g = 2^{-1}$, one has $\rho(s) = \sqrt{ss_e + s^2[\ln(s) - \ln(s_e) - 1]}$.

5.4 Projection-based coordinates for underactuated systems

Consider again the (not necessarily underactuated) mechanical system (5.2), but now with an additional viscous damping term:

$$\mathbf{M}(q)\ddot{q} + \mathbf{C}(q,\dot{q})\dot{q} + \mathbf{D}(q)\dot{q} + \mathbf{G}(q) = \mathbf{B}_u u. \tag{5.42}$$

The matrix-valued function $\mathbf{D} : \mathbb{R}^{n_q} \to \mathbb{R}^{n_q \times n_q}$ is assumed to be smooth, and thus bounded, i.e. $\exists k_D < 0$ such that $\|\mathbf{D}(q)\| \leq k_D$ for all $q \in \mathbb{R}^{n_q}$.

Suppose an s-parameterized maneuver of the form (5.9) (see Def. 3.2) is known for this system, corresponding to the pair (Φ, ρ) with both $\Phi : \mathcal{S} \to \mathbb{R}^{n_q}$ and $\rho : \mathcal{S} \to \mathbb{R}_{\geq 0}$ smooth. That is, the maneuver's state curve is traced out by

$$x_s(s) = \mathrm{col}\left(\Phi(s), \Phi'(s)\rho(s)\right).$$

Its control curve $u_s(\cdot)$, on the other hand, can be found in a similar manner to (5.15). Namely, since $\mathcal{F}(s) := x_s'(s)$ can be written as

$$\mathcal{F}(s) = \mathrm{col}\left(\mathcal{F}_1(s), \mathcal{F}_2(s)\right) := \mathrm{col}\left(\Phi'(s), \Phi'(s)\rho'(s) + \Phi''(s)\rho(s)\right), \tag{5.43}$$

one can find $u_s = u_s(s)$ from

$$u_s = \mathbf{B}_u^\dagger \mathbf{B}_u u_s = \mathbf{B}_u^\dagger\left[\mathbf{M}(\Phi)\mathcal{F}_2\rho + \mathbf{C}(\Phi, \mathcal{F}_1)\mathcal{F}_1\rho^2 + \mathbf{D}(\Phi)\mathcal{F}_1\rho + \mathbf{G}(\Phi)\right], \tag{5.44}$$

where we have omitted the s-argument as to shorten the notation.

Our main aim in this section will be to harness the specific structure of the equations of motion of the mechanical system (5.2) as to derive general expressions for the transverse linearization corresponding of the excessive transverse coordinates we have previously introduced in Section 4.6. Specifically, we provide will explicit expressions for the transverse linearization, thus avoiding having to solve a matrix equation as in [38] (see Thm. 4 therein). This in fact allows one to obtain expressions for the transverse linearization of *any* set of transverse coordinates, including those in [34].

5.4.1 Structure of the transverse dynamics

Suppose $x_s : \mathcal{S} \to \mathbb{R}^n$ traces out a non-trivial periodic orbit $\mathcal{O}$. Further suppose that a $\mathcal{C}^2$-smooth projection operator $p = p(x)$ for this orbit is known (see Definition 4.5). Since the system (5.42) is of second order, the excessive transverse coordinates

$$e_\perp = x - (x_s \circ p)(x)$$

can be written as $e_\perp = \mathrm{col}(e_1, e_2)$, where

$$e_1 := q - \Phi(p), \tag{5.45a}$$

$$e_2 := \dot{q} - \Phi'(p)\rho(p). \tag{5.45b}$$

Clearly

$$\dot{e}_1 = \dot{q} - \Phi'(p)\dot{p} = \mathcal{F}_1(p)\big[\rho(p) - \dot{p}\big] + e_2, \tag{5.46}$$

whereas by adding and subtracting $\mathbf{M}(q)\mathbf{F}(q, \dot{q}, p)$ on the right-hand side of (5.2), with

$$\mathbf{F}(q, \dot{q}, s) := \mathbf{M}(q)\mathcal{F}_2(s)\rho(s) + \mathbf{C}(q, \dot{q})\dot{q} + \mathbf{D}(q)\dot{q} + \mathbf{G}(q), \tag{5.47}$$

one obtains

$$\dot{e}_2 = \ddot{q} - \mathcal{F}_2(p)\dot{p} = \mathcal{F}_2(p)\big[\rho(p) - \dot{p}\big] + \mathbf{M}^{-1}(q)\left[\mathbf{B}_u u - \mathbf{F}(q, \dot{q}, p)\right]. \tag{5.48}$$

Consider now a control law of the following form:

$$u = \mathbf{U}(x, p(x)) + v. \tag{5.49}$$

Here $v = v(x) \in \mathbb{R}^m$ is some orbitally stabilizing feedback to be defined, while the $\mathcal{C}^1$-smooth mapping $\mathbf{U} : \mathbb{R}^{2n_q} \times \mathcal{S} \to \mathbb{R}^m$ consists of two parts:

$$\mathbf{U}(x, s) = \mathbf{U}_0(q, s)) + \mathbf{U}_{e_2}(x, s)\big(\dot{q} - \Phi'(s)\rho(s)\big). \tag{5.50}$$

Here $\mathbf{U}_0$ and $\mathbf{U}_{e_2}$ are such that, for all $s \in \mathcal{S}$ and any $x \in \mathbb{R}^{n_q}$, it holds that

$$\mathbf{U}_0(\Phi(s), s) \equiv u_s(s) \quad \text{and} \quad \|\mathbf{U}_{e_2}(x, s)\| \leq c_1 + c_2 \left\|\dot{q} - \Phi'(s)\rho(s))\right\|, \tag{5.51}$$

for some real numbers $c_1, c_2 > 0$. Using the vector function $\mathbf{F}(\cdot)$ defined in (5.47), some possible candidates for $\mathbf{U}(\cdot)$ are the following:

$$\mathbf{U}_s(s) = \mathbf{B}_u^\dagger \mathbf{F}\big(\Phi(s), \Phi'(s)\rho(s), s\big) = u_s(s), \tag{5.52a}$$
$$\mathbf{U}_q(q,s) = \mathbf{B}_u^\dagger \mathbf{F}\big(q, \Phi'(s)\rho(s), s\big), \tag{5.52b}$$
$$\mathbf{U}_x(x,s) = \mathbf{B}_u^\dagger \mathbf{F}\big(q, \dot{q}, s\big). \tag{5.52c}$$

Here (5.52a) and (5.52a) both correspond to $\mathbf{U}_{e_2} = \mathbf{0}_{m\times 1}$, whereas (5.52c) corresponds to

$$\mathbf{U}_0(q,s) = \mathbf{B}_u^\dagger \mathbf{F}\big(q, \Phi'(s)\rho(s), s\big), \tag{5.53a}$$
$$\mathbf{U}_{e_2}(x,s) = \mathbf{B}_u^\dagger \left[2\mathbf{C}\big(q, \Phi'(s)\big)\rho(s) + \mathbf{C}(q, \big(\dot{q} - \Phi'(s)\rho(s)\big) + \mathbf{D}(q)\right]. \tag{5.53b}$$

Note that the above expressions for $\mathbf{U}_{e_2}$ are easily derived from Property *ii)* in Assumption 5.1. Indeed, for any projection operator $p = p(x)$, we may in a vicinity of $\mathcal{O}$ write

$$\mathbf{C}(q,\dot{q}) = \mathbf{C}\big(q, \Phi'(p)\big)\Phi'(p)\rho^2(p) + 2\mathbf{C}\big(q, \Phi'(p)\big)\rho(p)e_2 + \mathbf{C}(q, e_2)e_2.$$

We now define

$$A_{e_2}(x,s) := \begin{bmatrix} \mathbf{I}_{n_q} \\ \mathbf{M}^{-1}(q)\left[\mathbf{B}_u\mathbf{U}_{e_2}(x,s) - 2\mathbf{C}\big(q, \Phi'(p)\big)\rho(p) - \mathbf{C}\big(q, e_2(x)\big) - \mathbf{D}(q)\right] \end{bmatrix}, \tag{5.54}$$

as well as

$$f_0(q,s) := \begin{bmatrix} \mathbf{0}_{n_q\times 1} \\ \mathbf{M}^{-1}(q)\left[\mathbf{B}_u\mathbf{U}_0(q,s) - \mathbf{F}\big(q, \Phi'(s)\rho(s), s\big)\right] \end{bmatrix}, \tag{5.55a}$$
$$B(q) := \begin{bmatrix} \mathbf{0}_{n_q\times m} \\ \mathbf{M}^{-1}(q)\mathbf{B}_u \end{bmatrix}. \tag{5.55b}$$

Note here that, by Assumption 5.1 and (5.51), there exist a pair of constant real numbers $a_0, a_1 > 0$ such that

$$\|A_{e_2}(x, p(x))e_2\| \le a_0 \|e_2\| + a_1 \|e_2\|^2$$

for all $x \in \mathbb{R}^n$ and all $e_2 \in \mathbb{R}^{n_q}$. Moreover, both $f_0(\cdot)$ and $B(\cdot)$ are everywhere bounded, $B(\cdot)$ has full rank, and $f_0(\Phi(s), s) \equiv 0$ for all $s \in \mathcal{S}$.

Using the above, the equations governing the system's dynamics can then be written in the following form:

Lemma 5.21. *Let $p : \mathfrak{X} \to \mathcal{S}$ be a $\mathcal{C}^2$-smooth projection operator (see Def. 4.5) which is well defined in a neighborhood $\mathfrak{X} \subset \mathbb{R}^n$ of the orbit $\mathcal{O}$. Suppose u is taken according to* (5.49) *for some $\mathbf{U}(\cdot)$ of the form* (5.50) *satisfying* (5.51)*. Then, within $\mathfrak{X}$, the system* (5.42) *can be written as*

$$\dot{x} = \mathcal{F}(p)\rho(p) + f_0(q, \rho) + A_{e_2}(x, p)e_2 + B(q)v,$$

where $A_{e_2}(\cdot)$ is defined in (5.54)*, while $f_0(\cdot)$ and $B(\cdot)$ are defined in* (5.55)*.* □

Consider now the Jacobian matrix of $e_\perp$:

$$De_\perp(x) = \mathbf{I}_n - \mathcal{F}(p)Dp(x).$$

Using Lemma 5.21, the time derivative of $e_\perp$ is

$$\dot{e}_\perp = De_\perp(x)\dot{x} = De_\perp(x)\big[\mathcal{F}(p)\rho(p) + f_0(q, \rho) + A_{e_2}(x, p)e_2 + B(q)v\big]. \quad (5.56)$$

Note here that if the projection operator only depends on the generalized coordinates, not their velocities, i.e. $\frac{\partial}{\partial \dot{q}}p(x) \equiv 0$ for all $x \in \mathbb{R}^n$, then

$$De_\perp(x)B(x) = \begin{bmatrix} \mathbf{0}_{n_q \times m} \\ D_q p(q)\mathbf{M}^{-1}(q)\mathbf{B}_u \end{bmatrix},$$

where $D_q p(q) = \frac{\partial}{\partial q}p(x)$. Moreover,

$$\begin{aligned} \dot{e}_1 &= \mathcal{F}_1(p)\big[\rho(p) - D_q p(q)\big] + e_2 \\ &= \mathcal{F}_1(p)\big[1 - D_q p(q)\mathcal{F}_1(p)\big]\rho(p) + \big(\mathbf{I}_{n_q} - \mathcal{F}_1(p)D_q p(q)\big)\, e_2 \end{aligned}$$

can then also be easily deduced from (5.46).

5.4.2 Transverse linearization

Using the structure of the transverse dynamics (5.56), we will now derive explicit expressions for the transverse linearization associated with $e_\perp$ about the maneuver's orbit.

To this end, we define

$$A_{e_1}(q, s) := \begin{bmatrix} \mathbf{0}_{n_q \times 1} \\ \mathbf{M}^{-1}(q)\frac{\partial}{\partial q}\left[\mathbf{B}_u\mathbf{U}_0(q, s) - \mathbf{F}\big(q, \Phi'(s)\rho(s), s\big)\right] \end{bmatrix} \quad (5.57)$$

and

$$A_p(q, s) = \frac{\partial}{\partial s}\left[\mathcal{F}(s)\rho(s)\right] + \begin{bmatrix} \mathbf{0}_{n_q \times 1} \\ \mathbf{M}^{-1}(q)\frac{\partial}{\partial s}\left[\mathbf{B}_u\mathbf{U}_0(q, s) - \mathbf{F}\big(q, \Phi'(s)\rho(s), s\big)\right] \end{bmatrix}. \quad (5.58)$$

Recall the definition of $A_{e_2}(\cdot)$ given in (5.54), and denote $B_s(s) = B\big(\Phi(s)\big)$. Let $A_s(s) := A_p\big(\Phi(s), s\big)\mathcal{P}(s) + \hat{A}_\perp(s)$ where $\mathcal{P}(s) = Dp(x_s(s))$ and

$$\hat{A}_\perp(s) := \big[A_{e_1}\big(\Phi(s), s\big)\ ,\ A_{e_2}\big(x_s(s), s\big)\big]. \tag{5.59}$$

The first-order variational system about the orbit is then given by

$$\dot{\boldsymbol{\delta}}_x = A_s(s)\boldsymbol{\delta}_x + B_s(s)v, \tag{5.60}$$

where $s = s(t) \in \mathcal{S}$ again is a solution to $\dot{s} = \rho(s)$. Moreover, by recalling the notation $\mathcal{E}_\perp(s) := De_\perp(x_s(s))$, the following can be deduced from (4.56):

Proposition 5.22. *Suppose the conditions in Lemma 5.21 hold. Then the matrix-valued functions $A_\perp(\cdot)$ and $B_\perp(\cdot)$, defined by*

$$\begin{aligned} A_\perp(s) &:= \mathcal{E}_\perp(s)\hat{A}_\perp(s) - \mathcal{F}(s)\mathcal{F}^\mathsf{T}(s)D^2p(x_s(s))\rho(s), \\ B_\perp(s) &:= \mathcal{E}_\perp(s)B\big(\Phi(s)\big), \end{aligned}$$

with $\hat{A}_\perp(s)$ defined in (5.59)*, correspond to the transverse linearization associated with $e_\perp$ (see Corollary 4.31). That is,*

$$\dot{\boldsymbol{\delta}}_{e_\perp} = A_\perp(s)\boldsymbol{\delta}_{e_\perp} + B_\perp(s)v, \tag{5.61a}$$

$$0 = \mathcal{P}(s)\boldsymbol{\delta}_{e_\perp}, \tag{5.61b}$$

with $s = s(t)$. □

Note that one can use the above expression to compute the transverse linearization for any other set of transverse coordinates for this class of mechanical systems. Indeed, denote by $z_\perp : \mathbb{R}^{2n_q} \to \mathbb{R}^{2n_q-1}$ a set of transverse coordinates as by Definition 4.11. According to Lemma 4.15, we may then write $e_\perp(x) = \mathcal{E}_\perp(p)\mathcal{Z}_\perp^\dagger(p)z_\perp + \big(\,\|z_\perp\|^2\big)$, where $\mathcal{Z}_\perp(s) := Dz_\perp(x_s(s))$. Conversely, $z_\perp(x) = \mathcal{Z}_\perp(p)e_\perp + \big(\,\|e_\perp\|^2\big)$ by Lemma 4.29. Hence, if $\boldsymbol{\delta}_{e_\perp}(t)$ solves (5.61) and $\boldsymbol{\delta}_{z_\perp}(t)$ is the state of the first-order approximation system of the dynamics of $z_\perp$ about the desired orbit $\mathcal{O}$, then

$$\boldsymbol{\delta}_{e_\perp}(t) = \mathcal{E}_\perp(s(t))\mathcal{Z}_\perp^\dagger(s(t))\boldsymbol{\delta}_{z_\perp}(t) \quad \text{and} \quad \boldsymbol{\delta}_{z_\perp}(t) = \mathcal{Z}_\perp(s(t))\boldsymbol{\delta}_{e_\perp}(t).$$

Consequently,

$$\begin{aligned} \dot{\boldsymbol{\delta}}_{z_\perp} &= \big[\mathcal{Z}_\perp(s)A_\perp(s) + \mathcal{Z}_\perp'(s)\rho(s)\mathcal{E}_\perp(s)\big]\,\mathcal{Z}_\perp^\dagger(s)\boldsymbol{\delta}_{z_\perp} + \mathcal{Z}_\perp(s)B_\perp(s)v \\ &= \Big[\mathcal{Z}_\perp(s)\hat{A}_\perp(s) + \mathcal{Z}_\perp'(s)\rho(s)\mathcal{E}_\perp(s)\Big]\,\mathcal{Z}_\perp^\dagger(s)\boldsymbol{\delta}_{z_\perp} + \mathcal{Z}_\perp(s)B_s(s)v. \end{aligned} \tag{5.62}$$

Note also that, unlike the transverse linearization derived in Section 4.4, which we recall was completely independent of the choice of projection operator, the above does in fact have such a dependence through $\mathcal{E}_\perp(s) = \mathbf{I}_n - \mathcal{F}(s)\mathcal{P}(s)$. This, however, is simply due to the factorization of $A_s(s)$, which allowed us to omit the matrix-valued function $A_p(s)$ in the transverse linearization (5.61). Thus, if $\mathbf{U}(\cdot)$ does not depend on a particular choice of projection operator, then one can simply set $\mathcal{P}(s) = \mathcal{F}^\mathsf{T}(s)/\left\|\mathcal{F}(s)\right\|^2$ such that $\mathcal{E}_\perp(s)\mathcal{Z}_\perp^\dagger(s) = \mathcal{Z}_\perp^\dagger(s)$ in the above.

Transverse linearization for VHC-based coordinates

Let an s-parameterized maneuver be known, and suppose there exists a smooth scalar function $\theta : \mathbb{R}_{\geq 0} \to \mathbb{R}$, as well as a smooth vector-valued function $\mathcal{Q} : \mathbb{R}_{\geq 0} \to \mathbb{R}^{n_q}$, such that $\mathcal{Q}(\theta(t)) \equiv \Phi(s(t))$ for all $t \geq 0$. For simplicity's sake, we will assume that the last element of $\mathcal{Q}(\theta)$ is equal to θ. Thus, the function $y = y(q)$ and its derivative, which are defined by

$$y := L_y\left(q - \mathcal{Q}(q_{n_q})\right), \quad \dot{y} := L_y\left(\dot{q} - \mathcal{Q}'(q_{n_q})\dot{q}_{n_q}\right), \quad L_y := [\mathbf{I}_{n_q-1}, \mathbf{0}_{n_q\times 1}], \tag{5.63}$$

both vanish on the desired orbit. Since the zero-level set of the function $y(q)$ corresponds to a specific relation between the generalized coordinates of the system, it is commonly referred to as a vector of *virtual holonomic constraints.*

We associate with $\mathcal{Q}(\cdot)$ the two-dimensional zero-dynamics set

$$\mathfrak{C} = \left\{(q, \dot{q}) \in \mathbb{R}^{n_q} \times \mathbb{R}^{n_q} : \; y(q) = 0, \; \dot{y}(q, \dot{q}) = 0\right\},$$

some times referred to as the *constraint manifold* [31]. For any solution remaining entirely within $\mathfrak{C}$, there must necessarily be some function $\theta(t)$ that solves the reduced dynamics (5.21) associated with $\mathcal{Q}(\theta)$, that is

$$\alpha_i(\theta)\ddot{\theta} + \beta_i(\theta)\dot{\theta}^2 + \gamma_i(\theta) = 0, \quad i = 1, 2, \ldots, m.$$

Suppose that $\alpha_i(\theta) \neq 0$ holds everywhere for some $j \in \{1, 2, \ldots, m\}$. For this particular equation, we then omit the j-subscript in the following and write $\alpha(\theta) = \alpha_j(\theta)$ etc. As was demonstrated in Section 5.3.2 (see also [33, 105]), the function

$$I(\theta_0, \theta, \dot{\theta}_0, \dot{\theta}) := \Psi(\theta_0, \theta)\alpha^2(\theta)\dot{\theta}^2 - \alpha^2(\theta_0)\dot{\theta}_0^2 + 2\int_\theta^\theta \Psi(\theta_0, \tau)\alpha(\tau)\gamma(\tau)d\tau \tag{5.64}$$

retains its zero value along such a solution.

In light of the above, consider the following vector of transverse coordinates:

$$z_\perp = \operatorname{col}\big(y, \dot{y}, I(\theta_0, q_{n_q}, \dot{\theta}_0, \dot{q}_{n_q})\big) \tag{5.65}$$

with y and $\dot{y}$ defined in (5.63) and $I(\cdot)$ in (5.64). Clearly $\|z_\perp(x)\| \equiv 0$ for all $x \in \mathcal{O}$, while the Jacobian matrix

$$Dz_\perp(x) = \begin{bmatrix} \mathbf{I}_{n_q-1} & -L_y \mathcal{Q}'(q_{n_q}) & \mathbf{0}_{n_q-1} & \mathbf{0}_{(n_q-1)\times 1} \\ \mathbf{0}_{n_q-1} & -L_y \mathcal{Q}''(q_{n_q})\dot{q}_{n_q} & \mathbf{I}_{n_q-1} & -L_y \mathcal{Q}'(q_{n_q}) \\ \mathbf{0}_{1\times(n_q-1)} & \partial_\theta I(q_{n_q}, \dot{q}_{n_q}) & \mathbf{0}_{1\times(n_q-1)} & \alpha^2(q_{n_q})\dot{q}_{n_q} \end{bmatrix}$$

with $\partial_\theta I(\theta, \dot{\theta}) = \alpha(\theta)(\beta(\theta)\dot{\theta}^2 + \gamma(\theta)) - \frac{2\delta(\theta)}{\alpha(\theta)} I$, has (full) rank equal to $2n_q - 1 = n - 1$ when evaluated along $\mathcal{O}$; indeed

$$Dz_\perp(x_\star(t)) = \begin{bmatrix} \mathbf{I}_{n_q-1} & -L_y \Phi'(\theta) & \mathbf{0}_{n_q-1} & \mathbf{0}_{(n_q-1)\times 1} \\ \mathbf{0}_{n_q-1} & -L_y \Phi''(\theta)\dot{\theta} & \mathbf{I}_{n_q-1} & -L_y \Phi'(\theta) \\ \mathbf{0}_{1\times(n_q-1)} & -\alpha^2(\theta)\ddot{\theta} & \mathbf{0}_{1\times(n_q-1)} & \alpha^2(\theta)\dot{\theta} \end{bmatrix}, \tag{5.66}$$

where $x_\star(t) := \operatorname{col}\big(\mathcal{Q}(\theta(t)), \mathcal{Q}'(\theta(t))\dot{\theta}(t)\big) \equiv x_s(s(t))$.

It is important to note that the above function $\theta = \theta(t)$ does not necessarily correspond to an s-parameterization. For example, it may instead correspond to a T-periodic solution encircling an equilibrium of type center. Nevertheless, since we have assumed knowledge of an s-parameterization, there necessarily exists a function $\vartheta : \mathcal{S} \to \mathbb{R}^{n_q}$ such that $\vartheta(s(t)) \equiv \theta(t)$ for all $t \geq 0$ and $\dot{s} = \rho(s)$ if the orbit is closed. That is, $\Phi(s) = \mathcal{Q}(\vartheta(s))$ and $x_s(s) = \operatorname{col}\big(\mathcal{Q}(\vartheta(s)), \mathcal{Q}'(\vartheta(s))\vartheta'(s)\rho(s)\big)$, such that $\mathcal{Z}_\perp(s) = Dz_\perp(x_s(s))$. Hence, for some control law of the form (5.49), the resulting transverse linearization associated with $z_\perp(\cdot)$ can be obtained from (5.62).

5.5 Example: Upright oscillations of the Cart-Pendulum System

Consider the cart-pendulum system shown Figure 5.3. The system has two degrees of freedom, corresponding to the generalized coordinates $q = \operatorname{col}(x_c, \varphi) \in \mathbb{R}^2$. The cart is actuated, whereas the pendulum is not, meaning that the system has one degree of underactuation. To keep the derivations short, we consider unit masses, as well as consider the pendulum bob to be a point mass, while its rod is considered to be massless and of unit length.

With the coordinate convention shown in Figure 5.3, the system's dynamic equations of motion are

$$2\ddot{x}_c + \cos(\varphi)\ddot{\varphi} - \sin(\varphi)\dot{\varphi}^2 = u, \tag{5.67a}$$

$$\ddot{\varphi} + \cos(\varphi)\ddot{x}_c - g\sin(\varphi) = 0, \tag{5.67b}$$

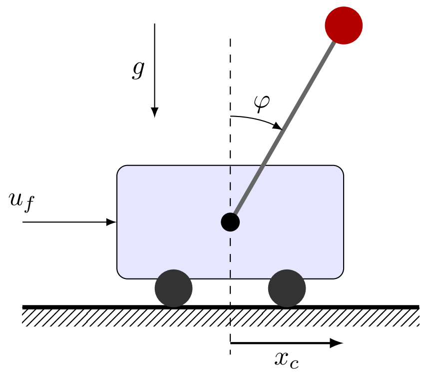

Figure 5.3: Schematic of the cart-pendulum system. It consists of an unactuated pendulum attached to an actuated cart, which can be controlled in the horizontal direction by an external force u_f.

where $g = 9.81\,\mathrm{m\,s^{-2}}$ is the gravitational acceleration. Thus

$$\mathbf{M}(q) = \begin{bmatrix} 2 & \cos(\varphi) \\ \cos(\varphi) & 1 \end{bmatrix}, \ \mathbf{C}(q, \dot{q}) = \begin{bmatrix} 0 & -\sin(\varphi)\dot{\varphi} \\ 0 & 0 \end{bmatrix}, \ \mathbf{G}(q) = \begin{bmatrix} 0 \\ -g\sin(\varphi) \end{bmatrix},$$

and $\mathbf{B}_u = \mathrm{col}(1, 0)$ corresponds to (5.2) for (5.67).

The task we will consider is the following: To generate (asymptotically) orbitally stable oscillations about the unstable upright equilibrium of the pendulum. In addition to solving this problem using the methods we considered so far in this chapter, we will first demonstrate how this can be done using a similar approach as a means of comparison. More specifically, we will utilize the virtual holonomic constraints (VHC) approach of [33] to generate such an orbit, and then the utilize the VHC-based transverse coordinates considered in Section 5.4.2 as to construct an orbitally stabilizing feedback controller. Note that, in addition to highlight the subtle differences between these approaches, the VHC-based method will also be utilized in an example in Chapter 8, where we will build from it a *robust* orbitally stabilizing control law using ideas within the realm of sliding mode control.

5.5.1 Virtual holonomic constraints–based approach

Orbit generation

As in Reference [33], we are looking to generate an orbit of (5.67a) upon which the virtual holonomic constraints $y(q) := x_c + a\sin(\varphi)$ vanishes for some $a \in \mathbb{R}$. As we did towards the end of Section 5.4.2, we will, for some smooth function $\theta : \mathbb{R}_{\geq 0} \to \mathbb{R}$, associate with $y(q)$ a vector-valued function

$$\mathcal{Q}(\theta) = \begin{bmatrix} -a\sin(\theta) \\ \theta \end{bmatrix}. \tag{5.68}$$

Obviously, $y(\mathcal{Q}(\theta)) \equiv 0$ for all $\theta \in \mathbb{R}$. The task at hand will therefore be to search for a T-periodic function $\theta : \mathbb{R}_{\geq 0} \to \mathbb{R}$, i.e. $\theta(t+T) = \theta(t)$, of minimal periodicity $T > 0$, such that $q_\star(t) = \mathcal{Q}(\theta(t))$ is a solution to (5.67a) under some continuous control input $u_f^\star(t)$.

Let us begin by assuming the invariance of $q_\star = \mathcal{Q}(\theta)$, such that $\dot{q}_\star = \mathcal{Q}'(\theta)\dot{\theta}$ and $\ddot{q}_\star(t) = \mathcal{Q}'(\theta)\ddot{\theta} + \mathcal{Q}''(\theta)\dot{\theta}^2$, with $\mathcal{Q}'(\theta) = \frac{d}{d\theta}\mathcal{Q}(\theta)$. From (5.67a) it is then clear that

$$(1-2a)\cos(\theta)\ddot{\theta} + (2a-1)\sin(\theta)\dot{\theta}^2 = u_f^\star \tag{5.69a}$$

$$(1 - a\cos^2(\theta))\ddot{\theta} + a\cos(\theta)\sin(\theta)\dot{\theta}^2 - g\sin(\theta) = 0, \tag{5.69b}$$

must hold for all $t \in \mathbb{R}_{\geq 0}$ along any solution of the form $q_\star(t) = \mathcal{Q}(\theta(t))$. Specifically, the $\mathcal{C}^2$-smooth function $\theta = \theta(t)$ must satisfy (5.69b), with the corresponding nominal control input $u_f^\star(t)$ found from (5.69a). Since (5.69b) is the reduced dynamics (see (5.22)) associated with $\mathcal{Q}(\theta)$, we recall from Lemma 5.5 that the equilibrium point $\theta = \theta_e = 0$ is a center if $a > 1$.

Moreover, in a similar manner to Proposition 5.12 (see also [33, Thm. 1]), the function $I(\cdot)$ defined by (5.64), which here is given by

$$\begin{aligned} I(\theta, \dot{\theta}, \theta_0, \dot{\theta}_0) = \frac{1}{2}(1 - a\cos^2(\theta))\Big[&(1 - a\cos^2(\theta))\dot{\theta}^2 \\ &- (1 - a\cos^2(\theta_0))\dot{\theta}_0^2 + 2g(\cos(\theta) - \cos(\theta_0))\Big], \end{aligned} \tag{5.70}$$

retains its zero value along any solution of (5.69b) with initial conditions $(\theta_0, \dot{\theta}_0)$. Hence, by taking $a > 1$, we can, for some $\theta_0 < 0$ sufficiently close to the center equilibrium, set $\dot{\theta}_0 = 0$ and find the velocity $\dot{\theta}(t)$ of the corresponding solution from $I(\theta, \dot{\theta}, \theta_0, 0) = 0$ until we possibly again have, for some $\theta \in \mathbb{R}$, that $\dot{\theta} = 0$. Due to the solutions of the reduced dynamics being mirrored across the horizontal axis in the phase plane, any such found T-periodic solution is therefore given by $(\theta(t), \dot{\theta}(t))$ for $t \in [0, T/2)$, and by $(\theta(t), -\dot{\theta}(t))$ for $t \in [T/2, T)$.

Choosing an s-parameterization and a projection operator

Suppose now that such a nontrivial, T-periodic solution $\theta_\star(t) = \theta_\star(t+T)$ of (5.69b) which encircles its (center) equilibrium point $(0, 0)$ has been found. The next step is then to obtain an s-parameterization and a projection operator[5]. In this regard, first note that we cannot use θ to parameterize the curve as $\dot{\theta}(t)$ will not be strictly positive everywhere along the orbit. Instead, we observe that the time derivative of $s(t) = \operatorname{atan2}(-\dot{\theta}(t), \theta(t))$, with $\operatorname{atan2}(\cdot)$ denoting the four-quadrant arctangent function, is given by

$$\dot{s}(t) = \frac{\dot{\theta}^2(t) - \theta(t)\ddot{\theta}(t)}{\theta^2(t) + \dot{\theta}^2(t)}.$$

If $\dot{s}(t) > 0$ for all $t \in [0, T)$, then we can always find the unique function $\rho : [0, 2\pi) \to \mathbb{R}_{\geq 0}$ satisfying $\dot{s}(t) \equiv \rho(s(t))$. Moreover, we can then find a pair of functions, $(\vartheta(s), \dot{\vartheta}(s))$, satisfying $\vartheta(s(t)) \equiv \theta(t)$ and $\dot{\vartheta}(s(t)) \equiv \dot{\theta}(t)$, such that

$$x_s(s) = \begin{bmatrix} \mathcal{Q}(\vartheta(s)) \\ \mathcal{Q}'(\vartheta(s))\dot{\vartheta}(s) \end{bmatrix} \quad \text{and} \quad p(x) = \operatorname{atan2}(-\dot{\varphi}, \varphi) \tag{5.71}$$

correspond, respectively, to an s-parameterization and a projection operator (see Def. 3.2 and Def. 4.5, respectively) for the target motion.

Feedback transformation and transverse coordinates

Given a periodic solution to (5.69b) with initial condition $(\theta_0, \dot{\theta}_0)$, we have the following candidates for transverse coordinates: $z_\perp = \operatorname{col}(y, \dot{y}, I)$ where

$$\begin{bmatrix} y \\ \dot{y} \\ I \end{bmatrix} := \begin{bmatrix} x_c + a\sin(\varphi) \\ \dot{x}_c + a\cos(\varphi)\dot{\varphi} \\ \frac{1}{2}\alpha(\varphi)\left[\alpha(\varphi)\dot{\varphi}^2 - \alpha(\varphi_0)\dot{\varphi}_0^2 + 2g(\cos(\varphi) - \cos(\varphi_0))\right] \end{bmatrix}, \tag{5.72}$$

with $\alpha(\varphi) := 1 - a\cos^2(\varphi)$. Indeed, by (5.70) one has $\|z_\perp(x_s(s))\| \equiv 0$ for all $s \in \mathcal{S}$, while both $z_\perp$ and its Jacobian matrix (see (5.66)) are locally well defined if $a\cos^2(\vartheta(s)) \neq 1$ for all $s \in [0, 2\pi)$.

Before linearizing the dynamics of these coordinates along the periodic orbit, we first introduce the following feedback transformation:

$$u_f = \frac{\sin(\varphi)(2a-1)}{1 - a\cos^2(\varphi)}\left(\dot{\varphi}^2 - g\cos(\varphi)\right) + \frac{1 + \sin^2(\varphi)}{1 - a\cos^2(\varphi)}u, \quad u \in \mathbb{R}. \tag{5.73}$$

It is well defined close to $\varphi = 0$, but grows unboundedly when $\varphi \to \arccos(1/\sqrt{a})$. Note that this transformation is partially feedback linearizing [13], in the sense that it results in $\ddot{y} = u$.[6] Thus the transverse dynamics

[5]Choosing a projection operator is not strictly necessary already at this this stage, but it can be convenient to do so while simultaneously choosing the parameterization.

[6]Notice from $\ddot{y} = u$ the possibility of pre-stabilizing the $(y, \dot{y})$-subspace by taking $u = \hat{u} - \hat{k}_y y - \hat{k}_{\dot{y}}\dot{y}$ for any constant gains $\hat{k}_y, \hat{k}_{\dot{y}} > 0$.

can be written as $\frac{d}{dt}z_\perp = \hat{A}_\perp(\varphi(t),\dot{\varphi}(t))z_\perp + \hat{B}_\perp(\varphi(t),\dot{\varphi}(t))u$, where

$$\hat{A}_\perp(\varphi,\dot{\varphi}) := \begin{bmatrix} 0 & 1 & 0 \\ 0 & 0 & 0 \\ 0 & 0 & \dot{\varphi}\frac{2a\cos(\varphi)\sin(\varphi)}{1-a\cos^2(\varphi)} \end{bmatrix}$$

and $\hat{B}_\perp(\varphi,\dot{\varphi}) := \mathrm{col}\big(0, 1, -\dot{\varphi}(1-a\cos^2(\varphi))\cos(\varphi)\big)$. The transverse linearization can then, in turn, be obtained by simply using the previously found parameterization $s \mapsto (\vartheta(s), \dot{\vartheta}(s))$; namely,

$$\dot{\boldsymbol{\delta}}_{z_\perp} = \mathcal{A}_\perp(s)\boldsymbol{\delta}_{z_\perp} + \mathcal{B}_\perp(s)K(s)u \tag{5.74}$$

where $s = s(t)$, $\mathcal{A}_\perp(s) = \hat{A}_\perp(\vartheta(s),\dot{\vartheta}(s))$ and $\mathcal{B}_\perp(s) = \hat{B}_\perp(\vartheta(s),\dot{\vartheta}(s))$.

Designing an orbitally stabilizing feedback

We will consider a periodic orbit similar to the one constructed in [33]. Specifically, we consider the orbit corresponding to (5.68) with $\theta(t) = \theta(t+T)$ the solution to (5.69b) for

$$a = 1.5 \quad \text{and} \quad (\theta_0, \dot{\theta}_0) = (0, 0.5). \tag{5.75}$$

Using (5.70), one can find that the amplitude of the induced oscillations of the pendulum is approximately 0.113 rad, such that the transverse coordinates are well defined when $|\varphi| < \sqrt{(1/a)} \approx 0.62\,\text{rad}$ as then $a\cos^2(\varphi) > 1$.

Using the transverse coordinates (5.72) and the feedback transformation (5.73), as well as using the parameterization and projection operator given by (5.71) (note that these are then also locally well defined), a nominal LQR-based feedback controller was designed for the system using Proposition 4.23 for the found transverse linearization. Specifically, the PRDE (4.35) with $\mathcal{Q}_\perp = \mathbf{I}_3$, $\Gamma_\perp = 10$ and $\kappa = 0$ was solved using Gusev's SDP method [177] which we considered in Chapter. 4.4.2, in which $\mathcal{R}_\perp(s)$ was approximated by a truncated Fourier series of order 100 for 500 evenly spaced sampling points. The elements of the resulting feedback matrix

$$K_\perp(s) = [K_y(s), K_{\dot{y}}(s), K_I(s)] = -\Gamma_\perp(s)\mathcal{B}_\perp^\intercal(s)\mathcal{R}_\perp(s)$$

are shown in Figure 5.4. The results from simulating the closed-loop system with initial conditions $x_0 = \mathrm{col}(-1, 0, 0, 0)$ are shown in Figure 5.5.

5.5.2 Suggested approach using synchronization functions

We will now again consider the task of generating orbitally stabilizing oscillations of the cart-pendulum system. Rather than using the VHC-based

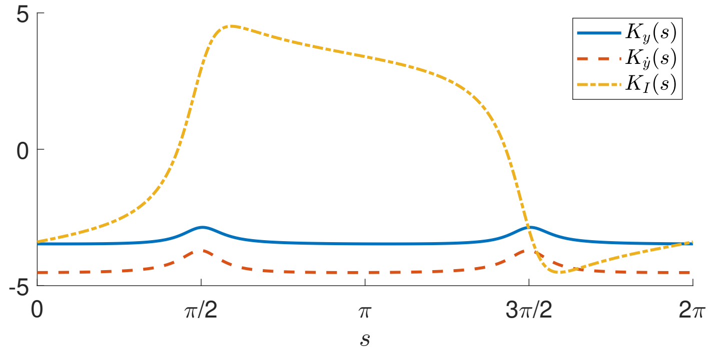

Figure 5.4: Elements of the nominal feedback matrix $K_\perp(s)$ found by solving the PRDE (4.35).

method as in the previous section, we will instead attempt to generate an s-parameterized orbit; specifically, one which is similar to the orbit induced by VHC-based method using the theory outlined in Section 5.3. We will then design an orbitally stabilizing control law based on the excessive transverse coordinates introduced in Section 4.5, using the specific structure of an underactuated mechanical system as we derived in Section 5.4.

Generating an s-parameterized periodic orbit

Consider the following vector of synchronization functions:

$$\Phi(s) = \text{col}\left(X(s), \Theta(s)\right).$$

Here both $X : \mathcal{S} \to \mathbb{R}$ and $\Theta : \mathcal{S} \to \mathbb{R}$ are smooth, while $\mathcal{S} = [0, 2\pi)$. The resulting reduced dynamics (5.22) associated with Φ is given by

$$\underbrace{\left(\Theta' + X' \cos(\Theta)\right)}_{\alpha(s)} \ddot{s} + \underbrace{\left(X'' + \Theta'' \cos(\Theta)\right)}_{\beta(s)} \dot{s}^2 \underbrace{-g \sin(\Theta)}_{\gamma(s)} = 0. \tag{5.76}$$

Our aim will now be choose the pair $\left(X(s), \Theta(s)\right)$ such that: 1) there exists a strictly positive, $\mathcal{C}^1$ function $\rho : \mathcal{S} \to \mathbb{R}_{>0}$, which is the unique positive solution to (5.23), i.e.

$$\alpha(s)\rho'(s)\rho(s) + \beta(s)\rho^2(s) + \gamma(s) = 0;$$

and 2), the resulting orbit, i.e.

$$\mathcal{O} = \left\{x \in \mathbb{R}^4 : \; x = \text{col}\left(\Phi(s), \Phi'(s)\rho(s)\right), \quad s \in \mathcal{S}\right\},$$

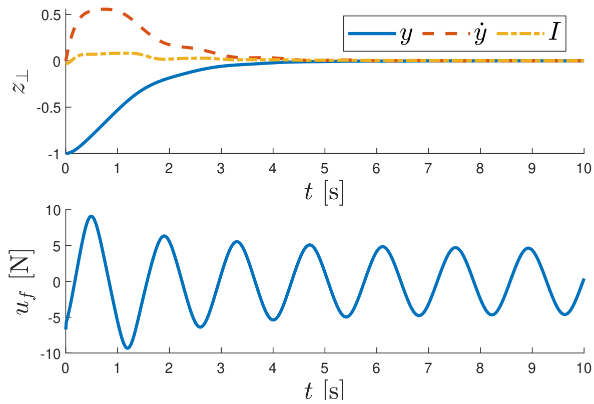

(a) Transverse coordinates and control input vs. time.

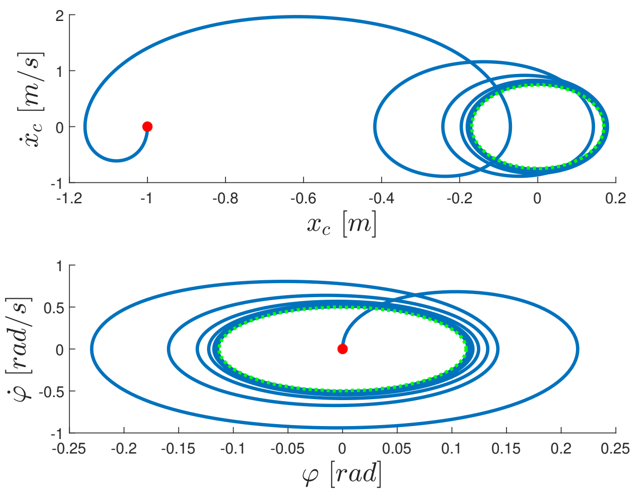

(b) Phase portraits.

Figure 5.5: Response of the cart-pendulum system under the VHC-based orbitally stabilizing feedback constructed in Section 5.5.1.

is similar to the one we generated in Section 5.5.1. Note that if such a function $\rho(\cdot)$ is found, then we have by (5.15) that the control curve of the corresponding maneuver is traced out by

$$u_s(s) = \big(2X' + \Theta' \cos(\Theta)\big)\,\rho'\rho + \big(2X'' + \Theta'' \cos(\Theta) - (\Theta')^2 \sin(\Theta)\big)\,\rho^2, \tag{5.77}$$

where the s-arguments on the right-hand side has been omitted as to shorten the notation.

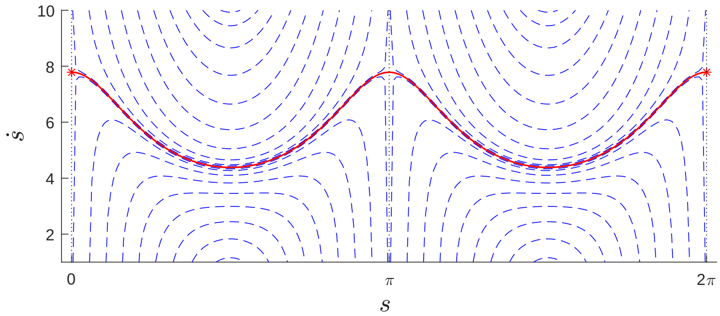

Figure 5.6: Phase portrait of the reduced dynamics (5.76) with (5.78). The red curve represents the positive solution $\dot{s} = \rho(s)$ over the interval $[0, 2\pi)$ for $a_2 = 0.5$.

Choosing synchronization functions: In order to find an orbit similar to the one constructed using the VHC-based approach in the previous section, we will consider

$$X(s) = -1.5 \sin\big(a_2 \cos(s)\big) \quad \text{and} \quad \Theta(s) = a_2 \cos(s). \tag{5.78}$$

Comparing it to the VHC (5.68), i.e. $\mathcal{Q}(\theta) = \mathrm{col}(-1.5\sin(\theta), \theta))$, it is clear that we are attempting to find a constant parameter $a_2 \in \mathbb{R}$ such that $\theta(t) \approx a_2 \cos(s(t))$, with $\theta(t)$ the solution to (5.69b) and $s(t)$ the solution to (5.76). Essentially, we want to pick a_2 to get the appropriate amplitude of the oscillations of the pendulum, as compared to VHC approach of [33] in which the amplitude is instead determined by the initial conditions $(\theta_0, \dot{\theta}_0)$. Hence, whereas the VHC-based approach provided a family of periodic solutions around the equilibrium, there can exist only one (positive) function $\rho(\cdot)$ for each choice of a_2 which simultaneously solves the reduced dynamics and ensures that $s(t)$ evolves from $s_0 = 0$ to $s_T = 2\pi$. For example, the red curve highlighted in Fig. 5.6 is the unique (positive) solution for the case when $a_2 = 0.5$. Note here that, even though

$$\alpha(s) = a_2 \sin(s) \big(1.5 \cos\big(a_2 \cos(s)\big) - 1\big)$$

vanishes for $s = s_s \in \{0, \pi, 2\pi\}$, the function $\rho(s)$ nevertheless crosses the vertical asymptotes that are visible in Fig. 5.6. Indeed, these singular points are all simple (see Def. 5.11), as $\lim_{s \to s_s} \delta(s)/\alpha(s) = 0$ since $\delta(s) = \beta(s) - \alpha'(s) = -1.5 a_2^2 \sin^2(s) \sin(\Theta(s))$ and $-\gamma(s_s)/\beta(s_s) > 0$.

Orbitally stabilizing feedback design

We found that the periodic orbit corresponding to $a_2 = 0.1129$ was very close to the periodic orbit which was constructed using the VHC approach.

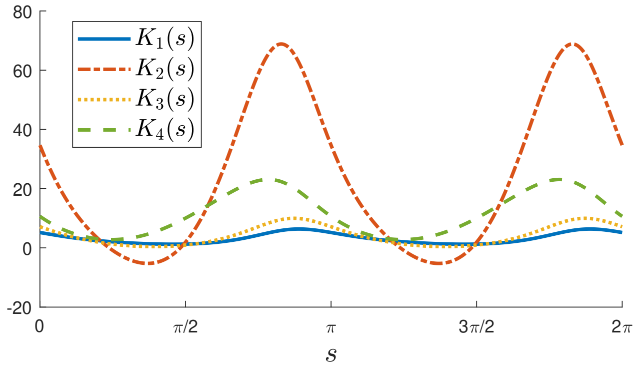

Figure 5.7: Elements of the nominal feedback matrix $K(s)$ found by solving the projected PRDE (4.96) using the SDP formulation (4.99).

Our aim will therefore now be to construct an orbitally stabilizing feedback for this orbit using the excessive transverse coordinates introduced in Section 4.5. To this end, we will begin by choosing a projection operator for this orbit.

Choosing a projection operator: Observe that upon the desired orbit, the angle of the pendulum and its angular velocity must evolve in time according to $\varphi_\star(t) = \Theta(s(t)) = a_2\cos(s(t))$ and $\dot{\varphi}_*(t) = \Theta'(s(t))\rho(s) = -a_2\sin(s(t))\rho(s(t))$. Hence, sufficiently close to the orbit, we can find s as the root of the following implicit equation:

$$h(x,s) = s - \operatorname{arctan2}\left(\dot{\varphi}, -\varphi\rho(s)\right) = 0. \tag{5.79}$$

Here $\operatorname{arctan2}(\cdot)$ denotes the four-quadrant arctangent function. We can therefore utilize Lemma 4.8 in order to obtain a projection operator, $p = p(x)$, which only depends on φ and $\dot{\varphi}$. Moreover, for this operator we have $Dp(x) = \rho(p)\left[\dot{\varphi}, -\varphi\right] / \big(\dot{\varphi}^2 + \varphi^2\rho^2(p) - \varphi\dot{\varphi}\rho'(p)\big)$.

Designing a PrjPRDE-based control law: Consider the control law (5.49) with $\mathbf{U}(\cdot)$ taken as (5.52a), that is $u_f = u_s\big(p(x)\big) + v$. We will utilize Proposition 4.44 in order to design an LQR-based feedback of the form (4.97), i.e. $v = K(p)e_\perp$. In order to find an approximate solution to the the projected periodic Riccati differential equation (PrjPRDE) (4.96) we used the semidefinite programming (SDP) problem formulation (4.99), by taking the matrix function $R(s)$ as a trigonometric polynomial of order 50 and by using 500 evenly spaced grid points over the interval $[0, 2\pi)$. In the PrjPRDe we took with $\mathcal{Q} = \mathbf{I}_4$, $\Gamma = 10$ and $\kappa = 0.2$. The resulting SDP was solved using the YALMIP toolbox [200] and the SDPT3 solver [201]. The resulting solution satisfied (4.96) within a maximum error norm of less than 1×10^{-7} for all $s \in [0, 2\pi)$. The elements of the resulting feedback matrix $K(s) = \big[K_1(s), K_2(s), K_3(s), K_4(s)\big]$ are shown in Figure 5.7.

Results from numerical simulation: In order to implement the control law, the projection operator was found by searching for the root of the implicit equation (5.79) using MATLAB's `fzero` function, which is based on an algorithm similar to Brent's method [165]. Note that a naive implementation of Newton's method was also tested for this purpose, and was found to have a similar convergence rate to the desired root, and resulted in the closed-loop system having almost the exact same response.

The results from simulating the system with the initial conditions $x_0 = \mathrm{col}(-1, 0, 0, 0)$ are shown in Figure 5.5.2. The obtained response can be seen to be more aggressive than the response under the VHC-based feedback shown in Figure 5.5. This is likely due to both the large control gains (see Fig. 5.7) and that the magnitude of transverse coordinate $I(\cdot)$ used in the VHC approach is generally less than the magnitude of $e_2 = \mathrm{col}(e_{2,1}, e_{2,2})$.

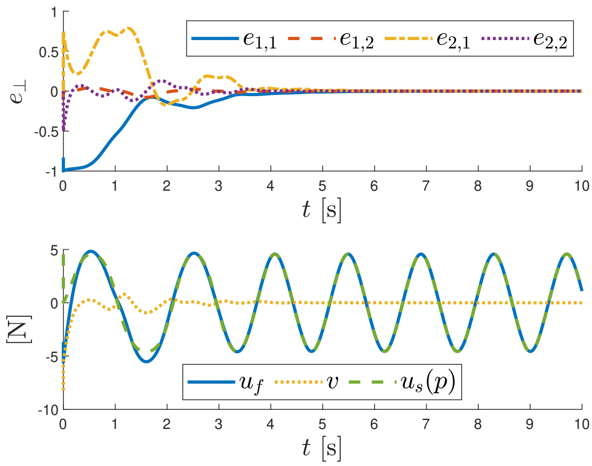

(a) Transverse coordinates and control inputs vs. time.

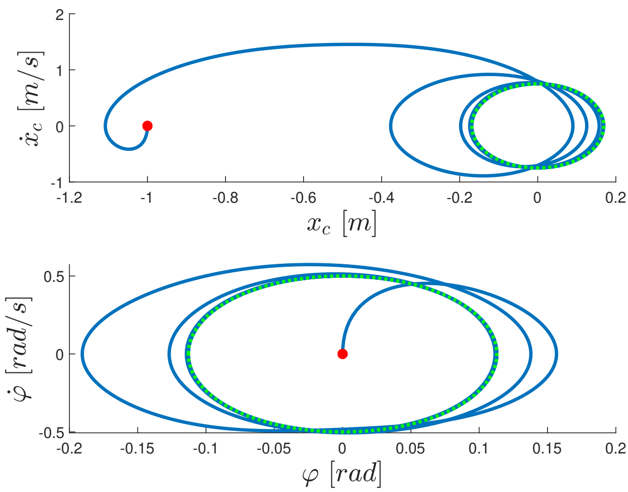

(b) Phase portraits.

Figure 5.8: Response of the cart-pendulum system under the orbitally stabilizing feedback constructed in Section 5.5.2.

Chapter 6

Orbital Stabilization of Point-to-Point Maneuvers

In this chapter, we consider the problem of stabilizing, via continuous static state-feedback, heteroclinic orbits corresponding to so-called point-to-point (or rest-to-rest) maneuvers. This is achieved by defining a projection operator which allows one to "merge" the Jacobian linearization at the equilibrium points on the orbit's boundaries with a transverse linearization along it.

6.1 Introduction

A *point-to-point* (PtP) motion is perhaps the most fundamental of all motions in robotics: Starting from rest at a certain configuration (point), the task is to steer the system to rest at a different goal configuration. Often it can also be beneficial, or even necessary, to know a smooth maneuver which connects the two configurations. Indeed, it provides guarantees that the controls remain within the admissible range along the nominal motion, and that neither any kinematic- nor dynamics constraints are violated along it.

We have already seen in Chapter 5 a possible approach for solving the nontrivial task of planning such (open-loop) PtP maneuvers in an underactuated mechanical system. Assume, therefore, that such an open-loop maneuver is known. The task we are looking to solve in this chapter is therefore that of designing an orbitally stabilizing feedback controller for this motion.

By definition, the boundaries (or end points) of any PtP motion must correspond to (forced) equilibrium points of the dynamical system. Hence, as opposed to the (closed) periodic orbits we have mainly considered so far in this thesis, we now also have to take into consideration these equilibria on the boundaries of the maneuver when designing an orbitally stabilizing feedback for it. This directly excludes regular transverse coordinates–based methods such as [33, 34, 56], which would then require some form of control switching and/or orbit jumping à la [202, 203]. This of course does not mean that such methods cannot be modified in some (switching- or jumping-free) manner as to solve such tasks. Rather, it means that one must detect, in some continuous fashion, when one should only stabilize the transverse direction and when one should also stabilize the tangential direction to account for the equilibria.

Regarding this latter point, the idea of using projections onto the orbit as proposed in [22, 47] can, as we will later see, be modified for this purpose. Indeed, through the use of an s-parameterization for such maneuvers together with the an appropriate projection operator, stabilizing the origin of the projection-based error function first introduced in Section 4.3 in fact corresponds to stabilizing the desired orbit (together with its boundary points). The novel approach we propose in this chapter for stabilizing the zero-level set of this error function combines a transverse linearization, similar to that in [26], with the standard Jacobian linearization about the equilibrium points on the boundaries.

Outline. The chapter is organized as follows. In Section 6.2, the problem statement is given and the concept of an s-parameterized point-to-point maneuver is introduced. In Section 6.3 we define projection operators for this type of maneuvers. Conditions upon an orbitally stabilizing feedback for a PtP maneuver, as well as how to design one are stated in Section 6.3.4. A nonprehensile manipulation example is then considered in Section 6.4.

6.2 Problem formulation

Consider again a nonlinear control-affine system

$$\dot{x} = f(x) + B(x)u \tag{6.1}$$

with state $x \in \mathbb{R}^n$ and with $(m < n)$ controls $u \in \mathbb{R}^m$. It is assumed that both $f : \mathbb{R}^n \to \mathbb{R}^n$ and the columns of the full-rank matrix function $B : \mathbb{R}^n \to \mathbb{R}^{n\times m}$, denoted $b_i(\cdot)$, are twice continuously differentiable ($\mathcal{C}^2$).

Let the pair $(x_e, u_e) \in \mathbb{R}^n \times \mathbb{R}^m$ correspond to an equilibrium of (6.1), i.e., $f(x_e) + B(x_e)u_e \equiv \mathbf{0}_{n\times 1}$. If we denote

$$A(x, u) := Df(x) + \sum_{i=1}^{m} Db_i(x)u_i, \tag{6.2}$$

then the (forced) equilibrium point x_e is said to be *linearly stabilizable* if there exists some $K \in \mathbb{R}^{m\times n}$ such that $A(x_e, u_e) + B(x_e)K$ is Hurwitz [40].

That is, the full-state feedback $u = u_e + K(x - x_e)$ then renders x_e a locally exponentially stable equilibrium of (6.1).

The concept of s-parameterized point-to-point maneuvers

Suppose (x_α, u_α) and (x_ω, u_ω), $x_\alpha \neq x_\omega$, are linearly stabilizable equilibrium points of (6.1). For $\mathcal{S} := [s_\alpha, s_\omega] \subset \mathbb{R}$, $s_\alpha < s_\omega$, we will assume knowledge of three functions,

$$x_s : \mathcal{S} \to \mathbb{R}^n, \quad u_s : \mathcal{S} \to \mathbb{R}^m, \quad \text{and} \quad \rho : \mathcal{S} \to \mathbb{R}_{\geq 0}, \tag{6.3}$$

which correspond to an s-parameterization (cf. Asm. 3.1 and Def. 3.2) of a point-to-point (PtP) maneuver

$$\mathcal{M} := \{(x, u) \in \mathbb{R}^n \times \mathbb{R}^m : \; x = x_s(s), \; u = u_s(s), \; s \in \mathcal{S}\}$$

of (6.1), whose boundaries are (x_α, u_α) and (x_ω, u_ω).

Definition 6.1. The triplet (x_s, u_s, ρ) in (6.3) is an *s-parameterization* of the PtP maneuver $\mathcal{M}$ of (6.1) if:

P1 $x_s(\cdot)$ is $\mathcal{C}^2$, while $u_s(\cdot)$ and $\rho(\cdot)$ are $\mathcal{C}^1$;

P2 $\rho(s_\alpha) = \rho(s_\omega) \equiv 0$, as well as $\rho(s) > 0$ for all $s \in \operatorname{int} \mathcal{S}$;

P3 $\|\mathcal{F}(s)\| > 0$ for all $s \in \mathcal{S}$, where $\mathcal{F}(s) := x_s'(s)$;

P4 $x_s : \mathcal{S} \to \mathbb{R}^n$ is one-to-one;

P5 $\mathcal{F}(s)\rho(s) = f(x_s(s)) + B(x_s(s))u_s(s)$ for all $s \in \mathcal{S}$;

P6 $(x_s(s_i), u_s(s_i)) = (x_i, u_i)$ for both $i \in \{\alpha, \omega\}$. □

Comparing the above definition to Definition 3.2, it is clear that Definition 6.1 further specifies that $\rho(s_\omega) = \rho(s_\alpha) \equiv 0$, as well as the additional boundary condition **P6**. Due to the properties **P1** − **P6**, it follows that the maneuver's projection upon state space, that is

$$\mathcal{O} := \{x \in \mathbb{R}^n : \; x = x_s(s), \quad s \in \mathcal{S}\}, \tag{6.4}$$

is compact and consist of a (forced) *heteroclinic orbit* of (6.1) and its limit points. For simplicity's sake, we will therefore refer to the set $\mathcal{O}$ as the maneuver's orbit. As before, **P5** ensures that it is a controlled invariant set of (6.1), with the evolution of curve parameter as a function of time, $s = s(t)$, governed by the autonomous differential equation

$$\dot{s} = \rho(s). \tag{6.5}$$

By the chain rule we have

$$\dot{x}_\star(s(t)) = x_s'(s(t))\dot{s}(t) = \mathcal{F}(s(t)\rho(s(t)),$$

which inserted into the left-hand side of the expression in **P5** demonstrates that $\mathcal{M}$ is consistent with the dynamics (6.1). Hence, whereas $\|\dot{x}_\star(s(t))\| \equiv 0$ for $s(t) \in \{s_\alpha, s_\omega\}$, the key aspect of such an s-parameterization is that Property **P3** holds for $x_s(\cdot)$, as $\rho(\cdot)$ instead vanishes at the boundaries. Notice, however, that as we assume $\rho(\cdot)$ to be $\mathcal{C}^1$ and $\rho(s_\alpha) = \rho(s_\omega) \equiv 0$, the rate at which $s(\cdot)$ convergence to s_ω (resp. s_α) in positive (resp. negative) time from within $\mathcal{S}$ can be at most exponential, which would correspond to $\rho'(s_\omega) < 0$ (resp. $\rho'(s_\alpha) > 0$).

By comparing the nominal state curve's arc length computed using a time-parameterization and the s-parameterization, that is

$$\mathfrak{L}_{\mathcal{O}} = \int_{-\infty}^{\infty} \|\dot{x}_\star(s(\tau))\| d\tau = \int_{s_\alpha}^{s_\omega} \|\mathcal{F}(\sigma)\| d\sigma,$$

it is also clear this is a compact representation of such a point-to-point motion.

For our purpose, however, the key property of such an s-parameterization is that it allows one to construct a projection operator for the maneuver's orbit, which by **P1** and **P4** is well-defined in a vicinity of $\mathcal{O}$.

The orbital stabilization problem and a reduction principle

The resulting orbital stabilization problem we are looking to solve in this chapter is essentially equivalent to Problem 3.3. For the reader's convenience, we nevertheless restate in here. For this purpose, recall the notation $\operatorname{dist}(\mathcal{O}, x) := \inf_{y\in\mathcal{O}} \|x - y\|$.

Problem 6.2. *(Orbital Stabilization) Find a mapping $k : \mathbb{R}^n \to \mathbb{R}^m$, which is locally Lipschitz in a neighborhood of $\mathcal{O}$ and satisfies $k(x_s(s)) \equiv u_s(s)$ for all $s \in \mathcal{S}$, such that the orbit $\mathcal{O}$ is asymptotically stable with respect to* (6.1) *under the control law $u = k(x)$. Namely, for every $\epsilon > 0$, there is a $\delta > 0$, such that for any solution $x(\cdot)$ of the closed-loop system satisfying* $\operatorname{dist}(\mathcal{O}, x(t_\alpha)) < \delta$, *it is implied that* $\operatorname{dist}(\mathcal{O}, x(t)) < \epsilon$ *for all $t \geq t_\alpha$ (*stability*), and that* $\operatorname{dist}(\mathcal{O}, x(t)) \to 0$ *as $t \to \infty$ (*attractivity*).*

Recall also that the asymptotic stability of $\mathcal{O}$ is equivalent to the *asymptotic orbital stability* (see Def. 2.2) of all the solutions upon it. Hence it is still well justified to refer to the above problem as an orbital stabilization problem even though the boundaries of $\mathcal{O}$ correspond to equilibrium points.

Observe also that since we are looking to stabilize a heteroclinic orbit upon which all solutions converge to x_ω, it follows that x_ω is necessarily asymptotically stable relative to $\mathcal{O}$. We need therefore only apply a reduction theorem [108–110] to arrive at the following conclusion:

Proposition 6.3. *A solution to Problem 6.2 implies the (local) asymptotic stability of x_ω with respect to the closed-loop system* (6.1) *under $u = k(x)$.*

Proof. The statement follows directly from, e.g., Corollary 7 in [110]. □

6.3 A projection-based orbital stabilization scheme

6.3.1 Projection operators for point-to-point maneuvers

So far in this thesis, the definition of a projection operator which has been used (see Def. 4.5) is only applicable to non-vanishing orbits, such as periodic orbits. The following definition therefore provides additional conditions in order to also account for the equilibrium points on the boundaries of $\mathcal{O}$ in the case of point-to-point maneuvers.[1]

Definition 6.4. (Projection operators for PtP maneuvers) Let $\mathfrak{X} \subset \mathbb{R}^n$ denote a simply-connected domain containing a neighborhood of $\mathcal{O}$, whose interior can partitioned into three disjoint, open subsets, $\mathcal{H}_\alpha$, $\mathcal{T}$, $\mathcal{H}_\omega$, such that $\mathrm{cl}(\mathfrak{X}) = \mathrm{cl}(\mathcal{H}_\alpha \cup \mathcal{T} \cup \mathcal{H}_\omega)$. Here

- $\mathcal{T}$ is an open tubular neighborhood of $\mathcal{O}$;
- $\mathcal{B}_\epsilon(x_\alpha)\backslash\mathcal{T} \subset \mathrm{cl}\,\mathcal{H}_\alpha$ and $\mathcal{B}_\epsilon(x_\omega)\backslash\mathcal{T} \subset \mathrm{cl}\,\mathcal{H}_\omega$, for some $\epsilon > 0$;
- $\mathrm{cl}(\mathcal{T}) \cap \mathrm{cl}(\mathcal{H}_i) \neq \emptyset \ \forall i \in \{\alpha, \omega\}$, $\mathrm{cl}(\mathcal{H}_\alpha) \cap \mathrm{cl}(\mathcal{H}_\omega) = \emptyset$.

A map $p : \mathfrak{X} \to \mathcal{S}$ is said be to a *projection operator* for $\mathcal{O}$ if it Lipschitz continuous and well defined within $\mathfrak{X}$, as well as satisfies

C1 $p(x_\star(s)) \equiv s$ for all $s \in \mathcal{S}$;

C2 $p(\mathcal{H}_\alpha) \equiv s_\alpha$, $p(\mathcal{H}_\omega) \equiv s_\omega$, and $p(\mathrm{int}\,\mathcal{T}) \in \mathrm{int}\,\mathcal{S}$;

C3 $p(\cdot)$ is $\mathcal{C}^r$, $r \geq 1$, within $\mathcal{H}_\alpha$, $\mathcal{T}$ and $\mathcal{H}_\omega$. □

In order to shed some light on the necessity of these requirements, we consider again the set

$$\Pi(s) := \{x \in \mathfrak{X} : p(x) = s\} \tag{6.6}$$

[1] We will also use Definition 6.4 in Chapter 7 when we consider the problem of orbitally stabilizing quasi-periodic orbits for a class of hybrid systems.

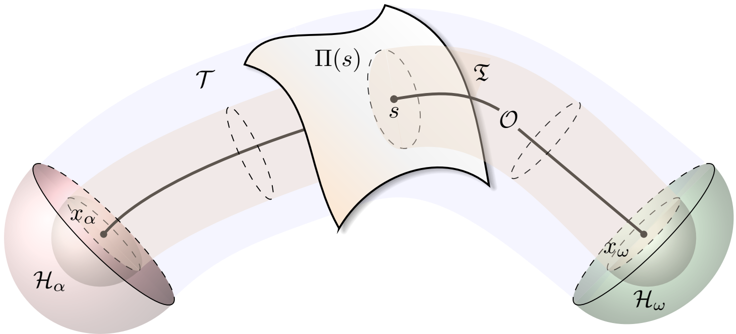

Figure 6.1: Illustration of the moving Poincaré section $\Pi(s)$ defined in (6.6) traveling along the orbit $\mathcal{O}$ which begins and terminates at x_α and x_ω, respectively. The gradient of the projection operator is assumed to be nonzero and well defined within the blue-shaded tubular neighborhood $\mathcal{T}$. Within darkly shaded hemispheres $\mathcal{H}_\alpha$ and $\mathcal{H}_\omega$, on the other hand, the gradient vanishes as the projection operator projects the states onto the respective equilibrium therein. The aim of this chapter is the construction of a positively invariant neighborhood $\mathfrak{T}$ within which all solutions converge to $\mathcal{O}$.

which we previously considered in Section 4.3. As is illustrated in Figure 6.1, for some $s \in \operatorname{int}\mathcal{S}$, it corresponds to a *moving Poincaré section* [54] as before, that is $(n-1)$-dimensional hypersurface whose tangent space at $x_s(s)$, denoted $\mathbf{T}\Pi(s)$, is orthogonal to

$$\mathcal{P}(s) := Dp(x_s(s)). \tag{6.7}$$

Thus by Condition **C1** (which also appeared in Def. 4.5), it follows that $\mathcal{P}(s)\mathcal{F}(s) \equiv 1$ for all $s \in \mathcal{S}$, from which, in turn, one can deduce that the surface $\Pi(s)$ is locally transverse to the direction of the nominal orbit's flow given by $\mathcal{F}(s)$. The tubular neighborhood $\mathcal{T}$ in the definition (consider the blue-shaded tube in Figure 6.1) is guaranteed to everywhere have a nonzero radius due Property **P4** in Definition 6.1. It can be taken as any connected subset of $\bigcup_{s\in\operatorname{int}\mathcal{S}}\Pi(s)$ such that the surfaces $\Pi(s_1)\cap\mathcal{T}$ and $\Pi(s_2)\cap\mathcal{T}$ are locally disjoint for any $s_1, s_2 \in \operatorname{int}\mathcal{S}$, $s_1 \neq s_2$. Thus, for any x within $\mathcal{T}$, $Dp(x)$ is nonzero, bounded, continuous, and normal to $\Pi(p(x))$ at x.

The main additions to Definition 6.4 compared to Definition 4.5 are therefore conditions **C2** and **C3**. These two conditions are needed in order to guarantee the existence of the two half-ball-like regions, $\mathcal{H}_\alpha$ and $\mathcal{H}_\omega$, which have nonzero measure and correspond to $\Pi(s_\alpha)$ and $\Pi(s_\omega)$, respectively (consider the darkly shaded semi-ellipsoids in Figure 6.1). As a consequence, $\|Dp(x)\| \equiv 0$ for all $x \in \operatorname{int}\mathcal{H}_\alpha \cup \operatorname{int}\mathcal{H}_\omega$, and hence $p(\cdot)$ is

$\mathcal{C}^r$ almost everywhere within $\mathfrak{X}$, except at $\mathfrak{X}_\alpha := \lim_{s\to s_\alpha^+}\Pi(s)$ and $\mathfrak{X}_\omega := \lim_{s\to s_\omega^-}\Pi(s)$, which correspond to the intersections $\mathcal{H}_\alpha \cap \mathcal{T}$ and $\mathcal{T}\cap\mathcal{H}_\omega$.

Recall the notation for the line segment, $\mathfrak{L}(a,b) := \{a+(b-a)\iota,\ \iota\in[0,1]\}$, which connects two points $a,b\in\mathbb{R}^n$. In regard to finding a projection operator satisfying the above definition, the following statement shows that the type of operators considered in Proposition 4.9 also provides a large family of such operators for this type of orbits as well.

Proposition 6.5. *Let the smooth matrix-valued function $\Lambda:\mathcal{S}\to\mathbb{M}^n_{\succeq 0}$ be such that $\mathfrak{h}(s) := \Lambda(s)\mathcal{F}(s)$ is of class $\mathcal{C}^r$ on $\mathcal{S}$, and $\mathcal{F}^{\mathsf{T}}(s)\Lambda(s)\mathcal{F}(s)>0$ holds for all $s\in\mathcal{S}$. Then there is an ϵ and a neighborhood $\mathfrak{X}\subset\mathbb{R}^n$ of $\mathcal{O}$, with $\mathcal{B}_\epsilon(x_s(s))\subset\mathfrak{X}$ for all $s\in\mathcal{S}$, such that*

$$p(x) = \mathop{\arg\min}_{\substack{s\in\mathcal{S}\\ \mathfrak{L}(x_s(s),x)\subset\mathcal{B}_\epsilon(x_s(s))}} \Big[(x-x_s(s))^{\mathsf{T}}\Lambda(s)(x-x_s(s))\Big] \tag{6.8}$$

is a projection operator for the s-parameterized PtP maneuver corresponding to $\mathcal{O}$ which is $\mathcal{C}^r$-smooth within $\mathcal{T}$. Moreover,

$$\mathcal{P}(s) := Dp(x_\star(s)) = \frac{\mathcal{F}^{\mathsf{T}}(s)\Lambda(s)}{\mathcal{F}^{\mathsf{T}}(s)\Lambda(s)\mathcal{F}(s)} \tag{6.9}$$

holds for its Jacobian matrix $Dp(\cdot)$ evaluated inside $\mathcal{T}$.

Proof. Even though the first part of the proof is essentially equivalent to that of Proposition 4.9, we repeat it here for completeness' sake.

Differentiating the terms inside the brackets in (6.8) with respect to s, we obtain the function

$$J(x,s) := (x-x_s(s))^{\mathsf{T}}\left[\Lambda'(s)(x-x_s(s)) - 2\Lambda(s)\mathcal{F}(s)\right].$$

Since $\frac{\partial}{\partial s}J(x,s)\big|_{x=x_s(s)} = 2\mathcal{F}^{\mathsf{T}}(s)\Lambda(s)\mathcal{F}(s)>0$, the function to be minimized is locally convex, implying that Condition **C1** in Definition 6.4, i.e. $s\equiv p(x_s(s))$ for all $s\in\mathcal{S}$, is satisfied. Note from Definition 6.1 that the curve $x_s(\cdot)$ has bounded curvature (Property **P1**) and is not self-intersecting (Property **P4**). Thus the implicit function theorem (see, e.g., [160, Thm. 3.1.10]) ensures that there exists, in a certain vicinity of each point on $\mathcal{O}$, a unique function $p(x)$ satisfying $J(x,p(x))\equiv 0$, which in turn implies that $p(x)$ solves (6.8). Thus, for $\mathfrak{X}\subset\mathbb{R}^n$ a sufficiently small neighborhood of $\mathcal{O}$, the requirement $\mathfrak{L}(x_s(p(x)),x)\subset\mathcal{B}_\epsilon(x_s(s))\subset\mathfrak{X}$ ensures the uniqueness of a solution to (6.8) within $\mathcal{T} := \{x\in\mathfrak{X}:\ J(x,p(x))=0\}$.

Denoting $e := x - x_s(p)$, then for $x \in \mathcal{T}$ [160, Cor. 3.1.11]

$$Dp(x) = \frac{\mathcal{F}^\mathsf{T}\Lambda - e^\mathsf{T}\Lambda'}{\mathcal{F}^\mathsf{T}\Lambda\mathcal{F} + e^\mathsf{T}\left[\frac{1}{2}\Lambda'' e - 2\Lambda'\mathcal{F} - \Lambda\mathcal{F}'\right]}.$$

Here we have omitted the p-arguments to shorten the notation, i.e. $\mathcal{F} = \mathcal{F}(p)$ etc. Hence $Dp(\cdot)$ is nonzero and of class $\mathcal{C}^r$ (as $\Lambda\mathcal{F}'$ is) within $\mathcal{T} \subset \mathbb{R}^n$, with $\mathcal{P}(s) := Dp(x_\star(s))$ given by (6.9) therein.

What remains is therefore to show the parts of **C2** and **C3** in Definition 6.4 relating to the sets $\mathcal{H}_\alpha$ and $\mathcal{H}_\omega$, within which $p(x) = s_\alpha$ and $p(x) = s_\omega$. Denote by $\mathfrak{X}_\alpha = \mathrm{cl}(\mathcal{H}_\alpha) \cap \mathrm{cl}(\mathcal{T})$ and $\mathfrak{X}_\omega = \mathrm{cl}(\mathcal{T}) \cap \mathrm{cl}(\mathcal{H}_\omega)$, respectively. Due to the expression for $Dp(\cdot)$ above, which is valid within $\mathcal{T}$, together with $\mathcal{P}\mathcal{F} = 1$, it follows that sufficiently close to x_ω the states will leave $\mathcal{T}$ if they go in the direction $\mathcal{F}(s_\omega)$ when on $\mathfrak{X}_\omega$, but the unique minimizer of (6.8) will nevertheless still be s_ω if x remains sufficiently close to $\mathfrak{X}_\omega$, even if $\Lambda(\cdot)$ is not positive definite, as long as $\mathfrak{X}$ is a sufficiently small neighborhood of $\mathcal{O}$. In order to show this, consider a point $x \in \mathfrak{X}\backslash\mathcal{T}$ lying sufficiently close to x_ω such that it can written as $x = x_{\Pi(s)} + c_s\mathcal{F}(s)$ for some $x_{\Pi(s)} \in \Pi(s) \subset \mathcal{T}$ and $c_s(x) > 0$. We are therefore looking for an s which minimizes the nonnegative function

$$\begin{aligned}&\big[(x_{\Pi(s)} - x_s(s))^\mathsf{T}\Lambda(s)(x_{\Pi(s)} - x_s(s))\\ &\quad + 2c_s(x)(x_{\Pi(s)} - x_s(s))^\mathsf{T}\Lambda(s)\mathcal{F}(s_\omega)c_s(x) + c_s(x)\mathcal{F}^\mathsf{T}(s_\omega)\Lambda(s)\mathcal{F}(s)\big]\end{aligned}$$

subject to $s \in \mathcal{S}$ and $\mathfrak{L}(x_s(s), x) \subset \mathfrak{X}$. Not considering the latter constraint, we have by the the Karush–Kuhn–Tucker (KKT) conditions [164, Theorem 12.1] that the following is necessary for s to be a minimizer to this constrained optimization problem: $J(x, s) - \mu_\alpha + \mu_\omega = 0$. Here $\mu_\alpha, \mu_\omega \geq 0$ are the Lagrange multipliers associated with the inequality constraints $s - s_\alpha \geq 0$ and $s_\omega - s \geq 0$, which must satisfy the complementary slackness conditions: $\mu_i(s - s_i) = 0$ for $i \in \{\alpha, \omega\}$. Since $J(x_{\Pi(s)}, s) = 0$, it is therefore necessary that

$$c_s\mathcal{F}^\mathsf{T}(s)\big[c_s\Lambda'(s) - \Lambda(s)\big]\mathcal{F}(s) + 2c_s\tilde{x}_{\Pi(s)}^\mathsf{T}\big[\Lambda'(s) - \Lambda(s)\big]\mathcal{F}(s) - \mu_\alpha + \mu_\omega = 0,$$

where $\tilde{x}_{\Pi(s)} := x_{\Pi(s)} - x_s(s)$. One can easily show that s_ω satisfies this equation for some $\mu_\omega > 0$. Moreover, for $\mathfrak{X}$ a sufficiently small neighborhood of $\mathcal{O}$, there cannot be a solution $s \in \mathrm{int}\,\mathcal{S}$ which does not violate $\mathfrak{L}(x_s(s), x) \subset \mathfrak{X}$. Indeed, by making $\mathfrak{X}$ small enough, one can guarantee that $-c_s\mathcal{F}^\mathsf{T}(s)\Lambda(s)\mathcal{F}(s)$ is the dominant term, which cannot be canceled by the Lagrange multipliers as $\mu_\alpha = \mu_\omega = 0$ if $s \in \mathrm{int}\,\mathcal{S}$. Using the same arguments about x_α with then $c_s(x) < 0$, the existence of $\mathcal{H}_\alpha$ and $\mathcal{H}_\omega$ in

Condition **C2** is therefore implied, and the requirements of **C3** are met. Thus all the conditions of Definition 6.4 are satisfied, which concludes the proof. □

6.3.2 Implicit representation of the orbit

Given a projection operator $p : \mathfrak{X} \to \mathcal{S}$ as by Definition 6.4 which is at least $\mathcal{C}^2$-smooth within $\mathcal{T}$, let the corresponding projection onto $\mathcal{O}$ be denoted $x_p(x) := (x_s \circ p)(x)$, and consider the function $e = e(x)$ previously considered in Section 4.3, defined by

$$e := x - x_p(x). \tag{6.10}$$

From the properties of $x_s(\cdot)$ and $p(\cdot)$ (see Def. 6.1 and Def. 6.4, respectively), it follows that e is well defined for $x \in \mathfrak{X}$, locally Lipschitz in a neighborhood of $\mathcal{O}$, and therefore r-times continuously differentiable almost everywhere therein. Most importantly, however, is the fact that the zero-level set of this function corresponds to the nominal orbit $\mathcal{O}$ which we aim to stabilize, while, locally, its magnitude is nonzero away from it.

Similarly to the previous chapters, our goal will therefore be to design a control law which (locally) drives the value of e to zero. In order to achieve this, the linearization of the dynamics of e about the orbit will again be our tool of choice. Yet, obtaining the linearization of e is not as straightforward for a PtP maneuver as it were for trivial- or periodic orbits. In fact, due to how we have defined projection operators, it will be a combination of these two linearization techniques. To better illustrate this fact, consider the half-balls $(\mathcal{H}_\alpha, \mathcal{H}_\omega)$ and the tube $\mathcal{T}$ introduced in Section 6.3.1. Clearly, whenever $x \in \operatorname{int} \mathcal{H}_i$ for a fixed $i \in \{0, f\}$, one has $e = x - x_i$ as $p(x) \equiv s_i$, and thus $De(x) = \mathbf{I}_n$ therein. For $x \in \mathcal{T}$, on the other hand, the function $e(\cdot)$ corresponds to a vector of excessive transverse coordinates (see Sec. 4.5). Hence its Jacobian matrix evaluated along the orbit inside $\mathcal{T}$ is given by

$$\mathcal{E}_\perp(s) := De(x_s(s)) = \mathbf{I}_n - \mathcal{F}(s)\mathcal{P}(s) \tag{6.11}$$

with $\mathcal{P}$ defined in (6.7). Recall from Lemma 4.28 that $\mathcal{E}_\perp(s)$ is a projection matrix which can be used to project any vector $x \in \mathbb{R}^n$ onto $\mathbf{T}\Pi(s)$. Our aim will therefore be to "merge" the regular (Jacobian) linearization about the equilibria on the boundaries of $\mathcal{O}$ with the a transverse linearization, corresponding to the first-order components of e which evolve upon $\mathbf{T}\Pi(s)$.

6.3.3 Merging two linearization techniques

In order to solve our current goal, namely the stabilization of the zero-level set of the function $e = e(x)$ defined by some projection operator $p = p(x)$

which is $\mathcal{C}^2$-smooth within $\mathcal{T}$, we will consider for (6.1) a control law of the form

$$u = u_s(p) + K(p)e. \tag{6.12}$$

Here the function $u_s(\cdot)$ provides the nominal control input upon the s-parameterized maneuver (see Def. 6.1) and $K : \mathcal{S} \to \mathbb{R}^{m\times n}$ is smooth. Note that, due to $p(\cdot)$ being locally Lipschitz in $\mathfrak{X}$, the (local) existence and uniqueness of a solution $x(t)$ to (6.1) is guaranteed by the Picard–Lindelöf theorem (see, e.g. [74, Thm. 2.2]) if u is taken according to (6.12), as the right-hand side of (6.1) is then locally Lipschitz in a neighborhood of $\mathcal{O}$.

Note that whenever $Dp(\cdot)$ is well defined, we have by the chain rule that the time derivative of e under (6.12) is given by

$$\dot{e} = De(x)\left(f(x) + B(x)\left[u_s(p) + K(p)e\right]\right), \tag{6.13}$$

where $p = p(x)$. As we have narrowed our scope to the control law (6.12), Problem 6.2 is therefore equivalent to the following:

Problem 6.6. *Find a smooth, matrix-valued function $K : \mathcal{S} \to \mathbb{R}^{m\times n}$ such that the origin of* (6.13) *is locally asymptotically stable.*

In order to attempt to find a solution to this problem, we will extract the first-order components of the right-hand side of (6.13) with respect to e. To this end, let

$$A_s(s) := A(x_s(s), u_s(s)) \quad \text{and} \quad B_s(s) := B(x_s(s)), \tag{6.14}$$

where $A(\cdot)$ is given by (6.2), as well as

$$A_{cl}(s) := A_s(s) + B_s(s)K(s). \tag{6.15}$$

We may then state the following.

Proposition 6.7. *Let $p : \mathfrak{X} \to \mathcal{S}$ be a projection operator as by Definition 6.4 which is $\mathcal{C}^2$-smooth within $\mathcal{T}$. Then there exists a neighborhood $\mathcal{N}(\mathcal{O})$ of $\mathcal{O}$, such that the time derivative of $e = e(x)$ can be written in the following forms within three specific subsets of $\mathcal{N}(\mathcal{O})$: If $x \in \mathcal{H}_i \cap \mathcal{N}(\mathcal{O})$ with $i \in \{\alpha, \omega\}$ fixed, then*

$$\dot{e} = A_{cl}(s_i)e + O(\|e\|^2); \tag{6.16}$$

whereas if $x(t) \in \mathcal{T} \cap \mathcal{N}(\mathcal{O})$, then

$$\dot{e} = \left[\mathcal{E}_\perp(p)A_{cl}(p) - \mathcal{F}(p)\mathcal{P}'(p)\rho(p)\right]\mathcal{E}_\perp(p)e + O(\|e\|^2), \tag{6.17}$$

where $p = p(x)$ and $\mathcal{P}'(s) = \mathcal{F}^{\mathsf{T}}(s)D^2p(x_s(s))$.

Proof. Recall that $De(x) = \mathbf{I}_n$ whenever x is within the interior of either $\mathcal{H}_\alpha$ or $\mathcal{H}_\omega$, whereas $De(x) = \mathbf{I}_n - \mathcal{F}(p)Dp(x)$ within $\mathcal{T}$. Hence, by assuming $p = s_i$ to be fixed, (6.16) follows by applying Taylor's theorem [160] to the right-hand side of (6.13) about x_i.

In order to obtain (6.17), we can artificially extend the curve $x_s(\cdot)$ at its boundaries in the appropriate direction along $\mathcal{F}(\cdot)$, thus allowing us to use Proposition 4.30 (note that this artificial extension is only needed if the curvature of $\mathfrak{X}_i \cap \mathcal{N}(\mathcal{O})$ is non-zero, as the line segment $\mathfrak{L}(x, x_p(x))$ might then cross it). Considering, for instance, s_ω, this extended curve can be of the form $x_s^e(s) = x_\omega + \mathcal{F}(s_\omega)(s - s_\omega) + \frac{1}{2}\mathcal{F}'(s_\omega)(s - s_\omega)^2$, as well as $u_s^e(s) = u_s(s_\omega) + u_s'(s_\omega)(s - s_\omega)$, for $s \geq s_\omega$. Hence, due to the criteria imposed on the orbit (see Def. 6.1), there always exists an $\epsilon > 0$ allowing for a natural concatenation of the chosen projection operator in the appropriate direction, specifically onto the right-open interval $[s_\omega, s_\omega + \epsilon)$, that preserves its smoothness.

Denote by p^e such an extended ($\mathcal{C}^2$-smooth) projection operator. It is such that $p(x) \equiv p^e(x)\ \forall x \in \mathcal{T}$, while associated with any point on $[s_\omega, s_\omega + \epsilon)$ there is a moving Poincaré section (see (6.6)) of dimension $n - 1$. This implies the existence of a (tubular) neighborhood enveloping the extended curve, within which, for all states satisfying $p^e(x) = s_\omega$, the line segment $\mathfrak{L}\big(x, (x_s \circ p^e)(x)\big)$ remains within this neighborhood. Denote by $F_\perp(x)$ the right-hand side of (6.13), and by $F_\perp^e(x)$ the corresponding function for the extended curves (x_s^e, u_s^e) with the projection operator p^e. Note that $F_\perp \equiv F_\perp^e$ for all x in $\mathcal{T}$. Hence the statement follows from the fact that the right-hand side of (6.17) is equivalent to that obtained by applying Proposition 4.30 to $F_\perp^e$ within a sufficiently small open subset of $\mathcal{T}$ containing the orbit.[2]

□

Consider the linear, time-invariant system

$$\dot{y} = A_{cl}(s_i)y, \quad y \in \mathbb{R}^n, \tag{6.18}$$

for some fixed $i \in \{\alpha, \omega\}$. It corresponds to the first-order approximation system of (6.16). Clearly it is also equivalent to the linearized system obtained from the Jacobian linearization of (6.1) under the linear control law $u = u_s(s_i) + K(s_i)(x - x_i)$ about the respective equilibrium point. By Corollary 4.31, the first-order approximation system of (6.17) about $\mathcal{O}$ (i.e.

[2]An alternative path to this result is to introduce the (minimizing) geodesic curve, $\gamma : [0, 1] \to \mathfrak{X}_i$, on the hypersurface $\mathfrak{X}_i$ connecting $x_p(x)$ and x. Since $Dp(x)$ (taken from within $\mathcal{T}$) is normal to $\mathfrak{X}_i$ for any $x \in \mathfrak{X}_i$, one has $Dp(\gamma(\tau))\gamma'(\tau) = 0\ \forall \tau \in [0, 1]$. Thus $F_\perp(x) = \int_0^1 \frac{\partial F_\perp}{\partial x}\big|_{\gamma(t)}\gamma'(t)dt = \int_0^1 \frac{\partial F_\perp}{\partial x}\big|_{\gamma(t)}\big(\mathbf{I}_n - \mathcal{F}(s_i)Dp(\gamma(t))\big)\gamma'(t)dt$, where $\gamma'(0) \to \mathcal{E}_\perp(p)e \in \mathbf{T}_{x_p}\Pi(p)$ as $e \to 0$.

the transverse linearization associated with e inside $\mathcal{T}$), on the other hand, is equivalent to the following system of differential-algebraic equations:

$$\dot{z} = \left[\mathcal{E}_\perp(s)A_{cl}(s) - \mathcal{F}(s)\mathcal{P}'(s)\rho(s)\right] z, \tag{6.19a}$$

$$0 = \mathcal{P}(s)z, \tag{6.19b}$$

where $z \in \mathbb{R}^n$ and with $s = s(t)$ a solution to (6.5).

As is well known (see, e.g., [44, Theorem 4.6]), the origin of (6.18) is exponentially stable at both s_α s_ω if, and only if, for any $Q_\alpha, Q_\omega \in \mathbb{M}^n_{\succ 0}$, there exist unique $L_\alpha, L_\omega \in \mathbb{M}^n_{\succ 0}$ satisfying a pair of the algebraic Lyapunov equations (ALEs):

$$A_{cl}^\mathsf{T}(s_\alpha)L_\alpha + L_\alpha A_{cl}(s_\alpha) = -Q_\alpha, \tag{6.20a}$$

$$A_{cl}^\mathsf{T}(s_\omega)L_\omega + L_\omega A_{cl}(s_\omega) = -Q_\omega. \tag{6.20b}$$

A similar statement can also be readily obtained for (6.19) using the exact same arguments as we used to prove Theorem 4.41 in Section 4.6.2:

Lemma 6.8. *Suppose there exist smooth matrix-valued functions $L, Q_\perp : \mathcal{S} \to \mathbb{M}^n_{\succ 0}$ such that the projected Lyapunov differential equation (PrjLDE)*

$$\begin{aligned}\mathcal{E}_\perp^\mathsf{T}(s)\big[A_{cl}^\mathsf{T}(s)\mathcal{E}_\perp^\mathsf{T}(s)L(s) + L(s)\mathcal{E}_\perp(s)A_{cl}(s) + Q_\perp(s)\big]\mathcal{E}_\perp(s)\\ + \rho(s)\mathcal{E}_\perp^\mathsf{T}(s)\big[L'(s) - (\mathcal{P}'(s))^\mathsf{T}\mathcal{F}^\mathsf{T}(s)L(s) - L(s)\mathcal{F}(s)\mathcal{P}'(s)\big]\mathcal{E}_\perp(s) = \mathbf{0}_n\end{aligned} \tag{6.21}$$

is satisfied for all $s \in \mathcal{S}$. Then the time derivative of the scalar function $V_\perp = z^\mathsf{T}L(s(t))z$, with $z = z(t)$ governed by (6.19), *is $\dot{V}_\perp = -z^\mathsf{T}Q_\perp(s(t))z$.* □

Note here that by (6.19b) we have $z^\mathsf{T}L(s)z = z^\mathsf{T}L_\perp(s)z$ where $L_\perp(s) := \mathcal{E}_\perp^\mathsf{T}(s)L(s)\mathcal{E}_\perp(s)$. Recall that, similarly to the ALEs, a solution of the form $L_\perp(s) = \mathcal{E}_\perp^\mathsf{T}(s)L_\perp(s)\mathcal{E}_\perp(s)$ satisfying the PrjLDE in the periodic case is unique (see Theorem 4.41). As the following statement demonstrates, the uniqueness of such a solution also holds whenever ρ vanishes on the boundaries of $\mathcal{S}$.

Proposition 6.9. *Let $\rho : \mathcal{S} \to \mathbb{R}_{\geq 0}$ be $\mathcal{C}^1$, as well as satisfy $\rho(s_\alpha) = \rho(s_\omega) \equiv 0$, $\rho'(s_\alpha) > 0$ and $\rho(s) > 0$ for all $s \in \operatorname{int}\mathcal{S}$. Then there exists a $\mathcal{C}^1$ solution $L : \mathcal{S} \to \mathbb{M}^n_{\succ 0}$ to* (6.21) *for some smooth $Q_\perp : \mathcal{S} \to \mathbb{M}^n_{\succ 0}$ if, and only if, there exists a unique, $\mathcal{C}^1$-smooth solution $L_\perp : \mathcal{S} \to \mathbb{M}^n_{\succeq 0}$ to*

$$\mathcal{E}_\perp^\mathsf{T}(s)\big[\rho(s)L_\perp'(s) + A_{cl}^\mathsf{T}(s)L_\perp(s) + L_\perp(s)A_{cl}(s) + Q_\perp(s)\Big]\mathcal{E}_\perp(s) = \mathbf{0}_n \tag{6.22}$$

satisfying $L_\perp(s) = \mathcal{E}_\perp^\mathsf{T}(s)L_\perp(s)\mathcal{E}_\perp(s)$ for all $s \in \mathcal{S}$.

Proof. Note that we will sometimes omit the s-arguments in the following as to shorten the notation.

Given a solution $L(s)$ to (6.21), let $L_\perp := \mathcal{E}_\perp^\top L\mathcal{E}_\perp$. Clearly $L_\perp = \mathcal{E}_\perp^\top L_\perp \mathcal{E}_\perp$ then holds as $\mathcal{E}_\perp^2 = \mathcal{E}_\perp$ by Lemma 4.28. Differentiating $L_\perp(s)$ with respect to s yields $L_\perp' = \left(\frac{d}{ds}\mathcal{E}_\perp^\top\right)L\mathcal{E}_\perp + \mathcal{E}_\perp^\top L'\mathcal{E}_\perp + \mathcal{E}_\perp^\top R\left(\frac{d}{ds}\mathcal{E}_\perp\right)$. By then using that $\left(\frac{d}{ds}\mathcal{E}_\perp\right)\mathcal{E}_\perp = -\mathcal{F}\mathcal{F}^\top D^2 p(x_s)$, and inserting the above expression for $L_\perp'$ into (6.22), one finds that (6.22) holds if $L(s)$ satisfies (6.21).

To show that the converse holds as well, let $L_\perp(s) = \mathcal{E}_\perp^\top(s)L_\perp(s)\mathcal{E}_\perp(s)$ solve (6.21). Taking then $L(s) := L_\perp(s) + h_L(s)\mathcal{P}^\top(s)\mathcal{P}(s)$, with $h_L : \mathcal{S} \to \mathbb{R}_{>0}$ an arbitrary smooth function, one can easily show, using the properties stated in Lemma 4.28, that $L(s)$ satisfies (6.21).

What remains is therefore to show that a solution

$$L_\perp(s) = \mathcal{E}_\perp^\top(s)L_\perp(s)\mathcal{E}_\perp(s)$$

to (6.21) is unique. In this regard, let $N_\perp : \mathcal{S} \to \mathbb{R}^{n\times n-1}$ be defined by (4.88). Following the exact same steps as in the proof of Theorem 4.41, one can show that a solution $L(s)$ to (6.22) implies that there is a solution to

$$\mathcal{L}_\perp'(s)\rho(s) = -\mathcal{A}^\top(s)\mathcal{L}_\perp(s) - \mathcal{L}_\perp(s)\mathcal{A}(s) - \mathcal{Q}_\perp(s), \tag{6.23}$$

where where $\mathcal{A}(s) := N_\perp^\dagger(s)\mathcal{E}_\perp(s)A_{cl}(s)N_\perp(s)$, while the matrix functions $\mathcal{L}_\perp(s) := N_\perp^\top(s)L(s)N_\perp(s)$ and $\mathcal{Q}_\perp(s) := N_\perp^\top(s)Q(s)N_\perp(s)$ are both sufficiently smooth and positive definite. In order to show uniqueness, we use the fact that $\rho(s_\alpha) = 0$. Hence, due to both $\mathcal{L}_\perp(s_\alpha)$ and $\mathcal{Q}_\perp(s_\alpha)$ being members of $\mathbb{M}_{\succ 0}^{n-1}$ and satisfying the algebraic Lyapunov equation (6.23) for $s = s_\alpha$, it follows that the constant matrix $\mathcal{A}(s_\alpha)$ must necessarily be Hurwitz, which in turn implies that $\mathcal{L}_\perp(s_\alpha)$ is unique [44, Theorem 4.6]. Since the right-hand side of (6.23) is continuously differentiable, and the derivative of the left-hand side evaluated at $s = s_\alpha$ equals $\mathcal{L}_\perp'(s_\alpha)\rho'(s_\alpha)$, it follows that it has a unique solution $\mathcal{L}_\perp(s)$. Consequently

$$\hat{L}_\perp(s) = \mathcal{E}_\perp^\top(s)L(s)\mathcal{E}_\perp(s) = (N_\perp^\dagger(s)\mathcal{E}_\perp(s))^\top\mathcal{L}_\perp(s)N_\perp^\dagger(s)\mathcal{E}_\perp(s)$$

is also unique, which concludes the proof. □

6.3.4 Conditions upon an orbitally stabilizing feedback

In Chapter 4 we saw that the (local) exponential stability of a closed orbit could be determined by finding a suitable Lyapunov function. Specifically, a positive (semi-) definite function $V = V(x)$ which could be written in a quadratic-like form. Take, for instance, the function

$$V = e^\top(x)L(p(x))e(x). \tag{6.24}$$

In the case of a trivial orbit (an equilibrium point) $x_e \in \mathbb{R}^n$, such that $L(p(x)) = L_e$ and $e = x - x_e$, then V is a Lyapunov function for the trivial orbit if L_e is a solution to an ALE as (6.20). For a periodic orbit, on the other hand, recall from Theorem 4.41 that $L(\cdot)$ then instead had to be a solution to some PrjLDE. Using (6.24) together with the fact that the orbit was closed, we could prove its local exponential stability (see Thm. 4.41).

In order to stabilize the type of orbits we consider in this chapter, specifically the compact set $\mathcal{O}$, we will provide additional conditions to ensure its stability. The main idea is simple: to look for a (smooth) matrix-valued function $L : \mathcal{S} \to \mathbb{M}^n_{\succ 0}$ which solves both the ALEs (6.20) and the PrjLDE (6.21) (or (6.22)), without necessarily requiring that $L(s_\omega) \succeq L(s_\alpha)$. Intuitively, by using Figure 6.1, such a solution would imply the following: First, due to (6.20a), any solution starting within a sufficiently small subset of $\mathcal{H}_\alpha$ containing x_α will either convergence onto x_α or be fed into the tube $\mathcal{T}$. Second, by (6.21), there is a sufficiently small tubular neighborhood of $\mathcal{O}$ contained within $\mathcal{T}$ which is positively invariant, such that the solutions within it either converge onto $\mathcal{O}$ or are funneled into $\mathcal{H}_\omega$. Third, due to (6.20b), there is a subset of $\mathcal{H}_\omega$ within which all solutions either converge directly to x_ω at an exponential rate, or back into a subset of $\mathcal{T}$. Lastly, all of these subsets can be taken as level sets of the function (6.24), which locally is strictly decreasing at an exponential rate. Hence (6.24) is a strict Lyapunov function for $\mathcal{O}$, ensuring its exponential stability.

With this in mind, the main contribution of this chapter follows:

Theorem 6.10. *Given a projection operator $p : \mathfrak{X} \to \mathcal{S}$ satisfying Definition 6.4 which is $\mathcal{C}^2$-smooth within $\mathcal{T}$, consider the closed-loop system* (6.1) *under the (locally Lipschitz) control law* (6.12). *If there exists a $\mathcal{C}^1$-smooth matrix-valued function $L : \mathcal{S} \to \mathbb{M}^n_{\succ 0}$ such that*

1. *For some $Q_\alpha, Q_\omega \in \mathbb{M}^n_{\succ 0}$, $L_\alpha = L(s_\alpha)$ and $L_\omega = L(s_\omega)$ satisfy the algebraic Lyapunov equations* (6.20)*;*

2. *For some smooth $Q_\perp : \mathcal{S} \to \mathbb{M}^n_{\succ 0}$, $L_\perp(s) := \mathcal{E}_\perp^\top(s) L(s) \mathcal{E}_\perp(s)$ satisfies the projected Lyapunov differential equation* (6.22) *for all $s \in \mathcal{S}$.*

Then

a) *The final equilibrium, x_ω, is asymptotically stable;*

b) *The set $\mathcal{O}$, defined in* (6.4), *is exponentially stable;*

c) *There exists a pair of numbers, $\mu, \upsilon \in \mathbb{R}_{>0}$, such that the time derivative of the locally Lipschitz function $V(\cdot)$, defined in* (6.24), *satisfies $\dot{V}(x) \le -\mu V(x)$ for almost all x in $\mathfrak{T} = \{x \in \mathbb{R}^n : \ V(x) < \upsilon\}$.*

Proof. By the reduction principle stated in Corollary 11 in [110], *a*) is implied by *b*). Moreover, since the (forward) invariance of $\mathcal{O}$ holds due to the existence of the maneuver (see Property **P5** in Def. 6.1) and the properties of projection operators (see Def. 6.4), we also claim that *c*) implies *b*). Thus, before showing that the theorem's hypotheses imply *c*), we will validate this claim.

To this end, let us first note that $x \mapsto V(x)$ is not differentiable at the hypersurfaces $\mathfrak{X}_\alpha := \lim_{s\to s_\alpha^+} \Pi(s)$ and $\mathfrak{X}_\omega := \lim_{s\to s_\omega^-} \Pi(s)$ (see (6.6) for the definition of Π), but it is locally Lipschitz everywhere else in the projections operator's domain $\mathfrak{X}$. Since V is locally Lipschitz in $\mathfrak{X}$ (as p is), we have that the hypersurfaces $\mathfrak{X}_\alpha$ and $\mathfrak{X}_\omega$ have Lebesgue measure zero by Rademacher's theorem (see, e.g., [204]). This fact will allow us to validate the previously stated claim by utilizing Clarke's generalized directional derivative (based on his generalized gradient [204, Thm. 8.1]) and the comparison lemma [44] (see also Theorems 3.1 and 3.2 in [112]).

Denote $V_*(t) = V(x(t))$ and consider the upper-right (Dini) derivative $V_*^+(t)$ of $V_*(t)$, defined by $V_*^+(t) := \limsup_{h\to 0^+} \frac{1}{h}\left[V_*(t+h) - V_*(t)\right]$. At any $x = x(t)$, this is equivalent to (see, e.g., [169]):

$$V^+(x) = \limsup_{h\to 0^+} \frac{1}{h}\left[V(x + hf_{cl}(x)) - V(x)\right].$$

Here $f_{cl}(x) := f(x) + B(x)\big[u_s(p) + K(p)e\big]$ corresponds to the right-hand side of the closed-loop system (6.1), which, as we recall, is locally Lipschitz and thus guaranteeing (local) existence and uniqueness of solutions. Note, moreover, that $\|V^+(x)\| \le l_V \|f_{cl}(x)\|$ for some Lipschitz constant $l_V > 0$. It is known that Clarke's generalized gradient [204] can be used to show that the following holds:

$$V^+(x) \le V^\circ(x) = \limsup_{y\to x} \left\{DV(y)f_{cl}(x) :\ y \notin \mathfrak{X}_\alpha \cup \mathfrak{X}_\omega\right\}.$$

Hence *c*) implies $V_*^+(t) \le -\mu V_*(t)$ holding for all $t \ge t_0$ if the system is initialized within some neighborhood $\mathcal{T} \subset \mathfrak{X}$ of $\mathcal{O}$ at time t_0. Thus *c*) $\implies$ *b*) follows from the comparison lemma (see, e.g., [44, 169]).

What remains is therefore to show that the theorem's hypotheses imply *c*). Under the assumption that V is differentiable at some x in $\mathfrak{X}$, one finds, using the shorthand notation $p = p(x)$, that its time derivative is equal to

$$\dot{V} = \dot{e}_\perp^\top R(p)e_\perp + e_\perp^\top\left[R'(p)Dp(x)\dot{x}\right]e_\perp + e_\perp^\top R(p)\dot{e}_\perp. \tag{6.25}$$

Hence, whenever x is within the interior of either of the sets $\operatorname{int}\mathcal{H}_i$, $i \in \{\alpha, \omega\}$, where $\|Dp(x)\| = 0$, one has by (6.16) and the ALEs (6.20) that the following holds therein:

$$\dot{V} = -e_\perp^\top Q_i e_\perp + O(\|e_\perp\|^3). \tag{6.26}$$

Whenever x is in $\mathcal{T}$, one instead has $Dp(x)\dot{x} = \rho(p(x)) + O(\|e_\perp\|)$ (this follows from the first-order Taylor expansion about $x_\star(p(x))$ and by using (6.5)). Thus by (6.17), (4.47) and (6.25) we obtain, for $x \in \mathcal{T}$:

$$\begin{aligned}\dot{V} =& e_\perp^\top \mathcal{E}_\perp^\top \big[A_{cl}^\top \mathcal{E}_\perp^\top R + R\mathcal{E}_\perp A_{cl} \\ &+ \rho\big[R' - (\mathcal{P}')^\top \mathcal{F}^\top R - R\mathcal{F}\mathcal{P}'\big]\big]\mathcal{E}_\perp e_\perp + O(\|e_\perp\|^3).\end{aligned}$$

Since a solution $R_\perp(s)$ to (6.22) implies a solution to (6.21) (see Prop. 6.9), we thus obtain, using also (4.47), that

$$\dot{V} = -e_\perp^\top Q_\perp(p) e_\perp + O(\|e_\perp\|^3). \tag{6.27}$$

Thus, by (6.26) and (6.27), there exists some constant $\mu > 0$ such that the differential inequality $\dot{V} \leq -\mu V$ holds almost everywhere within a neighborhood $\mathcal{N}$ of $\mathcal{O}$ where $\|e_\perp\|$ is sufficiently small. This concludes the proof $\square$

Recall from Proposition 4.43 that if (6.21), or equivalently (6.22), is satisfied for one projection operator $p(\cdot)$, then for any other projection operator $\hat{p}$ the resulting PrjLDE (6.21) corresponding to $u = u_s(\hat{p}) + K(\hat{p})\big[\mathbf{I}_n - \mathcal{F}(\hat{p})\mathcal{P}(\hat{p}) + \mathfrak{F}(\hat{p})\hat{\mathcal{P}}(\hat{p})\big]\hat{e}$ will also be satisfied. Here $\mathcal{P}(s) = Dp(x_s(s))$, $\hat{\mathcal{P}}(s) = D\hat{p}(x_s(s))$ and $\hat{e} = x - x_s(\hat{p})$, while $\mathfrak{F} : \mathcal{S} \to \mathbb{R}^n$ is some arbitrary smooth function. Hence, in addition to the linear stabilizability of the two equilibrium points, it is necessary that the non-vanishing part of the orbit $\mathcal{O}$ is linearly *transversely* stabilizable for a solution to Theorem 6.10 to exist. However, given such a solution for one projection operator, an equivalent solution might not necessarily exist for another due to the boundary equilibria. Thus, before we move on to showing how such a feedback can be constructed, we will apply the method to a simple fully-actuated, one-degree-of-freedom system as to highlight the effect of the projection operator upon the resulting feedback controller.

Example 6.1. Consider the double integrator

$$\ddot{q} = u, \quad q(t), u(t) \in \mathbb{R},$$

with state vector $x = \mathrm{col}(q, \dot{q})$. Starting from rest at q_α, the task is to drive the system to rest at q_ω ($> q_\alpha$) along the curve $x_s(s) = \mathrm{col}(s, \rho(s))$. Here $s \in \mathcal{S} := [q_\alpha, q_\omega]$ and $\rho(s) := \kappa(s - q_\alpha)(q_\omega - s)^2$ for some constant

$\kappa > 0$. As $\|\mathcal{F}(s)\|^2 = 1 + (\rho'(s))^2 \geq 1$, this is an s-parameterization as by Definition 6.1.

Suppose $p(\cdot)$ is a projection operator in line with Def. 6.4 (we will provide some candidates for this operator shortly). Using $p = p(x)$, we define

$$e_1 := q - p, \quad e_2 := \dot{q} - \rho(p) \quad \text{and} \quad u_s(p) := \rho'(p)\rho(p),$$

such that $u = u_s(p) - k_1 e_1 - k_2 e_2$ is of the form of (6.12). Let us therefore check when this feedback, corresponding to a constant $K = [-k_1, -k_2]$, satisfies the conditions in Theorem 6.10 for a given $p(\cdot)$

We begin by considering the ALEs (6.20). Their solutions necessarily correspond to the constant matrices $A_{cl}(s_\alpha)$ and $A_{cl}(s_\omega)$ being Hurwitz, which is the case only if $k_1, k_2 > 0$ as

$$A_{cl} := \begin{bmatrix} 0 & 1 \\ -k_1 & -k_2 \end{bmatrix}.$$

Suppose, therefore, in the following that $k_1, k_2 > 0$ and let $L \in \mathbb{M}^2_{\succ 0}$ be the corresponding unique solution to $A_{cl}^{\mathsf{T}} L + L A_{cl} = -2\mathbf{I}_2$. We may then consider the (locally Lipschitz) Lyapunov function candidate $V = 2^{-1} e^{\mathsf{T}} L e$, with $e = \mathrm{col}(e_1, e_2)$, whose origin evidently corresponds to the desired orbit. Within the interiors of $\Pi(q_\alpha)$ and $\Pi(q_\omega)$, with $\Pi(\cdot)$ defined in (6.6), where $\|Dp\| = 0$, we then have $\dot{V} = -\|e\|^2$. To determine the stability of the orbit as a whole, we therefore need to check that we also have contraction within some tubular neighborhood contained in $\mathcal{T}$ for the chosen projection operator. We consider two different such operators next.

By taking inspiration from [22], let us first consider the projection operator corresponding to taking $\Lambda = L$ in (6.8). Using (6.9), we then observe that $\mathcal{E}_\perp^{\mathsf{T}}(s) L \mathcal{F}(s) = \mathbf{0}_{1\times 2}$ for all $s \in \mathcal{S}$. Hence (6.22) is everywhere satisfied for $L_\perp = L$ and $Q = \mathbf{I}_2$ (see [22] for further details). Moreover, we have $\dot{V} = -\|e\|^2$ for all x such that $p(x) \in (q_\alpha, q_\omega)$.

Consider now instead the operator obtained by taking $\Lambda = \mathrm{diag}(1, 0)$ in (6.8). This is equivalent to $p(x) = \mathrm{sat}_{q_\alpha}^{q_\omega}(q)$, where $\mathrm{sat}_a^b(\cdot)$ is the saturation function with lower- and upper bound a and b, respectively. (A specific example of using this operator is shown in Figure 6.2.) Clearly then $e_1 \equiv 0$ for $q \in [q_\alpha, q_\omega]$, while it can be shown that $\dot{e}_2 = -(k_2 + \rho'(p))e_2$. Thus, the time derivative of the above Lyapunov function candidate now satisfies

$$\dot{V} = -L_{22}(k_2 + \rho'(p))e_2^2 = -L_{22}(k_2 + \rho'(p))\|e\|^2$$

whenever $q \in (q_\alpha, q_\omega)$, with $L_{22} > 0$ the bottom-right element of L. We can therefore ensure that V will be strictly decreasing everywhere inside the tube

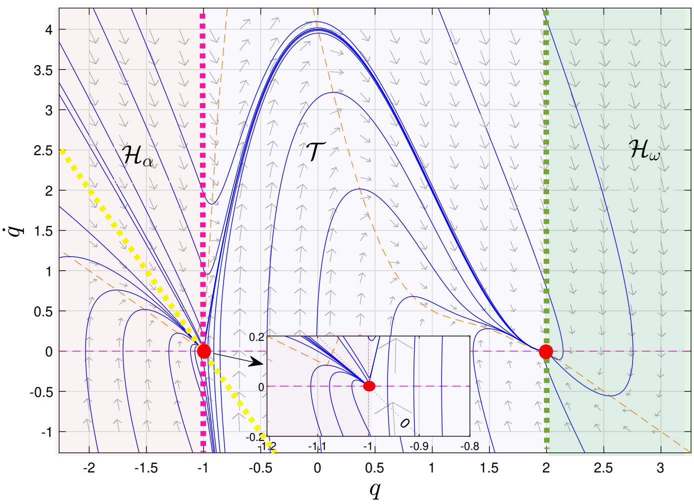

Figure 6.2: Phase portrait of $\ddot{q} = u$, with u corresponding to Example 6.1 for $q_\alpha = -1$, $q_\omega = 2$, $\kappa = 1$, $p(x) = \mathrm{sat}_{q_\alpha}^{q_\omega}(q)$ and $k_1 = k_2 = 4$. The level curve $\dot{q} + 2(q+1) = 0$ crossing $(q_\alpha, 0)$ is illustrated by the yellow, dotted line.

(except, of course, on the nominal orbit) by taking, e.g., $k_2 > \sup_{s\in\mathcal{S}} |\rho'(s)|$. This is nevertheless in contrast to the previous operator (i.e. $\Lambda = L$) where $k_2 > 0$ could be taken arbitrarily small and still ensure contraction, thus highlighting the dependence of the feedback $K(\cdot)$ upon the choice of $p(\cdot)$.

Avoiding solutions getting "trapped" about the initial equilibrium

Under a control law (6.12) satisfying the conditions in Theorem 6.10, any solution of (6.1) initialized in vicinity of $\mathcal{O}$ will converge either directly to the initial equilibrium x_α, which is rendered partially unstable (a "saddle"), or onto $\mathcal{O}\backslash\{x_\alpha\}$ and then onward to x_ω. However, since we have assumed ρ to be continuously differentiable on the whole of $\mathcal{S}$, the divergence away from x_α on $\mathcal{M}$ is at most exponential. Moreover, it implies that the system's states can get "trapped" if they enter the region of attraction of x_α. Indeed, they will then converge toward x_α at an exponential rate, but never enter into the tube $\mathcal{T}$ from within which they can converge to x_ω. An example of this behavior can be observed in Figure 6.2, where the solutions which either start or enter into the region $\mathcal{H}_\alpha$ (shaded in red) and lie below the curve $\dot{q} + 2(q+1) = 0$ (highlighted in yellow) cannot enter into the tube $\mathcal{T}$.

Both of these issues can, however, be resolved by some ad hoc modification to the controller (6.12). For example, one can simply limit the codomain of the projection operator used in (6.12). For an operator of the form (6.8), this would correspond to

$$p(x) = \underset{\substack{s\in[s_\alpha+\epsilon, s_\omega]\\ \mathfrak{L}(x_\star(s),x)\subset\mathfrak{X}}}{\arg\min} \Big[(x - x_s(s))^{\mathsf{T}}\Lambda(s)(x - x_s(s))\Big]$$

for some sufficiently small $\epsilon > 0$. Here ϵ may be taken as a constant (static approach); or, alternatively, one can let $\epsilon \in [0, \epsilon_M]$ be a bounded dynamic variable, e.g. $\dot\epsilon = \lambda_\epsilon \cdot \mathrm{sign}\big(\delta_\epsilon - \|x - x_\alpha\|\big)$ for small $\epsilon_M, \delta_\epsilon, \lambda_\epsilon > 0$ (dynamic approach). Note that if the latter dynamic option is chosen, then the resulting control law will necessarily no longer be truly static in a neighborhood of x_α. Such a scheme can always be justified, as it may be considered as a bounded, vanishing disturbance which can be made as small as one likes through the choice of ϵ (or ϵ_M).

Finite-time PtP maneuvers

As an alternative way of handling the issue of solutions getting "trapped" about x_α, especially the slow convergence away from it when confined to $\mathcal{O}$, one can instead consider maneuvers where x_α is finite-time repellent with respect to $\mathcal{O}$. If also x_ω is finite-time attractive, then we refer to such a maneuver as a *finite-time* PtP maneuver. Similarly to the terminal sliding mode controller considered in Chapter 3, $\rho(\cdot)$ of course cannot be Lipschitz about s_α and/or s_ω for such a maneuver (see, e.g., [112, 117, 118]). For instance, taking $\rho(s) = \kappa|s - q_\alpha|^a|q_\omega - s|^b$ in Example 6.1, one has

$$\rho'(s) = \kappa\left(a\lceil s - q_\alpha\rfloor^{a-1}|q_\omega - s|^b + b\lceil q_\omega - s\rfloor^{b-1}|s - q_\alpha|^a\right).$$

where $\lceil x\rfloor^a = \mathrm{sgn}\,x\,|x|^a$. Hence, if $a, b \in (0.5, 1)$, then $\rho'(\cdot)$ discontinuous at q_α and q_ω, whereas

$$u_s(s) = \rho'(s)\rho(s) = \kappa^2\left(a\lceil s - q_\alpha\rfloor^{2a-1}|q_\omega - s|^{2b} + b\lceil q_\omega - s\rfloor^{2b-1}|s - q_\alpha|^{2a}\right)$$

is not. Note, however, that similarly to the control law (3.34), if $p(x) = \mathrm{sat}_{q_\alpha}^{q_\omega}(q)$, then any orbitally stabilizing feedback cannot be Lipschitz (in terms of e) about x_ω either. This is due to the fact that $\rho'(s) \to -\infty$ as $s \to s_\omega$, which can result in additional attractive equilibrium points if not compensated for by an appropriately chosen feedback controller.

Note also that for such a maneuver to exist in the solution space of an underactuated mechanical system (see Chapter 5), the reduced dynamics (5.22) must a have certain type of singular point at the respective boundaries. Take, for example, $s\ddot s + (1 - a)\dot s^2 - bs(s - c) = 0$ with $a > 3/2$ and

$b, c > 0$. It has a heteroclinic orbit connecting $s_\alpha = 0$ and $s_\omega = c$. Here s_α is not only an equilibrium point, but also a singular point of the type considered in [193] which we briefly discussed in Section 5.3.2, making it finite-time repellent with respect to the heteroclinic orbit.

6.3.5 Constructing an orbitally stabilizing feedback

As shown in Example 6.1, one can combine Theorem 6.10 with a specific projection operator as in [22].

Corollary 6.11. *If there exist $\mathcal{C}^1$-smooth, matrix-valued functions $L, Q : \mathcal{S} \to \mathbb{M}^n_{\succ 0}$ satisfying, for all $s \in \mathcal{S}$,*

$$\rho(s)L'(s) + A_{cl}^\mathsf{T}(s)L(s) + L(s)A_{cl}(s) = -Q(s). \tag{6.28}$$

Then $L(s)$ satisfies the conditions in Theorem 6.10 if $x_s(\cdot)$ is of class $\mathcal{C}^3$ and $p(\cdot)$ is taken as in Proposition 6.5 with $\Lambda(s) = L(s)$. □

Corollary 6.11 clearly shows the possibility of finding a matrix $K(\cdot)$ of feedback gains that solves Problem 6.6 by solving a differential Riccati equation. However, it also forces one to use a particular projection operator (see Proposition 6.5), which generally requires one to solve an optimization problem at each iteration. Meanwhile, Example 6.1 showed that it also can be possible to find projection operators which are very simple, e.g. operators only depending on the configuration variables of the system. This motivates the need for a method which allows one to attempt to find a solution for any choice of projection operator. Thus, let $B_\perp(s) := \mathcal{E}_\perp(s)B_s(s)$ and

$$A_\perp(s) := \mathcal{E}_\perp(s)A_s(s) - \rho(s)\mathcal{F}(s)\mathcal{F}^\mathsf{T}(s)D^2p(x_s(s))\mathcal{E}_\perp(s).$$

The following statement, which is a slight modification of the differential linear matrix inequality approach (differential LMI) of Proposition 4.46, can be used to obtain such a method.

Proposition 6.12. *Given a projection operator $p(\cdot)$ which is $\mathcal{C}^2$-smooth within $\mathcal{T}$, suppose that for some strictly positive, smooth function $\lambda : \mathcal{S} \to \mathbb{R}_{>0}$, there exists a pair of smooth matrix-valued functions*

$$Y : \mathcal{S} \to \mathbb{R}^{m\times n} \quad \textit{and} \quad W : \mathcal{S} \to \mathbb{M}^n_{\succ 0},$$

which, for all $s \in \mathcal{S}$, satisfy the matrix inequality

$$\begin{aligned}\rho(s)W'(s) - W(s)A_\perp^\mathsf{T}(s) - A_\perp(s)W(s) - Y^\mathsf{T}(s)B_\perp^\mathsf{T}(s)\\ - B_\perp(s)Y(s) - \lambda(s)[\mathcal{E}_\perp(s)W(s) + W(s)\mathcal{E}_\perp^\mathsf{T}(s)] \succeq \mathbf{0}_n.\end{aligned} \tag{6.29}$$

Further suppose that for some $K_\alpha, K_\omega \in \mathbb{R}^{m\times n}$, which are such that $(A_s(s_\alpha)+B_s(s_\alpha)K_\alpha)$ and $(A_s(s_\omega)+B_s(s_\omega)K_\omega)$ are both Hurwitz, one has

$$K_\alpha W(s_\alpha) = Y(s_\alpha) \quad \textit{and} \quad K_\omega W(s_\omega) = Y(s_\omega). \tag{6.30}$$

Then by taking $K(s) = Y(s)W^{-1}(s)$, the matrix function $L(s) = W^{-1}(s)$ satisfies all the conditions in Theorem 6.10.

Proof. That there exist a smooth matrix-valued function $Q_\perp : \mathcal{S} \to \mathbb{M}^n_{\succ 0}$ such that $L = W^{-1} \in \mathbb{M}^n_{\succ 0}$ solves the PLDE (6.21) follows from the proof of Proposition 4.46. Thus we only need to demonstrate that the ALEs (6.20) are also satisfied. To this end, we note that the constant matrix $A_{cl}(s_\alpha) = A_s(s_\alpha) + B_s(s_\alpha)Y(s_\alpha)W^{-1}(s_\alpha)$ is Hurwitz. Thus by Theorem 1 in [183], there exists a matrix $\hat{Q}_\alpha \in \mathbb{M}^n_{\succ 0}$ such that $\mathrm{sym}\big[A_s(s_\alpha)W(s_\alpha) + B_s(s_\alpha)Y(s_\alpha)\big] = -2^{-1}\hat{Q}_\alpha$, where $\mathrm{sym}[A] = 2^{-1}(A + A^\mathsf{T})$. For $L(s_\alpha) = W^{-1}(s_\alpha)$ we may therefore take $Q_\alpha = W^{-1}(s_\alpha)\hat{Q}_\alpha W^{-1}(s_\alpha)$ in (6.20a). Since the exact same arguments can be used for the point s_ω, the statement follows. □

In order to find a solution pair (W, Y) to Proposition 6.12, one can use some transcription method as to discretize the differential LMI (6.29) into a finite set of LMIs. One can then attempt to find an approximate solution using semi-definite programming (SDP). In regard to handling the constant stabilizing matrices K_α and K_ω in the resulting SDP formulation, there are two main options:

1) Add, for both $s \in \{s_\alpha, s_\omega\}$, the LMI constraints

$$W(s)A_s^\mathsf{T}(s) + A_s(s)W(s) + Y^\mathsf{T}(s)B_s(s) + B_s(s)Y(s) \prec \mathbf{0}_n;$$

2) Add the equality constraints (6.30), in which some stabilizing matrices K_α and K_ω have already been found.

In case of the latter option, one can for example use LQR: Take, for both $i \in \{0, f\}$,

$$K_i = -\Gamma_i^{-1}B_s^\mathsf{T}(s_i)R_i,$$

where $R_i \in \mathbb{M}^n_{\succ 0}$ solves the algebraic Riccati equation

$$A_s^\mathsf{T}(s_i)R_i + R_iA_s(s_i) - R_iB_s(s_i)\Gamma_i^{-1}B_s^\mathsf{T}(s_i)R_i = -Q_i \tag{6.31}$$

given some $\Gamma_i \in \mathbb{M}^m_{\succ 0}$ and $Q_i \in \mathbb{M}^n_{\succ 0}$.

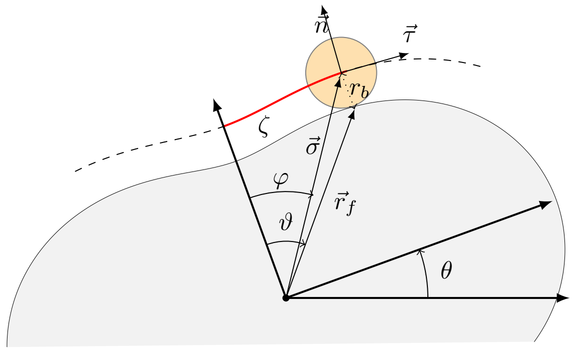

Figure 6.3: The coordinate convention used in Section 6.4.1, with frame having the form of the "butterfly" robot.

6.4 Application to non-prehensile manipulation

We will now apply the feedback design approach outlined in Section 6.3.4 as to solve the following non-prehensile manipulation [5] problem: Generate an asymptotically orbitally stable PtP maneuver corresponding to a ball rolling between any two points upon an actuated planar frame.[3] In order construct such a maneuver, we will utilize the synchronization function-based approach we considered in Chapter 5, specifically Theorem 5.18. To this end, we begin by describing the system model and provide some necessary assumptions.

6.4.1 System description and mathematical model

Consider a rigid ball of (effective) radius r_b rolling without slipping upon the boundary of a solid, actuated frame as seen in Figure 6.3. The edge of the frame is traced out by the polar coordinates $(\vartheta, r_f(\vartheta))$, that is $\vec{r}_f(\vartheta) = r_f(\vartheta)\,\mathrm{col}\big(\sin(\vartheta), \cos(\vartheta)\big)$, with $\vartheta \in \mathcal{I} \subseteq \mathbb{S}^1$ and where the scalar function $r_f : \mathcal{I} \to \mathbb{R}_{>0}$ is smooth. Note that this representation can be used to describe several well-known nonlinear systems, including the following three systems which are depicted in Figure 6.4:

- the ball-and-beam [205] ($r_f(\vartheta) = \frac{\text{const.}}{\cos(\vartheta)}$);
- the disk-on-disk [206] ($r_f(\vartheta) = \text{const.}$);
- as well as the so-called butterfly robot [4, 144].

[3]To fully appreciate the difficulty of the problem we are attempting to solve, we recommend watching an excellent video on the topic made by Brian Douglas, which is available through the link: `https://youtu.be/V30e77x8BQA`.

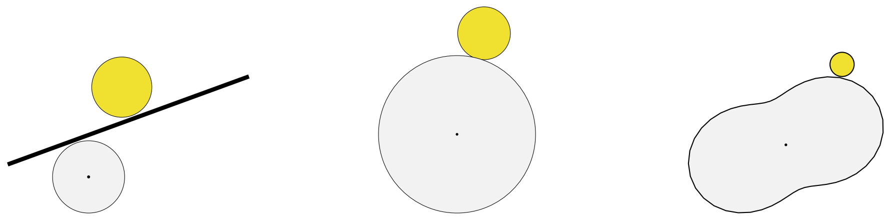

(a) Ball-and-beam. **(b)** Disk-on-disk. **(c)** The "butterfly" robot.

Figure 6.4: Examples of underactuated, nonlinear systems within the class of systems considered in Section 6.4.1, in which a yellow ball can be indirectly controlled through its contact with an actuated (gray) frame.

For later, we note that the frame of the butterfly robot, which is a smooth figure-of-eight–shaped Jordan curve, for example can be of the following form [144]:

$$r_f(\vartheta) = a - b\cos(2\vartheta), \quad a, b \in \mathbb{R}_{>0}. \tag{6.32}$$

In order to derive the equations governing the dynamics of these types of systems, we will make the following assumptions, for which the validity of the latter two must be checked for any found motion of the system:

A1. The ball's center traces out a smooth curve when it traverses the frame, i.e., there are no cusps (see, e.g., [207];

A2. The ball is always in contact with the frame;

A3. The ball always rolls without slipping.

Let θ and φ be defined as shown in Figure 6.3, such the position of the ball's center in the frame's body-fixed frame is given by the vector $\vec{\sigma} = \vec{\sigma}(\varphi)$ depicted in Figure 6.3. Given the arc length $\zeta_f(\vartheta) = \int_\alpha^\vartheta \|\vec{r}_f{}'(\mu)\|\, d\mu$, we denote by $\vec{\tau}_f(\vartheta) = \frac{d\vec{r}_f}{d\zeta_f}(\vartheta)$ the unit tangent vector to $\vec{r}_f$ at ϑ, and by $\vec{n}_f(\vartheta) = \vec{k} \times \vec{\tau}_f(\vartheta)$, $\vec{k} := \mathrm{col}(0,0,1)$, the corresponding unit normal vector. Note that if Assumption **A1** holds, then there exists a diffeomorphism $\vartheta = h(\varphi)$. Hence the unit tangent and normal vectors to $\vec{\sigma}(\varphi)$ (see Figure 6.3) are found by $\vec{n}(\varphi) = (\vec{n}_f \circ h)(\varphi)$ and $\vec{\tau}(\varphi) = (\vec{\tau}_f \circ h)(\varphi)$. Moreover, since clearly $\vec{\sigma}(\varphi) = (\vec{r}_f \circ h)(\varphi) + r_b \vec{n}(\varphi)$, the arc length is

$$\zeta(\varphi) = \int_\alpha^\varphi \|\vec{\sigma}'(\mu)\|\, d\mu = \int_\alpha^\varphi \left\| \Big(\frac{d\vec{r}_f}{d\vartheta} \circ h\Big)(\mu) + r_b \Big(\frac{d\vec{n}_f}{d\vartheta} \circ h)(\mu)\Big) \right\| |h'(\mu)|\, d\mu.$$

Using the Frenet formula [207], i.e. $\vec{n}_f(\vartheta) = -\kappa_f(\vartheta)\vec{\tau}_f(\vartheta$, where κ_f is the signed curvature of $\vec{r}_f$ at ϑ, this can be written as

$$\zeta = \int_0^{\vartheta} \left|1 - r_b\kappa_f(\mu)\right| \left\|\vec{r}_f{}'(\mu)\right\| d\mu,$$

which clearly shows the need for Assumption **A1** to hold.

As in [144], we take $q = \mathrm{col}(\theta, \varphi)$ as generalized coordinates. Assuming **A1**-**A3** holds, one finds, by using the above derivations, that the mechanical system's kinetic- and potential energy can be completely determined from q and $\dot{q}$. By using the Euler Lagrange equations and the procedure outlined in Section 5.2, one therefore finds that the system's dynamic equations of motion can be written in the form (5.2), i.e.,

$$\mathbf{M}(q)\ddot{q} + \mathbf{C}(q, \dot{q})\dot{q} + \mathbf{G}(q) = \mathbf{B}_u u, \tag{5.2}$$

where $\mathbf{B}_u = \mathrm{col}(1, 0)$, as well as

$$\begin{aligned}
\mathbf{M}(q) &= \begin{bmatrix} J_f + J_b + m\|\vec{\sigma}\|^2 & -\big(m\vec{\sigma}\cdot\vec{n} + \frac{J_b}{r_b}\big)\zeta' \\ -\big(m\vec{\sigma}\cdot\vec{n} + \frac{J_b}{r_b}\big)\zeta' & \big(\frac{J_b}{r_b^2} + m\big)\zeta'^2 \end{bmatrix}, \\
\mathbf{C}(q, \dot{q}) &= \begin{bmatrix} c_{11}\dot{\varphi} & c_{11}\dot{\theta} - c_{12}\dot{\varphi} \\ -c_{11}\dot{\theta} & \Big(\frac{J_b}{r_b^2} + m\Big)\zeta'\zeta''\dot{\varphi} \end{bmatrix}, \\
\mathbf{G}(q) &= \mathrm{col}\left(m\vec{g}\cdot\big(\big(\frac{d}{d\theta}\mathrm{Rot}(\theta)\big)\vec{\sigma}\big), m\vec{g}\cdot\big(\mathrm{Rot}(\theta)\vec{\tau}\zeta'\big)\right).
\end{aligned}$$

Here $c_{11} := m\zeta'\vec{\sigma}\cdot\vec{\tau}$, $c_{12} := \big(m\vec{\sigma}\cdot\vec{n} + \frac{J_b}{r_b}\big)\zeta'' + c_{11}\kappa\zeta'$ and $\vec{g} = \mathrm{col}(0, g)$; m denotes the ball's mass; J_f and J_b are the the moments of inertia of the frame and ball, respectively; $\kappa(\varphi)$ is the signed curvature of $\vec{\sigma}(\varphi)$; $g = 9.81\,\mathrm{m\,s^{-2}}$ is the gravitational acceleration; and Rot $\in \mathbf{SO}(2)$ is the counterclockwise planar rotation matrix.

6.4.2 Maneuver design

We will now utilize the procedure outlined in Section 5.3.4 to plan PtP maneuvers for such systems. For this purpose, let $\psi(\varphi)$ denote the *tangential angle* of the polar curve at φ. Namely, the angle such that the unit tangent vector $\vec{\tau}$ at φ can be written as $\vec{\tau} = \mathrm{col}(\cos(\psi), \sin(\psi))$; or equivalently, the angle such that $\frac{\partial\psi}{\partial\zeta} = \kappa$ (recall that ζ is the arc length and $\kappa = \kappa(\varphi)$ is the signed curvature of $\vec{\sigma}(\varphi)$). Hence ψ is trivial for systems with constant curvature, e.g., $\psi \equiv 0$ for the ball-and-beam system and $\psi = -\varphi$ for the disk-on-disk.

With this in mind, consider

$$\Phi(s) = \operatorname{col}\big(\Theta(s) - \psi(s), s\big), \quad s \in \mathcal{S} \subseteq \mathbb{S}, \tag{6.33}$$

for some smooth, scalar function $\Theta(\cdot)$. Simply put, if one takes $\Theta = 0$, then the vector of synchronization functions (6.33) aligns $\vec{\tau}$ with the fixed horizontal axis (see Figure 6.3), such that the ball can be consider as to be rolling on a horizontal surface. The function $\Theta(\cdot)$ can therefore be used to slow down or speed up the rolling motion by altering the artificial "slope" upon which the ball rolls.

For this vector of synchronization functions $\Phi(\cdot)$, one finds that the scalar functions $\alpha(\cdot)$ and $\gamma(\cdot)$ which appear in corresponding reduced dynamics (5.22), that is

$$\alpha(s)\ddot{s} + \beta(s)\dot{s}^2 + \gamma(s) = 0, \tag{6.34}$$

are given by

$$\alpha(s) = \left(\frac{J_b}{R}\left(\kappa + \frac{1}{R}\right) + m(1 + \vec{\sigma}\cdot\vec{\kappa})\right)\zeta'^2 - \left(m\vec{\sigma}\cdot\vec{n} + \frac{J_b}{R}\right)\zeta'\Theta', \tag{6.35a}$$

$$\gamma(s) = mg\zeta'\sin(\Theta(s)). \tag{6.35b}$$

From this and Lemma 5.5, the following can be deduced:

Proposition 6.13. *A point $s_e \in \mathcal{S}$, for which $\alpha(s_e) \neq 0$, is an equilibrium point of* (6.34) *if $\Theta(s_e) \equiv 0$. Moreover, it is a center if $\Theta'(s_e)/\alpha(s_e) > 0$, or a saddle if $\Theta'(s_e)/\alpha(s_e) < 0$.* □

One can therefore choose the equilibrium points of (6.34) freely through the choice of Θ. This, in turn, can be utilized to find a solution satisfying the conditions in Theorem 5.18 for the existence of a heteroclinic orbit in the second-order system (6.34). More specifically, let Θ be taken such that: $\alpha(s) \neq 0$ on $\mathcal{S}$; $\Theta'(s_\alpha)/\alpha(s_\alpha) \leq 0$ and $\Theta'(s_\omega)/\alpha(s_\omega) \leq 0$; as well as $\Theta(s_e) = 0$ and $\Theta'(s_e)/\alpha(s_e) > 0$ for some $s_e \in \operatorname{int}\mathcal{S}$. Then Condition (5.41) corresponds to the existence of a separatrix connecting s_α and s_ω, for which the corresponding function $\rho : \mathcal{S} \to \mathbb{R}_{\geq 0}$ can be found from (5.32). We utilize this procedure in the following example.

6.4.3 Simulation example: The butterfly robot

As an example, we will consider the "butterfly" robot (BR) given by (6.32), with the values of the system parameters given in Table 6.1. The specific task we will consider is to steer the ball from $\varphi_\alpha = 0\,\text{rad}$ to $\varphi_\omega = 2\,\text{rad}$.[4]

[4]Stabilizing a heteroclinic orbit of the BR has been considered previously in [208]. In that paper, the authors use several simplifying assumptions, including that the ball is a

Table 6.1: Parameter values of the butterfly robot used in the simulations.

m [kg]	r_b [m]	J_b [kg m^2]	J_f [kg m^2]	a [m]	b [m]
3.0×10^{-3}	1.09×10^{-2}	5.8×10^{-7}	8.9×10^{-4}	1.14×10^{-1}	3.9×10^{-2}

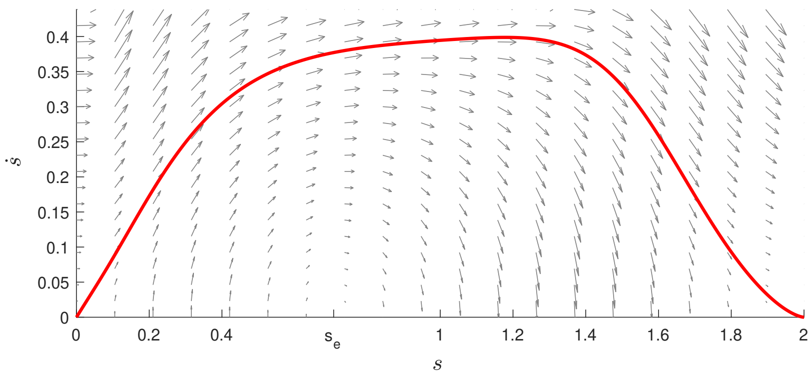

Figure 6.5: Phase portrait of (6.34), with the red curve $\dot{s} = \rho(s)$ the unique solution of (6.34) satisfying **P2** in Definition 6.1.

Motion planning: In light of Proposition 6.13, we will consider the synchronization functions (6.33) with

$$\Theta(s) = k(s - s_\alpha)(s - s_e)(s_\omega - s)^2, \tag{6.36}$$

where $s_\alpha = 0$, $s_e \approx 0.707$, $s_\omega = 2$, and $k = 0.01$. The corresponding unique (positive) solution to (6.34) of the form $\dot{s} = \rho(s)$ found using the integrability of the reduced dynamics, i.e. (5.27), and satisfying Property **P2** in Definition 6.1, is the red curve in Figure 6.5. The corresponding nominal control input found from (5.15) can be seen in Figure 6.6, where it is measured relative to the right vertical axis.

Projection operator: We took $\Lambda = \mathrm{diag}(0, 1, 0, 0)$ in (6.8) with $\mathcal{S} := [s_\alpha, s_\omega]$, which is equivalent to $p(x) = \mathrm{sat}_{s_\alpha}^{s_\omega}(\varphi)$, with $\mathrm{sat}_a^b : \mathbb{R} \to [a, b]$ the saturation function. Following the discussion in Section 6.3.4, it was implemented as $p(x) = \mathrm{sat}_{s_\alpha+\epsilon}^{s_\omega}(\varphi)$, where the dynamic variable $\epsilon \in [0, \epsilon_M]$ was governed by $\dot{\epsilon} = \epsilon_M \mathrm{sign}\big(\epsilon_M - \|x - x_\alpha\|\big)$ with $\epsilon_M = 10^{-3}$ (similar results were obtained with a constant $\epsilon = \epsilon_M$).

point mass that is sliding. The crucial difference, however, is that, as opposed to our method, their approach is limited to a very specific orbit, and it uses an energy-based control strategy with separate "swing-up" and "balance" controllers.

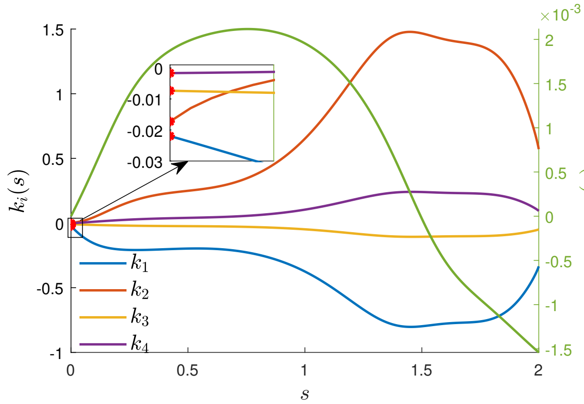

Figure 6.6: Found elements of $K(s) = [k_1(s), k_2(s), k_3(s), k_4(s)]$ (left axis) and the nominal control input $u_s(s)$ (right axis).

Control design: Since the Jacobian linearization is controllable (and therefore stabilizable) at both $x_\alpha = x_s(s_\alpha)$ and $x_\omega = x_s(s_\omega)$, we computed a pair of constant LQR-based feedback matrices $K_\alpha, K_\omega \in \mathbb{R}^{m\times n}$ by solving the algebraic Riccati equations (6.31) using the `CARE` command in MATLAB with $\Gamma_\alpha = \Gamma_\omega = 10^5$ and $Q_\alpha = Q_\omega = \mathbf{I}_4$. Note that the magnitude of Γ_α and Γ_ω here simply reflects the small parameter values (see Table 6.1). We then took $\lambda = 0.5$, and formulated a semidefinite programming (SDP) problem following Proposition 6.12 with the equality constraints (6.30). In order to transcribe the differential LMI (6.29) into a finite number of LMIs, we took the elements of the matrix functions W and Y as sixth-order Beziér polynomials, and took (6.29) evaluated at 200 evenly spaced points as LMI constraints in the SDP. The resulting SDP was then solved using the YALMIP toolbox for MATLAB [200] together with the SDPT3 solver [201]. Figure 6.6 shows the elements of the obtained $K(s) = Y(s)W^{-1}(s) \in \mathbb{R}^{1\times 4}$.

Simulation results: The response of the system when starting with the initial conditions $x(0) = x_\alpha + \mathrm{col}(0.1, -0.3, 0, 0)$ is shown in Figure 6.7, with some snapshots of the system's configuration shown in Figure 6.8. As the states are initially within the half-ball corresponding to x_α, it can be seen that the controller therefore first brings the states close to x_α, after which they then follow the nominal orbit to x_ω. Notice also that the normal force F_n between the ball and the frame is everywhere positive, meaning that the previously made assumption that the ball does not depart from the frame is not violated.

Figure 6.9 shows the system response for the initial conditions $x(0) = x_\omega + \mathrm{col}(0.1, 0.1, 0, 0)$. Interestingly, these initial conditions do not lie in

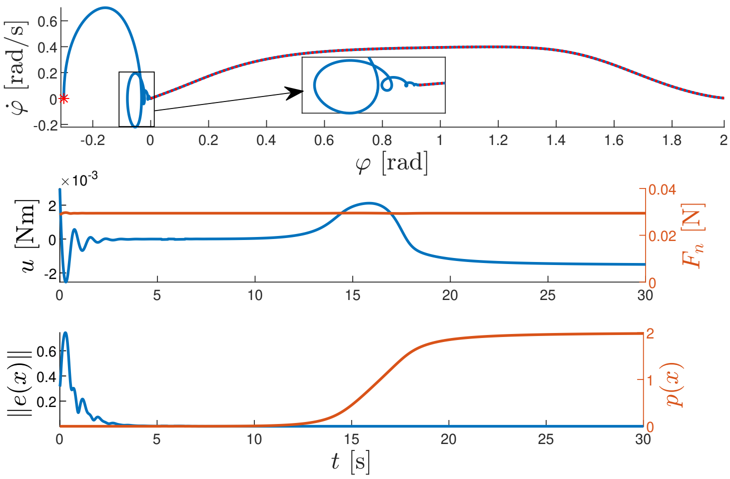

Figure 6.7: Response of the BR system initialized close to x_α.

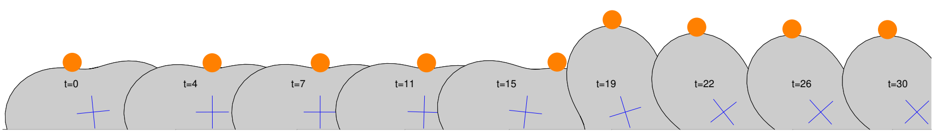

Figure 6.8: Snapshots of the configuration of the "butterfly" robot system corresponding to the response shown in Fig. 6.7.

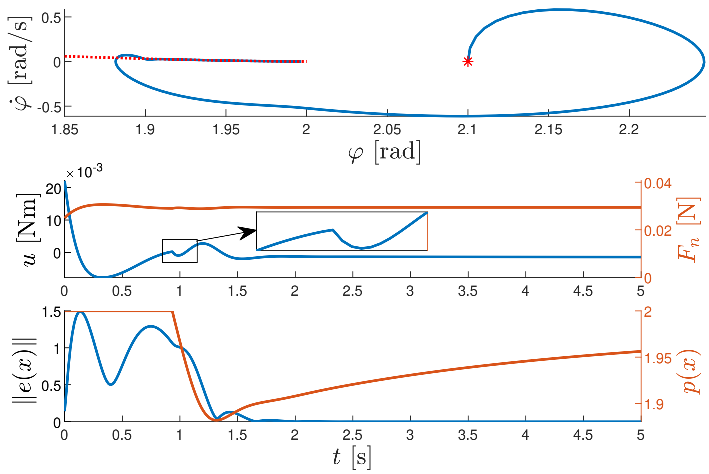

Figure 6.9: Response of the BR system initialized close to x_ω.

the region of attraction of the linear feedback $u = u_s(s_\omega) + K(s_\omega)(x - x_\omega)$. Notice also that φ becomes less than 2 rad just before $t = 1$ s, at which the gradient of the projection operator has a discontinuity. It can be seen that the smoothness of the control signal is violated at this time instant, but it is clear from the highlighted rectangle that Lipschitz continuity is preserved.

To test the sensitivity of the closed-loop system to noise and perturbations, we again simulated the system with the initial conditions $x(0) = x_\alpha + \text{col}(0.1, -0.3, 0, 0)$ but with a small amount of white noise added to the measurements passed to the controller, with the actual mass of the ball, m_b, being 10% larger than that assumed, as well as with the matched disturbances $10^{-4}\sin(t)$ added to the right-hand side of (5.2). The resulting system response is shown in Figure 6.10. As seen in Figure 6.11, even with a 90% reduction in the ball's mass, as well as noise and a matched disturbance, the control law is still able to bring the states close to x_ω (ensuring its practical stability), although it is clear that the controller's maneuver-following capabilities have significantly deteriorated.

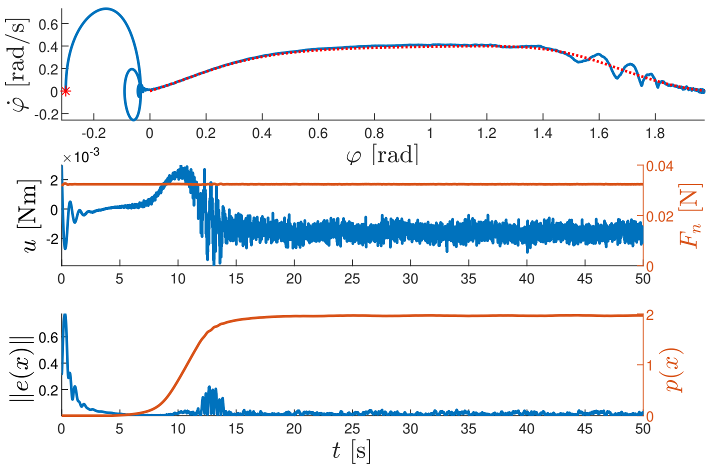

Figure 6.10: Response of the BR system initialized close to x_α, with white noise added to all the state measurements, with the mass of the ball increased by 10% and subject to a small matched disturbance.

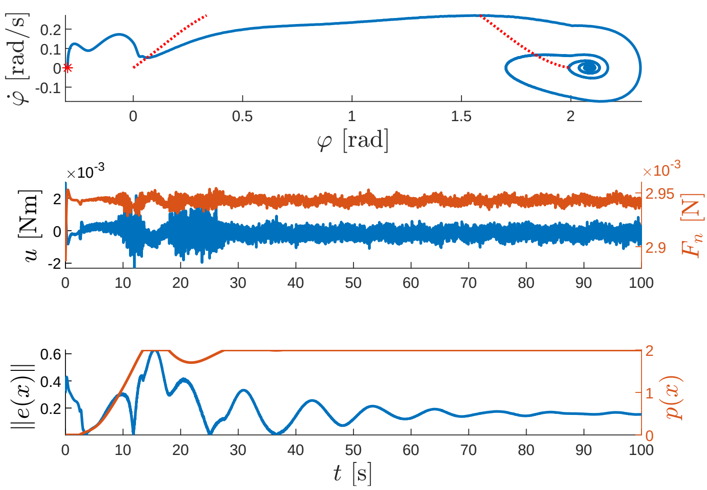

Figure 6.11: Response of the "butterfly" robot when the mass of the ball is 90% smaller, with noise and a matched disturbance.

Chapter 7

Orbital Stabilization of Cycles in Hybrid Systems

The problem of stabilizing (hybrid) periodic orbits of a class of hybrid dynamical systems is considered in this chapter. A numerical framework for finding such orbits for a class of hybrid underactuated mechanical systems is also presented.

7.1 Introduction

There are a variety of dynamical systems whose behaviors cannot be descried by a single set of ordinary differential equations with a locally Lipschitz continuous right-hand side. An example is an oscillatory system subject to dry friction due to the discrete nature of dry (Coulomb) friction. Other examples include systems which can experience short-lived events resulting in either an abrupt change (jump) in the system's states or a complete change of its mode. The latter case may for instance correspond to the time instant at which a loss of contact occurs between two rigid bodies (e.g. the ball departing from the frame of the butterfly robot; see Sec. 6.4); whereas the former may correspond to certain systems experiencing collisions or impacts. If such abrupt changes occur on a sufficiently small time interval, then idealizing these events as instantaneous, discrete transitions between different phases (modes) of the dynamical system might be justified. Such an idealization gives rise to a *hybrid dynamical system* [209, 210], where the system's dynamics are represented by a series of continuous-time dynamics which can be interconnected by discrete jump events. These events are triggered when the system's states (in the given mode) hits certain switching surfaces while simultaneously satisfying certain transitioning laws (guards).

A solution of a hybrid dynamical system, a hybrid trajectory, may therefore consist of a series of sub-arcs, each corresponding to a different mode with its own set of differential equations. If the continuous-time dynamics in each mode are sufficiently smooth, then a linearization about the trajectory's sub-arcs can be carried out in the usual manner to obtain the first-order variational system (see Sec. 2.3). Moreover, if two sub-arcs of a trajectory, each governed by its own set of differential equations, are connected by a continuous transition, then the two linearizations in each sub-arc can be concatenated together using the so-called *Saltation matrix* [211], thus possibly allowing for characterization of the stability of a hybrid trajectory from the first-order approximation. Indeed, by using the concept of Saltation matrices, Aizerman and Gantmakher [90] obtained a generalization of the Andronov–Vitt theorem (Thm. 2.8) in the case of a hybrid periodic trajectory consisting only of such continuous transitions; see also [26]. Furthermore, as to also allow for discrete jumps in the value of the states at the transitions, a similar construction to the Saltation matrix was proposed by Müller [212].

Our aim in this chapter is to utilize constructions similar to the Saltation matrix and its extension by Müller [212] for the purpose of orbitally stabilizing feedback design. For simplicity's sake, we will limit our studies to hybrid periodic orbits (cycles) along which a single, discrete jump in the values of the states occurs. Note, however, that the approach we suggest in Section 7.2.1 can readily be extended to orbits along which an order series of such jumps occurs, as well as to those where the continuous-time dynamics change in between the discrete transitions. Note also that the approach is both conceptually similar to- and inspired by the approach proposed in [198, 213], where a specific set of transverse coordinates for hybrid periodic trajectories of underactuated mechanical systems was considered.

In the approach we suggest in this chapter, the same projection-based function considered in Chapter 6 will be utilized. A statement (see Thm. 7.2) will also be provided which allows for the construction of an orbitally stabilizing feedback by solving a semidefinite programming problem (cf. Prop. 4.46 and Thm. 6.12). In addition to the orbital stabilization scheme, we also present a method for planning hybrid cycles of underactuated mechanical systems. Specifically, using the theory of synchronization functions outlined in Chapter 5, we propose a series of steps allowing for an efficient numerical implementation of the motion planning procedure proposed in [198].

Outline: The chapter is organized as follows. We formulate the problem of orbital stabilization of a cycle for a class of hybrid dynamical systems in Section 7.2.1, as well as state the necessary assumptions and define the notion of an s-parameterization for such orbits. In the sections 7.2.2-7.2.3 we introduce and prove the proposed orbital stabilization method. In Section 7.3 we suggest a numerical framework allowing one to search for hybrid cycles using nonlinear programming. The problem of generating an orbitally stabilizing walking gait of a three-link biped robot is considered as an example in Section 7.4.

7.2 Projection-based orbital stabilization

7.2.1 Problem formulation

Consider a hybrid dynamical system of the form

$$\dot{x} = f(x) + B(x)u, \qquad x \notin \mathbf{\Sigma}_-, \tag{7.1a}$$

$$\mathbf{\Sigma}_+ \ni x^+ = \mathbf{J}(x^-), \qquad x^- \in \mathbf{\Sigma}_-. \tag{7.1b}$$

Here $x \in \mathbb{R}^n$ is the state and $u \in \mathbb{R}^m$ the controls. Both $f(\cdot)$ and the $B(\cdot)$ are assumed to be of class $\mathcal{C}^2$ as in the previous chapters, while the jump map $\mathbf{J} : \mathbf{\Sigma}_- \to \mathbf{\Sigma}_+$ is assumed to be $\mathcal{C}^1$ on $\mathbf{\Sigma}_-$. The switching surfaces $\mathbf{\Sigma}_+$ and $\mathbf{\Sigma}_-$ are defined by

$$\mathbf{\Sigma}_- = \{x \in \mathbb{R}^n : \ \sigma_-(x) = 0, \ \upsilon(x) \geq 0\}, \tag{7.2a}$$

$$\mathbf{\Sigma}_+ = \{x \in \mathbb{R}^n : \ \sigma_+(x) = 0\}, \tag{7.2b}$$

with $\sigma_\pm \in \mathcal{C}^2(\mathbb{R}^n, \mathbb{R})$, while $\upsilon \in \mathcal{C}^0(\mathbb{R}^n, \mathbb{R}^l)$ for some positive integer l (commonly $\upsilon = \pm\dot{\sigma}_-$ with $\|D\sigma_- B\| = 0$). Note that we will use the superscripts "$-$" and "$+$" throughout this chapter to denote the values of a function immediately before or after an instantaneous jump, respectively.

Knowledge of an s-parameterized hybrid periodic maneuver

For simplicity's sake, we will only consider maneuvers which undergo a single jump, after which the states are returned to the maneuver's starting point and the motion is repeated. We will refer to a maneuver corresponding such a hybrid cycle as as hybrid periodic maneuver. Specifically, let $x_a, x_b \in \mathbb{R}^n$, $x_a \neq x_b$, denote two points in state space for which the following hold:

$$x_a \in \mathbf{\Sigma}_+, \quad x_b \in \mathbf{\Sigma}_-, \quad \text{and} \quad x_a = \mathbf{J}(x_b). \tag{7.3}$$

Similarly to the previous chapter, we will assume that we know an s-*parameterization* of a hybrid periodic maneuver, that is

$$\mathcal{M} := \{(x, u) \in \mathbb{R}^n \times \mathbb{R}^m : \ x = x_s(s), \ u = u_s(s), \ s \in \mathcal{S}\},$$

whose boundaries correspond to x_a and x_b. Unlike the point-to-point maneuvers in Chapter 6, however, these boundary points are not (forced) equilibrium points of the dynamical system, and consequently they are not invariant limit points of the corresponding orbit. Thus, rather than the subscripts "α" and "ω", we instead use "a" and "b", which, in regard to the instantaneous jump, may be interpreted as to simply mean "after" and "before", respectively.

We define next the notion of an s-parameterization for this type of maneuver:

Definition 7.1. For $\mathcal{S} := [s_a, s_b] \subset \mathbb{R}$, $s_a < s_b$, a triplet of functions (x_s, u_s, ρ) of the form

$$x_s : \mathcal{S} \to \mathbb{R}^n, \quad u_s : \mathcal{S} \to \mathbb{R}^m, \quad \text{and} \quad \rho : \mathcal{S} \to \mathbb{R}_{\geq 0}, \tag{7.4}$$

is said to constitute an *s-parameterization* of the hybrid periodic maneuver $\mathcal{M}$ of (6.1) if:

P1 $x_s(\cdot)$ is $\mathcal{C}^2$, while $u_s(\cdot)$ and $\rho(\cdot)$ are $\mathcal{C}^1$;

P2 $x_s(s_a) = x_a$ and $x_s(s_b) = x_b$, with x_a and x_b satisfying (7.3);

P3 $\rho(s) > 0$ for all $s \in \mathcal{S}$;

P4 $\|\mathcal{F}(s)\| > 0$ for all $s \in \mathcal{S}$, where $\mathcal{F}(s) := x_s'(s)$;

P5 $x_s : \mathcal{S} \to \mathbb{R}^n$ is one-to-one;

P6 $\mathcal{F}(s)\rho(s) = f(x_s(s)) + B(x_s(s))u_s(s)$ for all $s \in \mathcal{S}$;

P7 $D\sigma_+(x_a)\mathcal{F}(s_a) \neq 0$ and $D\sigma_-(x_b)\mathcal{F}(s_b) \neq 0$. □

Thus the differences between an s-parameterized point-to-point maneuver (see Def. 6.1) and a hybrid periodic one as we consider it here are mainly threefold: 1) the maneuver's boundaries satisfy the jump condition (7.3) rather than corresponding to equilibrium points; 2) since the time-scaling function ρ does not vanish at the boundaries, the orbit's period can be computed by

$$T_s = \int_{s_a}^{s_b} \frac{1}{\rho(\tau)} d\tau > 0; \tag{7.5}$$

3) the additional strong transversality- (or "non-grazing impact-") conditions (see also [56]):

$$D\sigma_+(x_a)\mathcal{F}(s_a) \neq 0 \quad \text{and} \quad D\sigma_-(x_b)\mathcal{F}(s_b) \neq 0. \tag{7.6}$$

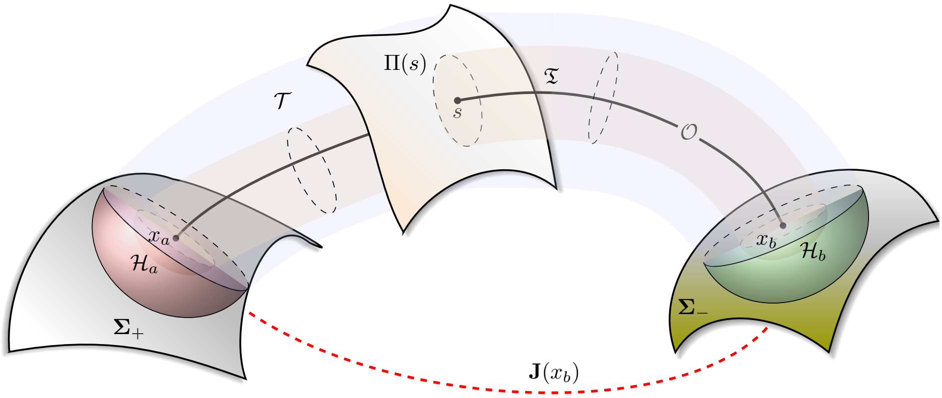

Figure 7.1: Illustration of the moving Poincaré section $\Pi(s)$ defined by (6.6) traveling along the orbit $\mathcal{O}$. Unlike the point-to-point maneuvers considered in the previous chapter, the orbit now begins and terminates at points $x_a \in \boldsymbol{\Sigma}_+$ and $x_b \in \boldsymbol{\Sigma}_-$ corresponding to the jump condition $x_a = \mathbf{J}(x_b)$. The gradient of the projection operator is assumed to be nonzero and well defined within the blue-shaded tubular neighborhood $\mathcal{T}$, but vanishes within darkly shaded hemispheres $\mathcal{H}_a$ and $\mathcal{H}_b$ if the moving Poincaré section does not align with the switching surfaces.

The orbital stabilization problem

As in the previous chapters, we will denote by $\mathcal{O} \subset \mathbb{R}^n$ the maneuver's orbit:

$$\mathcal{O} := \{x \in \mathbb{R}^n : \; x = x_s(s), \quad s \in \mathcal{S}\}\,. \tag{7.7}$$

The task we will consider is again to solve the orbital stabilization problem for $\mathcal{O}$; see Problem 3.3. Namely, to render $\mathcal{O}$ exponentially stable with respect to (7.1) using some static state-feedback control law $u = k(x)$, with $k : \mathbb{R}^n \to \mathbb{R}^m$ locally Lipschitz in a neighborhood of $\mathcal{O}$.

7.2.2 Projection-based coordinates

As in Chapter 6, we will consider the function $e = e(x)$, defined by

$$e(x) := x - x_p(x) = x - (x_s \circ p)(x). \tag{7.8}$$

Here $p : \mathfrak{X} \subset \mathbb{R}^n \to \mathcal{S}$ is a projection operator satisfying Definition 6.4 which is at least $\mathcal{C}^2$-smooth within the tubular neighborhood $\mathcal{T}$.[1] Recall

[1]Such a projection operator has to be used now as well due to the fact that we do not know a continuation of the state curve $x_s(\cdot)$ beyond the interval $\mathcal{S} = [s_a, s_b]$.

that such an operator $p(\cdot)$ is well defined and locally Lipschitz within the closure of its domain $\mathrm{cl}\,\mathfrak{X} = \mathrm{cl}\,(\mathcal{H}_a \cup \mathcal{T} \cup \mathcal{H}_b)$ (see Figure 7.1), with $Dp(x)$ being nonzero and $\mathcal{C}^1$ for all $x \in \mathcal{T}$, while $Dp(x) \equiv 0$ when x is within the interior of $\mathcal{H}_i := \{x \in \mathfrak{X} :\ p(x) = s_i\}$ for both $i \in \{a, b\}$.

The moving Poincaré section might not align with the switching surfaces

Recall that for any $x \in \mathcal{T} \subset \mathfrak{X}$, the set

$$\Pi(s) = \{x \in \mathfrak{X} :\ p(x) = s\}$$

illustrated in Figure 7.1, corresponds to a moving Poincaré section. Further recall that when the system's states lie upon such a hypersurface, the function (7.8) may be viewed as an excessive set of transverse coordinates upon it. Thus, its "first-order components" lie on $\mathbf{T}\Pi(p)$, with $\mathbf{T}\Pi(s) := \big\{x \in \mathbb{R}^n :\ \mathcal{P}(s)x = 0\big\}$ the tangent space of $\Pi(s)$ at $x_s(s)$.

This, however, raises the question: How to ensure the stability of the zero-level set of e, i.e. the orbit $\mathcal{O}$, if the moving Poincaré section induced by $p(\cdot)$ does not (locally) align with one (or both) of the switching surfaces? Such a scenario is illustrated by the red- and green-shaded regions of $\mathcal{H}_a$ and $\mathcal{H}_b$ in Figure 7.1, and even more clearly about x_b by the red-shaded region in Figure 7.2. Specifically, the issue which arises in such a scenario is how to determine the orbit's stability characteristics from the first-order approximation of the e-dynamics if the states leave the tubular neighborhood.

Several methods have been proposed in regard to either handling or avoiding this misalignment issue. For instance, an orthogonal coordinate transformation is utilized in [214] such that the nominal orbit in the new coordinates is orthogonal to the switching surface at the point of intersection. In [56], and more recently [215], one instead defines the projection operator such that its gradient locally aligns with the switching surfaces.

In this chapter, however, we will utilize an approach similar to the one proposed by Freidovich and collaborators in [198, 213], whose development is similar in both its structure and idea to the Saltation matrix mentioned in this chapter's introduction. While their approach is constructed for a specific set of $(n-1)$ transverse coordinates for underactuated mechanical systems, we consider it here for the function e defined in (7.8).

Handling the misalignment between the switching surfaces and the moving Poincaré sections on the orbit's boundaries

Consider a point $\boldsymbol{\delta}_e^- \in \mathbf{T}\Pi(s_b)$ lying within the red-shaded region in Figure 7.2. We want to find its projection, denoted $\boldsymbol{\delta}_x^-$, upon $\mathbf{T\Sigma}_-$ along $\mathcal{F}(s_b)$.

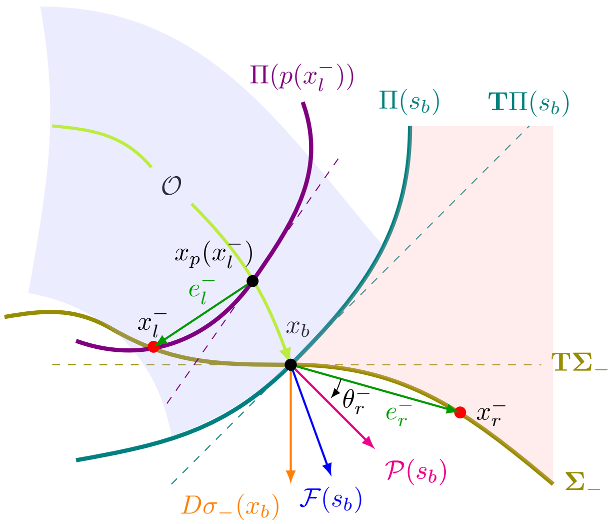

Figure 7.2: Illustrates two different states crossing the switching surface $\mathbf{\Sigma}_-$, whose tangent space at x_b does not align with the tangent space of the final moving Poincaré section $\Pi(s_b)$. Whereas the left crossing point, x_l^-, lies within the blue-shaded tube where the gradient of the projection operator is nonzero, the right crossing point, x_r^-, lies in the red zone within which $p(x) \equiv s_b$.

That is, we are looking for a number κ such that $\boldsymbol{\delta}_x^- = \boldsymbol{\delta}_e^- + \kappa\mathcal{F}(s_b) \in \mathbf{T\Sigma}_-$. To this end, we note that $D\sigma_-(x_b)\boldsymbol{\delta}_x^- = D\sigma_-(x_b)\left[\boldsymbol{\delta}_e^- + \kappa\mathcal{F}(s_b)\right] \equiv 0$, implying $\kappa = -(D\sigma_-(x_b)\boldsymbol{\delta}_e^-)/(D\sigma_-(x_b)\mathcal{F}(s_b))$. Hence

$$\boldsymbol{\delta}_x^- = \left(\mathbf{I}_n - \frac{\mathcal{F}(s_b)D\sigma_-(x_b)}{D\sigma_-(x_b)\mathcal{F}(s_b)}\right)\boldsymbol{\delta}_e^-.$$

By similar arguments, one can easily show that $\boldsymbol{\delta}_e^+ = \mathcal{E}_\perp(s_a)\boldsymbol{\delta}_x^+$ is the projection of $\boldsymbol{\delta}_x^+ \in \mathbf{T\Sigma}_+$ onto $\mathbf{T}\Pi(s_a)$ along $\mathcal{F}(s_a)$.

With this in mind, we define the projection matrix

$$\mathrm{P}_{\mathbf{T}\Sigma_-} := \left(\mathbf{I}_n - \frac{\mathcal{F}(s_b)D\sigma_-(x_b)}{D\sigma_-(x_b)\mathcal{F}(s_b)}\right), \tag{7.9}$$

for which clearly $\mathrm{P}_{\mathbf{T}\Sigma_-}\mathcal{F}(s_b) = \mathbf{0}_{n\times 1}$, and therefore $\mathrm{P}_{\mathbf{T}\Sigma_-}\mathcal{E}_\perp(s_b) = \mathrm{P}_{\mathbf{T}\Sigma_-}$. Indeed, if the tangent surface of $\mathbf{\Sigma}_-$ at x_b aligns with the tangent of the moving Poincaré section $\Pi(s_b)$ (see Figure 7.2), then $\mathrm{P}_{\mathbf{T}\Sigma_-} \equiv \mathcal{E}_\perp(s_b)$.

Now note that the Jump condition (7.3), i.e. $x_a = \mathbf{J}(x_b)$, implies $\boldsymbol{\delta}_x^+ = D\mathbf{J}(x_b)\boldsymbol{\delta}_x^-$. Thus by combining this with the projection matrices obtained above, we find that $\boldsymbol{\delta}_e^+ = \mathbf{J}_\perp \boldsymbol{\delta}_e^-$, where

$$\mathbf{J}_\perp := \mathcal{E}_\perp(s_a) D\mathbf{J}(x_b) \left(\mathbf{I}_n - \frac{\mathcal{F}(s_b) D\sigma_-(x_b)}{D\sigma_-(x_b)\mathcal{F}(s_b)} \right). \tag{7.10}$$

The matrix (7.10) will be a vital part of the method we will soon propose for designing an orbitally stabilizing control law. Roughly speaking, we will use it to state a condition, specifically a linear matrix inequality, which ensures that the discrete jump will not locally destabilize the cycle.

7.2.3 Method for orbitally stabilizing feedback design

In order to stabilize the orbit (7.7), we will again take inspiration from the approach in Chapter 6. We will consider a controller of the form

$$u = u_s(p) + K(p)\mathcal{E}_\perp(p)e \tag{7.11}$$

where $p = p(x)$ and with $K : \mathcal{S} \to \mathbb{R}^m$ smooth. Here $\mathcal{E}_\perp(s) := \mathbf{I}_n - \mathcal{F}(s)\mathcal{P}(s)$ is the projection matrix having the properties previously stated in Lemma 4.28, with $\mathcal{P}(s)$ corresponding to $Dp(x_s(s))$ evaluated within the tube $\mathcal{T}$. The difference between (7.11) and the control law (6.12) considered in Chapter 6 is therefore that we only consider the projection of e onto $\mathbf{T}\Pi(p)$ by passing it through $\mathcal{E}_\perp(p)$. Using again Figure 7.2, the following paragraph provides some motivation for this modification:

Suppose the system's solution crosses the last moving Poincaré section, $\Pi(s_b)$, at the end of $\mathcal{T}$ and enters into $\mathcal{H}_b$, which is illustrated by the red-shaded region in Figure 7.2. If this happens sufficiently close to x_b, we want the solution to eventually hit the switching surface, which on $\Pi(s_b)$ lies in the direction of $\mathcal{F}(s_b)$. This means that, ideally, the control law should not act on the the parts of e lying in the span of $\mathcal{F}(s_b)$ for $x \in \mathcal{H}_b$. Hence we use $\mathcal{E}_\perp(p)e$ in the control law (7.11) rather than just e, which in fact could end up deteriorating the performance by "forcing" the controller to also act upon perturbation in the direction of $\mathcal{F}(s_b)$ when x is within $\mathcal{H}_b$. The same reasoning can be applied in regard to trajectories passing through $\mathcal{H}_a$.

Let $A_s(s) := A(x_s(s), u_s(s))$ and $B_s(s) := B(x_s(s))$, with $A(x,u) := Df(x) + \sum_{i=1}^m Db_i(x)u_i$, and denote $B_\perp(s) := \mathcal{E}_\perp(s)B_s(s)$ as well as

$$A_\perp(s) := \mathcal{E}_\perp(s)A_s(s) - \rho(s)\mathcal{F}(s)\mathcal{F}^\mathsf{T}(s)D^2p(x_s(s))\mathcal{E}_\perp(s).$$

We will again take inspiration from [183] and suggest an approach utilizing a differential linear matrix inequality (LMI) in order to find a stabilizing feedback. While we have seen the use of such differential LMIs before in Chapter 4 and Chapter 6 (see Prop. 4.46 and Thm. 6.12, respectively), the addition of an LMI which utilized the constructed jump map $\mathbf{J}_\perp$ defined in (7.10) to account for the discrete jump is the main novelty here.[2]

Theorem 7.2. *Suppose that for some function $\lambda \in \mathcal{C}^0(\mathcal{S}, \mathbb{R}_{>0})$, there exist smooth matrix-valued functions $Y : \mathcal{S} \to \mathbb{R}^{m\times n}$ and $W : \mathcal{S} \to \mathbb{M}^n_{\succ 0}$ satisfying*

$$\begin{aligned}\rho(s)W'(s) - W(s)A_\perp^\top(s) - A_\perp(s)W(s) - Y(s)^\top B_\perp^\top(s) - B_\perp(s)Y(s) \\ - 2^{-1}\lambda(s)[\mathcal{E}_\perp(s)W(s) + W(s)\mathcal{E}_\perp^\top(s)] \succeq \mathbf{0}_n\end{aligned} \tag{7.12}$$

for all $s \in \mathcal{S}$. Further suppose that

$$\begin{bmatrix} W(s_b)(1-\mu) & W(s_b)\mathbf{J}_\perp^\top \\ \mathbf{J}_\perp W(s_b) & W(s_a) \end{bmatrix} \succeq 0 \tag{7.13}$$

for some $0 < \mu \ll 1$ and with $\mathbf{J}_\perp$ defined in (7.10). Then, by taking for the hybrid system (7.1) the control law (7.11) with

$$K(s) := Y(s)W^{-1}(s)\mathcal{E}_\perp(s), \tag{7.14}$$

the hybrid periodic orbit (7.7) is rendered asymptotically stable.

Proof of Theorem 7.2

For the closed-loop system

$$\dot{x} = f_{cl}(x) := f(x) + B(x)\left[u_s(p) + K(p)e\right], \tag{7.15}$$

consider the following Lyapunov-like[3] function candidate for the orbit $\mathcal{O}$ defined in (7.7):

$$V_\perp := e^\top \mathcal{E}_\perp^\top(p) W^{-1}(p)\mathcal{E}_\perp(p)e. \tag{7.16}$$

We will in the following show that: 1) the differential LMI (7.12) guarantees that $V_\perp$ is strictly decreasing within a subset of the tube $\mathcal{T}$ containing $\mathcal{O}$; 2) the LMI (7.13) both ensures that $V_\perp$ is not increasing over the jump if x_- is sufficiently close to x_b, and that this is true even if the system's solution enter into either one- or both of $\mathcal{H}_a$ and $\mathcal{H}_b$. Combined, these claims guarantee the existence of a tubular neighborhood of $\mathcal{O}$ lying entirely between the switching surfaces $\mathbf{\Sigma}_+$ and $\mathbf{\Sigma}_-$, within which $V_\perp$ decays to zero. This, combined with the properties of $V_\perp$ listed in the following statement, proves the validity of Theorem 7.2.

[2]Note that similar conditions to the one in Theorem 7.2 for handling the discrete jumps have been proposed for differential Riccati equations and "standard" transverse coordinates; see [216].

[3]A Lyapunov-like function, or non-monotonic Lyapunov function [217], is a strictly positive function which unlike a "regular" Lyapunov function may momentarily increase in value, but is locally bounded and strictly decreasing when evaluated over the whole cycle.

Lemma 7.3. *There is a neighborhood of the orbit $\mathcal{O}$ within which the function $V_\perp = V_\perp(x)$, defined in (7.16), is locally Lipschitz, as well as nonzero everywhere therein expect on the orbit where it vanishes.*

Here the local Lipschitz property of $V_\perp$ is inherited from the projection operator, whereas the latter property follows from the fact that $V_\perp$ can vanish only if $\mathcal{E}_\perp(p)e = 0$, which we in turn claim can only locally occur on $\mathcal{O}$ for $x \in \mathfrak{X}$. Indeed, let $\epsilon > 0$ be some (sufficiently small) number such that $\mathcal{N}_\epsilon \backslash \{\mathbf{\Sigma}_- \cup \mathbf{\Sigma}_+\}$, with

$$\mathcal{N}_\epsilon := \{x \in \mathbb{R}^n : \ \mathrm{dist}(\mathcal{O}, x) \leq \epsilon\},$$

consists of three connected regions. Let $\mathfrak{M}_\epsilon \subset \mathcal{N}_\epsilon$ denote the region lying between $\mathbf{\Sigma}_-$ and $\mathbf{\Sigma}_+$ as well as its intersection with these two surfaces. Thus $\mathfrak{M}_\epsilon$ is a tubular neighborhood of $\mathcal{O}$ whose ends align with the switching surfaces. This allows us to state the following statement, from which the above lemma follows.

Claim 7.4. *There is an $\epsilon > 0$ such that $\|\mathcal{E}_\perp(p(x))e(x)\| \equiv 0$ within $\mathfrak{M}_\epsilon$ only if $x \in \mathcal{O}$.*

Proof. From (4.47), we know that $\mathcal{E}_\perp(p(x))e(x)$ does not locally vanish for x in $\mathcal{T}$. What we need to check is therefore what occurs if there are regions within $\mathfrak{M}_\epsilon$ where $\|Dp\|(x) \equiv 0$, thus corresponding to some subset of $\mathcal{H}_a$ or $\mathcal{H}_b$. To this end, we note from Claim 4.7 that $\|\mathcal{P}(s)\| = \sqrt{1+\tan^2(\varphi(s))}/\|\mathcal{F}(s)\|$, where $\varphi(s) \in (-\frac{\pi}{2}, \frac{\pi}{2})$ denotes the angle between $\mathcal{P}^\mathsf{T}(s)$ and $\mathcal{F}(s)$ in their common plane. Thus

$$\begin{aligned}\mathcal{E}_\perp(s_b)e &= e - \mathcal{F}(s_b)\mathcal{P}(s_b)e = e - \mathcal{F}(s_b)\|\mathcal{P}(s_b)\|\,\|e\|\cos(\theta)\\ &= e - \frac{\mathcal{F}(s_b)}{\|\mathcal{F}(s_b)\|}\sqrt{1+\tan^2(\varphi(s))}\,\|e\|\cos(\theta)\end{aligned}$$

where θ is the angle between $e = x - x_b$ and $\mathcal{P}^\mathsf{T}(s_b)$ in their common plane. Setting this to equal to zero implies

$$\frac{e}{\|e\|} = \frac{\mathcal{F}(s_b)}{\|\mathcal{F}(s_b)\|}\sqrt{1+\tan^2(\varphi(s))}\cos(\theta),$$

which can only occur when e and $\mathcal{F}(s_b)$ are colinear. This is, however, impossible for sufficiently small e due to the non-grazing condition (7.6) and the fact that $\sigma_- \in \mathcal{C}^2$ (the curvature of the switching surface is bounded). As we can use the exact same arguments about x_a, the claim is true. □

Contraction within a tubular neighborhood

Consider now the tube

$$\mathcal{T} := \{x \in \mathfrak{X} : \; \|Dp\| \neq 0\}.$$

Using the same arguments as in the proof of Theorem 6.10, the differential LMI (7.12) implies that there exists a $\zeta > 0$, as well as a small tubular neighborhood of $\mathcal{N}$ of $\mathcal{O}$, such that

$$\dot{V}_{\perp} \leq -\lambda(p) e^{\mathsf{T}} W^{-1}(p) e + O(\|e\|^3) \leq -\zeta V_{\perp}$$

whenever x is in $\mathcal{T} \cap \mathcal{N}$. Hence, for a solution $x(t)$ of (7.15) remaining in $\mathcal{T} \cap \mathcal{N}$ over some time interval $[t_a, t]$ before eventually either leaving $\mathcal{T}$ or hitting $\mathbf{\Sigma}_{-}$, one has $V_{\perp}(t) \leq V_{\perp}(t_a) \exp\{-\zeta(t - t_a)\}$ by the comparison principle (see, e.g. [169, Theorem 1.1],[44, Lemma 3.4])). In fact, from this and the continuous dependence of the solutions to (7.15) on the initial conditions (see, e.g., [44, Theorem 3.5]) in the absence of any discrete dynamics, it follows that for any $\epsilon > 0$, there is a $\delta > 0$, such that by taking $x(t_1) \in \mathcal{T}$ satisfying $\|x(t_1) - x_a\| < \delta$, then, for T_s as in (7.5), there is a $t_2 \in [T_s - \epsilon, T_s + \epsilon]$ such that $x(t) \in \mathcal{T}$ for all t in $[t_1, t_2]$, $x(t_2) \in \mathcal{T}$ satisfies $\|x(t_2) - x_b\| < \epsilon$, and, moreover, $V_{\perp}(t_2) \leq V_{\perp}(t_1) \exp\{\epsilon - \eta\}$, with $\eta := \int_{s_a}^{s_b} \lambda(\tau)/\rho(\tau) d\tau$.

Thus, we need to show that the theorem's hypotheses ensure that the value of $V_{\perp}$ does not increases over a jump even if a solution has entered into either $\mathcal{H}_a$ or $\mathcal{H}_b$ while remaining sufficiently close to x_a and x_b, respectively.

Non-increasing jump condition

Lemma 7.5. *If the LMI* (7.13) *holds, then there exists a real number $c > 0$ such that if $\|x_b - x^{-}\| < c$, then the function $V_{\perp} = V_{\perp}(x)$, defined in* (7.16), *is non-increasing over the resulting jump.*

Proof. For some continuous function $h : \mathbb{R}^n \to \mathbb{R}^l$, $l \geq 1$, which is differentiable at a point $y \in \mathbb{R}^n$, we will in the following write

$$h(x) = h(y) + Dh(y)(x - y) + R_h^1(x - y),$$

where $\left\|R_h^1(z)\right\| \in o(\|z\|)$ as $z \to 0$. If, moreover, h is of class $\mathcal{C}^2$, then we replace $R_h^1(\cdot)$ by $R_h^2(\cdot)$ which satisfies $\left\|R_h^2(z)\right\| \in O(\|z\|^2)$.

We begin by noting that as $\mathbf{J}(\cdot)$ has been assumed to be differentiable at $x_b = x_s(s_b)$, we can, for x in a small neighborhood of x_b, write

$$\mathbf{J}(x) = \mathbf{J}(x_b) + D\mathbf{J}(x_b)(x - x_b) + R_{\mathbf{J}}^1(x - x_b). \tag{7.17}$$

For some $\mathbf{\Sigma}^+ \ni x^+ = \mathbf{J}(x^-)$, with $x^- \in \mathbf{\Sigma}^-$ close to x_b, it follows that

$$x^+ - x_a = D\mathbf{J}(x_b)(x^- - x_b) + R^1_{\mathbf{J}}(x^- - x_b). \tag{7.18}$$

Now, since $\sigma_- \in \mathcal{C}^2$ and $\sigma_-(x_b) \equiv 0$, we can write

$$\sigma_-(x) = D\sigma_-(x_b)(x - x_b) + R^2_{\sigma_-}(x - x_b).$$

Observe that for any $x^- \in \mathbf{\Sigma}^-$ such that $\sigma_-(x^-) \equiv 0$, this implies

$$D\sigma_-(x_b)(x^- - x_b) = -R^2_{\sigma_-}(x^- - x_b). \tag{7.19}$$

Recall here the projection matrix $\mathrm{P}_{\mathbf{T}\Sigma_-}$, defined in (7.9), which satisfies $\mathrm{P}_{\mathbf{T}\Sigma_-}\mathcal{F}(s_b) = \mathbf{0}_{n\times 1}$. Using this property, we can infer that

$$\mathrm{P}_{\mathbf{T}\Sigma_-}(x^- - x_b) = \mathrm{P}_{\mathbf{T}\Sigma_-}\mathcal{E}_\perp(s_b)(x^- - x_b) = (x^- - x_b) + \mathcal{F}(s_b)\hat{R}^2_{\sigma_-} \tag{7.20}$$

where $\hat{R}^2_{\sigma_-} := R^2_{\sigma_-}/(D\sigma(x_b)\mathcal{F}(s_b))$. Inserting this into (7.18) yields

$$x^+ - x_a = D\mathbf{J}(x_b)\left[\mathrm{P}_{\mathbf{T}\Sigma_-}\mathcal{E}_\perp(s_b)(x^- - x_b) - \mathcal{F}(s_b)\hat{R}^2_{\sigma_-}\right] + R^1_{\mathbf{J}}(x^- - x_b). \tag{7.21}$$

Let us denote $x_p^\pm = x_p(x^\pm)$, such that $x^\pm = e^\pm + x_p^\pm$. We have $x^- - x_b = e^- + x_p^- - x_b$. Hence $x^- - x_b = e^-$ whenever $x_p^- = x_b$, which corresponds to $x^- \in \mathcal{H}_b$ (see the red-shaded region in Figure 7.2); if not, then $x^- \in \mathcal{T}$ (see the blue-shaded tube).

Now, take note of the fact that for any $x \in \mathfrak{X}$ we can write $x_b = x_p(x) + \int_{p(x)}^{s_b}\mathcal{F}(\tau)d\tau =: x_p(x) + F_b(x)$. Expanding $F_b(x) := \int_p^{s_b}\mathcal{F}(\tau)d\tau$ about x_b yields

$$F_b(x) = -\mathcal{F}(s_b)\mathcal{P}(s_b)(x - x_b) + R^2_{F_b}(x - x_b),$$

and hence

$$x - x_b = e - F(x) = e + \mathcal{F}(s_b)\mathcal{P}(s_b)(x - x_b) + R^2_{F_b}(x - x_b).$$

Thus we may by (7.21) write

$$x^+ - x_a = D\mathbf{J}(x_b)\mathrm{P}_{\mathbf{T}\Sigma_-}\mathcal{E}_\perp(s_b)e^- + \hat{R}^1_{\mathbf{J}}(x^- - x_b), \tag{7.22}$$

where $\hat{R}^1_{\mathbf{J}}(x^-) = R^1_{\mathbf{J}}(x^-) - D\mathbf{J}(x_b)\mathcal{F}(s_b)\hat{R}^2_{\sigma_-} + r^-(x^-)$ with

$$r^-(x^-) = \begin{cases} \mathbf{0}_{n\times 1}, & \text{if } x_p(x^-) = x_b, \\ D\mathbf{J}(x_b)\mathrm{P}_{\mathbf{T}\Sigma_-}\mathcal{E}_\perp(s_b)R^2_{F_b}(x^- - x_b), & \text{otherwise.} \end{cases}$$

Consider now the left-hand side of (7.21). Similarly to the above analysis about the end of the cycle, we also have at the beginning that $x^- + x_a = e^+$ whenever $x_p^+ = x_a$, whereas

$$\begin{aligned} x^+ - x_a &= e^+ + \int_{s_a}^{p(x)} \mathcal{F}(\tau)d\tau =: e^+ + F_a(x) \\ &= e^+ + \mathcal{F}(s_a)\mathcal{P}(s_a)(x^+ - x_a) + R^2_{F_a}(x^+ - x_a). \end{aligned}$$

Hence $\mathcal{E}_\perp(s_a)(x^+ - x_a) = \mathcal{E}_\perp(s_a)e^+ + r_+(x^+)$, where

$$r^+(x^+) = \begin{cases} 0, & \text{if } x_p(x^+) = x_a, \\ \mathcal{E}_\perp(s_a)R^2_{F_a}(x^+ - x_a), & \text{otherwise.} \end{cases}$$

If we therefore multiply both sides of (7.22) from the left by $\mathcal{E}_\perp(s_a)$ and replace $x^+ - x_a$ using (7.18), we find that

$$\mathcal{E}_\perp(s_a)e^+ = \mathbf{J}_\perp \mathcal{E}_\perp(s_b)e^- + R^1_{\mathbf{J}_\perp}(x^- - x_b), \tag{7.23}$$

where $R^1_{\mathbf{J}_\perp}(x - x_b) := \mathcal{E}_\perp(s_a)\big[\hat{R}^1_{\mathbf{J}}(x^- - x_b) - r^+(x^+ - x_a)\big]$ and with $\mathbf{J}_\perp$ defined by (7.10).

Now in order to help us compute $V_\perp^+$ and $V_\perp^-$, we first note that, by the fundamental theorem of calculus, we can, for any $s \in \mathcal{S}$, write

$$\mathcal{E}_\perp^\mathsf{T}(p)W^{-1}(p)\mathcal{E}_\perp(p) = \mathcal{E}_\perp^\mathsf{T}(s)W^{-1}(s)\mathcal{E}_\perp(s) + \int_s^p \frac{d}{d\tau}\big[\mathcal{E}_\perp^\mathsf{T}(\tau)W^{-1}(\tau)\mathcal{E}_\perp(\tau)\big]d\tau,$$

where the magnitude of the integral term is $O(\|x - x_s(s)\|)$ as $x \to x_s(s)$. Hence

$$\begin{aligned} V_\perp^- &= (e^-)^\mathsf{T}\mathcal{E}_\perp^\mathsf{T}(s_b)W^{-1}(s_b)\mathcal{E}_\perp(s_b)e^- + O(\|x^- - x_b\|^3), \\ V_\perp^+ &= (e^+)^\mathsf{T}\mathcal{E}_\perp^\mathsf{T}(s_a)W^{-1}(s_a)\mathcal{E}_\perp(s_a)e^+ + O(\|x^+ - x_a\|^3). \end{aligned}$$

By again replacing $x^+ - x_a$ using (7.18), as well as utilizing (7.23) and the fact that $\left\|R^1_{\mathbf{J}_\perp}(x^- - x_b)\right\| \in o(\|x^- - x_b\|)$ as $x^- \to x_b$, we can here write

$$V_\perp^+ = (e^-)^\mathsf{T}\mathcal{E}_\perp^\mathsf{T}(s_b)\mathbf{J}_\perp^\mathsf{T}W^{-1}(s_a)\mathbf{J}_\perp^\mathsf{T}\mathcal{E}_\perp(s_b)e^- + o(\|x^- - x_b\|^2).$$

Noting that, due to the properties of the Schur complement (see, e.g. [181, Thm. 1.12]), the LMI (7.12) implies

$$W(s_b)(1-\mu) - W(s_b)\mathbf{J}_\perp^\mathsf{T}W^{-1}(s_a)\mathbf{J}_\perp W(s_b) \succeq 0, \tag{7.24}$$

and therefore

$$V_\perp^+ \le (1-\mu)(e^-)^\mathsf{T}\mathcal{E}_\perp^\mathsf{T}(s_b)W^{-1}(s_b)^\mathsf{T}\mathcal{E}_\perp(s_b)e^- + o(\|x^- - x_b\|^2).$$

Hence $V_\perp^+ \le (1-\mu)V_\perp^- + o(\|x^- - x_b\|^2)$. Since $V_\perp^- \neq 0$ if $\|x^- - x_b\| \neq 0$ is sufficiently small by Claim 7.4, we have that $V_\perp^-$ is $O(\|x^- - x_b\|^2)$ but not $o(\|x^- - x_b\|^2)$ as $x^- \to x_b$. It thus follows that for any $\mu > 0$, there is a $c > 0$, such that $\|x^- - x_b\| < c$ implies $V_\perp^+ \le V_\perp^-$. This concludes the proof of Lemma 7.5. $\square$

Handling the red zones

While we have showed so far that the Lyapunov-like function candidate $V_\perp$ is decreasing in time when sufficiently close to the orbit within the tube $\mathcal{T}$, as well as non-increasing over the jump, our aim is now to study the behavior when a solution enters into either one or both of the sets

$$\begin{aligned}\mathcal{H}_a &:= \{x \in \mathfrak{X} : \ p(x) = s_a, \ \|Dp(x)\| = 0\},\\ \mathcal{H}_b &:= \{x \in \mathfrak{X} : \ p(x) = s_b, \ \|Dp(x)\| = 0\}.\end{aligned}$$

Note that the red-shaded region Figure 7.2 provides an illustration of $\mathcal{H}_b$.

More specifically, let $x(\cdot)$ denote a trajectory of the closed-loop system (7.15) remaining in some small neighborhood of $\mathcal{O}$, which first leaves the tube $\mathcal{T}$, hits $\mathbf{\Sigma}_-$, then undergoes a jump, and eventually enters into the tube again. We will show that if $x(\cdot)$ was sufficiently close to x_b when it left $\mathcal{T}$ (e.g. by entering $\mathcal{H}_b$ or hitting $\mathbf{\Sigma}_-$), then the value of $V_\perp$ has not increased the next time it enters $\mathcal{T}$ if the LMI (7.13) holds. Since similar arguments can be used to investigate both $\mathcal{H}_a$ and $\mathcal{H}_b$, we will mainly focus on $\mathcal{H}_b$ for the sake of brevity.

We first note that, due to Lemma 7.5, such an investigation is only of interest if $\mathcal{H}_b \cap \mathbf{\Sigma}_- \cap \mathcal{B}_\epsilon(x_b)\backslash\{x_b\}$ is non-empty for some arbitrarily small $\epsilon > 0$. Suppose, therefore, in the following that this is the case, and consider a point $x_{\Pi_b} \in \Pi(s_b)$ lying on the boundary between $\mathcal{T}$ and $\mathcal{H}_b$. Due to the non-grazing condition (7.6) and the fact that $\sigma_- \in \mathcal{C}^2$, it is guaranteed that for x_{Π_b} sufficiently close to x_b, there exists a number $q > 0$ such that $x_{\Pi_b} + q\mathcal{F}(s_b)\rho(s_b) \in \mathbf{\Sigma}_-$. Thus, let $x(\cdot)$ denote a solution of the closed-loop system (7.15) which is equal to x_{Π_b} at some time instant t_{Π_b}, i.e. $x(t_{\Pi_b}) = x_{\Pi_b}$. Then, due to the local existence and uniqueness of the solutions to (7.15), the following holds: for any $\epsilon > 0$, there is a $\delta > 0$, such that if $\|x_b - x_{\Pi_b}\| < \delta$, then there exists a (finite) time instant $t_- > t_{\Pi_b}$ such that

$x(t_-) \in \mathbf{\Sigma}_-$ and $\|x(t_-) - x_b\| < \epsilon$.[4] For such a solution, clearly

$$x(t) = x_{\Pi_b} + (t - t_{\Pi_b})\mathcal{F}(s_b)\rho(s_b) + \int_{t_{\Pi_b}}^{t} \left[f_{cl}(x(\tau)) - \mathcal{F}(s_b)\rho(s_b)\right] d\tau$$

holds for all $t \in [t_{\Pi_b}, t_-]$. Subtracting x_b from both sides results in

$$e(t) = e_{\Pi_b} + (t - t_{\Pi_b})\mathcal{F}(s_b)\rho(s_b) + \int_{t_{\Pi_b}}^{t} \left[f_{cl}(x(\tau)) - \mathcal{F}(s_b)\rho(s_b)\right] d\tau, \quad (7.25)$$

where e_{Π_b} denotes the value of e when it crossed the last moving Poincaré section $\Pi(s_b)$ immediately before $x(\cdot)$ enters $\mathcal{H}_b$.

Using (7.19), we find

$$(t_- - t_{\Pi_b})\rho(s_b) = \frac{D\sigma_-(x_b)\left[-e_{\Pi_b} - \int_{t_{\Pi_b}}^{t_-}\left[f_{cl}(x(\tau)) - \mathcal{F}(s_b)\rho(s_b)\right] d\tau\right]}{D\sigma_-(x_b)\mathcal{F}(s_b)} - R_{\sigma_-}^2$$

which inserted into (7.25) yields

$$\mathrm{P}_{\mathbf{T}\Sigma_-} e^- = \mathrm{P}_{\mathbf{T}\Sigma_-}\mathcal{E}_\perp(s_b)e^- = \mathrm{P}_{\mathbf{T}\Sigma_-}\left[e_{\Pi_b} + \int_{t_{\Pi_b}}^{t_-} f_{cl}(x(\tau))d\tau\right]. \quad (7.26)$$

Here the matrix $\mathrm{P}_{\mathbf{T}\Sigma_-}$ is as defined in (7.9), and thus satisfies $\mathrm{P}_{\mathbf{T}\Sigma_-}\mathcal{F}(s_b) \equiv \mathbf{0}_{n\times 1}$. We claim that this implies $\mathrm{P}_{\mathbf{T}\Sigma_-}e^- = \mathrm{P}_{\mathbf{T}\Sigma_-}e_{\Pi_b} + R_{\Pi_b}(e_{\Pi_b})$ with $\|R_{\Pi_b}(e_{\Pi_b})\| = o(\|e_{\Pi_b}\|)$. Indeed,

$$\mathrm{P}_{\mathbf{T}\Sigma_-}\int_{t_{\Pi_b}}^{t_-} f_{cl}(x(\tau))d\tau = \mathrm{P}_{\mathbf{T}\Sigma_-}\int_{t_{\Pi_b}}^{t_-} \big[f_{cl}(x(\tau)) - \mathcal{F}(s_b)\rho(s_b)\big]d\tau$$

where, for some Lipschitz constant $l_{f_{cl}} > 0$,

$$\begin{aligned}\|f_{cl}(x(t)) - \mathcal{F}(s_b)\rho(s_b)\| &\le l_{f_{cl}}\|x(t) - x_b\| = l_{f_{cl}}\|x(t) - x_{\Pi_b} + e_{\Pi_b}\| \\ &\le l_{f_{cl}}\big(\|x(t) - x_{\Pi_b}\| + \|e_{\Pi_b}\|\big)\end{aligned}$$

due to the right-hand side of (7.15) being locally Lipschitz continuous. Clearly, $\|x(t) - x_{\Pi_b}\| \to 0$ as $\|e_{\Pi_b}\| \to 0$. Moreover, by defining $\Upsilon(\tau) := \sigma_-(\xi(\tau))$ where $\xi(\tau) := x\big((t_- + t_{\Pi_b})\tau + t_{\Pi_b}\big)$, we have $\Upsilon(1) - \Upsilon(0) = -\Upsilon(0) = \int_0^1 \Upsilon'(\tau)d\tau$, and hence (cf. Hadamard's lemma)

$$-\sigma_-(x_{\Pi_b}) = (t_- - t_{\Pi_b})\int_0^1 D\sigma_-(\xi(\tau))f_{cl}(\xi(\tau))d\tau.$$

[4]The time instant t_- can be determined from the *time-to-impact* function, $T_I(\cdot)$, i.e. $t_- - t_{\Pi_b} = T_I(x_{\Pi_b})$, which by [135, Lemma 3] is continuous in a neighborhood of x_{Π_b}.

Since $\sigma_-(x_{\Pi_b}) = O(\|e_{\Pi_b}\|)$ and the integral is non-zero for x_- sufficiently close to x_b due to the non-grazing condition (7.6), it follows that $|t_- - t_{\Pi_b}| = O(\|e_{\Pi_b}\|)$. Thus $\mathrm{P}_{\mathbf{T}\Sigma_-} e^- = \mathrm{P}_{\mathbf{T}\Sigma_-} e_{\Pi_b} + R_{\Pi_b}(e_{\Pi_b})$ is indeed true as claimed.

Denote now by $e^+ = e(t_+)$ the value of $e(t)$ immediately after the jump. Suppose that $x(t_+)$ lies in $\mathcal{H}_a$, and that it crosses Π_{s_a} at the time instant $t_{\Pi_a} > t_+$, where we denote $e_{\Pi_a} = e(t_{\Pi_a})$. Similarly to before the jump, we now perform a (first-order) projection along $\mathcal{F}(s_a)$ and use the fact that $e_{\Pi_a} = \mathcal{E}_\perp(s_a)e_{\Pi_a} + \mathcal{F}(s_a)R_{\Pi_a}(e_{\Pi_a})$ where $\|R_{\Pi_a}(e_{\Pi_a})\| = O(\|e_{\Pi_a}\|^2)$. This now results in $\mathcal{E}_\perp(s_a)e_{\Pi_a} = \mathcal{E}_\perp(s_a)e^+ + R_+(e^+)$ with $\|R_+(e^+)\| = o(\|e^+\|)$. Hence, by copying the steps at the end of the proof for Lemma 7.5, one can show that if the value of $\|e\|$ is sufficiently small when leaving the tube $\mathcal{T}$, then the value of $V_\perp$ when the system's trajectory returns to the tube again will be less than or equal to its value when it left the tube, even if the trajectory of the closed-loop system passed through $\mathcal{H}_b$ and/or $\mathcal{H}_a$. Hence there necessarily exists a small neighborhood of $\mathcal{N}$ of $\mathcal{O}$, specifically the interior of a level set of the function $V_\perp$, such that by initializing the system upon any of the moving Poincaré sections $\Pi(\cdot)$ within $\mathcal{N}$, then the states will return to this section within a finite amount of time without ever leaving $\mathcal{N}$, and the value of $V_\perp$ is γ-times less than its previous value for some $0 < \gamma < 1$. As a consequence, the hybrid periodic orbit $\mathcal{O}$ is asymptotically stable, which concludes the proof of Theorem 7.2.

7.2.4 Stronger statement for a differential-algebraic system

While Theorem 7.2 provided sufficient conditions for the existence of an orbitally stabilizing feedback for the hybrid cycle, we will in this section show, using a linear comparison system, that it is in fact somewhat conservative. Moreover, we will at the same time demonstrate that rather than using a positive definite matrix function $W(\cdot)$ and its inverse, one can alternatively use a positive semidefinite matrix function and its pseudoinverse.

Let $\chi(t) \in \mathbb{R}^n$ and consider the following system of differential-algebraic equations with a discrete jump:

$$\left.\begin{aligned} \dot{\chi}(t) &= A_\perp(s)\chi(t) + B_\perp(s)v, \\ \dot{s} &= \rho(s), \\ 0 &= \mathcal{P}(s)\chi, \end{aligned}\right\} \quad s \in \mathcal{S} := [s_a, s_b], \tag{7.27a}$$

$$\left.\begin{aligned} \chi^+ &= \mathbf{J}_\perp \chi^-, \\ s^+ &= s_a, \end{aligned}\right\} \quad s^- = s_b. \tag{7.27b}$$

Here the matrix-valued functions are as defined before Theorem 7.2. One can therefore view this system as the transverse Linearization associated with e, defined in (7.8), when the states are within the tube $\mathcal{T}$. Any misalignment between the moving Poincaré sections at the ends of the tube and the switching surfaces are again handled through the respective projections along $\mathcal{F}(s_a)$ and $\mathcal{F}(s_b)$, which are incorporated into the linear mapping $\mathbf{J}_\perp$ defined in (7.10).

Recall that $W^\dagger \in \mathbb{R}^{n\times n}$ is the unique pseudoinverse of $W \in \mathbb{R}^{n\times n}$ if it satisfies the following four conditions:

$$W^\dagger W W^\dagger = W^\dagger,\ W W^\dagger W = W,\ (W W^\dagger)^\mathsf{T} = W W^\dagger,\ (W^\dagger W)^\mathsf{T} = W^\dagger W.$$

Using the properties of the pseudoinverse, we can as an alternative to the differential LMI (7.12) instead consider a projected differential LMI. In much the same way as a solution $W(\cdot)$ to (7.12) may be viewed as the inverse of some solution to a Riccati equation (see, e.g., (4.96)), the solution we suggest may be viewed as the pseudoinverse of a positive semidefinite solution to a projected Riccati equation as in Proposition 4.45. Unlike the more restrictive condition in Theorem 7.2, which ensures that the Lyapunov function candidate (7.16) is non-increasing over a discrete jump, the following statement for (7.27) only requires a similar function to be decreasing when evaluated over the whole cycle.

Proposition 7.6. *Suppose that for some constant $\omega \in \mathbb{R}_{>0}$ and function $\lambda \in \mathcal{C}^0(\mathcal{S}, \mathbb{R}_{>0})$, there exist smooth matrix-valued functions $Y_\perp : \mathcal{S} \to \mathbb{R}^{m\times n}$ and $W_\perp : \mathcal{S} \to \mathbb{M}^{n\times n}_{\succeq 0}$, satisfying*

$$Y_\perp(s)\mathcal{E}_\perp^\mathsf{T}(s) \equiv Y_\perp(s) \quad \text{and} \quad W_\perp(s) \equiv \mathcal{E}_\perp(s) W_\perp(s)\mathcal{E}_\perp^\mathsf{T}(s) \succeq \omega \mathcal{E}_\perp(s)\mathcal{E}_\perp^\mathsf{T}(s), \tag{7.28}$$

as well as

$$\begin{aligned}\mathcal{E}_\perp(s)\Big[\rho(s)W_\perp'(s) - W_\perp(s)A_s^\mathsf{T}(s) - A_s(s)W_\perp(s) \\ - Y(s)^\mathsf{T}B_s^\mathsf{T}(s) - B_s(s)Y(s) - \lambda(s)W_\perp(s)\Big]\mathcal{E}_\perp^\mathsf{T}(s) \succeq \mathbf{0}_n\end{aligned} \tag{7.29}$$

for all $s \in \mathcal{S}$. Further suppose that

$$\begin{bmatrix} W_\perp(s_b)(\eta - \mu) & W_\perp(s_b)\mathbf{J}_\perp^\mathsf{T} \\ \mathbf{J}_\perp W_\perp(s_b) & W_\perp(s_a)\end{bmatrix} \succeq 0, \tag{7.30}$$

where $\eta := \exp\left\{\int_{s_a}^{s_b} \lambda(\tau)/\rho(\tau)d\tau\right\}$ and μ is arbitrarily small. Then, under the control law $v = K(s)\chi$ with

$$K(s) := Y(s)W_\perp^\dagger(s) = Y(s)\left[W_\perp(s) + \mathcal{F}(s)\mathcal{F}^\mathsf{T}(s)h(s)\right]^{-1} \tag{7.31}$$

for some arbitrary smooth function $h : \mathcal{S} \to \mathbb{R}_{>0}$, the solutions of the system (7.27) are bounded and the origin $\chi = 0$ is exponentially attractive.

Remark 7.7. If the conditions in Proposition 7.6 are met, then it can be more computationally effective to use the inverse expression on the right-hand side of (7.31) as it avoids the expensive computation of the pseudoinverse of $W_\perp$. Their equivalence is easily seen by using the properties of $Y_\perp$ and $W_\perp$ stated in (7.28), which imply that $W(s) = W_\perp(s) + \mathcal{F}(s)\mathcal{F}^\mathsf{T}(s)h(s)$ is positive definite, with its inverse given by $W^{-1}(s) = W_\perp^\dagger(s) + \mathcal{P}^\mathsf{T}(s)\mathcal{P}(s)h^{-1}(s)$ where $W_\perp^\dagger(s) = \mathcal{E}_\perp^\mathsf{T}(s)W_\perp^\dagger(s)\mathcal{E}_\perp(s)$.

Proof. Let the controller be taken as (7.31) in the continuous part of (7.27), and consider the Lyapunov-like function candidate

$$V_\perp = \chi^\mathsf{T} W_\perp^\dagger(s)\chi. \tag{7.32}$$

As stated in Remark 7.7, since $W_\perp(s) \equiv \mathcal{E}_\perp(s)W_\perp(s)\mathcal{E}_\perp^\mathsf{T}(s)$, its pseudoinverse $W_\perp^\dagger$ must in turn satisfy $W_\perp^\dagger(s) \equiv \mathcal{E}_\perp^\mathsf{T}(s)W_\perp^\dagger(s)\mathcal{E}_\perp(s)$. Indeed, it is a straightforward consequence of the properties of the pseudoinverse, e.g.,

$$W_\perp W_\perp^\dagger W_\perp = \mathcal{E}_\perp W_\perp \mathcal{E}_\perp^\mathsf{T} W_\perp^\dagger \mathcal{E}_\perp W_\perp \mathcal{E}_\perp^\mathsf{T} = W_\perp,$$

where we have omitted the s-argument for brevity. Hence (7.32) is strictly positive for all $\|\chi\| \neq 0$. In order to prove the statement, we therefore need to show that $V_\perp$ is strictly decreasing over each iteration of the cycle.

Let us begin by showing that $V_\perp$ is strictly decreasing in the continuous phase. If $u = K(s)\chi$ is taken as in the proposition, then by differentiating $V_\perp$ with respect to time, we obtain

$$\dot{V}_\perp = \chi^\mathsf{T}\left[\rho\frac{d}{ds}W_\perp^\dagger + \left(A_\perp + B_\perp Y_\perp W_\perp^\dagger\right)^\mathsf{T} W_\perp^\dagger + W_\perp^\dagger\left(A_\perp + B_\perp Y_\perp W_\perp^\dagger\right)\right]\chi. \tag{7.33}$$

Note now that the assumptions upon $W_\perp$ implies the relation $W_\perp W_\perp^\dagger \mathcal{E}_\perp \equiv \mathcal{E}_\perp$, from which, in turn,

$$(\mathbf{I}_n - W_\perp(s)W_\perp^\dagger(s))\mathcal{E}_\perp(s) = 0 \tag{7.34}$$

can easily be deduced. Using this, together with the fact that for any matrix $X \in \mathbb{R}^{n\times n}$ one has

$$\begin{aligned} W_\perp^\dagger X &= W_\perp^\dagger X + W_\perp^\dagger X W_\perp(\mathbf{I}_n - W_\perp^\dagger W_\perp)W_\perp^\dagger \\ &= W_\perp^\dagger(XW_\perp)W_\perp^\dagger + W_\perp^\dagger X(\mathbf{I}_n - W_\perp W_\perp^\dagger), \end{aligned}$$

we obtain the following relation: $W^\dagger(s)A_s(s)\mathcal{E}_\perp(s) = W^\dagger(s)(A(s)W(s))W^\dagger(s)$. Moreover, since [218, Thm. 4.3]

$$\dot{W}_\perp^\dagger = -W_\perp^\dagger \dot{W}_\perp W_\perp^\dagger + (W_\perp^\dagger)^2\dot{W}_\perp(\mathbf{I}_n - W_\perp W_\perp^\dagger) + (\mathbf{I}_n - W_\perp^\dagger W_\perp)\dot{W}_\perp(W_\perp^\dagger)^2,$$

we have that $\mathcal{E}_\perp^\mathsf{T}(s)\left[\frac{d}{ds}W_\perp^\dagger(s)\right]\mathcal{E}_\perp(s) = -W_\perp^\dagger(s)W_\perp'(s)W^\dagger(s)$. Using these relations, we can rewrite (7.33) as

$$\dot{V}_\perp = \chi^\mathsf{T} W_\perp^\dagger \left[-\rho W_\perp' + W_\perp A_s^\mathsf{T} + Y_\perp^\mathsf{T} B_s^\mathsf{T} + A_s W_\perp + B_s Y_\perp\right] W_\perp^\dagger \chi,$$

where we have omitted the s-arguments to save space. Using (7.29), we get

$$\dot{V} \leq -\lambda(s)\chi^\mathsf{T} W_\perp^\dagger(s)\,[W_\perp(s)]\,W_\perp^\dagger(s)\chi = -\lambda(s)V_\perp.$$

Thus for any $t \geq t_a$ such that $s(t) \leq s_b$ with $s(t_a) = s_a$, we have

$$V_\perp(t) \leq V_\perp(t_a)\exp\left\{-\int_{s_a}^{s(t)} \lambda(\tau)/\rho(\tau)d\tau\right\} \tag{7.35}$$

by the comparison principle [44, 169], implying that $V_\perp$ is strictly decreasing at an exponential rate during the continuous phase.

We will now prove that if (7.30) holds, then $V_\perp^{-,k+1} < V_\perp^{-,k}$ where $V_\perp^{-,k} \neq 0$ denotes the value of $V_\perp$ immediately after the k-th jump. If this holds, then both the boundedness of solutions and exponential attractivity of the origin $\chi = 0$ is necessarily guaranteed. To this end, let us begin by noting that

$$V_\perp^+ = (\chi^+)^\mathsf{T} W_\perp^\dagger(s_a)\chi^+ = (\chi^-)^\mathsf{T}\mathbf{J}_\perp^\mathsf{T} W_\perp^\dagger(s_a)\mathbf{J}_\perp\chi^-. \tag{7.36}$$

Without loss of generality, we will assume $s(t_a) = s_a$ such that $V_\perp^{-,0} = V_\perp(t_a)$. Thus immediately before the first jump one has $V_\perp^+ \leq \eta^{-1}V_\perp(t_a)$ by (7.35). As to ensure our aim of $V_\perp^- \leq (1-\iota)V(t_a)$ for some arbitrarily small $\iota > 0$, it is therefore by (7.36) sufficient that

$$W_\perp^\dagger(s_b)(\eta - \mu) - \mathbf{J}_\perp^\mathsf{T} W_\perp^\dagger(s_a)\mathbf{J}_\perp \succeq 0$$

where $\mu = \eta\iota$. Multiplying from both sides by $W_\perp(s_b)$, one obtains

$$W_\perp(s_b)(\eta - \mu) - W_\perp(s_b)\mathbf{J}_\perp^\mathsf{T} W_\perp^\dagger(s_a)\mathbf{J}_\perp W_\perp(s_b) \succeq 0. \tag{7.37}$$

Note now that $(\mathbf{I}_n - W_\perp(s_a)W_\perp^\dagger(s_a))\mathbf{J}_\perp = 0$ due to (7.34) for $\mathbf{J}_\perp$ taken according to (7.10). Hence, by the generalized Schur complement (see, e.g., [181, Th. 1.20]), the above matrix inequality holds if and only if (7.30) holds. This concludes the proof. □

7.3 Orbit generation for underactuated hybrid mechanical systems

In this section, we will consider the problem of planning hybrid cycles of underactuated mechanical systems whose states may undergo instantaneous (discrete) jumps if they enter a certain region of state space. More specifically, we will propose a method which allows for an effective numerical implementation of the theoretical procedure proposed in [198].

The continuous-time dynamics of the systems we consider are given by the Euler-Lagrange equations previously considered in Section 5.2, namely

$$\mathbf{M}(q)\ddot{q} + \mathbf{C}(q,\dot{q})\dot{q} + \mathbf{G}(q) = \mathbf{B}_u u. \tag{7.38}$$

Here $q, \dot{q} \in \mathbb{R}^{n_q}$ are the vectors of generalized coordinates and -velocities, while $u \in \mathbb{R}^m$ is the vector of the $m < n_q$ independent controls. Denoting by $x(t) := \mathrm{col}\big(q(t), \dot{q}(t)\big) \in \mathbb{R}^n$ the state vector at time $t \in \mathbb{R}_{\geq 0}$, then as with (7.1), the system is assumed to undergo a discrete jump governed by $\mathbf{J} : \mathbf{\Sigma}^- \to \mathbf{\Sigma}^+$ when the states enter $\mathbf{\Sigma}^- \subset \mathbb{R}^n$, with the switching surfaces of the form as in (7.2).

7.3.1 A preliminary trajectory optimization problem

The problem we will now consider is that of finding a hybrid cycle of the system (7.38), corresponding to an s-parameterization as of Definition 7.1. To this end, we begin by stating the following *trajectory optimization problem* (TCP) in Lagrange form [17, 21]:

Problem 7.8 (Trajectory optimization problem)**.** *Given a $\mathcal{C}^2$-smooth function $\mathfrak{O} : \mathbb{R}^{n_q} \times \mathbb{R}^{n_q} \times \mathbb{R}^n \to \mathbb{R}_{\geq 0}$, minimize*

$$\int_0^T \mathfrak{O}\left(q_\star(\tau), \dot{q}_\star(\tau), u_\star(\tau)\right) d\tau \tag{7.39}$$

with respect to $\big(x_a, x_b, T, x_\star(t), u_\star(t)\big)$ where $x_\star(t) = \mathrm{col}\big(q_\star(t), \dot{q}_\star(t)\big)$, subject to the following: $(x(t), u(t)) = (x_\star(t), u_\star(t))$ satisfying the system dynamics (7.38) *for all $t \in [0, T]$; the boundary conditions*[5]

$$x_\star(0) = x_a \in \mathbf{\Sigma}_+, \tag{7.40a}$$

$$x_\star(T) = x_b \in \mathbf{\Sigma}_-, \tag{7.40b}$$

$$x_a = \mathbf{J}\big(x_b\big); \tag{7.40c}$$

[5]For certain tasks one might have that (at least parts of) x_a and x_b are specified in advance.

as well as any other (well-behaved) constraints, represented by

$$\mathfrak{H}\big(T, q_\star(t), \dot{q}_\star(t), u_\star(t)\big) \leq 0_{r\times 1} \tag{7.41}$$

for some vector-valued function $\mathfrak{H} : \mathbb{R}_{\geq 0} \times \mathbb{R}^{n_q} \times \mathbb{R}^{n_q} \times \mathbb{R}^m \to \mathbb{R}^r$. □

There exist a variety of different ways of solving this problem by transcribing it into a nonlinear programming problem, including (multiple-) shooting-based methods [17] and collocation-based methods [18, 20, 21]. Regardless of the method which is used to find an approximate solution to this problem, the found solution will evidently correspond to an s-parameterization of a hybrid periodic orbit of (7.38) as by Definition 7.1 if $\|\dot{x}(t)\| \neq 0$ for all $t \in [0, T]$.

7.3.2 Synchronization function-based orbit optimization

Rather than a time-parameterized solution to the above trajectory optimization problem, we are looking for a continuously differentiable s-parameterized solution in the following, more general form:

$$x_s(s) = \mathrm{col}\,\big(\Phi(s), \Phi'(s)\rho(s)\big)\big).$$

For this purpose, we will again utilize the synchronization function–based approach and corresponding results stated in Section 5.3. Our main aim will be to formulate the orbit-generation problem in such a way that it facilities the (effective) use of numerical optimization in order to find an approximate s-parameterized orbit.

To this end, let $\Phi(s) = \Phi(s; \mathbf{c}) : \mathcal{S} \to \mathbb{R}^n_q$ denote a smooth vector of synchronization functions, each of which consisting of a finite numbers basis functions. The coefficients of these basis functions are all stacked together into the coefficient vector $\mathbf{c} \in \mathbb{R}^l$, which will be among the decisions variables in the resulting optimization problem.

Recall from Section 5.3.1 that for $x_s(\cdot)$ to correspond to an s-parameterized orbit of (7.38) over the fixed interval $\mathcal{S} = [s_a, s_b]$, then

$$\mathfrak{A}(s)\rho'(s)\rho(s) + \mathfrak{B}(s)\rho^2(s) + \mathfrak{G}(s) = \mathbf{B}_u u_s(s) \tag{5.11}$$

must hold for all $s \in \mathcal{S}$. Further recall from Lemma 5.3 that given knowledge of the pair (Φ, ρ), the $\mathcal{C}^1$ function $u_s : \mathcal{S} \to \mathbb{R}^m$, corresponding to the nominal control input on the orbit, can be computed from

$$u_s(s) = \mathbf{B}_u^\dagger \left[\mathfrak{A}(s)\rho'(s)\rho(s) + \mathfrak{B}(s)\rho^2(s) + \mathfrak{G}(s)\right]$$

where $\mathbf{B}_u^\dagger \mathbf{B}_u = \mathbf{I}_m$. Thus, for a specific choice of the coefficient vector $\mathbf{c}$, we know that the continuous-time dynamics (7.38) are satisfied if we can find a function $\rho : \mathcal{S} \to \mathbb{R}_{>0}$ which simultaneously satisfies the following m equations (see (5.18)) for all $s \in \mathcal{S}$:

$$\alpha_i(s)\rho'(s)\rho(s) + \beta_i(s)\rho^2(s) + \gamma_i(s) = 0, \quad i = 1, 2, \ldots, m.$$

In order to avoid having to handle singular points in the numerical search, we will assume the following in the sequel:

Assumption 7.9. $\alpha_1(s) \neq 0$ for all $s \in \mathcal{S}$.

By Lemma 5.9, we therefore have the following: If for some $a, b \in \mathbb{R}_{\geq 0}$, the equality

$$\Psi_1(s_a, s_b)\alpha_1^2(s_b)b^2 - \alpha_1^2(s_a)a^2 + 2\int_{s_a}^{s_b} \Psi_1(s_a, \tau)\alpha_1(\tau)\gamma_1(\tau)d\tau \equiv 0 \quad (7.42)$$

holds, with $\Psi_i(s_a, s_b) = \exp\left\{2\int_{s_a}^{s_b}\big(\delta_i(\tau)/\alpha_i(\tau)\big)d\tau\right\}$, then there exists a function $\rho : \mathcal{S} \to \mathbb{R}_{\geq 0}$, which is $\mathcal{C}^1$ almost everywhere, satisfies

$$\alpha_i(s)\rho'(s)\rho(s) + \beta_i(s)\rho^2(s) + \gamma_i(s) = 0,$$

for all $s \in \mathcal{S} := [s_a, s_b]$, as well as $\rho(s_a) = a$ and $\rho(s_b) = b$. If, moreover, $\rho(s) > 0$ for all $s \in \mathcal{S}$, then it is smooth on this interval. Supposing

$$\left[\alpha_1(s)\beta_i(s) - \alpha_i(s)\beta_1(s)\right]\rho^2(s) + \alpha_1(s)\gamma_i(s) - \alpha_i(s)\gamma_1(s) = 0, \quad i = 2, \ldots, m, \quad (7.43)$$

also hold for all $s \in \mathcal{S}$, then $x_s(s)$ corresponds to an s-parameterized orbit of the continuous-time dynamics, which is driven by the corresponding nominal control input function:

$$u_s(s) = \mathbf{B}_u^{\dagger}\left[\left(\mathfrak{B}(s)\alpha_1(s) - \beta_1(s)\mathfrak{A}(s)\right)\rho^2(s) + \alpha_1(s)\mathfrak{G}(s) - \mathfrak{A}(s)\gamma_1(s)\right]/\alpha_1(s). \quad (7.44)$$

The key idea of the motion planning scheme proposed in [198] when applied to the approach we here present, is that one only requires (7.42) and (7.43) to hold, with $u_s(\cdot)$ found from (7.44), rather than checking (5.11) directly. Our aim will now be structure the motion planning problem proposed [198] in such a away that it can be effectively solved using numerical optimization. For simplicity's sake, we will to this end also make the following additional assumption:

Assumption 7.10. $\delta_1(s) \equiv 0$ for all $s \in \mathcal{S}$.

If Assumption 7.10 holds, then $\Psi_1(\cdot) \equiv 1$. Recall from Lemma 5.6 that this allows us to write (7.42) in terms of $\rho(\cdot)$ as

$$\alpha_1^2(s)\rho^2(s) - \alpha_1^2(s_a)\rho^2(s_a) + 2\int_{s_a}^{s} \alpha_1(\tau)\gamma_1(\tau)d\tau = 0, \tag{7.45}$$

thus avoiding the nested integrals appearing in regard to the integration of $\Psi(\cdot)$. As we have previously mentioned in Section 5.3.2, this property is not uncommon; for instance, it is always satisfied whenever a passive (unactuated) degree of freedom acts as a pivot in an open kinematic chain (see e.g. the arguments in [99]), which is the case for bipedal walkers with passive ankles (cf. Sec. 7.4). Thus, to best clarify the method presented, we will assume this property to hold for $i = 1$ hereinafter. It is, however, important to note that this property is not strictly necessary for the method we will propose, although it certainly simplifies both the overall procedure and its numerical evaluation, possibly also increasing the speed and convergence of the resulting numerical search.

Restating the trajectory optimization problem

By using $x_s(s) = \mathrm{col}\big(\Phi(s), \Phi'(s)\rho(s)\big)$ with $\Phi(s) = \Phi(s; \mathbf{c})$, we may reformulate the trajectory optimization problem (TCP) stated in Problem 7.8 as instead being a search for the coefficients $\mathbf{c}$ and the function $\rho(\cdot)$. To this end, let us fix the interval $\mathcal{S} = [s_a, s_b] \subset \mathbb{R}$, $s_a < s_b$. Similarly, let us assume that the basis functions of which the rows of $\Phi(\cdot)$ are built have been fixed, whereas their coefficients, which we recall have been lumped into $\mathbf{c} \in \mathbb{R}^l$, will be decision variables in the numerical search. Thus, under the assumption that $\dot{s}(t) = \rho(s(t)) > 0$, we may replace $x_\star(t)$ and $u_\star(t)$ in Problem 7.8 with $x_s(s(t))$ and $u_s(s(t))$, respectively. The resulting reformulation of the TCP as an "orbit optimization problem" can then be stated:

Problem 7.11. *Given the functions $\mathfrak{O}(\cdot)$ and $\mathfrak{H}(\cdot)$ as in Problem 7.8, minimize, with respect to $\big(x_a, x_b, \mathbf{c}, \rho(s)\big)$, the objective function*

$$\int_{s_a}^{s_b} \frac{1}{\rho(\tau)} \mathfrak{O}\left(\Phi(\tau), \Phi'(\tau)\rho(\tau), u_s(\tau)\right) d\tau, \tag{7.46}$$

with $u_s(s)$ found from (7.44), subject to the following: (7.45), (7.43), and $\rho(s) > 0$ for all $s \in \mathcal{S}$; the boundary conditions

$$x_s(s_a) = x_a \in \mathbf{\Sigma}_+, \quad x_s(s_b) = x_b \in \mathbf{\Sigma}_-, \quad \text{and} \quad x_a = \mathbf{J}\big(x_b\big); \tag{7.47a}$$

as well as

$$\mathfrak{H}\big(T_s, \Phi(s), \Phi'(s)\rho(s), u_s(s)\big) \leq 0_{r\times 1} \tag{7.48}$$

where $T_s = \int_{s_a}^{s_b} \big(1/\rho(\tau)\big)d\tau$. □

Transcribing the reformulated TCP into a nonlinear program

Since the objective (7.46) is evaluated over a constant interval, it is natural to discretize the problem using some numerical quadrature rule, such as, for example, a Gauss-Legendre quadrature [195]. Thus, for some quadrature of order ν, we denote the set of ordered quadrature nodes lying in $\mathcal{S}$ by $\{\hat{s}_j\}_{j=1}^{\nu}$, while $\{w_j\}_{j=1}^{\nu}$ denotes the set of the corresponding quadrature weights. If $\hat{s}_1 \neq s_a$ and/or $\hat{s}_\nu \neq s_b$, then we denote $\hat{s}_0 = s_a$ and $\hat{s}_{\nu+1} = s_b$ in order to also include the end points. We also introduce a set of $\nu+2$ new decision variables, grouped into $\mathbf{R} := \{\varrho_j\}_{j=0}^{\nu+1}$, which may be interpreted as the values of the function $\rho(\cdot)$ evaluated at certain discrete points:

$$\varrho_0 = \rho(s_a), \quad \varrho_j = \rho(\hat{s}_j) \quad \text{for} \quad j = 1, 2, \dots, \nu, \quad \varrho_{\nu+1} = \rho(s_b). \tag{7.49}$$

Let $\bar{u}_s^j$ correspond to (7.44) computed at $\hat{s}_j$ using $\rho(\hat{s}_j) = \varrho_j$, that is

$$\bar{u}_s^j = \mathbf{B}_u^\dagger \left[\frac{\left(\mathfrak{B}(\hat{s}_j)\alpha_1(\hat{s}_j) - \beta_1(\hat{s}_j)\mathfrak{A}(\hat{s}_j)\right)\varrho_j^2 + \alpha_1(\hat{s}_j)\mathfrak{G}(\hat{s}_j) - \mathfrak{A}(\hat{s}_j)\gamma_1(\hat{s}_j)}{\alpha_1(\hat{s}_j)} \right].$$

Using the chosen quadrature rule, the following (discretized) approximation of the objective function (7.46) can then be obtained:

$$\mu \sum_{j=1}^{\nu} w_j \frac{1}{\varrho_j} \mathfrak{O}\left(\Phi(\hat{s}_j), \Phi'(\hat{s}_j)\varrho_j, \bar{u}_s^j\right). \tag{7.50}$$

Here $\mu \in \mathbb{R}$ is some quadrature-dependent scaling factor, e.g. $\mu = (s_b - s_a)/2$ for a Gaussian quadrature.

In regard to the constraints, we first note that, since $\rho(\cdot)$ is required to be a strictly monotonically increasing function in s, the following inequality constraints must be added to the numerical search:

$$\varrho_j \geq 0, \quad j = 0, \dots, \nu+1. \tag{7.51}$$

Note also that it is here possible to replace the zero on the right-hand side with a small, positive number as to ensure $\rho(\hat{s}_j) > 0$. However, this can easily be avoided by simply initializing all the decision variables ϱ_j with a value different from zero. Indeed, $\varrho_j \equiv 0$ then cannot occur if the remaining decision variables are initialized properly due to ϱ_j appearing in the denominator in (7.50). Similar arguments can also be applied as to ensure that Assumption 7.9 holds by adding the inequality constraint

$$(-1)^h \alpha(\hat{s}_j) \geq 0, \quad j = 0, \dots, \nu+1, \tag{7.52}$$

for a fixed $h \in \{0,1\}$ chosen prior to the search.

The boundary constraints (7.47) are taken with $x_a = \mathbf{J}(x_b)$ and

$$\mathrm{col}(\Phi(s_a), \Phi'(s_a)\varrho_0) = x_a \in \mathbf{\Sigma}_+, \quad \mathrm{col}(\Phi(s_b), \Phi'(s_b)\varrho_{\nu+1}) = x_b \in \mathbf{\Sigma}_-, \tag{7.53}$$

Regarding the dynamical constraints, for each $i \in \{2,\dots,m\}$ and $j \in \{0,\dots,\nu+1\}$, one can add

$$\left|[\alpha_1(\hat{s}_j)\beta_i(\hat{s}_j) - \alpha_j(\hat{s}_j)\beta_1(\hat{s}_j)]\,\varrho_j^2 + \alpha_1(\hat{s}_j)\gamma_i(\hat{s}_j) - \alpha_j(\hat{s}_j)\gamma_1(\hat{s}_j)\}\right| \leq \epsilon \tag{7.54}$$

for some $\epsilon \geq 0$ taken sufficiently small, as to account for (7.43). Furthermore, the introduction of the new decision variables also allows one to divide the integral dynamics constraint (7.45) in a multiple-shooting fashion into $\nu+1$ constraints of the form:

$$\alpha_a(\hat{s}_j)^2\varrho_j^2 - \alpha_a(\hat{s}_{j-1})^2\varrho_{j-1}^2 + 2\tilde{\mu}\Delta\hat{s}_j\sum_{k=1}^{\nu}\tilde{w}_k\alpha(\tilde{s}_k)\gamma(\tilde{s}_k) = 0 \tag{7.55}$$

for all $j \in \{1,2,\dots,\nu+1\}$. Here $\Delta\hat{s}_j := \hat{s}_j - \hat{s}_{j-1}$, while the integral in (7.45) is approximated using some quadrature rule of order $\tilde{\nu}$ with node-weight pairing $\{(\tilde{s}_k, \tilde{w}_k)\}_{k=1}^{\nu}$ and scaling factor $\tilde{\mu}$.

Lastly, the additional constraints (7.48) (assuming they do not contain any integral constraints) are evaluated at each node, i.e.,

$$\mathfrak{H}\big(T_s, \Phi(\hat{s}_j), \Phi'(\hat{s}_j)\varrho_j, \bar{u}_s^j\big) \leq 0_{r\times 1}, \quad j = 0,\dots,\nu+1, \tag{7.56}$$

where $T_s = \mu\sum_{j=1}^{\nu} w_j\big(1/\varrho_j\big)$.

The resulting nonlinear program can then be stated as follows:

Nonlinear minimization problem: Minimize, with respect to the decision variables $\big(x_a, x_b, \mathbf{c}, \mathbf{R}\big)$, the objective function (7.50) subject to the constraints (7.51)-(7.56).

Note that the particular structure of this nonlinear optimization problem makes the gradients of the constraints and the objective function, as well as the Hessian of the corresponding Lagrangian function, in terms of the decision variables easily attainable, although we omit the explicit expressions due to their length. Note also that both the Hessian of the Lagrangian and the gradients of the constraints will result in quite sparse matrices in general, with the level of sparsity generally depending on the choice of synchronization functions.

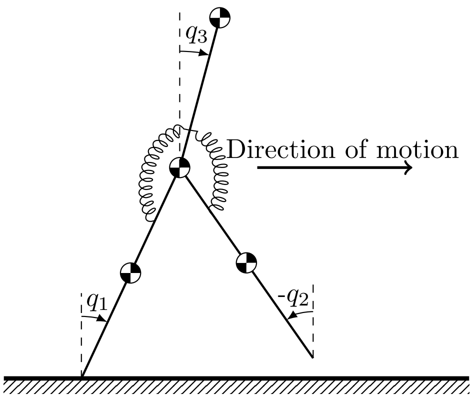

Figure 7.3: Schematic of the three-link biped system.

7.4 Example: Three-link biped with one actuator

Since the discovery by McGeer [219] that a simple bipedal mechanism situated on an inclined slope and powered only by gravity could exhibit stable walking as a natural mode, there has been a large body of research conducted in regard to dynamic walking of bipedal robots; see, e.g., [1, 2, 104, 136, 213, 220], to name but a few. Since the equations governing the dynamics of such systems often can be accurately represented as a underactuated mechanical systems with hybrid dynamics, both the orbit-generation scheme we proposed in Section 7.3, as well as the orbital stabilization approach based on Theorem 7.2, are well suited for such systems.

7.4.1 Problem formulation and system description

Consider the following task: Create a stable, symmetric gait of a three-link biped robot with two degrees of underactuation. The simple robot structure, shown in Figure 7.3, is a commonly used testbed in regard to hybrid motion planning and control; see, e.g., [99, 135, 216]. It consists of three links connected together through a central hip joint, with two linear springs attached between its torso and each of its legs.

For simplicity's sake, we will assume that the initial, desired configuration $q^{\star}(0)$ is given, such that the final configuration $q^{\star}(T)$, which should occur after some finite amount of time $T > 0$, can be found directly from the assumption of a symmetric gait:

$$q_2^{\star}(T) = q_1^{\star}(0), \quad q_1^{\star}(T) = q_2^{\star}(0), \quad q_3^{\star}(T) = q_3^{\star}(0). \tag{7.57}$$

Here $q_1^{\star}(0)$ can be computed from the desired step length L_{step} by $q_1^{\star}(0) = -\arcsin\left(L_{step}/(2r)\right)$ with r denoting the length of the stance leg.

Table 7.1: Parameters of the three-link biped system [216].

Parameters	**Legs**	**Hip**	**Torso**
Mass [kg]	$m = 5$	$M_h = 15$	$M_t = 10$
CoM [m]	$r/2 = 0.5$	$r = 1$	$l = 1$
Length [m]	$r = 1$		
Gravitational acceleration		$g = 9.81\,\mathrm{m\,s^{-2}}$	
Spring stiffness		κ [$\mathrm{N\,m^{-1}}$], to be found	

The matrix-valued functions $\mathbf{M}(\cdot)$, $\mathbf{C}(\cdot)$ and $\mathbf{G}(\cdot)$ corresponding to the system's continuous-time dynamics (7.38) are taken as in [216], which in turn are identical to those in [135] with the addition of linear springs. The velocity impact map is taken from [135] and is of the form $\dot{q}_+ = \mathbf{J}_{\dot{q}}(q_-)\dot{q}_-$, such that the discrete jump map is given by $\mathbf{J}(x) = \operatorname{diag}(\mathbf{J}_q q, \mathbf{J}_{\dot{q}}(q)\dot{q})$, with $\mathbf{J}_q$ corresponding to relabeling in (7.57) written compactly as $q_\star(0) = \mathbf{J}_q q_\star(T)$. The physical parameters of the system are taken from [135] (see Table 7.1), with the spring stiffness K left as a possible additional decision variable in our search.

7.4.2 Results from numerical optimization

We considered the task of finding symmetric gaits of length $L_{step} = 0.5\,\mathrm{m}$ and with initial lean angle $q_3^\star(0) = 0.2\,\mathrm{rad}$ using the nonlinear optimization procedure outlined at the end of Section 7.3.2.[6] As an objective function to minimize, we considered

$$\frac{1}{g m_T L_{step}} \int_0^T \sum_{i=1}^m \left|(\mathbf{B}_u^i u_i)^\mathsf{T} \dot{q}\right| dt \tag{7.58}$$

corresponding to the energetic cost of transport (CoT) of the system over one step. Here m_T denotes the total mass of the system and $\mathbf{B}_u^i$ denotes the i-th column of $\mathbf{B}_u$. Note that this objective function is not everywhere continuously differentiable due to the absolute value function, such that its gradient is not well defined whenever $\mathbf{B}_u^i u_i = 0$. While this can be resolved using, e.g., slack variables [21], we found that, even without any such modifications, the performance of the numerical search[7] was comparable to that of the smooth objective $\sum u_i^2$ and led to a lower CoT.

[6] We used the squares of the variables in (7.49) as decision variables in our search.

[7] The optimization problems were solved using the *fmincon* command in MATLAB running the interior-point algorithm solver on a 64bit operating system with an Intel Core I7 2.8 GHz processor. Gradients of the constraints and objective were provided to the solver, whilst the Hessian of the Lagrangian was estimated using the BFGS algorithm.

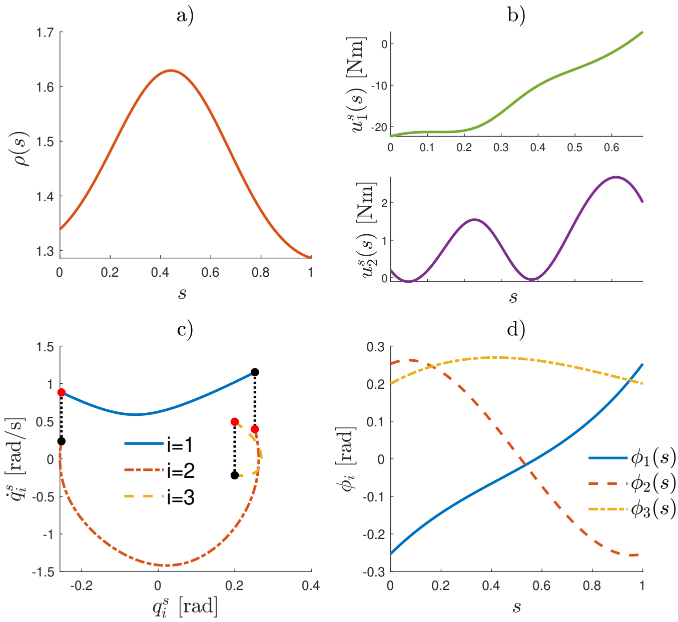

Figure 7.4: Gait found with $\mathfrak{b} = 3$ and two actuators: a) solution of the reduced dynamics; b) control inputs; c) phase portraits of the system coordinates (initial points in red); and c) synchronization functions

We used Gauss–Legendre quadratures [195] for computing the objective (7.50) and integral dynamics constraints (7.55), with the order of the quadratures taken as $\nu = 50$ and $\tilde{\nu} = 5$, respectively. We took $\mathcal{S} = [0, 1]$, with the synchronization functions given by Bézier polynomials of order $\mathfrak{b}$, whose first and last parameters are taken according to (7.57), with the remaining initialized as zero. Since none of the nodes of a Guass–Lequadre quadrature lies on the integration boundaries, the total number of decision variables, $\{\mathbf{c}, \mathbf{R}, K\}$, thus equaled $3\mathfrak{b} + \nu$. Before the numerical search, all the decision variables contained in $\mathbf{R}$ were initialized with a value of one.

One degree of underactuation

We first considered the system with two actuators, $u = \mathrm{col}(u_1, u_2)$, and

$$\mathbf{B}_u = \begin{bmatrix} -1 & 0 & 1 \\ 0 & -1 & 1 \end{bmatrix}^{\mathsf{T}}. \tag{7.59}$$

In order to compare to [99, 135], we took $\mathfrak{b} = 3$, as well as set $K = 0$ and omitted it as an decision variable. The search converged after 119 iterations

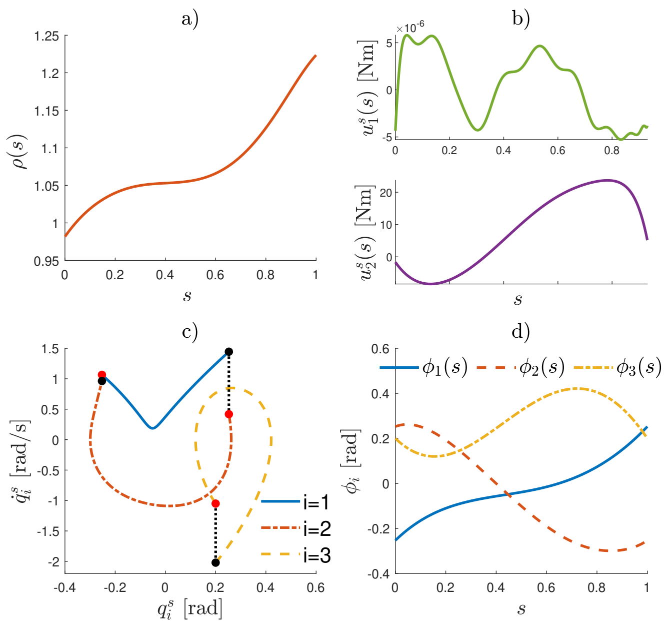

Figure 7.5: Gait found with $\mathfrak{b} = 9$ and one actuator: a) solution of the reduced dynamics; b) control inputs; c) phase portraits of the system coordinates (initial points in red); and c) synchronization functions.

and took approximately 18.5 s on average. The resulting gait, having a CoT of approximately $3.16 \cdot 10^{-2}$, can be seen in Figure 7.4 .

Two degrees of underactuation

Next, we considered the system with only a single actuator, here denoted by u_2, with the new input mapping matrix taken as $\mathbf{B}_u = \mathrm{col}(1, -1, 0)$. In (7.54) we took $\epsilon = 10^{-5}$. Moreover, we added K as an optimization variable with initial value $20\,\mathrm{N\,m^{-1}}$, as well as took the order of the Bézier polynomials as $\mathfrak{b} = 9$. The gait found from the solving the resulting optimization problem is shown in Figure 7.5. It had a CoT of approximately $7.19 \cdot 10^{-2}$, with the search converging after 954 iterations and taking approximately 74 s on average. Denoting by $u_1^s(s)$ the left-hand side of (7.43), one can also see from Plot b) that $|u_1^s(s)| < \epsilon$. Thus the found solution corresponds to an almost feasible gait, in which $u_1^s(\cdot)$ can be seen as a small perturbation that must be handled by the feedback controller.

7.4.3 Orbital stabilization and numerical simulation

We considered the task of designing a control law for the the found gait shown in Figure 7.5 using Theorem 7.2.

Projection operator: As $\phi_1(s) > 0$ for all $s \in [0,1]$, we took the projection operator as

$$p(x) = \arg\min_{s\in\mathcal{S}} \left(q_1 - \Phi_1(s)\right)^2. \tag{7.60}$$

The tubular neighborhood of the gait's orbit corresponding to this projection operator is therefore $\mathcal{T} = \{x \in \mathbb{R}^n : \ |q_1| < |\arcsin\left(L_{step}/(2r)\right)|\}$, within which

$$Dp = \frac{1}{\phi_1'(p)}[1, \mathbf{0}_{1\times n_q}], \quad D^2p = -\frac{\phi_1''(p)}{(\phi_1'(p))^3}\,\mathrm{diag}(1, \mathbf{0}_{1\times n_q}).$$

Control design: In order to design an orbitally stabilizing feedback for this gait, we utilized the differential LMI approach corresponding to Theorem 7.2. In order to facilitate the search for a solution to Theorem 7.2 using convex optimization, we needed to discretize the differential LMI (7.12) in some way. To this end, we again used the approach considered in Section 6.4.3 and represented each element of $W(s)$ and $Y(s)$ as Beziér polynomials of order $\mathfrak{r} = 20$:

$$W(s) = \sum_{i=0}^{\mathfrak{r}} \mathfrak{B}_{i,\mathfrak{r}}(s)W_i \quad \text{and} \quad Y(s) = \sum_{i=0}^{\mathfrak{r}} \mathfrak{B}_{i,\mathfrak{r}}(s)Y_i.$$

Here $\mathfrak{B}_{i,\mathfrak{r}}(s)$ are the Bernstein basis polynomials of degree $\mathfrak{r}$, while $W_i \in \mathbb{M}^6_{\succeq 0}$ and $Y_i \in \mathbb{R}^{1\times 6}$ were the coefficients we were looking to find. To restrict the search space, the the following constraints were added to the search:

$$10^{-3}\mathbf{I}_6 \preceq W_i \preceq 10^5\mathbf{I}_6 \quad \text{and} \quad -\mathbb{1}_{1\times 6} \leq \ Y_i \leq \mathbb{1}_{1\times 6}.$$

The differential LMI (7.12), with $\lambda(s) = (10^{-2} + s(1-s))$, evaluated at 200 evenly spaced points over $[0,1]$ was taken as LMIs in the search, while $\mu = 10^{-4}$ was used in the jump LMI (7.13). The resulting semidefinite programming problem was then solved using the YALMIP toolbox for MATLAB [200] together with the SDPT3 solver [201].

Simulation results: Denoting by $y_i = q_i - \phi_i(p)$ and $z_i = \dot{q}_i - \phi_i'(p)\rho(p)$, the response of the closed-loop system when starting with the initial conditions

$$x_a = x_s(s_a) + \mathrm{col}(0.1, -0.1, 0.1, -0.1, 0.0, -0.2) \tag{7.61}$$

is shown in Figure 7.6. The sensitivity of the designed control law with respect to perturbations away from the hybrid cycle is clearly seen by the large spike in the control input signal at the end of the first step, as shown in Figure 7.6(a).

Figure 7.7 shows the closed-loop system's response for the initial conditions

$$x_a = x_s(s_a) + \mathrm{col}(-0.2, 0.1, 0.1, 0.4, 0.4, 0.5). \tag{7.62}$$

Notice that these initial conditions lie outside of the tubular neighborhood-part, given by $\mathcal{T} = \{x \in \mathbb{R}^n : \ |q_1| < |\arcsin{(L_{step}/(2r))}|\}$, of the domain of the projection operator (7.60). The resulting switch which occurs at approximately $t = 0.3\,\mathrm{s}$ when the states enter into $\mathcal{T}$ is clearly visible in Figure 7.6(a).

To test the possibility of limiting the magnitude of the applied control signal when perturbed away from the hybrid cycle, we also simulated the system with a control input signal which saturated at certain bounds. Remarkably, even when saturating u at $\pm 30\,\mathrm{N\,m}$, the control law is still stabilizing when initializing the system at both (7.61) and (7.62). The response for the initial conditions (7.62) is shown in Figure 7.8. It is clear that, even though the control law does stabilize the cycle also with saturation, the convergence is slower than without saturation (see Fig. 7.7), and leads to a significantly different response.

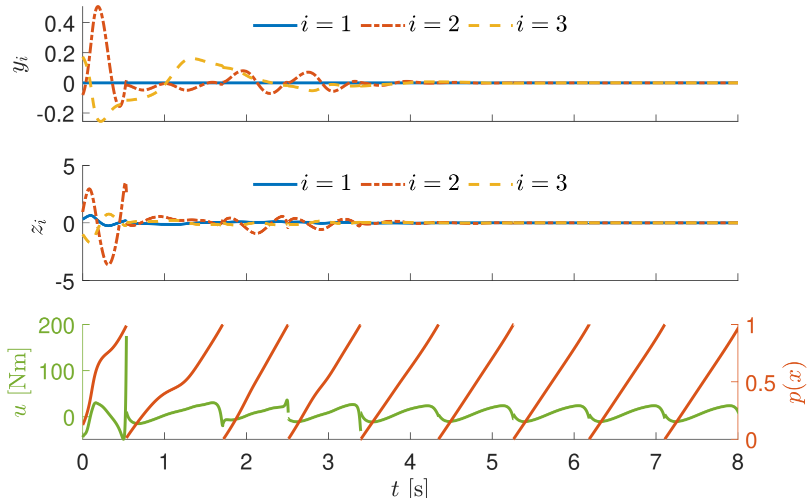

(a) Evolution of the transverse coordinates, the control input and the projection operator.

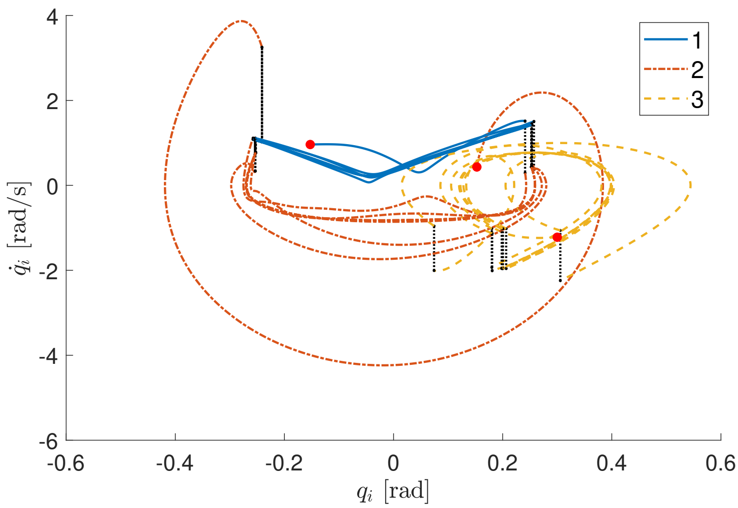

(b) Link angles plotted against their velocities. Initial conditions are highlighted in red.

Figure 7.6: from simulating the closed-loop system with perturbed initial conditions (7.61) and a single actuator.

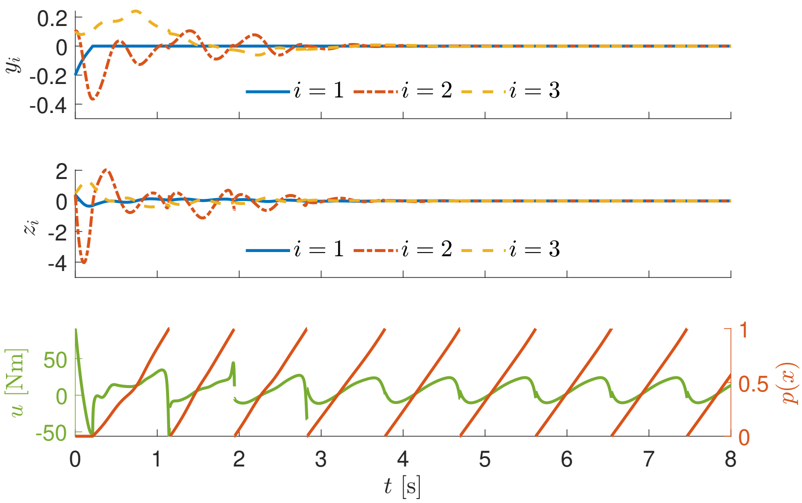

(a) Evolution of the transverse coordinates, the control input and the projection operator.

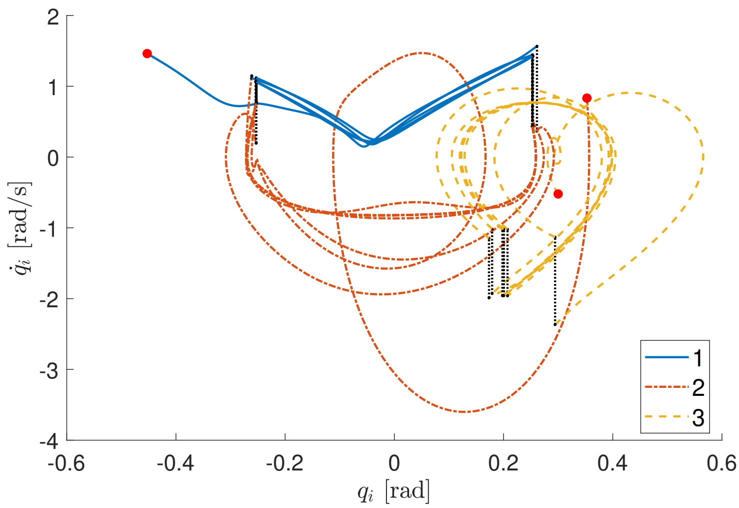

(b) Link angles plotted against their velocities. Initial conditions are highlighted in red.

Figure 7.7: from simulating the closed-loop system with perturbed initial conditions (7.62) and a single actuator.

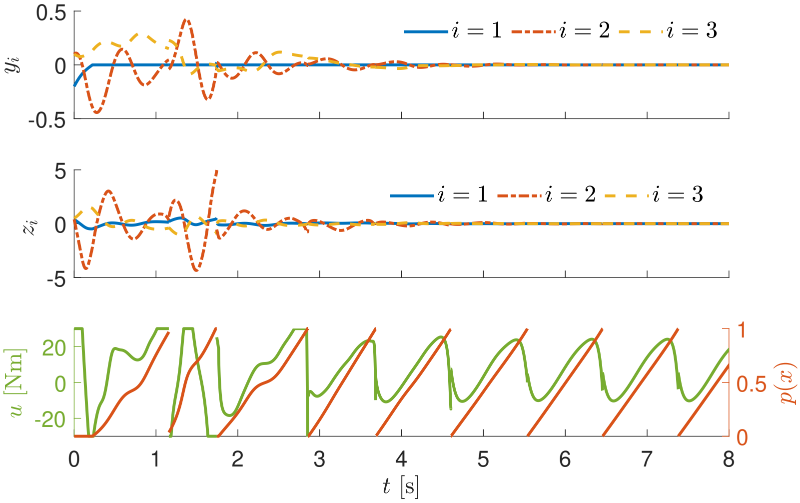

(a) Evolution of the transverse coordinates, the control input and the projection operator.

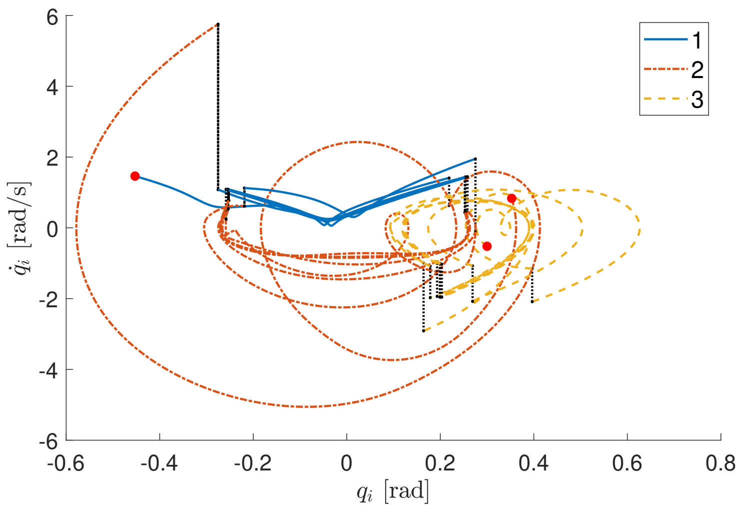

(b) Link angles plotted against their velocities. Initial conditions are highlighted in red.

Figure 7.8: Results from simulating the closed-loop system with perturbed initial conditions (7.62) and a single actuator saturated at $\pm 30\,\mathrm{N\,m}$.

Chapter 8

Robust Orbital Stabilization via Sliding Mode Control

In this chapter, we present a method that allows one to add a robustifying feedback extension to an existing orbitally stabilizing feedback for a trivial or periodic orbit utilizing the sliding-mode control (SMC) methodology.

8.1 Introduction

Motivational example

Suppose we are interested in stabilizing the origin of the system

$$\dot{y} = h(y) + B\left(u + \Delta(y,t)\right), \quad y \in \mathbb{R}^n, \quad u \in \mathbb{R}^m.$$

Here $h : \mathbb{R}^n \to \mathbb{R}^n$ is $\mathcal{C}^2$ and satisfies $\|h(0)\| = 0$; $B \in \mathbb{R}^{n\times m}$ has full rank; and $\Delta(\cdot) \in \mathbb{R}^m$ is some unknown perturbation which is piecewise continuous in both its arguments, as well as everywhere upper bounded by a known constant $\Delta_M > 0$. Further suppose a constant matrix $K \in \mathbb{R}^{m\times n}$ is known such that all the eigenvalues of $H^{cl} := Dh(0) + BK$ have strictly negative real parts; that is, the control law $u = k(y) := Ky$ would (locally) exponentially stabilize the origin if there were no perturbations.

Since the perturbation Δ is unknown, it cannot be directly canceled by feedback. Moreover, since it might be non-zero even at the origin, a continuous static state-feedback cannot exponentially stabilize the origin of the perturbed system in general. Thus, we instead aim to utilize our knowledge of the matrix K to design a static *discontinuous* control law following the sliding mode control (SMC) methodology [60, 62, 63], with its well-known insensitivity to certain matched perturbations. Specifically, we are looking to find a smooth, vector-valued *switching function* $\sigma : \mathbb{R}^n \to \mathbb{R}^m$, $\sigma(0) = 0$, with the property that the system's states converge to the origin at an exponential rate if they are confined to the *sliding manifold/surface*, defined by $\Sigma = \{y \in \mathbb{R}^n : \ \sigma(y) = \mathbf{0}_{m\times 1}\}$. Yet, this immediately raises the question: How to construct such a switching function?

The concept of equivalent control

In order to answer the above question, we need to somehow determine what the solutions of the closed-loop system are when we have confined the system's state to the sliding manifold using a discontinuous controller. To this end, we can use the concept of *equivalent control* introduced by Utkin [60, 62, 112]. Specifically, we can study the solutions in the *ideal sliding mode* on Σ by setting $\dot{\sigma} = \mathbf{0}_{m\times 1}$ and solving for the equivalent control $u = u_{eq}$. Inserting the found u_{eq} back into (8.18), one can analyze the system's behavior when confined to the sliding manifold (8.22). While the equivalent control which is "experienced" by the system will not in general be equal to the actual discontinuous control input which is applied to the system, it may intuitively be considered as the low-frequency component of the applied signal which keeps the states on Σ despite the matched perturbations.

It thus follows that if we can construct a switching function $\sigma(\cdot)$ such that the equivalent control in the ideal sliding mode on Σ is

$$u_{eq} = Ky - \Delta + O(\|y\|^2),$$

then the origin is locally exponentially stable (in the sliding mode) as desired.

We demonstrate next how one might construct such a switching function if the Jacobian linearization of the nominal (perturbation-free) system about the origin has a particular invariant subspace.

Real invariant subspaces of the linearization

Let $\sigma(y) = Sy$ for some full-rank matrix $S \in \mathbb{R}^{m\times n}$. By setting $\dot{\sigma} = \mathbf{0}_{m\times 1}$ following the equivalent control approach, one obtains

$$S\left[h\left(y_\sigma\right) + B\left(u_{eq} + \Delta(y_\sigma, t)\right)\right] = \mathbf{0}_{m\times 1}$$

where $y_\sigma \in \sigma^{-1}(0) = \ker(S)$. Assuming SB is nonsingular, the equivalent control is therefore

$$u_{eq} = -\Delta(y_\sigma, t) - (SB)^{-1}S\left[Hy_\sigma + O(\|y_\sigma\|^2)\right].$$

Hence $Ky_\sigma = -(SB)^{-1}SHy_\sigma$ is required for the equivalent control to have the desired properties. Consequently, the following must hold:

$$Sy = \mathbf{0}_{m\times 1} \quad\implies\quad SH^{cl}y = \mathbf{0}_{m\times 1}.$$

From this, we can make the following observation: the matrix S is a full-rank left annihilator of an invariant subspace of the linear system $\dot{z} = H^{cl}z$ of co-dimension m. By the Hartman–Grobman theorem (see Section 2.3), we know that this invariant subspace corresponds to a locally invariant (stable) manifold of the nonlinear system $\dot{\chi} = h(\chi) + BK\chi$ of the same dimension. As a consequence, if, in a sufficiently small neighborhood of the origin, we can bring the system's states onto the sliding manifold and then remain there, then all the states will converge to the origin despite of any matched perturbations.

How to extend this to periodic orbits?

Our main objective in this chapter is to extend these ideas also to nontrivial periodic orbits of nonlinear dynamical systems. Namely, we aim to utilize the local equivalence between the stable invariant manifolds of the nominal (nonlinear) closed-loop system and the stable invariant subspaces of the corresponding first-order approximation system along such an orbit. Yet, how to construct a time-invariant switching function $\sigma(\cdot)$ for this purpose may not be immediately obvious. Indeed, as opposed to the case of a trivial orbit, linearizing a nonlinear system about a periodic solution results in a time-varying (periodic) system with one zero characteristic exponent (see Sec. 2.3.1). This implies that one must find a real invariant subspace of appropriate dimension among the remaining independent solutions. However, any annihilator of such a subspace will be time-varying in general. Thus, one first needs to construct such a subspace, and then, more importantly, design from its annihilator the time-invariant switching function.

It is a constructive procedure for solving the above problem which is the main contribution of this chapter. More specifically, we suggest for this purpose the following three-step approach:[1]

1) *Transverse linearization:* Derive the linear periodic system corresponding to the first approximation (linearization) along the nominal orbit of the dynamics of a set of $(n-1)$ transverse coordinates, whose origin correspond to the nominal orbit;

2) *Floquet–Lyapunov transformation:* Transform this linear periodic system into a linear time-invariant system through a real Floquet–Lyapunov factorization of its state transition matrix;

[1] This idea is inspired by the method proposed by Freidovich and Gusev [67] in regard to a specific procedure for mechanical systems. The approach we here present builds upon and generalizes their ideas, as well as expand their applicability to a larger class of systems and provides a constructive procedure for obtaining the desired switching function.

3) *Invariant subspace–based switching function design:* Construct a switching function for this linear time-invariant system, corresponding to an annihilator of one of its real invariant subspaces whose co-dimension equals the number of independent control variables.

Outline: The above three-step approach is presented in a top-to-bottom way in the next three sections: We first demonstrate how to use invariant subspaces to design switching functions for stabilizing the origin of linear time-invariant systems in Sec. 8.2, corresponding to step 3) above. Then in Sec. 8.3 the same is done for linear time-periodic systems using Floquet–Lyapunov transformations, which is used in step 2). We then consider robust orbital stabilization of periodic orbits for nonlinear systems in Sec. 8.4, with the chapter's main result stated in Section 8.4.2. The remainder of the chapter is then organized as follows: A suggestion for a simple unit vector-based sliding mode control law for the nonlinear system is given in Sec. 8.4.3, which is briefly compared to a Lyapunov redesign based controller in Sec. 8.4.4. Then the concrete task of stabilizing upright oscillations of the cart-pendulum system subject to both matched- and unmatched uncertainties is considered as an illustrative example in Section 8.5.

8.2 Invariant subspace–based SMC design for LTI systems

In this section, we will show how invariant subspaces can be used to construct switching functions for linear time-invariant (LTI) systems with matching perturbations:

$$\dot{y} = Ay + B\left(u + \Delta(y,t)\right), \quad y \in \mathbb{R}^{\bar{n}}, \quad u \in \mathbb{R}^{\bar{m}}. \tag{8.1}$$

Here $A \in \mathbb{R}^{\bar{n}\times\bar{n}}$ is constant and $B \in \mathbb{R}^{\bar{n}\times\bar{m}}$ is of full rank. The matched perturbation term $\Delta : \mathbb{R}^{\bar{n}} \times \mathbb{R}_{\geq 0} \to \mathbb{R}^{\bar{m}}$ consists of system uncertainties and unknown external disturbances, but has a known upper bound $\Delta_M \in \mathbb{R}_{\geq 0}$,

Our aim is to design a sliding manifold on which the stability of the nominal closed-loop system is preserved and matched perturbations are rejected. Specifically, under the assumption of the stabilizability of the pair (A, B), we are in light of the motivational example in the chapter's introduction looking to solve the following problem:

Problem 8.1. *Given a matrix $K \in \mathbb{R}^{\bar{m}\times\bar{n}}$ such that $A_{cl} := A + BK$ is a Hurwitz (stable) matrix, find a full-rank matrix $S \in \mathbb{R}^{\bar{m}\times\bar{n}}$ such that, when restricted to the manifold*

$$\Sigma := \{y \in \mathbb{R}^{\bar{n}} : \ \sigma(y) := Sy = 0\}, \tag{8.2}$$

the system (8.1) *experiences the equivalent control* $u_{eq} = Ky - \Delta(y,t)$.

As mentioned in Section 8.1, a solution to Problem 8.1 is of course not only of use in regard to linear systems per say. Indeed, the system (8.1) may, for example, correspond to a nonlinear dynamical system after a (feedback) linearization has been performed about some operating point. Problem 8.1 can therefore also be viewed as a way for formulating the problem of switching surface design for such systems. For instance, given, say, an underactuated mechanical system (see Ch. 5), it allows one to constructed such a surface from the Jacobian linearization, given only knowledge of a $\mathcal{C}^1$-smooth exponentially stabilizing control law for the unperturbed system.

The following statement provides sufficient conditions which ensure that a matrix S is a solution to Problem 8.1.

Lemma 8.2. *If* $S \in \mathbb{R}^{\bar{m}\times\bar{n}}$ *is such that*

1. $\det(SB) \neq 0$,
2. $Sy = 0 \implies SA_{cl}y = 0$,

then it is a solution to Problem 8.1.

Proof. Following the equivalent control approach, [62] we set $S\dot{y}^* \equiv 0$ when y^* is confined to the sliding manifold (8.2) to obtain $S\left[Ay^* + B\left(u_{eq} + \Delta\right)\right] \equiv 0$. By adding and subtracting BKy^* inside the brackets, this can be equivalently rewritten as

$$S\left[A_{cl}y^* + B\left(u_{eq} + \Delta - Ky^*\right)\right] \equiv 0.$$

Since $Sy^* = 0$ implies $SA_{cl}y^* = 0$ (condition 2.) and the square matrix SB is nonsingular (condition 1.), the above equality must correspond to the unique equivalent control $u_{eq} = Ky^* - \Delta$. Hence (8.1) evolves as if $\dot{y}^* = A_{cl}y^*$ in the ideal sliding mode. □

Similarly to the motivating example in the previous section, the fact that such a solution S must be nonsingular (condition 1.) and be such that $SA_{cl}y = 0$ if $Sy = 0$ (condition 2.) implies that S must be a left annihilator of a real invariant subspace of A_{cl}, thus corresponding to a (controlled) (A,B)-invariant subspace of of the unperturbed system (8.1) [40, 221] (note that we will briefly show how to derive a basis for such subspaces in the next section). Necessarily, any such subspace must also be equivalent to a real A_{cl}^{T}-invariant subspace of the same dimension. That is, $SA_{cl} = \mathcal{A}_\sigma S$ for some Hurwitz matrix $\mathcal{A}_\sigma \in \mathbb{R}^{\bar{m}\times\bar{m}}$. For instance, if $\bar{m} = 1$, then it follows that S must be a left eigenvector of A_{cl}; a fact which was utilized in the similar type of scheme proposed in [222] for single input systems.

The existence of such a matrix S therefore boils down to the existence of a real A_{cl}-invariant subspace, for which there are three obvious possibilities:

S1. There does not exist any real invariant subspace of A_{cl} satisfying the conditions of the Lemma, that is, either no subspace of codimension $\bar{m}$ or $\operatorname{rank} SB < \bar{m}$ for any annihilator;

S2. There exists exactly one subspace of codimension $\bar{m}$ satisfying the conditions of the Lemma;

S3. There exist more than one such subspace.

It is important to note that there is no guarantee that such a subspace will exist in general for an arbitrary stabilizing matrix K. Thus, in the case of situation S1, one is forced to either find an alternative feedback matrix K, use alternative methods to construct S directly[2], design a robustifying feedback extension utilizing other approaches (e.g., through Lyapunov redesign techniques [44, 64, 223]) or to use dynamic methods such as integral sliding mode control [63].

Having the possibility to choose a particular surface among many, as in situation S3, is of course the most desirable. Indeed, this provides one with the possibility to pick a subspace having certain properties, such as choosing the subspace which has the fastest convergence (that whose largest (negative) exponent has the largest magnitude), etc. This also provides motivation for utilizing this approach beyond just for robustification purposes, in the sense that it can also be used to drive the system onto a prespecified subspace having some desired properties (see the example in Sec. 3.3 regarding adding a robustifying feedback extension).

Since determining the real, invariant subspaces of a matrix plays such a pivotal role in our approach, we briefly review how to compute these subspaces, before we move on to showing how robustifying feedback extensions can be designed for the LTI system given a solution to Lemma 8.2.

8.2.1 Real, invariant subspaces of LTI systems

Consider the following task: For a matrix $A \in \mathbb{R}^{\bar{n}\times\bar{n}}$, find all its, real invariant subspaces of dimension $d < \bar{n}$. Or put slightly differently: find any

[2] Knowledge of a stabilizing matrix K is of course not needed for constructing a sliding manifold for LTI systems. Indeed, there exist several well-known approaches for designing the matrix S directly; see e.g. Chapter 2.2 in [63] or Chapter 7 in [62].

subspace $\aleph^d \subset \mathbb{R}^{\bar{n}}$ spanned by d linear independent vectors $v_1, v_2, \ldots, v_d \in \mathbb{R}^{\bar{n}}$ such that $Ax \in \aleph^d$ for all $x \in \aleph^d$.

In this regard, recall the well-known fact that any (possibly complex) invariant subspace of a matrix $A \in \mathbb{R}^{\bar{n}\times\bar{n}}$ is spanned by its generalized eigenspaces [74]. Let, therefore, $\lambda_j \in \mathbb{C}$, $j = 1, 2, \ldots, \bar{n}$, denote the eigenvalues of A. We also denote by $\mathrm{alg}(\lambda_j)$ the algebraic multiplicity of λ_j (i.e., its multiplicity as a root of the characteristic polynomial of A) and by $\mathrm{geo}(\lambda_j)$ its geometric multiplicity (i.e., the number of independent eigenvectors corresponding to λ_j). Associated with each eigenvalue λ_j (discounting its multiplicity) there is a real eigenspace $\mathfrak{E}_j$ spanned by the imaginary and real parts of the corresponding eigenvectors and generalized eigenvectors of A [224]. Specifically,

$$\mathfrak{E}_j = \mathrm{span}_{\iota\in\mathbb{R}} \left\{ e^{\mathrm{Re}(\lambda_j)\iota} \cos\left(\mathrm{Im}(\lambda_j)\iota\right) \sum_{\alpha=1}^{\mathrm{alg}(\lambda_j)} b_j^\alpha \iota^{\alpha-1}, \right.$$
$$\left. e^{\mathrm{Re}(\lambda_j)\iota} \cos\left(\mathrm{Im}(\lambda_j)\iota\right) \sum_{\alpha=1}^{\mathrm{alg}(\lambda_j)} b_j^\alpha \iota^{\alpha-1} \right\}$$

for some real vectors $a_j^\alpha, b_j^\alpha \in \mathbb{R}^{\bar{n}}$.

For example, let λ_j^r denote a strictly real eigenvalue of A. Then any vector in the eigenspace $\mathfrak{E}_{\lambda_j^r} := \ker\left(\lambda_j^r \mathbf{I}_{\bar{n}} - A\right)$ spans a real, one-dimensional invariant subspace of A. Moreover, if $\dim(\mathfrak{E}_{\lambda_j^r}) = \mathrm{geo}(\lambda_j^r) = d > 1$, then the basis vectors of $\mathfrak{E}_{\lambda_j^r}$ can be used to generate real, invariant subspaces of all dimensions up to and including d.

More generally, one can utilize the fact that any real, square matrix has a real Jordan form [225, Thm. 3.4.1.5]: there exists a nonsingular matrix $V \in \mathbb{R}^{\bar{n}\times\bar{n}}$ and a block diagonal matrix $J \in \mathbb{R}^{\bar{n}\times\bar{n}}$ such that $AV = VJ$. Thus, let us denote $J_1^r, \ldots, J_{k_r}^r$ the blocks of J corresponding to the real eigenvalues of A, and let $V_i^r = [v_{i,1}^r, \ldots, v_{i,k_i^r}^r] \in \mathbb{R}^{\bar{n}\times k_i^r}$ denote the corresponding columns of V such that $AV_i^r = V_i^r J_i^r$. Note that this is equivalent to a Jordan chain:

$$(A - \mathbf{I}_{\bar{n}}\lambda_i^r)\, v_{i,1}^r = 0, \quad (A - \mathbf{I}_{\bar{n}}\lambda_i^r)\, v_{i,2}^r = v_{i,1}^r, \;\ldots\; (A - \mathbf{I}_{\bar{n}}\lambda_i^r)\, v_{i,k_i^r}^r = v_{i,(k_i^r-1)}^r.$$

Then, for any positive integer $\mu \le k_i^r$, one may construct a real, invariant, μ-dimensional subspace of A spanned by the real, linearly independent generalized eigenvectors $v_{i,1}^r, v_{i,2}^r, \ldots, v_{i,\mu}^r$. Furthermore, given two different such generalized eigenspaces, denoted $\{v_{i,1}^r, v_{i,2}^r, \ldots, v_{i,k_i^r}^r\}$ and $\{v_{j,1}^r, v_{j,2}^r, \ldots, v_{j,k_j^r}^r\}$, one can construct invariant subspaces of any dimension less than or equal to $k_r^i + k_r^j$; for example, $\aleph^3 = \mathrm{span}\{v_{i,1}^r, v_{j,1}^r, v_{j,2}^r\}$, with $i \neq j$, would be a three-dimensional invariant subspace, and so on.

For the complex conjugate eigenvalue pairs of A, denoted $\{\lambda_i^c, \overline{\lambda_i^c}\}$, this, however, cannot be applied directly as the corresponding generalized eigenspaces, that is $\mathfrak{E}_{\lambda_i^c}^{\bar{n}} := \ker\left(\lambda_i^c \mathbf{I}_{\bar{n}} - A\right)^{\bar{n}}$, are then spanned by complex generalized eigenvectors $v_{i,1}^c, v_{i,2}^c, \ldots, v_{i,k_c^i}^c$. In order to generate real, invariant subspace from these complex eigenspaces, one can instead use the fact that for any $v_i^c \in \mathfrak{E}_{\lambda_i^c}$, its complex conjugate satisfies $\overline{v_i^c} \in \overline{\mathfrak{E}_{\lambda_i^c}^{\bar{n}}} := \ker\left(\overline{\lambda_i^c}\mathbf{I}_{\bar{n}} - A\right)^{\bar{n}}$. Thus for a complex eigenvalue λ_i^c and its corresponding eigenvector v_i^c, the space spanned by $\{\mathrm{Re}[v_i^c], \mathrm{Im}[v_i^c]\}$ is a two-dimensional invariant subspace of A. In terms of the real Jordan form, let $J_1^c, \ldots, J_{k_c}^c$ be the Jordan blocks corresponding to the complex conjugate eigenvalue pairs $\{\lambda_i^c, \overline{\lambda_i^c}\}$ for $i = 1, \ldots, k_c$. Then for $V_i^c = [\mathcal{V}_1^c, \ldots, \mathcal{V}_{k_c}^c] \in \mathbb{R}^{\bar{n}\times 2k_c}$, where

$$\mathcal{V}_i^c := \left[\mathrm{Re}[v_{i,1}^c], \mathrm{Im}[v_{i,1}^c]\right] \in \mathbb{R}^{\bar{n}\times 2}, \tag{8.3}$$

one has $AV_i^c = V_i^c J_i^c$, such that for any positive integer $\mu \leq k_c$, one can construct a real, invariant subspace of even dimension 2μ, spanned by $\mathcal{V}_1^c, \mathcal{V}_1^c, \ldots, \mathcal{V}_\mu^c$. Hence pairs of complex conjugate eigenvalues may only generate invariant subspaces of even dimension, from which the two following well-known statements can be concluded:

Fact 8.3. *A matrix $A \in \mathbb{R}^{\bar{n}\times\bar{n}}$ has real invariant subspaces of all even dimensions less than $\bar{n}$, while it has real invariant subspaces of odd dimensions if, and only if, it has at least one real eigenvalue.*

Fact 8.4. *If $\bar{n}$ is odd, then $A \in \mathbb{R}^{\bar{n}\times\bar{n}}$ has real, invariant subspaces of all dimensions less than $\bar{n}$.*

Recall that the nominal closed-loop system is required to have a real invariant subspace of a specific dimension for there to exist a solution to Problem 8.1 of the form as in Lemma 8.2. The suggested approach is therefore heavily reliant on the chosen nominal feedback matrix K. Meanwhile, it also makes it particularly well-suited when used together with pole-placement techniques for finding K. Indeed, since one then can, at least to some extent, freely choose the characteristic polynomial of the nominal closed-loop system using, e.g., Ackermannn's formula [226], one can always guarantee the existence of a specific invariant subspace. The following example[3] demonstrates how this allows one to find a solution to Problem 8.1.

Example 8.1. Consider a chain of two integrators written in the form as

[3]The author is grateful to Prof. Leonid Freidovich for suggesting this example.

in (8.1), that is

$$A = \begin{bmatrix} 0 & 1 & 0 \\ 0 & 0 & 1 \\ 0 & 0 & 0 \end{bmatrix} \qquad \text{and} \qquad B = \begin{bmatrix} 0 \\ 0 \\ 1 \end{bmatrix}. \tag{8.4}$$

Taking, for some real number $\varrho > 0$,

$$K = \begin{bmatrix} -\varrho^3 & -3\varrho^2 & -3\varrho \end{bmatrix},$$

the characteristic polynomial of $A_{cl} := A + BK$ is $(\lambda + \varrho)^3$. Thus all its eigenvalues equal ϱ, while the corresponding eigenvectors all given by $v_\varrho = \text{col}(1/\varrho^2, -1/\varrho, 1)$. The matrices in the Jordan form of A_{cl}, $A_{cl} = VJV^{-1}$, are consequently

$$J = \begin{bmatrix} -\varrho & 1 & 0 \\ 0 & -\varrho & 1 \\ 0 & 0 & -\varrho \end{bmatrix} \qquad \text{and} \qquad V = \begin{bmatrix} \frac{1}{\varrho^2} & \frac{2}{\varrho^3} & \frac{3}{\varrho^4} \\ -\frac{1}{\varrho} & -\frac{1}{\varrho^2} & -\frac{1}{\varrho^3} \\ 1 & 0 & 0 \end{bmatrix}.$$

The only two-dimensional invariant subspace of A_{cl} is therefore spanned by the first two columns of V. This subspace has the left annihilator

$$S = \begin{bmatrix} \varrho^2 & 2\varrho & 1 \end{bmatrix},$$

which in turn is a left eigenvector of A_{cl} corresponding to the left eigenvalue $-\varrho$, i.e. $SA_{cl} = -\varrho S$. Since evidently $SB = 1$, this S satisfies all the conditions of Lemma 8.2 and is therefore a solution to Problem 8.1.

The above example is in fact just a particular version of the eigenvalue-placement approach as described in [63, Sec. 2.2.2], although it is here derived from a slightly different point of view. We can easily generalize it to any single-input system given by a chain of integrators:

$$\dot{y}_1 = y_2, \quad \dot{y}_2 = y_3, \quad \ldots, \quad \dot{y}_{\bar{n}} = u.$$

Indeed, if one takes $u = K_{\bar{n}} y$, with (here $\binom{\cdot}{\cdot}$ denotes the binomial coefficient)

$$K_m := \left[-\varrho^m, -m\varrho^{m-1}, \ldots, -\binom{m}{i}\varrho^i, \ldots, --\binom{m}{2}\varrho^2, -m\varrho \right],$$

then the characteristic polynomial of the matrix A_{cl} is $(\lambda + \varrho)^{\bar{n}}$. Similarly to the above example, A_{cl} only has one invariant subspace of co-dimension one. This subspace has the left annihilator

$$S = \left[\varrho^{\bar{n}-1}, (\bar{n}-1)\varrho^{\bar{n}-2}, \ldots, \binom{\bar{n}-1}{i}\varrho^{i-1}, \ldots, (\bar{n}-1)\varrho, 1 \right],$$

which therefore satisfies all the conditions of Lemma 8.2. Note that, by setting $Sy = 0$, we can make the same observation as in [63], namely that we then can write $y_{\bar{n}}$ in terms of $y_1, y_2, \ldots, y_{\bar{n}-1}$, i.e. $y_{\bar{n}} = K_{\bar{n}-1}\operatorname{col}(y_1, \ldots, y_{\bar{n}-1})$, such that the matrix corresponding to the reduced-order system

$$\dot{y}_1 = y_2,\ \dot{y}_2 = y_3,\ \ldots \quad \dot{y}_{\bar{n}-1} = -\varrho^{\bar{n}-1}y_1 - (\bar{n}-1)\varrho^{\bar{n}-2}y_2 - \cdots - (\bar{n}-1)\varrho y_{\bar{n}-1},$$

has the characteristic polynomial $(\lambda + \varrho)^{\bar{n}-1}$.[4]

The above example was based on an invariant subspace constructed from a system with only real eigenvalues. The following example shows how a real invariant subspace can be generated from a pair of complex conjugate eigenvalues using (8.3).

Example 8.2. Consider again the three-dimensional LTI system in Example 8.1, with A and B given by (8.4). Consider now instead

$$K = \begin{bmatrix} -1 & -2 & -2 \end{bmatrix}.$$

The corresponding matrix $A_{cl} := A + BK$ has one real eigenvalue, $\lambda^r = -1$, and a pair of complex conjugate eigenvalues $(\lambda^c, \overline{\lambda^c})$, with $\lambda^c = \frac{1}{2}(-1 + \sqrt{-3})$. The eigenvectors corresponding to λ^r and λ^c are

$$v^r = \operatorname{col}\big(1, -1, 1\big) \quad \text{and} \quad v^c = \operatorname{col}\big(-1 + \sqrt{-3}, -1 - \sqrt{-3}, 2\big).$$

The only real, invariant, two-dimensional subspace is that spanned by

$$[\operatorname{Re}[v^c], \operatorname{Im}[v^c]] = \begin{bmatrix} -1 & \sqrt{3} \\ -1 & -\sqrt{3} \\ 2 & 0 \end{bmatrix}.$$

Clearly $S = [1, 1, 1]$ is a left annihilator for this space, and $SB = 1$, meaning that this S satisfies the conditions of Lemma 8.2. Indeed, $SA_{cl} = -S$.

8.2.2 Sliding mode control design

Suppose now a sliding surface $\sigma(y) = Sy$, with S satisfying Lemma 8.2, is known. The next step is then to design a control law ensuring that the sliding manifold (8.2) is reached in finite time despite of the matched perturbation. The following statement is useful in this regard.

[4] Using similar arguments to the backstepping-based assignment proposed in e.g. [227], one can alternatively assign arbitrary real eigenvalues, $-\lambda_1, \ldots, -\lambda_{\bar{n}} < 0$, by taking $u = u(y_1, \ldots, y_{\bar{n}})$ such that $\dot{\kappa}_{\bar{n}} = -\lambda_{\bar{n}}\kappa_{\bar{n}}$, where $\kappa_{i+1} = \dot{\kappa}_i + \lambda_i\kappa_i$ with $\kappa_1 = y_1$.

Lemma 8.5. *Let $S \in \mathbb{R}^{\bar{m}\times\bar{n}}$ satisfy Lemma 8.2 and suppose u is taken as*

$$u = Ky + (SB)^{-1}v \tag{8.5}$$

in (8.1) *for some $v \in \mathbb{R}^{\bar{m}}$. Then*

$$\dot{\sigma} = \mathcal{A}_\sigma\sigma + v + SB\Delta(y,t) \tag{8.6}$$

holds for $\sigma := Sy$ outside of the sliding manifold Σ, with $\mathcal{A}_\sigma := SA_{cl}S^\dagger$ Hurwitz.

Proof. Firstly, we can always write $y = S^\dagger\sigma + (\mathbf{I}_{\bar{n}} - S^\dagger S)y$. Here $S^\dagger$ is taken as the unique Moore–Penrose pseudoinverse of S, i.e. $SS^\dagger = \mathbf{I}_{\bar{m}}$, although any full-rank right inverse may be used instead. Using this in $\dot{\sigma} = S\dot{y}$, together with the fact that $SA_{cl}(\mathbf{I}_{\bar{n}} - S^\dagger S)y \equiv \mathbf{0}_{\bar{m}\times 1}$ for all $y \in \mathbb{R}^n$ if S satisfies Lemma 8.2, one obtains (8.6) by inserting (8.5) into (8.1).

Secondly, since S annihilates a stable invariant subspace of A_{cl}, spanned by a set of its (real) generalized eigenvectors, the matrix $\mathcal{A}_\sigma \in \mathbb{R}^{\bar{m}\times\bar{m}}$ is necessarily Hurwitz, with its spectrum a subset of the spectrum of A_{cl}. Indeed, if $S_\perp \in \mathbb{R}^{\bar{n}\times(\bar{n}-\bar{m})}$ is a basis of $\ker\{S\}$, then there exists a nonsingular matrix $Y \in \mathbb{R}^{\bar{m}\times\bar{m}}$, as well as a possibly singular matrix $Z \in \mathbb{R}^{(\bar{n}-\bar{m})\times\bar{m}}$ and a block diagonal Hurwitz matrix $J \in \mathbb{R}^{\bar{n}\times\bar{n}}$ such that $A_{cl} = VJV^{-1}$ is a real Jordan form [225, Ch. 3.4] of A_{cl}, with

$$V = \begin{bmatrix} S_\perp & S_\perp Z + S^\dagger Y \end{bmatrix} \quad \text{and} \quad V^{-1} = \begin{bmatrix} S_\perp^\dagger - ZY^{-1}S \\ Y^{-1}S \end{bmatrix}.$$

By partitioning J as

$$J = \begin{bmatrix} J_{11} & J_{12} \\ J_{21} & J_{22} \end{bmatrix}$$

where

$$J_{11} \in \mathbb{R}^{(\bar{n}-\bar{m})\times(\bar{n}-\bar{m})},\ J_{12} \in \mathbb{R}^{(\bar{n}-\bar{m})\times\bar{m}},\ J_{21} \in \mathbb{R}^{\bar{m}\times(\bar{n}-\bar{m})},\ J_{22} \in \mathbb{R}^{\bar{m}\times\bar{m}},$$

one can show that $\mathcal{A}_\sigma = SA_{cl}S^\dagger = Y[J_{22} - J_{21}Z]Y^{-1}$. Due to the specific structure of the real Jordan form and the fact that $S_\perp$ spans an invariant subspace of A_{cl}, namely $S_\perp = S_\perp J_{11}$, we must here have $J_{21} \equiv \mathbf{0}_{\bar{m}\times(\bar{n}-\bar{m})}$. Hence the eigenvalues of $\mathcal{A}_\sigma$ are the eigenvalues of J_{22}, which in turn correspond to a subset of the spectrum of A_{cl}. □

There exist several control strategies in the literature which may here be used to ensure that the origin of (8.6) is reached in finite time despite of the perturbation Δ. As an example of such a controller, we provide next a unit-vector approach [63].

Proposition 8.6. *Let $\mathcal{A}_\sigma := SA_{cl}S^\dagger$ be as in Lemma 8.5 and let $P \in \mathbb{M}^{\bar{m}\times\bar{m}}_{\succ 0}$ be the unique solution to the Lyapunov equation*

$$\mathcal{A}_\sigma^\top P + P\mathcal{A}_\sigma = -Q$$

for some $Q \in \mathbb{M}^{\bar{m}\times\bar{m}}_{\succ 0}$. Then the control law (8.5)*, with*

$$v = \begin{cases} -\mu\frac{\sigma}{\|\sigma\|} & \text{if} \quad \|\sigma\| \neq 0, \\ 0 & \text{if} \quad \|\sigma\| = 0, \end{cases} \tag{8.7}$$

for some

$$\mu \geq \frac{1}{\lambda_{min}(P)}\left[\frac{1}{2}\mu_\star + \lambda_{max}(P)\|SB\|\Delta_M\right], \quad \mu_\star > 0,$$

guarantees that the sliding manifold (8.2) *is reached in finite time.*

Proof. It is well known that $\mathcal{A}_\sigma$ being Hurwitz guarantees the existence of a unique solution to the Lyapunov equation [44]. Consider, therefore, the Lyapunov function candidate $V_\sigma := \sigma^\top P\sigma$, such that by (8.6),

$$\begin{aligned} \frac{d}{dt}V_\sigma &= \sigma^\top\left(\mathcal{A}_\sigma^\top P + P\mathcal{A}_\sigma - \frac{2\mu}{\|\sigma\|}P\right)\sigma + 2\sigma^\top PSB\Delta(y,t) \\ &\leq -\lambda_{min}(Q)\|\sigma\|^2 + 2\left[\lambda_{max}(P)\|SB\|\Delta_M - \mu\lambda_{min}(P)\right]\|\sigma\|. \end{aligned}$$

From the lower bound of μ one consequently obtains $\frac{d}{dt}V_\sigma \leq -\alpha V_\sigma - \beta\sqrt{V_\sigma}$ with $\alpha := \lambda_{min}(Q)/\lambda_{max}(P)$ and $\beta := \mu_\star/\sqrt{\lambda_{max}(P)}$. Using standard argument (see, e.g., Ch. 14.1.1 in [44]) it can therefore be concluded that the sliding manifold Σ is reached in finite time, with the settling time t_s satisfying the inequality $t_s \leq 2\alpha^{-1}\ln\left(\alpha\beta^{-1}\sqrt{V_\sigma(0)} + 1\right)$; see [228]. □

Remark 8.7. By taking inspiration from the similar type of scheme proposed in [222], it is possible to relax the matching condition in regard to the disturbances and uncertainties acting on the system. Specifically, if

$$\Delta(y,t) = B\Delta_{matched}(y,t) + \Delta_{unmatched}(y,t),$$

then a control law of the form as (8.5) and (8.7) will asymptotically stabilize the origin $y = 0$ if the matrix $S \in \mathbb{R}^{\bar{m}\times\bar{n}}$ satisfying the conditions in Lemma 8.2, can be taken such that $\left\|\left(\mathbf{I}_{\hat{n}} - B(SB)^{-1}S\right)\Delta_{unmatched}(y,t)\right\| \leq \eta_1\|y\|$ and $\|S\Delta_{unmatched}(y,t)\| \leq \eta_2\|Sy\|$ both hold for some sufficiently small constants $\eta_1, \eta_2 \geq 0$. □

We also remark that while the well-known chattering effect [62, 63] is the main drawback of the controller (8.7), methods for alleviating and attenuating this effect using continuous approximations of (8.7) do exist; see, for example, [44, 64, 223]. Although note that these methods only ensure convergence to a boundary layer of the sliding manifold. Alternatively, the structure of (8.5) may also allow (depending on the disturbance) for the possibility of utilizing multivariable super-twisting algorithms [65, 229].

Example 8.3. Consider again the system in Example 8.2 with the switching function taken as $\sigma(y) = Sy$ for $S = [1, 1, 1]$. Since $S^{\dagger} = \mathrm{col}(1/3, 1/3, 1/3)$, we have $\mathcal{A}_{\sigma} := SA_{cl}S^{\dagger} = -1$. Hence $\mathcal{A}_{\sigma}$ clearly corresponds to the real eigenvalue of the remaining one-dimensional invariant subspace of A_{cl}. Taking the control law according to (8.5), we find from Lemma 8.5 that

$$\dot{\sigma} = -\sigma + v + \Delta(y,t),$$

with $\Delta(\cdot)$ containing the unknown perturbations acting on the system. Since, e.g., $\mathcal{A}_{\sigma}^{\mathsf{T}} + \mathcal{A}_{\sigma} = -2$, Proposition 8.6 ensures that the control law (8.5) with the following relay-based robustifying feedback extension

$$v = -\mu\lceil\sigma\rfloor^{0}, \quad \mu > \Delta_M \geq |\Delta(y,t)|,$$

with $\lceil\cdot\rfloor^{\alpha} := \mathrm{sgn}(\cdot)\,|\cdot|^{\alpha}$, makes the states converge to the sliding manifold $\Sigma = \left\{y \in \mathbb{R}^3 : \; Sy = 0\right\}$ within a finite amount of time. Alternatively, if, say $|\dot{\Delta}(y,t)| \leq \mu$, then other controllers, such as the continuous super-twisting algorithm [63, 230], $v = -\mu_p\lceil\sigma\rfloor^{\frac{1}{2}} + w$ with $\dot{w} = -\mu_d\lceil\sigma\rfloor^{0}$ and appropriately chosen gains $\mu_p, \mu_d > 0$, can of course be used instead.

8.3 Switching function design for linear periodic systems

In the previous section we saw how to design a switching function for LTI systems using the knowledge of a stabilizing feedback. As such a linear system may have been obtained through the linearization of a nonlinear system about one of its nominal equilibrium points, such an approach therefore provides a means to construct robustifying feedback extensions for nonlinear systems utilizing first-order approximation about the desired hyperbolic equilibrium. Yet, as we are mainly concerned with periodic orbits in this chapter, where the linearization along the nominal solution instead results in a linear time-periodic (LTP) system, we need some way of bridging the gap between LTI- and LTP systems in order to apply such an approach directly. This is what we will aim to do in this section. Specifically, we will provide conditions which a switching function for an LTP system must satisfy as to correspond to specific invariant subspace; and , most importantly, we will show how (and when) we can transform an LTP system into an LTI system using a real-valued Floquet–Lyapunov transformation, thus allowing us to directly apply Lemma 8.2.

The types of system we will now consider are LTP systems of the form

$$\dot{y} = A(t)y + B(t)\left(u + \Delta(y,t)\right), \ t \in \mathbb{R}_{\geq 0}, \ y \in \mathbb{R}^{\bar{n}}, \ u \in \mathbb{R}^{\bar{m}}, \tag{8.8}$$

with continuous, bounded, T-periodic matrix functions $A(t) = A(t+T)$ and $B(t) = B(t+T)$ of minimal period $T > 0$. As before, $\Delta(\cdot) \in \mathbb{R}^{\bar{m}}$ is unknown but has known upper bound Δ_M.

In a similar manner to the LTI systems in the previous section, we assume that a continuous, T-periodic matrix function $K : \mathbb{R}_{\geq 0} \to \mathbb{R}^{\bar{m}\times\bar{n}}$ is known such that the origin of the perturbation-free closed-loop system, given by

$$\dot{\chi} = A_{cl}(t)\chi, \quad A_{cl}(t) := A(t) + B(t)K(t), \tag{8.9}$$

is exponentially stable. Recall in this regard that if we denote by $\Phi_{A_{cl}}(\cdot) \in \mathbb{R}^{\bar{n}\times\bar{n}}$ the *state-transition matrix* (STM), i.e. the unique solution to

$$\frac{d}{dt}\Phi_{A_{cl}}(t,t_0) = A_{cl}(t)\Phi_{A_{cl}}(t,t_0), \quad \Phi_{A_{cl}}(t_0,t_0) = \mathbf{I}_{\bar{n}}, \tag{8.10}$$

then the exponential stability of (8.8) is equivalent to all the eigenvalues of the *Monodromy matrix* (see, e.g., Section 2.3.1)

$$\mathfrak{M}_{A_{cl}} := \Phi_{A_{cl}}(T,0) \tag{8.11}$$

having magnitudes strictly less than one.

Assuming knowledge of such a matrix $K(\cdot)$, the problem we are looking to solve in section is the following:

Problem 8.8. *Find a $\mathcal{C}^1$ matrix function $S : \mathbb{R}_{\geq 0} \to \mathbb{R}^{\bar{m}\times\bar{n}}$, such that the forward invariance of the relation $S(t)y(t) \equiv 0$ for all $t \geq t_0$ corresponds to the system* (8.8) *experiencing the equivalent control*

$$u_{eq}(t) = K(t)y(t) - \Delta(y(t),t)$$

for all $t \geq t_0$.

Although this problem is naturally more challenging than Problem 8.1 as the matrix $S(\cdot)$ might be time-varying (periodic), solutions can be found using our knowledge of the state-transition matrix.

Lemma 8.9. *Let $X_0 \in \mathbb{R}^{\bar{n}\times(\bar{n}-\bar{m})}$ be of full rank and suppose the $\mathcal{C}^1$ matrix function $S : \mathbb{R}_{\geq 0} \to \mathbb{R}^{\bar{m}\times\bar{n}}$ is a left annihilator of the range space of $\Phi_{A_{cl}}(t,0)X_0$ at time t, that is*

$$\|S(t)\Phi_{A_{cl}}(t,0)X_0 p\| \equiv 0$$

for all $p \in \mathbb{R}^{(\bar{n}-\bar{m})}$ and any $t \geq 0$. Then $S(t)$ is a solution to Problem 8.8 if $\operatorname{rank}[S(t)B(t)] = \bar{m}$ *for all $t \in \mathbb{R}_{\geq 0}$. Moreover, if $S(t)$ is to be T-periodic, i.e. $S(t) = S(t+T)$ for any $t \geq 0$, then X_0 must be a basis of an invariant subspace of $\mathfrak{M}_{A_{cl}}$ of codimension $\bar{m}$.*

Proof. First note that at each time $t \in \mathbb{R}_{\geq 0}$ one must have

$$\frac{d}{dt}\left[S(t)\Phi_{A_{cl}}(t,0)X_0\right] = \dot{S}(t)\Phi_{A_{cl}}(t,0)X_0 + S(t)A_{cl}(t)\Phi_{A_{cl}}(t,0)X_0 = 0$$

which implies the relation $\dot{S}(t)\Phi_{A_{cl}}(t,0)X_0 = -S(t)A_{cl}(t)\Phi_{A_{cl}}(t,0)X_0$.

Now assuming the forward invariance of $S(t)y(t) = 0$, it follows that

$$\frac{d}{dt}\left(S(t)y(t)\right) = \dot{S}(t)y + S(t)\left(A(t)y + B(t)(u_{eq} + \Delta)\right) \equiv 0.$$

Therefore, as if $S(t)y(t) = 0$ then $y(t) = \Phi_{A_{cl}}(t,0)X_0 p$ for some $p \in \mathbb{R}^{\bar{n}-\bar{m}}$, we obtain, using the above relation, that

$$\begin{aligned} -S(t)A_{cl}(t)y + S(t)\left(A(t)y + B(t)(u_{eq} + \Delta)\right) &= S(t)B(t)\left[u_{eq} + \Delta - K(t)y\right] \\ &\equiv 0. \end{aligned}$$

Due to the assumption that $\operatorname{rank}[S(t)B(t)] = \bar{m}$, the equivalent control is thus uniquely given by $u_{eq} = K(t)y - \Delta$ as desired.

To derive the stated condition for the T-periodicity of $S(\cdot)$, recall the following well-known property of the STM [25, 74]: $\Phi_{A_{cl}}(t+T,0) = \Phi_{A_{cl}}(t,0)\mathfrak{M}_{A_{cl}}$. Thus if $S(t) = S(t+T)$ for all $t \geq 0$, then

$$\begin{aligned} \|S(t)\Phi_{A_{cl}}(t,0)X_0 p\| &= \|S(t+T)\Phi_{A_{cl}}(t+T,0)X_0 p\| \\ &= \|S(t)\Phi_{A_{cl}}(t,0)\mathfrak{M}_{A_{cl}}X_0 p\| \\ &= 0 \end{aligned}$$

for any $p \in \mathbb{R}^{(\bar{n}-\bar{m})}$ and all $t \geq 0$. It follows that there must be some nonsingular matrix $N \in \mathbb{R}^{(\bar{n}-\bar{m})\times(\bar{n}-\bar{m})}$ such that $\mathfrak{M}_{A_{cl}}X_0 = X_0 N$, or equivalently, the columns of X_0 form a basis of an invariant subspace of $\mathfrak{M}_{A_{cl}}$. □

The question of how to generate and numerically construct such a matrix function $S(\cdot)$ therefore arises. For this purpose, suppose we can smoothly transform the LTP system (8.8) into an LTI one. This would allow us to readily use the theory outlined in the previous section, in particular Lemma 8.2. We demonstrate how this can be achieved utilizing a *Floquet–Lyapunov* (FL) transformation next.

8.3.1 Preliminaries: Floquet–Lyapunov (FL) theory

Let $A : \mathbb{R}_{\geq 0} \to \mathbb{R}^{\bar{n}\times\bar{n}}$ be a bounded and continuous matrix function, and consider the linear time-varying (LTV) system:

$$\dot{y} = A_{cl}(t)y, \quad y \in \mathbb{R}^{\bar{n}}, \quad t \in \mathbb{R}_{\geq 0}. \tag{8.12}$$

Denote by $\Phi_{A_{cl}}(\cdot)$ the STM, i.e. $y(t) = \Phi_{A_{cl}}(t,\tau)y(\tau)$ for all $t,\tau \in \mathbb{R}_{\geq 0}$ (see (8.10)), and suppose there exists a real, constant, $\bar{n}\times\bar{n}$ matrix F and a nonsingular, $\mathcal{C}^1$ matrix function $L : \mathbb{R}_{\geq 0} \to \mathbb{R}^{\bar{n}\times\bar{n}}$ such that $\Phi_{A_{cl}}(\cdot)$ can be factorized as follows:

$$\Psi_{A_{cl}}(t,0) = L(t)e^{Ft} \quad \forall t \in \mathbb{R}_{\geq 0}. \tag{8.13}$$

The coordinate transformation $y(t) = L(t)z(t)$ is then said to be a (real) *Lyapunov transformation*, while the system (8.12) is said to be *real-reducible*, in the sense that $\dot{z} = Fz$ is time invariant.

While it is well known that not all LTV systems of the form (8.12) are reducible, Floquet [231] showed that all LTP systems are. If for a T-periodic matrix $A_{cl}(t)$ there is some matrix function $L(t) = L(t+cT)$, with c an integer, such that (8.13) holds, then $y(t) = L(t)z(t)$ is therefore said to be a cT-periodic *Floquet–Lyapunov* (FL) *transformation*, while (8.13) will be referred to as a cT-periodic FL *factorization*.

In the following, we will therefore take the matrix $A_{cl}(\cdot) \in \mathbb{R}^{\bar{n}\times\bar{n}}$ in (8.12) to be both continuous and T-periodic. It is known that a real, $2T$-periodic FL factorization always exists for LTP systems of the form (8.12) [61, 232, 233]. The following statement demonstrates this fact (see also Theorem 3.1 in [232] for a generalization of this theorem.)

Theorem 8.10 (Real FL Transformation [61]). *If $A_{cl}(t) = A_{cl}(t+T)$ in* (8.12) *is continuous, then there always exists a real, continuously differentiable, nonsingular matrix function $L(t)$, as well as real, commuting matrices F and Y, i.e. $FY = YF$, satisfying*

$$L(t+2T) = L(t), \qquad L(t+T) = L(t)Y, \qquad Y^2 = \mathbf{I}_{\bar{n}},$$

such that (8.13) *holds for the LTP system* (8.12).

The existence of real, T-periodic FL factorizations, however, depends upon the spectrum of the Monodromy matrix $\mathfrak{M}_A$. That is to say, since any such factorization (8.13) naturally must satisfy

$$\mathfrak{M}_{A_{cl}} = \Phi_{A_{cl}}(T, 0) = e^{FT}, \tag{8.14}$$

the existence of a real matrix F is dependent on the existence of a real (matrix) logarithm of $\mathfrak{M}_{A_{cl}}$, i.e. $\log \mathfrak{M}_{A_{cl}} = FT$. Using this, together with the fact that $\Phi_{A_{cl}}(t, 0)$ is nonsingular for all $t \in \mathbb{R}_{\geq 0}$, the following statement is just a well-known, straightforward consequence of Theorem 1 in [234].

Lemma 8.11. *The LTP system* (8.12) *has a real, T-periodic FL factorization of the form* (8.13) *if, and only if, each Jordan block corresponding to an eigenvalue of $\mathfrak{M}_{A_{cl}}$ with negative real part appears an even number of times.*

For the sake of completeness, we will in the next section briefly outline some methods for obtaining a real FL factorization.

8.3.2 Constructing Floquet–Lyapunov factorizations

There are several ways of computing real (cT-period) Floquet–Lyapunov (FL) factorization for LTP systems. These are mainly grouped into either direct- or indirect methods.

In the case of direct approaches (see e.g. [233]) one uses knowledge of the state transition matrix to find $L(\cdot)$ and F directly from (8.13). The existence of a real matrix F in Theorem 8.10, for instance, then follows from the fact that the Monodromy matrix, $\mathfrak{M}_A$, is real; indeed, using Lemma 3 in [233], we have

$$\mathfrak{M}_{A_{cl}}^2 = \overline{\mathfrak{M}_{A_{cl}}}\mathfrak{M}_{A_{cl}} = e^{TB}e^{T\overline{B}} = e^{T(B+\overline{B})} = e^{2TF} \tag{8.15}$$

such that $F = (B + \overline{B})/2$ for some possibly complex matrix B.

In the indirect approach suggested in [235], on the other hand, one assumes that $F \in \mathbb{R}^{\bar{n}\times\bar{n}}$ satisfying (8.13) is known for some cT-periodic matrix $L(t)$. By then substituting (8.13) into (8.10), one obtains the matrix differential equation

$$\frac{d}{dt}L(t) = A_{cl}(t)L(t) - L(t)F \tag{8.16}$$

which must hold for all $t \geq 0$. Moreover, since $\frac{d}{dt}L^{-1}(t) = -L^{-1}(t)\dot{L}(t)L^{-1}(t)$ for any smooth, nonsingular square matrix function $L(\cdot)$, it follows that

$$\frac{d}{dt}L^{-1}(t) = -L^{-1}(t)A_{cl}(t) + FL^{-1}(t) \tag{8.17}$$

must be satisfied for all $t \geq 0$ as well. Hence either (8.16) or (8.17) can be solved for $L(t)$ or $L^{-1}(t)$, respectively, using the fact that that $L(0) = L^{-1}(0) = \mathbf{I}_{\bar{n}}$. Note that the converse is also true [61]:

Corollary 8.12. *If there exists a matrix $F \in \mathbb{R}^{\bar{n}\times\bar{n}}$ and a cT-periodic, nonsingular matrix function $L : \mathbb{R}_{\geq 0} \to \mathbb{R}^{\bar{n}\times\bar{n}}$, $L(0) = \mathbf{I}_{\bar{n}}$, satisfying the matrix differential equation* (8.16)*, then* (8.13) *is a real, cT-periodic FL factorization of* (8.10)*.*

One therefore has two natural options for finding an FL factorization:

1) Integrate (8.10) to find the Monodromy matrix and then obtain F from (8.15), such that $L(t)$ can be found either from (8.13) directly or by integrating (8.16);

2) Or as suggested in [235], find both F and $L(t)$ simultaneously by solving (8.16) as a boundary value problem using $L(0) = L(cT) = L(t)Y$ for some $k \in \{1, 2\}$, and by taking $\dot{F} = 0$.

See also [236] and [237] for alternative ways of computing real factorizations.

8.3.3 FL Transformation–based switching function design

We will now apply the Floquet–Lyapunov (FL) theory outlined in the previous sections in order to solve Problem 8.8.

Proposition 8.13. *Let the pair $(L(t), F)$ be a real, cT-periodic FL factorization of the closed-loop system* (8.9) *for some positive integer c, and suppose the matrix F has a real, invariant subspace $\aleph$ of co-dimension $\bar{m}$. If $\hat{S} \in \mathbb{R}^{\bar{m}\times\bar{n}}$ is a full rank left-annihilator of $\aleph$, that is $\hat{S}z = 0$ for all $z \in \aleph$ and* $\text{rank}[\hat{S}L^{-1}(t)B(t)] = \bar{m}$ *for all $t \in [0, cT)$, then the matrix function $S(t) := \hat{S}L^{-1}(t)$ is a solution to Problem 8.8.*

Proof. Assume, without loss of generality, that the relation $\sigma(t) = S(t)y(t) \equiv 0$ is forced for $t \geq 0$. Following the equivalent control approach [62, 63], we then set

$$\dot{\sigma}(t) = \hat{S}\left[\frac{dL^{-1}}{dt}(t)y + L^{-1}(t)\left(A(t)y + B(t)(u_{eq} + \Delta)\right)\right] \equiv 0.$$

Here $\frac{d}{dt}L^{-1}(t)$ can be found from (8.17), such that the above reduces to

$$\begin{aligned}
\dot{\sigma} &= \hat{S}\left[FL^{-1}(t)y - L^{-1}(t)\big(A_{cl}(t) - A(t)\big)y + L^{-1}(t)B(t)(u_{eq} + \Delta)\right] \\
&= \hat{S}\left[Fz - L^{-1}(t)B(t)K(t)y + L^{-1}(t)B(t)(u_{eq} + \Delta)\right] \\
&= \hat{S}Fz + S(t)B(t)\left[u_{eq} - K(t)y + \Delta\right] \equiv 0.
\end{aligned}$$

Now, as $\aleph$ is F-invariant and $\hat{S}$ annihilates $\aleph$, we here have that $\hat{S}z = \hat{S}Fz \equiv 0$ for all $z \in \aleph$. As we have assumed $[S(t)B(t)]$ to be invertible, it therefore follows that the equivalent control corresponds to $u_{eq}(t) = K(t)y(t) - \Delta(y(t), t)$ as desired. □

Remark 8.14. As is clear from the proof, this statement can easily be extended to any real-reducible, linear, time-varying system.

Recall from Theorem 8.10 that a real FL factorization always exists for $c = 2$, whereas the existence of a T-periodic factorization follows from Lemma 8.11. The following statements demonstrates that a $2T$-periodic factorization may in fact result in a T-periodic $S(t)$.

Corollary 8.15. *Let the triplet $(L(t), F, Y)$ denote a real, $2T$-periodic FL factorization of the closed-loop system (8.9) as in Theorem 8.10 and let the conditions of Proposition 8.13 hold. Then the matrix function $S(t) := \hat{S}L^{-1}(t)$ is T-periodic if $\hat{S} = \hat{S}Y$.* □

This is just a consequence of the fact that $L^{-1}(T) = Y$. For $\hat{S} = \hat{S}Y$ to be satisfied, however, it is clear that the rows of $\hat{S}$ must be linear combinations of the left eigenvectors of Y corresponding to its unitary eigenvalues. This may of course also sometimes be possible even when $Y \neq I_{\bar{n}}$ as $Y^2 = \mathbf{I}_{\bar{n}}$ (the matrix Y is involutory), and hence all its eigenvalues satisfy $\lambda_Y^2 = 1$.

8.4 Sliding manifold design for nonlinear systems

By taking inspiration from the statements in the previous sections, our aim will now be to design robustifying feedback extensions for periodic orbits of a class of nonlinear dynamical systems.

8.4.1 Problem formulation

Consider the nonlinear control-affine system (4.1) now subject to an unknown matched perturbation:

$$\dot{x} = f(x) + B(x)\left(u + \Delta(x, t)\right). \tag{8.18}$$

As before, $x(t) \in \mathbb{R}^n$ denotes the state at time $t \in \mathbb{R}_{\geq 0}$, and $u(t) \in \mathbb{R}^m$ represents the control inputs, with $m \leq n$. Moreover, $f : \mathbb{R}^n \to \mathbb{R}^n$ is assumed to be $\mathcal{C}^2$, while the columns of $B(\cdot) \in \mathbb{R}^{n\times m}$, denoted $b_i : \mathbb{R}^n \to \mathbb{R}^n$, $i \in \{1, \ldots, m\}$, are linearly independent and (locally) Lipschitz continuous. As in the previous sections, the perturbation term $\Delta : \mathbb{R}^n \times \mathbb{R}_{\geq 0} \to \mathbb{R}^m$, consisting of system uncertainties and unknown external disturbances, is assumed to be piecewise continuous in both its arguments (with the respective sets of any discontinuity points having zero Lebesgue measure); moreover, it has a known upper bound $\Delta_M > 0$, that is,[5]

$$\sup_{x\in\mathbb{R}^n, t\in\mathbb{R}_{\geq 0}} \|\Delta(x,t)\| \leq \Delta_M. \tag{8.19}$$

It is assumed that a bounded, T-periodic solution $x_\star(t) = x_\star(t+T)$ of the nominal (i.e. perturbation-free) and undriven (i.e. $u \equiv 0$) system is known for some $T > 0$, whose orbit we denote by

$$\mathcal{O} := \big\{x \in \mathbb{R}^n \,|\; x = x_\star(t),\ t \in [0,T)\big\}. \tag{8.20}$$

That is, $\dot{x}_\star(t) = f(x_\star(t))$ and $0 < \|f(x_\star(t))\| < \infty$ hold for all $t \in \mathbb{R}_{\geq 0}$. It will further be assumed that a $\mathcal{C}^2$-mapping $k : \mathbb{R}^n \to \mathbb{R}^m$ is known, satisfying $k(x_\star(t)) \equiv 0$, which (locally) renders $x_\star(t)$ an exponentially orbitally stable solution (see Def. 2.2) of the nominal closed-loop system, described by

$$\dot{\chi} = f(\chi) + B(\chi)k(\chi), \quad \chi \in \mathbb{R}^n. \tag{8.21}$$

The fact that $k(\cdot)$ renders $x_\star(\cdot)$ an exponentially orbitally stable solution of the disturbance-free system (8.21) does of course in no way guarantee that it will also be an (asymptotically) orbitally stable solution of (8.18) in the presence of the matched perturbation given by $B(x)\Delta(x,t)$. In fact, it may no longer be a solution of the closed-loop system at all. For this reason, we consider the task of utilizing the knowledge of $k(\cdot)$ to instead design a *robust* controller which also renders $x_\star(\cdot)$ an asymptotically orbitally stable solution of the system (8.18).

To utilize the SMC methodology, our aim will be to construct a time-invariant switching function, $x \mapsto \sigma(x)$, $\sigma : \mathbb{R}^n \to \mathbb{R}^m$, which has the property that its zero-level set, given by

$$\Sigma := \{x \in \mathbb{R}^n :\ \sigma(x) = \mathbf{0}_{m\times 1}\}, \tag{8.22}$$

defines a sliding manifold upon which all solutions sufficiently close to the desired orbit converges to it. As in the previous sections, we will again turn to Utkin's equivalent control concept in order to help us construct such a switching function. Using our prior knowledge of the nominal feedback $k(\cdot)$, the problem we now are aiming to solve can be formulated as follows:

[5] While the restrictions upon $\Delta(\cdot)$ are here taken to be quite conservative for simplicity's sake, they can be somewhat relaxed. For example, the proposed scheme can be extended to a disturbance term of the form $\Delta : \mathbb{R}^n \times \mathbb{R}^m \times \mathbb{R}_{\geq 0} \to \mathbb{R}^m$, for which a (Filippov) solution to the unforced system (8.18) (locally) exists and $\|\Delta(x,u,t)\| \leq \Delta_0 + \Delta_u\|u\| + \alpha(x,t)$ is satisfied given known constants $\Delta_0, \Delta_u \in \mathbb{R}_{\geq 0}$ and a known class $\mathcal{K}$-function $\alpha : \mathbb{R}^n \times \mathbb{R}_{\geq 0} \to \mathbb{R}_{\geq 0}$.

Problem 8.16. *Find a time-invariant, $\mathcal{C}^2$-smooth switching function $\sigma : \mathbb{R}^n \to \mathbb{R}^m$ such that there exists a tubular neighborhood of the orbit $\mathcal{O}$, within which, when restricted to the* sliding manifold (8.22)*, the resulting equivalent control for the system* (8.18) *is of the form*

$$u_{eq} = \hat{k}(x) - \Delta(x, t) \tag{8.23}$$

where $\hat{k} : \mathbb{R}^n \to \mathbb{R}^m$ is a $\mathcal{C}^1$ mapping satisfying, for all $y \in \mathcal{O}$,

$$\hat{k}(y) \equiv 0 \qquad \text{and} \qquad D\hat{k}(y) = Dk(y).$$

That is, the first-order approximations of $\hat{k}(\cdot)$ and $k(\cdot)$ along $\mathcal{O}$ are equal.

Remark 8.17. The use of Utkin's equivalent control method ensures that the control "experienced" by the system when confined to the manifold (8.22) corresponds to (8.23), which is both disturbance rejecting and asymptotically orbitally stabilizing. Thus, any motion (of reduced order) of the system (8.18) in sliding mode may be considered to evolve as if $\dot{x} = f(x) + B(x)\hat{k}(x)$. The mapping $\hat{k}(\cdot)$ is considered rather than the known feedback $k(\cdot)$ as it allows for an added level of flexibility in the design of the switching function (adding or removing higher order terms) while still maintaining the local orbitally stabilizing feedback properties.

Notice also the absence of an explicit form of a sliding mode control law in Problem 8.16. Indeed, as previously stated, the main focus of this chapter is not the design of sliding mode controllers per se, but rather the design of sliding manifolds on which the orbit (8.20) is asymptotically stable. Of course, if such a manifold is given, then some sort of sliding mode control law—be that a relay-type, unit-vector, higher-order, etc.—is necessary in order to bring the system's states onto it in finite time. While the choice of such a control law is important in regard to aspects such as, for example, chattering attenuation and the required assumptions upon the unknown disturbance term, it does not affect the corresponding equivalent control (8.23), which instead is completely determined by the choice of switching function. Hence, the tasks of designing and stabilizing the corresponding sliding manifold may be considered separately, with our focus in this thesis mainly on the former.

To clearly see why a solution to Problem 8.16 is desirable, we can study the ideal sliding equation. It is obtained by inserting the equivalent control into the dynamical system (8.18):

$$\dot{x}_\sigma = f(x_\sigma) + B(x_\sigma)\hat{k}(x_\sigma).$$

The corresponding first-order approximation system about the solution $x_\star(\cdot)$ is necessarily equivalent to that of the nominal system (8.21), namely $\dot{\boldsymbol{\delta}}_x = A_{cl}(t)\boldsymbol{\delta}_x$. By the Andronov–Vitt theorem (see Thm. 2.8), it follows that $x_\star(\cdot)$ is an exponentially orbitally stable solution of the ideal sliding mode equation. As we can tie the solutions of this system to those of (8.18) when in sliding mode using Utkin's equivalent control method [60, 62], the following statement can be concluded:

Proposition 8.18. *Let $\sigma : \mathbb{R}^n \to \mathbb{R}^m$ be a solution to Problem 8.16. Then there exists a tubular neighborhood $\mathcal{N}$ of the orbit $\mathcal{O}$, such that if the states of the system* (8.18) *are restricted to $\Sigma := \{x \in \mathbb{R}^n : \ \sigma(x) = \mathbf{0}_{m\times 1}\}$ within $\mathcal{N}$, then all solutions of* (8.18) *converges to $\mathcal{O}$, rendering $x_\star(\cdot)$ exponentially orbitally stable in the ideal sliding mode.* □

As previously mentioned, our suggested approach for solving this problem is, roughly speaking, to construct the switching function such that the corresponding sliding manifold corresponds to a particular real, invariant subspace of the first-order approximation system. Due to the connection with the linearized system, we therefore begin by defining the following continuous and bounded, T-periodic matrix functions:

$$B_t(t) := B(x_\star(t)), \quad K(t) := Dk(x_\star(t)), \quad A_{cl}(t) := Df(x_\star(t)) + B_t(t)K(t).$$

Moreover, we let the corresponding state-transition matrix (STM) $\Phi_{A_{cl}}(\cdot)$ and Monodromy matrix $\mathfrak{M}_{A_{cl}}$ be defined according to (8.10) and (8.11), respectively. With this notation in place, the following statement provides sufficient conditions for a switching to be a solution to Problem 8.16.

Lemma 8.19. *Let $\sigma : \mathbb{R}^n \to \mathbb{R}^m$ be $\mathcal{C}^2$, and define the T-periodic matrix function $S(t) := D\sigma(x_\star(t))$. If $\sigma(x_\star(t)) \equiv 0$, as well as*

1. $\det[S(t)B_t(t)] \neq 0$,
2. $S(t)x = 0 \implies \Big[\dot{S}(t) + S(t)A_{cl}(t)\Big]\, x \equiv 0$,

are satisfied for all $t \in [0, T)$, then $\sigma(\cdot)$ is a solution to Problem 8.16.

Remark 8.20. It is not difficult to see that condition 2. together with the fact that $S(t) = D\sigma(x_\star(t))$ must be T-periodic, implies by Lemma 8.9 that $S(t)$ must be a left annihilator of the range space of $\Phi_{A_{cl}}(t, 0)X_0$, with X_0 a basis of a real, invariant subspace of the Monodromy matrix $\mathfrak{M}_{A_{cl}}$ of codimension m. This has an important implication: only the eigenvalues of the Monodromy matrix that correspond to its subspace with basis X_0

need to have a magnitude strictly less than one. Hence, there may exist a sliding manifold on which all solution are exponentially orbitally stable even though the feedback $k(\cdot)$ is not fully orbitally stabilizing, but only stabilizes a particular subspace of the first-order approximation system.

Proof. In order to show convergence to $\mathcal{O}$ within some nonzero tubular neighborhood when restricted to Σ, let $\tau : \mathbb{R}^n \to [0, T)$ be the solution to

$$\tau(x) = \arg\min_{t\in[0,T)} \|x - x_\star(t)\|^2, \tag{8.24}$$

for a given $x \in \mathbb{R}^n$ about $\mathcal{O}$. Clearly $\tau(\cdot)$ is a projection operator onto the time-parameterized curve $x_\star(t)$. Hence, from Proposition 4.9 (see also the work of Leonov [54]), the time derivative of $\tau = \tau(x)$ is well defined in a neighborhood of $\mathcal{O}$. Moreover, the equation governing its dynamics may be written in the form

$$\dot{\tau} = 1 + f_{||}(\tau, \tilde{x}) + B_{||}(\tau, \tilde{x})u$$

where $\tilde{x} := x - x_\star(\tau)$ and $f_{||}(\tau, 0) = 0$. Recall also from Lemma 4.29 that a $\mathcal{C}^2$ function $x \mapsto h(x)$ can, sufficiently close to $\mathcal{O}$, be equivalently rewritten in the following form using $\tau(\cdot)$ and $\tilde{x}$:

$$h(x) = h(x_\star(\tau)) + Dh(x_\star(\tau))\tilde{x} + R_h(x).$$

Here R_h is $\mathcal{C}^1$ and satisfies $\|R_h(x)\| = O(\|\tilde{x}\|^2)$. We can therefore write

$$\begin{aligned}\sigma(x) &= S(\tau)\tilde{x} + R_\sigma(x),\\ f(x) &= f(x_\star(\tau)) + A_t(\tau)\tilde{x} + R_f(x),\\ k(x) &= K(\tau)\tilde{x} + R_k(x),\end{aligned}$$

with $A_t(\tau) := Df(x_\star(\tau))$ and where we have used that $\sigma(x_\star(t)) = k(x_\star(t)) \equiv \mathbf{0}_{m\times 1}$. Thus, by differentiating $\sigma(\cdot)$ with respect to time one obtains

$$\dot{\sigma}(x) = \dot{S}(\tau)\tilde{x} + S(\tau)(\dot{x} - \dot{x}_\star(\tau)) + \frac{d}{dt}R_\sigma(x).$$

Inserting for $\dot{x}$, as well as using the fact that $S(\tau)\dot{x}_\star(\tau) = S(\tau)\dot{\tau}\frac{d}{d\tau}x_\star(\tau) \equiv 0$, this becomes

$$\begin{aligned}\dot{\sigma}(x) &= \dot{S}(\tau)\tilde{x} + S(\tau)\big(f(x) + B(x)\big[u + \Delta\big]\big) + \frac{d}{dt}R_\sigma(x)\\ &= \Big[\dot{S}(\tau) + S(\tau)A_t(\tau)\Big]\,\tilde{x} + S(\tau)B(x)\big[u + \Delta\big] + \hat{R}\\ &= \Big[\dot{S}(\tau) + S(\tau)A(\tau)\Big]\,\tilde{x} + S(\tau)\left(B_t(\tau) + \tilde{B}(x)\right)\big[u + \Delta\big] + \hat{R},\end{aligned}$$

where $\tilde{B}(x) := B(x) - B(x_\star(\tau))$, $\hat{R} := S(\tau)R_f + \frac{d}{dt}R_\sigma$. By adding and subtracting $S(\tau)B_t(\tau)K(\tau)\tilde{x}$, the above may be equivalently rewritten as

$$\begin{aligned}\dot{\sigma}(x) =& \Big[\dot{S}(\tau) + S(\tau)A_{cl}(\tau)\Big]\tilde{x} - S(\tau)B_t(\tau)K(\tau)\tilde{x} \\ &+ S(\tau)\big(B_t(\tau) + \tilde{B}(x)\big)\big[u + \Delta\big] + \hat{R}.\end{aligned}$$

With this in mind, suppose the sliding manifold Σ has been rendered forward invariant such that $\sigma(x) = S(\tau)\tilde{x} + R_\sigma(x) \equiv 0$. This implies that $\tilde{x} = X_S(\tau) - S^\dagger(\tau)R_\sigma(x)$ for some $X_S(\tau) \in \ker\{S(\tau)\}$, and in which $S^\dagger(\tau)$ is a full-rank right inverse of $S(\tau)$ such that $S(\tau)S^\dagger(\tau) = \mathbf{I}_m$ for all $\tau \in [0, T)$. By now proceeding according to the equivalent control approach [62], we set $\dot{\sigma}(x) \equiv 0$. Hence, by using condition 2. in Lemma 8.19, the equivalent control u_{eq} must therefore satisfy

$$\begin{aligned}&\big[\mathbf{I}_m + \big(S(\tau)B_t(\tau)\big)^{-1}S(\tau)\tilde{B}(x)\big](u_{eq} + \Delta) \\ &\quad = K(\tau)\tilde{x} - \big(S(\tau)B_t(\tau)\big)^{-1}\Big[\Big(\dot{S}(\tau) + S(\tau)A_{cl}(\tau)\Big)S^\dagger(\tau)R_\sigma(x) + \hat{R}\Big].\end{aligned}$$

Since we have assumed the columns of $B(\cdot)$ to be locally Lipschitz in some region containing the orbit, there necessarily exists a Lipschitz constant $l_B > 0$ such that $\|\tilde{B}(x)\| \le l_B\|\tilde{x}\|$ holds therein. It follows that for sufficiently small $\tilde{x}$, the matrix function $\Lambda(x) := \mathbf{I}_m + (S(\tau)B_t(\tau))^{-1}S(\tau)\tilde{B}(x)$ is nonsingular. This, in turn, implies that, locally, the equivalent control is of the form $u_{eq} = \hat{k}(x) - \Delta$ with

$$\begin{aligned}\hat{k}(x) := \Lambda^{-1}(x)\Big(K(\tau)\tilde{x} - \big(S(\tau)B_t(\tau)\big)^{-1} \\ \times\Big[\Big(\dot{S}(\tau) + S(\tau)A_{cl}(\tau)\Big)S^\dagger(\tau)R_\sigma(x) + \hat{R}\Big]\Big).\end{aligned}$$

What remains is therefore to show that $\hat{k}(\cdot)$ is equal to $k(\cdot)$ in the first approximation along $\mathcal{O}$. Indeed, if this is the case, then necessarily $u_{eq} = -\Delta(x_\star(t), t)$ on $\mathcal{O} \subset \Sigma$, illustrating the insensitivity to the matched disturbance. To this end, we first note that $\Lambda^{-1}(x_\star(t)) = \mathbf{I}_m$ for all $t \in [0, T)$. Moreover, since the Jacobian matrix of $\tilde{x}$ evaluated along the nominal motion is given by $D\tilde{x}(x_\star(t)) = \mathbf{I}_n - \dot{x}_\star(t)\dot{x}_\star^\mathsf{T}(t)/\|\dot{x}_\star(t)\|^2$ (see Prop. 4.9), as well as that $\|K(t)\dot{x}_\star(t)\| \equiv 0$ for all $t \in [0, T)$, the relation $K(t)D\tilde{x}(x_\star(t)) \equiv K(t)$ always holds. Since all the terms inside the brackets on the right-hand inside of the expression for $\hat{k}(\cdot)$ are necessarily of order no less than two with respect to $\tilde{x}$ as $\|\tilde{x}\| \to 0$, we can conclude that $D\hat{k}(x_\star(t)) \equiv K(t)$, and thus $\hat{k}(\cdot)$ equals $k(\cdot)$ in the first-order approximation as desired. This concludes the proof. $\square$

Although Lemma 8.19 provides sufficient conditions for a mapping to be a solution to Problem 8.16, it does not provide a constructive procedure for obtaining such a switching function. We therefore demonstrate next how one can design such a function using a Floquet–Lyapunov transformation, by first transforming the orbital stabilization problem into the task of stabilizing the origin of a set of transverse coordinates.

8.4.2 Nonlinear switching function design

Preliminaries: Transverse coordinates and projection operators

This chapter's main results utilizes the three principal components of this thesis which were introduced in Chapter 4: a projection operator, a set of transverse coordinates, and the corresponding transverse linearization. For the sake of convenience, we briefly recall the main aspects of each of these components, as well as the notion of an s-parameterization, next.

s-parameterization: Let the curve $x_s : \mathcal{S} \to \mathcal{O}$, with $\mathcal{S} := [0, s_T)$, denote a known s-parameterization of the periodic orbit (8.20) as by Assumption 4.3; namely, $s \mapsto x_s(s)$ is $\mathcal{C}^2$-smooth, as well as satisfies

$$\|\mathcal{F}(s(t))\| > 0 \quad \text{and} \quad x_\star(t) \equiv x_s(s(t)) \tag{8.25}$$

for all $t \in [0, T)$, with $\mathcal{F}(s) := \frac{d}{ds} x_s(s)$. Here $s : [0, T) \to \mathcal{S}$ is a homeomorphism, strictly monotonically increasing in time, with its nominal time evolution over $\mathcal{S}$ governed by the autonomous differential equation

$$\dot{s} = \rho(s), \tag{8.26}$$

given a known strictly-positive, $\mathcal{C}^1$ function $\rho : \mathcal{S} \to \mathbb{R}_{\geq 0}$ such that $f(x_s(s)) = \rho(s)\mathcal{F}(s)$. Thus $s = s(t)$ can be considered as a rescaling of time along the orbit $\mathcal{O}$, with $s = t$ if one takes $\rho = 1$ on $[0, T)$.

Projection operator: We assume knowledge of a $\mathcal{C}^2$ projection operator $p : \mathbb{R}^n \supset \mathfrak{X} \to \mathcal{S}$ as by Definition 4.5. That is, within the open tubular neighborhood $\mathfrak{X}$ of the orbit $\mathcal{O}$, $p(\cdot)$ projects any $x \in \mathfrak{X}$ onto a unique point on $\mathcal{S}$ and satisfies $s \equiv p(x_s(s))$ for all $s \in \mathcal{S}$.

Transverse coordinates: In order to also have some measure of the deviation from the orbit, we will further assume that a set of $(n-1)$ transverse coordinates, denoted $z_\perp = z_\perp(x)$, are known for the orbit $\mathcal{O}$. Recall from Definition 4.11 that this is equivalent to the vector-valued function $z_\perp : \mathbb{R}^n \to \mathbb{R}^{n-1}$ being of class $\mathcal{C}^2$, as well as satisfying $\|z_\perp(y)\| = 0$ and $\operatorname{rank}[Dz_\perp(y)] = n - 1$ for all $y \in \mathcal{O}$.

Transverse linearization: Given such a set of transverse coordinates, the corresponding transverse dynamics are given by

$$\frac{d}{dt}z_\perp = f_\perp(x) + g_\perp(x)(u + \Delta(x,t)), \tag{8.27}$$

where $f_\perp(x) := Dz_\perp(x)f(x)$ and $B_\perp(x) := Dz_\perp(x)g(x)$. A key part of our approach is to utilize the transverse linearization corresponding to the perturbation-free system (i.e. for $\Delta = 0$). That is, the linear, T-periodic system (see Thm. 4.22)

$$\dot{\boldsymbol{\delta}}_{z_\perp} = \mathcal{A}_\perp(s(t))\boldsymbol{\delta}_{z_\perp} + \mathcal{B}_\perp(s(t))u, \tag{8.28}$$

where $\mathcal{A}_\perp(s) := Df_\perp(x_s(s))\mathcal{Z}_\perp^\dagger(s)$ and $\mathcal{B}_\perp(s) := g_\perp(x_s(s))$ for $\mathcal{Z}_\perp(s) := Dz_\perp(x_s(s))$.

With the above in mind, note that we may apply Lemma 4.15 as to rewrite the stabilizing feedback $k(\cdot)$ in terms of the pair $(p, z_\perp)$ close to $\mathcal{O}$ (see also Prop. 4.26):

$$k(x) = K_\perp(p(x))z_\perp(x) + R_k(x) \tag{8.29}$$

where $\|R_k(x)\| = O(\|z_\perp\|^2)$ and

$$K_\perp(s) := Dk(x_s(s))\mathcal{Z}_\perp^\dagger(s). \tag{8.30}$$

Hence, by using (8.28) and (8.26), the transverse linearization of the unperturbed closed-loop system (8.21) may be written as a differential equation in the independent variable s:

$$\frac{d}{ds}\chi_\perp = \frac{1}{\rho(s)}\left[\mathcal{A}_\perp(s) + \mathcal{B}_\perp(s)K_\perp(s)\right]\chi_\perp =: \frac{1}{\rho(s)}\mathcal{A}_\perp^{cl}(s)\chi_\perp. \tag{8.31}$$

That is, $\chi_\perp(s(t)) = \boldsymbol{\delta}_{z_\perp}(t)$, with $\boldsymbol{\delta}_{z_\perp}(t)$ a solution to (8.28) under $u = K_\perp(s(t))\boldsymbol{\delta}_{z_\perp}(t)$. In the following, we will denote by $\Phi_\perp^{cl}(\cdot)$ the state transition matrix corresponding to (8.31):

$$\frac{d}{ds}\Phi_\perp^{cl}(s) = \frac{1}{\rho(s)}\mathcal{A}_\perp^{cl}(s)\Phi_\perp^{cl}(s), \quad \Phi_\perp^{cl}(0) = \mathbf{I}_{n-1}, \quad s \in \mathcal{S}. \tag{8.32}$$

Recall now from theorems 2.10 and 4.22 the fact that the periodic orbit of (8.21) being (locally) exponentially stable is equivalent to the exponential stability of the origin of transverse linearization (8.31). Moreover, recall that this, in turn, is equivalent to all the $(n-1)$ characteristic multipliers, i.e. the eigenvalues of the Monodromy matrix[6], $\mathfrak{M}_\perp^{cl} := \Phi_\perp^{cl}(s_T)$, having magnitudes strictly less than one. Our aim will now be to utilize this fact as to construct a matrix function $S_\perp : \mathcal{S} \to \mathbb{R}^{m\times n}$ solving Problem 8.8 for linear-periodic system (8.31), such that the function $\sigma(x) := S_\perp(p(x))z_\perp(x)$ is a solution to Problem 8.16.

Main statement

We are now ready to state the main result of this chapter.

Theorem 8.21. *Suppose there exists a $\mathcal{C}^1$-smooth, nonsingular, s_T-periodic matrix function $L : \mathcal{S} \to \mathbb{R}^{(n-1)\times(n-1)}$ and a Hurwitz matrix $F \in \mathbb{R}^{(n-1)\times(n-1)}$ such that the state transitions matrix of* (8.31), *defined in* (8.32), *admits the real, s_T-periodic FL factorization:*

$$\Phi_\perp^{cl}(s) = L(s)e^{sF}.$$

Further suppose that there exists a full-rank matrix $\hat{S} \in \mathbb{R}^{m\times n}$ such that

1. $\det[\hat{S}L^{-1}(s)\mathcal{B}_\perp(s)] \neq 0,$
2. $\hat{S}z = 0 \implies \hat{S}Fz = 0,$

for all $s \in \mathcal{S}$. Then, for any projection operator $p(\cdot)$ (see Def. 4.5), the function

$$\sigma(x) := S_\perp(p(x))z_\perp(x), \quad \textit{with} \quad S_\perp(s) := \hat{S}L^{-1}(s), \tag{8.33}$$

solves Problem 8.16. As a consequence, the solutions of the system (8.21) *when its states are restricted to*

$$\Sigma := \{x \in \mathbb{R}^n : \ \sigma(x) = \mathbf{0}_{m\times 1}\}$$

sufficiently close the periodic orbit $\mathcal{O}$ converge to $\mathcal{O}$ at an exponential rate.

Remark 8.22. The existence of a real s_T-periodic FL factorization is assumed in Theorem 8.21 rather than a $2s_T$-periodic factorization, which, as we recall from Theorem 8.10, is always guaranteed to exist. This restriction is due to the image of the projection operator $p(\cdot)$ being equal to $[0, s_T)$. More precisely, given a triplet $(L(t), F, Y)$ corresponding to a real, $2s_T$-periodic factorization (see, e.g., Theorem 8.10 or Theorem 3.1 in [232]), we would be limited to only recovering the subinterval $[0, s_T)$ through $p(\cdot)$,

[6]Note here that, while the state transition matrix with s-parameterization is only defined for $s \in \mathcal{S}$, one can simply take $\hat{\Phi}_\perp^{cl}(t, 0) := \Phi_\perp^{cl}(s(t))$ for $t \in [0.T)$, such that, e.g., $\hat{\Phi}_\perp^{cl}(t + kT, 0) = \Phi_\perp^{cl}(s(t))(\mathfrak{M}_\perp^{cl})^k$ for $t \in [0, T)$.

but by our definition of $S_\perp(s)$ and considering a factorization as in Theorem 8.10, we would naturally require continuity of $S_\perp(\cdot)$ at $s = s_T$. This then corresponds to the same condition as in Corollary 8.15, namely

$$S_\perp(s_T) = \hat{S}Y = S_\perp(0) = \hat{S}.$$

Hence, the rows of $\hat{S}$ must then be linear combinations of the eigenvectors of Y corresponding to its unitary eigenvalues, which is trivially true whenever $Y = \mathbf{I}_{n-1}$, i.e. when one has an s_T-periodic factorization.

Remark 8.23. The existence of an FL factorization of course does not imply the existence of a (unique) real, invariant subspace of F satisfying the conditions of the Theorem. See the discussion after Lemma 8.2 for further details in this regard.

Remark 8.24. In the special cases when the dynamical system (8.18) is so-called *transversely feedback linearizable* [30, 146], then one can instead simply utilize the theory outlined in Section 8.2, in particular Lemma 8.2, in order to find a solution to Problem 8.16. More specifically, since there then exist (at least locally) transverse coordinates and a smooth feedback transformation $u = a(x)+b(x)v$, $v \in \mathbb{R}^m$, such that the transverse dynamics (8.27) can be written as $\frac{d}{dt}z_\perp = Az_\perp + B\big(v + (b(x))^{-1}\Delta(x,t)\big)$, where the pair (A, B) is controllable, the statements in Section 8.2 are readily applicable.

Proof. It is here enough to show that (8.33) satisfies the requirements in Lemma 8.19. In this regard, $\|\sigma(x_s(s))\| \equiv 0$ is trivially satisfied due to the fact that $\|z_\perp(x_s(s))\| \equiv 0$, whereas

$$D\sigma(x_s(s))B(x_s(s)) = S_\perp(s)Dz_\perp(x_s(s))B(x_s(s)) = S_\perp(s)\mathcal{B}_\perp(s)$$

demonstrates that $\operatorname{rank}[S(t)B_t(t)] = m$ always holds as well.

In order to show that Condition 2. in Lemma 8.19 also is satisfied for any $x \in \ker\{S(s(t))\}$, we note that the equivalent expression to (8.17) for (8.31) can be written as

$$\rho(s)\frac{d}{ds}L^{-1}(s) = -L^{-1}(s)\mathcal{A}_\perp^{cl}(s) + FL^{-1}(s). \tag{8.34}$$

Recall here that $\rho(s)$ is such that $\dot{s} = \rho(s)$, and must consequently equal $\rho(s) = \|f(x_s(s))\|/\|\mathcal{F}(s)\|$ for $\mathcal{F}(s) := \frac{d}{ds}x_s(s)$. By differentiating $S(t) = D\sigma(x_\star(t))$, we therefore obtain (using the notation $\mathcal{Z}_\perp(s) := Dz_\perp(x_s(s))$)

$$\begin{aligned}\dot{S}(s(t)) &= \frac{d}{dt}\left(\hat{S}L^{-1}(s)\mathcal{Z}_\perp(s)\right)\\ &= S_\perp(s)\left[\big(-\mathcal{A}_\perp^{cl}(s) + L(s)FL^{-1}(s)\big)\mathcal{Z}_\perp(s) + \rho(s)\frac{d}{ds}\mathcal{Z}_\perp(s)\right].\end{aligned}$$

Now, since $S(s) = \hat{S}L^{-1}(s)\mathcal{Z}_\perp(s)$, it follows that $x \in \ker\{S(s)\}$ corresponds to either $x \in \mathrm{span}\{f(x_s(s))\}$ or $x = \mathcal{Z}_\perp^\dagger(s)L(s)(\mathbf{I}_n - \hat{S}^\dagger\hat{S})x$. Taking therefore $x = f(x_s(s))$ and using that $\mathcal{Z}_\perp(s)f(x_s(s)) \equiv 0$, it is easy to see that Condition 2. in Lemma 8.19 is satisfied due to the fact that

$$\frac{d}{dt}\left[\mathcal{Z}_\perp(s)f(x_s(s))\right] = \rho(s)\left[\frac{d}{ds}\mathcal{Z}_\perp(s)\right]f(x_s(s)) + \mathcal{Z}_\perp(s)A_{cl}(s)f(x_s(s)) = 0.$$

Hence we need only demonstrate that the following always holds:

$$\left[\dot{S}(s) + S_\perp(s)\mathcal{Z}_\perp(s)A_{cl}(s)\right]\mathcal{Z}_\perp^\dagger(s)L(s)(\mathbf{I}_n - \hat{S}^\dagger\hat{S}) = \mathbf{0}_n. \tag{8.35}$$

From the definition of the matrix function $\mathcal{A}_\perp^{cl}$ (see (8.31)), it can be shown that $\mathcal{A}_\perp^{cl}(s) = \left[\mathcal{Z}_\perp(s)A_{cl}(s) + \rho\frac{d}{ds}Dz_\perp(x_s(s))\right]\mathcal{Z}_\perp^\dagger(s)$. Using this together with the above expression for $\dot{S}(s)$, (8.35) reduces to

$$S_\perp(s)\left[L(s)FL^{-1}(s)\mathcal{Z}_\perp(s)\right]\mathcal{Z}_\perp^\dagger(s)L(s)(\mathbf{I}_n - \hat{S}^\dagger\hat{S}) = \hat{S}F(\mathbf{I}_n - \hat{S}^\dagger\hat{S}) = 0$$

where we have used that $\hat{S}Fz \equiv 0$ for all $z \in \ker\{\hat{S}\} = \{z \in \mathbb{R}^n : z = (\mathbf{I}_n - \hat{S}^\dagger\hat{S})z\}$, This concludes the proof.[7] $\square$

8.4.3 Some comments on sliding mode control design

Although it is the design of sliding manifolds which is the main focus of this chapter, we will in this section also partly demonstrate how the presented scheme allows for adding a robustifying feedback extension to an existing orbitally stabilizing feedback. We begin by providing the following statement, which acts as a useful stepping stone towards the design of such extensions.

Lemma 8.25. *For some projection operator $x \mapsto p(x)$ (see Def. 4.5), let*

$$\sigma(x) := S_\perp(p(x))z_\perp(x) = \hat{S}L^{-1}(p(x))z_\perp(x)$$

be a switching function according to Theorem 8.21. If the controller in (8.18) *is taken as*

$$u = k(x) + v, \quad v \in \mathbb{R}^m, \tag{8.36}$$

[7]Alternatively, the statement can be proven by utilizing the fact that (8.31) is real reducible (the existence of a real FL factorization has been assumed) in order to invoke Theorem 25 in the work of Massera [39]. This allows one to conclude that the origin of the transverse dynamics (8.27) is locally asymptotically stable when in sliding mode, and, therefore, by Proposition 1.5 in the paper by Hauser and Chung [41], that the solution $x_\star(\cdot)$ is exponentially orbitally stable.

then the dynamics of $\sigma(x)$ outside of the sliding manifold Σ are governed by

$$\dot{\sigma} = \mathfrak{A}_\sigma \sigma + S_\perp(p)\big[\mathcal{B}_\perp(p) + \tilde{B}_\perp(z_\perp, p)\big]\big(v + \Delta(x,t)\big) + R_\sigma(z_\perp, p), \quad (8.37)$$

with $p = p(x)$, and where $\mathfrak{A}_\sigma := \hat{S}F\hat{S}^\dagger \in \mathbb{R}^{m\times m}$ is Hurwitz, while $\|\tilde{B}_\perp(z_\perp, s)\| = O(\|z_\perp\|)$ and $\|R_\sigma(z_\perp, s)\| = O(\|z_\perp\|^2)$ for all $s \in \mathcal{S}$.

Remark 8.26. The known nominal feedback $k(x)$ does not have to be included in (8.36) due to the equivalent control (8.23) when confined to the sliding manifold. However, its inclusion has two clear benefits: 1) it allows reducing the magnitude of the gains used in the (discontinuous) extension v, which may help to alleviate chattering; and 2) it can increase the rate of convergence to the sliding manifold, especially when the system states are far away from it.

Proof. Firstly, recall from (8.29) that we may write $k(x) = K_\perp(p(x))z_\perp + R_k(x)$ in which $\|R_k(x)\| = O(\|z_\perp\|^2)$. Using this, together with Lemma 4.15 and the fact that $f_\perp(\cdot)$ is continuously differentiable (as $f(\cdot)$ and $z_\perp(\cdot)$ are assumed to be of class $\mathcal{C}^2$) we may then rewrite (8.27) in the following equivalent form using again the shorthand notation $p = p(x)$:

$$\frac{d}{dt}z_\perp = \mathcal{A}_\perp^{cl}(p)z_\perp + \left[\mathcal{B}_\perp(p) + \tilde{g}_\perp(z_\perp, p)\right](v + \Delta(x,t)) + R_\perp. \quad (8.38)$$

Here $R_\perp(z_\perp, s) := R_{f_\perp}(z_\perp, s) + B(x)R_k(z_\perp, p)$ and $\tilde{g}_\perp(z_\perp, s) := g_\perp(z_\perp, s) - \mathcal{B}_\perp(s)$ satisfy, respectively, $\|R_\perp(z_\perp, s)\| = O(\|z_\perp\|^2)$ and $\|\tilde{g}_\perp(z_\perp, s)\| \leq l_{\tilde{g}_\perp}\|z_\perp\|$ for all $s \in \mathcal{S}$. Note that $l_{\tilde{g}_\perp} > 0$ is a Lipschitz constant for $\tilde{g}_\perp$, whose (local) existence is guaranteed as $Dz_\perp$ is of class $\mathcal{C}^1$ and the columns of $B(\cdot)$ are locally Lipschitz.

With the above in mind, we can differentiate (8.33) with respect to time and use (8.34) to obtain

$$\begin{aligned}\dot{\sigma} &= \dot{S}_\perp(p)z_\perp + S_\perp(p)\left[\mathcal{A}_\perp^{cl}(p)z_\perp + \left[\mathcal{B}_\perp(p) + \tilde{g}_\perp(z_\perp, p)\right](v + \Delta) + R_\perp\right] \\ &= \hat{S}\left[-L(p)^{-1}\mathcal{A}_\perp^{cl}(p) + FL^{-1}(p)\right]\frac{\dot{p}}{\rho(p)}z_\perp \\ &\quad + S_\perp(p)\left[\mathcal{A}_\perp^{cl}(p)z_\perp + \left[\mathcal{B}_\perp(p) + \tilde{g}_\perp(z_\perp, p)\right](v + \Delta) + R_\perp\right].\end{aligned}$$

As $\dot{p} = Dp(x)\dot{x}$ and $\rho(s) = Dp(x_s(s)f(x_s(s)) = f(x_s(s))/\|\mathcal{F}(s)\|$, we may here, in the same manner as with (8.38), use Lemma 4.15 in order to write

$$\begin{aligned}\dot{p} =& \rho(p) + Df_\parallel(x_s(p))\big(\mathbf{I}_n - \mathcal{F}(p)Dp(x_s(p))\big)\mathcal{Z}_\perp^\dagger(p)z_\perp \\ &+ B_\parallel(x)(v + \Delta(x,t)) + R_{f_\parallel}(z_\perp, p),\end{aligned} \quad (8.39)$$

where $f_{\|}(x) := Dp(x)f(x)$ and $B_{\|}(x) := Dp(x)B(x)$, while $\|R_{f_{\|}}(z_{\perp}, s)\| = O(\|z_{\perp}\|^2)$. Using now the relation $\hat{S}F(\mathbf{I}_{n-1} - \hat{S}^{\dagger}\hat{S}) \equiv 0$ and the fact that we can always write, for any $s \in \mathcal{S}$, $z_{\perp} = L(s)\hat{S}^{\dagger}\sigma + (\mathbf{I}_{n-1} - L(s)\hat{S}^{\dagger}S_{\perp}(s))z_{\perp}$, it follows from the expression above that $\dot{\sigma}$ can be written in the form (8.37) with

$$
\begin{aligned}
\tilde{B}_{\perp}(z_{\perp}, s) &= \tilde{g}_{\perp}(z_{\perp}, s) + L(s)\left(\frac{d}{ds}L^{-1}(s)\right) z_{\perp}B_{\|}(x),\\
R_{\sigma}(z_{\perp}, s) &= S_{\perp}(s)\Big[R_{\perp}(z_{\perp}, s) + L(s)\left(\frac{d}{ds}L^{-1}(s)\right) z_{\perp}R_{f_{\|}}(z_{\perp}, s)\\
&\qquad + L(s)\left(\frac{d}{ds}L^{-1}(s)\right) z_{\perp}Df_{\|}(x_s(s))\big(\mathbf{I}_n - \mathcal{F}(s)\mathcal{P}(s)\big)\mathcal{Z}_{\perp}^{\dagger}(s)z_{\perp}\Big].
\end{aligned}
$$

Lastly, since $\hat{S}$ annihilates a stable invariant subspace of F, spanned by some of its (real) generalized eigenvectors, $\mathfrak{A}_{\sigma}$ must necessarily be Hurwitz, with its spectrum a subset of the spectrum of F; see the proof of Lemma 8.5 for more details. This concludes the proof. □

Utilizing the particular structure of (8.37), the next step is to design a feedback extension $v \in \mathbb{R}^m$ in (8.36) such that the sliding manifold (8.22), that is

$$\Sigma := \{x \in \mathfrak{X} : \ \sigma(x) := S_{\perp}(p(x))z_{\perp}(x) \equiv 0\},$$

is reached in finite time. In a similar manner to the control law proposed in Proposition 8.6 for the LTI system, we will suggest for this purpose a unit-vector approach of the form

$$
v = \begin{cases} -\zeta(x)\left(S_{\perp}(p(x))\mathcal{B}_{\perp}(p(x))\right)^{-1}\frac{\sigma(x)}{\|\sigma(x)\|} & \text{if} \quad \sigma \neq 0,\\ \mathbf{0}_{m\times 1} & \text{if} \quad \sigma = 0, \end{cases} \tag{8.40}
$$

for some strictly positive, $\mathcal{C}^1$ mapping $\zeta : \mathbb{R}^n \to \mathbb{R}_{\geq 0}$.

Unfortunately, due to the nonlinearity of the dynamical system (8.21), providing a general guarantee that this control scheme, i.e. (8.36) with (8.40), will always be (even locally) successfully is something which we have not been able to prove without additional assumptions. Essentially, the main problem in this regard is the fact that the nominal orbitally stabilizing feedback $k(\cdot)$ is only assumed to be *locally* stabilizing for the perturbation-free system. There is, therefore, a possibility that the unknown perturbations may cause the system states to escape, in finite time, the region of attraction of the nominal feedback before the robustifying extension (8.40) has brought the system's states onto the sliding manifold. Nevertheless, in what follows, we will attempt to derive some conditions upon the gain ζ, together with additional assumptions, which ensures the (local) success of this control scheme.

We begin by noting that, since $\mathfrak{A}_\sigma$ in (8.37) is Hurwitz, there is a unique solution $P \in \mathbb{M}^m_{\succ 0}$ to the Lyapunov equation

$$\mathfrak{A}_\sigma^\mathsf{T} P + P\mathfrak{A}_\sigma = -2Q$$

for any $Q \in \mathbb{M}^m_{\succ 0}$. Given such a matrix P, let us consider the Lyapunov function candidate

$$V_\sigma = \frac{1}{2}\sigma^\mathsf{T}(x)P\sigma(x).$$

We have

$$\begin{aligned}\dot{V}_\sigma &= 2^{-1}\sigma^\mathsf{T}\left[\mathfrak{A}_\sigma^\mathsf{T} P + P\mathfrak{A}_\sigma - 2\frac{\zeta}{\|\sigma\|}P\right]\sigma + \sigma^\mathsf{T} PW \\ &\leq -\left(\lambda_{\min}(Q)\|\sigma\| + \lambda_{\min}(P)\zeta - \lambda_{\max}(P)\|W\|\right)\|\sigma\|,\end{aligned}$$

where $W := -S_\perp \tilde{B}_\perp (S_\perp \mathcal{B}_\perp)^{-1}\zeta\frac{\sigma}{\|\sigma\|} + S_\perp(\mathcal{B}_\perp + \tilde{B}_\perp)\Delta + R_\sigma$. Recalling from Theorem 8.21 that $S_\perp(s)\mathcal{B}_\perp(s)$ is nonsingular for all $s \in \mathcal{S}$, there necessarily exist positive constants, $c_0, \hat{c}_0 > 0$, such that $\|S_\perp(s)\mathcal{B}_\perp(s)\| \leq c_0$ and $\|(S_\perp(s)\mathcal{B}_\perp(s))^{-1}\| \leq \hat{c}_0$. Furthermore, we will assume that a pair of smooth class $\mathcal{K}$ functions (see Def. 4.2 in [44]), denoted by $c_1, c_2 : \mathbb{R}_{\geq 0} \to \mathbb{R}_{\geq 0}$, are known such that for all $s \in \mathcal{S}$:

$$\|S_\perp(s)\tilde{B}_\perp(z_\perp, s)\| \leq c_1(\|z_\perp\|) \quad \text{and} \quad \|R_\sigma(z_\perp, s)\| \leq c_2(\|z_\perp\|). \tag{8.41}$$

This means that W has the upper bound:

$$\|W\| \leq \zeta\hat{c}_0 c_1(\|z_\perp\|) + (c_0 + c_1(\|z_\perp\|))\Delta_M + c_2(\|z_\perp\|).$$

We may therefore ensure that $\dot{V}_\sigma$ is (locally) negative definite by taking ζ as to satisfy

$$\zeta > \frac{\lambda_{\max}(P)(c_0 + c_1(\|z_\perp\|))\Delta_M + \lambda_{\max}(P)c_2(\|z_\perp\|) - \lambda_{\min}(Q)\|\sigma\|}{\lambda_{\min}(P) - \lambda_{\max}(P)\hat{c}_0 c_1(\|z_\perp\|)}.$$

For some $0 < \upsilon \ll 1$, this is always possible within

$$\mathcal{N}(\upsilon) := \left\{x \in \mathfrak{X} : \|z_\perp(x)\| \leq c_1^{-1}\left(\frac{\lambda_{\min}(P)(1-\upsilon)}{\lambda_{\max}(P)\hat{c}_0}\right)\right\}, \tag{8.42}$$

as then $0 < \upsilon\lambda_{\min}(P) \leq \lambda_{\min}(P) - \lambda_{\max}(P)\hat{c}_0 c_1(\|z_\perp\|)$ for all $z_\perp \in \mathcal{N}(\upsilon)$. Indeed, taking

$$\zeta(x) = \frac{\sqrt{\lambda_{\max}(P)}}{\upsilon\lambda_{\min}(P)}\left[\mu_\star + \sqrt{\lambda_{\max}(P)}\left((c_0 + c_1(\|z_\perp(x)\|))\Delta_M + c_2(\|z_\perp(x)\|)\right)\right] \tag{8.43}$$

ensures that $\dot{V}_\sigma < -\mu_\star\sqrt{V_\sigma} - V_\sigma\lambda_{min}(Q)/\lambda_{max}(P)$ for all $z_\perp \in \mathcal{N}(\upsilon)\backslash\{\mathbf{0}\}$.

It is, however, important to note that this alone does not guarantee that the sliding manifold will be reached, as the system states may escape $\mathcal{N}(\upsilon)$ beforehand. This can be resolved through additional assumptions, for example requiring local input-to-state stability of the transverse dynamics

$$\frac{d}{dt}z_\perp = f_\perp(x) + g_\perp(x)(k(x) + v + \Delta(x,t)) \tag{8.44}$$

with respect to the input $(v + \Delta)$, for v taken within a certain admissible range. For the sake of brevity, we will in the following statement which summarizing the above simply assume the forward invariance of $\mathcal{N}(\upsilon)$ with respect to (8.44):

Proposition 8.27. *Let the conditions in Lemma 8.25 be satisfied and consider* (8.44) *with the feedback extension* (8.40). *Suppose that by taking* $\zeta : \mathbb{R}^{n-1} \to \mathbb{R}_{\geq 0}$ *satisfying* (8.43) *for some* $\upsilon \in (0,1)$, *the tube* $\mathcal{N}(\upsilon)$ *is forward invariant with respect to the transverse dynamics* (8.44). *Then any solution of the nonlinear system* (8.18), *starting inside* $\mathcal{N}(\upsilon)$, *reaches the sliding manifold* (8.22) *in finite time.* □

It is clear that the above statement, as it stands, has several limitations. Indeed, besides the difficult-to-check assumption of the forward invariance of the transverse dynamics, it does in fact not provide a guarantee that the desired periodic orbit will be rendered asymptotically stable by the suggested control law. The reason for this is simple: While we do know that the sliding manifold will be reached when starting inside the tube $\mathcal{N}(\upsilon)$, we cannot guarantee that it will be reached sufficiently close to the desired orbit as to guarantee convergence to it. This, in turn, is because the convergence upon the sliding manifold, which is inherited from $k(\cdot)$, will generally only be local.

Yet, even in the light of the aforementioned limitations, Proposition 8.27 nevertheless shows that it can in fact be possible to design a *static* state-feedback control law which rejects any matched perturbation on the desired periodic orbit. Moreover, due to the generality of the problem considered, it is not at all surprising that further (system-specific) assumptions are likely needed in order to guarantee that the resulting closed-loop system will converge to the desired orbit. We leave this as a topic for future work.

8.4.4 An alternative Lyapunov redesign approach

Besides the SMC scheme we have proposed in this chapter, which is comprised of the specific switching-function design (Theorem 8.21) and a unit-vector controller (Proposition 8.27), there are of course also other methods which can be used to construct robustifying feedback extension to an existing orbitally stabilizing feedback controller. In fact, we previously mentioned in Section 8.1 some relevant candidates for this purpose for LTI systems which are also relevant in the nonlinear case, including: changing the unit-vector controller, using an integral sliding mode approach (see, e.g., [63, 238]), or using Lyapunov redesign techniques [44]. In regard to swapping out the unit-vector controller, the possibility of instead using multivariable extensions of the super-twisting algorithm [65, 229] is particularly interesting. Of course, such a dynamic control scheme requires that the perturbation term is Lipschitz continuous, but in turn ensures a continuous control signal.

In order to provide a relevant candidate to compare our suggested SMC approach to, we will here suggest a Lyapunov redesign technique similar to the designs suggested in [44, 64, 223]), which also results in a static state-feedback controller. We will still assume knowledge of an s-parameterization, a projection operator and a set of transverse coordinates as introduced at the beginning of Section 8.4.2. Taking the controller as (8.36), i.e. $u = k(x)+v$, the transverse dynamics can thus be written in the form (8.38). Moreover, since the periodic orbit $\mathcal{O}$ has been assumed to be exponentially stable with respect to the perturbation-free closed-loop system (8.21), there exists, for any $Q \in \mathcal{C}^0(\mathcal{S}, \mathbb{M}^{n-1}_{\succ 0})$, a solution $L_\perp \in \mathcal{C}^1(\mathcal{S}, \mathbb{M}^{n-1}_{\succ 0})$ to the periodic differential Lyapunov equation (4.32), i.e.

$$\rho(s)L_\perp'(s) + (\mathcal{A}_\perp^{cl})^\mathsf{T}(s)L_\perp(s) + L_\perp(s)\mathcal{A}_\perp^{cl}(s) = -Q(s). \tag{4.32}$$

Similarly to Lemma 4.20, we therefore consider the function

$$V_\perp(x) = z_\perp^\mathsf{T}(x)L_\perp(p(x))z_\perp(x). \tag{8.45}$$

Using (8.38) and by following similar steps to those in the proof of Lemma 4.20, the time derivative of $V_\perp$ can be written as

$$\dot{V}_\perp = -z_\perp^\mathsf{T} Q(p)z_\perp + 2z_\perp^\mathsf{T} L_\perp(p)g_\perp(x)\left[v + \Delta(x,t)\right] + O(\|z_\perp\|^3), \tag{8.46}$$

where $g_\perp(x) = Dz_\perp(x)B(x)$, $z_\perp = z_\perp(x)$ and $p = p(x)$. Following the standard route of the *Lyapunov redesign controller* (LRC) approach (see, e.g., [44]), our aim will now be to choose $v = v(x)$ in such a way that the term $z_\perp^\mathsf{T} L(p)g_\perp(x)\left[v + \Delta(x,t)\right]$ is negative semidefinite for $\|z_\perp\|$ sufficiently small. Indeed, this ensures that $\dot{V}_\perp < 0$ for all $x \in \mathcal{N}\backslash\mathcal{O}$, with $\mathcal{N}$ some (sufficiently) small neighborhood of $\mathcal{O}$.

Towards the goal of designing such an extension, we define

$$\xi(x) := g_\perp^\mathsf{T}(x) L_\perp(p(x)) z_\perp(x), \tag{8.47}$$

as well as

$$\Xi(x) := \begin{cases} \frac{\xi(x)}{\|\xi(x)\|} & \text{if} \quad \|\xi(x)\| \neq 0, \\ \mathbf{0}_{m\times 1} & \text{if} \quad \|\xi(x)\| = 0. \end{cases} \tag{8.48}$$

Given the above definitions of ξ and Ξ, the following provides an alternative robustifying feedback extension:

$$u = k(x) - \zeta(x)\Xi(x). \tag{8.49}$$

Here $\zeta : \mathbb{R}^n \to \mathbb{R}_{\geq 0}$ is a smooth function, which must be taken sufficient large as to dominate the disturbance term Δ. Indeed, it is clear from (8.46) that asymptotic stability of the periodic orbit is ensured under (8.49) if the following term is non-positive within a small neighborhood of $\mathcal{O}$:

$$z_\perp^\mathsf{T} L(p) g_\perp(x) \left(v + \Delta(x,t)\right) = \xi^\mathsf{T}(x) \left(v + \Delta(x,t)\right).$$

Taking the controller according to (8.49), which is evidently equivalent to $v = -\zeta(x)\Xi(x)$, we have that

$$\begin{aligned} \xi^\mathsf{T}(x) \left(v + \Delta(x,t)\right) &= \xi^\mathsf{T}(x)\Delta(x,t) - \zeta(x) \|\xi(x)\| \\ &\leq \|\xi(x)\| \left(\Delta(x,t) - \zeta(x)\right). \end{aligned}$$

From this, the following may readily be concluded.

Proposition 8.28. *Let $\zeta : \mathbb{R}^n \to \mathbb{R}_{\geq 0}$ be such that $\zeta(x) > \|\Delta(x,t)\|$ is satisfied for all $x \in \mathbb{R}^n$ and any $t \in \mathbb{R}_{\geq 0}$. If the control law is taken as* (8.49)*, then the periodic orbit* (8.20) *is asymptotically stable with respect to the nonlinear system* (8.21)*.* □

A slight drawback of the control law (8.49) is the fact that $g_\perp(x)$, and consequently $Dz_\perp(x)$, are required in order to compute $\xi(x)$. Thus, in order to provide a simpler alternative, we define

$$\hat{\xi}(s, z_\perp) := \mathcal{B}_\perp^\mathsf{T}(s) L_\perp(s) z_\perp, \tag{8.50}$$

as well as

$$\hat{\Xi}(s, z_\perp) := \begin{cases} \frac{\hat{\xi}(s,z_\perp)}{\|\hat{\xi}(s,z_\perp)\|} & \text{if} \quad \|\xi(s, z_\perp)\| \neq 0, \\ \mathbf{0}_{m\times 1} & \text{if} \quad \|\xi(s, z_\perp)\| = 0. \end{cases} \tag{8.51}$$

As opposed to $g_\perp(x)$ used in $\xi(\cdot)$, the term $L_\perp(s)\mathcal{B}_\perp(s)$ can be computed offline and stored using, e.g., splines or look-up tables. The resulting alternative to (8.49) is therefore to take

$$v = -\hat{\zeta}(x)\hat{\Xi}(p(x), z_\perp) \tag{8.52}$$

in (8.36) for some smooth function $\hat{\zeta} : \mathbb{R}^n \to \mathbb{R}_{\geq 0}$. However, by inserting this choice for v into the expression for $\dot{V}_\perp$ given by (8.46), it is clear that it does not guarantee that all perturbations will be rejected in general. One way of resolving this issue is to simply add an additional assumption upon the structure of $g_\perp(\cdot)$. For instance, that the following relation holds sufficiently close to $\mathcal{O}$:

$$g_\perp(x) = \mathcal{B}_\perp(p(x))\mathcal{B}_\perp^\dagger(p(x))g_\perp(x) =: \mathcal{B}_\perp(p(x))\mathfrak{G}(x). \tag{8.53}$$

With this condition in place, the following statement, which we leave somewhat imprecise for the sake of brevity, shows that asymptotic stability of the orbit also can be be achieved with this control law as long as $\hat{\zeta}(\cdot)$ is taken sufficiently large.

Proposition 8.29. *Suppose there exists some real number $c > 0$ such that, for all $\|z_\perp\| \leq c$, the continuous matrix function $\mathfrak{G} : \mathbb{R}^n \to \mathbb{R}^{m\times m}$, defined in* (8.53)*, is of full rank and its symmetric part is positive definite therein. Then one can always find some smooth function $\hat{\zeta} : \mathbb{R}^n \to \mathbb{R}_{\geq 0}$, taken to be sufficiently large, such that*

$$u = k(x) - \hat{\zeta}(x)\hat{\Xi}(p(x), z_\perp) \tag{8.54}$$

with $\hat{\Xi}$ taken according to (8.51)*, renders the periodic orbit* (8.20) *asymptotically stable with respect to the nonlinear system* (8.21)*.*

Remark 8.30. As the condition (8.53) is quite restrictive, it is important to remark that the LRC (8.54) can also be asymptotically orbitally stabilizing even when the condition does not hold. Essentially, this is due to the assumed Lipschitz continuity of the columns of $B_\perp(\cdot)$ and the leading quadratic term in the above expression for $\dot{V}_\perp$: Whenever the perturbation terms appearing in (8.46) cannot be compensated for by LRC, i.e. when $\text{span}(g_\perp(x)) \neq \text{span}(\mathcal{B}_\perp(p(x))$, the order of this term with respect to (8.46) will be $O(\|z_\perp\|^2)$, implying that the LRC will be stabilizing if this term is less in magnitude than the quadratic term $z_\perp^\mathsf{T} Q_\perp(p(x))z_\perp$.

Proof. Recall again from (8.46) that the asymptotic stability of the periodic orbit is ensured under (8.36) if v is taken such that the following term is non-positive within a small neighborhood of $\mathcal{O}$:

$$
\begin{aligned}
z_\perp^{\mathsf{T}} L(p) g_\perp(x)\,(v + \Delta(x,t)) &= z_\perp^{\mathsf{T}} L(p)\mathcal{B}_\perp(p(x))\mathfrak{G}(x)\,(v+\Delta(x,t)) \\
&= \hat{\xi}^{\mathsf{T}}(p(x), z_\perp)\mathfrak{G}(x)\,(v+\Delta(x,t))\,.
\end{aligned}
$$

Taking $v = -\hat{\zeta}(x)\hat{\Xi}(p(x), z_\perp)$ in the above, it is clear that the term

$$
-\hat{\xi}^{\mathsf{T}}(p(x), z_\perp)\mathfrak{G}(x)\hat{\zeta}(x)\hat{\Xi}(p(x), z_\perp)
$$

is only equal to zero within $\|z_\perp\| \leq c$ if $\left\|\hat{\xi}\right\| = 0$, and strictly negative otherwise. It is also clear that the term involving the perturbation Δ vanishes whenever $\left\|\hat{\xi}\right\| = 0$. As a consequence, it will always be possible to find some smooth function $\hat{\zeta}$ such that

$$
\hat{\xi}^{\mathsf{T}}(p(x), z_\perp)\mathfrak{G}(x)\Delta(x,t) - \hat{\xi}^{\mathsf{T}}(p(x), z_\perp)\mathfrak{G}(x)\hat{\zeta}(x)\hat{\Xi}(p(x), z_\perp) \leq 0
$$

within $\|z_\perp\| \leq c$ if Δ is bounded. This concludes the proof. □

8.5 Case study: Oscillation control of the Cart-Pendulum system

In order to construct a switching surface of the form (8.33) utilizing the method outlined in Section 8.4, the following four basic ingredients first have to be obtained:

1) A desired periodic solution of a nominal model of the system, with some known s-parameterization of the form (8.25);

2) A projection operator for the s-parameterized orbit (see Def. 4.5);

3) A set of transverse coordinates for the solution (see Def. 4.11);

4) An exponentially orbitally stabilizing state feedback $k(\cdot)$ for the nominal (perturbation-free) system.

In Chapter 5, specifically Section 5.5.1, we demonstrated how all these ingredients can be obtained in the case of orbitally stable oscillation control of the cart-pendulum system using the VHC-based approach of [33]. In this section, we will therefore revisit this example and utilize the control law obtained in Section 5.5.1 for construct a robust orbitally stabilizing feedback extension using the theory outlined Section 8.4.

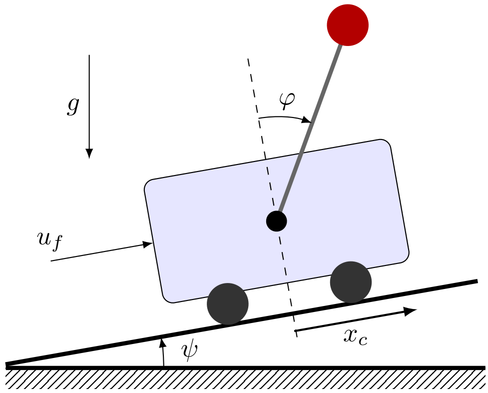

Figure 8.1: Schematic of the cart-pendulum system.

8.5.1 System model

In this section, we will differentiate between the "real" (actual) model of the system dynamics, which we do not know exactly, and the nominal (approximation) model we used in Section 5.5 to construct the desired periodic solution and to design the nominal orbitally stabilizing feedback.

Real dynamical model: The schematic of the system and the coordinate convention now used is shown in Figure 8.1. The cart is situated on a ramp of constant inclination ψ and is driven by an external force u_f, with the pendulum being unactuated as before. The equations of motion are now

$$(m_c + m_p)\ddot{x}_c + m_p l_p \cos(\varphi)\ddot{\varphi} - m_p l_p \sin(\varphi)\dot{\varphi}^2 \qquad (8.55a)$$
$$+g(m_c + m_p)\sin(\psi) = u_f - \upsilon_c \text{sign}(\dot{x}_c) + d_x(t),$$
$$(m_p l_p^2 + J_p)\ddot{\varphi} + m_p l_p \cos(\varphi)\ddot{x}_c - m_p l_p g \sin(\varphi - \psi) = -\upsilon_p \text{sign}(\dot{\varphi}) + d_p(t). \qquad (8.55b)$$

Here $g = 9.81\,\text{m}\,\text{s}^{-2}$ is the gravitational acceleration; m_c and m_p denote the mass of the cart and pendulum bob, respectively; l_p is the length of the pendulum and J_p is its moment of inertia; υ_c and υ_p are dry friction coefficients; while $d_x(t)$ and $d_p(t)$ are smooth, bounded, time-varying disturbances.

Nominal (disturbance-free) model used for trajectory generation and in the nominal feedback synthesis: Recall the equations of motion for the nominal system considered in Section 5.5:

$$2\ddot{x}_c + \cos(\varphi)\ddot{\varphi} - \sin(\varphi)\dot{\varphi}^2 = u_f, \qquad (8.56a)$$
$$\ddot{\varphi} + \cos(\varphi)\ddot{x}_c - g\sin(\varphi) = 0. \qquad (8.56b)$$

Comparing this to (8.55), it is clear that this corresponds to the following set of assumptions: zero inclination of the ramp ($\psi = 0$), no friction ($\upsilon_c = \upsilon_p = 0$), unit masses ($m_c = m_p = 1$), the pendulum is as a point mass of unit length ($l_p = 1$ and $J_p = 0$) and zero disturbances ($d_x = d_p = 0$).

8.5.2 Constructing a switching function

Our aim will now be to design a switching function of the form (8.33) for the cart-pendulum system using the VHC-based orbitally stabilizing feedback designed for the nominal system in Section 5.5.1. More specifically, we will utilize the linearized transverse dynamics of the closed-loop system,

$$\dot{\boldsymbol{\delta}}_{z_\perp} = \left[\mathcal{A}_\perp(s) + \mathcal{B}_\perp(s)K_\perp(s)\right]\boldsymbol{\delta}_{z_\perp} =: \mathcal{A}_\perp^{cl}(s)\boldsymbol{\delta}_{z_\perp},$$

corresponding to (5.74) under the control law $u = K_\perp(p)z_\perp$, with the elements of $K_\perp(\cdot)$ as in Figure 5.4.

In order to construct a switching function of the form (8.33), we first need to find: 1) a real 2π-periodic FL factorization of the state-transition matrix of (8.31), and then 2) a full-rank left-annihilator of a real invariant subspace of F of co-dimension m.[8] To find an FL factorization $(L(s), F, Y)$ for (8.31), we used the boundary value problem formulation proposed in [235], where an initial condition for F was found by integrating (8.10) and using (8.15). This resulted in $Y = \mathbf{I}_3$, i.e. $L(\tau)$ was 2π-periodic as required, while the found matrix F was approximately given by

$$F \approx \begin{bmatrix} 0.0843 & 1.1269 & 0.8987 \\ -3.4618 & -4.4920 & -3.1910 \\ 0.4531 & 0.4799 & -0.0735 \end{bmatrix}.$$

The three real eigenvalue-eigenvector pairs of this matrix F are in turn approximately given by

$$\begin{aligned}
(\lambda_1, \upsilon_1) &\approx \Big(-2.97, \mathrm{col}(0.32, -0.94, 0.11)\Big), \\
(\lambda_2, \upsilon_2) &\approx \Big(-1.06, \mathrm{col}(0.68, -0.73, 0.04)\Big), \\
(\lambda_3, \upsilon_3) &\approx \Big(-0.45, \mathrm{col}(0.02, -0.63, 0.78)\Big).
\end{aligned}$$

Hence F has three real invariant subspaces of co-dimension one:

$$\mathrm{span}\{\upsilon_1, \upsilon_2\}, \quad \mathrm{span}\{\upsilon_1, \upsilon_3\} \quad \text{and} \quad \mathrm{span}\{\upsilon_2, \upsilon_3\}.$$

[8] Since the system is mechanical, the dimension of the transverse dynamics will always be odd, that is $(n-1) = 2n_q - 1$. Thus by Fact 8.4, the system (8.31) must then have at least one such subspace. Although there is no guarantee that this subspace has an annihilator such that $S_\perp(s)\mathcal{B}_\perp(s)$ is nonsingular everywhere.

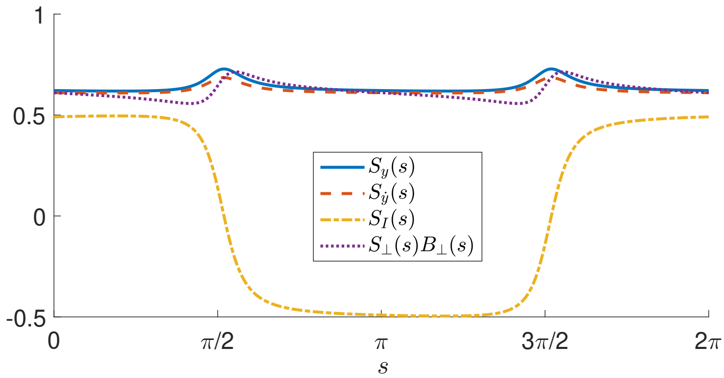

Figure 8.2: Elements of the designed switching function $S_\perp$ given by (8.33). Here $(S_\perp \mathcal{B}_\perp)$ is seen to be nonsingular.

Table 8.1: Parameters of the cart-pendulum system (8.55) used in simulation for the three considered scenarios.

Types of perturbations	m_c [kg]	m_p [kg]	l_p [m]	J_p [kg m^2]	ψ [rad]	υ_c [N]	υ_p [N m]	$d_x(t)$ [N]	$d_p(t)$ [N m]
None (nominal case)	1	1	1	0	0	0	0	0	0
Only matched	1	1	1	0	0	0.25	0	$0.1\sin(t)$	0
Matched & unmacthed	1.2	1.2	0.9	0.2	$5\pi/180$	0.25	0.1	$0.1\sin(t)$	$0.1\sin(t)$

However, only the subspace $\text{span}\{\upsilon_2, \upsilon_3\}$ had an annihilator that satisfied the nonzero-determinant condition in Theorem 8.21. We therefore took $\hat{S}$ such that $\hat{S}\upsilon_2 = \hat{S}\upsilon_3 \equiv 0$ (i.e. $\hat{S} \approx [0.62, 0.61, 0.48]$). The corresponding matrix function $S_\perp(s) = \hat{S}L^{-1}(s) = [S_y, S_{\dot{y}}, S_I]$ is shown in Figure 8.2, where $\big(S_\perp(s)\mathcal{B}_\perp(s)\big)$ can be seen to be separated from zero.

Note here that $\text{span}\{\upsilon_2, \upsilon_3\}$ consists of the two one-dimensional subspaces whose eigenvalues have the smallest magnitudes. Since solutions of the nominal (perturbation-free) system under just the LQR feedback may also partly correspond to the subspace spanned by υ_1, it is therefore to be expected that the convergence close to the orbit will (for the nominal system) be somewhat slower in general when confined to the corresponding sliding manifold.

8.5.3 Simulation results

Using the above designed switching function, we will now compare in simulations the control law (8.36) with feedback extension (8.40) to both the nominal LQR and the Lyapunov redesign controller (LRC) given by (8.49).

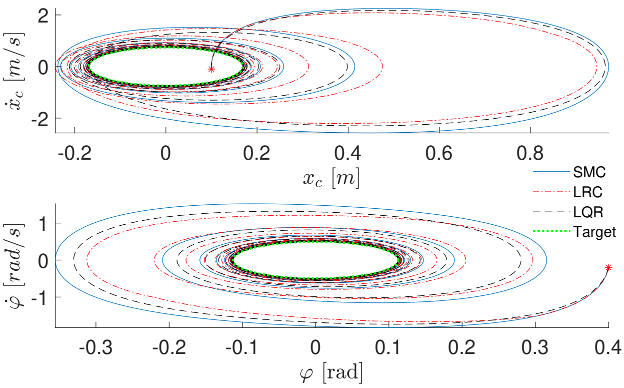

(a) Phase portraits.

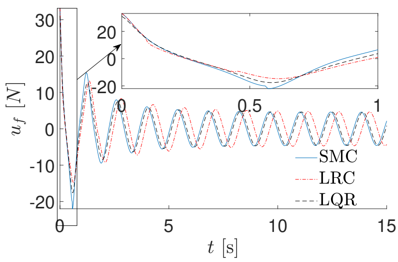

(b) Control input.

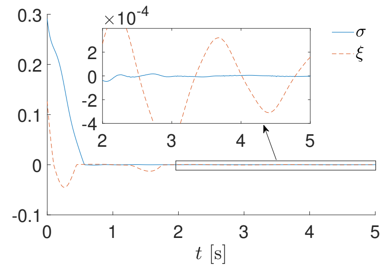

(c) Switching function σ and Lyapunov redesign function ξ.

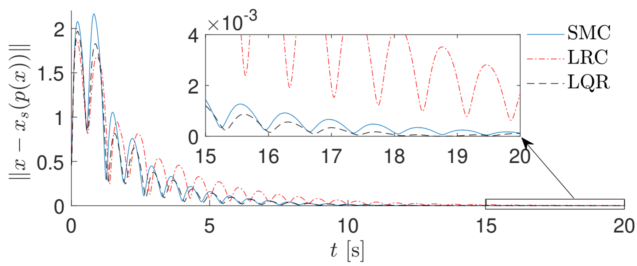

(d) Distance to orbit.

Figure 8.3: (Nominal model) Simulation results showing the performance of each controller, with $(\mu_1, \mu_2) = (0.5, 0.5)$, when implemented on the disturbance-free system; SMC (—), LRC ($-\cdot-$), LQR($--$), Target orbit ($\cdots$).

These were implemented as follows:

$$u_{LQR} = K_\perp(p)z_\perp, \qquad p = p(x), \qquad \text{(LQR)}$$

$$u_{SMC} = K_\perp(p)z_\perp - \mu_1 \;\text{sat}\left(\sigma(p, z_\perp)/\epsilon\right), \quad \sigma(s, z_\perp) := S_\perp(s)z_\perp, \qquad \text{(SMC)}$$

$$u_{LRC} = K_\perp(p)z_\perp - \mu_2 \;\text{sat}\left(\xi(p, z_\perp)/\epsilon\right), \quad \xi(s, z_\perp) := \mathcal{B}_\perp^\mathsf{T}(s)R_\perp(s)z_\perp. \qquad \text{(LRC)}$$

Here the saturation function sat$(\cdot)$ was used with $\epsilon = 10^{-3}$ rather than the signum function in order to mitigate chattering [44]. The gains $\mu_1, \mu_2 > 0$ in the SMC and LRC were taken as constants to facilitate the comparison between the controllers, as well as to highlight the effects of these gains with respect to the magnitude of any matched disturbances.

Each controller was tested on the system (8.55) for three different scenarios: without any perturbations (corresponding to the nominal system (8.56)), with only matched perturbations, and with both matched and unmatched perturbations. Table 8.1 contains the parameters used for each of these scenarios. The initial conditions were taken as

$$(x_c(0), \varphi(0), \dot{x}_c(0), \dot{\varphi}(0)) = (0.1, 0.4, -0.1, -0.2).$$

Nominal case: Figure 8.3 shows the simulation results when implemented on the nominal system (8.56), with the gains of the SMC and LRC taken as $(\mu_1, \mu_2) = (0.5, 0.5)$. Both the convergence to the orbit and the control inputs are seen to be fairly similar for all the control laws. As seen in (d), however, the LRC quickly drives the states close to the manifold $\xi \equiv 0$ such that u_{LRC} remains close to zero. This results in a slightly slower convergence to the target orbit for the LRC than the other two controllers. The SMC, on the other hand, can be seen in (c) to have a larger overshoot than the other controllers with respect to the projection operator–based distance measure $\|x - x_s(p(x))\|$, before eventually having a similar convergence rate to that of the nominal LQR after reaching the sliding manifold.

Matched perturbations: Figure 8.4 shows the performance of the three controllers when subject to only matched perturbations. The perturbation term had the upper bound $\Delta_M \leq 0.35$ (see Table 8.1) and the gains of the SMC and LRC were again taken as $(\mu_1, \mu_2) = (0.5, 0.5)$. As seen in (a), the LQR is unable to ensure convergence to the target orbit and instead settles into a perturbed orbit having a lower amplitude, whereas both the SMC and LRC are able to almost completely reject the disturbances. The effects of increasing the gains of both controllers can be seen in Figure 8.5. As one would expect, increasing the gain for the SMC is seen to decrease the time needed to reach the sliding manifold, slightly speeding up the convergence, but at the expense of both larger overshoot and increased peak actuator forces. The opposite behavior may be observed when increasing the gains of the LRC; it can be seen that the system's states are driven faster towards the manifold $\xi \equiv 0$, leading to slightly slower convergence to the target orbit, but reducing the overshoot.

Matched- and unmatched perturbations: Figure 8.6 shows the response of the system under the three controllers for $(\mu_1, \mu_2) = (4, 4)$ when

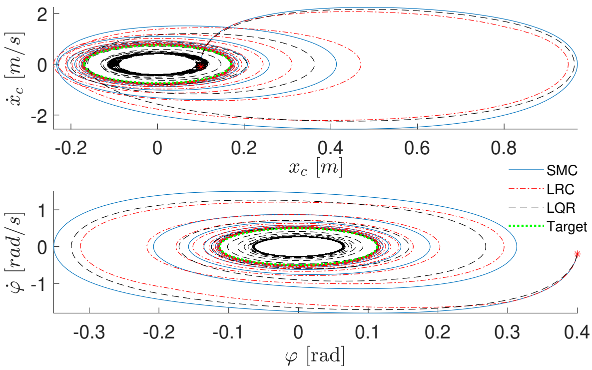

(a) Phase portraits.

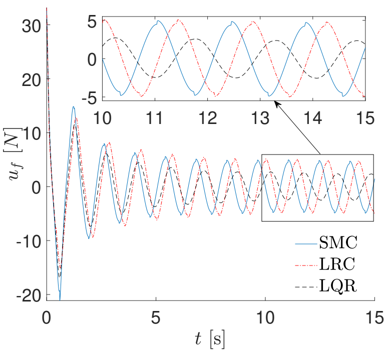

(b) Control input.

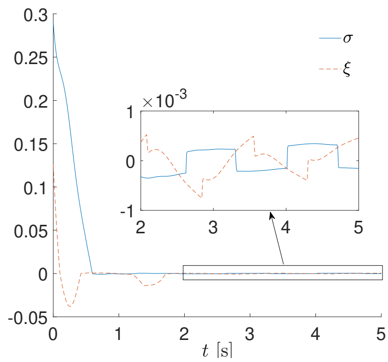

(c) Switching function σ and Lyapunov redesign function ξ.

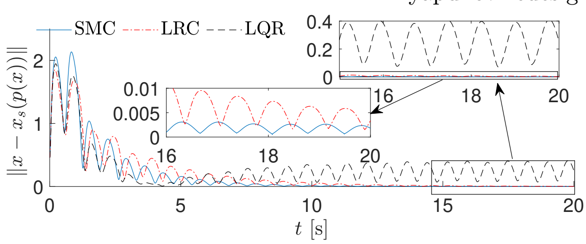

(d) Distance to orbit.

Figure 8.4: (Matched disturbances) Simulation results showing the performance of each controller, with $(\mu_1, \mu_2) = (0.5, 0.5)$, when subject to only matched disturbances; SMC (—), LRC ($- \cdot -$), LQR($- \, -$), Target orbit ($\cdots$).

subject to both matched and unmatched perturbations. The system under the LQR is seen to become unstable as the controller was unable to keep the angle of the pendulum within the region where the feedback (5.73) and

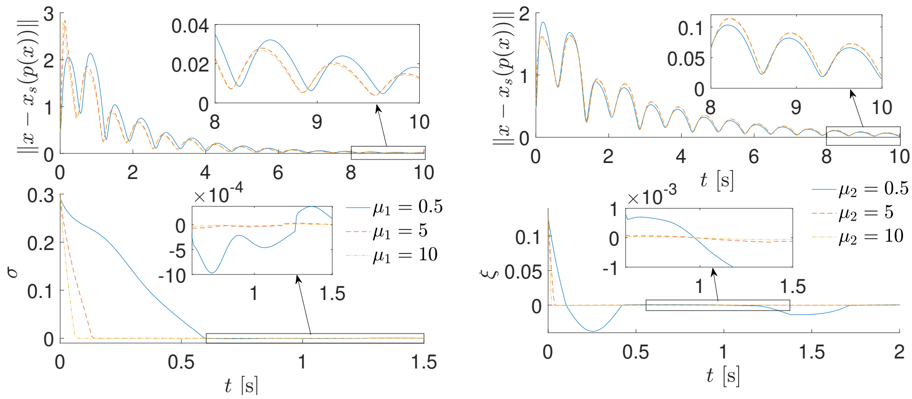

(a) Results for the SMC. Top: Distance to the orbit; Bottom: the switching function.

(b) Results for the LRC. Top: Distance to the orbit; Bottom: the LRC function ξ.

Figure 8.5: Gain comparison for the SMC (**a**) and LRC (**b**) when subject to matched disturbances; $\mu_i = 0.5$ (—), $\mu_i = 5$ ($- \cdot -$), $\mu_i = 10$ (— —).

the third transverse coordinate are well defined, corresponding to $|\varphi| < \sqrt{(1/a)} \approx 0.62\,\text{rad}$. To stay within this region, both the gain of the SMC and LRC had to be increased, with the SMC needing the largest increase for the considered initial conditions. It can again be seen from (b) and (c) in Figure 8.6 that the SMC is initially more aggressive than the LRC, leading to high peaks in the force applied to the cart and to a larger overshoot with respect to the target orbit. After the transient phase, however, the SMC settles into an orbit that is closer to the nominal orbit on average and which requires slightly less control forces than the settling orbit of the LRC.

Pure sliding mode controller and the effect of noise: Figure 8.7 shows the results for the different scenarios when taking in (5.73) the pure sliding mode controller given by

$$u = -\mu_1 \mathrm{sat}(\sigma(p, z_\perp)/\epsilon).$$

The gain had to be increased to maintain a similar performance in all three scenarios: $\mu_1 = 2$ for both the nominal case and with only matched perturbations, while it was increased to $\mu_1 = 6$ for the case also including unmatched perturbations. The similarity of these results compared to those under the controller (SMC) indicates that the equivalent control when confined to the manifold indeed corresponds to that of the designed LQR controller used in the switching function synthesis.

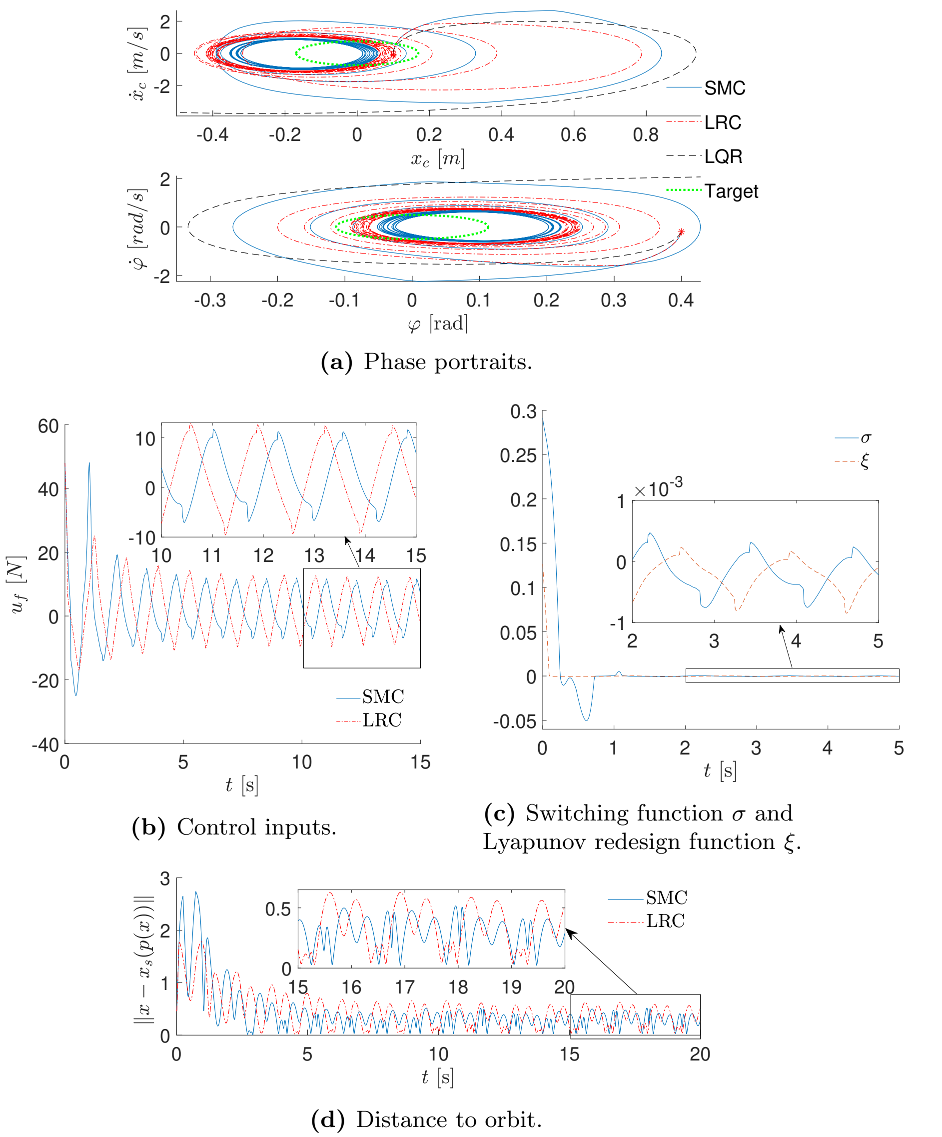

Figure 8.6: (Matched & unmacthed disturbances) Simulation results showing the performance of each controller, with $(\mu_1, \mu_2) = (4, 4)$; SMC (—-), LRC ($- \cdot -$), LQR($- \; -$), Target orbit ($\cdots$).

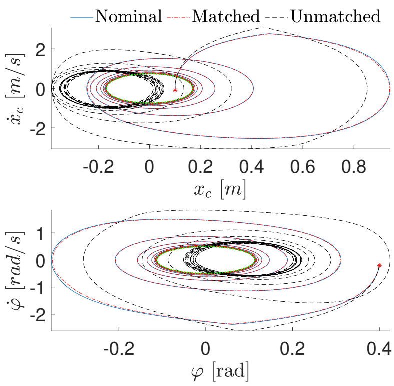

(a) Phase portraits.

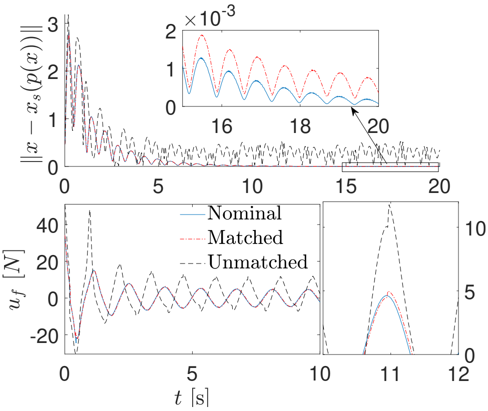

(b) Top: Distance to the orbit; Bottom: control input.

Figure 8.7: System response with only the sliding mode controller. The gain was taken as $\mu_1 = 2$ for both the nominal case (—) and with only matched disturbances ($- \cdot -$), while $\mu_1 = 6$ when subject to both matched and unmatched disturbances ($- -$).

Chapter 9

Conclusions and Further Work

9.1 Summary

A summary of each of the chapters in this thesis follows.

In Chapter 2, we introduced the notion of an orbit of smooth autonomous dynamical systems. Some of the key properties of such orbits were then stated, including that they cannot have self-intersection, as well as their inherent time invariance. It was also shown that Lyapunov's notion of stability is not well suited for characterising the stability of non-trivial orbits, motivating the notion of the *orbital stability* of a solution. A third stability notion, called Zhukovsky stability, was also introduced. It utilized a reparameterization to align perturbed trajectories in state space, making it a suitable stability notion also for non-trivial orbits. We saw that by using reparameterizations à la Zhukovsky, one could construct a so-called moving Poincaré section, upon which one could introduce *transverse coordinates.* A continuous representation of the stability characteristics of the orbit could then be obtained. This also facilitated the derivation of a certain type of linearization, a *transverse linearization*, which could be used to assess the stability of an orbit.

In Chapter 3, we formulated *the orbital stabilization problem.* The notion of an s-parameterization was also introduced, and an overview of the type of general control structure utilized throughout the thesis was provided. It was also shown how certain well-known controllers can be viewed as orbitally stabilizing controllers, including planar over- and critically-damped PD controllers, certain sliding mode controllers, and even certain reference-trajectory tracking controllers when viewing the trajectory as a curve in time–state space. Some alternative methods and related concepts were also discussed, such as energy shaping–based methods, path following, virtual holonomic constraints, transverse feedback linearization and contraction theory.

In Chapter 4, we presented methods for solving the orbital stabilization problem for periodic orbits. These methods were based on the combination of a certain set of (excessive) transverse coordinates and a projection operator. We showed that the combination of transverse coordinates and a projection operator allowed for a local change of coordinates, separating the transverse- and tangential dynamics. It was further showed that an exponentially orbitally stabilizing control law could be designed by solving some periodic differential matrix equation, e.g. a Riccati equation, derived using the corresponding transverse linearization. An easy-to-compute set of excessive transverse coordinates were then studied in detail. We saw that in order to stabilize the resulting transverse linearization, one has to take into account a certain transversality condition. Two main methods were suggested for orbitally stabilizing feedback design: a comparison-system approach applicable only to orthogonal coordinates, and approaches based on projected Lyapunov- and Riccati matrix differential equations.

In Chapter 5, a method for planning s-parameterized orbits of a class of underactuated mechanical systems was proposed. Inspired by the *virtual (holonomic) constraints approach*, this method utilized so-called *synchronization functions*, which are functions consisting of a finite number of basis functions parameterized by a scalar variable. By assuming that the system's states are synchronized according to these functions, an s-parameterized orbit corresponded to the scalar parameter being a monotonically increasing solution to a series of second-order differential equations. Some important aspects related to these *reduced dynamics* were then reviewed and studied, including their integrability, as well as their equilibria and singular points. Moreover, explicit expressions for the transverse linearization of the projection-based excessive transverse coordinates studied in Chapter 4 for mechanical control systems were also provided in Chapter 5.

In Chapter 6, we introduced a method for inducing, via locally Lipschitz continuous static state-feedback, an asymptotically stable heteroclinic orbit in a nonlinear control system. Our suggested approach used a particular s-parameterization of a known point-to-point maneuver, together with a particular projection operator as to merge a Jacobian linearization with a transverse linearization for the purpose of control design. Moreover, a possible way of constructing such a feedback by solving a semidefinite programming problem was suggested. It was demonstrated that the approach could be used to solve the challenging nonprehensile manipulation problem of rolling a ball, in a stable manner, between any two points upon a smooth actuated planer frame. This provided a general solution applicable to a number of well-known nonlinear systems, including the ball-and-beam, the disk-on-disk and the "butterfly" robot. The approach was successfully applied to the latter system in numerical simulations.

In Chapter 7, the problem of stabilizing (hybrid) periodic cycles of a class of hybrid dynamical systems was considered. Given knowledge of an s-parameterization of a hybrid cycle, along which the system's states undergo a single, discrete jump, a method was provided that allowed for its orbital stabilization. The main result was a statement providing sufficient conditions in this regard, by combining a differential linear matrix inequality with a linear matrix inequality accounting for the discrete jump occurring at the end of the cycle. In addition, a numerical framework based on synchronization functions for constructing such forced hybrid periodic cycles of underactuated mechanical systems with jumps was presented. It provided steps allowing for the discretization of the planning problem into a parametric nonlinear programming problem by using some numerical quadrature, e.g. Gauss–Legendre quadratures. The suggested orbit-generation approach and the orbital stabilization procedure were used in numerical simulations to generate an orbitally stable walking gait of a three-link biped robot with a single actuator.

In Chapter 8, the task of designing a robustifying feedback extension for a known orbitally stabilizing feedback controller in the case of trivial- and periodic orbits was considered. A new constructive procedure for generating a switching function was proposed, allowing for the use of sliding mode control extensions for disturbance rejection. The designed switching function corresponded to an annihilator of a specific real invariant subspace of a (transverse) linearization. For periodic orbits, it corresponded to a subspace of the Monodromy matrix of the first-order approximation (linearization) of a nominal model of the system. The switching function was constructed using a real Floquet–Lyapunov transformation of the state-transition matrix of the linearized dynamics of a set of transverse coordinates along the nominal orbit. A unit-vector-based approach was also suggested for stabilizing the corresponding sliding manifold in finite time. The efficacy of the proposed robustification procedure was demonstrated in numerical simulations, where it also was compared to a Lyapunov redesign technique. Specifically, it was applied to ensure orbitally stable oscillations about the up-right equilibrium of the Cart-Pendulum system subject to both matched- and unmatched perturbations.

9.2 Concluding remarks

In this thesis, we have studied the problem of orbital stabilization of various forced motions. While we have mainly focused on nonlinear and underactuated (mechanical) control systems, the methods which have been proposed can also readily be applied to linear and/or fully-actuated systems.

The orbital stabilization problem. In order to connect the concept of orbital stabilization with the well-established notion of an orbit of an autonomous system, we formulated in Chapter 3 a new control problem: *the orbital stabilization problem*. The resulting control objective is that of simultaneous generation and stabilization, via time-invariant state-feedback, of a desired (forced) orbit in the autonomous closed-loop system. Hence, orbital stabilization is a fundamental control objective, in which the aim is to ensure the asymptotic orbital (Poincaré) stability of all solutions upon the induced orbit. In light of the discussion in Chapter 2, it is therefore a less strict control objective than trajectory tracking, in which the aim is generally to ensure that the (non-autonomous) closed-loop systems admits the desired motion as an asymptotically Lyapunov stable solution.

Projection-based orbital stabilization. Despite the fundamentality of the orbital stabilization problem and the benefits of an orbitally stabilizing feedback, orbital stabilization has garnered little (direct) attention as a control objective beyond the task of stabilizing periodic orbits. Among the main aims of this thesis was therefore the development of a general-purpose method for designing orbitally stabilization feedback. Specifically, we aimed to provide a linearization-based approach which could be considered as a natural extension of methods utilizing the Jacobian linearization about a linearly stabilizable equilibrium point (i.e. a trivial orbit). Besides allowing stabilizing feedback to be designed using tools from linear control theory, this provides a means to obtain a (local) strict, time-invariant Lyapunov function. Such an approach will of course only guarantee local results, and should therefore always be weighed against alternative techniques which might exploit some inherent structure or other properties of the system.

The approach we suggested utilized a particular projection onto the desired orbit. This allowed an easy-to-compute function to be defined, whose zero-level set provided an implicit representation of the orbit. About a non-trivial periodic orbit, this function could be viewed as an excessive set of so-called *transverse coordinates* evolving upon a moving Poincaré section. In Chapter 4, explicit expression for the corresponding *transverse linearization* were derived, which had the same structure as the linearization obtained by Leonov (see Chapter 2). Remarkably, this transverse linearization has not, at least to the author's knowledge, been utilized before for control purposes. It was shown that an orbitally stabilizing feedback could be constructed by solving certain projected differential Riccati-like equations, allowing one to search for stabilizing feedback gains offline using semidefinite programming.

By imposing further conditions upon the projection operator, the approach was also extended to other orbits. In Chapter 6 it was used to stabilize heteroclinic orbits, corresponding to so-called point-to-point maneuvers, where a pair of algebraic Lyapunov equations were required to hold to account for the equilibrium points on the orbit's boundaries. The same type of projection operators was used in Chapter 7 to design an orbitally stabilizing feedback for hybrid cycles of a class of hybrid systems, with the addition of a linear matrix inequality based on a Saltation-like matrix to account for the discrete jump in the states at the end of the cycle.

Orbit generation using synchronization functions. In order to apply the suggested orbital stabilization approach, knowledge of a particular parameterization of the orbit to be stabilized was required. We called this parameterization an *s-parameterization*. By requiring that the parameter was a monotonically increasing function of time, it acted as a nonlinear time scaling, allowing the whole process from motion planning to control design to be carried out over a fixed interval, $\mathcal{S} \subset \mathbb{R}$, in terms of the parameter s. While an orbit with such a parameterization can be obtained using a variety of methods, we suggested in this thesis an approach based on so-called *synchronization functions* in Chapter 5 for underactuated mechanical systems. It was further shown in Chapter 7 that, under certain assumptions, this approach facilitated a procedure for transcribing a trajectory optimization problem into a parametric nonlinear program for a class of underactuated mechanical systems.

Robust orbital stabilization using sliding mode control. Methods for orbit generation and -stabilization, including those presented in this thesis, are often heavily reliant upon the mathematical model of the system. In order to enhance the robustness of such methods with respect to unknown (matched) perturbations, we proposed in Chapter 8 a new method for constructing a switching function to be used in the synthesis of a sliding mode controller for orbital stabilization of trivial or periodic orbits. Alongside alternative methods such as Lyapunov redesign, the suggested linearization-based technique allows one to add a *static* robustifying feedback extension to an orbitally stabilizing controller. Some limiting assumptions were however required to ensure stability of the closed-loop system under the suggested unit-vector controller also during the reaching phase.

9.3 Topics for future research

Future work will include both experimental validation, parametric (in-) sensitivity analyses and region of attraction estimation of the suggested control strategies. Below, we also outline some relevant topics for future research.

Objective function for the projected differential LMIs

In order to design orbitally stabilizing feedback for periodic motions, a projected Riccati differential equation was proposed in Section 4.6.3. Using the Schur complement and a specific objective function following Gusev's method, a solution could be found utilizing semidefinite programming. An alternative affine representation was given in Proposition 4.46 which avoided the use of the Schur complement. This differential-linear-matrix-inequality form (also used in Proposition 6.12, Theorem 7.2 and Proposition 7.6) thus lacks a clear candidate for an objective function to be used in the semidefinite program. Whereas the weighting matrices appearing in Riccati equations have a well-understood meaning in terms of the linear-quadratic-regulator (LQR) problem, thus providing one with a somewhat intuitive way of tuning the resulting feedback controller, the freedom in choosing the objective function for the affine representation might also be used for tuning purposes.

Curve stabilization

Some of the ideas in this thesis can be utilized to stabilize more general curves. Consider, for example, the curve $x_s(s) = \mathrm{col}\big(\phi(s), \phi'(s)\rho(s)\big)$ with

$$\phi(s) = s + \psi \sin\big(\eta(s - s_\alpha)/(s_\omega - s_\alpha)\big) \quad \text{and} \quad \rho(s) := \kappa|s - s_\alpha|^\alpha |s_\omega - s|^\beta$$

for the double integrator system $\ddot{q} = u$, $q, u \in \mathbb{R}$. Suppose $\mathcal{S} = [s_\alpha, s_\omega] = [0, 10]$, $\alpha = \beta = 3/4$, $\kappa = 0.1$, $\eta = 8\pi$ and $\psi = 5$. The finite-time point-to-point curve traced out by $x_s(\cdot)$ has several self-intersections. One can still utilize a *dynamic* projection operator of the form as in Propositions 4.9 and 6.5, by only looking over a sufficiently small moving subinterval of $\mathcal{S}$. Furthermore, since function $\rho(\cdot)$ is not Lipschitz at the boundaries of $\mathcal{S}$, such curves cannot be stabilized by a locally Lipschitz controller in general.

Stability during the reaching phase

As stated at the end of the concluding remarks, for the closed-loop system to be asymptotically stable under the robustifying (unit-vector) feedback extension proposed in Section. 8.4.3, quite limiting assumptions were required in Proposition 8.27. By utilizing certain system-specific structures, such as those of mechanical systems (cf. Assumption 5.1), one might obtain more constructive conditions for certain classes of systems.

Bibliography

References marked by an * were not directly consulted during the writing of this thesis.

[1] A. D. Kuo. ‘Choosing your steps carefully’. *IEEE Robotics & Automation Magazine* 14.2 (2007), 18–29.

[2] J. Reher and A. D. Ames. ‘Dynamic Walking: Toward Agile and Efficient Bipedal Robots’. *Annual Review of Control, Robotics, and Autonomous Systems* 4 (2020).

[3] M. T. Mason and K. M. Lynch. ‘Dynamic manipulation’. In: *IEEE/RSJ Int. Conf. on Intelligent Robots and Systems*. Vol. 1. IEEE. 1993, 152–159.

[4] K. M. Lynch, N. Shiroma, H. Arai and K. Tanie. ‘The roles of shape and motion in dynamic manipulation: The butterfly example’. In: *IEEE Int. Conf. on Robotics and Automation*. Vol. 3. IEEE. 1998, 1958–1963.

[5] F. Ruggiero, V. Lippiello and B. Siciliano. ‘Nonprehensile dynamic manipulation: A survey’. *IEEE Robotics and Automation Letters* 3.3 (2018), 1711–1718.

[6] K. M. Lynch and M. T. Mason. ‘Dynamic nonprehensile manipulation: Controllability, planning, and experiments’. *The Int. Journal of Robotics Research* 18.1 (1999), 64–92.

[7] M. W. Spong. ‘Underactuated mechanical systems’. In: *Control problems in robotics and automation*. Springer, 1998, 135–150.

[8] Y. Liu and H. Yu. ‘A survey of underactuated mechanical systems’. *IET Control Theory & Applications* 7.7 (2013), 921–935.

[9] A. S. Shiriaev, L. B. Freidovich and M. W. Spong. 'Controlled invariants and trajectory planning for underactuated mechanical systems'. *IEEE Trans. on Automatic Control* 59.9 (2014), 2555–2561.

[10] R. Olfati-Saber. 'Nonlinear control of underactuated mechanical systems with application to robotics and aerospace vehicles'. PhD thesis. Massachusetts Institute of Technology, 2001.

[11] J. Moreno-Valenzuela and C. Aguilar-Avelar. *Motion control of underactuated mechanical systems*. Vol. 1. Springer, 2018.

[12] R. Tedrake. *Underactuated Robotics. Algorithms for Walking, Running, Swimming, Flying, and Manipulation*. Downloaded on 23.02. 2022. URL: `http://underactuated.mit.edu`.

[13] M. W. Spong. 'Partial feedback linearization of underactuated mechanical systems'. In: *Proceedings of IEEE/RSJ Int. Conf. on Intelligent Robots and Systems (IROS'94)*. Vol. 1. IEEE. 1994, 314–321.

[14] S. Schaal and C. G. Atkeson. 'Robot juggling: implementation of memory-based learning'. *IEEE Control Systems Magazine* 14.1 (1994), 57–71.

[15] O. M. Andrychowicz, B. Baker, M. Chociej, R. Jozefowicz, B. McGrew, J. Pachocki, A. Petron, M. Plappert, G. Powell, A. Ray et al. 'Learning dexterous in-hand manipulation'. *The Int. J. of Robotics Research* 39.1 (2020), 3–20.

[16] S. Kuindersma. *Recent Progress on Atlas, the World's Most Dynamic Humanoid Robot*. Youtube video. Retrieved: 09.06.2021. 2020. URL: `https://youtu.be/EGABAx52GKI`.

[17] J. T. Betts. 'Survey of numerical methods for trajectory optimization'. *Journal of guidance, control, and dynamics* 21.2 (1998), 193–207.

[18] A. V. Rao. 'A survey of numerical methods for optimal control'. *Advances in the Astronautical Sciences* 135.1 (2009), 497–528.

[19] M. Posa, C. Cantu and R. Tedrake. 'A direct method for trajectory optimization of rigid bodies through contact'. *The Int. Journal of Robotics Research* 33.1 (2014), 69–81.

[20] D. A. Benson, G. T. Huntington, T. P. Thorvaldsen and A. V. Rao. 'Direct trajectory optimization and costate estimation via an orthogonal collocation method'. *Journal of Guidance, Control, and Dynamics* 29.6 (2006), 1435–1440.

[21] M. Kelly. 'An introduction to trajectory optimization: How to do your own direct collocation'. *SIAM Review* 59.4 (2017), 849–904.

[22] J. Hauser and R. Hindman. 'Maneuver regulation from trajectory tracking: Feedback linearizable systems'. *IFAC Proc. Vol.* 28.14 (1995), 595–600.

[23] W. Hahn. *Stability of motion*. Vol. 138. Springer, 1967.

[24] M. Urabe. *Nonlinear autonomous oscillations: Analytical theory*. Vol. 34. Elsevier, 1967.

[25] J. K. Hale. *Ordinary differential equations*. Robert E. Krieger Publishing Company, 1980.

[26] G. A. Leonov, D. Ponomarenko and V. Smirnova. 'Local instability and localization of attractors. From stochastic generator to Chua's systems'. *Acta Applicandae Mathematica* 40.3 (1995), 179–243.

[27] V. I. Zubov. *Theory of oscillations*. Vol. 4. World Scientific, 1999.

[28] M. Farkas. *Periodic motions*. Vol. 104. Springer Science & Business Media, 2013.

[29] G. Leonov. 'On stability in the first approximation'. *Journal of applied mathematics and mechanics* 62.4 (1998), 511–517.

[30] A. Banaszuk and J. Hauser. 'Feedback linearization of transverse dynamics for periodic orbits'. *Systems & control letters* 26.2 (1995), 95–105.

[31] A. Mohammadi, M. Maggiore and L. Consolini. 'Dynamic virtual holonomic constraints for stabilization of closed orbits in underactuated mechanical systems'. *Automatica* 94 (2018), 112–124.

[32] R. Ortega, B. Yi, J. G. Romero and A. Astolfi. 'Orbital stabilization of nonlinear systems via the immersion and invariance technique'. *Int. Journal of Robust and Nonlinear Control* (2018).

[33] A. Shiriaev, J. W. Perram and C. Canudas-de-Wit. 'Constructive tool for orbital stabilization of underactuated nonlinear systems: Virtual constraints approach'. *IEEE Trans. on Automatic Control* 50.8 (2005), 1164–1176.

[34] A. S. Shiriaev, L. B. Freidovich and S. V. Gusev. 'Transverse linearization for controlled mechanical systems with several passive degrees of freedom'. *IEEE Trans. on Automatic Control* 55.4 (2010), 893–906.

[35] B. Yi, R. Ortega, D. Wu and W. Zhang. 'Orbital stabilization of nonlinear systems via Mexican sombrero energy shaping and pumping-and-damping injection'. *Automatica* 112 (2020), 108661.

[36] M.-S. Park and D. Chwa. 'Orbital stabilization of inverted-pendulum systems via coupled sliding-mode control'. *IEEE Trans. on Industrial Electronics* 56.9 (2009), 3556–3570.

[37] R. Santiesteban, T. Floquet, Y. Orlov, S. Riachy and J.-P. Richard. 'Second-order sliding mode control of underactuated mechanical systems II: Orbital stabilization of an inverted pendulum with application to swing up/balancing control'. *Int. Journal of Robust and Nonlinear Control* 18.4-5 (2008), 544–556.

[38] S. S. Pchelkin, A. Shiriaev, A. Robertsson, L. B. Freidovich, S. A. Kolyubin, L. V. Paramonov and S. V. Gusev. 'On orbital stabilization for industrial manipulators: Case study in evaluating performances of modified PD+ and inverse dynamics controllers'. *IEEE Trans. on Contr. Sys. Tech.* 25.1 (2016), 101–117.

[39] J. L. Massera. 'Contributions to stability theory'. *Annals of Mathematics* (1956), 182–206.

[40] E. D. Sontag. *Mathematical control theory: deterministic finite dimensional systems.* Vol. 6. Springer Science & Business Media, 2013.

[41] J. Hauser and C. C. Chung. 'Converse Lyapunov functions for exponentially stable periodic orbits'. *Systems & Control Letters* 23.1 (1994), 27–34.

[42] P. Giesl and S. Hafstein. 'Review on computational methods for Lyapunov functions'. *Discrete & Continuous Dynamical Systems-B* 20.8 (2015), 2291.

[43] T. A. Johansen. 'Computation of Lyapunov functions for smooth nonlinear systems using convex optimization'. *Automatica* 36.11 (2000), 1617–1626.

[44] H. K. Khalil. *Nonlinear systems.* Vol. 3. Prentice Hall, 2002.

[45] R. E. Hindman. 'A nonlinear control design methodology using maneuvering ideas'. PhD thesis. University of Colorado at Boulder, 1999.

[46] R. Hindman and J. Hauser. 'Stability of manoeuvre regulation using arbitrary transverse foliations'. In: *Proceedings of the 1999 American Control Conf.* Vol. 6. IEEE. 1999, 4558–4562.

[47] S. A. Al-Hiddabi and N. H. McClamroch. 'Tracking and maneuver regulation control for nonlinear nonminimum phase systems: Application to flight control'. *IEEE Trans. on Control Systems Technology* 10.6 (2002), 780–792.

[48] P. Encarnaçao and A. Pascoal. 'Combined trajectory tracking and path following: an application to the coordinated control of autonomous marine craft'. In: *Proceedings of the 40th IEEE Conf. on Decision and Control (Cat. No. 01CH37228)*. Vol. 1. IEEE. 2001, 964–969.

[49] M. Urabe. 'Geometric study of nonlinear autonomous oscillations'. *Funkcialaj Ekvacioj* 1 (1958), 1–83.

[50]* G. Borg. *A condition for the existence of orbitally stable solutions of dynamical systems*. Elander, 1960.

[51] P. Hartman and C. Olech. 'On global asymptotic stability of solutions of differential equations'. *Trans. of the Amer. Math. Society* 104.1 (1962), 154–178.

[52] I. R. Manchester and J.-J. E. Slotine. 'Transverse contraction criteria for existence, stability, and robustness of a limit cycle'. *Systems & Control Letters* 63 (2014), 32–38.

[53] M. Surov, S. Gusev and L. Freidovich. 'Constructing Transverse Coordinates for Orbital Stabilization of Periodic Trajectories'. In: *2020 American Control Conf. (ACC)*. IEEE. 2020, 836–841.

[54] G. A. Leonov. 'Generalization of the Andronov-Vitt theorem'. *Regular and chaotic dynamics* 11.2 (2006), 281–289.

[55] A. Shiriaev, L. B. Freidovich and I. R. Manchester. 'Can we make a robot ballerina perform a pirouette? orbital stabilization of periodic motions of underactuated mechanical systems'. *Annual Reviews in Control* 32.2 (2008), 200–211.

[56] I. R. Manchester. 'Transverse dynamics and regions of stability for nonlinear hybrid limit cycles'. In: *18th IFAC World Congress*. Elsevier, 2011, 6285–6290.

[57] I. R. Manchester, U. Mettin, F. Iida and R. Tedrake. 'Stable dynamic walking over uneven terrain'. *The Int. Journal of Robotics Research* 30.3 (2011), 265–279.

[58] G. Leonov. 'The orbital stability of the trajectories of dynamic systems'. *Journal of Applied Mathematics and Mechanics* 54.4 (1990), 425–429.

[59] A. Shiryaev, R. R. Khusainov, S. N. Mamedov, S. V. Gusev and N. V. Kuznetsov. 'On Leonov's method for computing the linearization of transverse dynamics and analyzing Zhukovsky stability'. *Vestnik St. Petersburg University, Mathematics* 52.4 (2019), 334–341.

[60] V. Utkin. 'Variable structure systems with sliding modes'. *IEEE Trans. on Automatic control* 22.2 (1977), 212–222.

[61] V. Yakubovich and V. Starzhinskii. *Linear differential equations with periodic coefficients*. Vol. 2. Wiley, 1975.

[62] V. I. Utkin. *Sliding modes in control and optimization*. Springer Science & Business Media, 2013.

[63] Y. Shtessel, C. Edwards, L. Fridman and A. Levant. *Sliding mode control and observation*. Vol. 10. Springer, 2014.

[64] S. Gutman. 'Uncertain dynamical systems–A Lyapunov min-max approach'. *IEEE Trans. on Automatic Control* 24.3 (1979), 437–443.

[65] I. Nagesh and C. Edwards. 'A multivariable super-twisting sliding mode approach'. *Automatica* 50.3 (2014), 984–988.

[66] V. Utkin, A. Poznyak, Y. Orlov and A. Polyakov. 'Conventional and high order sliding mode control'. *Journal of the Franklin Institute* 357.15 (2020), 10244–10261.

[67] L. B. Freidovich and S. V. Gusev. *Method, system and computer program for controlling dynamic manipulations by a robot*. Patent application number: SE 1850676-6. 2018.

[68] C. F. Sætre and A. Shiriaev. 'On excessive transverse coordinates for orbital stabilization of periodic motions'. In: *IFAC World Congress 2020*. Elsevier, 2020, 9250–9255.

[69] C. F. Sætre and A. Shiriaev. 'On Orbital Stabilization as an alternative to Reference Tracking Control'. In: *16th Int. Workshop on Advanced Motion Control (AMC)*. IEEE. 2020, 91–97.

[70] C. F. Sætre, A. Shiriaev, S. Pchelkin and A. Chemori. 'Excessive transverse coordinates for orbital stabilization of (underactuated) mechanical systems'. In: *1st Virtual European Control Conf. (ECC)*. IEEE. 2020, 895–900.

[71] C. F. Sætre and A. Shiriaev. *Orbital Stabilization of Point-to-Point Maneuvers in Underactuated Mechanical Systems*. arXiv preprint (Accepted for publication in Automatica). 2022. arXiv: `2102.04966 [eess.SY]`.

[72] C. F. Sætre, A. Shiriaev and T. Anstensrud. 'Trajectory optimization and orbital stabilization of underactuated euler-lagrange systems with impacts'. In: *18th European Control Conf. (ECC)*. IEEE. 2019, 758–763.

[73] C. F. Sætre, A. S. Shiriaev, L. B. Freidovich, S. V. Gusev and L. M. Fridman. 'Robust orbital stabilization: A Floquet theory–based approach'. *Int. Journal of Robust and Nonlinear Control* 31.16 (2021), 8075–8108.

[74] G. Teschl. *Ordinary differential equations and dynamical systems*. Vol. 140. American Mathematical Soc., 2012.

[75] G. A. Leonov. 'Strange attractors and classical stability theory'. *Nonl. dyns. and sys. th.* 8.1 (2008), 49–96.

[76] A. L. Fradkov and A. Y. Pogromsky. *Introduction to control of oscillations and chaos*. Vol. 35. World Scientific, 1998.

[77] S. H. Strogatz. *Nonlinear dynamics and chaos with student solutions manual: With applications to physics, biology, chemistry, and engineering*. Second. CRC press, 2015.

[78] D. V. Efimov and A. L. Fradkov. 'Oscillatority of nonlinear systems with static feedback'. *SIAM journal on control and optimization* 48.2 (2009), 618–640.

[79] S. Mamedov, R. Khusainov, A. Klimchik, A. Maloletov and A. Shiriaev. 'Underactuated Mechanical Systems: Whether Orbital Stabilization Is an Adequate Assignment for a Controller Design?' *IFAC-PapersOnLine* (2020).

[80] A. A. Andronov, A. A. Vitt and S. E. Khaikin. *Theory of Oscillators*. first. Pergamom Press, 1966.

[81] W. J. Rugh. *Nonlinear system theory*. Johns Hopkins University Press Baltimore, MD, 1981.

[82] A. Loria and E. Panteley. 'Stability, as told by its developers'. *IFAC-PapersOnLine* 50.1 (2017), 5219–5230.

[83] A. M. Lyapunov. 'The general problem of the stability of motion'. *Int. J. control* 55.3 (1992). Orig. pub. 1892 (in Russian)., 531–534.

[84]* H. Poincaré. 'Mémoire sur les courbes définies par une équation différentielle (I)'. *J. de math. pures et app.* 7 (1881), 375–422.

[85]* N. Zhukovskij. 'On the solidity of motion'. *Collected Works* 1 (1948), 67–161.

[86] C. Ding. 'The limit sets of uniformly asymptotically Zhukovskij stable orbits'. *Computers & Mathematics with Applications* 47.6-7 (2004), 859–862.

[87] L. Arnold and V. Wihstutz. 'Lyapunov exponents: a survey'. In: *Lyapunov Exponents*. Springer, 1986, 1–26.

[88]* B. P. Demidovich. 'The orbital stability of bounded solutions of an autonomous system. I, II'. *Differentsial'nye uravneniya* 4.4 (1968), 575–588, 1359–1373.

[89] G. A. Leonov and N. V. Kuznetsov. 'Time-varying linearization and the Perron effects'. *Int. J. of bifurcation and chaos* 17.04 (2007), 1079–1107.

[90] M. A. Aizerman and F. R. Gantmakher. 'On the stability of periodic motions'. *Journal of Applied Mathematics and Mechanics* 22.6 (1958), 1065–1078.

[91] G. A. Leonov, A. Noack and V. Reitmann. 'Asymptotic orbital stability conditions for flows by estimates of singular values of the linearization'. *Nonlinear Analysis* 44 (2001), 1057–1085.

[92] F. R. Gantmacher. 'The theory of matrices'. *Chelsea* (1959).

[93] V. Yakubovich. 'A linear-quadratic optimization problem and the frequency theorem for nonperiodic systems. I'. *Siberian Mathematical Journal* 27.4 (1986), 614–630.

[94] P. Hartman. 'A lemma in the theory of structural stability of differential equations'. *Proceedings of the American Mathematical Society* 11.4 (1960), 610–620.

[95]* D. M. Grobman. 'Homeomorphism of systems of differential equations'. *Doklady Akademii Nauk SSSR* 128.5 (1959), 880–881.

[96] P. Hartman. 'On local homeomorphisms of Euclidean spaces'. *Bol. Soc. Mat. Mexicana* 5.2 (1960), 220–241.

[97]* A. Andronov and A. Vitt. 'On Stability in the Sense of Lyapunov'. *Zhurnal Eksperimental'noi i Teoreticheskoi Fisiki* 5 (1933), 381–382.

[98]* O. Perron. 'Die stabilitätsfrage bei differentialgleichungen'. *Mathematische Zeitschrift* 32.1 (1930), 703–728.

[99] E. R. Westervelt, C. Chevallereau, J. H. Choi, B. Morris and J. W. Grizzle. *Feedback control of dynamic bipedal robot locomotion*. CRC press, 2007.

[100] S. Bittanti, P. Bolzern and P. Colaneri. 'The extended periodic Lyapunov lemma'. *Automatica* 21.5 (1985), 603–605.

[101] P. Giesl, S. Hafstein and C. Kawan. 'Review on contraction analysis and computation of contraction metrics'. *arXiv preprint arXiv:2203.01367* (2022).

[102] J. M. Hollerbach. 'Dynamic scaling of manipulator trajectories'. In: *1983 American Control Conf.* IEEE. 1983, 752–756.

[103] D. Verscheure, B. Demeulenaere, J. Swevers, J. De Schutter and M. Diehl. 'Time-optimal path tracking for robots: A convex optimization approach'. *IEEE Trans. on Automatic Control* 54.10 (2009), 2318–2327.

[104] C. Chevallereau. 'Time-scaling control for an underactuated biped robot'. *IEEE Trans. on Robotics and Automation* 19.2 (2003), 362–368.

[105] A. Shiriaev, J. Perram, A. Robertsson and A. Sandberg. 'Explicit formulas for general integrals of motion for a class of mechanical systems subject to virtual constraints'. In: *2004 43rd IEEE Conf. on Decision and Control (CDC)(IEEE Cat. No. 04CH37601)*. Vol. 2. IEEE. 2004, 1158–1163.

[106] A. L. Fradkov and A. Y. Markov. 'Adaptive synchronization of chaotic systems based on speed gradient method and passification'. *IEEE Trans. on Circuits and Systems I: Fundamental Theory and Applications* 44.10 (1997), 905–912.

[107] G. Garofalo, C. Ott and A. Albu-Schäffer. 'Orbital stabilization of mechanical systems through semidefinite Lyapunov functions'. In: *2013 American Control Conf.* IEEE. 2013, 5715–5721.

[108] P. Seibert and J. Florio. 'On the reduction to a subspace of stability properties of systems in metric spaces'. *Annali di Matematica pura ed applicata* 169.1 (1995), 291–320.

[109] M. I. El-Hawwary and M. Maggiore. 'Reduction principles and the stabilization of closed sets for passive systems'. *IEEE Trans. on Automatic Control* 55.4 (2010), 982–987.

[110] M. I. El-Hawwary and M. Maggiore. 'Reduction theorems for stability of closed sets with application to backstepping control design'. *Automatica* 49.1 (2013), 214–222.

[111] V. Utkin, J. Guldner and M. Shijun. *Sliding mode control in electromechanical systems*. Vol. 34. CRC press, 1999.

[112] Y. V. Orlov. *Discontinuous systems: Lyapunov analysis and robust synthesis under uncertainty conditions*. Springer Science & Business Media, 2008.

[113] A. F. Filippov. 'Application of the theory of differential equations with discontinuous right-hand sides to non-linear problems in automatic control'. *IFAC Proceedings Vol.* 1.1 (1960), 933–937.

[114] A. F. Filippov. *Differential equations with discontinuous righthand sides: control systems*. Vol. 18. Springer Science & Business Media, 2013.

[115] V. A. Yakubovich, G. A. Leonov and A. K. Gelig. *Stability of stationary sets in control systems with discontinuous nonlinearities*. Vol. 14.

[116] L. Fridman, J. A. Moreno, B. Bandyopadhyay, S. Kamal and A. Chalanga. 'Continuous nested algorithms: The fifth generation of sliding mode controllers'. In: *Recent advances in sliding modes: From control to intelligent mechatronics*. Springer, 2015, 5–35.

[117] V. T. Haimo. 'Finite time controllers'. *SIAM Journal on Control and Optimization* 24.4 (1986), 760–770.

[118] S. P. Bhat and D. S. Bernstein. 'Finite-time stability of continuous autonomous systems'. *SIAM Journal on Control and Optimization* 38.3 (2000), 751–766.

[119] Y. Wu, X. Yu and Z. Man. 'Terminal sliding mode control design for uncertain dynamic systems'. *Systems & Control Letters* 34.5 (1998), 281–287.

[120] Y. Feng, X. Yu and Z. Man. 'Non-singular terminal sliding mode control of rigid manipulators'. *Automatica* 38.12 (2002), 2159–2167.

[121] M. Ruderman. 'Optimal terminal sliding-mode control for second-order motion systems'. *arXiv preprint arXiv:2001.09043* (2020).

[122] S. P. Bhat and D. S. Bernstein. 'Geometric homogeneity with applications to finite-time stability'. *Mathematics of Control, Signals and Systems* 17.2 (2005), 101–127.

[123] C. C. Chung and J. Hauser. 'Nonlinear control of a swinging pendulum'. *automatica* 31.6 (1995), 851–862.

[124] M. W. Spong. 'Energy based control of a class of underactuated mechanical systems'. *IFAC Proceedings Vol.* 29.1 (1996), 2828–2832.

[125] K. J. Åström and K. Furuta. 'Swinging up a pendulum by energy control'. *Automatica* 36.2 (2000), 287–295.

[126] J. G. Romero and B. Yi. 'Orbital stabilization of underactuated mechanical systems without Euler-Lagrange structure after of a collocated pre-feedback'. *arXiv preprint arXiv:2109.06724* (2021).

[127] B. Yi, R. Ortega, D. Wu and W. Zhang. 'Two Constructive Solutions to Orbital Stabilization of Nonlinear Systems via Passivity-based Control'. In: *2019 IEEE 58th Conf. on Decision and Control (CDC)*. IEEE. 2019, 2027–2032.

[128] B. Yi, R. Ortega, I. R. Manchester and H. Siguerdidjane. 'Path following of a class of underactuated mechanical systems via immersion and invariance-based orbital stabilization'. *arXiv preprint arXiv:2001.10325* (2020).

[129] A. P. Aguiar and J. P. Hespanha. 'Trajectory-tracking and path-following of underactuated autonomous vehicles with parametric modeling uncertainty'. *IEEE Trans. on automatic control* 52.8 (2007), 1362–1379.

[130] R. Skjetne, A. R. Teel and P. V. Kokotovic. 'Stabilization of sets parametrized by a single variable: Application to ship maneuvering'. In: *Proc. 15th int. Symp. Mathematical theory of networks and systems*. 2002.

[131] R. Skjetne, T. I. Fossen and P. V. Kokotović. 'Robust output maneuvering for a class of nonlinear systems'. *Automatica* 40.3 (2004), 373–383.

[132] A. P. Aguiar, D. B. Dačić, J. P. Hespanha and P. Kokotović. 'Path-following or reference tracking?: An answer relaxing the limits to performance'. *IFAC Proceedings Vol.* 37.8 (2004), 167–172.

[133] A. P. Aguiar, J. P. Hespanha and P. V. Kokotović. 'Performance limitations in reference tracking and path following for nonlinear systems'. *Automatica* 44.3 (2008), 598–610.

[134] C. Canudas-de-Wit. 'On the concept of virtual constraints as a tool for walking robot control and balancing'. *Annual Reviews in Control* 28.2 (2004), 157–166.

[135] J. W. Grizzle, G. Abba and F. Plestan. 'Asymptotically stable walking for biped robots: Analysis via systems with impulse effects'. *IEEE Trans. Automatic Control* 46.1 (2001), 51–64.

[136] C. Chevallereau, G. Abba, Y. Aoustin, F. Plestan, E. Westervelt, C. C. De Wit and J. Grizzle. 'Rabbit: A testbed for advanced control theory'. *IEEE Control Systems Magazine* 23.5 (2003), 57–79.

[137] E. R. Westervelt, J. W. Grizzle and D. E. Koditschek. 'Hybrid zero dynamics of planar biped walkers'. *IEEE Trans. Automatic Control* 48.1 (2003), 42–56.

[138] A. Shiriaev, A. Robertsson, J. Perram and A. Sandberg. 'Periodic motion planning for virtually constrained Euler–Lagrange systems'. *Systems & control letters* 55.11 (2006), 900–907.

[139] M. Maggiore and L. Consolini. 'Virtual holonomic constraints for Euler–Lagrange systems'. *IEEE Trans. on Automatic Control* 58.4 (2012), 1001–1008.

[140] A. Mohammadi. 'Virtual holonomic constraints for Euler-Lagrange control systems'. PhD thesis. University of Toronto (Canada), 2016.

[141] C. Canudas-de-Wit, B. Espiau and C. Urrea. 'Orbital stabilization of underactuated mechanical systems'. *IFAC Proceedings Vol.* 35.1 (2002), 527–532.

[142] A. Shiriaev, L. B. Freidovich, A. Robertsson and R. Johansson. 'Virtual-constraints-based design of stable oscillations of Furuta pendulum: Theory and experiments'. In: *Decision and Control, 2006 45th IEEE Conf. on.* IEEE. 2006, 6144–6149.

[143] A. S. Shiriaev, L. B. Freidovich, A. Robertsson, R. Johansson and A. Sandberg. 'Virtual-holonomic-constraints-based design of stable oscillations of Furuta pendulum: Theory and experiments'. *IEEE Trans. on Robotics* 23.4 (2007), 827–832.

[144] M. Surov, A. Shiriaev, L. Freidovich, S. Gusev and L. Paramonov. 'Case study in non-prehensile manipulation: planning and orbital stabilization of one-directional rollings for the "Butterfly" robot'. In: *IEEE Int. Conf. on Robotics and Automation.* 2015, 1484–1489.

[145] L. Herrera, Y. Orlov, O. Montano and A. Shiriaev. 'Model orbit output feedback tracking of underactuated mechanical systems with actuator dynamics'. *Int. Journal of Control* 93.2 (2020), 293–306.

[146] C. Nielsen and M. Maggiore. 'On local transverse feedback linearization'. *SIAM Journal on Control and Optimization* 47.5 (2008), 2227–2250.

[147] C. Nielsen. 'Set stabilization using transverse feedback linearization'. PhD thesis. University of Toronto, 2009.

[148] C. Nielsen, C. Fulford and M. Maggiore. 'Path following using transverse feedback linearization: Application to a maglev positioning system'. *Automatica* 46.3 (2010), 585–590.

[149] A. Akhtar, C. Nielsen and S. L. Waslander. 'Path following using dynamic transverse feedback linearization for car-like robots'. *IEEE Trans. on Robotics* 31.2 (2015), 269–279.

[150] W. Lohmiller and J.-J. E. Slotine. 'On contraction analysis for non-linear systems'. *Automatica* 34.6 (1998), 683–696.

[151] I. R. Manchester and J.-J. E. Slotine. 'Control contraction metrics: Convex and intrinsic criteria for nonlinear feedback design'. *IEEE Trans. on Automatic Control* 62.6 (2017), 3046–3053.

[152] V. Andrieu, B. Jayawardhana and L. Praly. 'Transverse exponential stability and applications'. *IEEE Trans. on Automatic Control* 61.11 (2016), 3396–3411.

[153] A. Pavlov, A. Pogromsky, N. van de Wouw and H. Nijmeijer. 'Convergent dynamics, a tribute to Boris Pavlovich Demidovich'. *Systems & Control Letters* 52.3-4 (2004), 257–261.

[154] P. Giesl. 'On a matrix-valued PDE characterizing a contraction metric for a periodic orbit'. *arXiv preprint arXiv:1808.02691* (2018).

[155] P. Giesl, S. Hafstein and I. Mehrabinezhad. 'Computation and verification of contraction metrics for periodic orbits'. *Journal of Mathematical Analysis and Applications* (2021), 125309.

[156] B. Yi and I. R. Manchester. 'On the equivalence of contraction and Koopman approaches for nonlinear stability and control'. *arXiv preprint arXiv:2103.15033* (2021).

[157] R. Wisniewski and T. N. Jensen. 'Algebraic Test for Asymptotic Stability of Periodic Orbits for Polynomial Systems'. *arXiv preprint arXiv:2112.05998* (2021).

[158] I. R. Manchester, J. Z. Tang and J.-J. E. Slotine. 'Unifying robot trajectory tracking with control contraction metrics'. In: *Robotics Research*. Springer, 2018, 403–418.

[159] R. Wang, R. Tóth and I. R. Manchester. 'Virtual Control Contraction Metrics: Convex Nonlinear Feedback Design via Behavioral Embedding'. *arXiv preprint arXiv:2003.08513* (2020).

[160] M. S. Berger. *Nonlinearity and functional analysis: lectures on non-linear problems in mathematical analysis*. Vol. 74. Academic press, 1977.

[161] S. G. Krantz and H. R. Parks. *The implicit function theorem: history, theory, and applications*. Springer Science & Business Media, 2013.

[162] S. G. Krantz and H. R. Parks. ‘Distance to C^k hypersurfaces’. *Journal of Differential Equations* 40.1 (1981), 116–120.

[163] R. L. Foote. ‘Regularity of the distance function’. *Proceedings of the American Mathematical Society* 92.1 (1984), 153–155.

[164] J. Nocedal and S. Wright. *Numerical optimization.* Springer Science & Business Media, 2006.

[165] R. P. Brent. *Algorithms for minimization without derivatives.* Courier Corporation, 2013.

[166] I. R. Manchester, M. M. Tobenkin, M. Levashov and R. Tedrake. ‘Regions of attraction for hybrid limit cycles of walking robots’. *IFAC Proc. Vol.* 44.1 (2011), 5801–5806.

[167] J. P. La Salle. *The stability of dynamical systems.* SIAM, 1976.

[168] H. Harvey. *PPlane.* MATLAB Central File Exchange. Retrieved February 2, 2021. 2021. URL: `https://www.mathworks.com/matlabcentral/fileexchange/61636-pplane`.

[169] T. Yoshizawa. *Stability theory and the existence of periodic solutions and almost periodic solutions.* Vol. 14. Springer-Verlag, New York, NY, 1975.

[170] S. Bittanti, P. Colaneri and G. De Nicolao. ‘A note on the maximal solution of the periodic Riccati equation’. *IEEE Trans. on automatic control* 34.12 (1989), 1316–1319.

[171] S. Bittanti and P. Colaneri. *Periodic systems: filtering and control.* Vol. 5108985. Springer Science & Business Media, 2009.

[172] S. Bittanti, A. J. Laub and J. C. Willems. *The Riccati Equation.* Springer Science & Business Media, 2012.

[173] B. Zhou and G.-R. Duan. ‘Periodic Lyapunov equation based approaches to the stabilization of continuous-time periodic linear systems’. *IEEE Trans. on Automatic Control* 57.8 (2012), 2139–2146.

[174] A. Varga. ‘On solving periodic differential matrix equations with applications to periodic system norms computation’. In: *Proc. of the 44th Conf. on Decision and Control.* IEEE. 2005, 6545–6550.

[175] A. Varga. ‘On solving periodic Riccati equations’. *Numerical Linear Algebra with Applications* 15.9 (2008), 809–835.

[176] S. V. Gusev, A. S. Shiriaev and L. B. Freidovich. ‘LMI approach for solving periodic matrix Riccati equation’. *IFAC Proceedings Vol.* 40.14 (2007), 254–256.

[177] S. V. Gusev, A. S. Shiriaev and L. B. Freidovich. ‘SDP-based approximation of stabilising solutions for periodic matrix Riccati differential equations’. *Int. J. of Control* 89.7 (2016), 1396–1405.

[178] S. Gusev, S. Johansson, B. Kågström, A. Shiriaev and A. Varga. ‘A numerical evaluation of solvers for the periodic Riccati differential equation’. *BIT Num. Mathematics* 50.2 (2010), 301–329.

[179] Y. Z. Chen, J. Q. Liu and S. B. Chen. ‘Comparison and uniqueness theorems for periodic Riccati differential equations’. *Int. Journal of Control* 69.3 (1998), 467–473.

[180] H. Abou-Kandil, G. Freiling, V. Ionescu and G. Jank. *Matrix Riccati equations in control and systems theory*. Birkhäuser, 2012.

[181] F. Zhang. *The Schur complement and its applications*. Vol. 4. Springer Science & Business Media, 2006.

[182] B. R. Barmish. ‘Necessary and sufficient conditions for quadratic stabilizability of an uncertain system’. *Journal of Optimization theory and applications* 46.4 (1985), 399–408.

[183] J. Bernussou, P. Peres and J. Geromel. ‘A linear programming oriented procedure for quadratic stabilization of uncertain systems’. *Systems & Control Letters* 13.1 (1989), 65–72.

[184] G. E. Dullerud and F. Paganini. *A course in robust control theory: a convex approach*. 1st ed. Springer Science & Business Media, 2005.

[185] I. R. Petersen and C. V. Hollot. ‘A Riccati equation approach to the stabilization of uncertain linear systems’. *Automatica* 22.4 (1986), 397–411.

[186] E. Ahbe, A. Iannelli and R. S. Smith. ‘A novel moving orthonormal coordinate-based approach for region of attraction analysis of limit cycles’. *Journal of Computational Dynamics (accepted)* (2022).

[187] T. Stykel. ‘Analysis and numerical solution of generalized Lyapunov equations’. PhD thesis. Institut für Mathematik, Technische Universität, Berlin, 2002.

[188] A. Albu-Schaeffer and C. Della Santina. ‘A review on nonlinear modes in conservative mechanical systems’. *Annual Reviews in Control* (2020).

[189] F. Bjelonic, A. Sachtler, A. Albu-Schäffer and C. Della Santina. ‘Experimental closed-loop excitation of nonlinear normal modes on an elastic industrial robot’. *IEEE Robotics and Automation Letters* 7.2 (2022), 1689–1696.

[190] M. W. Spong, S. Hutchinson, M. Vidyasagar et al. *Robot modeling and control.* Vol. 3. Wiley New York, 2006.

[191] F. Ghorbel, B. Srinivasan and M. W. Spong. 'On the uniform boundedness of the inertia matrix of serial robot manipulators'. *Journal of Robotic Systems* 15.1 (1998), 17–28.

[192] J. I. Mulero-Martínez. 'Uniform bounds of the coriolis/centripetal matrix of serial robot manipulators'. *IEEE Trans. on Robotics* 23.5 (2007), 1083–1089.

[193] M. O. Surov, S. V. Gusev and A. S. Shiriaev. 'New Results on Trajectory Planning for Underactuated Mechanical Systems with Singularities in Dynamics of a Motion Generator'. In: *2018 IEEE Conf. on Decision and Control (CDC).* IEEE. 2018, 6900–6905.

[194] D. Jordan, P. Smith and P. Smith. *Nonlinear ordinary differential equations: an introduction for scientists and engineers.* Vol. 10. Oxford University Press on Demand, 2007.

[195] P. J. Davis and P. Rabinowitz. *Methods of numerical integration.* Second edition. Academic Press, 1984.

[196] D. Jankuloski, M. Maggiore and L. Consolini. 'Further results on virtual holonomic constraints'. *IFAC Proceedings Vol.* 45.19 (2012), 84–89.

[197] A. Mohammadi, M. Maggiore and L. Consolini. 'When is a lagrangian control system with virtual holonomic constraints lagrangian?' *IFAC Proceedings Vol.* 46.23 (2013), 512–517.

[198] A. Shiriaev and L. Freidovich. 'Transverse linearization for impulsive mechanical systems with one passive link'. *IEEE Trans. Automatic Control* 54.12 (2009), 2882–2888.

[199] M. O. Surov, S. V. Gusev and A. S. Shiriaev. 'Shaping Stable Oscillation of a Pendulum on a Cart around the Horizontal'. *IFAC-PapersOnLine* 50.1 (2017), 7621–7626.

[200] J. Löfberg. 'YALMIP: A toolbox for modeling and optimization in MATLAB'. In: *Proc. of the CACSD Conf.* Vol. 3. Taipei, Taiwan. 2004.

[201] R. H. Tütüncü, K.-C. Toh and M. J. Todd. 'Solving semidefinite-quadratic-linear programs using SDPT3'. *Mathematical programming* 95.2 (2003), 189–217.

[202] P. X. La Hera, L. B. Freidovich, A. S. Shiriaev and U. Mettin. 'New approach for swinging up the Furuta pendulum: Theory and experiments'. *Mechatronics* 19.8 (2009), 1240–1250.

[203] S. Sellami, S. Mamedov and R. Khusainov. 'A ROS-based swing up control and stabilization of the Pendubot using virtual holonomic constraints'. In: *2020 Int. Conf. Nonlinearity, Information and Robotics (NIR)*. IEEE. 2020, 1–5.

[204] F. H. Clarke, Y. S. Ledyaev, R. J. Stern and P. R. Wolenski. *Nonsmooth analysis and control theory*. Vol. 178. Springer Science & Business Media, 2008.

[205] J. Hauser, S. Sastry and P. Kokotovic. 'Nonlinear control via approximate input-output linearization: The ball and beam example'. *IEEE Trans. on automatic control* 37.3 (1992), 392–398.

[206] J.-C. Ryu, F. Ruggiero and K. M. Lynch. 'Control of nonprehensile rolling manipulation: Balancing a disk on a disk'. *IEEE Trans. on Robotics* 29.5 (2013), 1152–1161.

[207] A. Belyaev. 'Plane and space curves. curvature. curvature–based features'. *Max–Planck–Institut für Informatik* (2004).

[208] M. Cefalo, L. Lanari and G. Oriolo. 'Energy-based control of the butterfly robot'. *IFAC Proceedings Vol.* 39.15 (2006), 1–6.

[209] R. Goebel, R. G. Sanfelice and A. R. Teel. 'Hybrid dynamical systems'. *IEEE Control Systems* 29.2 (2009), 28–93.

[210] A. J. Van Der Schaft and J. M. Schumacher. *An introduction to hybrid dynamical systems*. Vol. 251. Springer London, 2000.

[211] R. I. Leine and H. Nijmeijer. *Dynamics and bifurcations of non-smooth mechanical systems*. Vol. 18. Springer Science & Business Media, 2013.

[212] P. C. Müller. 'Calculation of Lyapunov exponents for dynamic systems with discontinuities'. *Chaos, Solitons & Fractals* 5.9 (1995), 1671–1681.

[213] L. B. Freidovich, A. S. Shiriaev and I. R. Manchester. 'Stability analysis and control design for an underactuated walking robot via computation of a transverse linearization'. *IFAC Proceedings Vol.* 41.2 (2008), 10166–10171.

[214] G. Song and M. Zefran. 'Stabilization of hybrid periodic orbits with application to bipedal walking'. In: *2006 American Control Conf.* IEEE. 2006, 6–pp.

[215] J. Z. Tang, A. M. Boudali and I. R. Manchester. 'Invariant funnels for underactuated dynamic walking robots: New phase variable and experimental validation'. In: *2017 IEEE Int. Conf. on Robotics and Automation (ICRA)*. IEEE. 2017, 3497–3504.

[216] P. X. M. La Hera, A. Shiriaev, L. Freidovich, U. Mettin and S. Gusev. 'Stable walking gaits for a three-link planar biped robot with one actuator'. *IEEE Trans. on Robotics* 29.3 (2013), 589–601.

[217] A. N. Michel, L. Hou and D. Liu. *Stability of dynamical systems: On the role of monotonic and non-monotonic Lyapunov functions.* Springer, 2015.

[218] G. H. Golub and V. Pereyra. 'The differentiation of pseudo-inverses and nonlinear least squares problems whose variables separate'. *SIAM Journal on numerical analysis* 10.2 (1973), 413–432.

[219] T. McGeer et al. 'Passive dynamic walking'. *Int. J. Robotics Res.* 9.2 (1990), 62–82.

[220] A. D. Ames, K. Galloway, K. Sreenath and J. W. Grizzle. 'Rapidly exponentially stabilizing control lyapunov functions and hybrid zero dynamics'. *IEEE Trans. on Automatic Control* 59.4 (2014), 876–891.

[221] G. Basile and G. Marro. 'Controlled and conditioned invariant subspaces in linear system theory'. *Journal of Optimization Theory and Applications* 3.5 (1969), 306–315.

[222] G. Perozzi, A. Polyakov, F. Miranda-Villatoro and B. Brogliato. 'Upgrading linear to sliding mode feedback algorithm for a digital controller'. In: *60th IEEE Conf. on Decision and Control.* 2021.

[223] M. Corless and G. Leitmann. 'Continuous state feedback guaranteeing uniform ultimate boundedness for uncertain dynamic systems'. *IEEE Trans. on Automatic Control* 26.5 (1981), 1139–1144.

[224] G. Haller and S. Ponsioen. 'Nonlinear normal modes and spectral submanifolds: existence, uniqueness and use in model reduction'. *Nonlinear dynamics* 86.3 (2016), 1493–1534.

[225] R. A. Horn and C. R. Johnson. *Matrix analysis.* Cambridge university press, 2012.

[226] J. Ackermann. 'Pole placement control'. *Control System, Robotics and Automation* 8.2011 (2009), 74–101.

[227] M. Krstic and M. Bement. 'Nonovershooting control of strict-feedback nonlinear systems'. *IEEE Trans. on Automatic Control* 51.12 (2006), 1938–1943.

[228] S. Yu, X. Yu, B. Shirinzadeh and Z. Man. ‘Continuous finite-time control for robotic manipulators with terminal sliding mode’. *Automatica* 41.11 (2005), 1957–1964.

[229] F. López-Caamal and J. A. Moreno. ‘Generalised multivariable supertwisting algorithm’. *Int. Journal of Robust and Nonlinear Control* 29.3 (2019), 634–660.

[230] A. Levant. ‘Sliding order and sliding accuracy in sliding mode control’. *Int. journal of control* 58.6 (1993), 1247–1263.

[231]* G. Floquet. ‘Sur les équations différentielles linéaires à coefficients périodiques’. *Annales scientifiques de l’École normale supérieure* 12 (1883), 47–88.

[232] P. Montagnier, C. C. Paige and R. J. Spiteri. ‘Real Floquet factors of linear time-periodic systems’. *Systems & control letters* 50.4 (2003), 251–262.

[233] J. Zhou. ‘Classification and characteristics of Floquet factorisations in linear continuous-time periodic systems’. *Int. Journal of Control* 81.11 (2008), 1682–1698.

[234] W. J. Culver. ‘On the existence and uniqueness of the real logarithm of a matrix’. *Proceedings of the American Mathematical Society* 17.5 (1966), 1146–1151.

[235] P. Montagnier, R. J. Spiteri and J. Angeles. ‘The control of linear time-periodic systems using Floquet–Lyapunov theory’. *Int. Journal of Control* 77.5 (2004), 472–490.

[236] S. Sinha, R. Paniyan and J. Bibb. ‘Liapunov-Floquet transformation: Computation and applications to periodic systems’. *Journal of vibration and acoustics* 118.2 (1996), 209–219.

[237] R. Castelli and J.-P. Lessard. ‘Rigorous numerics in Floquet theory: computing stable and unstable bundles of periodic orbits’. *SIAM Journal on Applied Dynamical Systems* 12.1 (2013), 204–245.

[238] M. Rubagotti, A. Estrada, F. Castaños, A. Ferrara and L. Fridman. ‘Integral sliding mode control for nonlinear systems with matched and unmatched perturbations’. *IEEE Trans. on Automatic Control* 56.11 (2011), 2699–2704.

ISBN 978-82-326-5510-6 (printed ver.)
ISBN 978-82-326-6639-3 (electronic ver.)
ISSN 1503-8181 (printed ver.)
ISSN 2703-8084 (online ver.)

NTNU

Norwegian University of
Science and Technology